

NASA CONFERENCE PUBLICATION

NASA CP-2075

(NASA-CP-2075) GOVERNMENT/INDUSTRY WORKSHOP
ON PAYLOAD LOADS TECHNOLOGY (NASA) 874 p HC
A99/MF A01 CSCL 22A

N79-20162

Unclass

G3/12 19898

GOVERNMENT/INDUSTRY WORKSHOP ON
PAYLOAD LOADS TECHNOLOGY

Papers presented at the Payload Loads Methodology Workshop
held at the Marshall Space Flight Center, Alabama,
on November 14, 15, and 16, 1978

Prepared by

NASA - George C. Marshall Space Flight Center
Marshall Space Flight Center, Alabama 35812

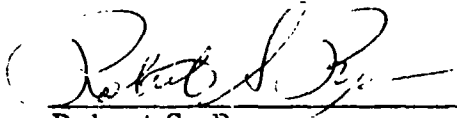


PAYLOAD LOADS METHODOLOGY WORKSHOP

MSFC, Morris Auditorium

November 14, 15, 16, 1978

A Payload Loads Methodology Workshop was held at Marshall Space Flight Center to explore ways of improving loads prediction accuracy, and efficiency areas. This document contains all the papers presented. A panel closed out the meeting. Panel members' viewpoints and their response to questions are included.



Robert S. Ryan
Workshop Coordinator

GOVERNMENT/INDUSTRY WORKSHOP ON
PAYLOAD FLIGHT LOADS PREDICTION METHODOLOGY

PAPERS PRESENTED

<u>Title</u>	<u>Presenter</u>
Payloads Loads Overview	R. Ryan, MSFC
Space Transportation System Payload Integration Process and Approaches for Loads	D. Wade, JSC
Spacecraft Dynamic Loads The Load Cycle Approach	Dr. E. R. Fleming Aerospace
Payload Lift-off Loads Reduction Feasibility Study	R. E. Gatto Rockwell
The SPAR System	W. D. Whetstone Engineering Information Systems, Inc.
Spacecraft Modal Testing Using Single Point Random and Multi-Shaker Sine Test Techniques	C. V. Stahle General Electric
Application of Perturbation Methods to Improve Analytical Model Correlation with Test Data	J. A. Garba, JPL
NASTRAN Modal Synthesis	J. Morgan Universal Analytics
Verification of Accuracy of Various Modal Methods	S. Yahata Rockwell

<u>Title</u>	<u>Presenter</u>
Time-Domain Data Analysis - A Promising New Technique	B. R. Hanks LaRC
A Comparison of Test Techniques Used During Modal Testing of ET Lox Tank	G. Johnston MSFC
Modeling of Shuttle Payload Bay Acoustic Environment	J. Young GSFC
STS Loads Impact on Syncom IV	S. Robinson Hughes Aircraft
Employment of Residual Mode Effects in Vehicle/Payload Dynamic Loads Analysis	R. N. Coppolino Aerospace
Comparison of Modal Synthesis Techniques - Effects on Modes, Frequencies, Loads	R. Hruda Martin Marietta
Sensitivity of Payload to Liftoff and Landing Loads Study	S. Yahata Rockwell
Summary of Voyager Design and Flight Loads	J. Chen, JPL
Loads Methodology for the Spacelab Transfer Tunnel	J. S. Moore, MSFC
Spacecraft Loads Analyses for the Titan/Centaur Launch Vehicle - A Case History	B. K. Wada, JPL
PAM Dynamic Loads Analysis Model Interfaces and Load Cycle Process	M. Markowitz MDAC
DATE Program Overview	W. B. Keegan GSFC

<u>Title</u>	<u>Presenter</u>
An Impedance Technique for Determining Low Frequency Payload Requirements	K. R. Payne Martin Marietta
Satellite Instrument Flexibility Specification Using Parameter Plane Stability Analysis	Dr. P. Likens Columbia University
Payload Z Load Alleviation Study	S. Yahata, Rockwell
Space Shuttle Payload Load Alleviation Using Bilinear Liquid Springs	C. D. Pengelley General Dynamics/ Convair
Low Response Suspension System for Orbiter Payloads	S. M. Church Boeing
Development of a Loads Criteria for Space Telescope	W. B. Haile Lockheed
Structural Criteria	N. Schlemmer, MSFC
An Approach for Establishing Preliminary Structural Design Requirements for Shuttle Payloads	J. I. McPherson MDAC
Estimation of Payload Loads Using Rigid Body Interface Accelerations	J. Chen, JPL
Mechanical and Loads Interface Definitions for Payload Retention	V. Durnell Ball Aerospace
Payload Response Measurements on Atlas/Centaur and Titan/Centaur Missions and Their Use in Development of Loads Criterion	T. Gerus, LeRC

**Delta Vehicle/Spacecraft Dynamic
Loads Analysis Modeling Techniques
and Forcing Function Development**

**M. Markowitz
MDAC**

**Spacelab Structural Assessment by
Comparative Analysis**

M. Tagg, MDTSCO

**A Generalized Modal Shock Spectra
Method for Spacecraft Loads Analysis**

M. Trubert, JPL

**The Application of Flight Data to Improving
Payload Response Prediction**

B. R. Hanks, LaRC

**Equivalent Pulse Determination for Stage
Zero Ignition of Titan/Centaur Forcing
Function Reconstruction**

M. Trubert, JPL

**Spacelab Payload and Shuttle Launched
Spacecraft Loads Analysis Methods**

**E. J. Kuhar
General Electric**

ORGANIZATION: SYSTEMS DYNAMICS LABORATORY	MARSHALL SPACE FLIGHT CENTER PAYLOAD LOADS OVERVIEW	NAME: R. RYAN DATE: NOVEMBER 1978
<p style="text-align: center;"><u>AGENDA</u></p> <ul style="list-style-type: none"> ○ ABSTRACT ○ THE PROBLEM DEFINED ○ THE KEY ISSUES ○ TRADES INVOLVED ○ APPROACH ○ TOOLS 		

PAYLOAD LOADS METHODOLOGY WORKSHOP

LOADS OVERVIEW

Robert S. Ryan

ABSTRACT

A fully operational Space Shuttle will offer science the opportunity to explore near earth orbit and finally interplanetary space on nearly a limitless basis. This multiplicity of payload/experiment combinations and frequency of launches places many burdens on dynamicists to predict launch and landing environments accurately and efficiently. However, our challenges do not stop there. Operational environments are usually mild from the loads standpoint, thus this part of the design criteria is stiffness and not strength driven. Herein lies the dilemma. The payload/experiments must survive the launch and landing environments, yet meet stringent requirements while in orbit. Two major problems are apparent in the attempt to design for the diverse environments: (1) Balancing the design criteria (loads, etc.) between launch and orbit operations, and (2) developing analytical techniques that are reliable, accurate, efficient, and low cost to meet the challenge of multiple launches and payloads. This paper deals with the key issues inherent in these problems, the key trades required, the basic approaches needed, and a summary of the state-of-the-art techniques.

<p>ORGANIZATION: SYSTEMS DYNAMICS LABORATORY</p>	<p>MARSHALL SPACE FLIGHT CENTER PAYLOAD LOADS OVERVIEW</p>	<p>NAME: R. RYAN DATE: NOVEMBER 1978</p>
<p style="text-align: center;"><u>THE PROBLEM DEFINED</u></p> <p>I. DESIGN REQUIREMENTS</p> <ul style="list-style-type: none"> o POTENTIAL CONFLICTING DESIGN REQUIREMENTS <ul style="list-style-type: none"> - TRANSPORTATION SYSTEM INDUCED <ul style="list-style-type: none"> o LAUNCH AND LANDING LOADS HIGH INERTIA o STRENGTH REQUIREMENTS o OPERATIONAL REQUIREMENTS o HIGH PERFORMANCE REQUIREMENTS, LOW LOADS o STIFFNESS REQUIREMENTS - ELIMINATES MANY OPTIONS FOR REDUCING COST, ETC. - COMPLEX SYSTEM TRADES REQUIRED BETWEEN: <ul style="list-style-type: none"> o LOADS o CONTROL o THERMAL o PERFORMANCE o OPERATIONAL WORKAROUNDS SUCH AS WIND BIASING NOT AVAILABLE 		

Chart 2

FILE NO.

ORGANIZATION: SYSTEMS DYNAMICS LABORATORY	MARSHALL SPACE FLIGHT CENTER PAYLOAD LOADS OVERVIEW	NAME: R. RYAN DATE: NOVEMBER 1978
<p style="text-align: center;"><u>THE PROBLEM DEFINED (CONT'D)</u></p> <p>II. PAYLOAD FLEXIBILITY</p> <ul style="list-style-type: none"> ○ WIDE RANGE OF PAYLOAD/EXPERIMENT COMBINATIONS PRODUCE: <ul style="list-style-type: none"> - PAYLOAD UNIQUE SENSITIVITIES - DYNAMIC TUNING/AMPLIFICATION - PAYLOAD UNIQUE DESIGN CRITERIA ○ A WIDE VARIETY OF ANALYSIS TOOLS (APPROACHES) REQUIRED <p>III. LOADS ANALYSIS</p> <ul style="list-style-type: none"> ○ ACCURATE TOOLS AVAILABLE <ul style="list-style-type: none"> - COMPLEX - TIME CONSUMING - POTENTIAL FOR INPUT ERROR ○ MULTIPLE PAYLOADS, QUICK TURNAROUND LAUNCH DICTATES: <ul style="list-style-type: none"> - ACCURACY - QUICK ASSESSMENT TIME - LOW COST - MINIMUM TESTING - MANY TRADE STUDIES 		

Chart 22

FILE NO.

R. RYAN

SYSTEMS DYNAMICS LAB

SPACE TELESCOPE LOADS CRITERIA

JULY 14, 1978

• LIFT OFF LOAD RESULTS USED TO ESTABLISH ΔL_S

PAYLOAD IDENTIFICATION	LOAD FACTOR	L-NOM	ΔL_S	RATIO $\Delta L_S/L_{NOM}$
SPACE LAB LONG MODULE	N _X ~ G'S	2.03	.42	.21
	N _Y ~ G'S	0.61	.78	1.28
	N _Z ~ G'S	1.32	.75	.57
SPACE LAB SINGLE PALLET	N _X ~ G'S	2.3	.81	.35
	N _Y ~ G'S	0.261	.19	.72
	N _Z ~ G'S	1.11	.24	.22
TDRS	N _X ~ G'S	2.72	.89	.33
	N _Y ~ G'S	0.297	.126	.42
	N _Z ~ G'S	2.66	1.93	.73
IUS + TDRS	N _X ~ G'S	2.74	.64	.31
	N _Y ~ G'S	0.20	.05	.25
	N _Z ~ G'S	1.17	.16	.14

3 SIGMA VALUE
 $\Delta L_S = 1.47 L_{NOM}$

MEAN VALUE

$\Delta L_S = .456 L_{NOM}$

L_{NOM} = PEAK VALUE, NOMINAL CASE

ΔL_S = 3 SIGMA INCREMENT DUE TO SHUTTLE SYSTEM PERTURBATIONS

NOTE: LOAD FACTORS PRESENTED BY ROCKWELL
 AT LOADS PANEL MEETING, 8 MARCH 1978

Chart 3

THE PROBLEM DEFINED

As stated in the introduction, the analyst faces two key problems. In the first place, the design requirements induced by the transportation system are of a different nature than the performance requirements due to mission operations in space. The high level acoustic environments and large static and dynamic loads drive toward strength design requirements, weight, and the potential requirement for isolation techniques, while the performance requirements drive toward stiffness requirements (chart 2). There is presently one payload under development where the performance requirements put the dynamic response of the payload system near resonance with the transportation system vehicle forcing functions. Either the system must take these loads or special isolation systems must be designed. As shown on chart 2, this leads to complex trades and elimination of options to reduce cost. Secondly, the large variety of payloads and requirements means that the analyst must have a whole cadre of approaches and analysis tools. Finally, although present analytical approaches are accurate, they are based on detailed modeling approaches, which require laborious efforts of compiling, sorting, and evaluating many pieces of data. This does not allow time for the required number of iteration cycles leading to improper trade assessments. Complex analysis approaches lead to input-type errors that are hard to find, further compounding the situation.

A large portion of the transportation system (Shuttle) design criteria is driven by max q environment, while payload loads result from short-term transient loads (inertial) at liftoff and landing. For max q environments, operational techniques such as wind biasing and wind constraints are available to reduce loads. This usually allows compensation for late changes in the environments without design changes. Due to the characteristics of payload loads, this option is not open. For payloads, you either fix the structure, develop an isolation system, or fly as is and take the risk.

THE PROBLEM DEFINED (CONT'D)

The problem is compounded by the fact that the Shuttle transportation system and the payload configurations are very complex, unsymmetrical, dynamic systems with high modal density. The opportunity for dynamic tuning is an ever present reality. Low damped systems that tune two or three subsystems are very sensitive to small parameter changes and require many combinations of parameter variations to develop design loads. Chart 3 shows the sensitivity of a Spacelab payload to variations in the Shuttle systems liftoff parameters, such as SRB thrust unbalance and thrust misalignment. Load changes shown as $\Delta L_s/LNOM$ are in the range of 15 to 120 percent. Clearly, this is a unique problem that must be faced for each payload.

There is a danger in stating problems, particularly when they seem insurmountable. However, in the case under discussion, this is not the case. For this problem, we start from a very strong analytical base and much experience. Also, the different classes of problems we need to solve are well defined. With the right focus and effort, the goals are reachable. On the next chart are the key issues involved in arriving at an answer.

KEY ISSUES PAYLOAD LOADS

ED1452

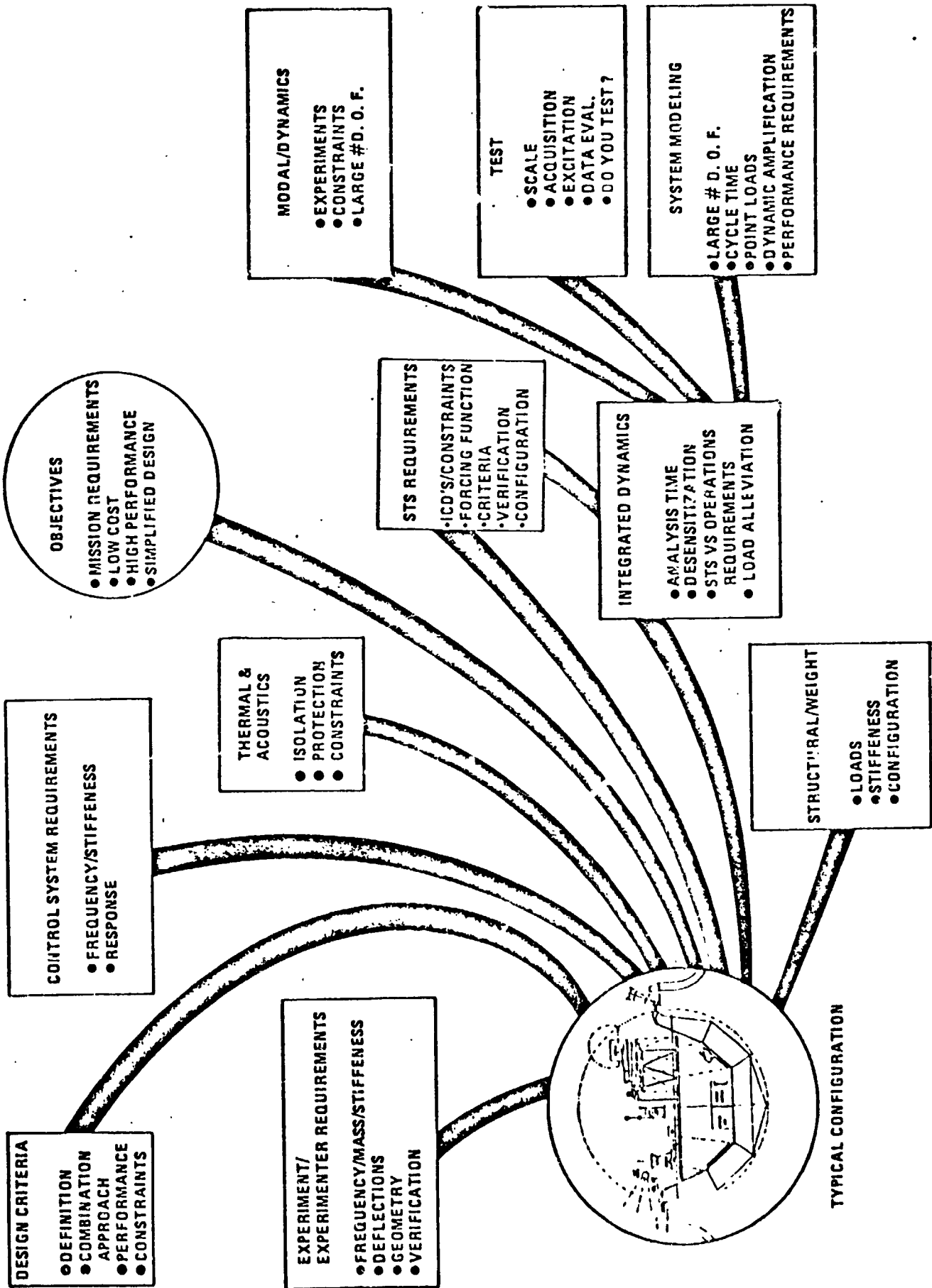


Chart 4

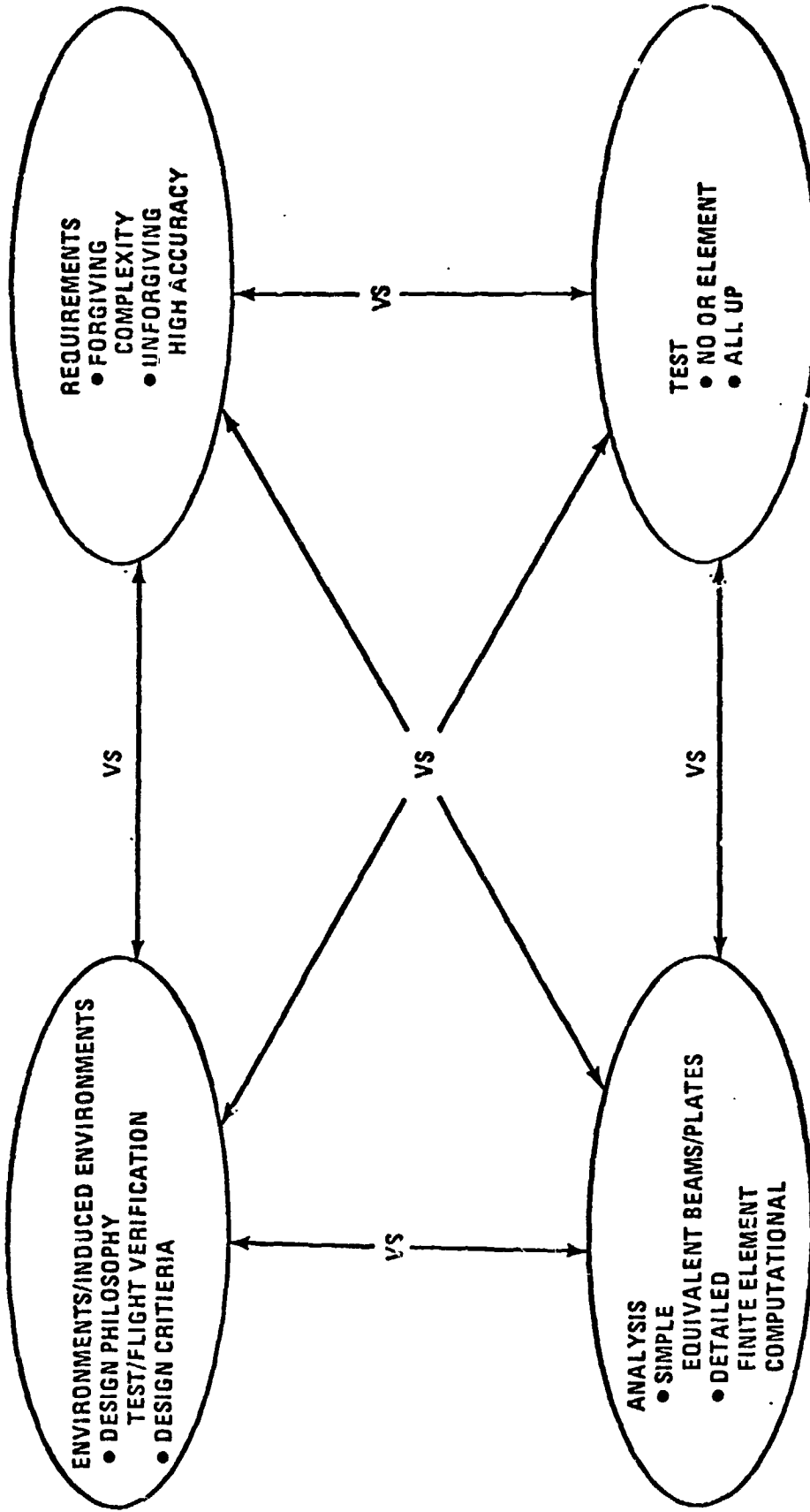
KEY PAYLOAD LOADS ISSUES

The various key issues from the structural dynamicist's viewpoint tend to focus in his own disciplines. This is a mistake. He must have a strong interaction in the development of the design criteria from the standpoint of philosophy, definition, combination approach, and performance since they drive the key issues in his own disciplines. The same is true with the control system and thermal requirements, since they have a direct input in the dynamicist's problem as well as being a key part of the many trades involved in the design criteria evolving from response and loads. In addition, the criteria for dynamics must satisfy the experiment requirements, the transportation system interfaces, etc. Neither can the performance criteria be avoided, since too conservative approaches lead to unacceptable weight penalties. With these complicating issues driving the dynamicist, he must consider the issues of his own discipline, while keeping them in the proper perspective with requirements from the other areas. Integrated dynamic analysis is composed of the subdisciplines modal/dynamic analysis, dynamic and static testing, and system modeling. The key issues in integrated dynamics are the cycle time, desensitization, performance criteria, balance between operational environment and transportation system environment, and requirements definition. Modal analysis is an important aspect of integrated analysis. The key issues here are the experiment model details, choice of modeling elements, large number of degrees of freedom, and the accuracy requirements on the dynamic characteristics. Closely coupled with these are the requirements for static and dynamic test. Key issues here are the level of testing, no testing, components, boundary conditions, substructure, environment load paths, full scale, and scale model. Key technical issues in the testing itself are test accuracy requirements, validity of the data, the excitation system and approach (random, sine, impulse, modal dwell), and the data acquisition system. Systems modeling has essentially the same issues as integrated dynamics, analysis cycle time, large number of degrees of freedom, decomposition, idealization, truncation, and modal selection criteria. Also, point loads such as arise from docking. The next chart deals with the trades required to optimally solve the problems.

<p>ORGANIZATION: SYSTEMS DYNAMICS LABORATORY</p>	<p>MARSHALL SPACE FLIGHT CENTER PAYLOAD LOADS OVERVIEW</p>	<p>NAME: R. RYAN</p>	<p>DATE: NOVEMBER 1978</p>
<p style="text-align: center;"><u>KEY TRADES</u></p> <ul style="list-style-type: none"> <input type="radio"/> CRITERIA <input type="radio"/> CONSTRAINTS <input type="radio"/> REQUIREMENTS <input type="radio"/> ANALYSIS <input type="radio"/> TEST <input type="radio"/> ISOLATION 			

Chart 5

PAYLOAD TECHNOLOGY



• TRADE DIFFERENT FOR EACH FLIGHT PHASE

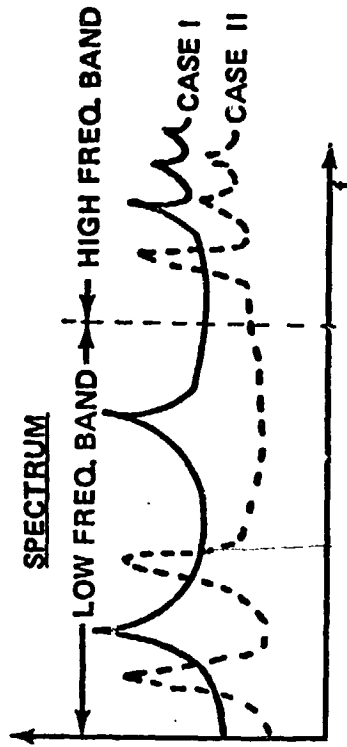
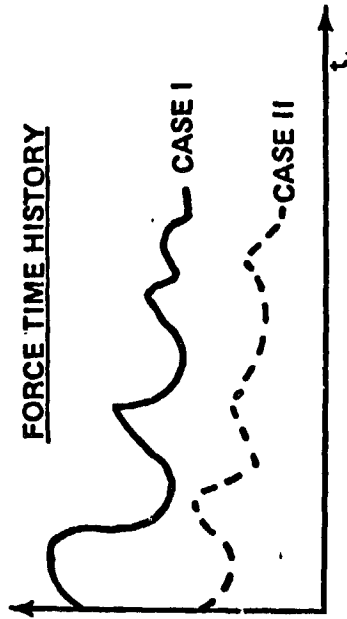
- LAUNCH
- OPERATIONS (ON-ORBIT)
- RETURN (LANDING)

ORGANIZATION: SYSTEMS DYNAMICS LABORATORY	MARSHALL SPACE FLIGHT CENTER PAYLOAD LOADS OVERVIEW	NAME: R. RYAN DATE: NOVEMBER 1978
<p style="text-align: center;"><u>CLASSES OF PAYLOADS</u></p> <p><u>CLASS I:</u> UNIQUE, SPECIAL PURPOSE PAYLOADS (SPACE TELESCOPE, HEAO)</p> <ul style="list-style-type: none"> ○ LARGE, EXPENSIVE, SENSITIVE UNITS ○ LONG OPERATIONAL LIFETIME ○ STRINGENT OPERATIONAL REQUIREMENTS ○ ACCURATE ENVIRONMENTS NECESSARY <p><u>CLASS II:</u> STANDARD CARRIERS (REUSABLE) WITH VARIOUS COMBINATIONS OF EXPERIMENT COMPLEMENTS (SPACELAB, LDEF)</p> <ul style="list-style-type: none"> ○ SHORT TERM OPERATIONS ○ SMALL TO MEDIUM SIZE EXPERIMENTS ○ CONSERVATIVE ENVIRONMENT CRITERIA ACCEPTABLE ○ IN GENERAL, NOT WEIGHT CRITICAL. CAN OFF LOAD EXPERIMENT COMPLEMENT. <p><u>CLASS III:</u> WEIGHT LIMITED (PERFORMANCE), REUSABLE STAGE PLUS PAYLOAD (IUS, SEPS, VIKING)</p> <ul style="list-style-type: none"> ○ TRANSPORTATION SYSTEM ENVIRONMENT CRITICAL ○ PAYLOAD DYNAMIC CHARACTERISTICS CRITICAL ○ STAGE/PAYLOAD DYNAMICS CAN INTERACT AND VIOLATE STS INTERFACE REQUIREMENTS 		

PAYLOAD/EXPERIMENT CONSTRAINT PROBLEM

APPROACH AND CONSIDERATIONS FOR DETERMINING PAYLOAD/EXPERIMENT FREQUENCY CONSTRAINTS.

FORCING FUNCTION: CRITERIA DICTATES THE REQUIREMENT FOR A WELL DEFINED FORCING FUNCTION WITH DISCRETE FREQUENCIES IDENTIFIED



CONSTRAINTS: A. SELECTION

- FREQUENCY SHOULD LIE BETWEEN LOW FREQUENCY BANDS AND HIGH FREQUENCY (ACOUSTIC/MECHANICAL) BANDS

B. PROBLEM

- MULTI AMPLIFICATION SOURCES TO BE AVOIDED
 - TRANSPORTATION SYSTEM
 - PAYLOAD DYNAMICS
 - EXPERIMENT DYNAMICS
- EXPERIMENT CARRYING RACK FREQUENCIES ARE FUNCTIONS OF EXPERIMENT MASS AND DYNAMICS.
- MANY SYSTEM TRADES OR CONSTRAINTS ARE REQUIRED
- SOFTENING SYSTEM TO REDUCE LANDING LOADS INCREASES COUPLING WITH LAUNCH SYSTEM.
- WEIGHT TRADES BETWEEN STIFFENING AND OFF LOADING TO MEET FREQUENCY CONSTRAINTS ARE COMPLEX

Chart 8

KEY TRADES

Turning now to the trades required to resolve these key issues and thus arrive at solutions to the three problems stated on chart 2, chart 6 depicts the four basic trade areas open to the engineer in arriving at an optimum answer. The trades indicated are not only between disciplines and design philosophy but must also consider simultaneously all mission phases, launch operations, and landing as has been explained previously. Before attacking these trades, it should be pointed out that this analysis development approach is unique for each type or class of payload and cannot be generalized further. In order to simplify the choices, three classes of payloads have been chosen (chart 7). The first class is composed of special purpose, long operation time payloads that require very accurate design criteria, hence are weighted towards the use of detailed time consuming analysis approaches. The second class is generally composed of reusable carriers with short operation time and many complements of experiments and are weighted toward simplified, quick analysis cycle time, conservative approaches. The third class, propulsion stages with attached payloads, is weighted toward very accurate, unconservative approaches with many trades in terms of isolation. These payloads are weight limited due to performance requirements.

Classifying payloads in terms of these classes and then performing the combinations of trades illustrated on chart 6 produce the optimum analysis/system approach. For example, if the choice is made to design conservatively without static and dynamic test, large safety factors are used for design. Simplified models and conservative analysis approaches are possible choices. If the system is very sensitive and weight critical, low safety factors, static and dynamic test, and detailed analysis would probably be the choice. In addition, frequency constraints, isolation, etc., can be used as part of the trades. In this case, a balance between low and high frequency environments must be obtained (chart 8). Also, in this case, the frequency content of environment must be predictable. The problems in carrying out this trade are indicated on the chart. If these conditions can be met, then simplified models and analysis approaches can be used at much reduced cost and time.

The analysis flow chosen is key to these trades and also to the optimum development of the design criteria. The next chart illustrates this.

PAYLOAD LOADS ANALYSIS FLOW

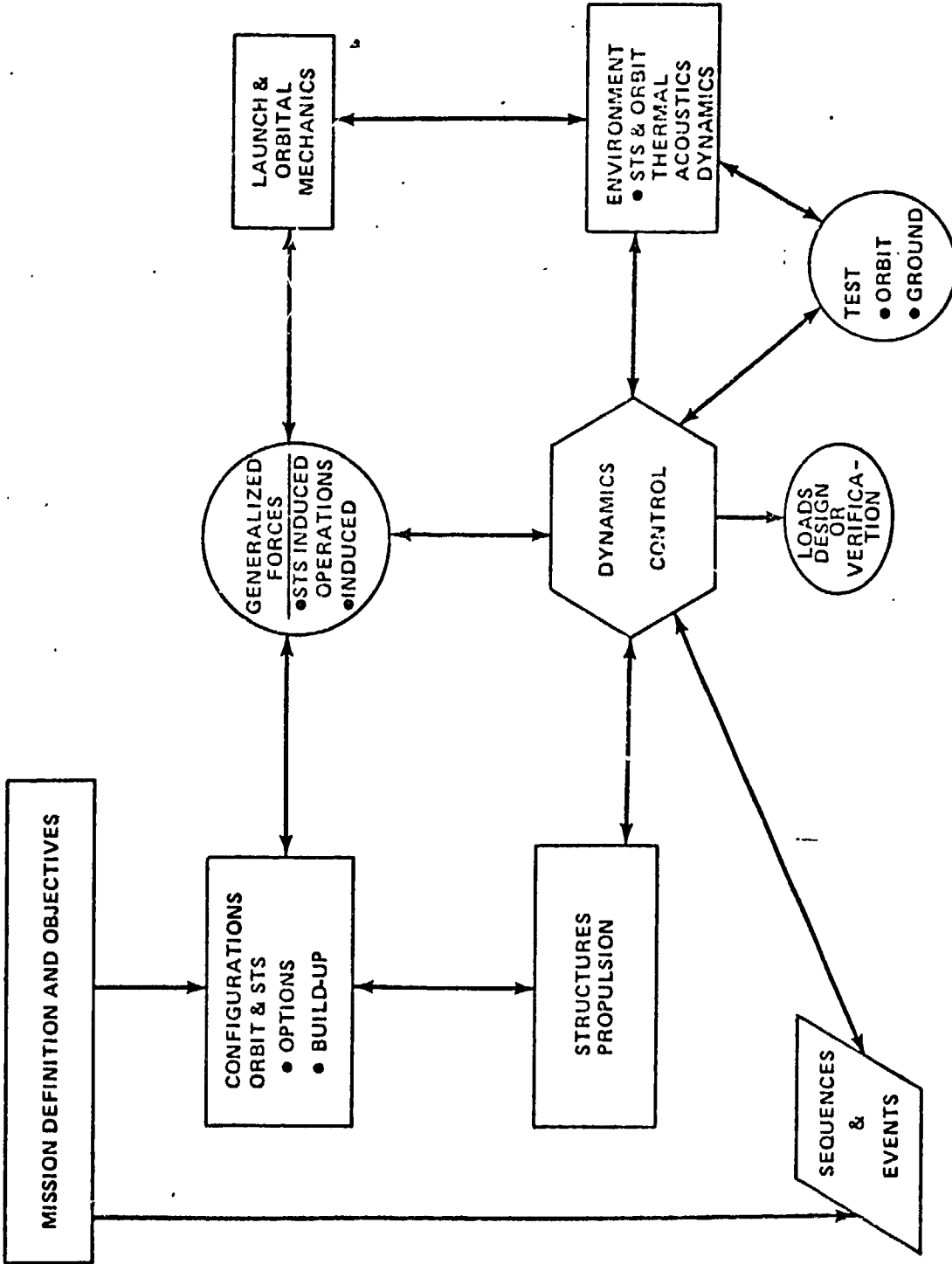


Chart 9

PAYLOAD LOADS ANALYSIS FLOW

The main emphasis on chart 9 is the need for proper interactive flow between the various disciplines and requirements. In a sense, this chart is redundant to what has been said previously; however, it is necessary to constantly remind ourselves that each discipline cannot work in a vacuum but the requirements of each discipline affects the requirements. This chart attempts to depict this interaction and is included as a means of stressing the requirement of the system approach in selecting our approaches for solving our problems.

● STRUCTURAL MODEL

- DISCRETE M & K , $[M] \{\ddot{q}\} + [K] \{q\} = \{F(t)\}$ -- COUPLED EQUATION
- MODAL MODEL, $[M_{eq}] \{\ddot{\eta}\} + [\omega^2 M_{eq}] \{\eta\} = \{\phi\}^T \{F(t)\}$

UNCOUPLED EQUATIONS

UNCOUPLED EQUATIONS RESULTING FROM MODAL MODEL MORE CONVENIENT FOR SOLUTION.

● MODAL MODEL

A. $[M]$, $[K]$ OF ALL UP SYSTEM

DIRECT OVERLAY OF $[M]$ & $[K]$ FOR SHUTTLE & PAYLOAD

B. MODAL SYNTHESIS

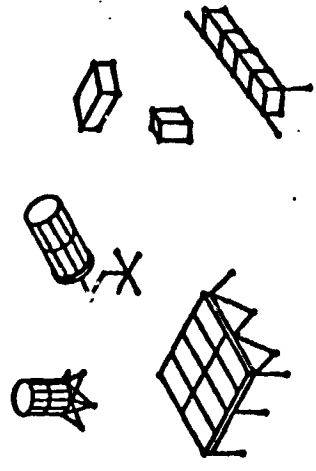


A → MOST ACCURATE
RESULTS IN LARGE EIGENVALUE PROBLEM
REQUIRING MUCH COMPUTER TIME -- EXPENSIVE

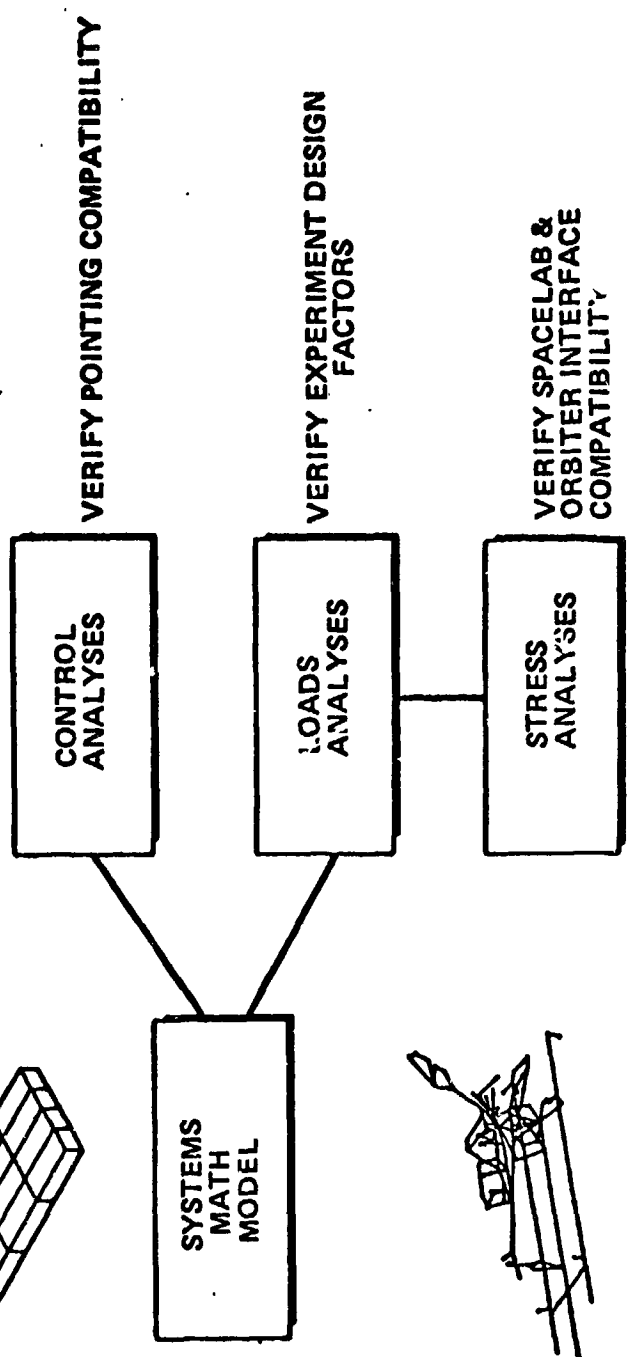
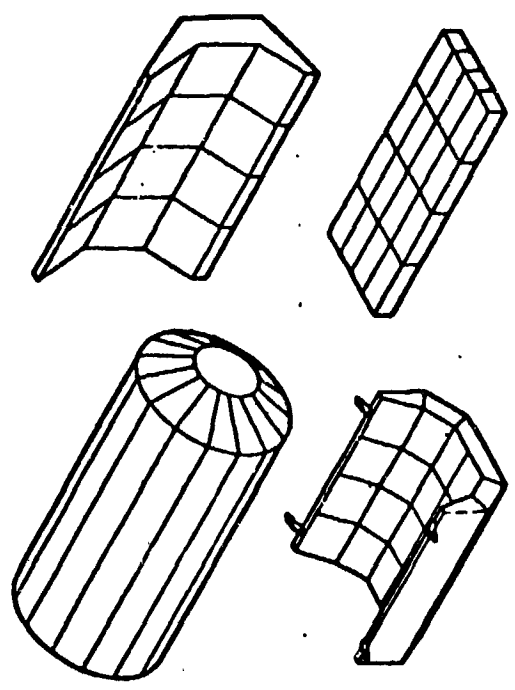
B → SMALLER EIGENVALUE PROBLEM
LESS COMPUTER TIME
SUBJECT TO CONVERGENCE ERRORS
REQUIRES INTERMEDIATE STEPS

PAYLOAD INTEGRATION MATH
MODEL DEVELOPMENT AND
INTEGRATION

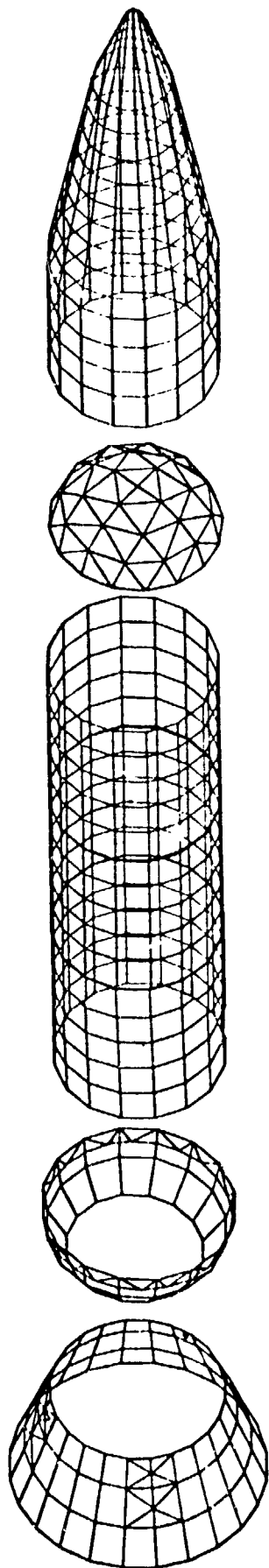
EXPERIMENTS



SPACELAB

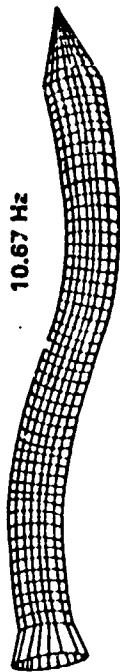


SRB MATH MODEL

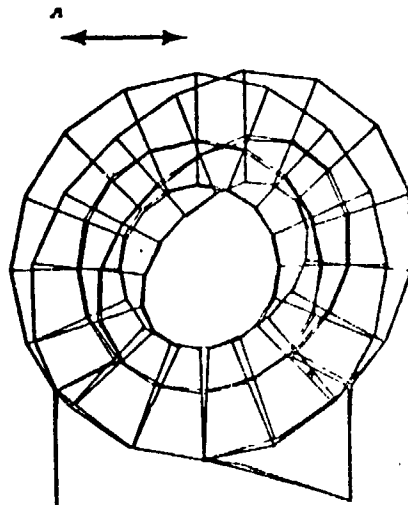


● CHARACTERISTICS

- NASTRAN FINITE ELEMENT MODEL WITH 10000 DEGREES OF FREEDOM
- ELASTIC PROPELLANT IDEALIZATION
- MODE SHAPES OF LIFTOFF CONFIGURATION
- FREE-FREE BENDING



2 Hz



● MODES WITH PROPELLANT PARTICIPATION

14 Hz

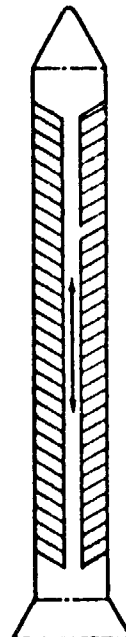


Chart 12

TOOLS

Tools available to analysts must be discussed in the three categories discussed under key issues: Integrated analysis, dynamic characteristics (structural model), and dynamic test. Chart 10 deals with the approaches available for characterizing the structure. Structural analysis can be broken into two large categories, discrete and modal. Here the differentiation between finite element, etc., used to arrive at these two classifications is not dealt with. These are the state-of-the-art tools known by and used by all. The choice between the two overall approaches is accuracy, time, and cost versus lower cost, time, and some loss of accuracy.

Chart 11 illustrates how a carrier payload, its experiments, and transportation system go together for the various analyses required. Careful observation of this large system leads quickly to the decision that the all-up discrete approach is not applicable to most payload loads problems.

Chart 12 depicts a detailed finite element model of the solid rocket booster, including its propellant showing the large number of degrees of freedom required to properly model this element of the Shuttle system. This model, however, could not be used directly in the overall Shuttle model. In this case, a very simplified model was chosen to represent the critical characteristics (modes, etc.) and forced to match the detailed model shown. The degrees of freedom using this simplified model were reduced several orders of magnitude without loss of accuracy in the overall systems model.

<p>ORGANIZATION: SYSTEMS DYNAMICS LABORATORY</p>	<p>MARSHALL SPACE FLIGHT CENTER PAYLOAD LOADS OVER VIEW</p>	<p>NAME: R. RYAN</p>
		<p>DATE: NOVEMBER 1978</p>
<p style="text-align: center;"><u>TESTING</u></p> <ul style="list-style-type: none"> ○ CONFIGURATIONS <ul style="list-style-type: none"> - SCALE MODEL - ELEMENTS - SUBSYSTEMS - ALL-UP ○ EXCITATION, DATA ACQUISITION, AND EVALUATION <ul style="list-style-type: none"> - MODAL SURVIFY <ul style="list-style-type: none"> ○ MULTI-SHAKER ○ SHAKER BLENDING AND DWELLING ○ GOODNESS CRITERIA ○ TIME CONSUMING TESTING - RANDOM, SINE, IMPULSE <ul style="list-style-type: none"> ○ SINGLE LARGE SHAKER ○ GOODNESS CRITERIA ○ SHORT TEST TIME ○ TIME CONSUMING EVALUATION APPROACHES 		

Chart 13

FILE NO.

U.S. GOVERNMENT PRINTING OFFICE: 1964 O-350-000

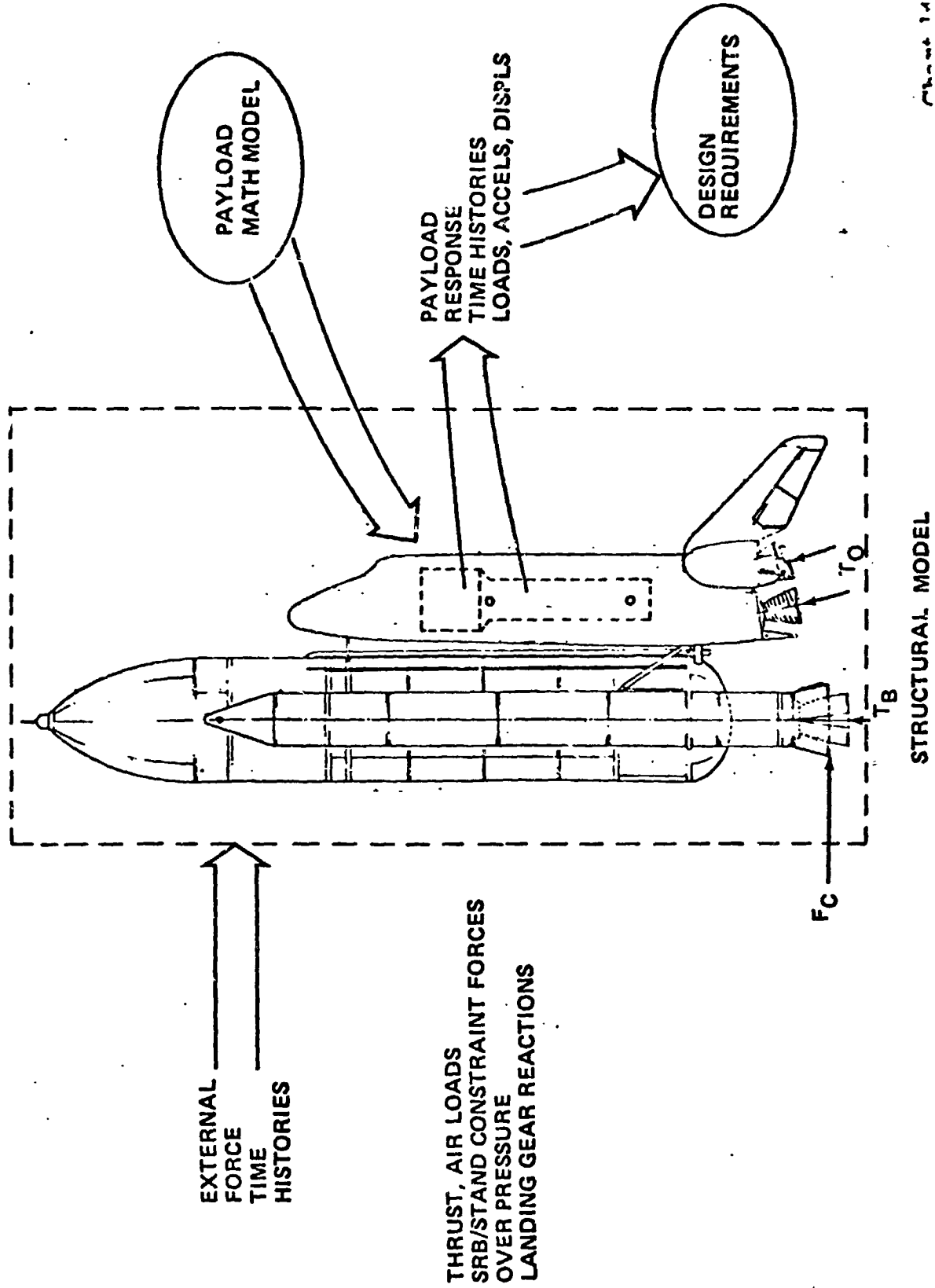
TESTING

Finally, we must deal with testing. Chart 13 lists the configuration choices. The advantages and disadvantages of each are well known and not repeated to save time and space. The same is true for the modal survey approaches. Using random testing for acquiring modal data is a fairly new comer. It has been used successfully for several space applications, MPT, one-eight scale all-up Shuttle, and many military payloads. Two potential advantages exist: (1) Acquiring accurate damping values, and (2) ability to drive response adequately from single or dual shaker points.

PAYLOAD LOADS APPROACHES

I. ALL-UP SYSTEM APPROACHES

- TIME RESPONSE DUE TO EXTERNALLY APPLIED FORCE TIME HISTORIES.



II. PAYLOAD SYSTEM APPROACHES

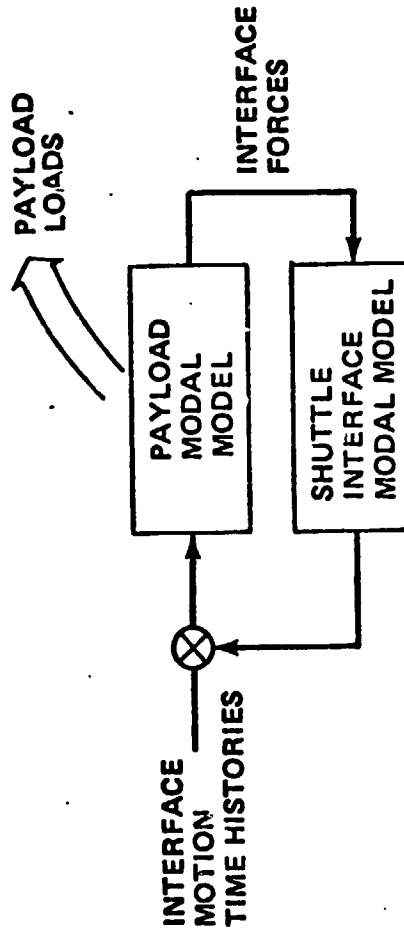
A. BASE MOTION

TIME RESPONSE OF PAYLOAD DUE TO
PAYLOAD/SHUTTLE INTERFACE MOTION



B. COUPLED BASEMOTION

SAME AS A EXCEPT ACCOUNTS FOR FEEDBACK
TO SHUTTLE INTERFACE.



ADVANTAGE: DOES NOT REQUIRE ALL-UP MODEL ANALYSES

A \Rightarrow SIMPLE HOWEVER ACCURACY IS QUESTIONABLE
DEPENDING UPON AMOUNT OF COUPLING A PARTICULAR
PAYLOAD AND SHUTTLE HAVE.

B \Rightarrow SUBJECT TO CONVERGENCE ERRORS
UNPROVEN

ADVANTAGE: USE OF FLIGHT MEASURED INTERFACE MOTION CAN
BE COMPLETED.

C. SHOCK SPECTRA & IMPEDANCE METHOD

ADVANTAGES:

SIMPLICITY – DOES NOT REQUIRE MODAL ANALYSIS OF ALL UP SYSTEM

DISADVANTAGES

- **SENSITIVE TO DAMPING ESTIMATES**
- **LEADS TO HEAVY STRUCTURAL WEIGHT**
- **MAY NOT ALWAYS BE CONSERVATIVE**

PAYLOAD LOADS APPROACHES

Using the structural model derived from its elements and all known forcing functions, the analyst can calculate the loads and derive the design criteria. Several techniques are available. Chart 14 depicts an all-up system approach which applies the total known forcing functions to the all-up system for each mission phase. The approach, though accurate, is costly and time consuming.

Moving from the all-up system approach to approaches where interface forces are applied directly to payload allows for more detailed payload models and reduces cost and time (chart 15). Two time response approaches are available, the base motion and coupled base motion. In the base motion approach, it must be assumed the payload does not change the transportation system response, thus interface accelerations are used as forcing functions on the payloads. This approach is simple. It is usually conservative; however, the accuracy is questionable since the coupling assumption is incorrect and the amount of conservatism remains unknown. The coupled base motion approach incorporates the coupling correctly between transportation system and payload; however, it is subject to convergence errors and is unproven. Both approaches can use flight measured interface motion if available.

Finally, the engineer can use impedance methods to calculate loads (chart 16). These approaches are simple and do not require modal analysis of the all-up system. This approach is very cost effective from the analysis standpoint, but the results are very sensitive to damping estimates used, can lead to weight penalties, and are not always conservative. It is very appealing because of the efficiency and low cost.

ORGANIZATION: SYSTEMS DYNAMICS LABORATORY	MARSHALL SPACE FLIGHT CENTER PAYLOAD LOADS OVERVIEW	NAME: R. RYAN DATE: NOVEMBER 1978
<p style="text-align: center;"><u>SUMMARY</u></p> <ul style="list-style-type: none"> ○ ACCURATE DYNAMIC ANALYSIS AND TESTING TOOLS ARE AVAILABLE. ○ TOOLS ARE TOO COSTLY FOR NEW PAYLOAD OPERATIONAL APPROACHES. ○ SOLUTION LIES IN BALANCE BETWEEN USE OF: <ul style="list-style-type: none"> - CONSTRAINTS - CRITERIA - SIMPLIFIED ANALYSIS - TRADES BETWEEN PERFORMANCE REQUIREMENTS AND TRANSPORTATION REQUIREMENTS - STATISTICAL COMBINATION APPROACHES FOR TOLERANCES, ETC. - UNCERTAINTY FACTORS - HIGHER SPEED COMPUTER TECHNIQUES - SPECIAL PURPOSE COMPUTERS 		

Chart 17

SUMMARY

In summary, the problem of payload prediction has been surveyed. Problems and concerns exist; however, the solutions appear on the horizon. There are very accurate dynamic analysis tools. In general, these tools are too costly to use for the new payload world facing us with the advent of the Space Shuttle Transportation System. Using a system approach that properly trades design between operational requirements and transportation requirements, frequency constraints, no test criteria, simplified dynamic models, unconservative combination approaches for tolerances, and detailed analysis where required will lead to the solutions of our problems.

PAYLOADS FLIGHT LOADS PREDICTION METHODOLOGY WORKSHOP

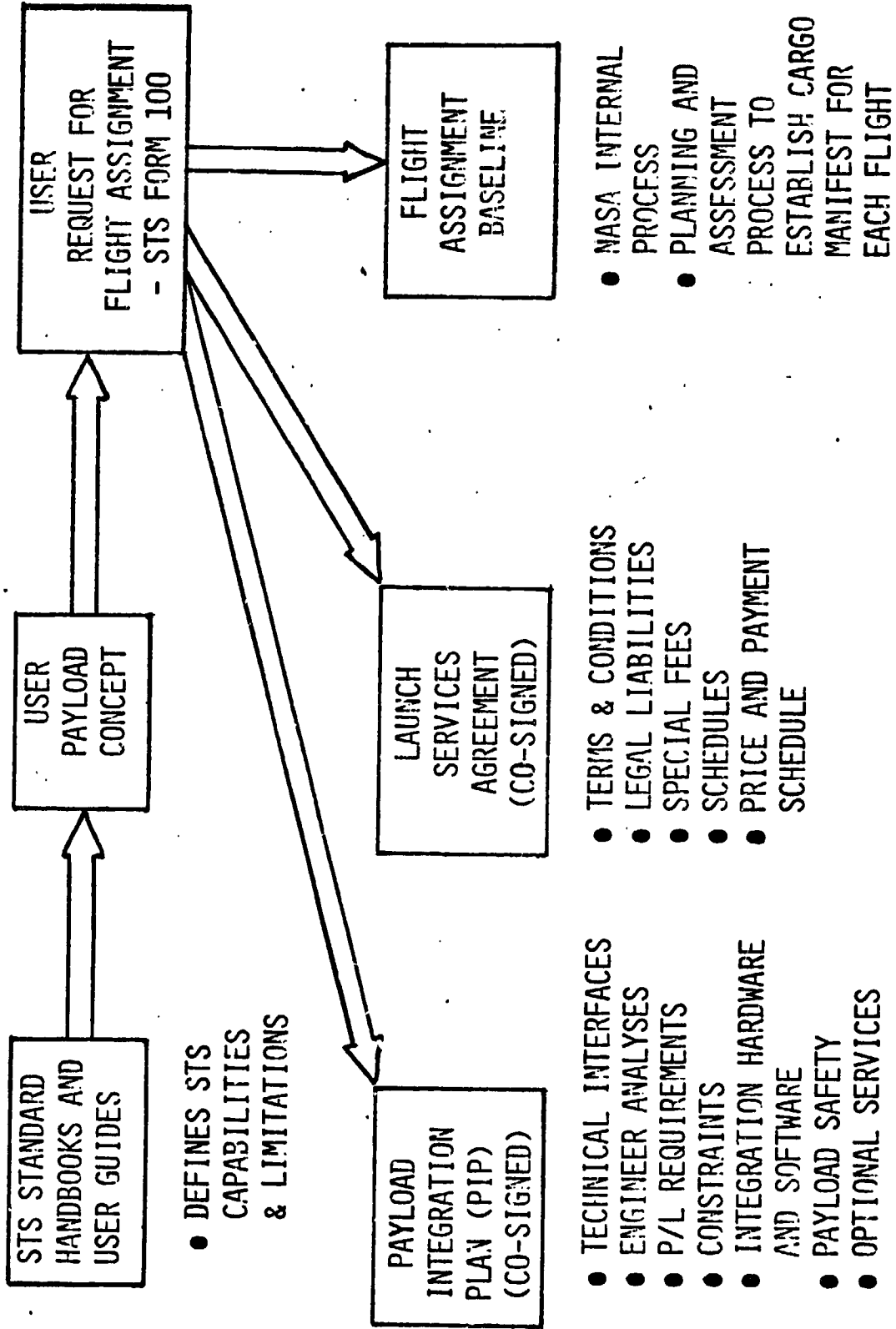
SPACE TRANSPORTATION SYSTEM PAYLOAD INTEGRATION PROCESS
AND APPROACHES FOR LOADS

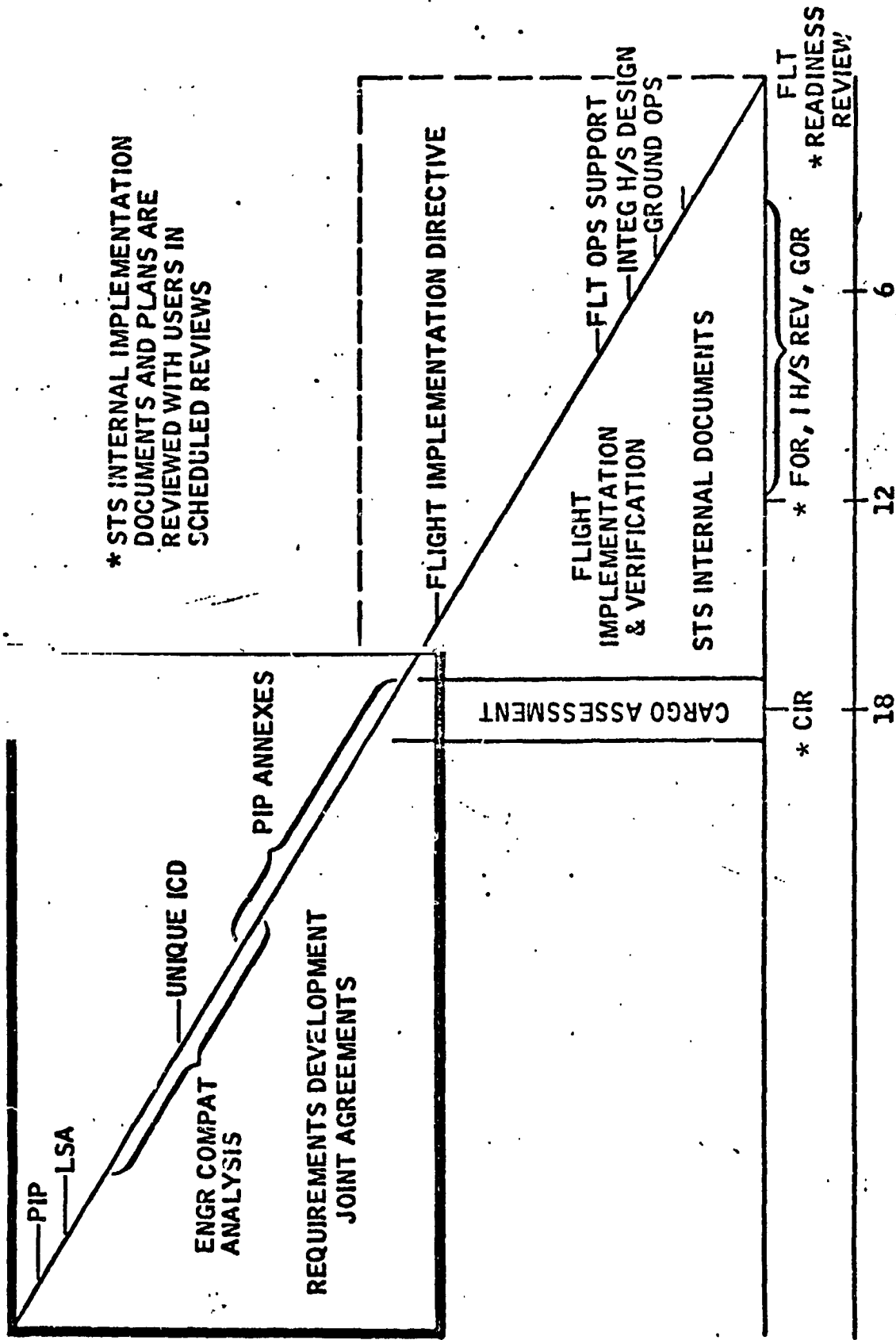
DON WADE

NOV. 14-16, 1978

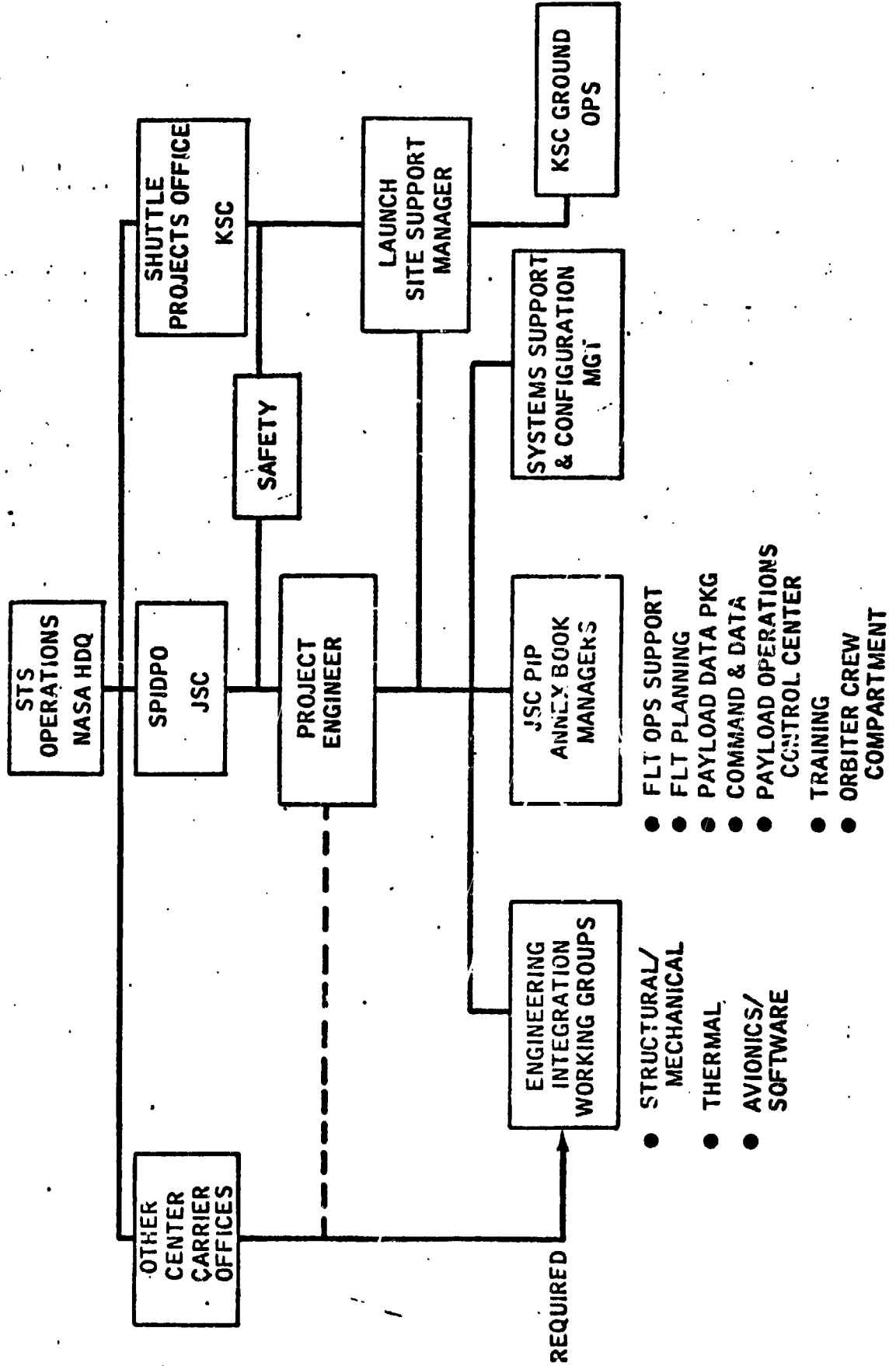
MSFC

SPACE TRANSPORTATION SYSTEM PAYLOAD INTEGRATION PROCESS





TIME PRIOR TO FLTS (MONTHS)



SEQUENCE OF EVENTS

- o INTEGRATION MEETING(S)
 - OVERVIEW OF SHUTTLE
 - OVERVIEW OF CARGO
- o PAYLOAD INTEGRATION PLAN
 - DEFINITION OF RESPONSIBILITIES/REQUIREMENTS
 - NUMBER OF LOAD CYCLES
 - o WHO DOES LOADS/DEFLECTIONS
 - o WHO PROVIDES MATH MODELS
 - o INTERFACE HARDWARE
 - o STRUCTURAL VERIFICATION PLAN
 - o SCHEDULE
- o INTERFACE CONTROL DOCUMENT
 - INTERFACE LOADS
 - CLEARANCES - INTERFACE & GENERAL
 - DEFINITION OF PHYSICAL INTERFACES
- o STRUCTURAL/MECHANICAL WORKING GROUP MEETINGS
 - ICD DEVELOPMENT AND MAINTAINENCE

SEQUENCE OF EVENTS

o STRUCTURAL/MECHANICAL WORKING GROUP (CONT'D)

- TECHNICAL INTERCHANGE

o SHUTTLE DATA

o PAYLOAD DATA

- PLANNING AND SCHEDULING OF ACTIVITIES

PRELIMINARY DESIGN LOADS AND DEFLECTIONS

o GIVEN IN ICD 2-19001 SHUTTLE ORBITER/CARGO STANDARD
INTERFACES (CORE ICD)

- PARA. 3.0 - PHYSICAL INTERFACES

- o PAYLOAD DYNAMIC ENVELOPE
- o ALLOWABLE TRUNNION TRAVEL

- PARA. 4.0 - STRUCTURAL INTERFACES

- o ORBITER INTERFACE ALLOWABLE LOADS
- o ORBITER DEFLECTIONS
- o LOAD FACTORS

TRANSIENT CONDITIONS

QUASI-STATIC CONDITIONS

EMERGENCY LANDING

- o ACOUSTIC LEVELS
- o RANDOM VIBRATION LEVELS

CARGO DEVELOPMENT LOADS/DEFLECTIONS CYCLE(S)

- o FUNDED BY CARGO ORGANIZATION (OPTIONAL SERVICE)
- o OPTIONS
 - JSC PERFORMS. CONTRACTOR SUPPLIES CARGO MATH MODEL AND LOAD TRANSFORMATION MATRIX
 - CONTRACTOR PERFORMS. JSC SUPPLIES SHUTTLE MATH MODEL AND FORCING FUNCTIONS (CONTRACTOR SPECIFIES MODAL SYNTHESIS METHOD)
 - UPPER STAGE CONTRACTOR PERFORMS. JSC SUPPLIES SHUTTLE MATH MODEL AND FORCING FUNCTIONS
- o LOAD/DEFLECTION CONDITIONS COMPUTED
 - OUTLINED IN SD77-SH-0214*
 - 8 LIFT-OFF CASES PLUS ADDITIONAL AS REQ'D.
 - 5 LANDING CASES PLUS ADDITIONAL AS REQ'D
 - QUASI-STATIC (MAX Q, BURN OUT, ENTRY, ATMOSPHERIC MANEUVER) 15 TO 22 CONDITIONS
- o SPACE SHUTTLE TRANSPORTATION SYSTEM. MODELS CONFIGURATION MANAGEMENT/CONTROL SYSTEM AND STANDARD ANALYSIS FOR PAYLOAD LOAD CYCLE.

CARGO DEVELOPMENT LOADS/DEFLECTIONS CYCLE(S) CONT'D)

- o CARGO INPUT DATA
 - FREE-FREE STIFFNESS AND MASS MATRICES
 - FREE-FREE MODE SHAPES AND FREQUENCIES
 - FIXED INTERFACE MODE SHAPES AND FREQUENCIES
 - MODAL TOPOLOGY AND DEGREE-OF-FREEDOM LIST
 - LOAD TRANSFORMATION MATRIX
 - RESULTS OF MODEL EQUILIBRIUM CHECKS

- o SHUTTLE INPUT DATA
 - SHUTTLE LIFT-OFF MODE SHAPES AND FREQUENCIES (2 CONFIGS)
 - SHUTTLE LIFT-OFF FORCING FUNCTIONS
 - ORBITER LANDING MODE SHAPES AND FREQUENCIES
 - ORBITER LANDING FORCING FUNCTIONS
 - ORBITER REDUCED STIFFNESS MATRIX (FIXED AT EXTERNAL TANK INTERFACE)
 - ORBITER THERMAL DEFLECTIONS
 - LOAD FACTORS FOR QUASI-STATIC ANALYSIS

- o CARGO OUTPUT DATA
 - OUTLINED IN SD77-SH-02L4.
 - INCLUDES LOAD FACTORS, INTERFACE LOADS, RELATIVE DEFLECTIONS, MAX/MIN CARGO ACCEL., AND OTHER LOAD TRANSFORMATION MATRIX INFO

CARGO DEVELOPMENT LOADS/DEFLECTIONS CYCLE(S) (CONT'D)

- o CONFIGURATION OPTIONS
 - ANALYZE CARGO IN MORE THAN ONE LOCATION, E.G., 3 SPACELAB PALLETS IN PAYLOAD BAY FOR EACH EVENT
 - o CHECKS PAYLOAD BAY POSITION DEPENDANCE
 - o CHECKS DYNAMIC INTERACTION
 - ANALYZE CARGO AS MANIFESTED FOR FLIGHT
 - o REDUCES UNCERTAINTIES DUE TO POSITION & DYNAMIC INTERACTION
 - o MANIFEST NOT USUALLY KNOWN AT TIME OF DEVELOPMENT CYCLE
- o DURATION OF LOAD CYCLE
 - 4 MONTHS AFTER RECEIPT OF CARGO MATH MODEL
- o VERIFICATION LOAD/DEFLECTION CYCLE
 - o FUNDED AND PERFORMED BY JSC (STANDARD SERVICE)
 - o REQUIRES TEST VERIFIED CARGO MODEL AND CARGO THERMAL DEFLECTIONS FROM CARGO ORGANIZATION
 - o USUALLY PERFORMED ABOUT 6 MONTHS BEFORE FLIGHT
 - o COMPLETE CARGO MANIFEST IS ANALYZED
 - o RESULTS ARE PROVIDED TO CARGO ORGANIZATION (INCLUDES LOAD TRANSFORMATION MATRIX DATA FOR CRITICAL STRUCTURE)

SUMMARY

- o LOADS/DEFLECTIONS REQUIREMENTS AND ANALYSIS RESPONSIBILITIES DOCUMENTED IN PAYLOAD INTEGRATION PLAN
- o LOADS/DEFLECTIONS DOCUMENTED AND CONTROLLED IN A STS/PAYLOAD INTERFACE CONTROL DOCUMENT
- o PRELIMINARY DESIGN LOADS BASED ON LOAD FACTORS FROM ICE .2-19001
- o SUBSEQUENT LOADS BASED ON COUPLED DYNAMIC AND QUASI-STATIC ANALYSIS
- o SEVERAL OPTIONS AVAILABLE FOR CARGO DEVELOPMENT LOADS
- o JSC PERFORMS FINAL (VERIFICATION) LOAD CYCLE

**SPACECRAFT DYNAMIC LOADS
THE LOAD CYCLE APPROACH**

**PRECEDING PAGE BLANK NOT FILMED
PRECEDING PAGE**

**E. R. FLEMING
AEROSPACE CORPORATION**

SPACECRAFT LOADS - THE LOAD CYCLE APPROACH

LOAD CYCLE APPROACH - ITERATIVE DETERMINATION OF LOADS, ACCOUNTING FOR EVOLUTION OF THE SPACECRAFT DESIGN

STEPS IN A LOAD ANALYSIS AND ASSOCIATED PROGRAM MILESTONES:

- PRELIMINARY DESIGN LOAD FACTORS - CONTRACT INITIATION
- PRELIMINARY LOAD CYCLE - COMPLETE AT PDR
- FINAL DESIGN LOAD CYCLE - COMPLETE AT CDR
- VERIFICATION LOAD CYCLE - COMPLETE PRIOR TO FIRST FLIGHT

VARIATIONS - VARIOUS POSSIBILITIES DEPENDING ON PROGRAM PECULIAR CONSIDERATIONS

SPACECRAFT LOADS - THE LOAD CYCLE APPROACH

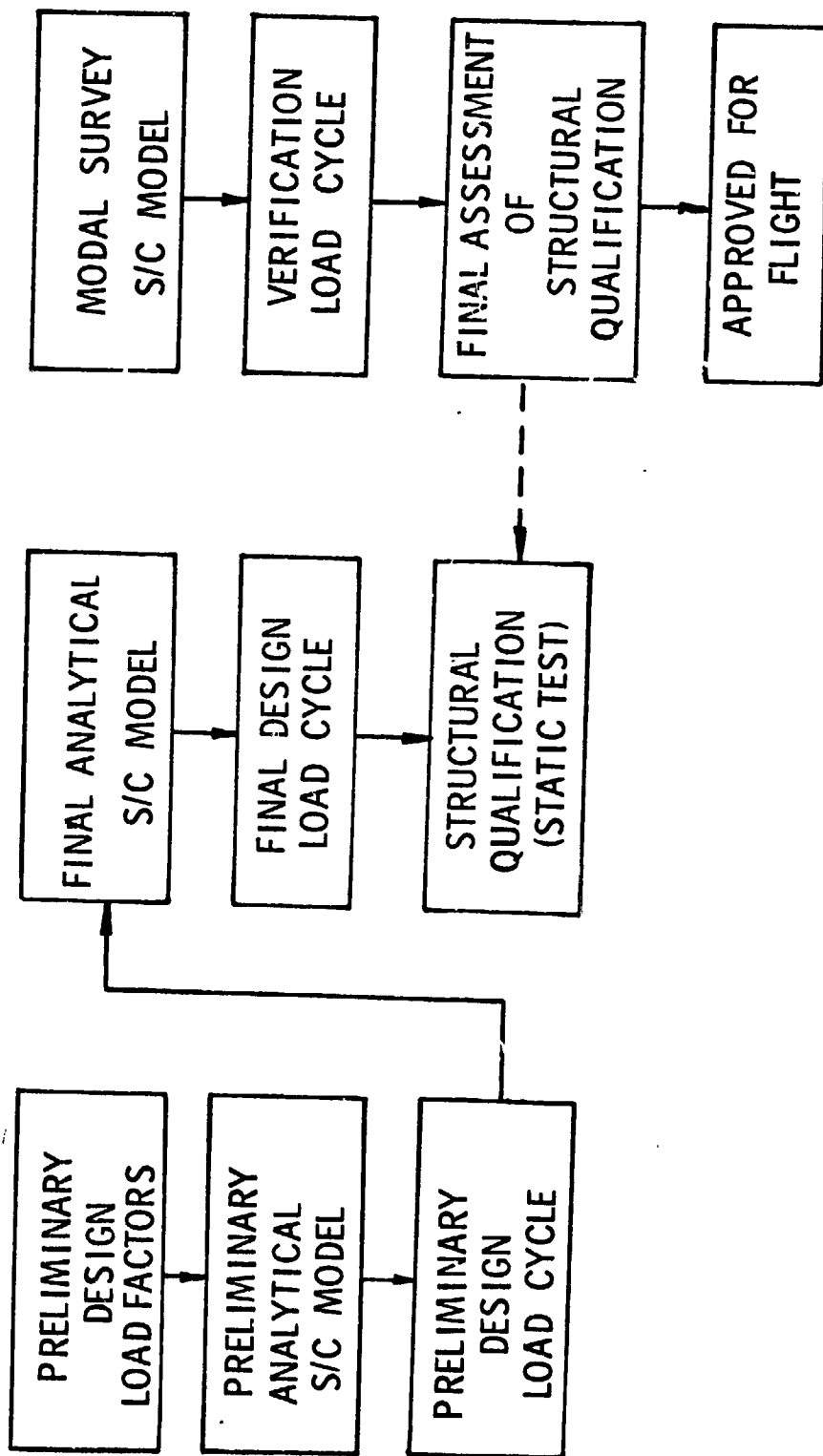
The subject of this presentation is the approach to spacecraft loads determination which the Aerospace Corporation recommends to the Air Force for most of its space programs. We call it the load cycle approach because it occurs in iterative cycles, each cycle being structured to accommodate the needs of the program as the spacecraft design evolves.

The steps enumerated on the chart call first for the establishment of a set of design load factors to which the spacecraft structure is initially sized. Subsequently, three distinct cycles of loads analysis are called for: The Preliminary, Final Design and Verification load cycles. These cycles are distinguished from each other largely by the spacecraft dynamic models employed for each one. The Preliminary and Final Design models are derived from finite element structural models and mass data appropriate to knowledge of the design at the time of the analysis. The Verification Load Cycle employs an experimentally derived dynamic model based on a modal survey of the actual spacecraft.

The time phasing of the load cycles is indicated on the chart by noting that the Preliminary Load Cycle should be completed by the time of the program's Preliminary Design Review (PDR); the Final Design Load Cycle should be completed at the time of the Critical Design Review (CDR); and the Verification Load Cycle should be completed as long before the first flight as possible.

The number and variety of load cycles described on the chart are typical of those performed for a program of average complexity. Variations can occur on any particular program. A typical variation consists of conducting more than the specified three load cycles for a program which undergoes significant design changes after program initiation. In other instances, considerations of program cost may dictate a reduction in the number of load cycles by eliminating the Preliminary Load Cycle. When this latter variation occurs there is a corresponding increase in the risk of expensive redesigns late in the program.

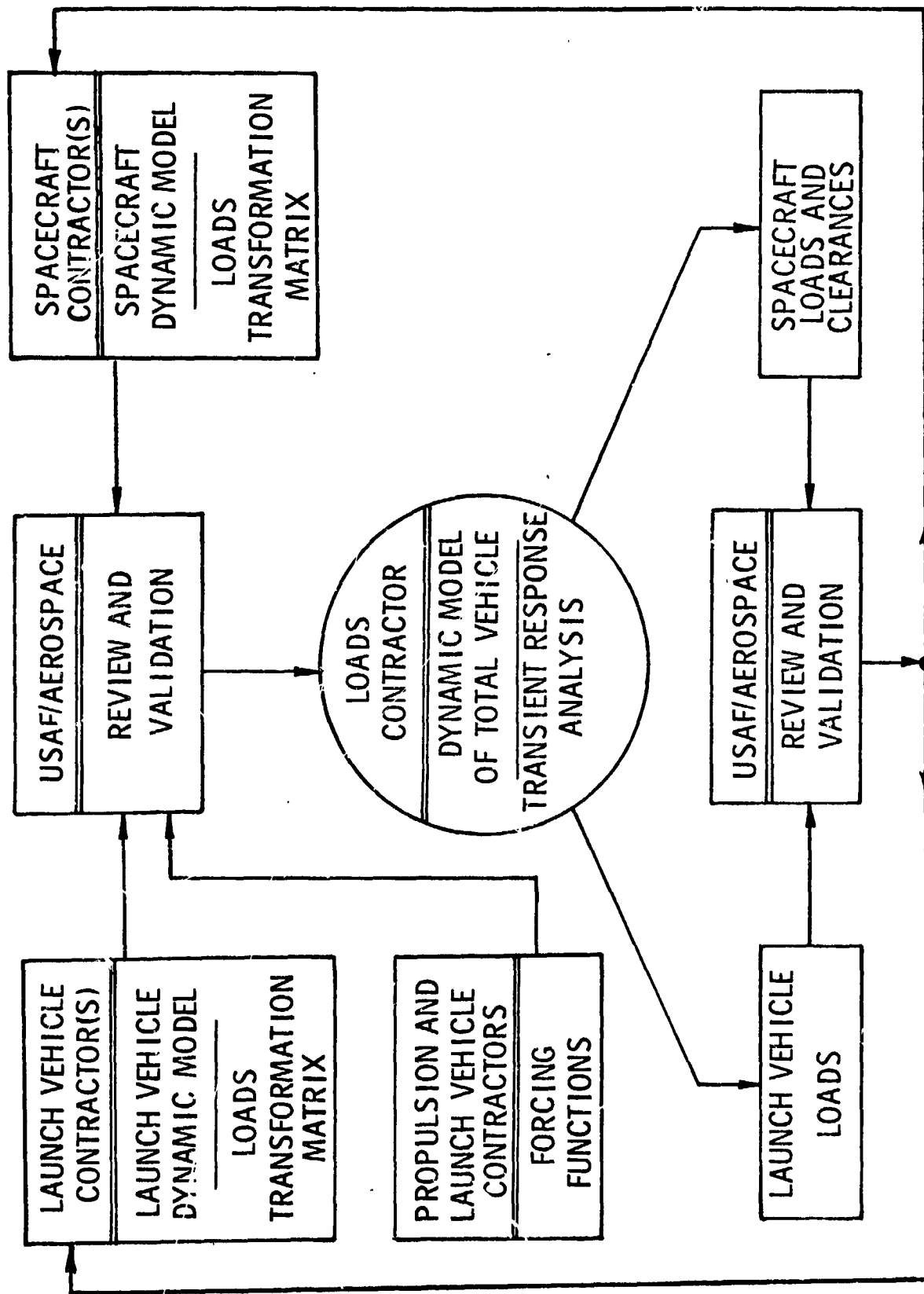
THE LOAD CYCLE PROCESS



THE LOAD CYCLE PROCESS

This chart shows, in flow diagram form, the iterative nature of the load cycle process. The Preliminary Load Cycle results in loads which may call for redesign of some structure. These changes, along with any others resulting from the maturing of the design are incorporated into a finite element structural model of what is hopefully the final design. This model is used in the Final Design Load Cycle. The loads resulting from this load cycle are, characteristically, the last set of loads available before the commitment is made to build the spacecraft hardware. Changes made to the design after this time are therefore extremely costly. In addition, the pace of a typical spacecraft program is usually one which makes it necessary to use the results of the Final Design Load Cycle as the basis for the static test. The modal survey provides the basis for the spacecraft dynamic model used in the Verification Load Cycle. The results of this load cycle are shown being compared with the static test loads to form the final assessment of structural qualification and approval for flight.

LOAD ANALYSIS INTERFACES



LOAD ANALYSIS INTERFACES

A number of contractors contribute to the performance of a load analysis. The chart depicts the interaction between these contractors.

The loads analysis itself is performed by the Loads Contractor shown in the center of the chart. This activity can be performed by the launch vehicle contractor, an upper stage contractor, or by any organization possessing the basic analysis capability. The contract for his work in this regard should be written in a manner which distinguishes it from any other supporting activity performed for the spacecraft program.

Basic data inputs to the Loads Contractor are made by the Spacecraft, Launch Vehicle, and Propulsion Contractors. These data are identified on the chart as the spacecraft and launch vehicle dynamic models, loads transformation matrices and the forcing functions. Each of these items is elaborated upon in subsequent charts.

The Aerospace Corporation is indicated on the chart acting in support of the Air Force, reviewing and validating the data inputs and the loads results. The Air Force Space and Missile Systems Organization (SAMSO) has issued a Commander's Policy which calls for the independent validation of the last (Verification) loads analysis performed for each SAMSO program. Although we are not SAMSO's exclusive agent for this activity, most of the independent loads verification analyses performed to date have been conducted by the Aerospace Corporation.

PRELIMINARY DESIGN LOAD FACTORS

SIMPLIFIED SPECIFICATION OF ACCELERATIONS AND THEIR SPATIAL DISTRIBUTIONS

- BEST ESTIMATE BASED ON PAST PREDICTIONS FOR SIMILAR CONFIGURATIONS
- ACCOUNTS FOR S/C CONFIGURATION PECULIARITIES
- PROVIDES FOR COMPONENT ACCELERATIONS HIGHER THAN GROSS ACCELERATIONS
- TAKES SPECIAL ACCOUNT OF LONG LEAD-TIME ITEMS

CRITERIA, ALONG WITH STIFFNESS AND CLEARANCE REQUIREMENTS, FOR BASIC STRUCTURAL DESIGN

MUST BE ADEQUATELY CONSERVATIVE

PRELIMINARY DESIGN LOAD FACTORS

Preliminary design load factors are the subject of this chart. Experience has shown that care taken with the development of these quantities pays significant dividends late in the program. Along with stiffness and clearance requirements, they form the basis for the general structural design of the spacecraft and, as such, have a primary influence on its dynamic characteristics and strength. Preliminary Design Load Factors, in the present context, are taken to mean a specified set of accelerations which can be used to design the spacecraft primary structure, the spacecraft adapter, the components and the local structure which supports the components.

Typically, two sets of Preliminary Design Load Factors are prescribed. One set pertains to the gross accelerations expected to be experienced by spacecraft during the various transient events which will take place during launch and ascent. These gross accelerations form the basis for design of the primary structure. A second set of accelerations, which apply to expected local accelerations, is also prescribed and these are used in the design of components and their supporting structure. The selection of these component load factors is an area in which conservatism pays particularly rich dividends. The unexpected high accelerations which may be discovered in the later load cycles are very often local in nature and preparation for this, in terms of conservative component design load factors, can often prevent costly redesign problems late in the program.

The general importance of conservatism in selecting Preliminary Design Load Factors cannot be overstressed. As noted above, they have a primary influence on the general structural arrangement selected by the designer. The need to cope, from the outset, with significant loads can force the designer to make structural efficiency a major objective in his overall design. Too often, optimistic initial estimates of load have given him the impression that he can compromise strength considerations in favor of his many other mission objectives. Later, when the design is modeled and higher loads are calculated, he finds that additional strength can only be obtained at the expense of significant weight, schedule and cost impact.

PRELIMINARY AND FINAL

DESIGN LOAD CYCLES

ANALYTICAL MODELING

- SPACECRAFT
- LAUNCH VEHICLE
- LAUNCH STAND
- LOAD TRANSFORMATION MATRICES

FORCING FUNCTIONS

- THRUST TIME HISTORIES - FLIGHT AND GROUND TEST DATA
- IGNITION OVERPRESSURE PULSES - MEASURED, PREDICTED
- GUSTS
- STEADY WINDS - WIND INDUCED OSCILLATIONS
- BUFFETING

TRANSIENT RESPONSE ANALYSES

- STATISTICAL TREATMENTS - "THREE SIGMA" LIMIT LOADS
- "WORST CASE" TREATMENTS
- UNCERTAINTY FACTORS

PRELIMINARY AND FINAL
DESIGN LOAD CYCLE

After the spacecraft structure has been designed and sized in accordance with the Preliminary Design Load Factors and when the other functional aspects of the design have been established, a series of load cycles is initiated based upon analytical models of the resulting design. This chart lists some of the key ingredients in these load cycles.

Analytical Modeling. Analytical modeling forms the basis for these load cycles and, as such, is an essential ingredient. Analytical models of both the spacecraft and the launch vehicle are required and these models must faithfully reproduce system dynamic characteristics throughout the frequency range in which significant structural loads may occur. The range up to about 50 Hz has been found to be important but, on occasion, higher frequency fidelity is required. Most of the critical transient events involve significant longitudinal excitation and the models must therefore reproduce at least the first longitudinal mode of the coupled launch vehicle/spacecraft system. The frequency of this mode, particularly for upper stage events, often exceeds 50 Hz.

Achievement of the required modeling fidelity requires careful treatment of the stiffness, mass and damping properties of the system. Extensive finite element modeling of the structure is usually required and experience has shown that attention to such details as separation joints and bearings is extremely important and experimental data are often invaluable in these instances. The acquisition of configuration peculiar experimental data for the spacecraft normally occurs after the Preliminary Load Cycle is well under way and the use of test-derived information is often an important distinguishing attribute of the Final Design Load Cycle. Spacecraft mass properties usually undergo significant evolution between these two load cycles as well. The spacecraft damping characteristics used in the Preliminary and Final Design Load Cycles are invariably simple estimates based on experience. Mode surveys of many different spacecraft have shown that modal viscous damping coefficients on the order of one percent of critical are the rule. The precise magnitude of this damping has not been found to be a critical parameter for most spacecraft transient loading events.

The dynamic model of the launch vehicle which is used in these load cycles (and in the Verification Load Cycle as well) is often a very mature one. Knowledge of launch vehicle characteristics evolves as flight experience is gained and models

for the standard boosters are reasonably well established today. While it has been found that many of the beam-like structural characteristics of expendable launch vehicles can be accurately derived by relatively simple analytical means, other features require extensive modeling work. For example, experience has shown that analytical prediction of the dynamic longitudinal behavior of a launch vehicle requires careful treatment of the fluid-structural interactions which take place in the propellant tanks. The engine support structure is usually another structurally complex system which requires extensive study to represent adequately. Often, both the engine and tankage behavior are only treated properly after flight measured structural response data are available for examination and the system has been remodeled.

The spacecraft and launch vehicle are modeled separately by their respective contractors and analytically coupled to each other by the loads contractor. This operation requires the use of modal synthesis techniques which take account of all significant structural aspects of the spacecraft-to-launch vehicle interface.

Treatment of the launch event requires analytical modeling, not only of the spacecraft/launch vehicle system, but also of the launch stand. Again, details play an important role. The nature of the interface between the stand and launch vehicle must be accurately accounted for in the model.

Finally, the modeling activity, in addition to providing an accurate representation of the system dynamic characteristics must also result in load transformation matrices (LTM's) which relate mass point inertial loads to internal member forces. In order to develop an LTM it is, of course, essential that the acceleration forces applied at mass points in the dynamic model be relatable to node point loads in the structural model. For this reason it is ideal that the dynamic model be derived directly from the model to be used for structural analysis. For this reason and also because the LTM forms the basis for deriving the static test loads, it has been found that the structural portion of the modeling effort is best performed by structures personnel in a contractor's organization.

Forcing Functions. Most of the critical flight events involve engine thrust transients - ignitions or shutdowns. It has been found that spacecraft transient response is highly sensitive to the detailed character of thrust transients and the only reliable source of such detailed information is high sample rate flight data. In the absence of such data, the results of ground test firings can sometimes be used, but usually with some compromise of confidence in the details. The use of analytical thrust-time predictions is limited to special instances and "specification" type thrust transients are rarely satisfactory. Propulsion personnel can play an important role in certifying the validity of any thrust transient used as a forcing function.

The engine ignition event can be accompanied by a "pressure pulse" phenomenon caused by reflection of exhaust gases from various parts of the launch pad facility. The forcing functions employed to date to simulate the effects of this phenomenon have been derived from limited experimental data and tailored to give reasonable agreement with measured spacecraft or launch vehicle response. Scale model "cold flow" testing has been employed as an aid in establishing some aspects of the phenomenon.

Gust induced forces are characteristically treated by determining the response of the launch vehicle/spacecraft system to a discrete gust having an idealized shape which is "tuned" over a range of wavelengths.

Some launch vehicle configurations are subject to the phenomenon of periodic vortex shedding in the presence of steady ground winds. This phenomenon poses a potential load problem for the launch vehicle and can be of significance for the spacecraft in that it establishes initial conditions for the launch event. Wind tunnel data provides the only source of information available for treating this problem.

The problem of establishing forcing functions to represent buffeting is a frustrating one. A sizable amount of experimental work was done on the subject during the early days of the space program. "Hammerhead" shapes were investigated in wind tunnels and a considerable volume of data were collected for specific shapes. Unfortunately the data is highly specialized and its application to new shapes is always questionable. Fortunately, acceleration response data for the cylinder-cone shapes characteristic of most current configurations show only modest response due to buffeting. Data from Titan III flights, however, indicates response during transonic flight which has been attributed to the effects of interaction between the large solid rocket motors

and the launch vehicle center body. Since the only data relevant to the phenomenon are flight response measurements, a procedure has been developed for scaling these flight data for application to new configurations. It involves identifying "similar" system modes for the flight tested and new spacecraft systems. The procedure is not completely satisfying and therefore requires the use of a safety factor.

Transient Response Analyses. After the dynamic models and forcing functions have been assembled the remaining task is determining the transient response information which is needed to verify the spacecraft design. The chart lists several considerations which bear on this design load issue. It was noted above that flight data should be utilized to obtain thrust transients. These transients vary from flight to flight and a sizeable family of them is necessary to form a representative ensemble. Analyses are conducted using each thrust transient and accelerations for each mass point, along with forces for each critical spacecraft member are calculated. Examination of these responses shows significant variability from case to case and statistical treatment is required to establish bounds for the design loads. Design limit load is usually taken as the "mean-plus-three-sigma" value of the calculated response. Used in this sense, mean-plus-three-sigma is meant to imply a probability of non-exceedance comparable to the three sigma level for a normally distributed statistical variable.

In instances where only limited amounts of forcing function data are available the small size of the sample should be accounted for. In instances where very small amounts of forcing function data are available, statistical treatment is not possible. In this event, worst case responses are multiplied by a factor to obtain limit load.

Confidence in the spacecraft analytical model should increase as the program matures. In the early stages of the program, when the Preliminary Load Cycle model is developed, knowledge of the structural and mass property details of the design is necessarily limited. It is recommended practice to account for this uncertainty by applying a multiplying factor of 1.5 to the calculated responses from this load cycle. When the analytical model for the Final Analytical Load Cycle is developed, knowledge of the design should be significantly improved and this "uncertainty factor" is usually reduced to 1.25.

THE SPACECRAFT MODE SURVEY

TEST OBJECTIVE - EXPERIMENTAL DETERMINATION OF ALL DYNAMIC PARAMETERS OF SIGNIFICANCE FOR LOADS ANALYSIS

- USUALLY REQUIRES MEASUREMENT OF ALL MODES WITH FREQUENCIES LESS THAN 50 Hz
 - MODAL QUALITY SUFFICIENT TO PERMIT DIRECT USE IN ANALYSIS
- TEST ARTICLE
- FLIGHT QUALITY SPACECRAFT STRUCTURE
 - SIMULATED COMPONENTS AND/OR SUBSYSTEMS AS APPROPRIATE
 - BOUNDARY CONDITIONS SIMULATING FLIGHT CONDITION
 - CANTILEVERED (WITH ADAPTER)
 - SYSTEM PECULIAR SUPPORT SYSTEMS
 - INSTRUMENTATION - SUFFICIENT TO DETECT MOTION OF ALL SIGNIFICANT MASSES

TESTING CRITERIA

- COMPLETENESS
- ORTHOGONALITY

THE SPACECRAFT MODE SURVEY

The commitment to construct the spacecraft is made at the CDR following completion of the Final Design Load Cycle. This chart addresses the spacecraft mode survey which occurs as soon as a suitable test article can be built and made available for testing.

Experience has shown that a spacecraft often experiences loads which depend upon the detailed character of its higher order modes, modes in the 20 to 50 Hz range. Further, it has been found that modifying analytical models to give good agreement with modal test results in this range is extremely difficult. As a consequence, the objective of the modal survey is the measurement of all modes, in the frequency range of interest, with sufficient accuracy to permit their direct use in the Verification Load Cycle.

The test article should be of flight quality in so far as its dynamic characteristics are concerned. Some simulation of sensitive components is usually necessary but the mass and stiffness properties of the simulators must accurately replicate those of the real equipment. Black boxes and solar cells are typical candidates for simulation. Occasionally, it may be desirable to remove certain subsystems from the test article to simplify the testing process. Solar arrays are a typical example. When this is done, the subsystem modes are determined in a separate test and coupled analytically to the measured spacecraft normal modes. The spacecraft test article must, of course, be suitably ballasted and instrumented so that modes will be obtained which will make this coupling practicable after the test.

For spacecraft which are launched on expendable launch vehicles, the mode survey is usually conducted with the spacecraft mounted on its adapter with the adapter grounded at its launch vehicle interface. Some Shuttle-launched spacecraft will require mode testing while mounted in their "cradles".

When the test is completed but before the set-up is torn down, the measured results should be subjected to as much scrutiny as possible to provide assurance that an adequate set of data have been acquired. Completeness of the set of measured modes, in the frequency range of interest, is judged by reviewing all of the sinusoidal sweep data obtained during the test. All indications of modal presence in the sweep data must be accounted for in the set of modes which were measured. Questions concerning missing modes must all be resolved. The quality of the measured modes themselves can be judged by a number of criteria. The precision of the "tuning" achieved during mode acquisition is a matter of judgement exercised by the test engineer during the test. After the set of modes

has been recorded, however, an orthogonality check is made to test the independence of the measured modes with respect to each other. An analytically derived mass matrix is necessary for performance of this orthogonality check. The matrix should be derived in a manner which is compatible with the instrumentation employed during the test. The orthogonality criterion applied to the measured modes requires that all off-diagonal terms in the generalized mass matrix $[\bar{M}]$ be less than 0.10, where

$$[\bar{M}] = [\phi]^T [m] [\phi]$$

and $[\phi]$ = matrix of measured modes normalized to unity for each modal generalized mass

$[m]$ = test article mass matrix

STATUS OF MODE SURVEY TESTING METHODS

CONVENTIONAL - MULTI SHAKER SINUSOIDAL SEARCH AND DWELL APPROACH

- MODES EXCITED ONE AT A TIME - PERMITS PHYSICAL OBSERVATION AND EVALUATION DURING TEST
- DEMONSTRATED EFFECTIVE ON NUMEROUS PROGRAMS
- PERFORMANCE OF TEST REQUIRES CONSIDERABLE AMOUNT OF TECHNIQUE AND EXPERIENCE
- TIME CONSUMING - ORDER OF WEEKS (INCLUDING DATA REDUCTION)

SINGLE POINT RANDOM - TRANSFER FUNCTION APPROACH

- MODES OBTAINED AFTER THE FACT THROUGH DATA REDUCTION
- MINIMAL TESTING TIME - ORDER OF DAYS (NOT INCLUDING DATA REDUCTION)
- TEST RELATIVELY SIMPLE TO PERFORM
- DATA REDUCTION REQUIRES SIGNIFICANT AMOUNT OF TIME AND JUDGEMENT
- EFFECTIVENESS FOR COMPLEX SPACECRAFT NOT YET ESTABLISHED

IMPROVED TESTING TECHNOLOGY REQUIRED

- OPTIMIZED TESTING/DATA REDUCTION TIME
- ENHANCED CLOSE MODE DISCRIMINATION

MODE SURVEY TESTING METHODS

The experimental determination of the normal modes of a complex spacecraft is a technically demanding problem. This chart lists some key features of current mode testing methods and comments on the current state of the testing technology.

The conventional method was, until relatively recently, the only technique employed for major mode surveys. It consists of applying sinusoidal excitation to the test article using several shakers which are physically located and driven in a manner which excites only one mode at a time. This technique, while difficult to execute, has the advantage that the modes are individually excited and can be subjected to close quantitative and qualitative examination, one at a time. It has the further advantage that data reduction is substantially completed as each mode is surveyed, so that a complete set of checks can be made before the test set-up is torn down. The technique has been employed with considerable success for many spacecraft programs.

The conventional technique has two significant shortcomings:

- (a) its use places major demands on the skill and perceptiveness of the test engineer, particularly in the matter of discriminating modes which are closely spaced in frequency, and
- (b) a considerable amount of time is required for its execution.

The time requirement is a particularly important disadvantage since conduct of the test requires the exclusive use of a test article which must be released at the earliest possible time for other testing purposes.

A second technique, called here the single point random (SPR) method, has received considerable attention of late. It makes use of an approach which is entirely different from the conventional one. Instead of exciting one mode at a time, the method calls for exciting several modes at once using a single shaker which delivers random force excitation. The measured excitation and response are then analytically processed to obtain transfer functions for each measurement station on the spacecraft. Modal parameters are then deduced by further analytical processing of these transfer functions. The test is relatively simple to perform. In principle, shaker locations can be selected before the test and application of the excitation is a routine process which can be performed in a short period of time. The data reduction process can be performed after the testing itself (i. e. the excitation) has been completed.

The test set-up can therefore be torn down at an early date and the test article can be released for other purposes.

At the present time the SPR method can be said to have two significant shortcomings:

- (a) Completion of the data reduction process requires a significant amount of time (more than a month for a complex spacecraft) and
- (b) The effectiveness of the method has not been established under a sufficient variety of circumstances to demonstrate that difficult modal discrimination problems can be solved with its use.

When SPR techniques are employed for a modal survey, the Aerospace Corporation currently recommends that verification of the results be obtained, after the fact, using a conventional sinusoidal search and dwell technique.

It is thus seen that improved modal testing technology is definitely needed. Research in this field should be aimed at improving existing techniques and at the development of new techniques as well. The objectives, as noted on the chart, must include optimizing both the testing and the data reduction time and must address the problem of close mode discrimination. There is work currently underway in this area. Modal testing problems have been the subject of a number of projects which have been pursued by the Air Force Flight Dynamics Laboratory, the Jet Propulsion Laboratory, the Langley Research Center and by several contractors. Also, we at Aerospace have had the subject under consideration for some time. Investigations by the various organizations range from seeking improvements to existing methodology to the development of entirely new techniques.

A common feature of most new methods is the avoidance of exciting individual modes, one at a time. Instead, modes are deduced by analytical means from forced or free decay response measurements. This approach treats the testing time problem admirably but leaves the mode discrimination problem open to question. Mode discrimination is a serious problem in the conventional, sinusoidal sweep and dwell test as well, but when modes are separately excited and observed the existence of the problem is apparent and measures can be taken to find a solution. The fundamental issue, then is how assurance can be acquired that valid modes have been obtained with the new methods in the absence of direct modal excitation and observation.

As noted later in this presentation, modal testing is a major contributor to the cost of the load cycle process. Improvements which would reduce this cost are sorely needed and it is recommended that current research to this end be both continued and enhanced.

THE VERIFICATION LOAD CYCLE

PROVIDES FINAL ASSURANCE OF LOAD ADEQUACY

SPACECRAFT DYNAMIC MODEL - TEST VERIFIED

- DIRECT USE OF MEASURED MODES - TEST ARTICLE DEVIATIONS FROM FLIGHT CONDITION CORRECTED ANALYTICALLY
- MODES ORTHOGONALIZED

UPDATED LOAD TRANSFORMATION MATRIX

LAUNCH VEHICLE MODEL AND FORCING FUNCTIONS LATEST AVAILABLE

UNCERTAINTY FACTOR - UNITY

PROVIDES BASIS FOR ASSESSING ADEQUACY OF STRUCTURAL QUALIFICATION

THE VERIFICATION LOAD CYCLE

The ultimate determination of spacecraft loads occurs in the Verification Load Cycle. This chart describes the salient features of this analysis.

The Verification Load Cycle occurs as soon as possible after the mode survey has been completed and the data has been reduced to suitable form for use in a loads analysis. This requires that the modes of separately tested subsystems be coupled to the measured spacecraft modes; that any other test article deviation from the flight condition be corrected and that the measured modes be orthogonalized. It has been found that this last step is desirable to insure mathematical compatibility of the resulting spacecraft representation with the model of the launch vehicle.

The launch vehicle model and the forcing functions employed in the Verification Load Cycle should incorporate any data necessary to account for knowledge gained after the Final Design Load Cycle. This is particularly true of any thrust transient data which may have been added to the statistical family as the result of additional flights.

The load transformation matrix is often updated between the Final Design and Verification Load Cycles. In particular, the timing of the Verification Load Cycle often permits the use of structural information acquired during the static test.

An uncertainty factor of 1.0 can be employed in the Verification Load Cycle if the spacecraft mode survey is considered adequate.

The results of the Verification Load Cycle, being the ultimate load determination, provide the criteria by which the adequacy of the spacecraft static test can be judged. Comparison of the member forces obtained from the load cycle with those induced during the static test provides the basis for this judgement and for final commitment to flight.

OBSERVATIONS ON THE LOAD CYCLE PROCESS

PROVIDES "MINIMUM WEIGHT" SPACECRAFT WITH HIGH CONFIDENCE IN
STRUCTURAL INTEGRITY

HIGHLY SPECIALIZED, TECHNICALLY SOPHISTICATED ACTIVITY
REQUIRES EXTENSIVE PRE-CONTRACT PLANNING AND CONTINUOUS
MANAGEMENT ATTENTION THROUGHOUT PROGRAM

EXPENSIVE - ORDER OF \$1,000,000 / PROGRAM

- DISTRIBUTION OF COSTS
 - SPACECRAFT ANALYTICAL MODELING 30%
 - MODE SURVEY 30%
 - LOAD CALCULATION 40%
 - 100%

IMPROVEMENTS HIGHLY DESIRABLE

- CONSERVATIVE DESIGN CRITERIA
- IMPROVED MODELING TECHNIQUES
- IMPROVED LOAD CALCULATION METHODS
- IMPROVED MODAL TESTING TECHNIQUES

OBSERVATIONS ON THE LOAD CYCLE PROCESS

This chart treats several final observations on the Load Cycle Process. The intent here is to note that the process has the potential of fulfilling its goals provided adequate attention is given to its planning and execution. On the other hand, it is also noted that the process, in its present state of development, leaves significant room for improvement.

The need for improvement is most dramatically underscored by the current high cost of the process. The quoted cost, in the neighborhood of one million dollars, is representative of a program which calls for three load cycles. An approximate distribution of these costs is shown on the chart.

As mentioned earlier, the Preliminary Load Cycle is occasionally eliminated in the interests of cost reduction. From the technical point of view, this entails some risk that excessive loads will be discovered late in the program. This risk can be partially offset, however, by employing more conservative preliminary design load factors than would otherwise be used. It is, of course conceivable that the entire load cycle process could be by-passed if sufficiently conservative design criteria were employed. This would require the use of conservative criteria for both loads and stiffness. A simple mode survey would still be required to demonstrate achievement of the stiffness (frequency) goals.

The cost breakdown indicates that modeling, together with loads calculation (which also involves a significant amount of modeling) accounts for seventy percent of the cost. Clearly, improvements in modeling technology could have a significant impact on load cycle costs. The need in the modeling area is for improvement in both accuracy and cost. There are strong indications that the number of modes required to achieve convergence in certain loads analyses can be dramatically reduced by employing residual stiffness techniques. This is an example of a step toward the goal of reducing costs while improving accuracy at the same time.

Finally, the mode survey is seen to account for nearly a third of the total load cycle cost. Again, technical improvement and cost reduction are both important goals. There are a number of promising activities now in progress in the modal survey field. These have already been alluded to and they deserve continued pursuit and encouragement.



PAYLOAD LIFT-OFF LOADS REDUCTION
FEASIBILITY STUDY

PRECEDING PAGE BLANK NOT FILMED

R. E. GATTO
NOVEMBER 14, 1978





STUDY OBJECTIVE & APPROACH

Integrated payload/Shuttle dynamic liftoff loads analysis have indicated substantially higher transverse accelerations for certain transition payloads, particularly those employing a cantilevered support in Shuttle, compared with accelerations imposed by their current expendable launch vehicles. In an effort to minimize payload structural modification transition costs, this study was undertaken to identify and assess techniques which potentially could reduce payload liftoff loads during Shuttle launch.

Several potential load reduction concepts were identified, as will be shown in subsequent charts. The study approach was to develop the appropriate forcing functions for each concept, and determine the resultant effect on loads for one payload of particular interest. The accompanying Shuttle ascent performance penalty, if any, also was determined. In addition, impacts on the Shuttle vehicle, launch facilities and/or launch operations were identified.





STUDY OBJECTIVE & APPROACH

OBJECTIVE

IDENTIFY AND ASSESS CONCEPTS WHICH WOULD RESULT IN REDUCED
PAYLOAD LOADS DURING SHUTTLE LAUNCH

APPROACH

DETERMINE, FOR EACH POTENTIAL LOAD REDUCTION CONCEPT:



- 0 REDUCTION IN PAYLOAD LIFTOFF DYNAMIC LOADS *
- 0 SHUTTLE ASCENT PERFORMANCE PENALTY
- 0 SHUTTLE VEHICLE MODIFICATIONS
- 0 LAUNCH FACILITIES MODIFICATIONS
- 0 LAUNCH OPERATIONS MODIFICATIONS

* SUBJECT OF PRESENT BRIEFING





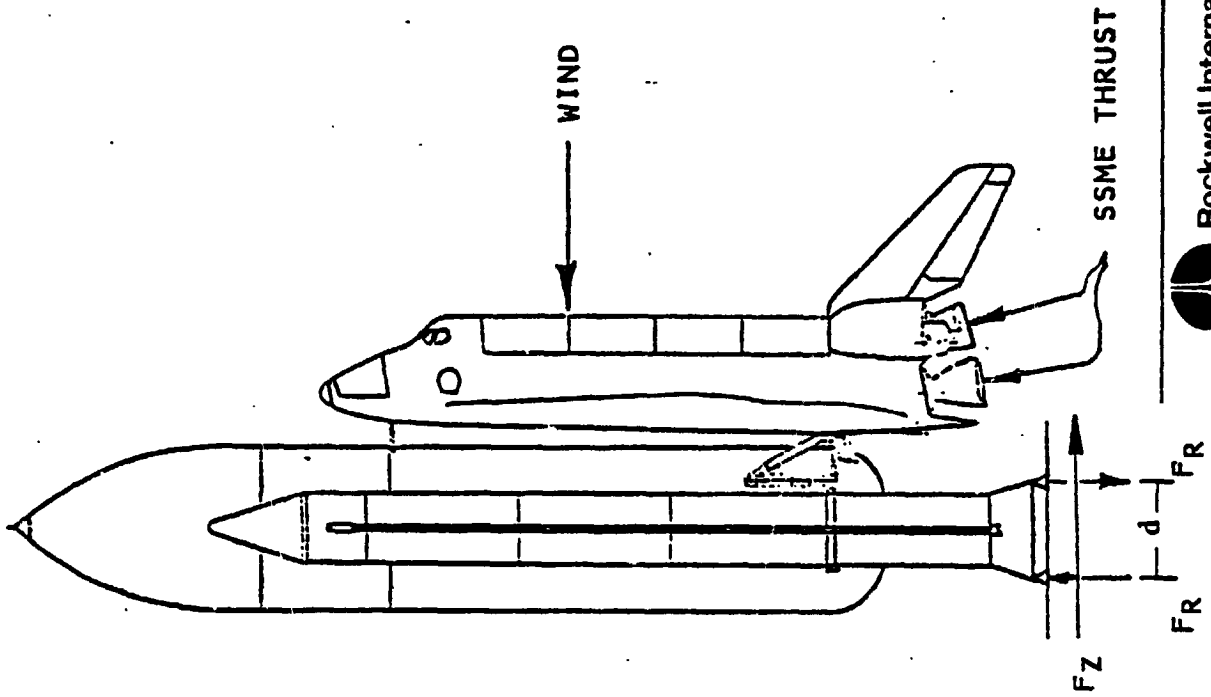
LIFTOFF CONFIGURATION

The facing chart shows the Shuttle liftoff configuration and the external forces acting on it just prior to SRB ignition and release. A worst case wind load (including gust) is acting upon the vehicle. The SSME engines are ignited and build up to 100% RPL. When all three engines are at 90% thrust or greater the SRB ignition signal is given. Prior to release the wind and SSME thrust forces are reacted at the base of the SRB's by the launch pad. These reactions include a horizontal force, F_x , due to the wind and the horizontal component of SSME thrust and the longitudinal reactions at the four support post positions on the aft skirt of each SRB. The post loads are due to both supporting the vehicle weight and reacting the over-turning moment due to wind and SSME forces.





LIFTOFF CONFIGURATION





LIFTOFF TWANG EFFECT

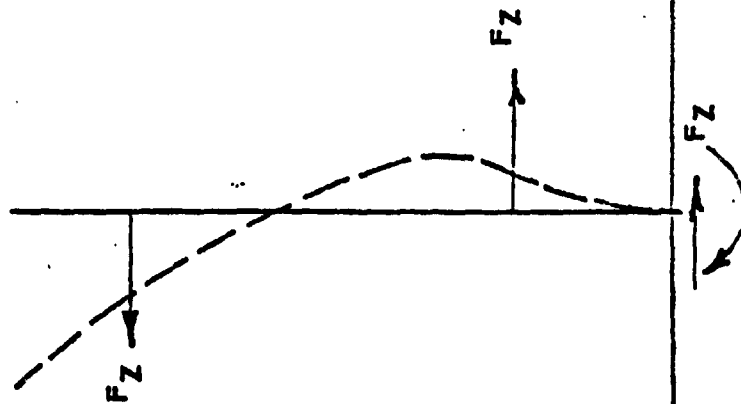
At the time of release a significant moment has built up at the base of each SRB to counteract the wind and SSME forces. The sketch on the left shows the deflected shape of the SRB's just prior to release. That in the middle shows the deflected shape just after liftoff. The forces at the base of the SRB's must decay rapidly to zero at the time of liftoff since there are no reacting forces once the vehicle leaves the pad. This rapid decay of base forces and change in deflected shape represents a shock input to the structure which would naturally respond at a much lower rate. The shock excites or "twangs" the vehicle causing it to vibrate significantly, mainly in its lower frequency structural modes. A time history of the base moment is shown on the last sketch on the right. The sharp drop-off of moment compared to the relatively slow buildup is very evident.



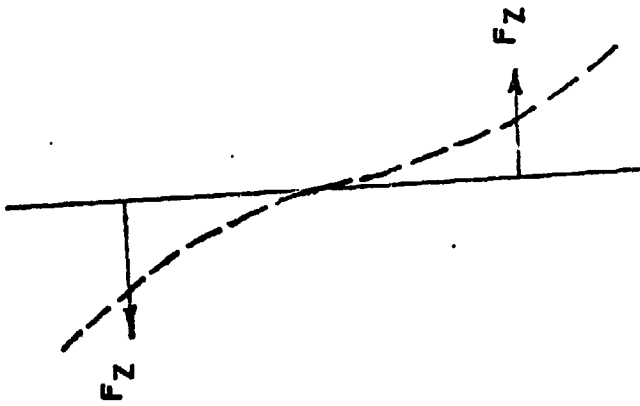


LIFTOFF 'TWANG' EFFECT

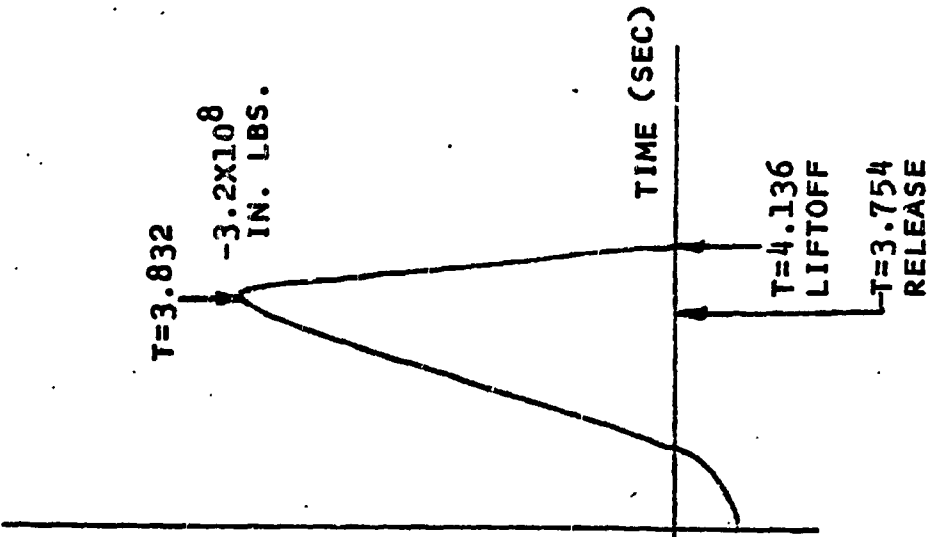
BEFORE LIFTOFF



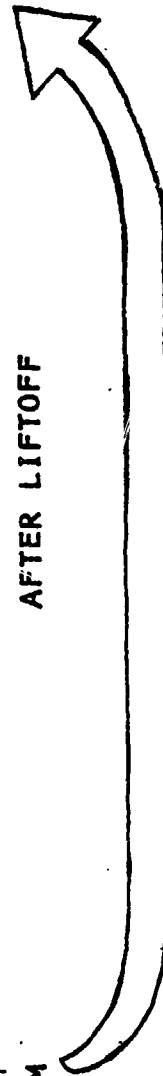
AFTER LIFTOFF



MOMENT



AFTER LIFTOFF





LIFT-OFF LOADS REDUCTION METHODS

The seven load reduction methods investigated during the study are listed. Due to time limitations in the present briefing, only the concepts indicated with a star will be discussed. The other concepts were found to be not feasible or ineffective.





LIFTOFF LOADS REDUCTION METHODS

- * 1. 2.75 SEC. SRB DELAY
- * 2. RELEASE @ 75% SSME, SSME GO TO 80% RFL
- 3. ONE SSME OUT (#1)
- * 4. TILT THE STACK
- 5. ET RESTRAINT
- 6. CONTROLLED RELEASE CONCEPT
- * 7. SLOW SRB BUILDUP

* TO BE DESCRIBED FURTHER





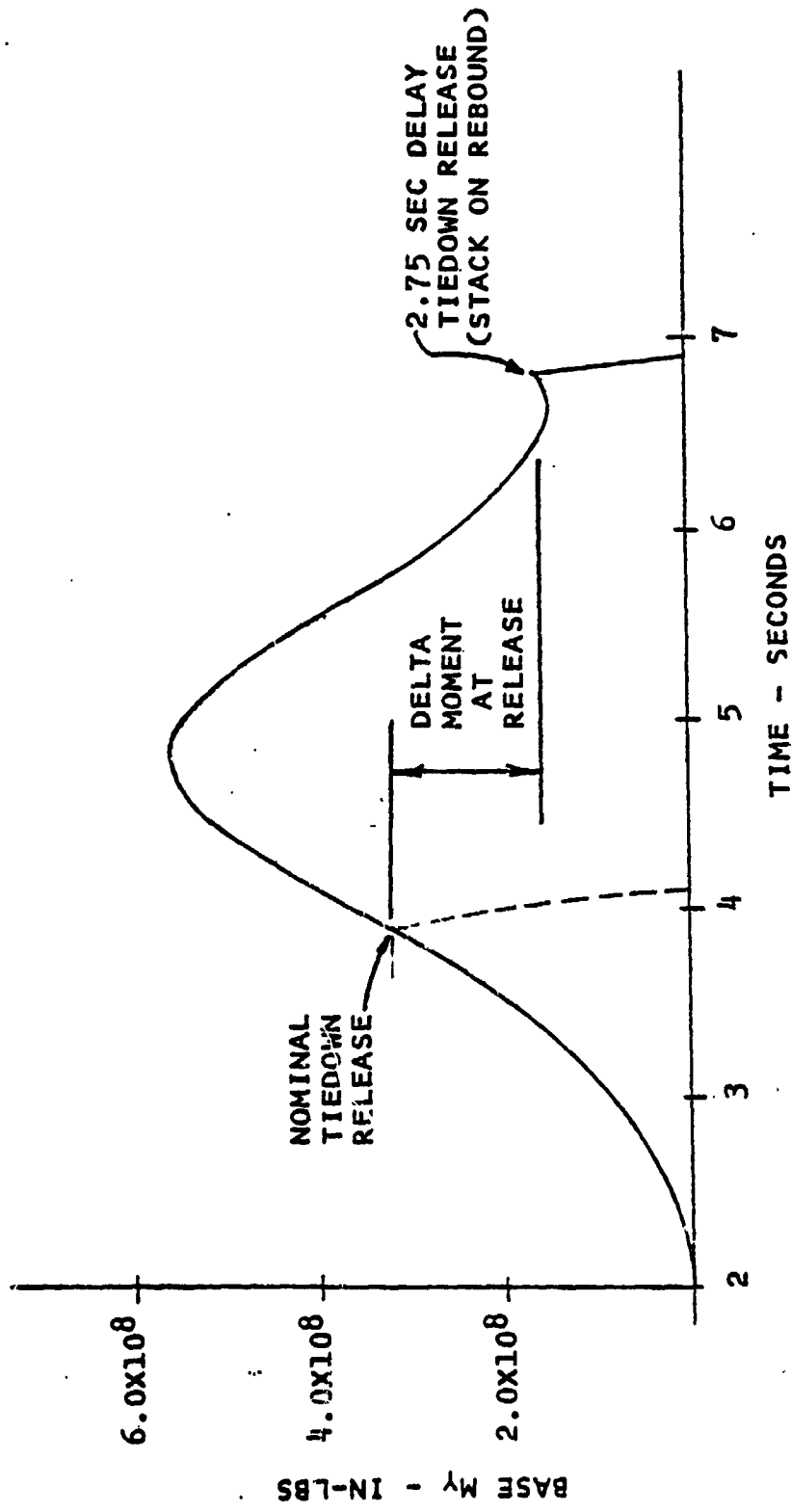
DELAYED SRB IGNITION BASE My VS. TIME

The facing chart shows the total SRB base bending moment (My) as a function of time. During a standard launch, the Shuttle vehicle is released with a large bending moment present at the base of the SRB's. The concept behind delaying release for 2.75 seconds is to let the moment buildup peak and then release the Shuttle vehicle on the rebound, when the base bending moment is in a trough. The effect of this delayed release on payload response is shown on the following chart.





DELAYED SRB IGNITION BASE MY VS. TIME





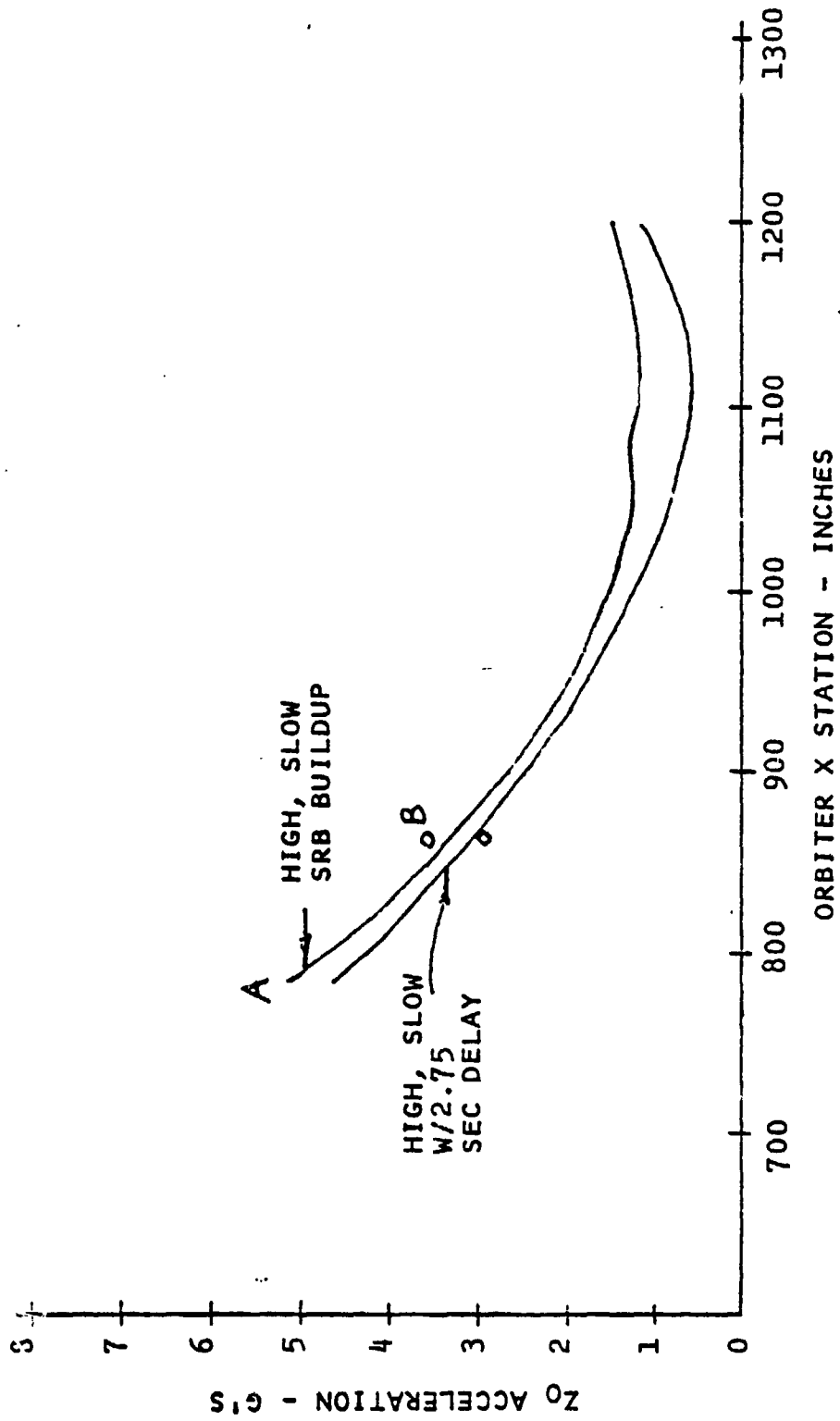
EFFECT OF DELAYED SRB IGNITION ON PAYLOAD LOADS

The amount of load reduction due to delaying the SRB ignition 2.75 seconds (slow SRB buildup) is shown on this chart. A 10% reduction was obtained at the front end of the PL (Point A) while that at Point B which represents secondary structure was reduced by 18%. The response at Point A would have to be reduced approximately 47% to be at the design landing value and that at Point B reduced about 38%. The small amount of response reduction obtained by this method would not warrant the loss of performance.





EFFECT OF DELAYED SRB IGNITION ON PAYLOAD LOADS





EFFECT OF THROTTLED BACK SSME'S ON PAYLOAD LOADS

Another loads reduction concept investigated involved throttling back the SSME's. At present, release occurs when the slowest engine reaches 90% thrust (the other 2 engines have already reached 100% thrust). With the throttled back SSME concept, release would occur when the lagging engine reaches 75% thrust and no engine is allowed to go above 80% thrust during the liftoff event.

A comparison of the payload loads for the nominal high, slow SRB case and the same case with throttled back SSME's is shown in the chart. The inserted diagram shows the change in base bending moment due to throttling the engines.

For this case a reduction of 21% was obtained at the tip (Point A) of the PL, but only a 11% reduction at Point B.

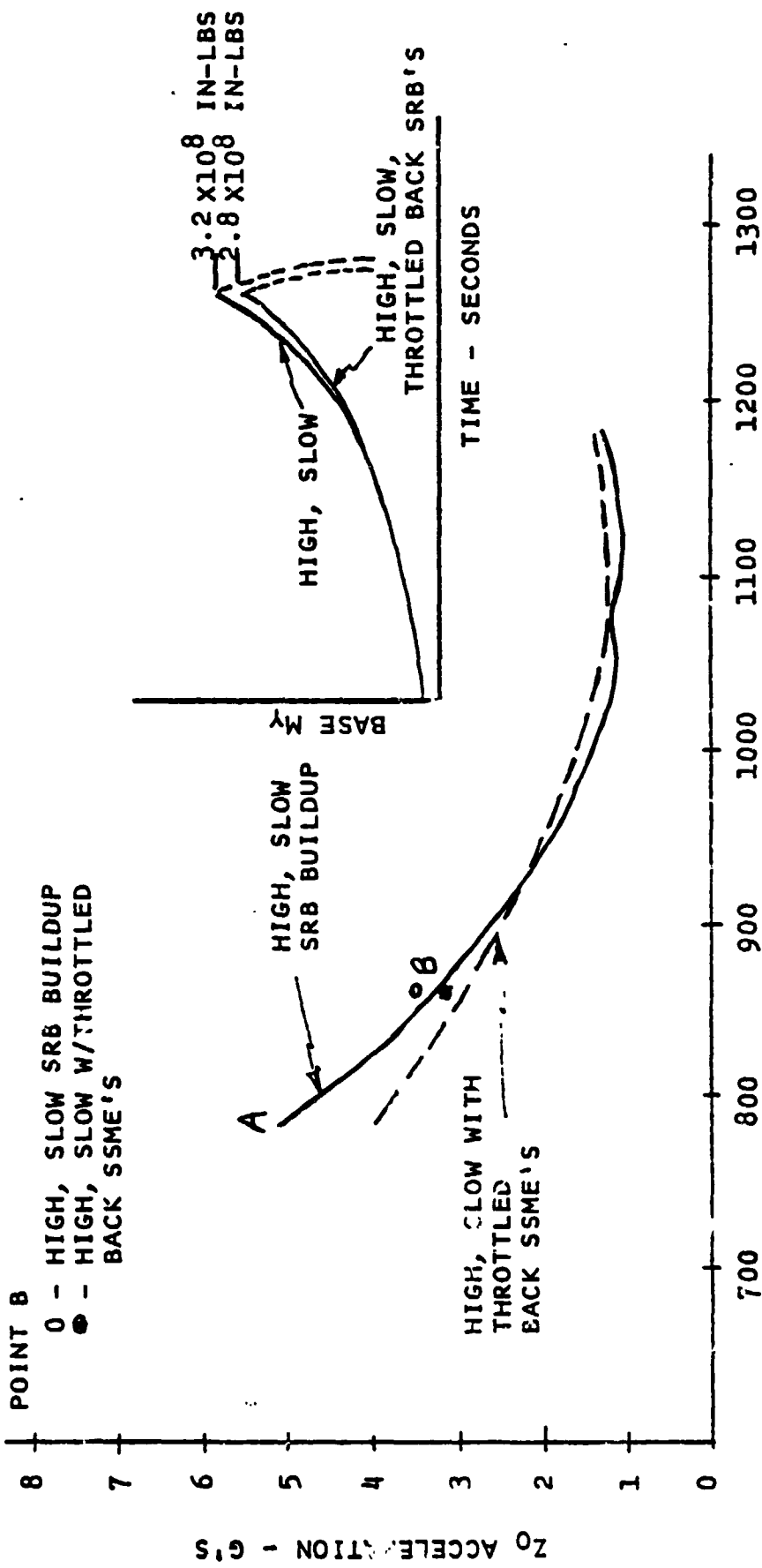




EFFECT OF THROTTLED BACK SSME'S ON PAYLOAD LOADS

POINT A IS THE CURVE VALUE AT THE TIP OF THE PYLD

- POINT B
- 0 - HIGH, SLOW SRB BUILDUP
 - - HIGH, SLOW W/THROTTLED BACK SSME'S





TILTED LAUNCH VEHICLE CONCEPT

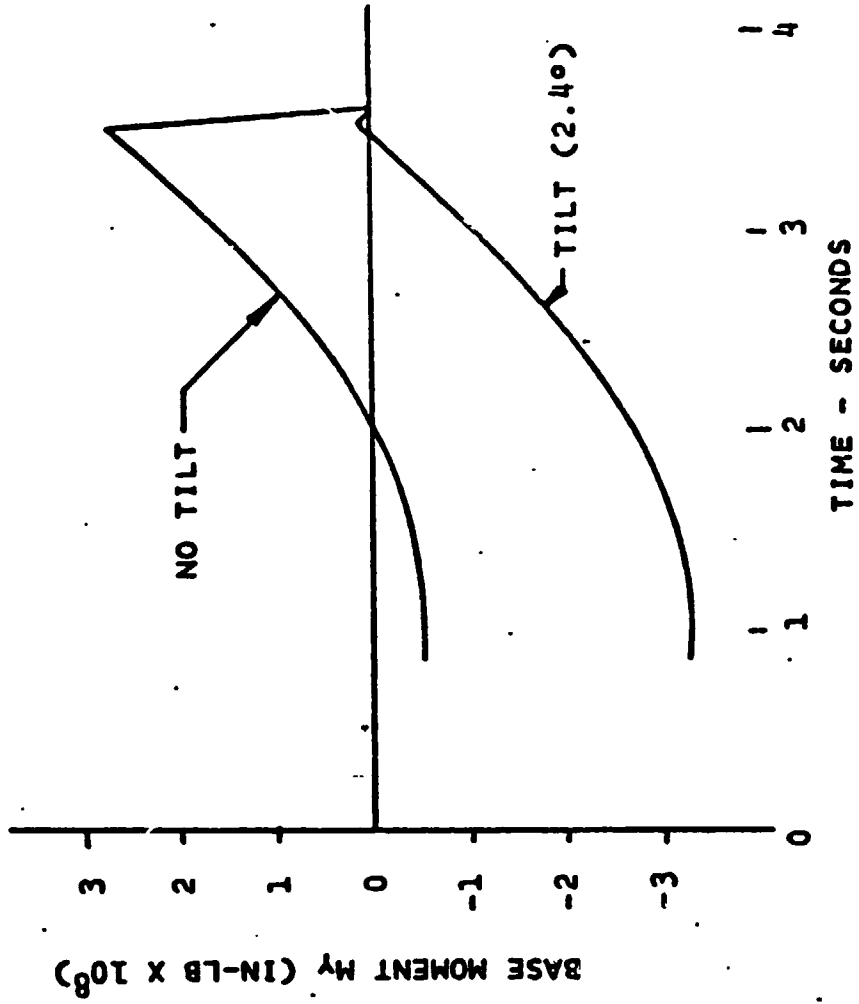
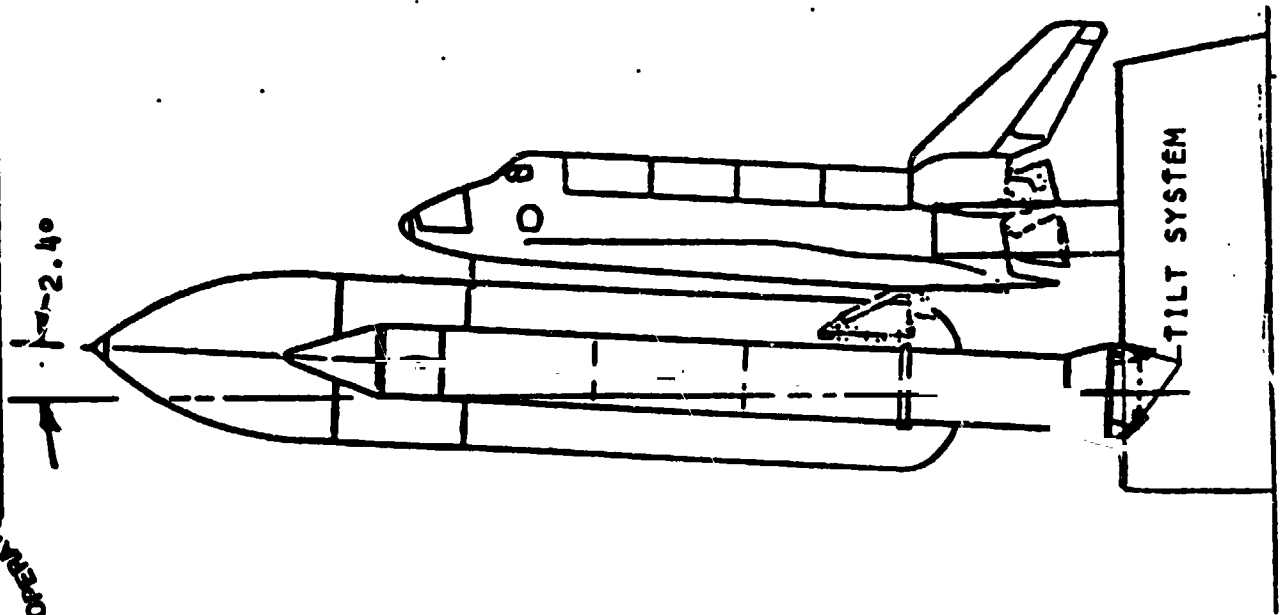
By far the most promising loads reduction concept investigated during this study involved tilting the Shuttle stack prior to liftoff. The concept being to pre-load the base of the SRB's with a moment opposite to the moment that would be built up by firing the main engines. Thus, instead of building up a high base bending moment and releasing the vehicle at its peak, the tilted case would start with a high base bending moment that would relieve as the SSME buildup began. Release would then occur when the base bending moment was close to zero.

The tilt angle would have to be determined in a trade study versus the impact to the base of the SRB's for an aborted lift-off (rebound). The impact to the SRB's may make this concept not viable.





TILTED LAUNCH VEHICLE CONCEPT





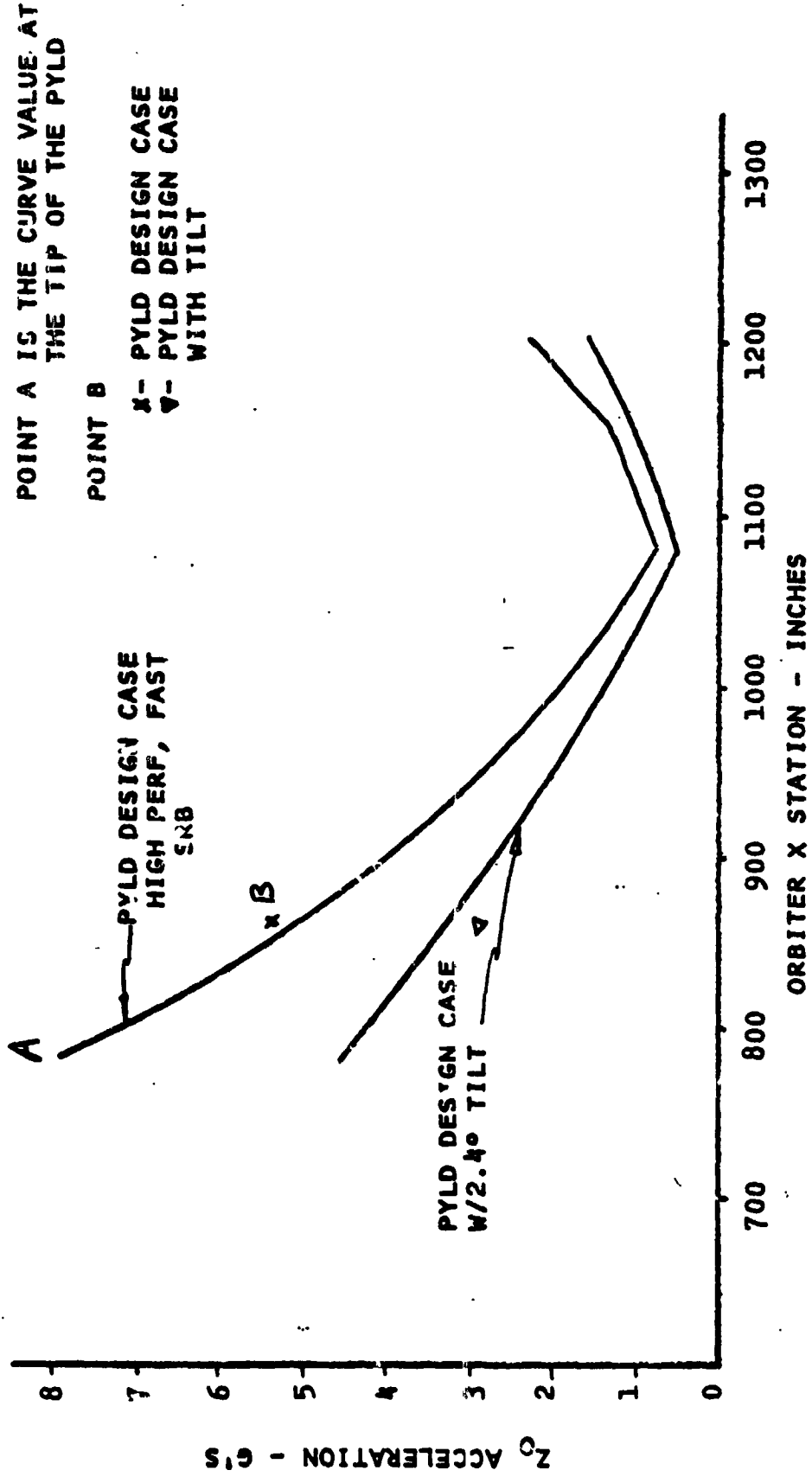
EFFECT OF TILTING SHUTTLE VEHICLE ON PAYLOAD DESIGN CASE

A significant reduction in liftoff response was obtained by tilting the vehicle. The results shown are for the fast buildup design case. A reduction of 41% occurred at the tip of the PL (Point A) and a reduction of 45% at Point B. The reduction at the tip is slightly less than that needed to equal the landing results while that at Point B is greater than required.





EFFECT OF TILTING SHUTTLE VEHICLE ON PAYLOAD DESIGN CASE





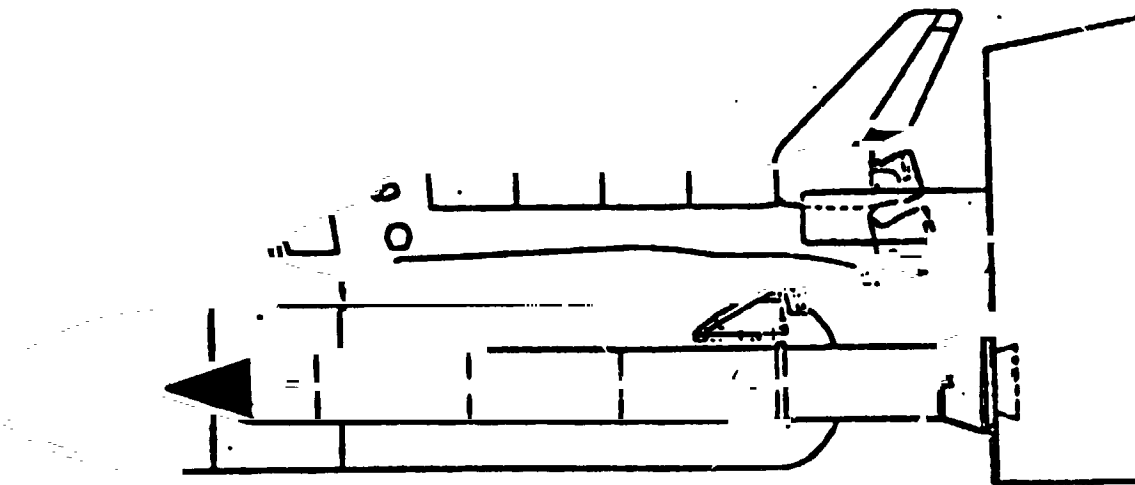
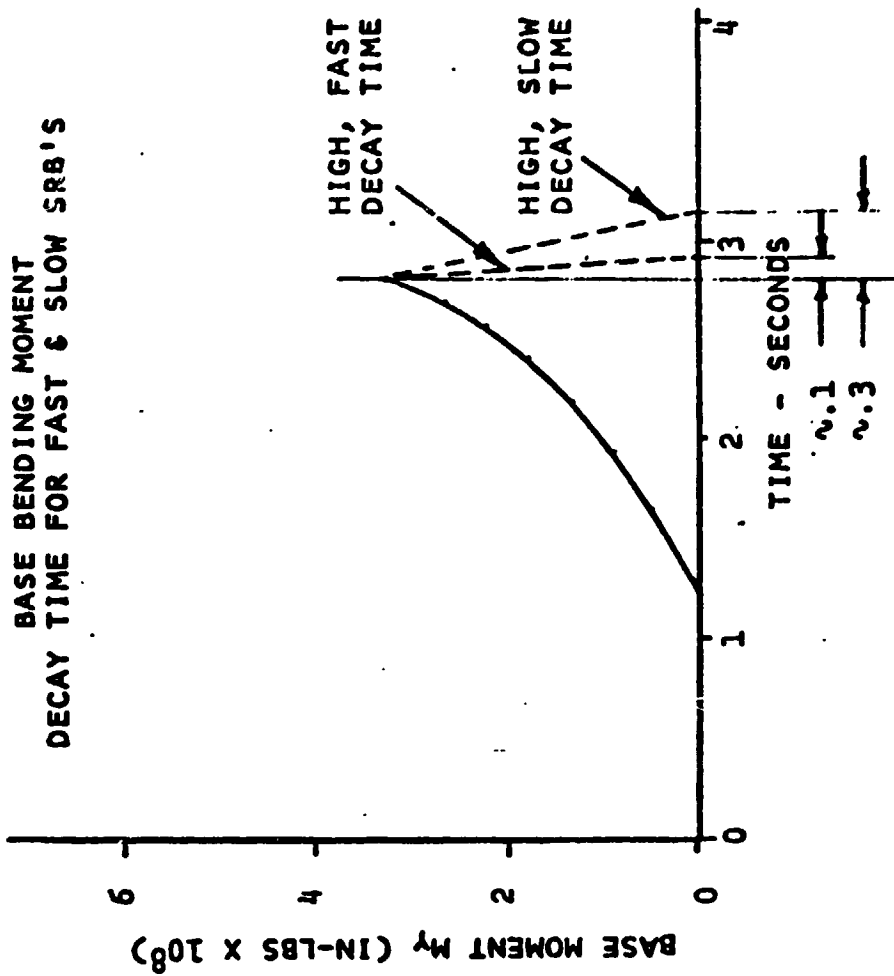
SLOW SRB THRUST BUILD UP

The decay times from the maximum base bending moment (M_y) can be seen in the figure for high performance SRB's with both a fast and slow thrust build up history. The faster the rise time to max thrust on the SRB's, the faster the Shuttle leaves the ground, and the faster the decay time for the max bending moment. As can be seen in the figure, the slow build up takes approximately three times as long to decay as does the fast build up SRB. Because of the much slower rate of decay the 'twang' effect on the vehicle at liftoff is reduced.





SLOW SRB THRUST BUILD UP





94

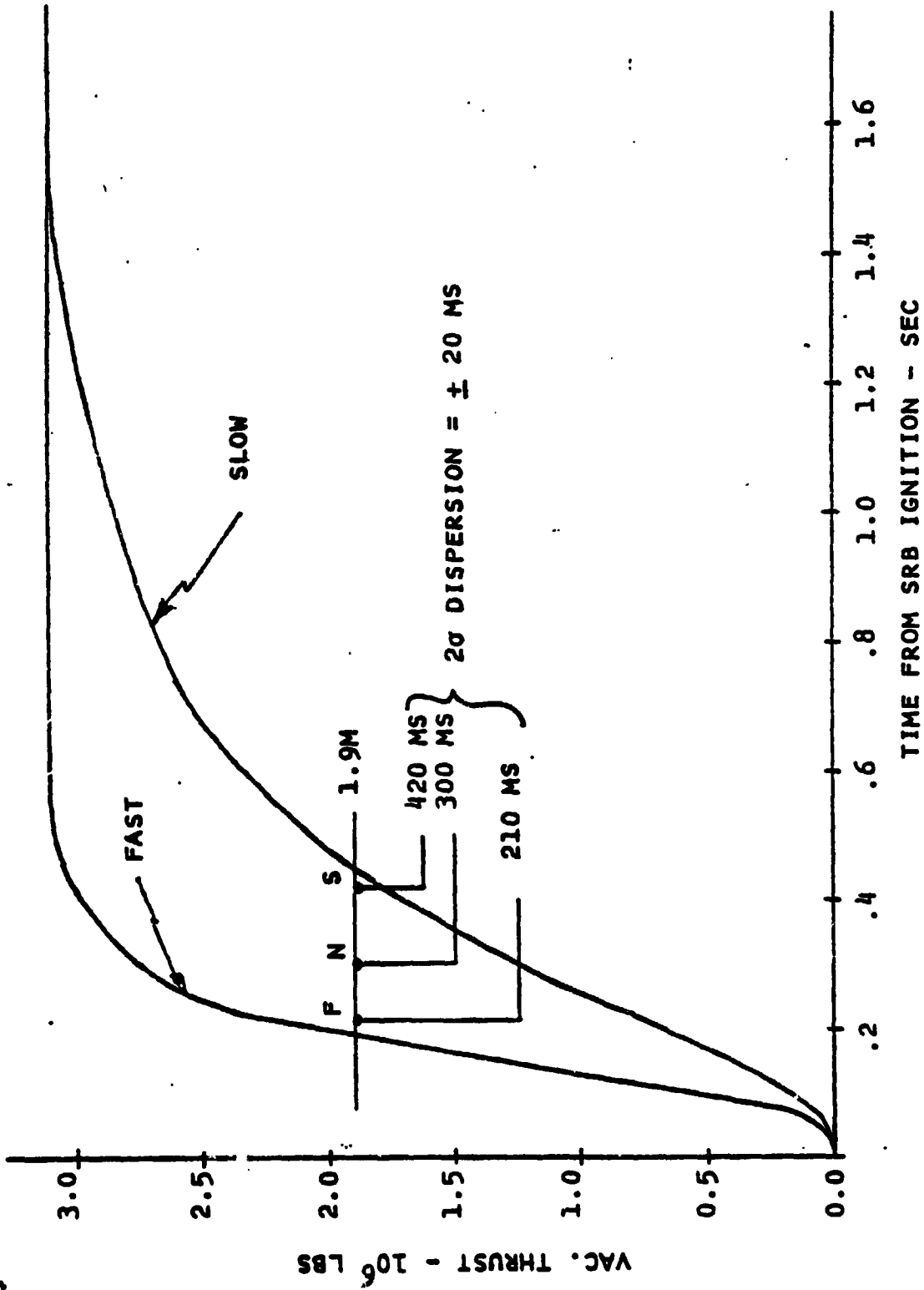
SRB THRUST BUILD UP - FAST & SLOW

The thrust build up curves for the fast and slow SRB conditions are shown in the opposing figure. S, N and F denote the spec values for slow, nominal and fast SRB build up times at a vacuum thrust of 1.9 million pounds. The fast and slow liftoff design cases are based on 2σ (+ 20 MS) dispersions about the fast and slow SRB times.





SRB THRUST BUILDUP





LIFTOFF LOADS COMPARISON - FAST VS. SLOW SRB BUILDUP

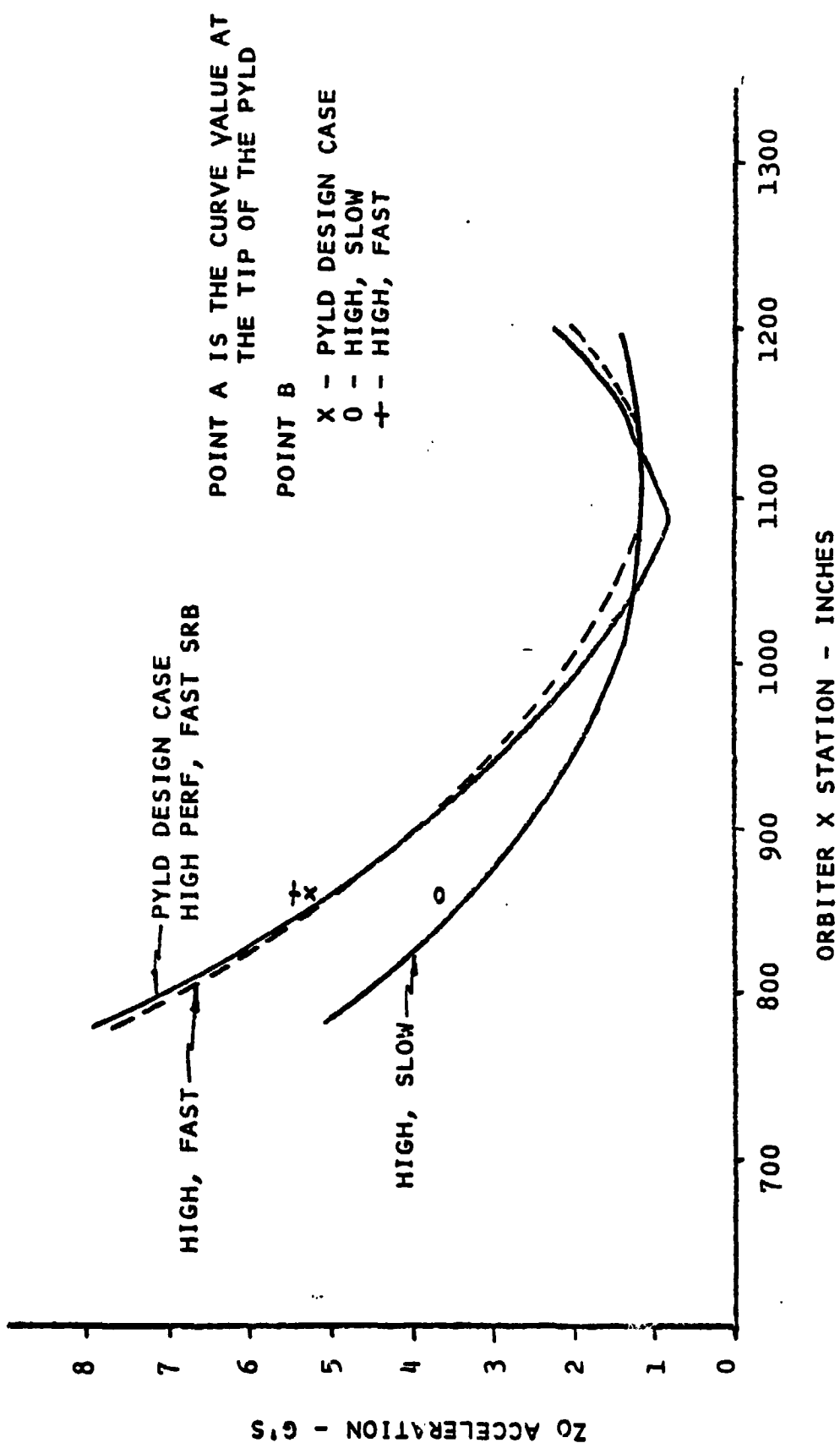
The facing figure shows a comparison of payload liftoff loads for two fast and one slow SRB buildup cases. The payload design case has high performance, fast buildup SRB's. All three SSME's have the same thrust buildup histories. The 2nd high performance, fast SRB case (dotted line) has engine #2 starting .333 sec. after engines #1 and #3. The two fast buildup cases are essentially identical forward of station 950 where it is desired to reduce liftoff load values. As can be seen from the figure significant load reduction (38% at the payload tip) would be realized if all SRB's fitted to the Shuttle had a slow rise time.



Space Transportation System
Integration & Operations Division
Space Systems Group



LIFTOFF LOADS COMPARISON FAST VS. SLOW SRB BUILDUP





LANDING LOADS VS. VARIATIONS ON LIFTOFF PAYLOAD DESIGN CASE LOADS

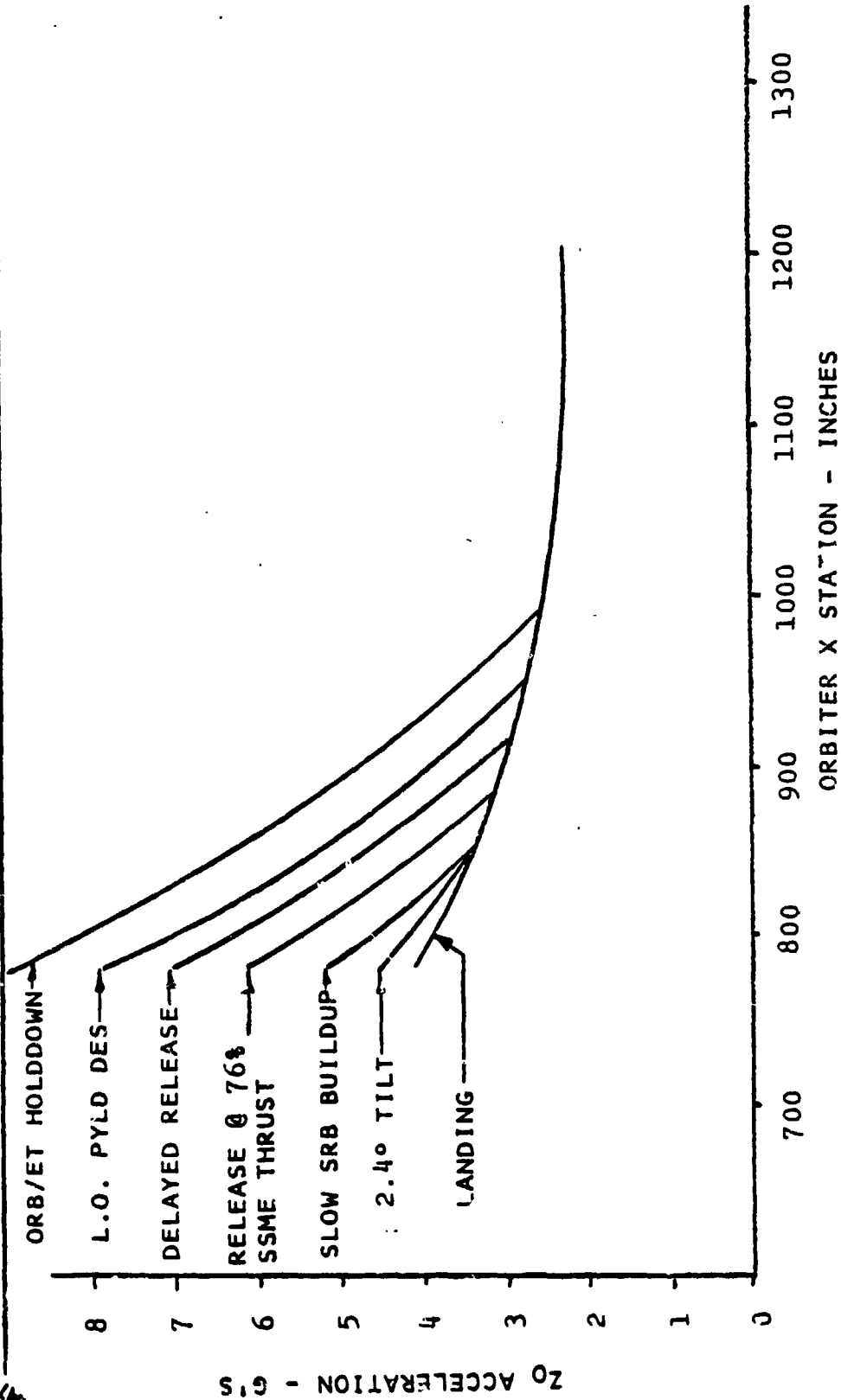
The opposite chart shows the payload liftoff design case with various load reduction methods applied to it versus the landing loads design case. The liftoff loads reduction cases plotted are: delayed SRB ignition (2.75 sec.), releasing the SRB's at 76% SSME thrust, high performance SRB with slow buildup, and tilting the Shuttle vehicle 2.4° before liftoff. The liftoff case that reduces the payload tip loads almost to the level of the landing loads is the 2.4° tilt case. Delaying SRB ignition 2.75 sec. reduces the payload design case loads the least (10%). The liftoff loads are not shown below the point at which they intersect the landing loads curve since they are always less than the landing loads near the base of the payload.



Space Transportation System
Integration & Operations Division
Space Systems Group



LANDING LOADS VS. VARIATIONS ON LIFTOFF PAYLOAD DESIGN CASE LOADS





SUMMARY OF RESULTS

A summary of the results obtained during this study are shown on the opposite chart. Of the seven methods investigated to reduce lift-off loads, tilting the stack is the most effective. One advantage of this method is that there is no loss in performance capability. There would be considerable launch facility impact, however, and the timeline must be changed to include the added operation of tilting the stack. Also a trade study would be required to determine the optimum tilt angle to minimize the impact to the SRB. Analysis results for this study must be considered preliminary.

The second best method of reducing payload response occurred with a slow SRB thrust buildup time history. This method does not seem realizable at this time, however. Initial SRB test data has shown that the engines have rise times very close to the current fast buildup case. In all probability, the SRB engines would have to be essentially redesigned in order to obtain the slow buildup history and still meet their other performance requirements.

All of the remaining methods investigated in this study do not give sufficient load reduction or would cause too severe an impact to the Shuttle system to be considered viable.



Rockwell International
Space Division



SUMMARY OF RESULTS

Load Reduction Concept	Liftoff Load Reduct. Pt. A. Pt. B.		Shuttle Ascent Performance Penalty	Shuttle Vehicle Impact	Launch Facilities Impact	Launch Operations
Delayed SRB Ignition	* 10%	* 18%	660 lbs.	Orbiter Acoustics. Software Mod.		
Release at 76% SSME thrust	* 23%	* 11%	None		None	None
Delayed Ignition of One SSME	* 31%	* 23%	120 lbs.	Safety hazard. Could not ignite last engine.		
Slow SRB Thrust Buildup	** 34%	** 33%	None	Would require SRB modification. Test data show fast buildup.		
Slow SRB Release	** 11%	** 6%	210 lbs	SRB skirt Mod.	SRB support Post Mod.	Install controlled release assemblies
Orbiter/ET Hold Down	** -14%	** -7%	300 lbs	Orbiter/ET fitting mod.	Added tie down points, fast retraction mechanism	Install half strut and release system
Tilted Stack	* 49%	* 44%	None	SRB base loads for L.O. abort.	Modify SRB support, tail service mast, crew & ET access arms	Timeline increased to include tilt operation
	* 47%**	* 38%**				

* Reduction required to equal landing results

** Reduction for slow buildup

*** Reduction for fast buildup

PRECEDING PAGE BLANK NOT FILMED

The SPAR System

November 1978

W. D. Whetstone

ENGINEERING INFORMATION SYSTEMS, INC.

5120 CAMPBELL AVENUE, SUITE 240

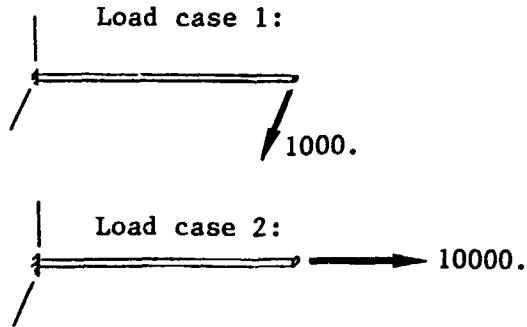
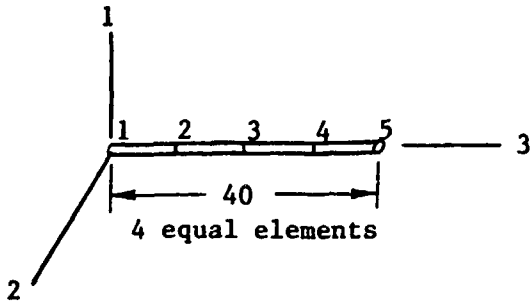
SAN JOSE, CALIFORNIA 95130

(408) 379-0730

The SPAR System

- SPAR provides a high-order language for solving a broad spectrum of engineering problems. The system consists of an array of independent processors, communicating automatically through a highly efficient general purpose engineering data base management system.
 - Advanced sparse matrix solution methods provide low execution costs, minimal central memory requirements, and large size capacity; permitting extremely fine meshes to be used. Static, buckling, and vibrational problems in the 10,000 to 20,000 DOF range are solved routinely. Maximum capacity, without substructuring, is typically in the 50,000 DOF range.
 - Highly effective in both interactive and batch operation. Major studies generally are best performed using a combination of both batch (RJE) and interactive runs. Graphics terminals, 30 cps thermal-printer terminals, and line printers all are used in various phases of typical applications.
 - All input is free-field. Extensive facilities are provided in areas such as mesh generation, data checking, automation of all aspects of problem definition, data base interrogation, and custom report generation.
 - Restarting and mixed batch/interactive operation is fully automated. To restart, the user needs only to reassign the file, or files, in which the data base resides, and resume execution as though the prior run had not been terminated.
 - The data base management system provides an automatic means of communicating with external programs, through ordinary sequential files, for purposes of obtaining source data or furnishing results. All information produced by the system is accessible in this way.
 - Effects of pre-stress may be included in all forms of static, dynamic, and buckling analysis.
 - The EIG eigensolver directly solves sparse high-order eigenproblems without using any form of DOF condensation. 10,000+ DOF vibrational and buckling eigenproblems are solved routinely. Costs are very low, particularly when modes from prior analyses are used as initial approximations.
- Extensive facilities for substructure and other forms of Rayleigh-Ritz analysis are provided for use where appropriate. Fully coupled 400+ DOF vibrational eigenproblems are solved routinely.
- Extensive dynamic analysis capability is provided: e.g. transient, random, shock spectrum, steady state. Any system state quantities may be tracked and/or recorded in the data base for use in subsequent studies. For example, the results of a complete vehicle response analysis may be recorded in the data base, and later used to define payload base excitation.
 - Extensive thermal element repertoire, including conduction, convection, radiation, and mass transport elements. Steady state and transient analysis of linear and nonlinear problems is performed. Common utilities, e.g. mesh generation, plotting, data entry routines, are shared by structural and thermal functions.

Example SPAR Runstream



Commands:

Explanation:

```

@XQT TAB
STAR1 5
TITLE'BEAM EXAMPLE
JOINT LOCATIONS
$ X Y Z
1 .0 .0 .0
2 .0 .0 10.
3 .0 .0 20.
4 .0 .0 30.
5 .0 .0 40.
MATERIAL CONSTANTS
1 10.+6, .3, .101, 1.-4
BEAM ORIENTATION
1 1 1 1.
E21 SECTION PROPERTIES
TUBE 1 2.0, 2.25
CONSTRAINT CASE 1
ZERO 1,2,3,4,5,6: 1
@XQT ELD
E21
1,2: 2,3: 3,4: 4,5
@XQT TOPO
@XQT E
@XQT EKS
@XQT K
@XQT INV
@XQT AUS
ALPHA: CASE TITLES
1'TRANSVERSE LOAD
2'AXIAL LOAD
SYSVEC: APPLIED FORCES
CASE 1: I=2: J=5: 1000.
CASE 2: I=3: J=5: 10000.
@XQT SSOL
@XQT GSF
@XQT PSF
@XQT VPRT
PRINT STATIC DISPLACEMENTS
PRINT STATIC REACTIONS
STOP
    
```

```

$ The model has 5 joints.
$ Create data set containing joint locations.
$ Create table of material constants
$ E, nu, rho, alpha for material 1.
$ Create table of orientation reference data.
$ Create table of cross section properties.
$ Tube #1 radii= 2.0, 2.25.
$ Create data set defining constraint case 1.
$ Zero all 6 motion components of joint 1.
. Define all elements.
$ Define all type E21 (general 2-node) elements.
$ Beams connect joints 1 and 2, 2 and 3, etc.
. Analyze element interconnection topology.
. Analyze element geometry.
. Create element stiffness matrices, etc.
. Create assembled system K.
. Create factored system K.
. Enter Arithmetic Utility System.
. Create data set named "CASE TITLES"
$ Create a data set named "APPLIED FORCES"
$ Page 1 (case 1) of "APPLIED FORCES"
$ Page 2 (case 2) of "APPLIED FORCES"
. Create data sets containing joint motions.
. Create data sets containing stresses.
. Produce Printed display of stresses.
    
```

Example - Data Base Table of Contents

Through the following commands, data base tables of contents may be obtained:

```
@XQT DCU          . DCU is the Data Complex Utility Program
TOC 1
```

The above commands cause a display of the following type to be produced:

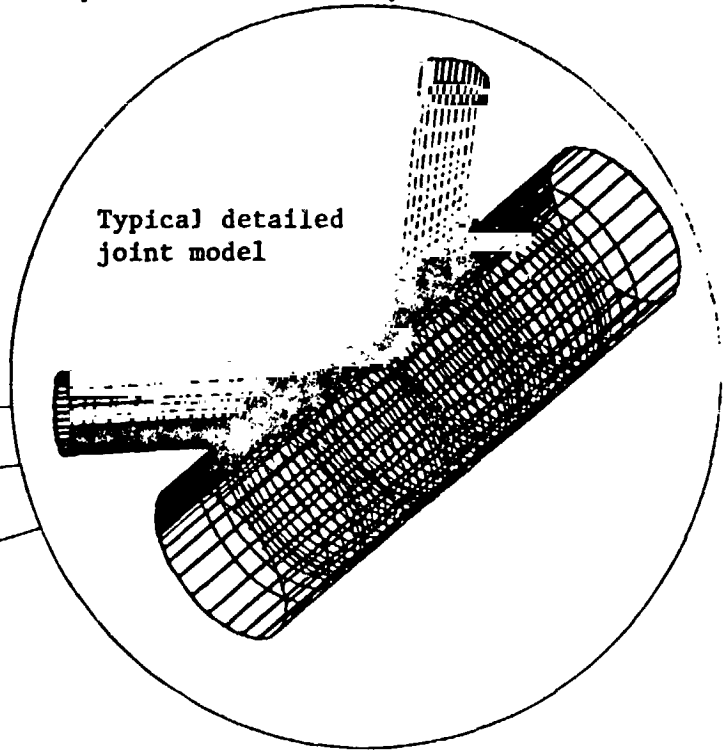
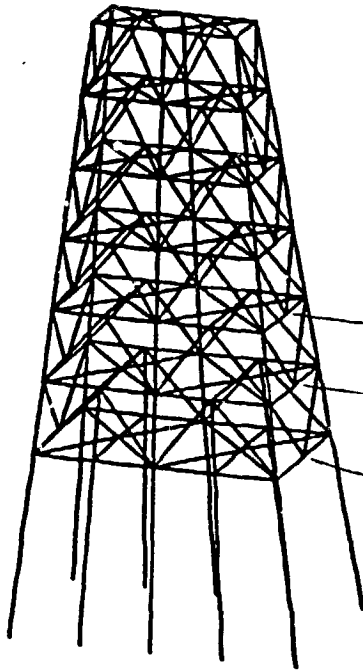
TABLE OF CONTENTS, LIBRARY 1
BEAM EXAMPLE

SEQ	RR	DATE	TIME	E R	WORDS	NJ	NI#NJ	T Y	DATA SET NAME				Processor by which created
									N1	N2	N3	N4	
1	17	110778	191116	0	18	1	18	0	JDF1	BTAB	1	8	TAB
2	18	110778	191116	0	5	5	5	0	JREF	BTAB	2	6	"
3	19	110778	191116	0	12	1	12	1	ALTR	BTAB	2	4	"
4	20	110778	191116	0	18	1	18	4	NDAL		0	0	"
5	21	110778	191116	0	15	5	15	1	JLOC	BTAB	2	5	"
6	22	110778	191116	0	10	1	10	i	MATC	BTAB	2	2	"
7	23	110778	191116	0	5	1	5	1	MREF	BTAB	2	7	"
8	24	110778	191116	0	31	1	31	1	BA	BTAB	2	9	"
9	26	110778	191116	0	5	5	5	0	CON		1	0	"
10	27	110778	191116	0	45	5	45	1	QJJT	BTAB	2	19	"
11	29	110778	191120	0	72	49	882	0	DEF	E21	1	2	ELD
12	61	110778	191120	0	2	1	2	0	GD	E21	1	2	"
13	62	110778	191120	0	15	1	15	4	GTIT	E21	1	2	"
14	63	110778	191120	0	20	1	20	0	DIR	E21	1	2	"
15	64	110778	191120	0	1	1	1	4	ELTS	NAME	0	0	"
16	65	110778	191120	0	1	1	1	0	ELTS	NNOD	0	0	"
17	66	110778	191120	0	1	1	1	0	ELTS	ISCT	0	0	"
18	67	110778	191120	0	15	1	15	0	NS		0	0	"
19	68	110778	191122	0	896	5	896	0	KMAP		9	3	TOPO
20	100	110778	191122	0	1792	5	1792	0	AMAP	EEEE	9	3	"
21	164	110778	191126	0	560	4	140	4	E21	EFIL	1	2	E, EKS
22	184	110778	191124	0	30	5	30	-1	DEM	DIAG	0	0	"
23	186	110778	191127	0	2240	5	2240	1	K	SPAR	36	0	K
24	266	110778	191129	0	3584	5	3584	1	INV	K	1	0	INV
25	394	110778	191131	0	30	1	15	4	CASE	TITL	1	1	AUS/ ALPHA
26	396	110778	191131	0	60	5	30	-1	APPL	FORC	1	1	AUS/SYSVEC
27	400	110778	191133	0	60	5	30	-1	STAT	DISP	1	1	SSOL
28	404	110778	191133	0	60	5	30	-1	STAT	REAC	1	1	"
29	408	110778	191135	0	208	4	208	-1	STRS	E21	1	1	GSF
30	416	110778	191135	0	208	4	208	-1	STRS	E21	1	2	"

DCU, the Data Complex Utility Program, enables user's to perform many data management functions, e.g. copying data sets from one library to another, disabling data sets, re-enabling previously disabled data sets, etc.

TYPICAL DYNAMIC ANALYSIS

Data exchange between all models is accomplished automatically via data base.



Analysis of frame model:

Vibrational modes

Joint force/moment eigenmatrices

Dynamic response, e.g. histories of generalized coordinates and time derivatives as required.

Joint motions, reactions, gross resultants (e.g. overturning moments), or any other state quantities.

Analysis of multiple detailed shell and/or 3D models of components:

Joint flexibility coefficients

Stress transformation matrices associated with unit force/moment resultants applied as membrane loads at edges.

Dynamic stress transformation matrices

Detailed dynamic stress response of the entire model, or of any number of selected key quantities.

Data base scanners,
graphic display generators,
custom report generators.

SPAR Structural Element Repertoire

Name	Description
E21	General beam elements such as channels, wide-flanges, angles, zees, tubes, etc.
E22	Beams for which the intrinsic stiffness matrix is given.
E23	Bar - Axial stiffness only.
E24	Plane beam.
E25	Zero-length element used to elastically connect geometrically coincident joints.

Two-dimensional (area) elements:

E31	Triangular membrane.
E32	Triangular plate.
E33	Triangular combined membrane and bending element.
E41	Quadrilateral membrane.
E42	Quadrilateral plate.
E43	Quadrilateral combined membrane and bending element.
E44	Quadrilateral shear panel.

Three-dimensional solids:

S41	Tetrahedron (pyramid).
S61	Pentahedron (wedge).
S81	Hexahedron (brick).

Compressible fluid elements:

F41	Tetrahedron (pyramid).
F61	Pentahedron (wedge).
F81	Hexahedron (brick).

Notes:

- Aeolotropic constitutive relations permitted, all area elements.
- Laminated cross sections permitted for E33, E43.
- Membrane/bending coupling permitted for E33, E43.
- E41, E42, E43, E44 may be warped.
- Aeolotropic constitutive relations permitted for 3-D solids.
- Non-structural mass permitted for line and area elements.

SPAR Processor Functions

Name	Function
TAB	Translates user inputs into data sets containing basic tables of information such as: <ul style="list-style-type: none">- Joint locations.- Material constants.- Element section properties.- Joint reference frame orientations.- Constraint conditions.
ELD	Produces data sets containing basic element definitions, i.e. connected joints, integers pointing to applicable lines in tables of section properties, material constants, etc.
E	Generates a system of data sets called the 'E-state,' consisting of individual element information packets containing data such as element geometry (dimensions, orientation), and literal section properties. E also forms the system diagonal mass matrix.
EKS	Computes element stiffness and stress influence matrices, and inserts them into the 'E-state'.
TOPO	Analyzes element interconnection topology, and produces data sets used to guide other SPAR processors in forming and factoring assembled system matrices.
K	Forms system elastic stiffness matrix.
M	Forms system consistent mass matrix.
KG	Forms system geometric (pre-stress) stiffness matrix.
FSM	Forms system matrices (dilatational strain energy, gravitational energy, kinetic energy) associated with fluid elements.
INV	Factors system matrices in SPAR's standard sparse-matrix format, e.g. K, K+Kg, K-cM.
AUS	The Arithmetic Utility System, containing an array of subprocessors in the following categories: <ul style="list-style-type: none">- Source data table construction and editing. For example, the following commands cause a 2 x 3 matrix to be created and stored in the data base in a data set named XYZ: <pre>TABLE(NI=2, NJ=3): XYZ J=1: 2.3 5.7 J=2: 3.4 4.2 j=3: 1.2 8.0</pre>

SPAR Processor Functions (continued)

Name	Function
AUS(cont)	<p>- Matrix arithmetic operations. For example, the following command causes a new data set, named KSUM, to be created and stored in the data base. KSUM is the sum of two matrices residing within data sets named K and KG. These matrices may be in any of a number of forms, e.g. total system matrices in sparse format:</p> $KSUM = SUM(K, KG)$ <p>- Special functions, including subprocessors used in performing substructure analysis.</p>
RMK	Translates arbitrary M and K data into SPAR format system matrices.
EQNF	Computes fixed-joint forces associated with thermal, dislocational, and pressure loading. Computes element generalized initial strain arrays.
SSOL	Computes joint motions and reactions due to static loading.
GSF	Produces data sets containing element stresses and internal loads.
PSF	Produces tabular stress reports from data sets generated by GSF.
ES	The Element State Processor, which will supersede GSF and PSF. ES performs an array of functions, including stress scans and automated production of dynamic stress transformation matrices.
EIG	Solves high-order eigenproblems involving system matrices in SPAR's sparse matrix format. Used to solve both vibrational and buckling eigenproblems.
CEIG	Computes complex modes and frequencies of damped, spinning structures. System matrices are in SPAR's standard sparse matrix format, permitting analysis of systems of very high order.
DR	Computes linear transient modal response.

SPAR Processor Functions (continued)

Name	Function
SYN	Synthesizes system M and K from substructure data in the form produced by AUS subprocessors SSPREP, SSM, and SSK.
STRP	General purpose eigensolver, full mass and stiffness matrices. Used primarily in analyzing systems synthesized by SYN.
SSBT	Substructure back-transformation processor. Computes joint motions in individual substructures from system state data in the form generated by SYN and STRP.
SM	The System Modification Processor. SM alters the basic definition of the structure to cause modes and frequencies to approach target values defined by the user. Typical applications include tuning finite element models to agree with dynamic test results, and design of vibration attenuators.
DCU	The Data Complex Utility Program. DCU performs utility operations such as printing data base tables of contents, copying data sets from file to file, printing selected items from data sets, and transferring data to or from programs outside the SPAR system.
VPRT	Prints reports of data in SPAR's SYSVEC (system vector) format, e.g. static displacements, reactions, vibrational or buckling eigenvectors.
PR	Generates reports of the results of dynamic response analyses. A variety of display formats are provided for the results of transient and random response studies.
PS	Prints designated parts of SPAR-format system matrices.
PLTA	Transforms user inputs into data sets detailing the composition of plots to be produced by PLTB.
PLTB	Produces plots of deformed or undeformed structure, stresses, etc.

Thermal Element Repertoire

Name	Description
	Conducting Elements:
K21	2 node line element
K31	3 node area element
K41	4 node area element
K61	6 node volume element
K81	8 node volume element
	Convection to a Known Temperature:
C21	2 node line element
C31	3 node area element
C41	4 node area element
	Fluid-Surface Convective Exchange:
C32	3 node line element
C42	4 node line element
C62	6 node area element
	Mass-Transport:
MT21	2 node line element
	Integrated Mass-Transport, Convective Exchange:
MT42	4 node line element
MT62	6 node area element
	Radiating Elements:
R21	2 node line element
R31	3 node area element
R41	4 node area element

Thermal Processor Functions

Name	Function
TGEO	Creation of primary thermal element network data structures.
SSTA	Computes steady state solutions, both linear and nonlinear.
TTRA	Computes transient solutions, both linear and nonlinear.



**GENERAL
ELECTRIC**



space division

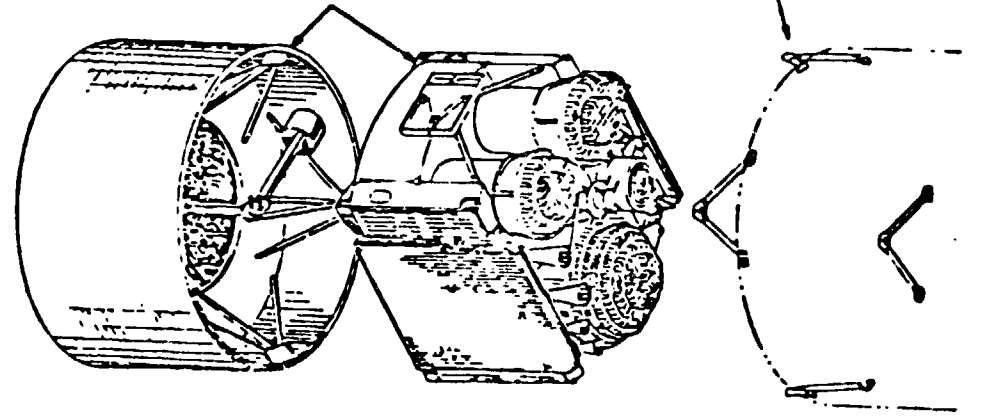
**SPACECRAFT MODAL TESTING USING
SINGLE POINT RANDOM AND
MULTI-SHAKER SINE
TEST TECHNIQUES**

**C. V. STAHL AND M. FERRANTE
GENERAL ELECTRIC CO. — SPACE DIVISION**

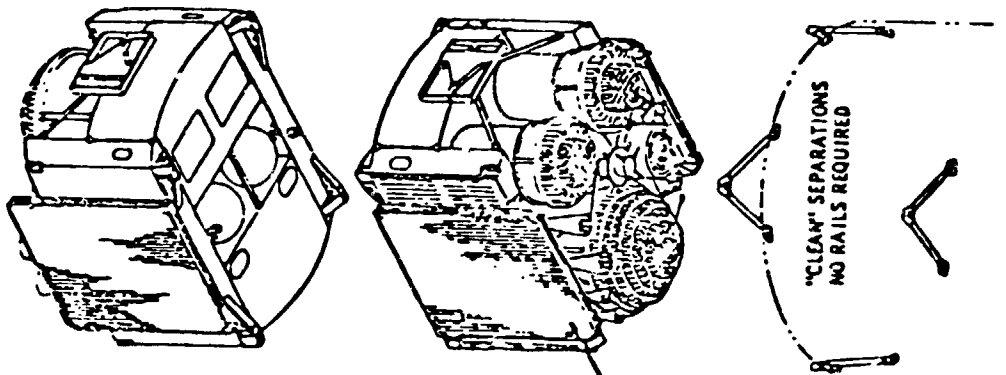
DSCS III STACKED LAUNCH CONFIGURATIONS



DSCS III/DSCS II LAUNCH



DSCS III/DSCS III LAUNCH



- DSCS II
INTERFACE
BASICALLY UNCHANGED
- SAME STATION
 - SAME SEPARATION HARDWARE
 - STIFF RADIAL LOAD PATH PROVIDED BY DSCS III

HARD MOUNT
SOLAR ARRAYS

TRUSS ADAPTER
REMAINS WITH
BOOSTER

"CLEAN" SEPARATIONS
NO RAILS REQUIRED



MODAL TEST OBJECTIVE AND CRITERIA



OBJECTIVE

- DEVELOP AN EXPERIMENTAL MODEL THAT INCLUDES ALL MODES WHICH ARE RESPONSIVE TO SIGNIFICANT LAUNCH TRANSIENTS (RESONANT FREQUENCIES, MODE SHAPES AND MODAL DAMPING COEFFICIENTS OF MODES BELOW 50 HERTZ).

CRITERIA

$$\phi_i^T M \phi_j = 1.0 \quad i = j$$

$$\leq 0.1 \quad i \neq j$$

OBJECTIVE AND CRITERIA CONSISTENT WITH VERIFICATION LOAD CYCLE REQUIREMENTS



**GENERAL
ELECTRIC**

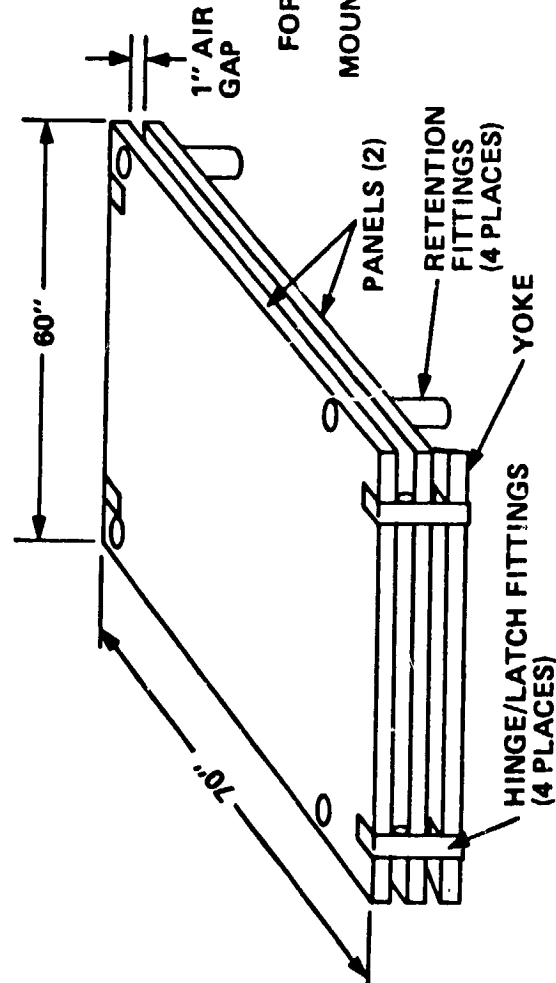
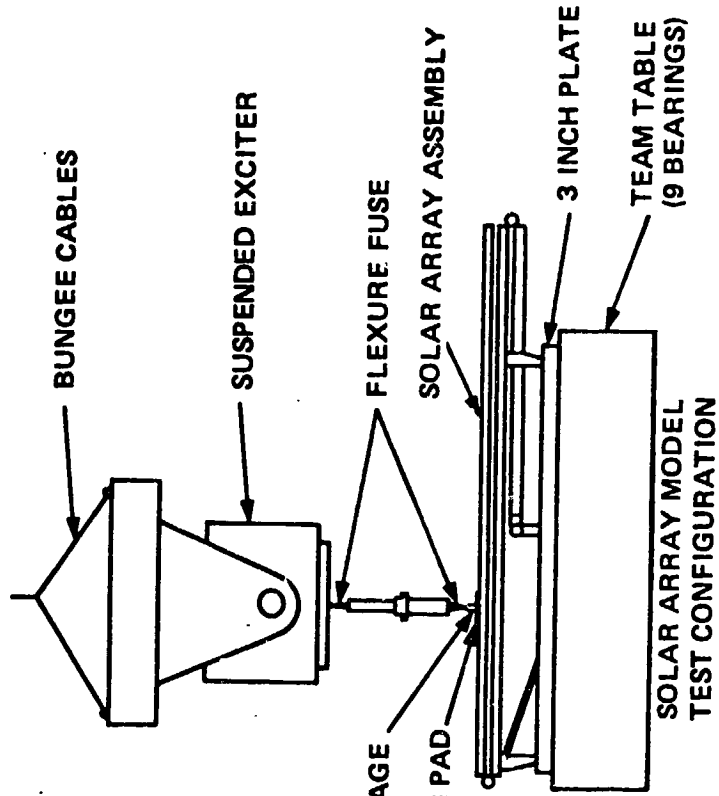
OVERALL APPROACH



- **SIMPLIFY TEST ARTICLE — SOLAR ARRAY AND CENTERBODY TESTED SEPARATELY**
 - ELIMINATES DUPLICATE MODES
 - REDUCES MODAL DENSITY
- **SINGLE POINT RANDOM EXCITATION (SPR)**
 - PRIMARY METHOD OF MEASUREMENT
 - EXCITATION VARIED TO EXCITE SELECTED MODES (5 LOCATIONS)
 - MEASURED MODES EDITED TO ELIMINATE DUPLICATES
- **MULTI-SHAKER SINE TESTING (MSS)**
 - MEASURE 15 MODES OF CENTERBODY (30 TO 50%)
 - VERIFY SINGLE POINT RANDOM TECHNIQUE

<p>MSS TECHNIQUE USED TO VALIDATE SPR TECHNIQUE</p>

SOLAR ARRAY MODAL TEST



DATA OBTAINED FROM THREE SHAKER LOCATIONS

- PANEL SURFACE DENSITY: 0.7 LB/FT²
- PANEL SIZE: 60" X 70"
- AIR GAP: 1 INCH

6



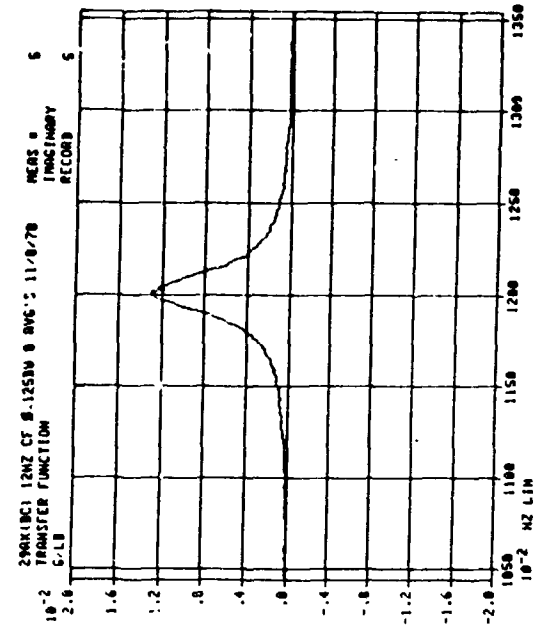
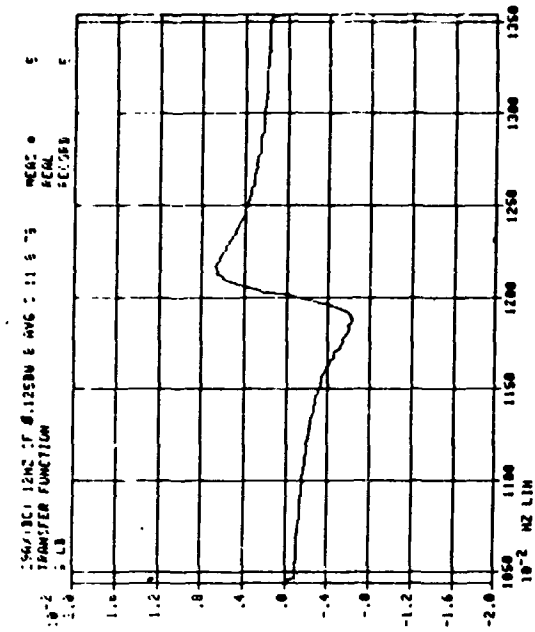
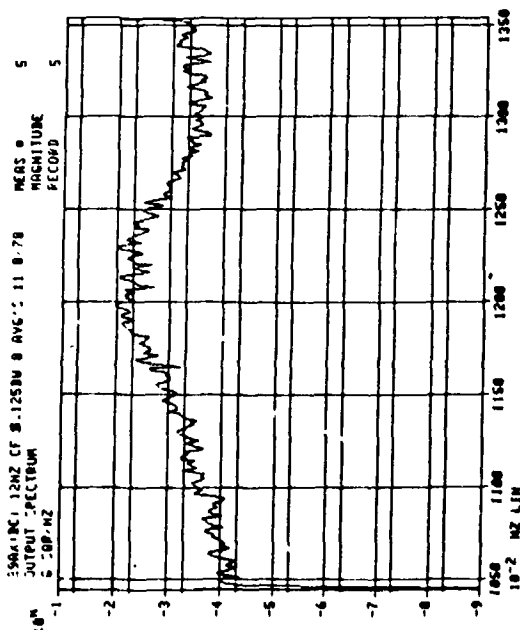
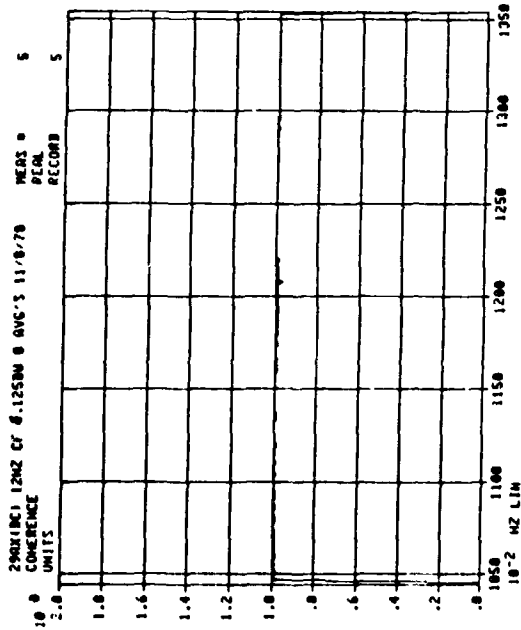
GENERAL ELECTRIC

118

STRUCTURAL TRANSFER FUNCTION DATA



space division



ORIGINAL PAGE IS OF POOR QUALITY



**GENERAL
ELECTRIC**

SOLAR ARRAY ORTHOGONALITY



Space division

MODE	1	2	3	4	5	6	7	8	9	10	11	12	13
FREQ	13.843	24.018	28.164	30.103	32.070	33.895	45.448	52.027	54.827	56.500	58.074	6A.626	71.411
C/C	3.234	1.938	0.844	1.632	1.060	1.563	1.076	1.402	0.971	1.306	1.379	0.644	1.226
1	1.000	-0.015	0.019	0.025	0.026	0.041	0.033	0.023	0.034	-0.017	0.020	0.078	0.016
2	1.000	0.005	0.005	-0.050	0.055	0.005	0.003	0.009	-0.088	-0.117	-0.003	-0.064	0.145
3	1.000	0.005	0.005	0.045	-0.025	0.016	0.024	0.005	-0.024	-0.041	0.043	0.013	-0.006
4	1.000	0.110	0.024	1.000	0.110	0.024	-0.175	-0.122	0.122	-0.067	-0.133	-0.043	-0.078
5	1.000	0.110	0.024	0.110	1.000	0.007	0.078	0.122	-0.057	-0.019	-0.032	-0.030	-0.110
6	1.000	0.019	0.005	0.005	0.005	1.000	-0.010	0.053	0.036	-0.023	0.023	0.003	0.008
7	1.000	0.019	0.005	0.005	0.005	0.005	1.000	-0.139	0.095	-0.024	0.008	-0.038	0.023
8	1.000	0.019	0.005	0.005	0.005	0.005	0.005	1.000	-0.053	0.018	-0.114	0.008	0.095
9	1.000	0.019	0.005	0.005	0.005	0.005	0.005	0.005	1.000	0.191	0.125	-0.129	0.051
10	1.000	0.019	0.005	0.005	0.005	0.005	0.005	0.005	0.005	1.000	0.116	-0.055	0.048
11	1.000	0.019	0.005	0.005	0.005	0.005	0.005	0.005	0.005	0.005	1.000	0.057	-0.157
12	1.000	0.019	0.005	0.005	0.005	0.005	0.005	0.005	0.005	0.005	0.005	1.000	-0.112
13	1.000	0.019	0.005	0.005	0.005	0.005	0.005	0.005	0.005	0.005	0.005	0.005	1.000

NUMBER OF TERMS ABOVE FOLLOWING THRESHOLD

0.02 0.04 0.06 0.08 0.10 0.12 0.14 0.16 0.18 0.20 0.22 0.24

57 40 27 22 17 10 5 3 1 0 0 0

LARGEST OFF DIAGONAL TERM = 0.191

TOTAL NUMBER OF OFF DIAGONAL TERMS = 78

APPROXIMATELY 6%
EXCEED 14

ORIGINAL PAGE IS
OF POOR QUALITY



**GENERAL
ELECTRIC**

TEST EQUIPMENT



space division

120

- 100 CHANNEL ANALOG MULTIPLEX SYSTEM WITH PATCH BOARD
- LARGE NUMBER OF RESPONSE MEASUREMENTS
 - 66 SOLAR ARRAY ACCELEROMETERS
 - 200 CENTERBODY ACCELEROMETERS
- SINGLE POINT RANDOM
 - HP 5451B (2 UNITS, ONE WITH 16 CHANNEL MULTIPLEXER)
 - LING MODEL 370 SHAKER (70 POUNDS RMS FORCE)
 - LING MODEL 385 SHAKER (500 POUNDS RMS FORCE)
 - KISTLER MODEL 9312A FORCE TRANSDUCER
- SINGLE SHAKER SINE
 - 4 SHAKERS (MB PM50'S)
 - 4 KISTLER MODEL 9312A FORCE TRANSDUCERS
 - SINGLE SERVO CONTROL WITH INDIVIDUAL GAIN CONTROLS
 - PHASELOCK
 - HP5451B

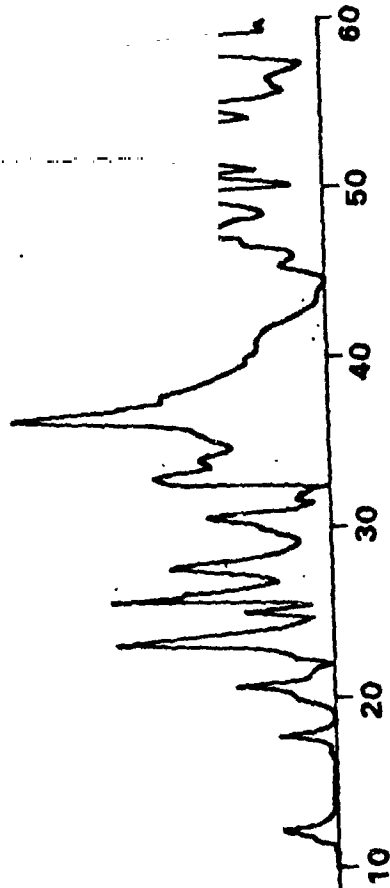
TWO EXCITATION SYSTEMS WITH
COMMON DATA ACQUISITION



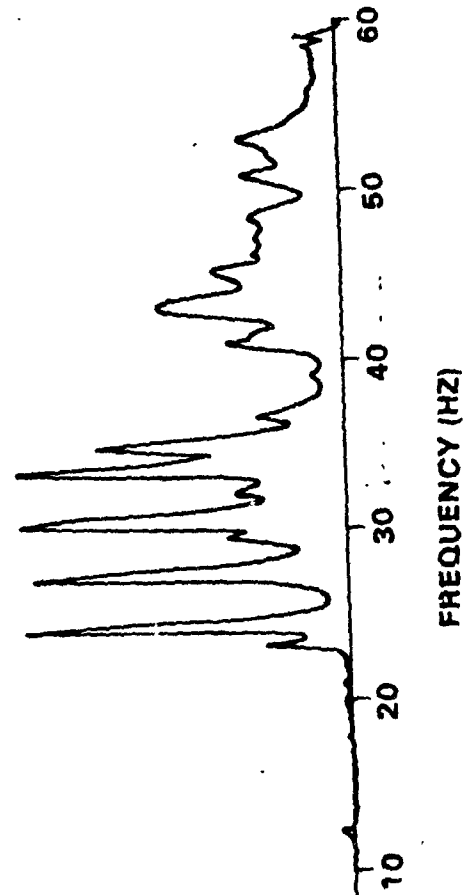
CENTER BODY SINE SWEEP TESTS



TOTAL RESPONSE
38Z



QUAD RESPONSE
4Z



APPROXIMATELY 40
MODES BETWEEN 10
AND 50 HERTZ



**GENERAL
ELECTRIC**



space division

MULTI-SHAKER SINE TECHNIQUE

- USE EXCITATION TO SUPPRESS MODES NEAR TARGET MODE
- ITERATE FORCE DISTRIBUTION FROM MODAL DEFLECTIONS AT SHAKER LOCATIONS

$$\{F_S\} = (\phi_S^T)^{-1} \{F_q\}$$

- VERIFY MODAL ISOLATION BY NARROW BAND SWEEPS

EXCITATION VARIED TO
SEPARATELY EXCITE TARGET MODES

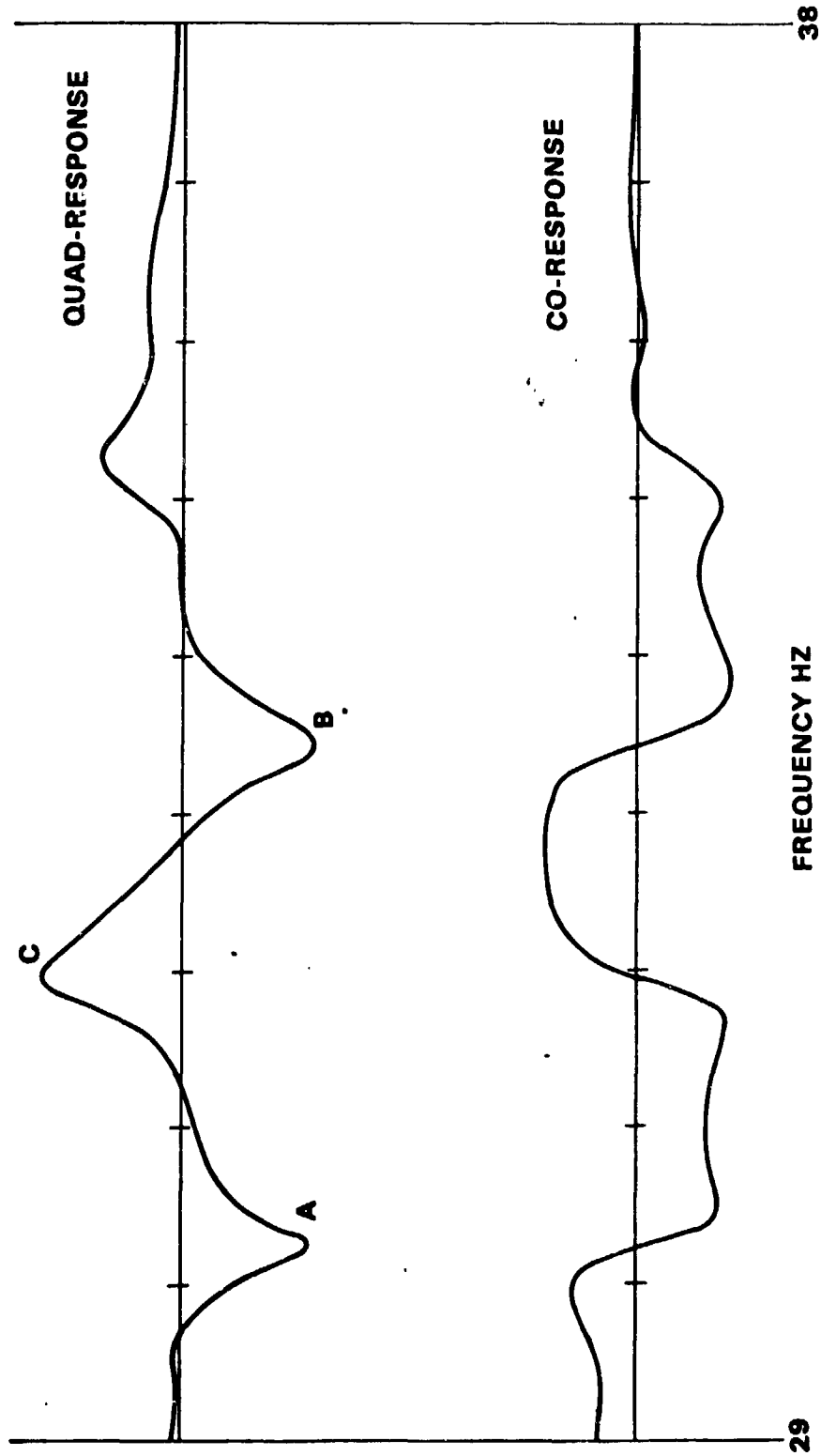


**GENERAL
ELECTRIC**

SINGLE SHAKER RESPONSE



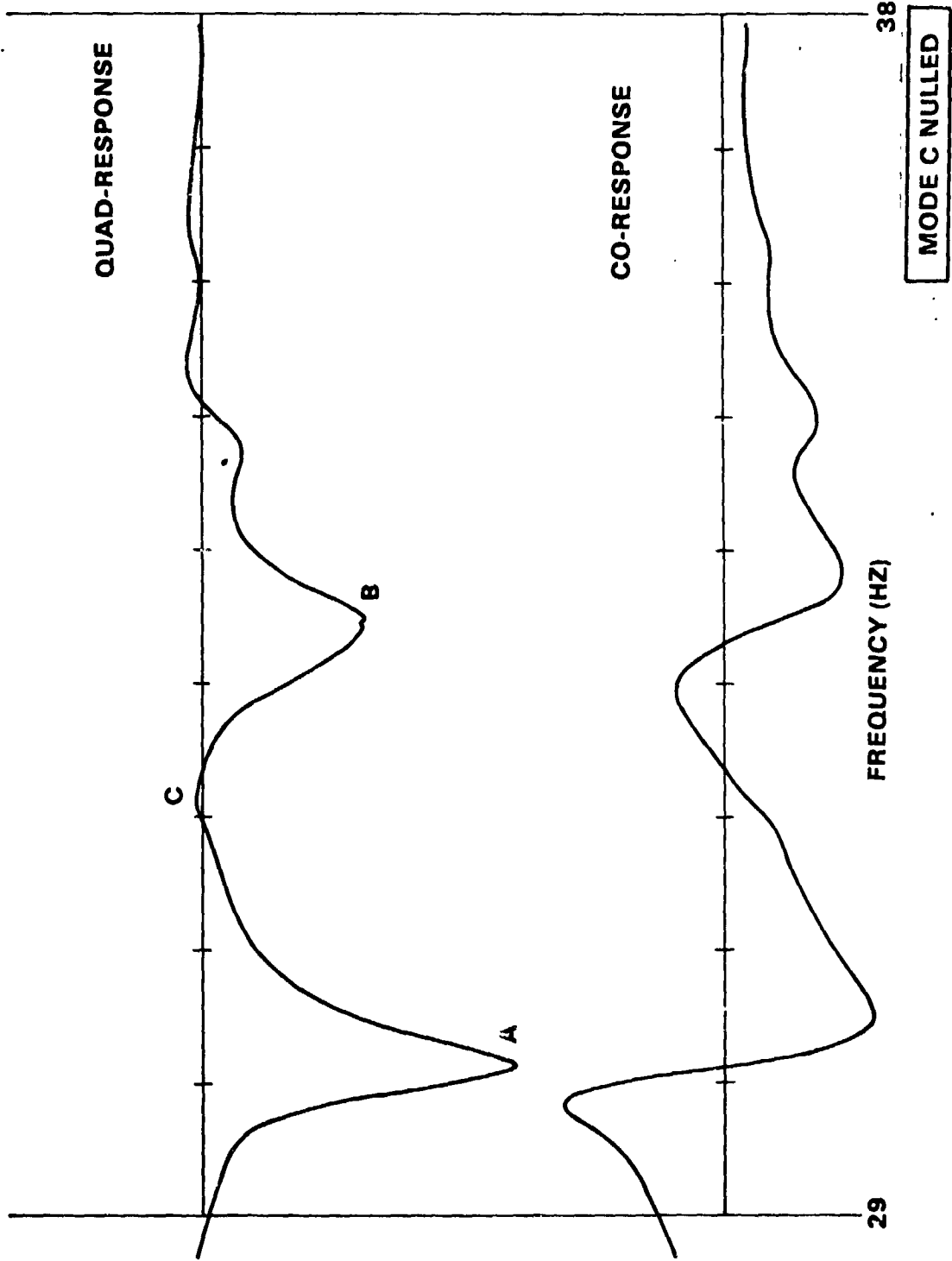
space division



12

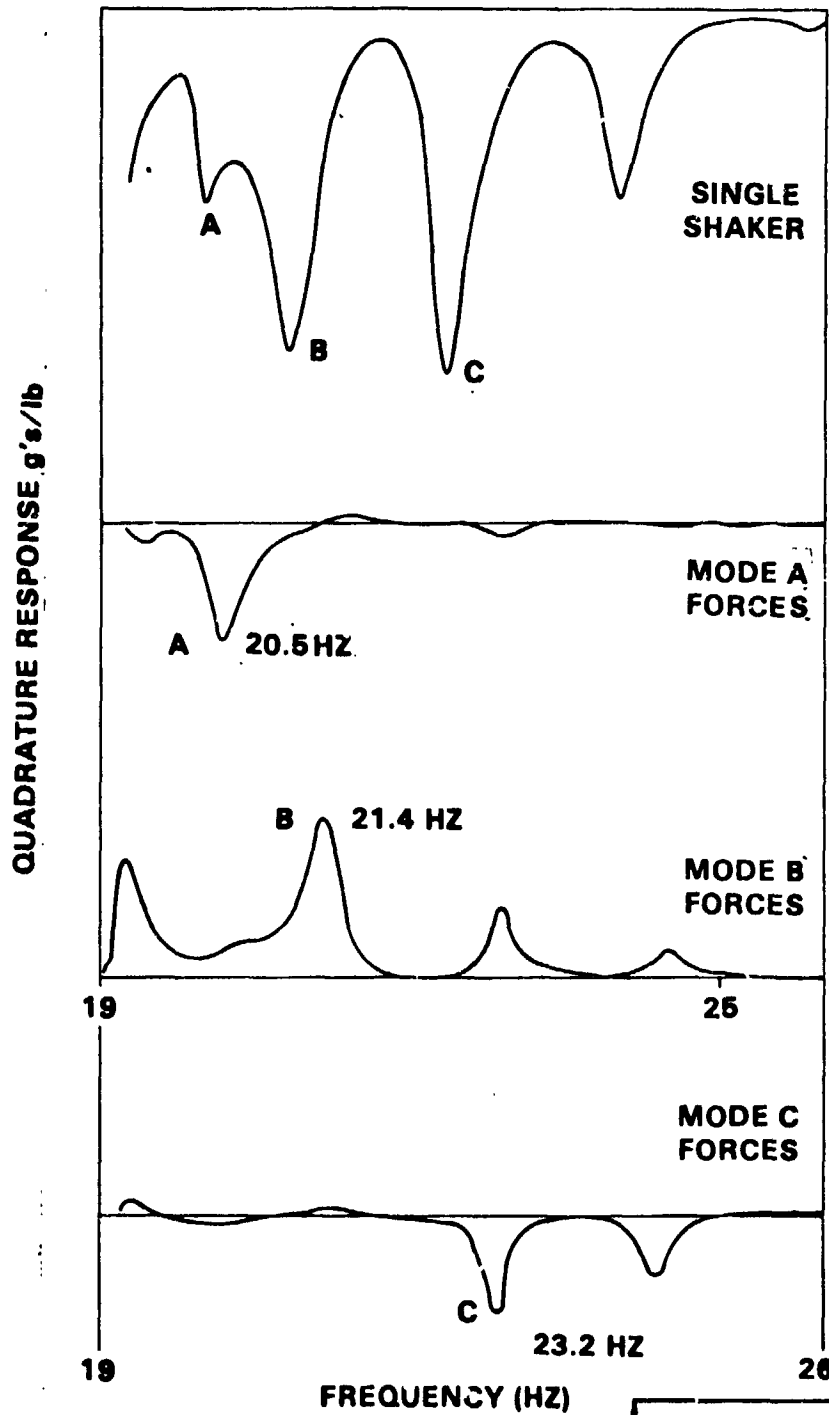


MULTI-SHAKER RESPONSE





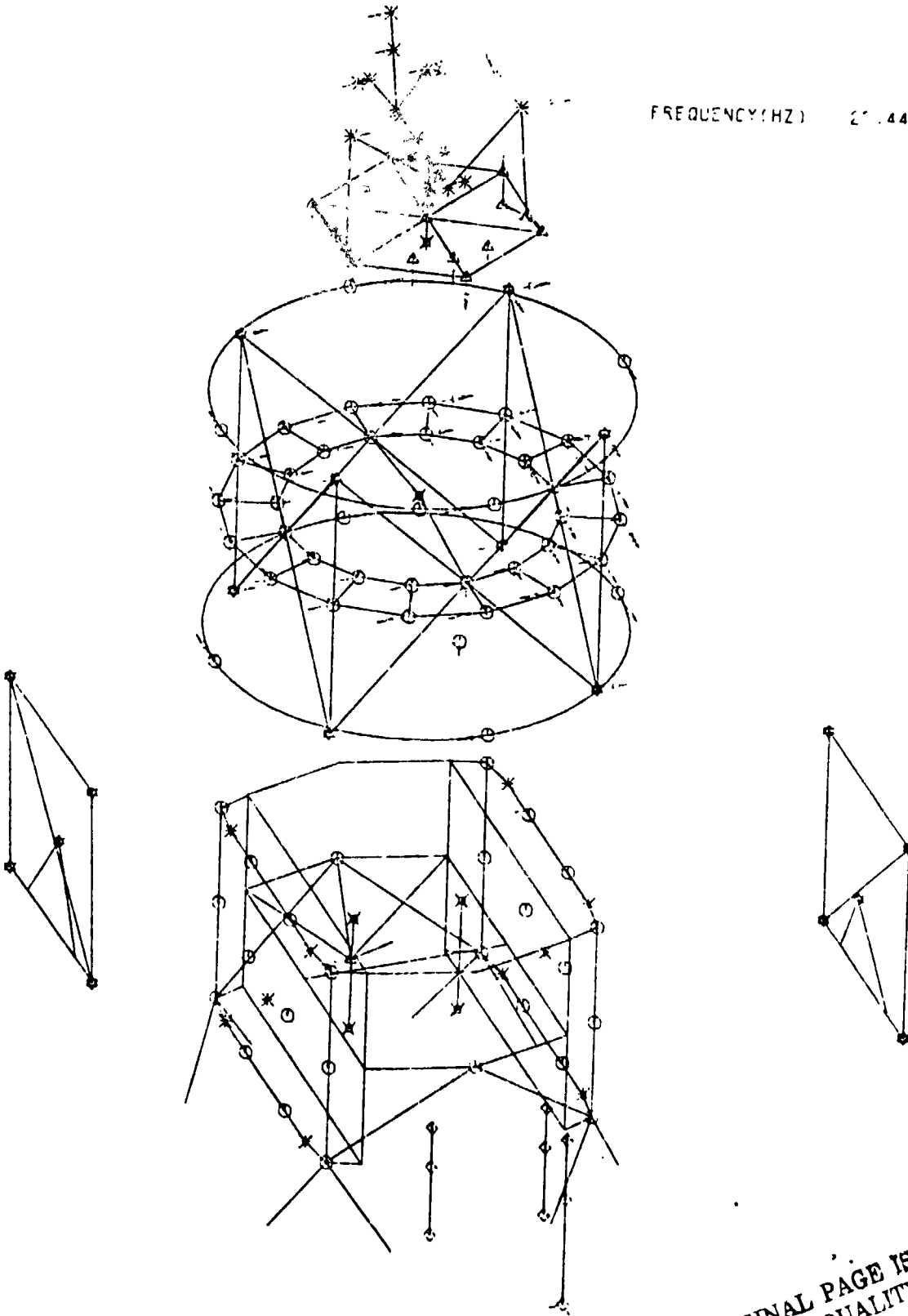
MULTI-SHAKER QUADRATURE RESPONSE



THREE SHAKERS
USED TO EMPHASIZE
INDIVIDUAL MODES

MS9903

FREQUENCY (HZ) 21.449

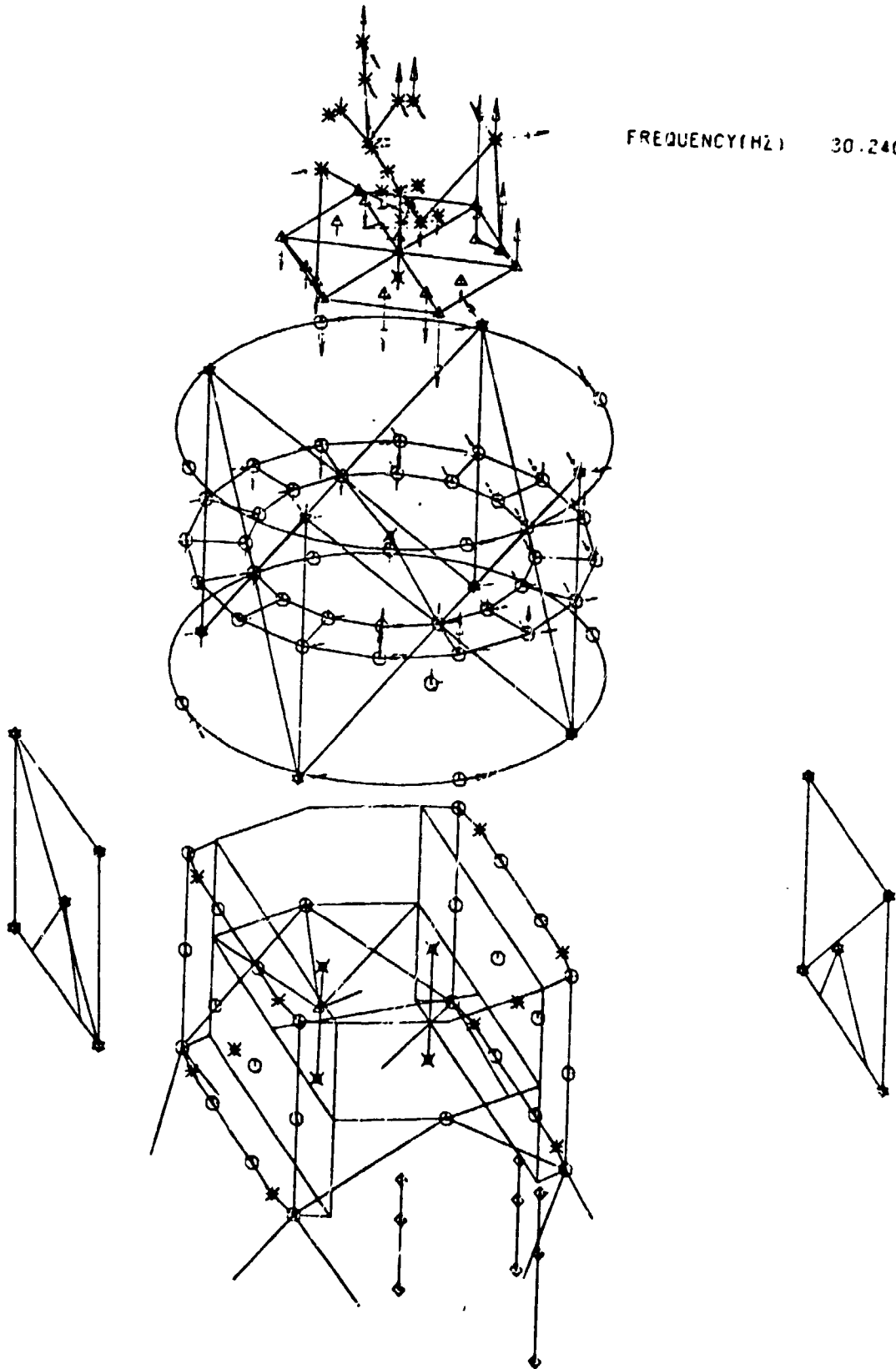


ORIGINAL PAGE IS
OF POOR QUALITY

41

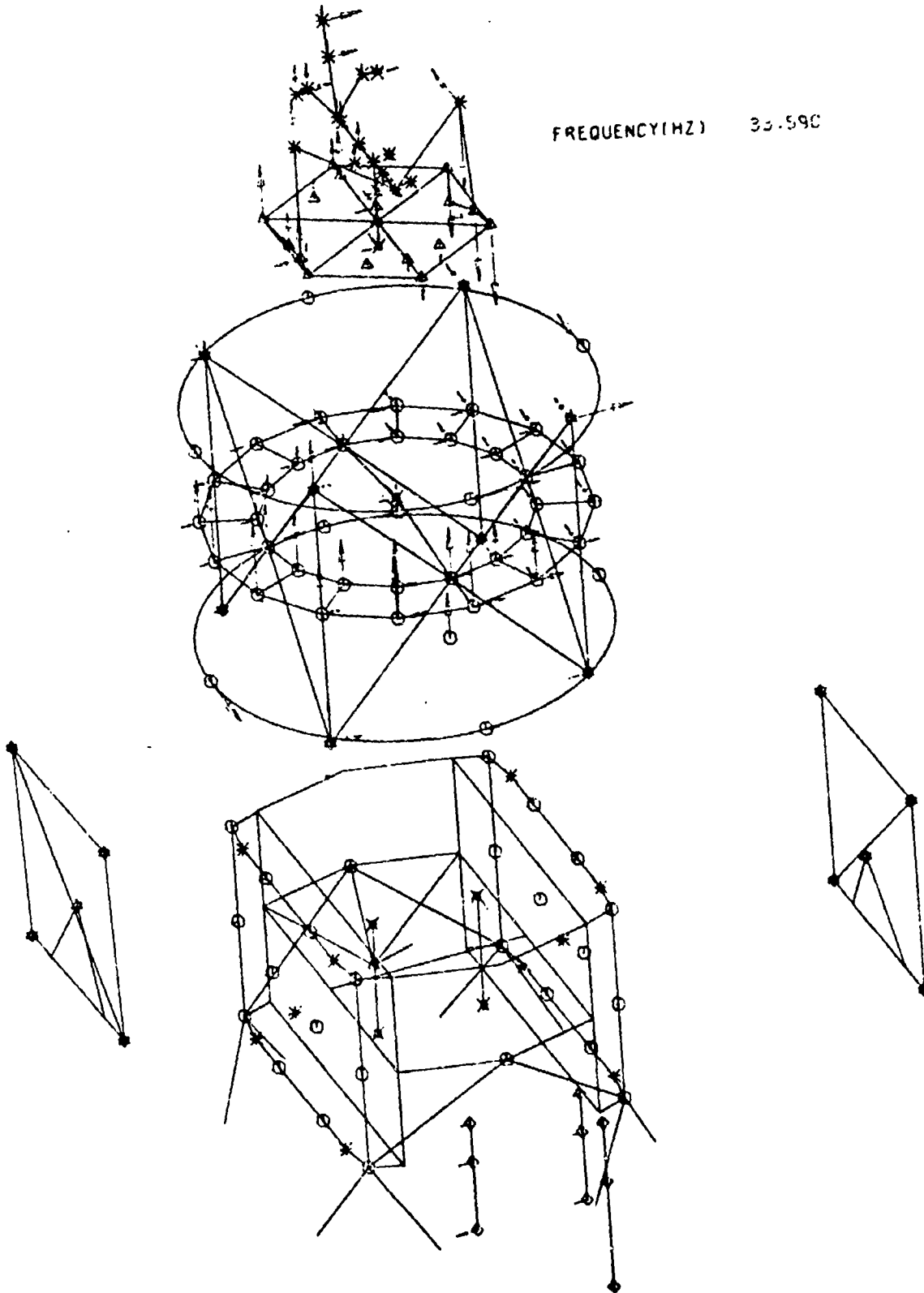
MSS003

FREQUENCY (HZ) 30.240



NC9004

FREQUENCY(HZ) 33.590





**GENERAL
ELECTRIC**

ORTHOGONALITY OF REPEATED MODES



	7	8	9	10	11	12
20.120	20.450	21.100	21.550	22.650	23.170	
0.	0.	0.	0.	0.	0.	R
0.227	0.156	-0.253	0.029	-0.021	-0.003	-0.003
0.053	0.036	0.254	-0.055	-0.014	-0.022	-0.022
0.048	0.024	-0.062	0.004	-0.000	0.022	0.022
0.127	-0.075	-0.249	0.110	0.015	0.003	0.003
-0.260	0.020	0.220	-0.027	0.150	0.124	0.124
-0.134	-0.219	-0.029	0.010	-0.045	-0.043	-0.043
1.000	0.910	0.272	-0.032	-0.140	-0.110	-0.110
0.210	1.000	0.221	-0.103	-0.023	-0.032	-0.032
0.275	0.221	1.000	-0.020	0.243	0.319	0.319
-0.036	-0.163	-0.026	1.000	-0.020	-0.025	-0.025
-0.140	-0.033	0.223	-0.020	1.000	0.989	0.989
-0.115	-0.032	0.310	-0.225	0.237	1.000	1.000
-0.010	-0.023	0.228	-0.020	0.131	0.177	0.177
0.010	-0.205	0.223	-0.110	-0.142	-0.114	-0.114
0.025	0.016	-0.014	0.015	-0.015	-0.013	-0.013
0.211	-0.241	-0.020	0.103	0.124	0.208	0.208
-0.260	0.002	0.176	-0.102	-0.017	-0.053	-0.053
1.014	0.000	-0.217	0.027	0.241	0.035	0.035

ORIGINAL PAGE #
ON FOUR

REPEATED MODES SHOW
IMPROVED ORTHOGONALITY



**GENERAL
ELECTRIC**

SUMMARY OF PRESENT RESULTS



space division

MULTI-SHAKER SINE TESTING

- o SMALL SHAKERS (< 50 POUNDS) ARE ADEQUATE
- o FORCE AMPLITUDE AND PHASE DISTORTED BY RESPONSE
- o NULL TECHNIQUE APPEARS TO IMPROVE ORTHOGONALITY

SINGLE POINT RANDOM

- o LARGER SHAKERS ARE NEEDED TO EXCITE STRUCTURE
- o EXCITATION AT STRUCTURAL "HARD POINTS" IS NEEDED TO OBTAIN ADEQUATE RESPONSE OVER THE COMPLETE FREQUENCY RANGE
- o DATA PROCESSING CAN BE AUTOMATED TO A LARGE DEGREE BUT IS TIME CONSUMING
- o REASONABLE RESULTS OBTAINED FOR SOLAR ARRAY
- o SIMULTANEOUS FITTING OF MODES IN A BAND APPEARS TO IMPROVE ORHTOGONALITY

PRECEDING PAGE BLANK NOT FILMED

**APPLICATION OF PERTURBATION
METHODS TO IMPROVE ANALYTICAL
MODEL CORRELATION WITH TEST DATA**

**Jay C. Chen
J.A. Garba
B.K. Wada**



JET PROPULSION LABORATORY



OBJECTIVES

• DEVELOP SYSTEMATIC METHOD FOR UPDATING ANALYTICAL MODELS
TO MATCH TEST DATA.

• GENERATE ALGORITHM COMPATIBLE WITH GENERAL PURPOSE COMPUTER
PROGRAMS SUCH AS NASTRAN.

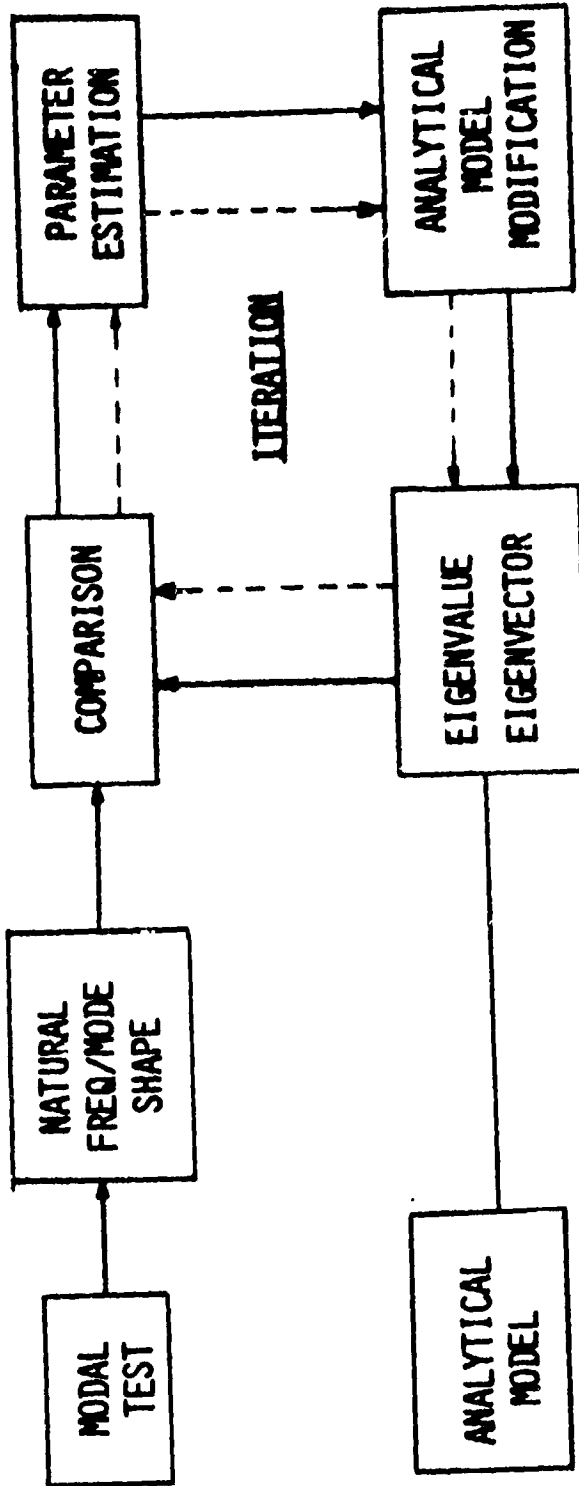


A P P R O A C H

- . SURVEY PUBLISHED METHODOLOGIES**
- . SELECT CANDIDATE METHODS**
- . EVALUATE METHODS USING ANALYTICALLY PERTURBED DATA**
- . APPLY METHODS TO REAL STRUCTURE TEST DATA**
- . DEVELOP IMPROVEMENTS IN METHODOLOGY**
- . DOCUMENT RESULTS**



ANALYSIS - TEST CORRELATION





C R I T E R I A

**THE FOLLOWING CHARACTERISTIC OF THE ANALYTICAL MODEL MUST SHOW
IMPROVED CORRELATION WITH TEST.**

- . FREQUENCY**
- . MODE SHAPE**
- . MODAL KINETIC ENERGY DISTRIBUTION**
- . STRAIN ENERGY DISTRIBUTION**
- . CROSS ORTHOGONALITY**
- . EFFECTIVE WEIGHT**
- . MODAL FORCE COEFFICIENTS**



SURVEY OF METHODS

. WHITE - MYA

ENERGY BALANCE

. HASSELMAN - WIGGINS

STATISTICAL VARIATIONS

EVALUATION OF DERIVATIVES

. BERMAN - KAMAN

TRANSFER FUNCTION APPROACH



WHITE'S FORMULATION

- $[M_0] \{\ddot{h}\} + [K_0] \{h\} = \{0\}$

$$\{h\} = \{\phi_0\} \{\xi\}$$

- $[1] \{\ddot{\xi}\} + [\omega_0^2] \{\xi\} = \{0\}$



SIMPLIFICATION

- $\{h\} = [\phi_0] \{\psi\} \implies [\bar{\psi}] = [\phi_0]^{-1} [\bar{h} \text{ exp}]$
- $\frac{1}{2} (n^2 + n)$ EQUATIONS $\implies [a_{ij}] + [b_{ij}] = [c_{ij}]$
- n EQUATIONS \implies USE ONE COL $\{\psi_i\}$
- ASSUME TEST MODE \equiv ANALYSIS MODE $\implies [\psi] = [I]$
AND USE DIAGONAL

$$\{\delta\} = [E_0]^{-1} \{\Omega^2 - \omega_0^2\}$$



WHITE'S FORMULATION (contd)

$$\bullet [\bar{K}] = [K_0] + \sum_{p=1}^P \delta_p [k]_p - [K_0] + [\Delta K_0]$$

$$\bullet [\bar{M}] = [M_0] + \sum_{q=1}^Q \delta_q [m]_q - [M_0] + [\Delta M_0]$$

$$\bullet [\bar{M}] \{\ddot{h}\} + [\bar{K}] \{h\} = \{0\}$$

$$\{h\} = [\phi_0] [\bar{\psi}] \{\gamma\}$$

$$\begin{aligned} \bullet [\bar{\psi}]^T [1] [\bar{\psi}] [\bar{\Omega}^2] - [\bar{\psi}]^T [\omega_0^2] [\bar{\psi}] &= \sum_{p=1}^P \delta_p [\bar{\psi}]^T [\phi_0]^T [k]_p [\phi_0] [\bar{\psi}] \\ &- \sum_{q=1}^Q \delta_q [\bar{\psi}]^T [\phi_0]^T [m]_q [\phi_0] [\bar{\psi}] [\bar{\Omega}^2] \end{aligned}$$

• UNDERLINE = TEST



APPLICATION OF WHITE'S METHOD

. VIKING PROPULSION SUBSYSTEM

THOROUGHLY ANALYZED AND TESTED
ACCEPTABLE CORRELATION
MODERATELY COMPLEX - 680 DOF

. PERTURBED ANALYTICAL MODEL

VERIFICATION OF METHOD
CONVERGENCE NOT GUARANTEED
CONVERGENCE NOT UNIFORM

. APPLICATION TO TEST DATA



MEMBER FACTOR CONVERGENCE OF PERTURBED ANALYTICAL MODEL

MEMBER GROUP	ORIGINAL PERTURBATION	ITERATION				
		1st	2nd	3rd	4th	5th
A	1.4	0.865	0.994	1.015	1.002	0.997
B	0.7	0.896	1.019	1.020	1.000	0.998
C	1.3	0.972	0.972	0.946	0.993	1.005
D	0.8	0.902	1.023	0.997	1.000	1.000
E	1.4	1.774	1.298	0.923	0.996	0.999
F	1.3	0.821	0.968	0.991	1.030	1.002
G	1.4	0.890	1.059	1.026	0.989	0.979



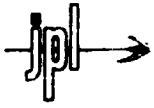
FREQUENCY CONVERGENCE OF PERTURBED ANALYTICAL MODEL

144

MODE NO.	ORIGINAL MODEL FREQUENCY,* Hz	PERTURBED MODEL FREQUENCY, Hz	ITERATION				
			1st, Hz	2nd, Hz	3rd, Hz	4th, Hz	5th, Hz
1	12.37	13.49	11.87	12.34	12.36	12.37	12.37
2	15.85	16.34	15.07	15.83	15.85	15.86	15.85
3	19.37	20.29	18.51	19.34	19.37	19.38	19.37
4	26.49	26.25	26.49	27.15	26.24	26.48	26.49
5	27.90	28.30	27.50	28.13	27.95	27.91	27.90
6	34.19	34.29	34.08	34.26	34.17	34.20	34.19
7	42.06	42.64	41.66	42.09	42.09	42.08	42.06
8	47.69	49.43	45.10	47.49	47.62	47.93	47.69
9	52.39	52.61	51.56	52.49	52.48	52.41	52.39
10	52.51	54.21	52.41	52.65	52.65	52.50	52.51
11	60.47	61.94	58.65	60.34	60.30	60.52	60.47
12	60.96	64.23	59.48	61.21	61.26	61.05	60.96

*CONSIDERED AS THE TEST DATA TO WHICH THE PERTURBED MODEL IS
TO CONVERGE.

11B



FREQUENCY COMPARISON OF TEST RESULTS AND ORIGINAL MODEL

<u>MODE NO.</u>	<u>FREQUENCY, Hz</u>	<u>ORIGINAL MODEL FREQUENCY, Hz</u>	<u>DIFFERENCE, Hz</u>	<u>DIFFERENCE, %</u>
1	12.95	12.37	0.58	4.5
2	17.66	15.85	1.81	10.2
3	20.80	19.37	1.43	6.9
4	22.97	26.49	-3.52	-15.3
5	28.33	27.90	0.43	1.5
6	32.76	34.19	-1.43	4.4
7	42.80	42.06	0.74	1.7
8	50.67	47.69	2.98	5.9
9	50.40	52.39	-1.99	3.9
10		52.51		
11		60.47		
12	65.38	60.96	4.42	6.8
RSS OF DIFFERENCE			7.29 Hz	



COMPARISON OF TEST FREQUENCIES TO THE ORIGINAL AND THE IMPROVED MODELS

MODE NO.	TEST FREQUENCY, HZ	ORIGINAL MODEL FREQUENCY, HZ.	MODEL A FREQUENCY, HZ	MODEL B FREQUENCY, HZ
1	12.95	12.37 (0.58)*	13.50 (-0.55)	13.42 (-0.47)
2	17.66	15.85 (1.81)	17.59 (0.07)	17.28 (0.38)
3	20.80	19.37 (1.43)	20.67 (0.13)	20.98 (-0.18)
4	22.97	26.40 (-3.52)	22.94 (0.03)	22.97 (0.00)
5	28.33	27.90 (0.43)	28.35 (-0.02)	28.34 (-0.01)
6	32.76	34.19 (-1.43)	32.74 (0.02)	32.76 (0.00)
	RSS OF DIFFERENCE	4.50	0.57	0.63

* THE VALUES IN PARENTHESES REFER TO THE DIFFERENCE: TEST FREQUENCY LESS MODEL FREQUENCY.



SUMMARY OF RESULTS

<u>CHARACTERISTIC</u>	<u>CORRELATION</u>
FREQUENCY	MUCH BETTER
MODE SHAPE	WORSE
KINETIC ENERGY	INCONCLUSIVE
CROSS ORTHOGONALITY	INCONCLUSIVE
EFFECTIVE WEIGHT	INCONCLUSIVE
MODAL FORCE COEFFICIENTS	WORSE



C O N C L U S I O N S

- . CONVERGENCE NOT UNIQUE
- . QUALITY OF IMPROVEMENT QUESTIONABLE
- . CORRELATIONS TO STIFFNESS QUESTIONABLE ON THE BASIS OF PHYSICAL REASONING
- . USE OF MODE SHAPE INFORMATION DESIRABLE

→ jpl

PARAMETER ESTIMATION

$$f(r_1, r_2, \dots, r_n) = f(\bar{r}_1, \bar{r}_2, \dots, \bar{r}_n) + \sum_{r_i = \bar{r}_i} \left(\frac{\partial f}{\partial r_i} \right) (r_i - \bar{r}_i) \quad (1)$$

$f(r_1, r_2, \dots, r_n)$ = TEST-MEASURED VALUE

$f(\bar{r}_1, \bar{r}_2, \dots, \bar{r}_n)$ = ANALYTICALLY OBTAINED VALUE

r_1, r_2, \dots, r_n = PARAMETERS (MASS AND/OR STIFFNESS) TO BE ESTIMATED

$\bar{r}_1, \bar{r}_2, \dots, \bar{r}_n$ = PARAMETER VALUES USED IN THE ANALYSIS

MATRIX FORMULATION

$$\{\Delta f\} = \left[\frac{\partial f}{\partial r} \right]_{r=\bar{r}} \{\Delta r\} \quad (2)$$

$$\{\Delta r\} = [S_{rr}] \left[\frac{\partial f}{\partial r} \right]^T \left([S_{rr}] \left[\frac{\partial f}{\partial r} \right] + [S_{\epsilon\epsilon}] \right)^{-1} \{\Delta f\} \quad (3)$$



JACOBIAN

$$\left[\frac{\partial f}{\partial r} \right] = \begin{bmatrix} \left[\frac{\partial \lambda}{\partial M} \right] & \left[\frac{\partial \lambda}{\partial K} \right] \\ \left[\frac{\partial \phi}{\partial M} \right] & \left[\frac{\partial \phi}{\partial K} \right] \end{bmatrix} \begin{bmatrix} \left[\frac{\partial M}{\partial r} \right] \\ \left[\frac{\partial K}{\partial r} \right] \end{bmatrix}$$

$$\frac{\partial \lambda}{\partial M}, \frac{\partial \lambda}{\partial K}, \frac{\partial \phi}{\partial M}, \frac{\partial \phi}{\partial K}$$

CAN BE EVALUATED BY APPROXIMATE METHODS

$$\frac{\partial M}{\partial r}, \frac{\partial K}{\partial r}$$

NEED ANALYTICAL FUNCTIONS

DIFFICULT IF NOT IMPOSSIBLE FOR COMPLEX STRUCTURE.

$\int p dt \rightarrow$

MATRIX PERTURBATION TECHNIQUE

IF MASS AND STIFFNESS MATRICES ARE AS FOLLOWS:

$$[M] = [M_0] + \Delta[M], \quad [K] = [K_0] + \Delta[K] \quad (1)$$

THEN

$$\left. \begin{aligned} \text{EIGENVECTORS: } [\Phi] &= [\phi_0] + \Delta[\phi_1] + \delta^2[\phi_2] + \dots \\ \text{EIGENVALUES: } [\lambda] &= [\lambda_0] + \Delta[\lambda_1] + \delta^2[\lambda_2] + \dots \end{aligned} \right\} \quad (2)$$

FROM PERTURBATION THEORY

$$\left. \begin{aligned} [\alpha] + [\alpha]^\top &= -[\phi_0]^\top [\Delta M] [\phi_0] \\ \Delta[\lambda_1] &= [\lambda_0] [\alpha] + [\alpha]^\top [\lambda_0] + [\phi_0]^\top [\Delta K] [\phi_0] \\ \Delta[\phi_1] &= [\phi_0] [\alpha] \end{aligned} \right\} \quad (3)$$

JACOBIAN

$$A. \quad \Delta \lambda_i \rightarrow [\Delta M] \text{ AND/OR } [\Delta K]$$

$$B. \quad \frac{\partial \lambda}{\partial \lambda_i} = \lim_{\Delta \lambda_i \rightarrow 0} \left(\frac{\Delta \lambda}{\Delta \lambda_i} \right), \quad \frac{\partial \phi}{\partial \lambda_i} = \lim_{\Delta \lambda_i \rightarrow 0} \left(\frac{\Delta \phi}{\Delta \lambda_i} \right) \quad (4)$$

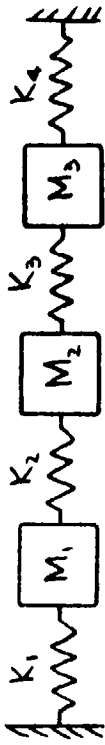


EVALUATION OF JACOBIAN

$$\left[\frac{\partial f}{\partial r} \right] = \begin{bmatrix} \frac{\partial \lambda}{\partial r} \\ \frac{\partial \phi}{\partial r} \end{bmatrix}$$

OBTAINED BY VARYING THE r 's BY SMALL AMOUNT AND CALCULATING THE VARIATION IN λ AND ϕ BY MATRIX PERTURBATION TECHNIQUE.

—jpl—→



PARAMETERS: $\gamma_1 = K_4$, $\gamma_2 = M_1$

$M_2 = M_3 = 4.0$, $K_1 = K_2 = K_3 = 3.0$

TARGET VALUES: $K_4 = 1.0$, $M_1 = 6.0$

EIGENVALUES: .25, 1.00, 2.25

EIGENVECTORS: $\begin{Bmatrix} 2.0 \\ 3.0 \\ 3.0 \end{Bmatrix}$, $\begin{Bmatrix} 1.0 \\ 0 \\ -1.0 \end{Bmatrix}$, $\begin{Bmatrix} 2.0 \\ -5.0 \\ 3.0 \end{Bmatrix}$

USED AS TEST DATA

ORIGINAL ANALYSIS: $K_4 = 0$, $M_1 = 6.0$

EIGENVALUES: .1406, .9091, 2.2003

EIGENVECTORS: $\begin{Bmatrix} 1.6384 \\ 2.8178 \\ 3.4689 \end{Bmatrix}$, $\begin{Bmatrix} 1.0499 \\ .1907 \\ -.9002 \end{Bmatrix}$, $\begin{Bmatrix} 2.1318 \\ -5.1166 \\ 2.6464 \end{Bmatrix}$

FIGURE 1. 3 DEGREES-OF-FREEDOM SAMPLE PROBLEM

Jpl →

TABLE 1

IDENTIFICATION OF 3 DOF SYSTEM

IDENTIFIED VALUES

CASE	DESCRIPTION OF MEASURED DATA	M_1	K_4	<u>IDENTIFIED VALUES</u>		
				1	2	3
	TARGET VALUES	6.0	1.0	.2500	1.0000	2.2500
	ORIGINAL ANALYTICAL VALUES	6.0	0.	.1406	.9091	2.2003
1	FIRST MODE $\lambda_1, \phi_{11}, \phi_{21}, \phi_{31}$	5.9916	1.0237	.2690 (.2523)	.9930 (1.0032)	2.2453 (2.2518)
2	THIRD MODE $\lambda_3, \phi_{13}, \phi_{33}$	5.9670	1.05535	.2778 (2590)	1.0011 (1.0127)	2.2502 (2.2572)
3	3-FREQUENCIES $\lambda_1, \lambda_2, \lambda_3$	5.7698	0.8781	.2516 (.2405)	1.0033 (1.0120)	2.2531 (2.2565)
4	FIRST MODE λ_1, ϕ_{31}	6.9852	.9023	.2499 (.2312)	.8835 (.9036)	2.1783 (2.1997)
5	SECOND MODE λ_2 ONLY	5.4523	.4430	.1983 (.1965)	.9999 (1.0060)	2.2539 (2.2586)



COMPARISONS OF FREQUENCY AND MODE SHAPE FOR HASSELMAN'S METHOD

		<u>ORIGINAL ANALYSIS</u>	<u>IESI</u>	<u>UPDATED</u>
2ND	FREQUENCY (Hz)	15.855	17.660	16.501
	OXIDIZER			
	X	.423	.418	.488
	Y	-.026	-.032	-.020
M	TANK			
	Z	.390	.544	.379
O				
	FUEL			
	X	.385	.407	.436
D	TANK			
	Y	-.013	-.010	-.008
	Z	-.136	-.090	-.180
E				
4TH	FREQUENCY (Hz)	26.487	22.970	27.229
	OXIDIZER			
	X	-.036	-.014	-.036
	Y	-.336	-.435	-.449
M	TANK			
	Z	.033	-.027	.036
O				
	FUEL			
	X	-.101	.017	-.125
D	TANK			
	Y	.661	1.000	.936
	Z	-.175	-.036	-.202
E				



S U M M A R Y

WHITE'S METHOD

**EASY TO MECHANIZE
CONVERGENCE NOT GUARANTEED
NEEDS ENGINEERING JUDGEMENT
NO MODEL IMPROVEMENT**

HASSELMAN'S METHOD

**JACOBIAN DIFFICULT TO EVALUATE FOR COMPLEX
3 DIMENSIONAL STRUCTURE**

MATRIX PERTURBATION - CHEN

**JACOBIAN EVALUATED BY MATRIX PERTURBATION
BEING APPLIED TO VIKING PROPULSION SYSTEM**

Application of Perturbation Methods to Improve Analytical Model Correlation with Test Data

J. A. Garba and B. K. Wada

Structures and Materials Section,
Jet Propulsion Lab.

APPRECIABLE EFFORT is being expended on the research and development of computer programs for the analytical simulation of structures. A parallel effort consists of the improvement of test methods to measure the dynamic characteristics of complex structures. Both of these have provided the engineer with valuable tools. The need has existed in the past and will exist in the future for capabilities to systematically update a mathematical model to more accurately represent the test data. Currently, most organizations use a "trial and error" approach to improve mathematical models. The demand in the future to correlate mathematical models with test data will be greater as the models become more complex. More reliance will be placed on test correlated analytical models to verify modifications, and some future requirements are for large structural systems which cannot be fully ground tested. For such systems confidence must be established by analyses with test verification of analytical models of subsystems or components.

The paper is limited to analysis/test correlation rather than "system identification," which aims to create a mathematical model that will reproduce the

test results. Analysis/test correlation is considered important because:

(1) The model is usually used to obtain structural design loads. Thus, it contains information vital to the structure, such as modal force coefficients.

(2) The model can be made physically meaningful to simulate the test conditions. Thus modifications to the model to simulate flight conditions are possible. The modifications may be a result of anticipated design changes or to eliminate some undesirable ground test condition, such as a gravitational force.

(3) The use of analysis/test correlated subsystems in obtaining system models using modal synthesis techniques result in better simulations.

The overall plan for the development of a method for the systematic correlation of analytical/test models is to evaluate the applicability of the published methodologies to "real structures", to apply new approaches as they are evolved during the effort, to select the most promising approach based upon the experiences, and then generate a computer program which is compatible to user oriented programs such as NASTRAN. The above

ABSTRACT

There are current and future requirements to develop a systematic method to update a mathematical model of a structure to more closely match the test data. The effort is cost effective since the number of reanalyses of a large structure will be reduced. Additionally, the mathematical model will more closely represent its test data.

This activity describes the positive and negative experiences in using a method published by C. W. White and an extension of the method. The results are based upon our understanding of the method as published.

steps are considered necessary to use technology developed to date, apply the methodology to a realistic problem (often the methodology has been shown to be successful only on simple problems or a mathematically constructed set of "test data"), and to obtain user experience prior to commitment of funds to develop a computer program. Many problems with various proposed methods are only fully realized after an attempt at its utilization.

This paper is an application of an approach published by C. White to the Viking Propulsion Subsystem (VPS) for which analytical models and modal test data are available. The VPS allows variation of the mass and stiffness, and is sufficiently complex. In addition, another method that evolved during the work will be presented. The attempt is to describe the experiences that were both successful and unsuccessful. The authors have applied C. White's method to the selected problem to the best of our ability. The theoretical development of C. White is repeated only to document our interpretation of his effort. In addition to using the actual VPS test data for correlation, a set of mathematically generated test data was also employed to evaluate the methodology. The resulting perturbed analytical model is representative of actual flight hardware and hence more realistic than the simple models usually used in such studies. Other methods such as those proposed by members of Wiggins and Kaman Corp. are in the review process and will be applied to the VPS to understand their merits.

The "best" methodology may not exist, but may be dependent on the accuracy desired, or the dynamic characteristics of significance for the model usage. The paper assumes that a correlation of most dynamic related characteristics is important. These characteristics include eigenvalues, eigenvectors, kinetic energy distribution, strain energy distribution, cross-orthogonality, effective weight, and modal force coefficients.

LINEAR PERTURBATION METHOD

The perturbation method follows the development by C. W. White, Refs. (1), * (2), and (3). Only the pertinent equations of the derivation are presented here.

Starting with the homogeneous equations of motion for the structure with negligible damping as

$$[M_0] \{\ddot{h}\} + [K_0] \{h\} = \{0\} \quad (1)$$

where

$\{h\}$ = global system absolute discrete displacement vector

$[M_0]$ = the initial model mass matrix

$[K_0]$ = the initial model stiffness matrix

*Numbers in parentheses designate References at end of paper.

a transformation from discrete to normal mode coordinates can be introduced as

$$\{h\} = [\phi_0] \{\xi\} \quad (2)$$

where

$\{\xi\}$ = normal mode or generalized coordinate vector

$[\phi_0]$ = eigenvector matrix obtained as the solution of the following equation

$$[M_0] [\phi_0] [\omega_0^2] = [K_0] [\phi_0] \quad (3)$$

where

$[\omega_0^2]$ = diagonal matrix of the system circular frequencies squared

Substituting Eq. (3) into Eq. (1) and premultiplying by $[\phi_0]^T$ leads to

$$[I] \{\ddot{\xi}\} + [\omega_0^2] \{\xi\} = \{0\} \quad (4)$$

by virtue of the normalization of $[\phi_0]$.

A linear perturbation in the nominal stiffness and mass matrices can now be introduced,

$$[K] = [K_0] + \sum_{p=1}^P \delta_p [k]_p = [K_0] + [\Delta K_0] \quad (5)$$

$$[M] = [M_0] + \sum_{q=1}^Q \delta_q [m]_q = [M_0] + [\Delta M_0] \quad (6)$$

where $[K]$ and $[M]$ are the perturbed system stiffness and mass matrices, respectively. The factors δ_p and δ_q denote the linear variations of the affected element stiffness and mass matrices. A total of P stiffness elements and Q mass elements are assumed to have been perturbed.

Using Eqs. (5) and (6), a perturbed eigenvalue problem similar to Eq. (2) can be formulated as

$$\left([I] + [\phi_0]^T [\Delta M_0] [\phi_0] \right) [\psi] [\Omega^2] = \left([\omega_0^2] + [\phi_0]^T [\Delta K_0] [\phi_0] \right) [\psi] \quad (7)$$

where

$[\psi]$ = eigenvector matrix of the perturbed problem

$[\Omega^2]$ = diagonal matrix of the perturbed system circular frequencies squared

The transformation from discrete to normal mode coordinates implied by Eq. (7) is

$$\{h\} = [\phi_0] [\psi] \{\gamma\} \quad (8)$$

where

$\{\gamma\}$ = the normal modes coordinate vector of the perturbed system

Equation (7) can be rewritten as

$$[I] [\psi] [\Omega^2] - [\omega_0^2] [\psi] = \sum_{p=1}^P \delta_p [\phi_0] [k]_p [\phi_0] [\psi] - \sum_{q=1}^Q \delta_q [\phi_0]^T [m]_q [\phi_0] [\psi] [\Omega^2] \quad (9)$$

In terms of model correlation, the terms in Eq. (9) can be interpreted as follows:

$[\omega_0^2]$ is related to the frequencies of the analytical model to be correlated

$[\Omega^2]$ is related to the measured frequencies

$[\phi_0]$ is the set of eigenvectors of the analytical model

$[\psi]$ is the set of eigenvectors relating the analytical to the experimental modes

The matrix $[\psi]$ has the property

$$[\psi] = [I] \quad (10)$$

for an unperturbed problem, meaning that there exists perfect correlation between test and analysis. For good, but not perfect correlation, the matrix $[\psi]$ is strongly diagonal, meaning that the size of the diagonal terms are much larger than the off-diagonal terms.

In terms of measured modes, the matrix $[\psi]$ can be obtained from

$$[\psi] = [\phi_0]^{-1} [h_{exp}] \quad (11)$$

where

$[h_{exp}]$ = a set of experimentally measured modes

Examining Eq. (9), the authors in Ref. (1) note that the right-hand side represents the potential and kinetic energy of the perturbed stiffness and mass elements. Eq. (9) can be rewritten as

$$[\psi]^T [I] [\psi] [\Omega^2] - [\psi]^T [\omega_0^2] [\psi] = [R] \quad (12)$$

where every term in matrix $[R]$ contains the $P + Q$ unknown δ 's.

In theory Eq. (12) leads to a set of equations that can be solved for the unknown factors δ . In practice there are several difficulties, namely:

(1) The solution of Eq. (11) for $[\psi]$ requires the inversion of a typically very large nonsymmetric matrix $[\phi_0]$.

(2) The measured modes, $[h_{exp}]$ usually contain fewer measurements than the original vector $\{h\}$ of the analysis requires. This leads to an incompatibility in the solution for $[\psi]$ in Eq. (11).

(3) Eq. (12) can be expanded into $1/2 (n^2 + n)$ equations in $P + Q$ unknowns, where n is the number of normal modes being considered. If the number of unknowns equals the number of equations, the solution can be obtained by matrix inversion. Otherwise, a least squares fit or a linear programming solution must be used depending on if the system is underdetermined or overdetermined.

Although Eq. (12) can lead to an exact solution, practical considerations require the search for a simplified approach, possibly leading to an iterative solution to the problem of determining the required factors δ . The authors, in Ref. (1), develop such a simplification as follows

If in Eq. (9) only the i -th column is considered, the equation simplifies to

$$\left(\Omega_i^2 [I] - [\omega_0^2] \right) \{\psi_i\} = [E]_i \{\delta\} \quad (13)$$

where columns of $[E]_i$ are

$$-\Omega_i^2 [\phi_0]^T [m]_q [\phi_0] \{\psi_i\}$$

or

$$[\phi_0]^T [k]_p [\phi_0] \{\psi_i\}$$

The solution of Eq. (13) is somewhat simplified from Eq. (12) but it is still restricted by the solution to Eq. (11). Further simplifications can be made by assuming that the perturbed modes are close to the original modes, then, from Eq. (10),

$$[\psi] \approx [I] \quad (14)$$

If, furthermore, in the formulation of the solution only the diagonal terms are considered, the set of equations simplify to

$$\{\Omega^2 - \omega_0^2\} = [E_0] \{\delta\} \quad (15)$$

which leads to

$$\{\delta\} = [E_0]^{-1} \{\Omega^2 - \omega_0^2\} \quad (16)$$

for the case where the number of the unknowns equals the modes under consideration, or

$$\{\delta\} = \left[\begin{matrix} [E_0]^T & [E_0] \end{matrix} \right]^{-1} [E_0]^T \{\Omega^2 - \omega_0^2\} \quad (17)$$

for a least squares fit solution where the number of equations exceed the unknown δ 's.

Equations (15) and (16) form the basis of the model correlation used herein. It should be noted that the simplifications used in the above derivation have eliminated the use of eigenvectors and rely solely on frequency correlation. While frequencies can be measured accurately, the method proposed by Eqs. (15) and (16) is essentially nothing more than an energy balance. The drawbacks of this will be discussed later in the application of this method. Since energy is a scalar and the eigenvectors are vectors, it is obvious that by using only frequency, rather than frequency and mode shape, the modal test data is not used to its full potential.

Before proceeding to apply the above method, let us consider an alternate formulation of the perturbation method as formulated by J. C. Chen, Refs. (4) and (5). Consider a system of equations for the structural system analogous to Eq. (1):

$$[M] \{\ddot{x}\} + [K] \{x\} = \{0\} \quad (18)$$

and introduce the linear perturbations:

$$\begin{aligned} [M] &= [M_0] + \epsilon [M_1] \\ [K] &= [K_0] + \epsilon [K_1] \\ [\phi] &= [\phi_0] + \epsilon [\phi_1] \end{aligned} \quad (19)$$

and

$$\begin{aligned} [\phi_0]^T [K_0] [\phi] &= \left[\omega_0^2 \right] \\ \{x\} &= [\phi] \{q\} \end{aligned} \quad (20)$$

where $\{q\}$ is the normal mode generalized coordinate. In the context of correlation, $[M_0]$, $[K_0]$ and $[\phi_0]$ refer to the analytical model, whereas $[M]$, $[K]$, and $[\phi]$ refer to the test values. Hence it is desirable to find ϵM_1 , and ϵK_1 , by perturbing a set of masses and stiffnesses and matching frequencies and mode shape. Substituting Eqs. (19) and (20) into Eq. (18), we obtain two sets of equations.

$$[\phi_0]^T [M] [\phi] \{\ddot{q}\} + [\phi_0]^T [K] [\phi] \{q\} = \{0\}$$

and

$$\begin{aligned} &[\phi_0 + \epsilon \phi_1]^T [M_0 + \epsilon M_1] [\phi_0 + \epsilon \phi_1] \{\ddot{q}\} \\ &+ [\phi_0 + \epsilon \phi_1]^T [K_0 + \epsilon K_1] [\phi_0 + \epsilon \phi_1] \{q\} = \{0\} \end{aligned} \quad (21)$$

Expanding Eq. (21) and neglecting the second-order terms and noting that

$$\begin{aligned} [\phi_0]^T [M] [\phi_0] &= [I] \\ [\phi_0]^T [M_0] [\phi_0] &= [I] \\ [\phi_0]^T [K] [\phi_0] &= \left[\Omega^2 \right] \end{aligned} \quad (22)$$

where as before the Ω and ω_0 related to the test and analytical frequencies, respectively, leads to

$$[I] \{\ddot{q}\} + \left[\Omega^2 \right] \{q\} = \{0\}$$

and

$$\begin{aligned} &\left([I] + [\phi_0]^T [M_0] [\epsilon \phi_1] \right. \\ &+ [\phi_0]^T [\epsilon M_1] [\phi_0] \\ &+ [\epsilon \phi_1]^T [M_0] [\phi_0] \left. \right) \{\ddot{q}\} + \left(\left[\omega_0^2 \right] \right. \\ &+ [\phi_0]^T [K_0] [\epsilon \phi_1] + [\phi_0]^T [\epsilon K_1] [\phi_0] \\ &+ [\epsilon \phi_1]^T [K_0] [\phi_0] \left. \right) \{q\} = \{0\} \end{aligned} \quad (23)$$

for the two equations to be equivalent, the coefficients are equated:

$$\left. \begin{aligned} [\phi_0]^T [\epsilon M_1] [\phi_0] &= - \left([\phi_0]^T [M_0] [\epsilon \phi_1] \right. \\ &\quad \left. + [\epsilon \phi_1]^T [M_0] [\phi_0] \right) \\ [\phi_0]^T [\epsilon K_1] [\phi_0] &= \left[\Omega^2 \right] - \left[\omega_0^2 \right] \\ &\quad - \left([\phi_0]^T [K_0] [\epsilon \phi_1] \right. \\ &\quad \left. + [\epsilon \phi_1]^T [K_0] [\phi_0] \right) \end{aligned} \right\} (24)$$

Since the eigenvectors are linearly independent of each other, any vector can be expressed as a linear combination of the complete set, thus

$$[\phi_1] = [\phi_0] [\alpha] \quad (25)$$

where the matrix $[\alpha]$ contains the linear factors. Using Eq. (25), we can establish the following relationships:

$$\left. \begin{aligned} [\phi_0]^T [M_0] [\epsilon \phi_1] &= [\epsilon \alpha] \\ [\phi_0]^T [K_0] [\epsilon \phi_1] &= \left[\omega_0^2 \right] [\epsilon \alpha] \end{aligned} \right\} (26)$$

Substituting Eqs. (26) and (24) and noting that in the notations used earlier

$$\left. \begin{aligned} [\phi_0]^T [\epsilon K_1] [\phi_0] &= \sum_{p=1}^P \delta_p [\phi_0]^T [k]_p [\phi_0] \\ &= [E_p] \{ \delta_p \} \\ [\phi_0]^T [\epsilon M_1] [\phi_0] &= \sum_{q=1}^Q \delta_q [\phi_0]^T [m]_q [\phi_0] \\ &= [E_q] \{ \delta_q \} \end{aligned} \right\} (27)$$

and

$$\left. \begin{aligned} [E_q] \{ \delta_q \} &= - \left([\epsilon \alpha] + [\epsilon \alpha]^T \right) \\ [E_p] \{ \delta_p \} &= \left[\Omega^2 \right] - \left[\omega_0^2 \right] \\ &\quad - \left(\left[\omega_0^2 \right] [\epsilon \alpha] \right. \\ &\quad \left. + [\epsilon \alpha]^T \left[\omega_0^2 \right] \right) \end{aligned} \right\} (28)$$

Eq. (28) can now be solved for either $\{ \delta_q \}$ or $\{ \delta_p \}$ by evaluating Eq. (26) with

$$[\epsilon \phi_1] = [\phi] - [\phi_0] \quad (29)$$

Since in the set of Eqs. (28) the effect of perturbations in mass and stiffness matrices are uncoupled, one has a choice of varying one or the other at a time in an iteration cycle, or one can separate the modes effected by mass and stiffness and use both of the equations in the same iteration cycle.

Each of the two Eqs. (28) lead to $1/2 (n^2 + n)$ equations in either P or Q unknowns, similar to the solution of Eq. (12).

On the surface it appears that the alternate formulation of Eqs. (28) has the advantage over Eq. (12) by making use of the measured mode shape information $[\epsilon \phi_1]$. The practical problems of applying Eq. (28) in model correlation will be discussed later.

CORRELATION MODEL

The Viking Propulsion Subsystem, which was an important structural subsystem of the Viking Orbiter,* was selected for correlating an analytical model with test results. It accounts for 70% of the Viking Orbiter weight, and the flight configuration contains large quantities of fluids with ullage.

The Viking Orbiter was designed by loads analysis. This process relies on a representative mathematical model to obtain flight loads to achieve a reliable design. A good correlation between the test results and analytical predictions is of paramount importance. Data obtained during the powered phase of the two Viking flights have shown very good correlation between predicted loads and flight measurements, Ref. (6).

Other considerations that make this subsystem appropriate for the application of the perturbation technique are:

(1) The structure was thoroughly tested and analyzed; the results are documented in Refs. (7)

*The Viking Orbiter is part of the Viking Spacecraft, which was flown successfully in 1975.

and (8). The eigenvalues, eigenvectors, and modal damping were experimentally determined by a modal test.

(2) An acceptable correlation between test and analysis was obtained previously. This correlation was achieved in a project environment with severe schedule constraints; it was obtained by inspection rather than a systematic fashion. The remaining differences appear small enough that perturbation theory is applicable for further correlation attempts.

(3) The structure is of moderate complexity. It contains thin-wall pressure vessels supported by beams. The local tank tab areas were modeled using the Guyan stiffness matrix reduction to generate superelements (Ref. (9)). It represents a sufficiently complex three-dimensional structure; a good test case for the various proposed methods for correlation. Usually the examples consist of either continuous beams representing launch vehicles, or three-dimensional structures using axial members only.

(4) The design of the major load carrying members was effected mainly by the lowest six normal modes. Some higher modes were of importance only in the design of local structure. The correlation thus could concentrate mainly on the lowest six modes.

(5) The variations of large masses were important unknown parameters. The effective masses of the fluids were important considerations. Extensive testing (Ref. (10)) was performed for their determination.

Several configurations of the propulsion subsystem were used in the modal test, these were (1) the flight configuration containing appreciable ullage volume in both the fuel and oxidizer tank, (2) both tanks completely filled with reference fluid with no ullage, and (3) both tanks empty. These configurations were chosen to verify the model independently of the effect of the fluid on the normal modes. The model discussed herein represents the second case, both tanks full.

The analytical model contains 677 static (stiffness) degrees of freedom and 84 dynamic (mass) degrees of freedom. There are a total of 5 types of tank tab superelement stiffness models, 117 plate elements and 184 beam elements.

Figure 1 shows the schematic of the analytical model including the coordinate system. Figure 2 is a photograph of the test hardware used in the modal test.

The frequency correlation between the test values and the best post test model, hereafter called the original model, is listed in Table 1. Note that there exists a one-to-one correspondence in all the modes except modes 10 and 11. The analysis shows that these are local thrust plate and engine modes that were not excited during the modal test. Since they are of no consequence in the design of primary structural members, these two modes will be dropped from any further discussion. The root sum squared (RSS) value of the frequency difference in Table 1 is 7.29 Hz.

ORIGINAL PAGE IS
OF POOR QUALITY

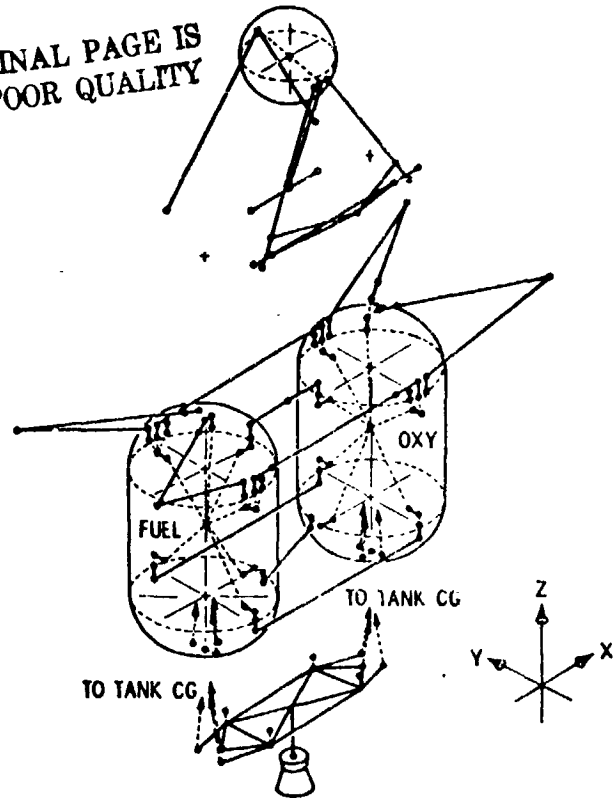


Fig. 1 - Schematic of the Viking propulsion subsystem finite element model

PERTURBED ANALYTICAL MODEL

Before the perturbation method was applied to the analytical model to obtain an improved test/analysis correlation with test data, the existing analytical model was perturbed. This perturbed model was then treated as the analytical model, and the existing analytical model was considered as the test data. The method developed earlier was applied to the assumed analytical model to try to reconstruct the original answers.

The purpose of this was two-fold:

(1) Check the methodology using the same analytical model which is to be used for the test/analysis correlation.

(2) Establish member/mode grouping for model convergence.

The perturbed model was generated by varying a set of member stiffnesses and retaining the masses unchanged. The members were selected based on the strain energy contribution to the lowest 12 normal modes. In the process of choosing the members to be perturbed, the strain energy contribution for the beam elements was separated by stiffness component. Thus the axial contribution was separated from bending and torsion. For the tank tabs modeled by superelements, a single perturbation constant was assigned for each of the groups varied.

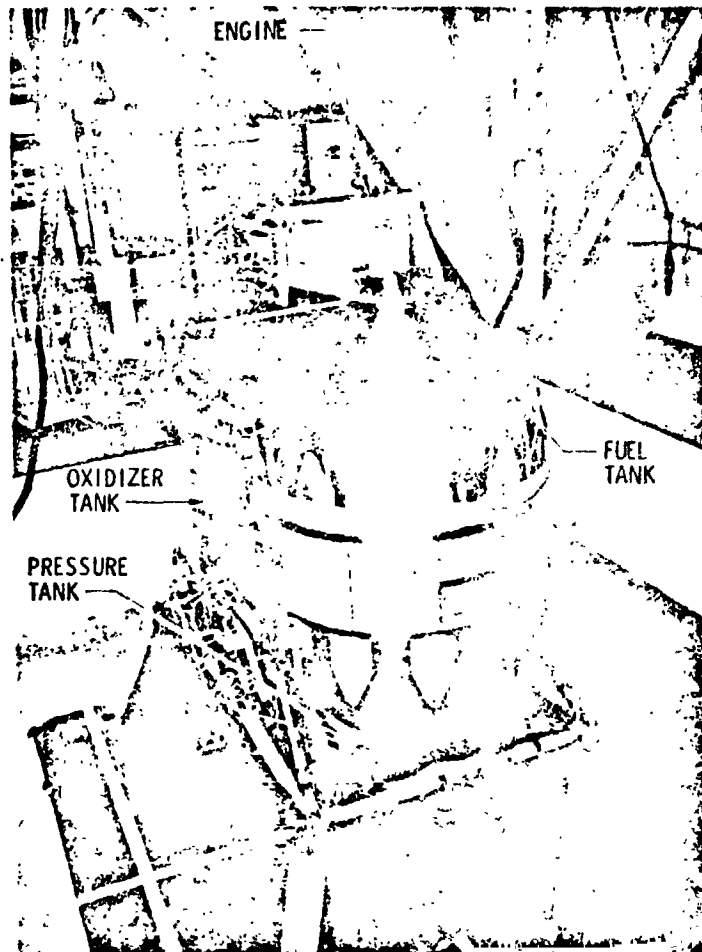


Fig. 2 - Propulsion subsystem modal test setup

A total of seven groups of members were selected to be perturbed. The member groups and the amount of original perturbation is listed in Table 2. This perturbation is similar to that used by C. W. White in Ref. (1), except that the perturbation in the referenced article was applied to axial members only on a relatively simple dynamic model. The method outlined in Refs. (1) to (3) was now used to systematically improve the model by applying Eqs. (16) and (17).

After carefully matching the strain energy and the affected normal modes, the model was indeed forced to converge in four iterations. The frequency convergence is shown in Table 3. The corresponding factors for the perturbed members are listed in Table 4. The factors are defined as the cumulative multipliers to be applied to the properties of the unperturbed original model. Thus a factor of 1.000 means that the group has the same properties as the original model.

Several important observations made in this exercise of applying the method to a perturbed analytical model are:

(1) Convergence is not guaranteed. As a matter of fact, the method diverged twice to factors that had no physical significance. Convergence was

Table 1 - Frequency Comparison of Test Results and Original Model

Mode No.	Frequency, Hz	Original Model Frequency, Hz	Difference, Hz	Difference, %	Mode Description
1	12.95	12.37	0.58	4.5	Oxidizer and fuel in Y, in phase
2	17.66	15.85	1.81	10.2	Oxidizer tank in Z
3	20.80	19.37	1.43	6.9	Oxidizer and fuel in Z
4	22.97	26.49	-3.52	-15.3	Oxidizer and fuel in Y out-of-phase
5	28.33	27.90	0.43	1.5	Fuel tank in Z
6	32.76	34.19	-1.43	4.4	Pressurant tank in θ_y
7	42.80	42.06	0.74	1.7	Local pressurant control assembly in X
8	50.67	47.69	2.98	5.9	Pressurant tank in Y
9	50.40	52.39	-1.99	3.9	Local pressurant control assembly in Z
10		52.81			Local thrust plate and nozzle
11		60.47			Local thrust plate and nozzle
12	65.38	60.90	4.48	6.8	Local pressurant control assembly in θ_y
RMS of difference			7.89 Hz		

Table 3 - Perturbed Analytical Model Member Grouping

Group	Description	Perturbation
A	Side bipods, 4 members supporting the tanks in a vertical plane	+40%
B	Top bipods, 4 members supporting the tanks in a horizontal plane	-30%
C	3-hole tank tabs, 4 superelements that form the link between the side bipods and the rigid tank	+30%
D	Top Siamese tank tabs, 2 superelements connecting the two tanks at the top	-30%
E	Bottom Siamese tank tabs, 2 superelements connecting the two planes at the bottom	+40%
F	Pressurant tank round members, 3 members supporting the pressurant tank	+30%
G	Pressurant control assembly (PCA) support struts, 4 members supporting the PCA	+40%

Table 3 - Frequency Convergence of Perturbed Analytical Model

Mode No.	Original Model Frequency, * Hz	Perturbed Model Frequency, Hz	Iteration				
			1st, Hz	2nd, Hz	3rd, Hz	4th, Hz	5th, Hz
1	12.37	13.49	11.87	12.34	12.36	12.37	12.37
2	15.85	16.34	15.07	15.83	15.85	15.86	15.85
3	19.37	20.29	18.51	19.34	19.37	19.38	19.37
4	26.49	26.25	26.49	27.15	26.24	26.48	26.49
5	27.90	28.30	27.50	28.13	27.95	27.91	27.90
6	34.19	34.29	34.08	34.56	34.17	34.20	34.19
7	42.06	42.64	41.66	42.09	42.09	42.08	42.06
8	47.69	49.43	45.10	47.49	47.62	47.93	47.69
9	52.39	52.61	51.96	52.49	52.48	52.41	52.39
10	52.51	54.21	52.41	52.65	52.65	52.50	52.51
11	60.47	61.94	59.65	60.34	60.30	60.52	60.47
12	60.96	64.23	59.48	61.21	61.26	61.05	60.96

*Considered as the test data to which the perturbed model is to converge.

Table 4 - Member Factor Convergence of Perturbed Analytical Model

Member Group	Original Perturbation	Iteration				
		1st	2nd	3rd	4th	5th
A	1.4	0.865	0.994	1.015	1.002	0.997
B	0.7	0.896	1.018	1.020	1.000	0.998
C	1.3	0.972	0.972	0.946	0.993	1.005
D	0.8	0.902	1.023	0.997	1.000	1.000
E	1.4	1.774	1.298	0.923	0.996	0.999
F	1.3	0.821	0.968	0.991	1.030	1.002
G	1.4	0.890	1.059	1.026	0.989	0.979

ORIGINAL PAGE IS OF POOR QUALITY

Table 5 - Comparison of Test Frequencies to the Original and the Improved Models

Mode No.	Test Frequency, Hz	Original Model Frequency, Hz	Model A Frequency, Hz	Model B Frequency, Hz
1	12.95	12.37 (0.58)*	13.50 (-0.55)	13.42 (-0.47)
2	17.66	15.85 (1.81)	17.59 (0.07)	17.28 (0.38)
3	20.80	19.37 (1.43)	20.67 (0.13)	20.98 (0.18)
4	22.97	26.49 (-3.52)	22.94 (0.03)	22.97 (0.00)
5	28.33	27.90 (0.43)	28.35 (-0.02)	28.34 (-0.01)
6	32.76	34.19 (-1.43)	32.74 (0.02)	32.76 (0.00)
7	42.80	42.06 (0.74)	42.85 (-0.05)	42.85 (-0.05)
8	50.67	47.69 (2.98)	50.32 (0.08)	50.48 (0.19)
9	50.40	52.39 (-1.99)	52.23 (-1.56)	52.40 (-2.00)
12	61.38	60.96 (4.42)	62.28 (3.10)	62.43 (2.95)
RSS of Difference:				
All 10 modes		7.29	3.52	3.62
First 6 modes		4.50	0.57	0.63

*The values in parentheses refer to the difference: test frequency less model frequency.

attained by not allowing the member factors to vary more than an arbitrary factor in each iteration. Thus, for example, if in the second iteration member group C was allowed to vary by 65%, the system soon diverged to a point where some other member group was removed totally, resulting in an unstable structure. This situation was corrected by regrouping the members and modes, even though the original group seemed perfectly logical. This arises because Eq. (15) is indeed nothing more than an energy balance. Thus unless the member groups are matched properly with the proper modes, physically unrealistic results are obtained. Mathematically a solution of Eq. (15) can be found that adds a multiple of one set of members and removes another set altogether. The energy is balanced, but the result is physically not reasonable. Unfortunately, the matching of modes and member groups is not that clear-cut, and logical matching does not assure physically reasonable results without some prior knowledge.

(2) Simple models such as the one used in Ref. 1 apparently can be made to converge not only uniformly, but also monotonically. Even with a most careful matching of modes and member groups the perturbed model did not converge uniformly.

(3) The alternate formulation of Eq. (18) failed to produce physically reasonable results in the first iteration, even though the matching of modes and member groups was the same as that used in Eq. (17). This method was not further pursued. The speculation is that the perturbations were too large for the alternate formulation leading to unreasonable perturbations in the mode shape $[\epsilon\phi_1]$ that in turn affected the solution of Eq. (28).

ANALYSIS/TEST CORRELATION

The previous section has established the feasibility of the perturbation method and has also revealed some of the shortcomings of the method when applied to a real-life structure. The method will now be used to try to improve the correlation between the test results and the analytical model of the Viking Propulsion Subsystem.

The approach will be that of applying Eqs. (16) and (17), or (28) in an iterative scheme. In proceeding in this manner it is fully realized that the convergence criterion is based on frequency alone and that the method consists of an energy balance. Once a reasonable frequency match is established the mode shape is checked to see if an improvement in the analytical model has been achieved.

The first step in applying the perturbation technique of Ref. 1 is to identify the major modal energy contributors, both potential and kinetic.

Then the major contributing elements are used with the affected modes to solve Eq. (16) or (17).

It was found that the lowest 5 modes all had appreciable strain energy contribution by the side bipods, top bipods, the 3-hole tank tab, and the top and bottom Siamese tank tabs, corresponding to groups A through E in the perturbed analytical model, Table 2. The kinetic energy in the first 5 modes was dominated by the fluid masses.

Numerous combinations of modes and member and mass groupings were used in the solution of Eqs. (16) or (17). The groupings allowed for variations in (1) stiffness only, (2) mass only, and (3) both stiffness and mass. None of the trials produced physically reasonable results. The solutions typically would indicate variations in member stiffnesses of in excess of $\pm 100\%$ and fluid masses of $\pm 30\%$. Use of Eq. (28) did not improve the results. None of these variations were considered physically reasonable. The systematic search for the perturbation factors using Eqs. (16) and (17) was hence abandoned.

Instead of a systematic search, the following procedure was used: one group of stiffness or mass elements was varied at a time trying to match the frequencies of from one up to four normal modes.

The group selected had the maximum energy content in these modes. The factor for the member group under consideration was calculated using a least squares fit approach, which is equivalent to solving Eq. (17) with one unknown. Consequently other member groups were used to improve the correlation.

Using the procedure described above, two improved models were obtained.

Model A: Started with variations in the member stiffnesses. Once this was exhausted, mass variations were used; twelve iterations were required.

Model B: Started with variations in the fluid masses. Once this was exhausted, member stiffness variations were used; seven iterations were required.

For either case the criteria for convergence was the minimization of the root sum square (RSS) or the frequency difference between the test model and the analytical model.

Table 5 shows the frequency comparison of the various models and the test data. Table 6 gives the perturbation factors, defined earlier, that are required to obtain the frequency improvement. It now remains to be seen if the model has indeed been improved. Since frequency by itself is not a measure of model correlation, the mode shape, cross orthogonality, kinetic energy distribution, effective weight (Refs. (11) and (12)), and force coefficients of the first 6 normal modes will be examined. Table 7 compares the modal deflections for the major masses of the test to the analytical deflections of the original analysis, Model A and Model B.

Table 6 - Perturbation Factors

Element	Model A	Model B
I. Stiffness		
Side bipods	1.397	1.227
Top bipods	1.328	1.000
3-hole tabs	1.179	1.089
Top Siamese tabs	0.754	0.865
Pressurant tank support round	1.401	1.685
Pressurant tank support square	0.813	0.813
PCA support struts	0.996	1.000
Shear tie	0.218	0.196
II. Mass		
Oxidizer lateral mass	1.000	0.933
Oxidizer longitudinal mass	1.000	0.900
Fuel lateral mass	1.000	0.933
Fuel longitudinal mass	1.000	0.936
Pressurant Control Assembly Inertia I_x	3.199	3.199
Pressurant Control Assembly Inertia I_y, I_z	1.050	1.050

Table 8 gives the cross-orthogonality matrix between the first six test modes and the corresponding analytical modes for the three analytical models. The cross orthogonality matrix [CO] is defined as

$$[CO] = \phi_T^T L_T L_A^T \phi_A \quad (30)$$

where

ϕ_T are the test modes or eigenvectors

ϕ_A are the analytical modes or eigenvectors

L_T Choleski decomposition of the test mass matrix, M_T

L_A Choleski decomposition of the analytical mass matrix, M_A

thus

$$\left. \begin{aligned} M_A &= L_A L_A^T \\ M_T &= L_T L_T^T \end{aligned} \right\} \quad (31)$$

The local kinetic energy distribution (Ref. (13)) of the major masses for the first six modes is listed in Table 9.

Table 10 lists the effective weight (Refs. (11) and (12)) as a percentage of the total weight for the test and the analytical models.

For purposes of member load calculations, the force coefficients are the most important correlation parameter. The force coefficients for the main load carrying members for the first five normal modes are shown in Table 11.

DISCUSSION OF RESULTS

Examining the results of the analysis/test correlation, the following observations can be made:

(1) The perturbation technique of Ref. (1) did not converge to produce a single unique model. Numerous other combinations of variations in stiffness and mass elements could produce similar frequency correlation to that shown for Models A and B.

Table 7 - Mode Shape Comparison

Mass Point and Direction	Test	Original	Model	Model	Test	Original	Model	Model	
		Analysis	A	B		Analysis	A	B	
		Mode 1				Mode 2			
Engine	X	-0.063	0.014	0.014	0.013	1.000	0.967	0.974	0.966
	Y	1.000	0.948	0.923	0.926	0.075	-0.010	-0.028	-0.028
	Z	0.016	0.052	0.056	0.056	0.221	0.150	0.104	0.118
Oxidizer tank	X	-0.004	0.008	0.008	0.008	0.418	0.423	0.459	0.420
	Y	0.634	0.548	0.531	0.579	-0.032	-0.026	-0.021	-0.023
	Z	0.009	0.037	0.038	0.038	0.544	0.390	0.269	0.337
Fuel tank	X	0.010	0.005	0.003	0.003	0.407	0.385	0.409	0.382
	Y	0.428	0.437	0.386	0.392	-0.010	-0.013	-0.005	-0.002
	Z	0.031	0.028	0.031	0.030	-0.090	-0.136	-0.114	-0.148
Pressurant tank	X	0.007	-0.008	-0.011	-0.011	-0.322	-0.178	-0.006	-0.139
	Y	-0.151	-0.177	-0.193	-0.177	0.029	0.007	0.004	0.008
	Z	0.012	0.036	0.037	0.037	0.243	0.126	0.074	0.093
RSS of difference			0.154	0.179	0.179		0.284	0.482	0.355
		Mode 3				Mode 4			
Engine	X	-1.000	-0.662	-0.290	-0.452	0.035	-0.043	-0.005	-0.007
	Y	-0.080	-0.080	-0.008	-0.014	0.638	0.425	0.448	0.442
	Z	0.809	0.708	0.471	0.363	0.039	-0.012	-0.005	0.007
Oxidizer tank	X	-0.682	-0.472	-0.298	-0.378	-0.014	-0.036	0.025	0.021
	Y	-0.044	-0.051	-0.073	-0.079	-0.435	-0.336	-0.267	-0.279
	Z	0.787	0.733	0.643	0.672	-0.027	0.033	-0.046	-0.043
Fuel tank	X	-0.451	-0.280	-0.161	-0.213	0.017	-0.101	-0.023	-0.023
	Y	-0.036	-0.239	0.060	0.061	1.000	0.661	0.638	0.644
	Z	0.826	0.675	0.294	0.440	-0.036	-0.175	-0.031	-0.050
Pressurant Tank	X	-0.445	-0.410	-0.353	-0.497	0.127	-0.129	0.097	0.088
	Y	0.180	0.048	0.030	0.042	-0.114	-0.109	-0.105	-0.098
	Z	0.830	0.742	0.497	0.390	-0.078	-0.084	-0.057	-0.055
RSS of difference			0.343	1.152	0.880		0.467	0.456	0.446
		Mode 5				Mode 6			
Engine	X	-0.007	0.004	-0.071	-0.118	-0.680	-0.007	-0.013	-0.012
	Y	0	0.059	0.005	0.005	-0.387	-0.055	-0.042	-0.042
	Z	0.314	0.212	0.265	0.242	0.088	-0.007	0.005	0.007
Oxidizer tank	X	0.193	0.139	0.080	0.123	0.041	-0.005	0.003	0
	Y	-0.040	-0.062	-0.025	-0.023	0.205	0.043	0.031	0.032
	Z	-0.108	-0.100	-0.071	-0.079	-0.082	-0.007	-0.009	-0.011
Fuel tank	X	0.228	0.144	0.129	0.153	0.077	0.008	0.005	0.007
	Y	0.073	0.109	0.031	0.029	-0.528	-0.078	-0.059	-0.080
	Z	0.613	0.435	0.545	0.494	0.309	0.015	0.029	0.031
Pressurant Tank	X	1.000	0.792	0.770	0.757	1.000	0.187	0.172	0.168
	Y	0.024	-0.016	0.011	0.008	0.212	0.027	0.016	0.016
	Z	0.268	0.175	0.253	0.218	-0.140	0.007	0.012	0.012
RSS of difference			0.334	0.305	0.331		1.074	1.096	1.098

ORIGINAL PAGE IS OF POOR QUALITY

Table 8 - Cross-Orthogonality Between Test Modes and Analytical Modes

Test Modes	Analytical Modes					
	M1	M2	M3	M4	M5	M6
Original Modes						
01	0.997968700	0.000000000	0.000000000	0.000000000	0.000000000	0.000000000
02	0.000000000	0.999999999	0.000000000	0.000000000	0.000000000	0.000000000
03	0.000000000	0.000000000	0.999999999	0.000000000	0.000000000	0.000000000
04	0.000000000	0.000000000	0.000000000	0.999999999	0.000000000	0.000000000
05	0.000000000	0.000000000	0.000000000	0.000000000	0.999999999	0.000000000
06	0.000000000	0.000000000	0.000000000	0.000000000	0.000000000	0.999999999
Model A Modes						
01	0.997968700	0.000000000	0.000000000	0.000000000	0.000000000	0.000000000
02	0.000000000	0.999999999	0.000000000	0.000000000	0.000000000	0.000000000
03	0.000000000	0.000000000	0.999999999	0.000000000	0.000000000	0.000000000
04	0.000000000	0.000000000	0.000000000	0.999999999	0.000000000	0.000000000
05	0.000000000	0.000000000	0.000000000	0.000000000	0.999999999	0.000000000
06	0.000000000	0.000000000	0.000000000	0.000000000	0.000000000	0.999999999
Model B Modes						
01	0.997968700	0.000000000	0.000000000	0.000000000	0.000000000	0.000000000
02	0.000000000	0.999999999	0.000000000	0.000000000	0.000000000	0.000000000
03	0.000000000	0.000000000	0.999999999	0.000000000	0.000000000	0.000000000
04	0.000000000	0.000000000	0.000000000	0.999999999	0.000000000	0.000000000
05	0.000000000	0.000000000	0.000000000	0.000000000	0.999999999	0.000000000
06	0.000000000	0.000000000	0.000000000	0.000000000	0.000000000	0.999999999

(2) The quality of the improved models is questionable. The only clearcut improvement achieved is in the frequency. It is not clear if it would not have been just as effective to retain the masses and stiffnesses of the original model and to adjust the frequencies (generalized stiffnesses) to match the test. The data show that the mode shape correlation of the original model with test data is generally better than that of the improved models. This is also true of the local kinetic energy, the effective weights, and the force coefficients. It is interesting to note that cross-orthogonality, which is often used as an indication of correlation, is an inconclusive indicator. The cross-orthogonality between the test modes and all three analytic modes is quite good and apparently insensitive to variations in mode shape.

(3) It is difficult to reconcile the perturbation factors listed in Table 6 with systematic model errors. Thus the required increase of the bipod areas by 40% does not seem physically reasonable. These are axial load carrying members that should not contain that high an inconsistency. The shear tie decrease in stiffness by 80% does have a physical explanation. During the modal test it was found that the shear link did act as a nonlinear

Table 9 - Kinetic Energy Distribution,
% of Total Kinetic Energy

Table 10 - Effective Weight Comparison,
% of Total Weight and Inertia

Mass Point and Direction	Test	Original Analysis	Model A	Model B	Test	Original Analysis	Model A	Model B
		<u>Mode 1</u>				<u>Mode 2</u>		
Oxidizer tank	X				23.6	34.0	46.0	37.3
	Y	76.6	66.2	74.6	73.6			
	Z				50.1	35.1	16.7	27.6
Fuel tank	X				13.8	16.7	21.3	18.0
	Y	16.0	24.3	16.5	19.1			
	Z				0.7	2.2	1.0	2.8
		<u>Mode 3</u>				<u>Mode 4</u>		
Oxidizer tank	X	27.0	19.3	14.5	16.3			
	Y					21.6	23.3	19.5
	Z	38.8	49.6	69.5	56.5			
Fuel tank	X	6.2	3.5	2.1	3.0	0	1.2	0
	Y					64.2	50.1	61.4
	Z	22.3	22.0	7.6	13.6	0.1	3.7	0
Pressurant tank	θ_y				2.7	0	4.3	4.3
	θ_z				2.8	0	3.9	3.9
		<u>Mode 5</u>				<u>Mode 6</u>		
Oxidizer tank	X	11.7	11.3	3.4	6.1			
	Y	0.4	2.0	0	0	2.3	3.3	1.8
	Z	3.5	5.7	2.4	3.1			
Fuel tank	X	6.3	6.4	4.4	6.7			
	Y	0.8	3.4	0	0	8.3	5.8	3.5
	Z	58.9	56.6	74.9	66.4			
Pressurant tank	θ_y	3.6	0	1.7	1.9	81.6	85.4	89.1
	θ_z					1.2	2.1	1.9

Direction	Test	Original Analysis	Model A	Model B	Test	Original Analysis	Model A	Model B
		<u>Mode 1</u>				<u>Mode 2</u>		
W_x					31.6	44.7	60.7	46.5
W_y	83.9	84.3	83.0	82.2	1.2	1.0	0	0
W_z	0	0.2	0.5	0.5	27.2	15.5	7.3	10.5
I_x	95.0	96.0	96.5	96.6	0	0.3	0	0
I_y					80.3	92.1	95.1	94.7
I_z	17.4	11.9	16.1	16.2				
		<u>Mode 3</u>				<u>Mode 4</u>		
W_x	31.6	21.7	16.9	20.6	0	1.4	0	0
W_y	1.2	2.4	0	0	4.8	2.4	1.5	6.4
W_z	62.1	74.9	72.6	72.9	1.0	0.3	1.2	0.8
I_x	0	0.3	0	0	1.9	0.6	2.7	2.4
I_y	14.6	6.5	0	3.2				
I_z	0	0	1.4	1.1	71.1	67.1	67.1	68.8
		<u>Mode 5</u>				<u>Mode 6</u>		
W_x	23.7	21.7	10.4	18.6	2.4	0	0	0
W_y					1.2	0	0	0
W_z	9.3	6.8	16.0	13.2				
I_y	0	0	2.4	0				
I_z	0.7	4.9	0	0.6	7.7	8.4	3.8	4.1

Table 11 - Force Coefficients, Newtons

Member No.	Test vs. Analysis	Mode No.				
		1	2	3	4	5
4	Test	-2527.5	343.0	-1183.7	-237.1	-194.4
	Original Analysis	-2548.4	502.2	-1055.6	-491.5	-186.4
	Model A	-2977.8	768.4	-535.5	-321.2	-437.1
	Model B	-2930.3	689.4	-496.8	-307.2	-324.9
3	Test	-297.1	-367.4	379.4	402.6	327.8
	Original Analysis	-328.3	-488.0	323.4	552.0	403.7
	Model A	-303.7	-619.8	77.0	345.2	343.1
	Model B	-332.0	-629.1	187.1	354.5	486.5
41	Test	2120.0	-1123.2	-487.5	836.3	-255.3
	Original Analysis	1900.3	-1086.7	-657.4	815.8	-137.5
	Model A	2089.5	-1338.8	-528.4	718.3	-217.2
	Model B	2094.6	-1289.1	-638.8	833.9	-270.3
40	Test	915.9	643.7	365.2	251.3	-235.8
	Original Analysis	1108.5	639.2	425.3	179.7	-434.1
	Model A	1328.9	724.5	474.1	246.7	-342.1
	Model B	1280.0	758.3	500.0	260.8	-353.2
12	Test	2213.9	367.4	-1310.9	191.7	277.1
	Original Analysis	2442.5	426.1	-1294.0	279.8	-318.7
	Model A	2845.2	723.6	-742.0	66.1	476.4
	Model B	2799.7	617.6	-1174.3	73.9	-357.4
11	Test	673.5	-442.2	355.4	-437.7	440.8
	Original Analysis	678.9	-481.7	258.4	-169.9	506.3
	Model A	797.0	-579.3	538.3	-312.7	609.5
	Model B	744.1	-604.5	-164.1	-323.6	562.5

spring due to monoball chatter. Modal test data was obtained in the linear region. Such a non-linear phenomenon does indeed reduce the effective spring constant, and it was found that the shear link had to be reduced in stiffness by 80% to match the test results of the fourth mode, the only mode which was affected by this member.

A mass decrease of up to 10% as shown for Model B is physically reasonable due to possible fluid slosh effects, even though the tanks were completely full and pressurized. The increase in the moment of inertia of the Pressurant Control Assembly (PCA) about the X axis by 300% is indeed acceptable because the model was found to be in error in the PCA moment of inertia and the calculated increase is well within the physically meaningful range.

(4) The data presented shows that it would be desirable to correlate using mode shape in addition to frequency. Since the mode shape is a vector rather than a scalar, this approach might be more fruitful. The use of mode shape data as suggested in Ref. (1) is impractical. Refs. (14), (15), and (16) use frequency and mode shape for model improvement. This method requires the evaluation of the derivatives of the eigenvalues and eigenvectors. In addition, it considers statistical error distributions for these test data and analyses. The method is successfully applied to a beam model of the Saturn V space vehicle. The feasibility of applying the method proposed by Refs. (14), (15), and (16) to a three-dimensional structure such as

the Viking Propulsion Subsystem has not been established.

CONCLUSION

The application of the method proposed by C. White to the VPS provided the authors with a good insight of the method's merits and limitations.

A comparison of this method to other published methods has not been made because other methods have not been tested as yet.

The larger objective of this work is to obtain insight into the merits and limitations of various methods, and to select one of these for an algorithm to be used for a computer program for model correlation. The program is to be comparable with NASTRAN.

Activities described herein are invaluable in a research and development activity leading to a user-oriented program. Especially since the proposed methods in the literature have been applied to a very limited number of real problems.

The use of analytically generated "test" results to illustrate different methodologies can be misleading. Algorithms that are successful on analytically generated "test" results may not be successful on real test data.

*This paper presents the results of one phase of research carried out at the Jet Propulsion Laboratory, California Institute of Technology, under Contract No. NAS 7-100 sponsored by the National Aeronautics and Space Administration. The effort was supported by Dr. A. Amos, Materials and Structures Division, Office of Aeronautics and Space Technology, National Aeronautics and Space Administration.

REFERENCES.

1. C. W. White and B. D. Maytum, "Eigensolution Sensitivity to Parametric Model Perturbations." The Shock and Vibration Bulletin, Bulletin 46, Part 5, Naval Research Lab., Washington, D. C., August 1976, pp. 123-133.
2. C. W. White and B. D. Maytum, "Eigensolution Sensitivity to Parametric Model Perturbations." Martin Marietta Corporation, Denver Division, Denver Colorado, Technical Report R-75-48628-001, April 1975.
3. C. W. White, "Dynamic Test Reflected Structural Model Methodology Report, Skylab Program." Martin Marietta Corporation, Denver Division, Denver, Colorado, Payload Integration Technical Report ED-2002-1577, December 19, 1972.
4. J. C. Chen and B. K. Wada, "Criteria for Analysis - Test Correlation of Structural Dynamic Systems." Journal of Applied Mechanics, Vol. 24, No. 2, pp. 471-477, June 1975.
5. J. C. Chen and B. K. Wada, "Matrix Perturbation for Structural Dynamic Analysis." Presented at the 17th AIAA/ASME/SAE Structures, Structural Dynamics, and Materials Conference, King of Prussia, Pennsylvania, May 5-7, 1976. Also to be published in the AIAA Journal, August 1977.
6. J. A. Garba, B. K. Wada, R. Bamford, and M. R. Trubert, "Evaluation of a Cost-Effective Loads Approach." Journal of Spacecraft and Rockets, Vol. 13, No. 11, pp. 675-683, November 1976.
7. B. K. Wada and J. A. Garba, "Dynamic Analysis and Test Results of the Viking Orbiter." ASME Winter Annual Meeting, ASME Paper 75-WA/Aero 7, Houston, Texas, November 30 - December 4, 1975.
8. G. R. Brownlee, F. D. Day, and J. A. Garba, "Analytical Prediction and Correlation for the Orbiter during the Viking Spacecraft Sinusoidal Vibration Test." The Shock and Vibration Bulletin, Bulletin 45, Part 3, Naval Research Lab, Washington, D. C., June 1975, pp. 37-57.
9. R. Bamford, B. K. Wada, J. Garba, and J. Chisholm, "Dynamic Analyses of Large Structural Systems." Synthesis of Vibrating Systems, The American Society of Mechanical Engineers, New York, N. Y. 1971.
10. W. H. Gayman, "Fluid Dynamics Tests of the Viking Orbiter Propellant Tank Configuration." PD 900-711, Jet Propulsion Laboratory, Pasadena, Calif., July 1975 (JPL Internal Document).
11. R. M. Bamford, B. K. Wada and W. H. Gayman, "Equivalent Spring Mass System for Normal Modes." Jet Propulsion Laboratory, Pasadena, California, Technical Memorandum 33-380, February 15, 1971.
12. B. K. Wada, R. Bamford and J. A. Garba, "Equivalent Spring-Mass System: A Physical Interpretation." The Shock and Vibration Bulletin, Bulletin 42, Part 5, Naval Research Lab, Washington, D. C., January 1972, pp. 215-225.
13. B. K. Wada, J. A. Garba and J. C. Chen, "Development and Correlation: Viking Orbiter Analytic Dynamic Model with Modal Test." The Shock and Vibration Bulletin, Bulletin 44, Part 2, August 1977, pp. 125-164.
14. J. D. Collins, G. C. Hart, T. K. Hasselman and B. Kennedy, "Statistical Identification of Structures." AIAA Journal, Volume 12, No. 2, pp. 185-180, February 1974.
15. J. D. Collins, G. C. Hart, T. K. Hasselman and B. Kennedy, "Model Optimization Using Statistical Estimation." The J. H. Wiggins Company, Redondo Beach, California, Technical Report No. 73-1087-2.
16. J. D. Collins, J. P. Young and L. A. Kiefling, "Methods and Applications of System Identification in Shock and Vibration." System Identification of Vibrating Structures, Mathematical Models from Test Data, American Society of Mechanical Engineers, New York, 1972.

ORIGINAL PAGE IS
FROM THE LIBRARY

NASTRAN MODAL SYNTHESIS

PRESENTED AT

PAYLOAD FLIGHT LOADS PREDICTION METHODOLOGY WORKSHOP

**GEORGE C. MARSHALL SPACE FLIGHT CENTER
HUNTSVILLE, ALABAMA**

NOVEMBER, 1978

PRESENTED BY

**UNIVERSAL ANALYTICS, INC.
LOS ANGELES, CALIFORNIA**

PRECEDING PAGE BLANK NOT FILMED

ORGANIZATION OF PRESENTATION

- NASTRAN MODAL SYNTHESIS FEATURES AND STATUS
- SUMMARY OF EQUATIONS
- ACCURACY OF MODAL SYNTHESIS APPROACHES
- PRODUCTION APPLICATION
- SUMMARY

GENERAL FEATURES OF NASTRAN MODAL SYNTHESIS

- NASTRAN AUTOMATED SUBSTRUCTURING PROVIDES FRAMEWORK
- USER-ORIENTED COMMANDS - COMBINE, REDUCE, MREDUCE, SOLVE, RECOVER, ETC.
- FREE, FIXED, OR MIXED BOUNDARY CONDITIONS FOR MODES CALCULATIONS
- DIAGNOSTIC OUTPUT AVAILABLE INCLUDING MODAL PARTICIPATION FACTORS AND MODAL KINETIC AND POTENTIAL ENERGY
- OPTIONS FOR USER (EXTERNAL) MODES AND COMPLEX MODES

GENERAL FEATURES OF NASTRAN MODAL SYNTHESIS

- LOADS ON INTERIOR POINTS INCLUDED
- RELATIVE MODAL DISPLACEMENTS PROVIDE DIRECT ASSESSMENT OF ACCURACY
- MODAL COORDINATES MAY BE CONSTRAINED
- EXACTLY ORTHOGONAL MODES NOT REQUIRED
- ANY NASTRAN EIGEN METHOD ALLOWED - GIVENS, FEER, INVERSE, HESSENBERG, COMPLEX INVERSE, ETC.
- MAY BE CONNECTED WITH NORMAL SUBSTRUCTURES
- FULL MULTI-STAGE CAPABILITIES
- EXACT STIFFNESS AND TOTAL MASS FOR ALL SUBSTRUCTURES

GENERAL FEATURES OF NASTRAN MODAL SYNTHESIS

A general purpose modal synthesis capability has been developed and incorporated into NASTRAN as an addition to the Automated Multi-Stage Substructuring System. The system is used by adding a special Substructure Control card deck after the Executive Control Deck. Substructures are assigned names by the user and may be REDUCED, ModalREDUCED, COMBINED, SOLVED, etc., by the use of a user-oriented control language. There are no restrictions on the number of substructures, the sizes of substructures, the types of modes computed, etc. Substructure models may be used in statics, normal modes, frequency and random response, and transient analyses. Numerous provisions for diagnostic output and capability for incorporation of computed models developed from test data or other analyses are provided.

SYSTEM STATUS

- INSTALLED IN THE NEXT NASTRAN RELEASE
- FIELD TESTED WITH MODIFIED LEVEL 16 (IBM AND CDC)
- TESTED WITH LARGF-ORDER ACTUAL PROBLEMS
- IN USE BY SEVERAL GROUPS

SYSTEM STATUS

NASTRAN modal synthesis was developed by UAI and has been in use for over one year. The system will be released in Level 17.5 NASTRAN early next year. The capability has been utilized by UAI, customers of several nationwide data centers, and by Goddard Space Flight Center personnel.

MODAL SYNTHESIS EQUATIONS

$$\begin{Bmatrix} U_B \\ - \\ - \\ U_I \end{Bmatrix} = \begin{bmatrix} I & 0 & 0 \\ G_{IB} & H_{IK} & H_{IO} \end{bmatrix} \begin{Bmatrix} U_B \\ Z_K \\ Z_O \end{Bmatrix}$$

$$G_{IB} = -K_{II}^{-1} K_{IB} \quad : \quad \text{GUYAN REDUCTION}$$

$$H_{IK} = \emptyset_{IK} - G_{IB} \emptyset_{BK} \quad : \quad \text{RELATIVE MODE SHAPES}$$

$$H_{IO} = K_{II}^{-1} (M_{II} G_{IB} + M_{IB}) \emptyset_{BO} \quad : \quad \text{INERTIA RELIEF SHAPES}$$

$$\{U_G\} = [H_{GH}] \{U_H\}$$

MODAL SYNTHESIS EQUATIONS

$$[K_{HH}] = \begin{bmatrix} H_{GH}^T & K_{GG} & H_{GH} \end{bmatrix}$$

$$= \begin{bmatrix} K_{BB} & 0 & 0 \\ 0 & \dots & \dots \\ 0 & \dots & K_{ZZ} \end{bmatrix}$$

MODES ARE STATICALLY
UNCOUPLED FROM
PHYSICAL DOF

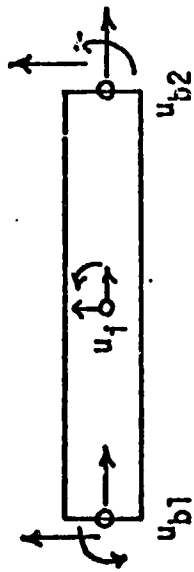
$$[M_{HH}] = \begin{bmatrix} H_{GH}^T & M_{GG} & H_{GH} \end{bmatrix}$$

MASS MATRIX IS COUPLED

MODAL SYNTHESIS EQUATIONS

A complete theoretical development of NASTRAN modal synthesis is presented in the NASTRAN Theoretical Manual. These charts summarize the form of the transformation matrix from the coordinates of one model, U_g , to the coordinates of that same model after modal reduction, U_h . The user defines which degrees of freedom are to remain as physical, U_b , and which degrees of freedom are to be fixed for the calculation of mode shapes and frequencies. The rows of ϕ_{ik} and ϕ_{bk} corresponding to fixed degrees of freedom are null.

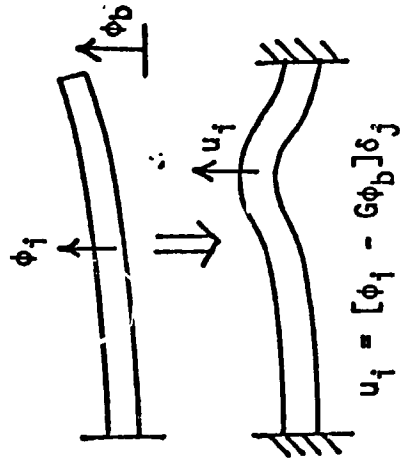
GENERALIZED COORDINATE SHAPE FUNCTIONS



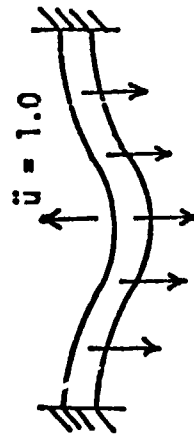
a) Component Substructure



b) Static Deflections, u_b



d) Modified Normal Modes



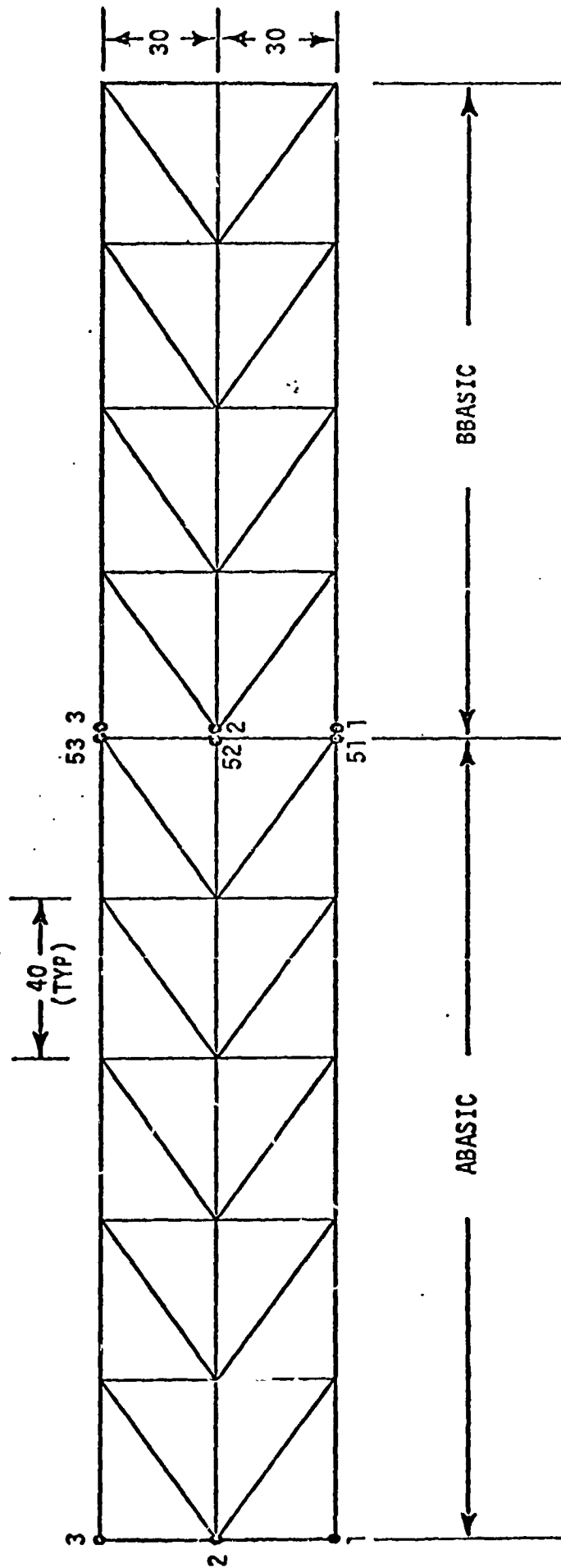
c) Inertia Relief, δ_0

GENERALIZED COORDINATE SHAPE FUNCTIONS

This slide illustrates the types of mode shape functions used in the formation of the transformation matrix for NASTRAN modal synthesis.

MODAL SYNTHESIS ACCURACY TEST PROBLEM

● - Boundary Points



NASTRAN MODAL SYNTHESIS ACCURACY PERCENT FREQUENCY ERRORS
WITH 20 ELASTIC DEGREES OF FREEDOM
TWO COMPONENT TRUSS PROBLEM

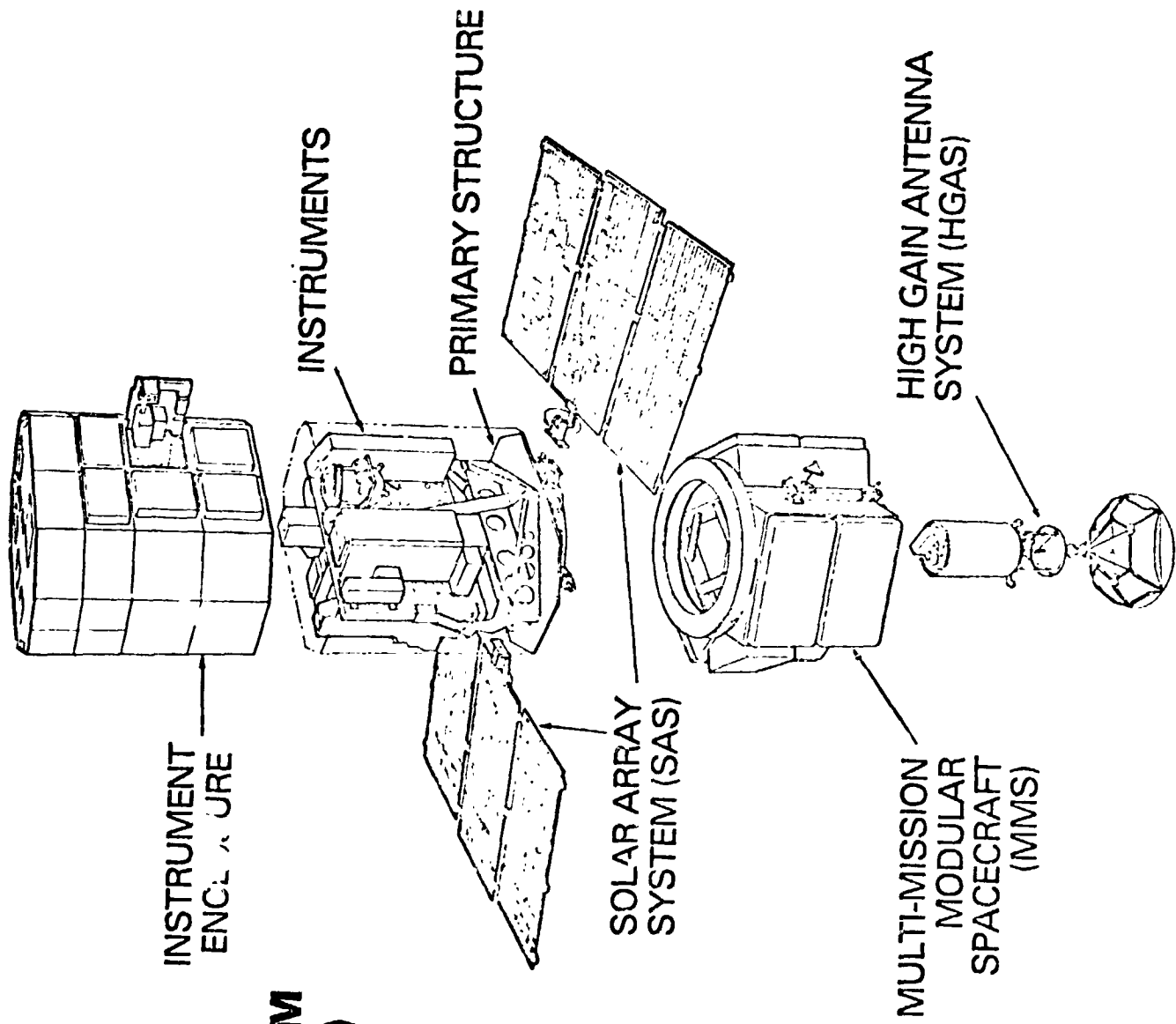
System Cantilevered Mode No.	NASTRAN Results				Hintz Results		
	Free Modes	Free w/I.h.	Cant. Modes	Cant. w/I.R.	Free w.I.R.	Hurty (Cant. Modes)	Cant. w/I.R.
1	8.92	.00034	.00043	.0034	.000017	.00074	9x10 ⁻⁹
2	1.21	.00902	.0017	0	.000061	.0018	3x10 ⁻⁶
3	7.67	.0135	.0098	.0061	.0138	.0096	.00584
4	1.08	.0023	.0096	.00002	.0024	.0092	.00002
5	6.00	.00083	.033	0	.00081	.034	.0014
6	0.85	.0020	.0098	.00060	.0020	.0103	.00054
7	0.61	.080	.947	.268	.083	.941	.264
8	1.58	.0071	.122	.021	.0058	.117	.018
9	.084	.00098	.59	.54	.00093	.80	.69
10	.030	.0041	.36	.40	.0045	.20	.25
11	.90	.021	.33	.98	.022	.30	1.03
12	3.30	.428	.49	12.3	.104	.28	11.1
13	4.01	5.35	.16		5.33	.14	
14	.244	7.87	.77		7.15	.72	
15	1.10		2.37			2.63	
16	.59		12.15			11.4	
17	6.69						

\ indicates freq. of
 first truncated mode

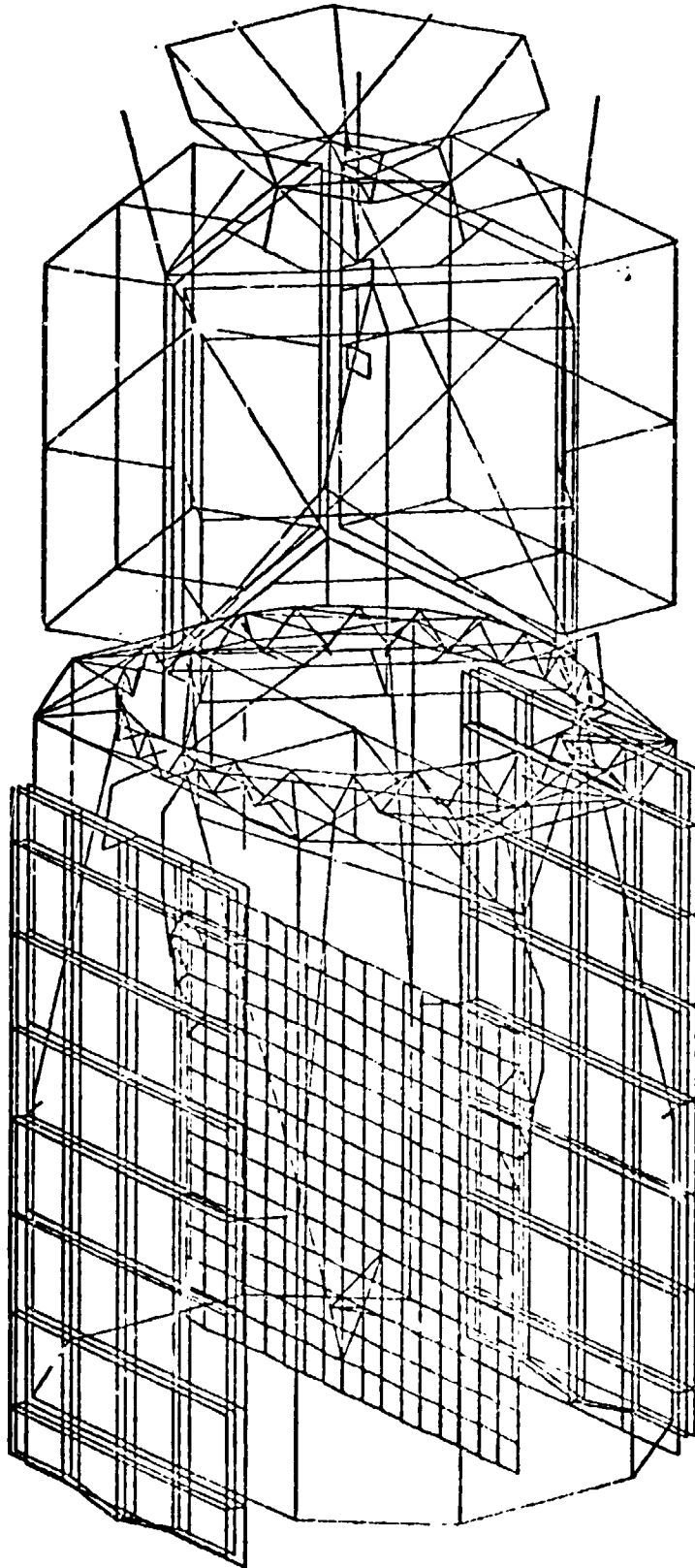
NASTRAN MODAL SYNTHESIS ACCURACY

Accuracy of NASTRAN modal synthesis methods is illustrated using a nine-cell truss model described by R.M. Hintz, "Analytical Methods in Component Modal Synthesis", AIAA Journal, Vol. 12, August 1975. The table presents percent error in frequency versus system mode number versus type of component modal synthesis option. The table indicates that use of the inertia relief shapes greatly reduces mode truncation errors.

SOLAR MAXIMUM MISSION (SMM) OBSERVATORY



SMM OBSERVATORY LAUNCH CONFIGURATION MODEL



SMM OBSERVATORY LAUNCH CONFIGURATION MODEL

These charts illustrate the structure and the analytical model of the Solar Maximum Mission Observatory. Twelve different NASTRAN models were coupled together using NASTRAN Automated Multi-Stage Substructuring and modal synthesis. The individual component models total more than 8000 degrees of freedom and the assembled model is represented by 20-50 physical degrees of freedom and approximately 50 modal coordinates. A total of 8 different models were built representing launch configuration, shuttle retrieval configuration, and 6 orbital configurations.

SUMMARY

- ACCURACY EQUAL OR BETTER THAN OTHER APPROACHES
- USER ORIENTED CONTROL
- FIELD TESTED AND DEBUGGED FOR 12 MONTHS
- NEW CAPABILITY PROVIDES MEANS FOR EFFICIENT DYNAMICS ANALYSES OF LARGE MODELS

SUMMARY

Testing of NASTRAN modal synthesis shows that the system is capable of producing the same levels of accuracy obtainable with different state-of-the-art modal synthesis methods. Differences in results may be obtained by selecting different types of component modes and types of solution vector recovery procedures.

The system is designed for ease of user control and automatically performs the bookkeeping task. Simple commands allow the user to access all data used by the NASTRAN Automated Substructuring and modal synthesis system.

The Automated Substructuring and modal synthesis system provides an effective tool for reducing computer resource requirements for large structural dynamics analyses. The system also serves as an effective project management tool because complex analyses are broken into many simpler and more manageable tasks.



VERIFICATION OF ACCURACY OF VARIOUS MODAL METHODS

BY M. A. MARTENS
NOVEMBER, 1978



Rockwell International
Space Division



AT THIS POINT IN TIME, ENOUGH DATA AND EXPERIENCE HAVE NOT BEEN ACCUMULATED TO PERMIT CONFIDENT PREDICTION OF LOW FREQUENCY DYNAMIC LOADS OF SHUTTLE/PAYLOAD CONFIGURATIONS BASED ON ANY CALCULATIONS SHORT OF A FULL COUPLED DYNAMIC LOADS ANALYSIS. IN PERFORMING THIS ANALYSIS WITH A MODAL APPROACH, A KEY OPERATION IS THE CALCULATION OF EIGENVALUES AND EIGENVECTORS OF THE COUPLED STRUCTURAL SYSTEM. NEARLY EVERY ASPECT OF THIS PAYLOAD ANALYSIS PROBLEM POINTS TO A COMPONENT MODE SYNTHESIS METHOD AS THE OBVIOUS APPROACH TO BE USED IN FORMULATING THE SYSTEM MODES. MANY COMPONENT MODE SYNTHESIS METHODS AND VARIATIONS HAVE BEEN DEVELOPED AND EXPOUNDED IN THE LITERATURE. THE SELECTION OF A SPECIFIC METHOD FOR IMPLEMENTATION IS AFFECTED BY RELATIVE ACCURACY, COST, AND CONVENIENCE, AS WELL AS PRACTICAL CONSIDERATIONS SUCH AS THE AVAILABILITY OF EXISTING SOFTWARE AND EXPERIENCE.

ROCKWELL INTERNATIONAL/SPACE SYSTEMS GROUP HAS BEEN INVOLVED IN SHUTTLE PAYLOAD LOADS PREDICTION WORK FOR SEVERAL YEARS NOW. OUR EARLY INVESTIGATIONS CONVINCED US THAT THE METHOD WHICH BEST FIT OUR NEEDS WAS TO REPRESENT THE SHUTTLE VEHICLES WITH A SET OF FREE-FREE MODES AUGMENTED WITH RESIDUAL FLEXIBILITY TERMS AS PROPOSED BY RUBIN AND MACNEAL. THE PAYLOAD COMPONENTS ARE USUALLY REPRESENTED EITHER AS FREE-FREE PHYSICAL MASS AND STIFFNESS MATRICES OR IN CRAIG-BAMPTON FIXED MODE FORM. WE SELECTED THIS METHOD NOT ONLY BECAUSE IT PROVIDES THE DESIRED COMPUTATIONAL ACCURACY AT REASONABLE COMPUTATIONAL COST, BUT BECAUSE IT IS PARTICULARLY AMENABLE TO THE INCORPORATION OF CONVENIENCE FEATURES, VALIDITY CHECKS, AND SOLUTION EVALUATION PROCEDURES.

AS OTHER COMPANIES AND AGENCIES BECAME INVOLVED IN THE LOW FREQUENCY STRUCTURAL DYNAMIC ANALYSIS OF SHUTTLE PAYLOADS, NASA-JSC AND ROCKWELL INTERNATIONAL/SSG WERE CALLED UPON TO PROVIDE THEM WITH COMPONENT MODE REPRESENTATIONS OF THE SHUTTLE VEHICLES. IN MANY INSTANCES, THEY HAD VERY LIMITED RESOURCES AVAILABLE FOR IMPLEMENTATION OF NEW METHODOLOGY, SUCH AS WOULD BE NEEDED TO INCLUDE THE RESIDUAL FLEXIBILITY TERMS USED AT ROCKWELL. SINCE THIS EARLY WORK DEALT WITH CONCEPTUAL DESIGN, THE DECISION WAS MADE TO PROVIDE THE FREE-FREE MODES OF THE SHUTTLE VEHICLES AND HERMIT SYNTHESIS TO BE DONE WITHOUT THE RESIDUAL FLEXIBILITY EFFECTS.

AS TIME PASSED, MORE AND MORE COMPANIES AND AGENCIES BECAME INVOLVED. THREE QUESTIONS DEVELOPED. FIRST, IS THE INACCURACY INHERENT IN THE CLASSICAL FREE-FREE SYNTHESIS METHOD (FREE-FREE MODES WITHOUT RESIDUAL FLEXIBILITY EFFECTS) SEVERE ENOUGH TO PRECLUDE ITS USE FOR OTHER THAN CONCEPTUAL DESIGN STUDIES? SECOND, ARE THE VARIOUS MODAL SYNTHESIS METHODS PREFERRED BY OTHER COMPANIES ADEQUATELY ACCURATE TO HANDLE THE PROBLEM AT HAND? THIRD, ARE MORE MODES REQUIRED TO OBTAIN A CONVERGENT SOLUTION THAN THE 200 MODES NORMALLY EMPLOYED BY ROCKWELL INTERNATIONAL/SSG.

THE OBJECTIVE OF THE STUDY IN THIS PRESENTATION WAS TO ANSWER THE ABOVE THREE QUESTIONS. ACTUALLY, THE FIRST QUESTION WAS ANSWERED IN AN EARLIER STUDY BUT SINCE PERTINENT DATA IS AVAILABLE, IT HAS BEEN INCLUDED HERE.



Rockwell International

Space Division



CHART 1

OBJECTIVES:

- 0 VERIFY THE ACCURACY OF VARIOUS MODAL METHODS.
- 0 INVESTIGATE MODAL CONVERGENCE.





ACTUALLY, ROCKWELL INTERNATIONAL/SSG HAD SUFFICIENT DISJOINTED EVIDENCE TO ANSWER THESE QUESTIONS TO OUR OWN SATISFACTION BUT IN ORDER TO PRESENT A CLEAR, ORDERLY SET OF DATA TO OTHER CONCERNED COMPANIES AND AGENCIES, A CONSISTENT SET OF SOLUTIONS WAS EXECUTED. VARIOUS COMPARISONS DEALING WITH THE QUESTIONS OF METHODOLOGY AND CONVERGENCE APPEAR IN THE LITERATURE. HOWEVER, SINCE THIS STUDY IS FOCUSED ON THE SPECIFIC PROBLEM OF SHUTTLE PAYLOAD ANALYSES, AND SINCE PROBLEM-DEPENDENT NUMERICAL EFFECTS MAY BE SIGNIFICANT, THE USE OF A SMALL ACADEMIC PROBLEM WAS REJECTED IN FAVOR OF A TYPICAL REAL PAYLOAD. ONE PAYLOAD AND ONE LIFTOFF CONDITION WERE SELECTED FOR THE STUDY. THE RESULTS, THEREFORE, ARE NOT ABSOLUTELY ALL INCLUSIVE BUT, RATHER, MAY BE INTERPRETED AS INDICATORS. THE FEATURES OF CONCERN HERE THAT ARE EXHIBITED BY THESE RESULTS ARE NOT EXPECTED TO CHANGE SIGNIFICANTLY FOR OTHER PAYLOADS OR FORCING FUNCTIONS.

FOUR FAIRLY REPRESENTATIVE METHODS LISTED IN CHART 2 WERE SELECTED FOR REPRESENTING THE SHUTTLE VEHICLES WITH AN EMPTY CARGO BAY. SEVERAL LEVELS OF MODAL TRUNCATION WERE ALSO SELECTED. ALL COMPARISONS WERE BASED ON SEVERAL ASPECTS OF RESPONSE RATHER THAN SOME EIGENVALUE OR EIGENVECTOR COMPARISON SCHEME BECAUSE RESPONSES ARE THE REAL SUBJECTS OF OUR CONCERN.



IMPLEMENTATION:

- 0 ONE LIFTOFF CONDITION (LP510 WITH 1P2 SRB)
- 0 USE 2-STAGE IUS-F/TDRS-7 (LOW SUSPENSION CRADLE)(RI MODIFIED VERSION)
- 0 INVESTIGATE FOUR METHODS OF REPRESENTING THE EMPTY SHUTTLE
 - 0 STIFFNESS AND MASS (NO SYNTHESIS)
 - 0 MACNEAL SYNTHESIS (FREE-FREE MODES WITH RESIDUAL FLEXIBILITY)
 - 0 CRAIG-BAMPTON SYNTHESIS (FIXED MODES)
 - 0 CLASSICAL FREE-FREE SYNTHESIS
- 0 USE SEVERAL LEVELS OF MODAL TRUNCATION
- 0 COMPARE VARIOUS ASPECTS OF RESPONSE
 - 0 SPACECRAFT NET LOAD FACTORS
 - 0 CARGO NET LOAD FACTORS
 - 0 SELECTED IUS MASS POINT LOAD FACTORS
 - 0 IUS/ORBITER INTERFACE FORCES
 - 0 SELECTED SPACECRAFT MASS POINT LOAD FACTORS
 - 0 SELECTED SPACECRAFT LTM RECOVERY ITEMS



THE STANDARD FOR COMPARISON IN THIS STUDY IS THE STIFFNESS AND MASS SOLUTION USING THE GREATEST NUMBER OF SYSTEM MODES. IN THIS SOLUTION, NO SYNTHESIS PROCEDURES WERE EMPLOYED IN THE REPRESENTATION OF THE SHUTTLE. RATHER, THE ENTIRE SHUTTLE SYSTEM OF ORBITER, EXTERNAL TANK, AND SOLID ROCKET BOOSTERS WAS REPRESENTED WITH MASS AND STIFFNESS MATRICES IN THE PHYSICAL COORDINATE SYSTEM. THE PAYLOAD WAS COMBINED WITH THE SHUTTLE IN DIRECT STIFFNESS FASHION. THE SYSTEM MODES WERE OBTAINED IN ONE VERY LARGE, EXPENSIVE EIGENANALYSIS. INACCURACY ASCRIBABLE TO APPROXIMATIONS IN THE SHUTTLE COMPONENT REPRESENTATION MAY BE TAKEN AS NONEXISTENT HERE. BY USING THE GREATEST NUMBER OF MODES IN THE TRANSIENT SOLUTION, THE EFFECTS OF MODAL TRUNCATION ARE MINIMIZED.

THE SPECIFIC GUIDELINES SHOWN WERE LAID DOWN AS CRITERIA FOR ACCEPTABLE VARIATION FROM THE STANDARD.



Rockwell International
Space Division



CRITERIA:

- 0 STANDARD FOR COMPARISON IS STIFFNESS AND MASS SOLUTION USING THE GREATEST NUMBER OF SYSTEM MODES (384).
- 0 DEFINITION OF ACCEPTABLE VARIATION FROM STANDARD:
 - 0 5% AT HEAVY MASS ITEMS AND PRIMARY STRUCTURE.
 - 0 10% AT SMALL MASSES AND FLEXIBLE APPENDAGES.

THE CONCLUSIONS THAT ARE SUPPORTED BY THIS STUDY ARE SHOWN ON CHART 4. IT DOES NOT SEEM LIKELY THAT MUCH SIGNIFICANCE SHOULD BE ATTACHED TO THE SLIGHTLY BETTER RESULTS OBTAINED WITH THE MACNEAL REPRESENTATION OVER THE CRAIG-BAMPTON REPRESENTATION. IT APPEARS THAT BOTH OF THESE METHODS YIELD VERY GOOD RESULTS FOR OUR PROBLEM. THE CLASSICAL FREE-FREE REPRESENTATION SHOWED UP QUITE POORLY. IT SHOULD BE NOTED THAT ALTHOUGH THE NUMERICAL RESULTS DOCUMENTED HERE FOR THE CLASSICAL FREE-FREE SOLUTION WERE ACTUALLY GENERATED AT ANOTHER COMPANY, CONSISTENT RUNS WERE PERFORMED AT ROCKWELL INTERNATIONAL/SPACE SYSTEMS GROUP WHICH PRODUCED SLIGHTLY DIFFERENT NUMERICAL ANSWERS BUT VERY MUCH THE SAME LEVEL OF ACCURACY.





CHART 4

CONCLUSIONS:

- 0 MODES OBTAINED FROM CRAIG-BAMPTON SYNTHESIS (FIXED MODES) YIELD RESPONSES THAT AGREE WITH THE STIFFNESS AND MASS SOLUTION TO WITHIN 2% WHEN THE SAME NUMBER OF SYSTEM MODES IS RETAINED.
- 0 MODES OBTAINED FROM MACNEAL SYNTHESIS (FREE-FRE E MODES WITH RESIDUAL FLEXIBILITY) YIELD RESPONSES THAT AGREE WITH THE STIFFNESS AND MASS SOLUTION TO WITHIN 1% WHEN THE SAME NUMBER OF SYSTEM MODES IS RETAINED.
- 0 MODES OBTAINED FROM CLASSICAL FREE-FREE SYNTHESIS YIELD RESPONSES THAT DIFFER FROM THE STIFFNESS AND MASS SOLUTION BY AS MUCH AS 11% AT THE SPACECRAFT C. G. AND BY UP TO 20% AND MORE AT INDIVIDUAL SPACECRAFT POINTS. THEREFORE, THIS METHOD IS NOT RECOMMENDED FOR ANYTHING BUT CONCEPTUAL DESIGN LOADS ASSESSMENTS.
- 0 TRUNCATION TO 200 SYSTEM MODES INTRODUCES AN ACCEPTABLE AMOUNT OF ERROR. (LESS THAN 3% AT HEAVY MASS ITEMS, AND LESS THAN 6% AT SPACECRAFT SMALL MASSES AND FLEXIBLE APPENDAGES.)



RESPONSE DATA FOR EACH SOLUTION ARE PRESENTED ON THIS AND THE FOLLOWING CHARTS. THE STIFFNESS AND MASS SOLUTIONS WITH THREE DIFFERENT LEVELS OF MODAL TRUNCATION ARE LISTED FOLLOWED BY TWO CRAIG-BAMPTON SOLUTIONS, A MACNEAL SOLUTION, AND A SOLUTION EMPLOYING THE CLASSICAL FREE-FREE COMPONENT REPRESENTATION. THE APPROACH LISTED APPLIES ONLY TO THE METHOD OF REPRESENTING THE SHUTTLE SIDE OF THE SHUTTLE/PAYLOAD INTERFACE. IN ALL SOLUTIONS EXCEPT THE LAST, THE PAYLOAD IS REPRESENTED IN EXACTLY THE SAME FASHION. THAT IS, THE IUS AND ASE ARE DESCRIBED BY 210 PHYSICAL DEGREES OF FREEDOM, WHILE THE SPACECRAFT MODEL CONSISTS OF 85 GENERALIZED DEGREES OF FREEDOM AND 48 PHYSICAL BOUNDARY DEGREES OF FREEDOM. THOUGH SEVERAL ASPECTS OF THE SOLUTION REPORTED IN THE LAST COLUMN ARE NOT CONSISTENT WITH THE OTHER SOLUTIONS, CONSISTENT RUNS WERE MADE AT ROCKWELL INTERNATIONAL/SSG, AS MENTIONED EARLIER, WHICH SUBSTANTIATE THE GENERAL LEVEL OF ACCURACY OF THIS METHOD. NOTE THAT THE CHARTS SHOW THE HIGHEST FREQUENCY INCLUDED FOR EACH COMPONENT REPRESENTED WITH GENERALIZED COORDINATES. SYSTEM MODES USED IN THE TRANSIENT SOLUTION ARE DESCRIBED BY THE NUMBER OF MODES AND THE HIGHEST FREQUENCY INCLUDED.

CHART 5 SHOWS GROSS SPACECRAFT ACCELERATION RESPONSES IN THE FORM OF ABSOLUTE MAXIMUM UNCORRELATED NET LOAD FACTORS. THE DATA CAN BE SEEN TO SUPPORT EACH OF THE FOUR CONCLUSIONS DISCUSSED IN CHART 4. AS COMPARED TO THE STANDARD SOLUTION IN THE FIRST COLUMN, BOTH THE CRAIG-BAMPTON AND THE MACNEAL SOLUTIONS LOOK VERY GOOD, WHILE THE INACCURACY IN THE CLASSICAL FREE-FREE SOLUTION IS OBVIOUS. TRUNCATION OF THE STIFFNESS AND MASS SYSTEM DOWN TO 200 MODES CAN BE SEEN TO STILL PRODUCE EXCELLENT RESULTS. MODE SETS SMALLER THAN 200 WERE NOT USED SINCE THE MODEST COST REDUCTION THAT COULD BE ACHIEVED COULD NOT, IN GENERAL, JUSTIFY THE INHERENT RISK.





METHODS STUDY
SC NET LOAD FACTOR COMPARISON

CHART 5

COMPONENT DEFINITION	APPROACH	K&M	K&M	K&M	CRAIG-BAMPTON	CRAIG-BAMPTON	MACNEAL	CLASSICAL FREE-FREE
IUS AND ASE		210 PHY			210 PHY	210 PHY	210 PHY	50 GEN
SC		48 PHY 85 GEN (49.9 HZ)			48 PHY 85 GEN (49.9 HZ)	48 PHY 85 GEN (49.9 HZ)	48 PHY 85 GEN (49.9 HZ)	48 PHY 85 GEN (49.9 HZ)
SHUTTLE		812 PHY			25 PHY 200 GEN (42.4 HZ)	25 PHY 200 GEN (42.4 HZ)	200 GEN (39.9 HZ)	300 IZ (61.4 HZ)
SYSTEM MODES USED		384 (60.0 HZ)	339 (50.0 HZ)	200 (25.1 HZ)	296 (42.3 HZ)	200 (25.1 HZ)	200 (25.1 HZ)	200
MAX X LF		3.094	3.095	3.088	3.094	3.092	3.087	2.85
MAX Y LF		.372	.372	.373	.373	.375	.373	- 8% .33
MAX Z LF		1.281	1.281	1.279	1.278	1.277	1.279	-11% 1.35 5%

CHART 6 SHOWS THE COMPARISON OF ABSOLUTE MAXIMUM UNCORRELATED TOTAL CARGO NET LOAD FACTORS. THE DATA IS SIMILAR TO THE PREVIOUS CHART.

CHART 7 SHOWS A COMPARISON OF ABSOLUTE MAXIMUM UNCORRELATED LOAD FACTORS AT SELECTED INDIVIDUAL IUS DEGREES OF FREEDOM.

CHART 8 SHOWS THE COMPARISON OF ABSOLUTE MAXIMUM UNCORRELATED INTERFACE FORCES EXERTED BY THE ORBITER ON THE IUS CRADLES.

CHART 9 SHOWS THE COMPARISON OF ABSOLUTE MAXIMUM UNCORRELATED LOAD FACTORS AT SELECTED INDIVIDUAL SPACECRAFT DEGREES OF FREEDOM.

CHART 10 SHOWS THE COMPARISON OF SELECTED ABSOLUTE MAXIMUM UNCORRELATED LOADS TRANSFORMATION RECOVERY ITEMS FOR THE SPACECRAFT.





METHODS STUDY
TOTAL CARGO NET LOAD FACTOR COMPARISON

CHART 6

COMPONENT DEFINITION	APPROACH	K&M	K&M	K&M	CRAIG-BAMPTON	CRAIG-BAMPTON	CRAIG-BAMPTON	MACNEAL	CLASSICAL FREE-FREE
IUS AND ASE		210 PHY			210 PHY	210 PHY	210 PHY	210 PHY	50 GEN
SC		48 PHY 85 GEN (49.9 HZ)			48 PHY 85 GEN (49.9 HZ)	48 PHY 85 GEN (49.9 HZ)	48 PHY 85 GEN (49.9 HZ)	48 PHY 85 GEN (49.9 HZ)	48 PHY 85 GEN (49.9 HZ)
SHUTTLE		812 PHY			25 PHY 200 GEN (42.4 HZ)	25 PHY 200 GEN (42.4 HZ)	25 PHY 200 GEN (42.4 HZ)	200 GEN (39.9 HZ)	300 GEN (61.4 HZ)
SYSTEM MODES USED		384 (60.0 HZ)	339 (50.0 HZ)	200 (25.1 HZ)	296 (42.3 HZ)	200 (25.1 HZ)	200 (25.1 HZ)	200 (25.1 HZ)	200
MAX X LF		2.903	2.902	2.901	2.903	2.904	2.901	2.901	
MAX Y LF		.151	.150	.150	.150	.150	.150	.150	
MAX Z LF		1.346	1.346	1.346	1.347	1.347	1.346	1.346	





SELECTED IUS LOAD FACTOR COMPARISONS

CHART 7

COMPONENT DEFINITION	APPROACH	K&M	K&M	K&M	CRAIG-BAMPTON	CRAIG-BAMPTON	CRAIG-BAMPTON	MACNEAL	CLASSICAL FREE-FREE
IUS AND ASE		210 PHY			210 PHY	210 PHY	210 PHY	210 PHY	50 GEN
SC		48 PHY 85 GEN (49.9 HZ)			48 PHY 85 GEN (49.9 HZ)	48 PHY 85 GEN (49.9 HZ)	48 PHY 85 GEN (49.9 HZ)	48 PHY 85 GEN (49.9 HZ)	48 PHY 85 GEN (49.9 HZ)
SHUTTLE		812 PHY			25 PHY 200 GEN (42.4 HZ)	25 PHY 200 GEN (42.4 HZ)	25 PHY 200 GEN (42.4 HZ)	200 GEN (39.9 HZ)	300 GEN (61.4 HZ)
SYSTEM MODES USED		384 (60.0 HZ)	339 (50.0 HZ)	200 (25.1 HZ)	296 (42.3 HZ)	200 (25.1 HZ)	200 (25.1 HZ)	200 (25.1 HZ)	200
IUS LARGE MOTOR		3.039 .206 1.407	3.039 .206 1.407	3.042 .205 1.409	3.039 .206 1.407	3.041 .205 1.409	3.041 .205 1.409	3.041 .205 1.409	2.985 .204 1.312
IUS SMALL MOTOR		3.122 .189 1.266	3.122 .189 1.266	3.121 .189 1.261	3.125 .189 1.272	3.127 .189 1.266	3.127 .189 1.266	3.120 .189 1.261	3.026 .149 1.286





METHODS STUDY
IUS/ORBITER INTERFACE FORCE COMPARISON

CHART 8

COMPONENT DEFINITION	APPROACH	K&M	K&M	K&M	CRAIG-BAMPTON	CRAIG-BAMPTON	MACNEAL	CLASSICAL FREE-FREE
IUS AND ASE		210 PHY			210 PHY	210 PHY	210 PHY	50 GEN
SC		48 PHY			48 PHY	48 PHY	48 PHY	48 PHY
		85 GEN (49.9 HZ)			85 GEN (49.9 HZ)	85 GEN (49.9 HZ)	85 GEN (49.9 HZ)	85 GEN (49.9 HZ)
SHUTTLE		812 PHY			25 PHY	25 PHY	200 GEN	300 GEN
SYSTEM MODES USED		384	339	200	200 GEN (42.4 HZ)	200 GEN (42.4 HZ)	200 GEN (39.9 HZ)	300 GEN (61.4 HZ)
		(60.0 HZ)	(50.0 HZ)	(25.1 HZ)	(42.3 HZ)	(25.1 HZ)	(25.1 HZ)	200
FWD ASE RHS 749X		1337	1320	1302	1304	1303	1295	1295
FWD ASE RHS 761Z		12512	12512	12512	12487	12485	12502	12502
AFT ASE RHS 753X		55636	55636	55638	55659	55659	55627	55627
AFT ASE RHS 762Z		14509	14509	14514	14514	14518	14512	14512
FWD ASE LHS 748X		1355	1345	1324	1321	1319	1319	1319
FWD ASE LHS 760Z		12084	12084	12088	12099	12099	12092	12092
AFT ASE LHS 754X		57044	57042	57056	57054	57078	57055	57055
AFT ASE LHS 763Z		15750	15751	15753	15754	15755	15750	15750
FWD ASE KEEL 750X		1946	1948	1940	1955	1963	1960	1960
FWD ASE KEEL 750Y		6047	6032	6033	6018	6038	6031	6031





SELECTED SC LOAD FACTOR COMPARISONS

CHART 9

APPROACH	K&M	K&M	CRAIG-- BAMPTON	CRAIG-- BAMPTON	K&M	K&M	CRAIG-- BAMPTON	CRAIG-- BAMPTON	MACNEAL	CLASSICAL FREE-FREE
IUS AND ASE	210 PHY		210 PHY	210 PHY			210 PHY	210 PHY	210 PHY	50 GEN
SC	48 PHY 85 GEN (49.9 HZ)		48 PHY 85 GEN (49.9 HZ)	48 PHY 85 GEN (49.9 HZ)			48 PHY 85 GEN (49.9 HZ)	48 PHY 85 GEN (49.9 HZ)	48 PHY 85 GEN (49.9 HZ)	48 PHY 85 GEN (47.9 HZ)
SHUTTLE	812 PHY		25 PHY 200 GEN (42.4 HZ)	25 PHY 200 GEN (42.4 HZ)			25 PHY 200 GEN (42.4 HZ)	25 PHY 200 GEN (42.4 HZ)	200 GEN (39.9 HZ)	300 GEN (67.4 HZ)
SYSTEM MODES USED	384 (60.0 HZ)		339 (50.0 HZ)	296 (42.3 HZ)	200 (25.1 HZ)		200 (25.1 HZ)	200 (25.1 HZ)	200 (25.1 HZ)	200
DOF										
349 +Y SA ANTENNA Z	4.249	4.360	4.360	4.360	4.003	4.003	4.360	4.077	4.020	4.090
350 +Y SA ANTENNA Y	2.944	2.950	2.950	3.004	2.752	2.752	3.004	2.805	2.757	2.470
381 NODE 1011 Z	2.895	2.887	2.887	2.953	2.924	2.924	2.953	2.948	2.929	3.001
382 NODE 1011 Y	1.382	1.381	1.381	1.411	1.344	1.344	1.411	1.351	1.337	1.135
215 PROPELLANT Z	1.265	1.266	1.266	1.260	1.261	1.261	1.260	1.259	1.261	1.409
216 PROPELLANT Y	.353	.353	.353	.353	.355	.355	.353	.357	.355	.333
217 PROPELLANT X	3.079	3.077	3.077	3.082	3.078	3.078	3.082	3.081	.355	2.991





METHODS STUDY
LTM RECOVERY COMPARISON

CHART 10

COMPONENT DEFINITION	APPROACH	K&M	K&M	K&M	CRAIG-BAMPTON	CRAIG-BAMPTON	CRAIG-BAMPTON	MACNEAL	CLASSICAL FREE-FREE
IUS AND ASE	210 PHY				210 PHY	210 PHY	210 PHY	210 PHY	50 GEN
SC	48 PHY				48 PHY	48 PHY	48 PHY	48 PHY	48 PHY
	85 GEN (49.9 HZ)				85 GEN (49.9 HZ)	85 GEN (49.9 HZ)	85 GEN (49.9 HZ)	85 GEN (49.9 HZ)	85 GEN (49.9 HZ)
SHUTTLE	812 PHY				25 PHY	25 PHY	25 PHY	200 GEN	300 GEN (67.4 HZ)
SYSTEM MODES USED	384		339	200	200 GEN (42.4 HZ)	200 GEN (42.4 HZ)	200	200	200
	(60.0 HZ)		(50.0 HZ)	(25.1 HZ)	(42.3 HZ)	(25.1 HZ)	(25.1 HZ)	(25.1 HZ)	(25.1 HZ)
LTM ROW	1200 Fx	1765	1765	1767	1761	1763	1763	1768	1391
	1201 Fy	650	650	648	655	651	651	647	433
	1202 Fz	4135	4136	4131	4137	4137	4137	4131	2629
	1203 Mx	34496	34496	34349	34650	34432	34432	34291	25527
	1204 My	61946	61939	62181	62028	62212	62212	62217	61348
1205 Mz	11201	11180	11516	11704	11718	11718	11516	6578	
Separation Plane	6089	6089	6075	6073	6073	6067	6067	6079	6750
	1812	1812	1819	1819	1819	1829	1829	1818	1629
	14722	14722	14688	14719	14719	14708	14708	14686	14241
	106788	106787	106600	107415	107149	107149	107149	106535	89116
	251294	251301	251732	250860	251071	251071	251071	251924	286571
Base of TRW Adaptor	29898	29505	29037	30237	30237	29021	29021	29041	32584
	6089	6089	6075	6073	6073	6067	6067	6079	6750
	1812	1812	1819	1819	1819	1829	1829	1818	1629
	14722	14722	14688	14719	14719	14708	14708	14686	14241
	172255	172253	172299	173142	173142	173216	173216	172205	147695
1216 My	471187	471193	471199	470242	470068	470068	471517	529919	
1217 Mz	29898	29505	29037	30237	30237	29021	29041	32584	



Rockwell International
Space Division



MacNeal's Method
of
Component Representation for Modal Synthesis
As Employed at Rockwell International/Space Division
for Shuttle Payload Analyses

by M. A. Martens

The shuttle liftoff or landing vehicle, exclusive of the payload, is treated as one component which, for the synthesis of system modes, is represented in the form described by MacNeal. Each payload component is represented in any convenient form which contains the orbiter-to-payload boundary degrees of freedom in physical coordinates (usually Craig-Bampton or physical stiffness and mass).

Rubin's extension to MacNeal's method is not used because, for the specific problem at hand, improvement in results sufficient to justify the increased cost have not been observed in our investigations. However, Rubin's paper (reference 1) provides a lucid explanation of the basic method and should be referred to for a more thorough development of this method. The equation numbers in this paper refer to the corresponding equations in the reference paper, though the inertial and dissipative terms have been deleted here.

Basically, the component is described by a subset of its free-free modes. However, to partially account for the degradation in the mathematical representation caused by modal truncation, the flexibility terms corresponding to the discarded modes are computed and included in the component representation. These residual flexibility terms (G_p) are found as the difference between the total flexibility (G) and the flexibility matrix (GN) obtained from the generalized stiffness matrix.

$$G_p = G - GN \quad (24)$$

Since the component is in an unconstrained state, special consideration must be given to obtain the "freed" total flexibility matrix. It has been shown that it may be computed from the rigid body modes (ϕ_R), physical mass matrix (M), and physical flexibility matrix (G_c). G_c is obtained by inverting the physical stiffness matrix with any arbitrary set of statically determinant constraints applied. Assuming the component eigenvectors are normalized to unit generalized mass, the total flexibility may be found as:

$$G = A^T G_c A \quad (21)$$

where

$$A = I - M \phi_R \phi_R^T \quad (17)$$

The G_N matrix may be found by inverting the non-zero diagonal partition (K_N) of the generalized stiffness matrix and transforming it back to physical coordinates.

$$GN = \phi_N K_N^{-1} \phi_N^T \quad (24)$$

The N partitions of the generalized stiffness and modal matrices refers to those partitions corresponding to all retained flexible body modes.

With these equations, G_p may be computed. The component may now be represented with a mass and stiffness matrix expressed in a coordinate system consisting of the selected free-free component modes (Q) and the physical boundary degrees of freedom (U_b), such that the equation for eigenanalysis is as follows:

$$\begin{bmatrix} K_Q + \phi_b^T G_{P_{bb}}^{-1} \phi_b & -\phi_b^T G_{P_{bb}}^{-1} \\ -G_{P_{bb}}^{-1} \phi_b & G_{P_{bb}}^{-1} \end{bmatrix} \begin{Bmatrix} Q \\ U_b \end{Bmatrix} + \begin{bmatrix} M_Q & 0 \\ 0 & 0 \end{bmatrix} \begin{Bmatrix} \ddot{Q} \\ \ddot{U}_b \end{Bmatrix} = \begin{Bmatrix} 0 \\ F_b \end{Bmatrix} \quad (30)$$

where

$M_Q = I$ (assuming modes normalized to unit generalized mass)

$K_Q =$ Generalized stiffness

$\phi_b =$ Partition of modal matrix containing the rows corresponding to boundary freedoms for all retained modes.

$G_{P_{bb}} =$ Boundary partition of residual flexibility matrix (square, symmetric).

This component representation is combined with the equations for all other components, adding equations in the same unknown (U_b) in direct stiffness fashion. The boundary loads sum to zero. Eigenvalues (λ^*) and eigenvectors (Q^* , U_b^*) are extracted in the usual manner from the system equations. At this point, the transient solution could be performed by passing the non-boundary applied loads through two coordinate transformations and the boundary loads through one. The residual flexibility terms would appear in the transformations. A more convenient approach is to transform the system modes back to the physical coordinate system before the transient solution. In order to obtain the non-boundary terms (subscript i = interior or non-boundary) of the system modes in the physical coordinate system,



the residual flexibility gives rise to additional terms in the transformation equation:

$$U_i^* = \phi_i Q^* + G_{Pib} G_{Pbb}^{-1} [U_b^* - \phi_b Q^*] \quad (32 \ \& \ 33)$$

Once the U_i^* and U_b^* portions of the system modes are available, the transient solution may proceed exactly as if these modes had been obtained without the use of a synthesis method.

In order to employ this method of component representation, inspection of equations 30, 32, and 33 reveals that the only component data required are the retained free-free modes, the corresponding generalized stiffness and mass matrices, and the columns of the residual flexibility matrix that correspond to the boundary degrees of freedom. Considerable savings can be achieved in the multiplication operations of equations 21 and 24 by computing only the required columns of the residual flexibility matrix.

Reference 1: Rubin, S., "Improved Component-Mode Representation for Structural Dynamic Analysis," AIAA Journal, Volume 13, Number 8, August 1975, pp. 995-1006.

M. Martens, 6/78

TIME-DOMAIN DATA ANALYSIS- A
PROMISING NEW TECHNIQUE

By

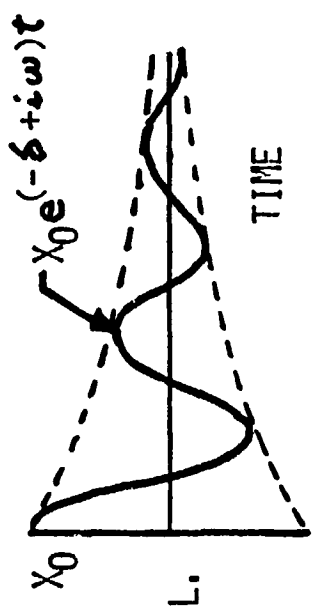
BRANTLEY R. HANKS

NASA LANGLEY RESEARCH CENTER

FREE DECAY TESTING

The ideal way to conduct modal tests on structural systems is by free decay following an initial impulse or displacement. This excitation method is free of forcing function distribution and loading effects as well as errors in forcing function wave form. However, complex structures have complicated free-decay responses which are difficult to analyze for modal content.

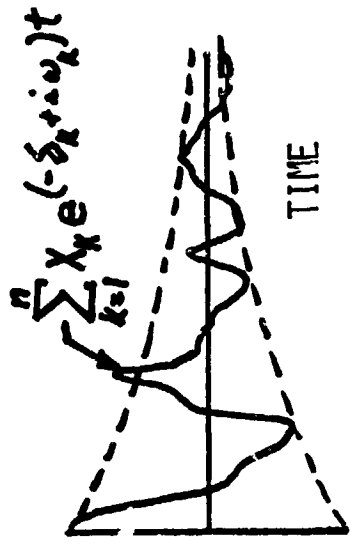
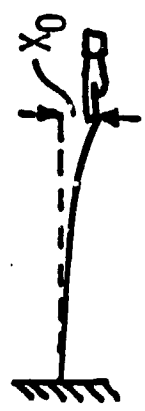
FREE-DECAY TESTING



AMPL.



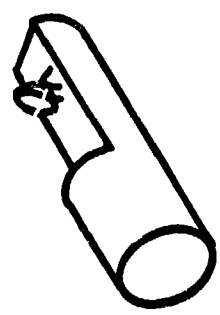
SIMPLE STRUCTURE



AMPL.



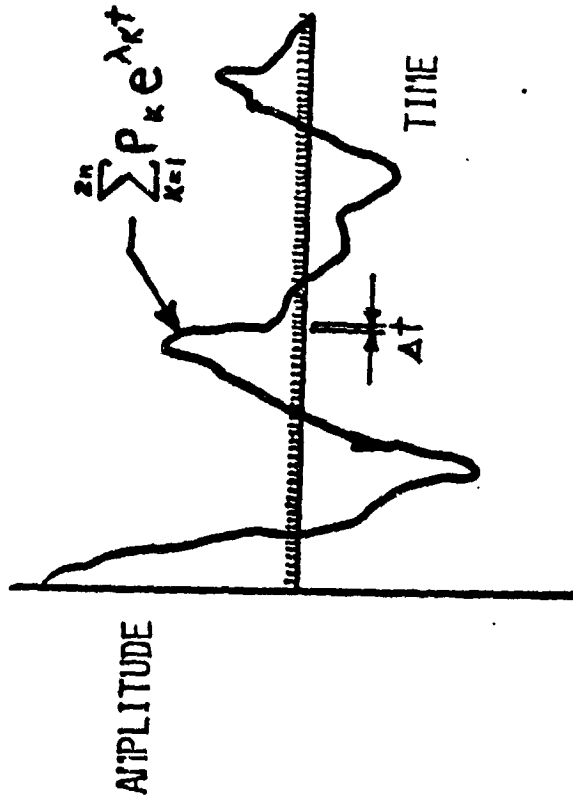
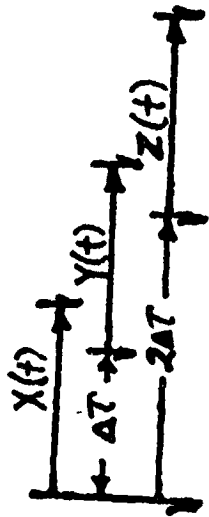
COMPLEX STRUCTURE



A NEW WAY OF ANALYZING FREE DECAY DATA

A method has been developed by S. R. Ibrahim of Old Dominion University, Norfolk, Virginia, for analyzing free-decay data for complex structures. The method analyzes blocks of sampled data from free-decay responses during three different segments of the decay signal. The three data blocks are of equal length but separated in time by some time, ΔT . They are arranged in a matrix format as shown to obtain an eigenvalue problem. The solution to this eigenvalue problem gives frequencies, damping, and mode shapes. There are no assumptions on spacing of modes (provided they are not duplicated exactly) or on magnitude of damping in the analysis.

A NEW WAY OF ANALYZING FREE-DECAY DATA
(IBRAHIM'S METHOD)



- STEPS:
1. ASSUME DATA FOLLOWS EQUATION SHOWN
 2. OBTAIN THREE SETS OF SAMPLED DATA X, Y, AND Z

3. FORM EIGENVALUE PROBLEM

$$\begin{bmatrix} Y \\ X \end{bmatrix} \begin{bmatrix} X \\ Y \end{bmatrix}^{-1} \begin{Bmatrix} P_k \\ Q_k \end{Bmatrix} = e^{\lambda_k \Delta t} \begin{Bmatrix} P_k \\ Q_k \end{Bmatrix}$$

WHERE Q_k IS $P_k e^{\lambda_k \Delta t}$

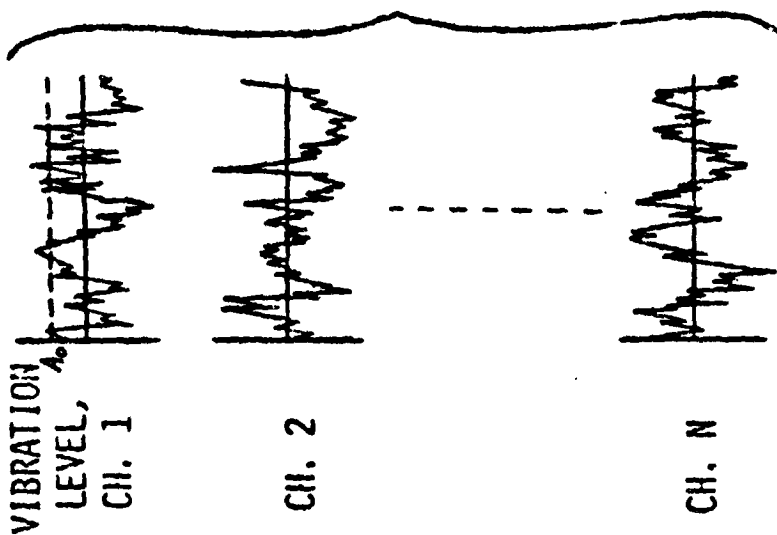
4. EIGENSOLUTION GIVES λ_k AND P_k FROM WHICH MODAL PARAMETERS ARE OBTAINED

TIME DOMAIN ANALYSIS OF RANDOM DATA

In cases where random excitation is present, free-decay responses can be obtained by the random decrement procedure. This consists of choosing some arbitrary "trigger" level (A_0) at which data sampling begins on a reference measurement (Channel 1). Each time the response passes through this level, with either positive or negative slope, a new sampling begins. A series of time responses for a single measurement is obtained each of which has a starting point at the trigger level. Adding these responses has the effect of cancelling random content, negative slopes cancel positive ones, and the result is an equivalent step input of level A_0 to the system. Remaining measurements are treated in the same manner with the start of each sampling controlled by the reference channel. A set of properly phased step input responses are obtained which can then be analyzed by the time domain method. By this procedure, no measurement of input force is necessary to obtain damping and, hence, the method is applicable to random flight data as well as laboratory data.

TIME DOMAIN ANALYSIS OF RANDOM DATA

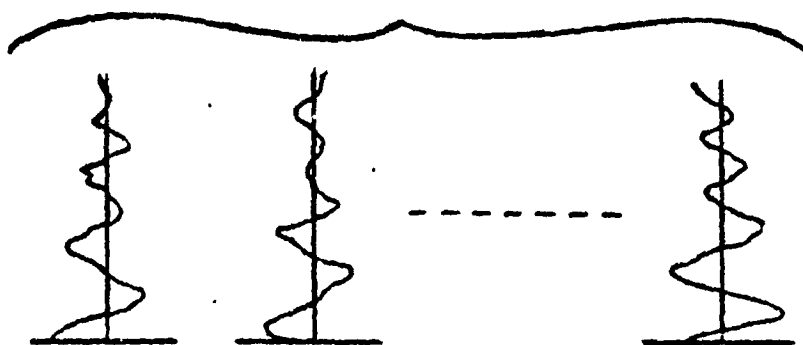
RANDOM FLIGHT RESPONSE



MULTI-CHANNEL
RANDOM
DECREMENT
ANALYSIS



DERIVED FREE RESPONSE



TIME
DOMAIN
ANALYSIS

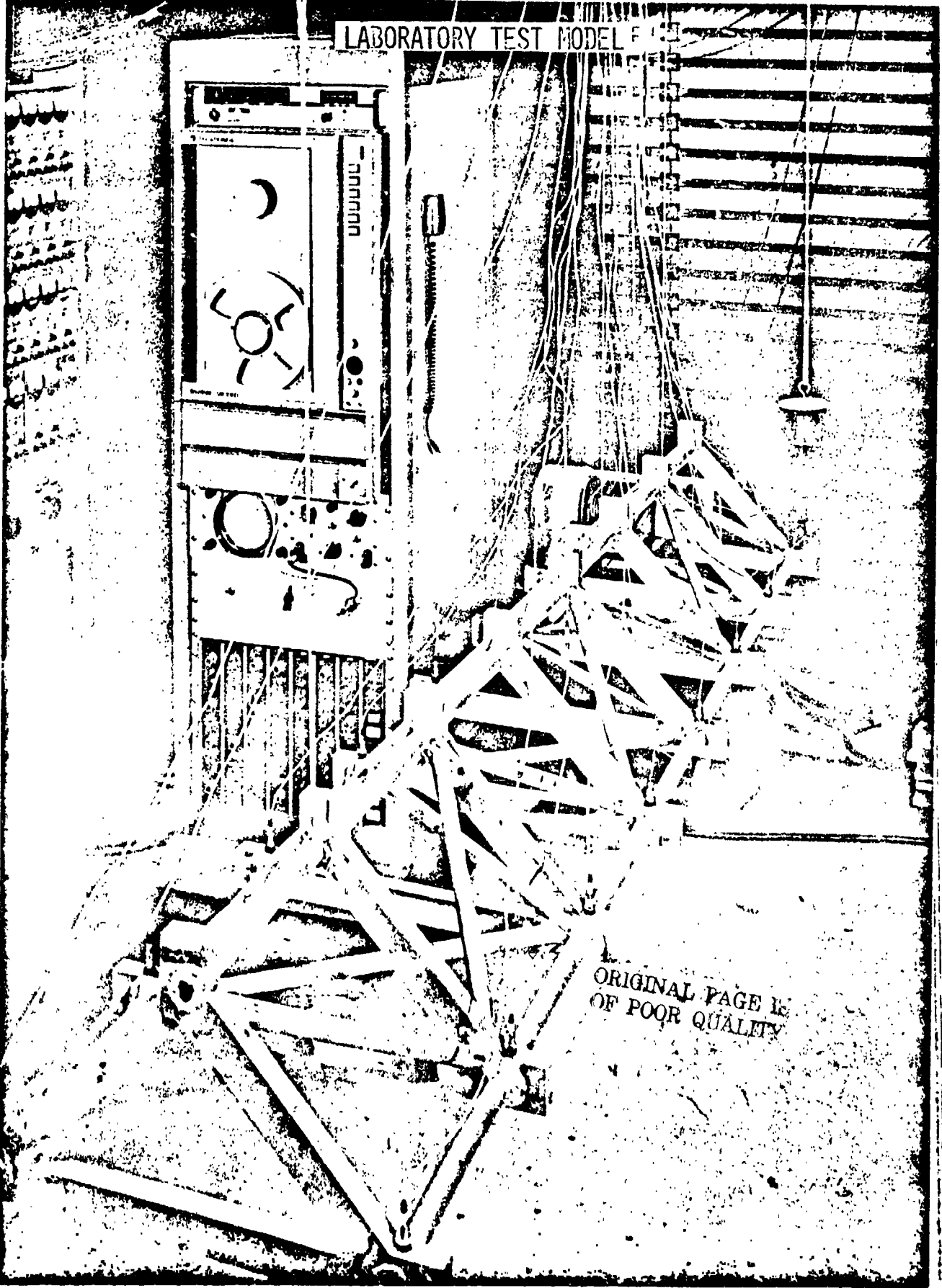


COMPLETE DYNAMIC
CHARACTERIZATION
WITHOUT INPUT
MEASUREMENT

LABORATORY TEST MODEL

The Ibrahim time domain modal data analysis method was first evaluated on a simple truss-type laboratory model shown in the figure. This model had been analyzed using NASTRAN and had been previously tested using a variety of sine and Fast Fourier Transform modal test methods. For the time domain tests, random excitation was applied at one end and then power to the exciter was cut and the motion allowed to decay out. Data was recorded during both random and free decay portions of the test. The time domain analysis method was applied to the data in both random decrement and free decay forms.

LABORATORY TEST MODEL



ORIGINAL PAGE IS
OF POOR QUALITY

MODAL FREQUENCIES - COMPARISON OF METHODS ON TEST MODEL

This chart shows a comparison of natural frequencies obtained on the laboratory test model by six test approaches and by NASTRAN analysis. Agreement is very good in all cases indicating that the two time domain methods are at least as accurate as other accepted methods. It is important to note that the time domain analysis used only 0.5 seconds of data in the free decay case and 2 seconds in the random decrement case. Damping and mode shape agreement among the methods was also very good.

MODAL FREQUENCIES - COMPARISON OF METHODS ON TEST MODEL

METHOD MODE ↗	NASTRAN	RESONANT DWELL	HARD-WIRED FFT (SWEEP)	TRANSIENT FFT SOFTWARE	RANDOM FFT SOFTWARE	FREE DECAY	RANDOM DEC/ FREE DECAY
1ST BENDING	73.4	74.6	74.4	74	74.1	74.2	74.2
1ST TORSION	80.1	79.7	78.8	79	78.8	78.7	78.8
1ST BEND (YAW)	117.3	120.7	119.4	119.5	119.6	119.9	120.3
2ND TORSION	158.9	158.5	156.9	156.5	156.5	156.6	156.6
2ND BENDING	159.2	163.1	161.9	161.5	161.6	162.0	161.8
3RD TORSION	218.8	219.1	216.9	216.5	216.5	216.5	216.5
3RD BENDING	244.7	246.7	245.0	244.5	245.0	245.0	245.0
2ND BEND (YAW)	253.1	263.2	261.2	261.0	261.0	259.6	260.7
4TH TORSION	284.1	283.7	281.3	280.5	281.0	281.0	280.8
4TH BENDING	314.9	316.3	325.0	324.5	325.0	325.3	325.3

VOYAGER PAYLOAD IN MODAL TEST SETUP

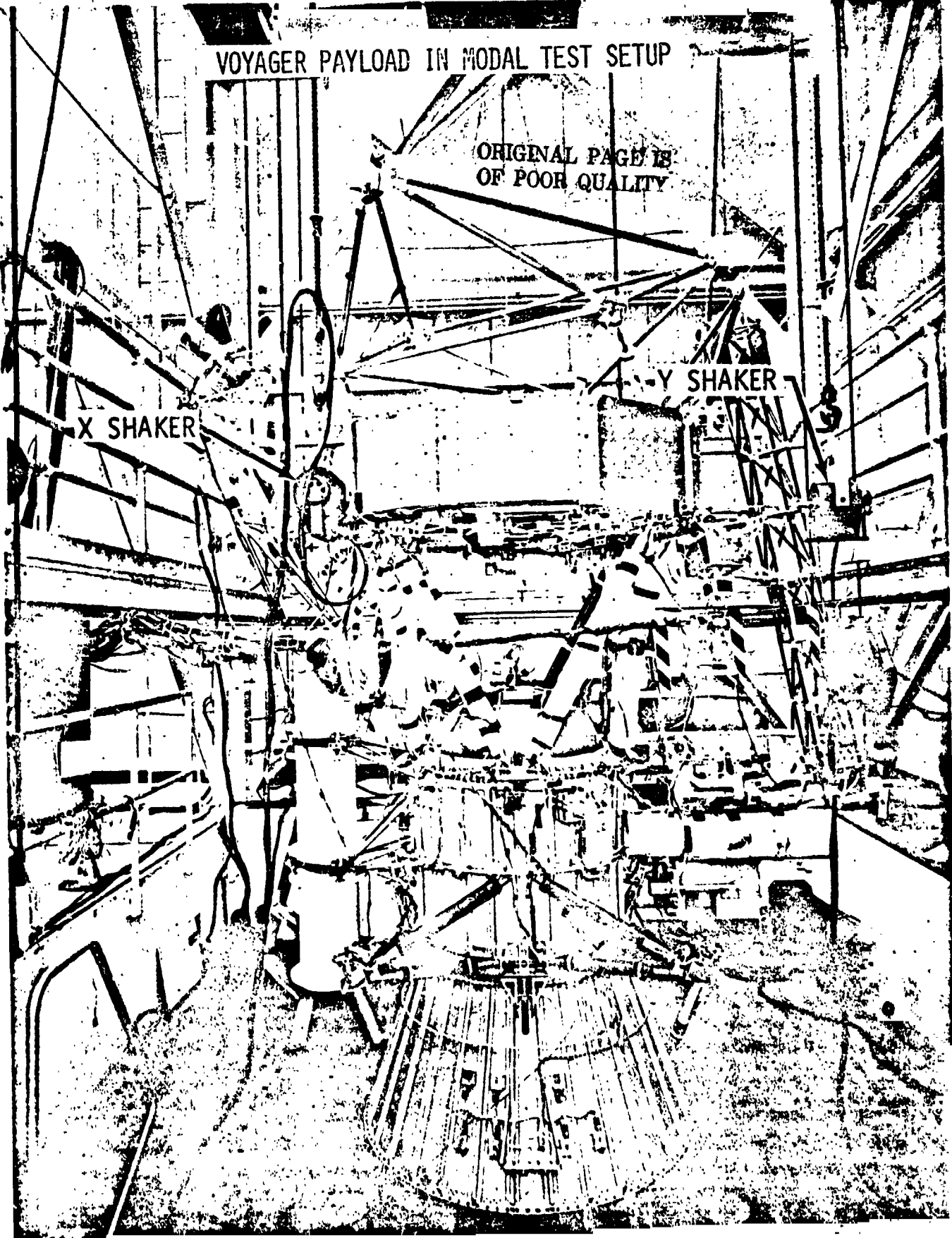
In order to evaluate the time domain test method in a more realistic case, random-excitation modal test data for the Voyager Jupiter/Saturn payload was obtained from the Jet Propulsion Laboratory (JPL). This data had previously been analyzed by JPL using an FFT analysis and compared with results of multiple shaker sine dwell tests. In order to provide a control for comparison of the time domain method with the previous methods, an additional FFT analysis was conducted at the Langley Research Center using the same data tapes used in the time domain analysis.

VOYAGER PAYLOAD IN MODAL TEST SETUP

ORIGINAL PAGE IS
OF POOR QUALITY

X SHAKER

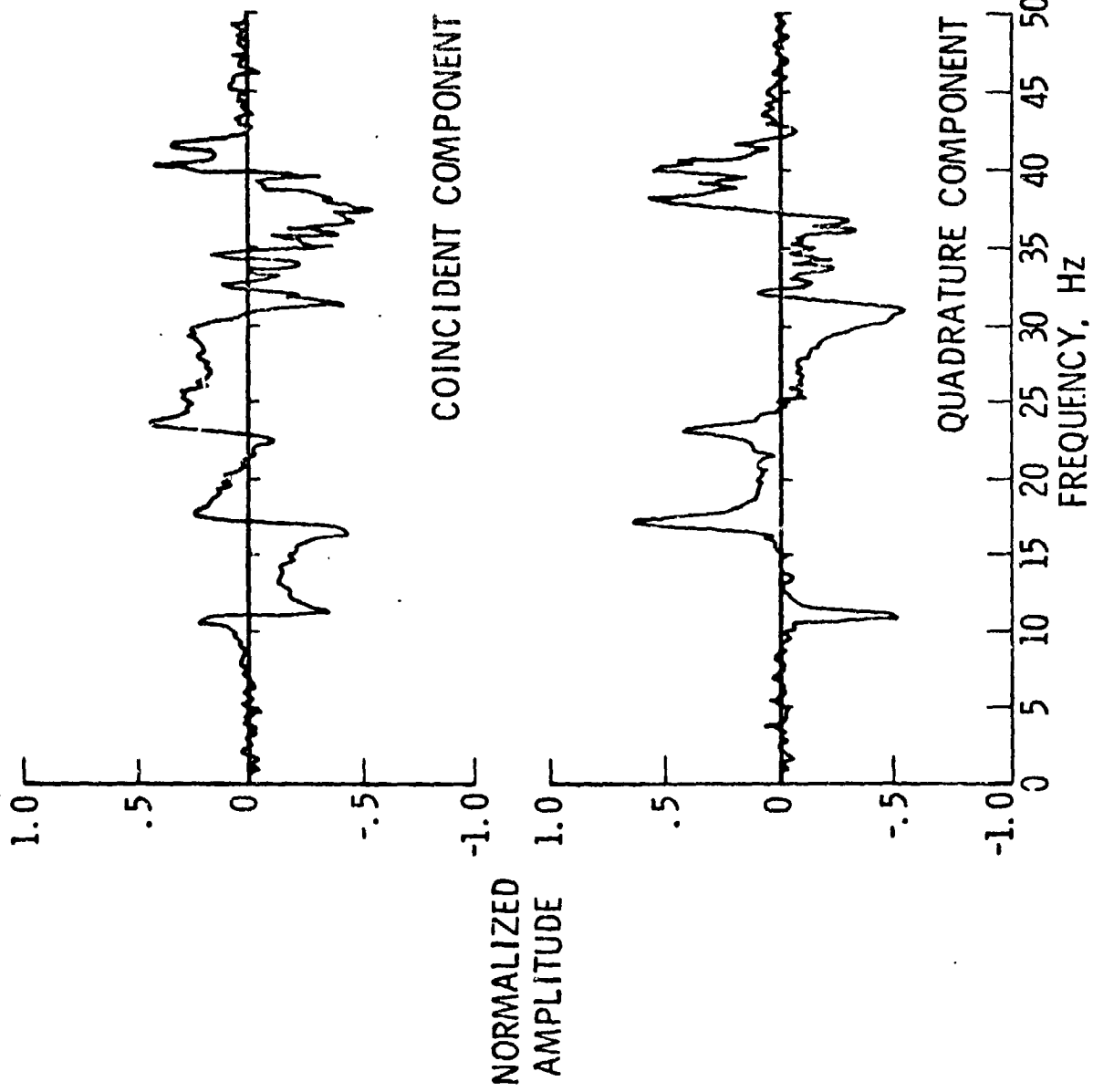
Y SHAKER



TYPICAL TRANSFER FUNCTION FOR VOYAGER PAYLOAD

This figure shows a typical transfer function obtained in FFT analysis of random data from the Voyager payload. The data is relatively clean below 20 Hz, begins to show some questionable shapes between 20 and 30 Hz indicating the possibility of buried modes, and between 30 and 45 Hz exhibits a considerable number of peaks which may or may not be modes. Visual examination of transfer functions from 26 measurements was used to detect strong clear peaks identifying modes in the control FFT analysis. The time domain analysis automatically selects the number of modes during the identification procedure.

TYPICAL TRANSFER FUNCTION FOR VOYAGER PAYLOAD



COMPARISON OF MODAL FREQUENCIES

This table shows the modal frequencies and mode description for the Voyager payload obtained by four different test and/or data analysis methods--the multiple point sine dwell (MPSD) tests, single point random (SPR) analysis at JPL and Langley Research Center (LRC), and the Ibrahim time domain (ITD) analysis. Agreement is generally good where the same modes are identified. The ITD method identified more modes than the others. A variety of subsequent studies of SPR data indicated that the additional modes identified by the ITD method are probably in the data either as weakly-excited modes or periodic noise. About 20 seconds of data was used in the ITD analysis, and the complete analysis process required 4 days as compared to several weeks for the other methods.

COMPARISON OF MODAL FREQUENCIES

<u>MODE NO.</u>	<u>MPSD</u>	<u>SPR-JPL</u>	<u>SPR-LRC</u>	<u>ITD</u>	<u>MODE DESCRIPTION</u>
1	10.5-10.7	10.92	10.97	10.95	1ST BENDING, Y
2	10.9-11.3	11.29	11.19	11.19	1ST BENDING, X
3	17.1-17.2	17.25	17.18	17.25	1ST TORSION
4	20.8		21.50	21.80	RTG
5				23.12	2ND TORSION + LECP
6	22.6-23.5	23.37	23.25	23.30	2ND TORSION
7				24.10	2ND TORSION + MAGNETOMETER
8	25.4-26.2			25.13	2ND BENDING, X
9	26.5-27.2	26.21	26.42	26.05	2ND BENDING, Y
10	27.3		27.97	27.81	SCAN PLATFORM, AXIAL
11			30.83	30.92	ANTENNA, Z
12	31.1	30.81	31.57	31.56	3RD BENDING, Y + ANTENNA
13		32.81	32.80	32.50	3RD BENDING, X
14				32.98	3RD TORSION
15				33.96	LECP, RTG TORSION
16				34.74	SCAN PLATFORM, X
17	35.2			35.94	RTG, X
18			37.09	36.81	SCIENCE APPENDAGE, X
19			38.70	38.75	SCIENCE APPENDAGE, X, ANTENNA
20				39.14	SCIENCE APPENDAGE, X, Z ROTATION
21	39.6-40.3	40.04	39.39	40.24	SCIENCE APPENDAGE, X
22			40.77	40.64	SCIENCE APPENDAGE, X
23		42.13	42.20	42.21	ANTENNA ROTATION, X
24				44.59	TANK ROT., SCIENCE APPENDAGE
25		44.80	44.80	44.80	HYDRAZENE TANK ROTATION
26	46.3		45.60	45.65	1ST AXIAL
27				48.04	TANK, APPENDAGE
28	52.9			50.69	RTG, SCAN PLATFORM, Z

COMPARISON OF DAMPING RATIO

This chart shows a comparison of damping ratio obtained for the modes of the previous table using the different test/data analysis methods. Agreement between the time domain analysis and the other methods is reasonable in most cases. A large error shown in mode 2 was traced to DC drift on the data. The very low damping of mode 5 was borne out by subsequent inspection of transfer functions. Modes 8, 9, and 10 show high damping in the ITD analysis. Subsequent observation of transfer functions produced neither proof or disproof of these values in light of the presence of other nearby modes.

COMPARISON OF DAMPING RATIO

<u>MODE NO.</u>	<u>MPSD</u>	<u>SPR-JPL</u>	<u>SPR-LRC</u>	<u>ITD</u>
1	.012-.015	.013	.020	.016
2	.012-.015	.024	.019	.069
3	.026-.031	.027	.033	.024
4	.027-.032		.030	.031
5				.002
6	.015-.023	.023	.025	.024
7				.021
8	.015-.018			.092
9	.011-.028	.016	.018	.100
10	.013-.014		.019	.061
11			.028	.019
12	POOR WAVE FORM	.029	.025	.021
13		.031	.034	.036
14				.030
15				.024
16				.023
17	.018-.022			.070
18			.026	.022
19			.040	.029
20				.047
21	.011-.016	.016	.030	.023
22			.017	.012
23		.003	.002	.001
24				.012
25		.008	.008	.009
26	.026-.036		.010	.018
27				.024
28	.012			.013

COMPARISON OF MODE SHAPES

This table shows a comparison of the mode shape for mode 2 for the different methods. The ITD method agrees reasonably well with the others. It should be noted that the ITD method suffered a significant disadvantage in this comparison because of inappropriate data for this type of analysis. The data was recorded in five groups with no common acceleration measurement between them as required for the ITD analysis. Hence, an undetermined phase and amplitude relationship existed between them. This relationship was estimated for the ITD analysis based on SPR analyses which used input force as the common measurement between data groups.

COMPARISON OF MODE SHAPES, MODE 2, X EXCITATION, X RESPONSE

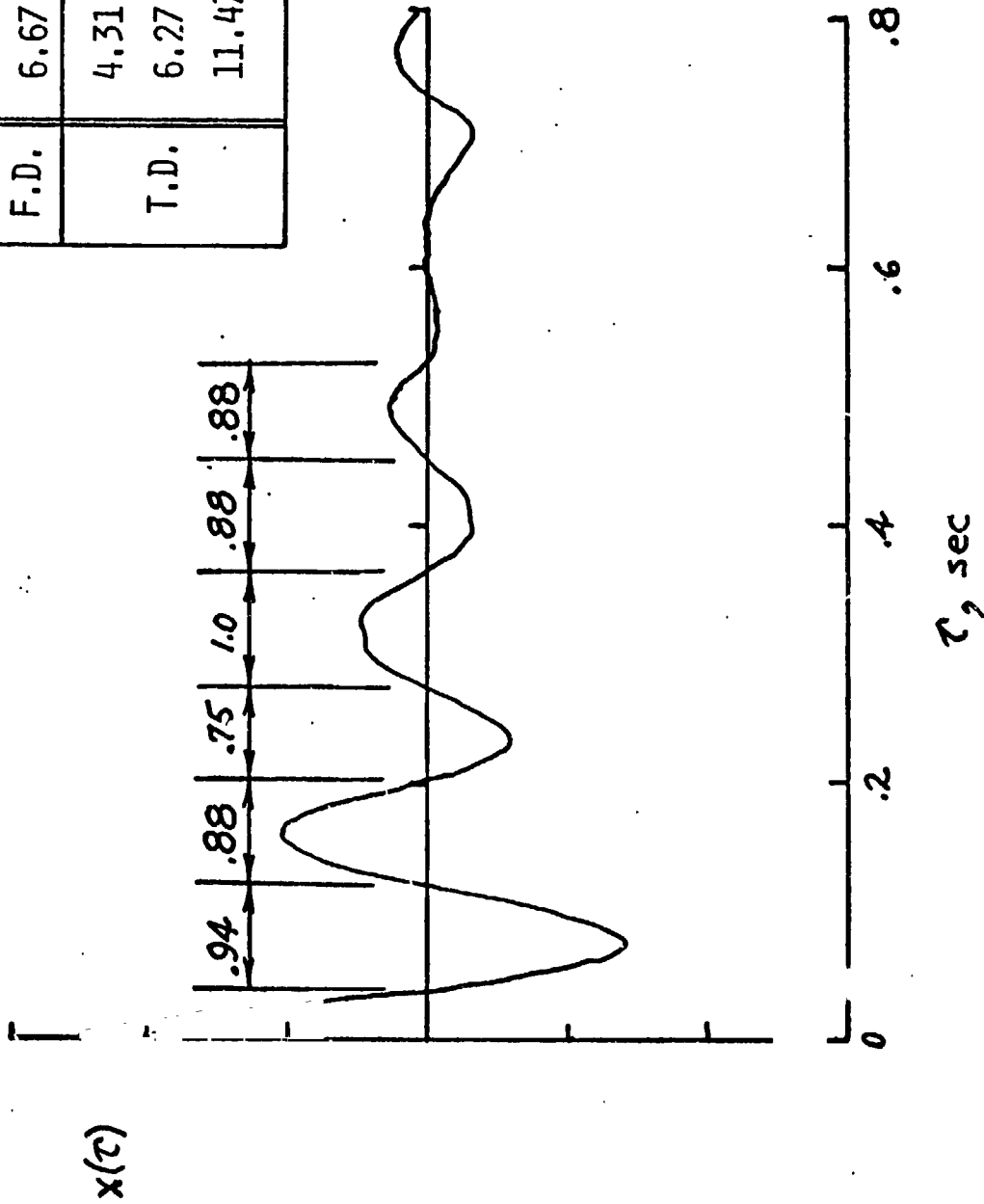
MEAS. No.	MEAS. DIR.	MPSD (10.9 Hz)		SPR-JPL (11.2 Hz)		SPR-LRC (11.2 Hz)		IID (11.1 Hz)	
		AMPL.	PHASE	AMPL.	PHASE	AMPL.	PHASE	AMPL.	PHASE
2	X	.532	0	.515	6	.574	-6	.351	3
4	X	1.000	0	1.000	0	1.000	0	1.000	0
5	X,Y	.348	-180	.459	176	.520	182	.469	-154
6	X	.526	-180	.515	176	.524	-182	.533	180
8	X	.648	1	.633	4	.661	-1	.661	-1
11	X,Y	.571	-179	.493	173	.441	-179	.841	163
13	X	.010	-99	.016	64	.014	65	.039	104
15	X,Z	.126	-183	.170	-178	.174	-185	.122	196
16	X,Y,Z	.299	177	.314	-179	.321	172	.321	172
17	X	.348	179	.341	-177	.341	-180	.283	63
19	X	.470	182	.487	-175	.490	-179	.490	-179
20	X	.148	179	.153	181	.148	-180	.215	-174
23	X,Y	.286	182	.257	-179	.228	-175	.417	-188
24	X	.834	-183	.816	-175	.575	-177	.575	-177
25	X,Y	.009	-172	.068	-15	.045	-19	.167	-116
26	X,Y	.042	-178	.047	-65	.024	-81	.025	107

TIME DOMAIN ANALYSIS OF FLIGHT DATA - B-1 HORIZONTAL TAIL

This figure shows the free decay response of the B-1 horizontal tail obtained by random decrement analysis of flight data. It appears to be a relatively clean single-mode response. However, closer inspection shows the period of each half cycle varies by as much as 33 percent indicating more than one frequency in the data. A frequency domain analysis yielded one frequency whereas the time domain method yielded three prominent ones.

TIME DOMAIN ANALYSIS OF FLIGHT DATA
B-1 HORIZONTAL TAIL

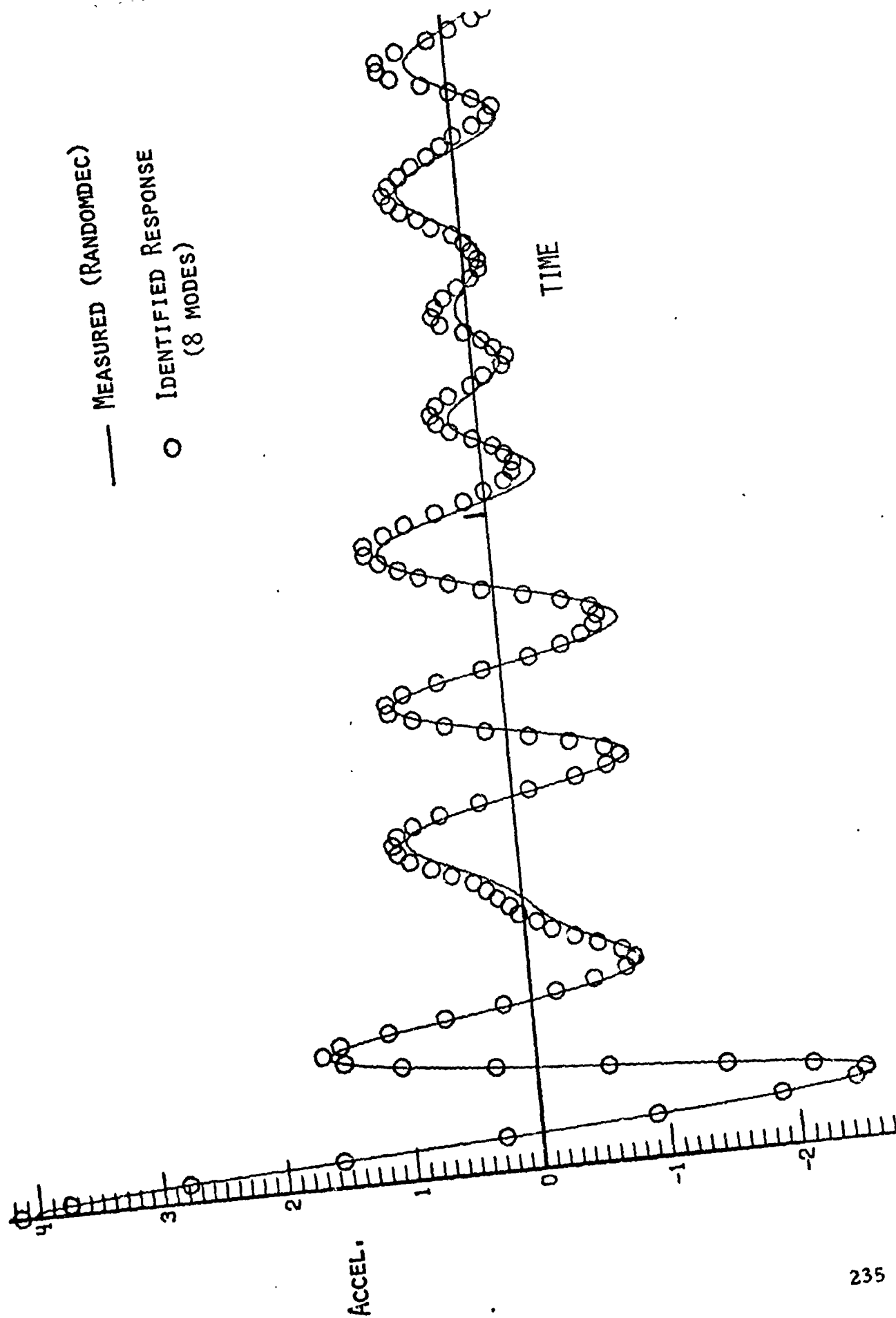
	FREQ.	DAMPING
F.D.	6.67	0.102
T.D.	4.31	0.068
	6.27	0.140
	11.47	0.031



COMPARISON OF TIME DOMAIN ANALYSIS WITH FLIGHT DATA - B-1 VERTICAL TAIL

A similar analysis of flight data from the vertical tail of the B-1 was conducted using the Ibrahim random decrement time domain method. Eight modes were identified. The identified frequencies and damping values were then curve fit to the original data obtaining the agreement shown in the figure. This curve fit procedure produces modal contribution factors which can be used for assessing prominence of modes in the response.

COMPARISON OF TIME DOMAIN ANALYSIS WITH FLIGHT DATA
B-1 VERTICAL TAIL



A COMPARISON OF TEST TECHNIQUES
USED DURING MODAL TESTING OF
ET LOX TANK

PRECEDING PAGE BLANK NOT FILMED

G. D. JOHNSTON
HOUSTON M. HAMMAC
A. D. COLEMAN

DYNAMICS TEST BRANCH
MARSHALL SPACE FLIGHT CENTER
HUNTSVILLE, AL 35812

PAPER PRESENTED AT THE
PAYLOAD FLIGHT LOADS PREDICTION METHODOLOGY WORKSHOP
MARSHALL SPACE FLIGHT CENTER
NOVEMBER 14-15, 1978

A COMPARISON OF TEST TECHNIQUES USED DURING
MODAL TESTING OF ET LOX TANK

G. D. Johnston, Houston M. Hammac, A. D. Coleman, NASA/MSFC

This presentation will briefly show the results of test data obtained from the modal test of the ET Lox Tank. A comparison will be made of data obtained using Multi-Point Sine tuning of modes with data obtained from Single-Point Random tests for the same condition. For the purpose of this presentation, only the liftoff condition will be used to make this comparison. A more detailed comparison of the remaining conditions and description of the test setup will be made in the published article.

This test was a major link in the verification chain of hydro-elastic analysis and test technique, and the results are being used to mathematically predict the modal characteristics of the entire External Tank. The general objective of this test program was to determine the symmetric and anti-symmetric hydro-elastic modal properties of a flight configuration test article. Specifically, the program was performed to experimentally determine vibrational frequencies, mode shapes, damping, and modal energy distribution of targeted modes selected from the pre-test analysis.

The test article consisted of a Support Ring, Intertank, and Lox Tank. Figure 1 shows the test article in Condition 1. The supporting special test equipment consisted of the Access Structure, Air Suspension System, Chromate Water Transfer System, the Pressure-Purge and Vent System, Shaker System, Digital Control System, and Data Acquisition system. The Access Structure and Air Suspension System are shown in Figure 1. A closeup view of one air bag pad is shown in Figure 2. Figure 3 is a schematic of the air suspension system. Figure 4 is a schematic of the Chromate Water Transfer System. Sodium mono-chromate was used as a corrosion inhibitor. The concentration was maintained between 200 and 350 parts per million. Figure 5 is a schematic of the Pressure-Purge and Vent System. The ullage pressure was maintained at 3.3 psig \pm 1.7 psig throughout the test except when the 1.6 psig and 8.0 psig condition were performed. Figure 6 shows the Digital Control System and Figure 7 is a portion of the Data Acquisition System.

One major feature of this test setup was the ability to cant the test article as much as thirteen degrees from vertical. This discussion will be limited to Condition 1 (0° cant and 487 inches of fluid with 3.3 psig ullage pressure). All of the test conditions where modal data were obtained are shown in Table 1.

A half-tank finite element model of the test article was generated for the analyses by the Martin Marietta Corporation. The choice of the half-tank was permitted by a convenient plane of symmetry and was required by the time and size constraints in the computer analysis that was performed. A detailed listing of the modal grid and finite elements used can be found in Appendices A and B of the MMC report number MMC-ET-SE21-5 dated

October 6, 1978. The model incorporated the structural elements of the Lox Tank, intertank, load ring, air support system, and the fluid. The finite element computer programs used are part of the Martin Marietta Aerospace Library known as FORMA. A detailed description of the modeling methods used and analysis procedure are found in Sections 4.0 and 5.0 of the MMC report number MMC-ET-SE21-5 dated October 6, 1978.

The Test Requirements Specification (MMC-ET-TM07) specified thirteen shaker positions as shown in Figure 8. In past modal tests, it has been the policy of MSFC to select force input points at those locations where mechanically induced energy is experienced by the structure to obtain direct transfer functions. An additional shaker position was added at the + Y Solid Rocket Booster attach point. This shaker position was selected to be the principal data point for the single point random excitation at the most critical condition of testing. The reasons for this decision were that 1) it would provide more direct transfer function data representing the SRB input, 2) it would provide a more complete data bank of modes for future analysis that possibly could be overlooked during multi-point sine testing, 3) it would provide an excellent opportunity to compare the two techniques and possibly improve on the current capability of single-point random testing. Also, it was deemed necessary to incorporate the single-point random capability because of the short period of time allowed, initially, for the entire test program. A total of three months was scheduled for all four conditions. It was reasoned that if one long delay was encountered after the test was started, single point random testing might be the only way data could be obtained for some of the final conditions. Single-point random data was obtained at three different input points during Conditions II and III. The driving points were at the ogive tip in the Z and Y directions and at the SRB crossbeam attach point on the + Y side of the Lox Tank.

This test did have a few "firsts" for MSFC. One, of course, is the first use of single-point random excitation to obtain modal data on a large scale structure. Another "first" was the canting of a large-liquid filled tank to 4° and 13° angles to obtain modal data. The cant angle did have dramatic effects on bulge modes and bending modes. These effects are covered in more detail in the test reports by MSFC and the MMC.

A modified Hewlett Packard Model 5451B digital system was used to perform the multi-point sine test. This system is shown in Figure 6 and contains a mini-computer and a fourier analyzer. It has the capability of controlling frequency, phase and amplitude of up to eight shakers simultaneously. It contains a 32 channel multiplexer to allow on-line recording of 32 force and acceleration measurements. At the beginning of a test condition, a wideband sweep would be performed at a single shaker position. From this sweep 31 transfer function plots were made to identify modal frequencies. These plots were of the real and imaginary values of each accelerometer. This process was repeated at several shaker locations to assure all modes

were identified. Narrowband sweeps in frequency steps of .01 hertz were performed where very high modal density was evident. Based on the sweep data and plots of the on-line data, shaker positions were selected to tune the targeted modes. To tune the modes, on-line measurements were monitored. Several parameters were used, but the principal ones were the Co-Quad values and the phase angle of these measurements. Lissajous and the driving point/acceleration phase angle was used in some cases. When the mode was tuned, all 202 accelerometers, driving point forces and fluid pressures were recorded on the Structural Data Acquisition System shown in Figure 7. After the data was recorded, a soft shaker dump was used to obtain modal decay data. The on-line measurements were recorded by the HP 5451B system and the damping calculations were made by curve fitting these decays automatically.

Single-point random tests were performed at the end of each test condition. Excitation for the SPR testing was provided by a Hewlett-Packard 5425 vibration control system. The drive spectrum was a shaped 5 to 50 hertz bandwidth ranging in composite force from 93 to 150 RMS force-pounds. Data was acquired with the same Hewlett-Packard 5451B modal system used to perform the MPS. Using the 32 channel multiplexer, all 202 measurements were recorded by seven sequential patchboards thru a patching matrix. Approximately thirty minutes of data were recorded of each measurement and stored on magnetic tape for later analysis.

The data was processed and analyzed employing a least squares curve fitting algorithm to obtain the mode shapes and modal coefficients. Tables II and III list the modal frequency and damping obtained from multi-point sine (MPS) and single-point random (SPR). It should be emphasized that due to insufficient time in the schedule, only one excitation point for single-point random was used to obtain data for Condition I. The only target modes not well matched with the multi-point sine data are three symmetric modes. All three unmatched modes have bending in the symmetric or Z Plane. Based on some of the analysis of data from Condition II, where three excitation points were used, the modal matching is even better.

A lot of shell modes are listed in the SPR column that do not appear in the MPS column. Again, due to insufficient time, the numerous shell modes could not be obtained using the MPS technique. This does, however, point out the great advantage of the SPR technique. The test article is now being installed for the static loads test, but we can continue investigating all the modes in the tank by curve fitting the data stored on tape.

The SPR data indicates excellent correlation with the MPS. The damping values agree very well and tend to verify that for this test condition the Lox Tank is a lightly damped structure. It must be realized that many of these modes will change and have considerably higher damping when the Lox Tank becomes an integral part of the Shuttle. There are two modes listed here, however, that will not be affected significantly

in the total assembly. In the opinion of the authors, the second and third bulge modes of the aft dome (12.76 and 18.95 hertz) will still have very low damping. These two modes are always the ones that present problems from the standpoint of 'POGO' and loads analysis. The second dome bulge mode was the strong POGO initiator in the Saturn V and Saturn IB vehicles. These modes should be observed carefully during MVGVT testing.

Appendix A contains a comparison of seven mode shapes corresponding to modal matches in Tables II and III. A more complete set of mode shapes will be published at a later date and will contain data from the remaining test conditions. Condition II presents some very interesting data because of the effect of the 13 degree cant angle. The math model did a reasonably good job of predicting the modes at the 13 degree attitude, but much more testing should be performed to assist in improving the math modeling techniques for in-flight cant angles.

<u>TEST CONDITIONS PERFORMED</u>					
<u>CONDITION</u>	<u>CANT ANGLE (DEGREES)</u>	<u>FLUID LEVEL (INCHES)</u>	<u>ULLAGE PRESS. (PSIG)</u>	<u>FLIGHT TIME (SECONDS)</u>	
* I	0	487	3.3	0	
* II	13	320.7	3.3	125	
* III	13	162	3.3	313	
IV	13	58	3.3	441	
* POST TEST	4	320.7	3.3	125	
POST TEST	0	320.7	1.6		
* POST TEST	0	320.7	3.3		
POST TEST	0	320.7	8.0		
POST TEST	0	384.5	3.3		
POST TEST	0	384.5	8.0		
POST TEST	0	218	3.3		
POST TEST	0	162	3.3		

* CONDITIONS THAT SINGLE-POINT RANDOM DATA OBTAINED

TABLE 1

ET LOX MODAL TEST DATA
COMPARISON OF FREQUENCY AND DAMPING
MULTI-POINT SINE VERSUS SINGLE POINT RANDOM

ANAL. MODE NO.	FREQUENCY, Hz			*DAMPING C/C _c		MODE DESCRIPTION
	ANAL.	MPS	SPR	MPS	SPR	
10	5.00	4.88	4.794	.016	.0032	M1, N2; SHELL (A)
12	4.75	4.90	4.969	.016	.0185	M1, N2; SHELL (S)
11	4.39		5.261		.0197	M1, N2; SHELL (S)
			5.655		.0155	
13	5.16	5.72	5.853	.022	.0158	M1, N0; BULGE (S)
			8.867		.0021	M1, N5; SHELL (S)
19	8.91	9.04		.011		M1, N1; BENDING (S)
29	9.68	9.18	9.192	.00319	.0026	M2, N3; SHELL (S)
16	8.93	9.48	9.407	.0067	.0057	M1, N1; BENDING (A)
		9.75	9.336	.020	.0122	M2, N7; SHELL (S)
			9.432		.0177	SHELL
			9.767		.0075	SHELL
26	12.96	12.76	12.748	** .00174	.00144	M2, N0; 2d SYS. BULGE
			12.832		.00238	SHELL & BULGE
			13.075		.00898	SHELL & BULGE, OGIVE
			13.332		.0010	SHELL, OGIVE
			13.650		.00535	SHELL & BENDING
22	12.79	13.73		.003		M2, N1; BENDING & SHELL
			13.798		.002	
27	13.17	14.08	14.057	.00165	.00338	M2, N1; BENDING (S)
			14.528		.0045	SHELL
			14.578		.0047	SHELL
			14.736		.0009	SHELL & OGIVE BULGE
			14.877		.0033	
			15.240		.0077	
			15.517		.00137	
			15.760		.00195	
			15.907		.0038	
			16.139		.0053	
			16.240		.0012	
32	15.30	16.54	16.603	.00323	.0030	; BENDING (S)
		16.56		.0029		DOMES BENDING & OGIVE SHELL
75	14.80	16.63	16.460	.0030	.0027	M3, N1; BENDING (A)
			16.950		.0079	SHELL

* ALL DAMPING VALUES ARE AVERAGE FROM ON-LINE MEASUREMENTS

** AVERAGE SYSTEM DAMPING. AFT DOME MEASUREMENTS INDICATE .11% DAMPING

TABLE II

ET LOX MODAL TEST DATA
COMPARISON OF FREQUENCY AND DAMPING
MULTI-POINT SINE VERSUS SINGLE POINT RANDOM

CONDITION I - 0° CANT, 487 INCHES FLUID LEVEL (LIFTOFF)

ANAL. MODE NO.	FREQUENCY, Hz			*DAMPING C/C _c		MODE DESCRIPTION
	ANAL.	MPS	SPR	MPS	SPR	
44	18.88	17.74	17.313	.0040	.0034	N2; DOME (S)
			17.563		.0078	
			17.679		.0014	
			17.864		.0020	
			18.082		.0017	
			18.316		.0161	
			18.464		.0033	
35	15.70	18.95	18.698	.0019	.0006	EXCELLENT MATCH; 3d SYS BULGE
			18.917		.0028	
			19.186		.0015	
43	18.81	19.29	19.491	.0015	.0015	M3, N1; BENDING (S)
			19.659		.0114	
36	19.50	19.68	19.849	.0051	.0037	N1; BENDING (A)
			20.091		.0029	
			20.211		.002	
48	20.92	21.26		.0010		M4, N1; BENDING (S)
41	21.72	21.57		.00148		N1; BENDING (A)
30	26.03	23.83		.015		CROSSBEAM, Z PLANE
		25.76		.0041		N0; DOME; N2; OGIVE
		45.41		.010		CROSSBEAM, X PLANE

* ALL DAMPING VALUES ARE AVERAGE FROM ON-LINE MEASUREMENTS.

TABLE III

ORIGINAL PAGE IS
OF POOR QUALITY

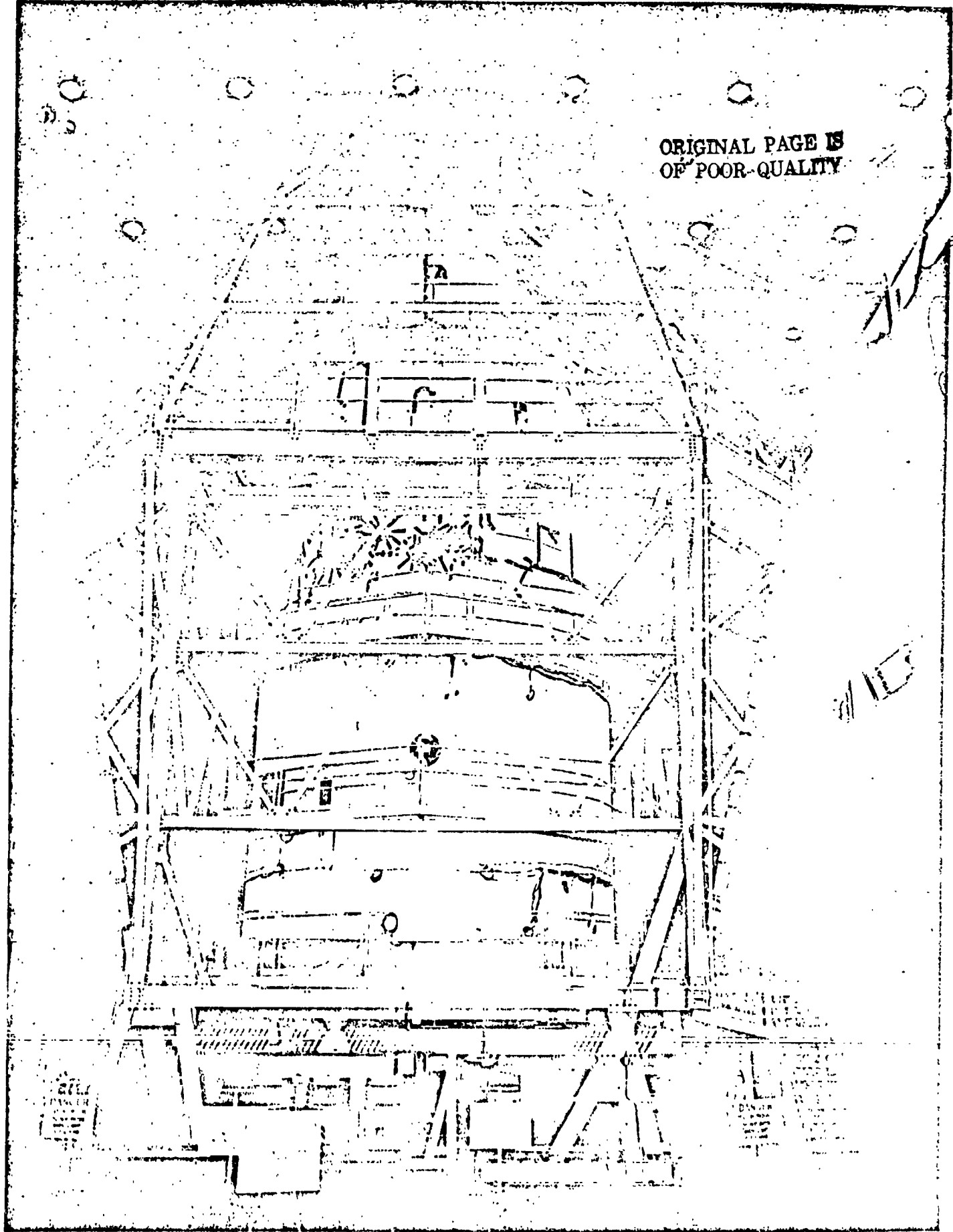
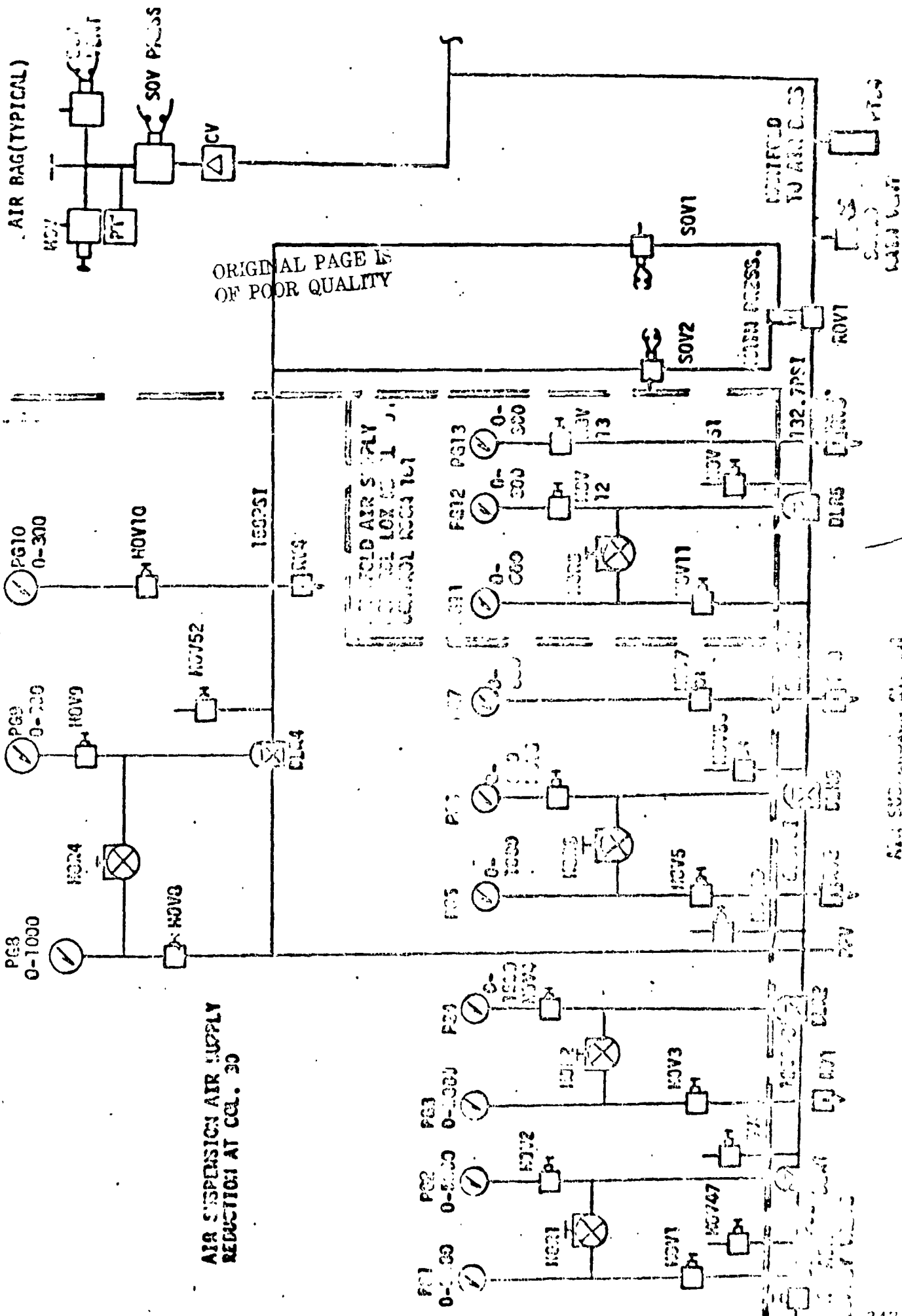


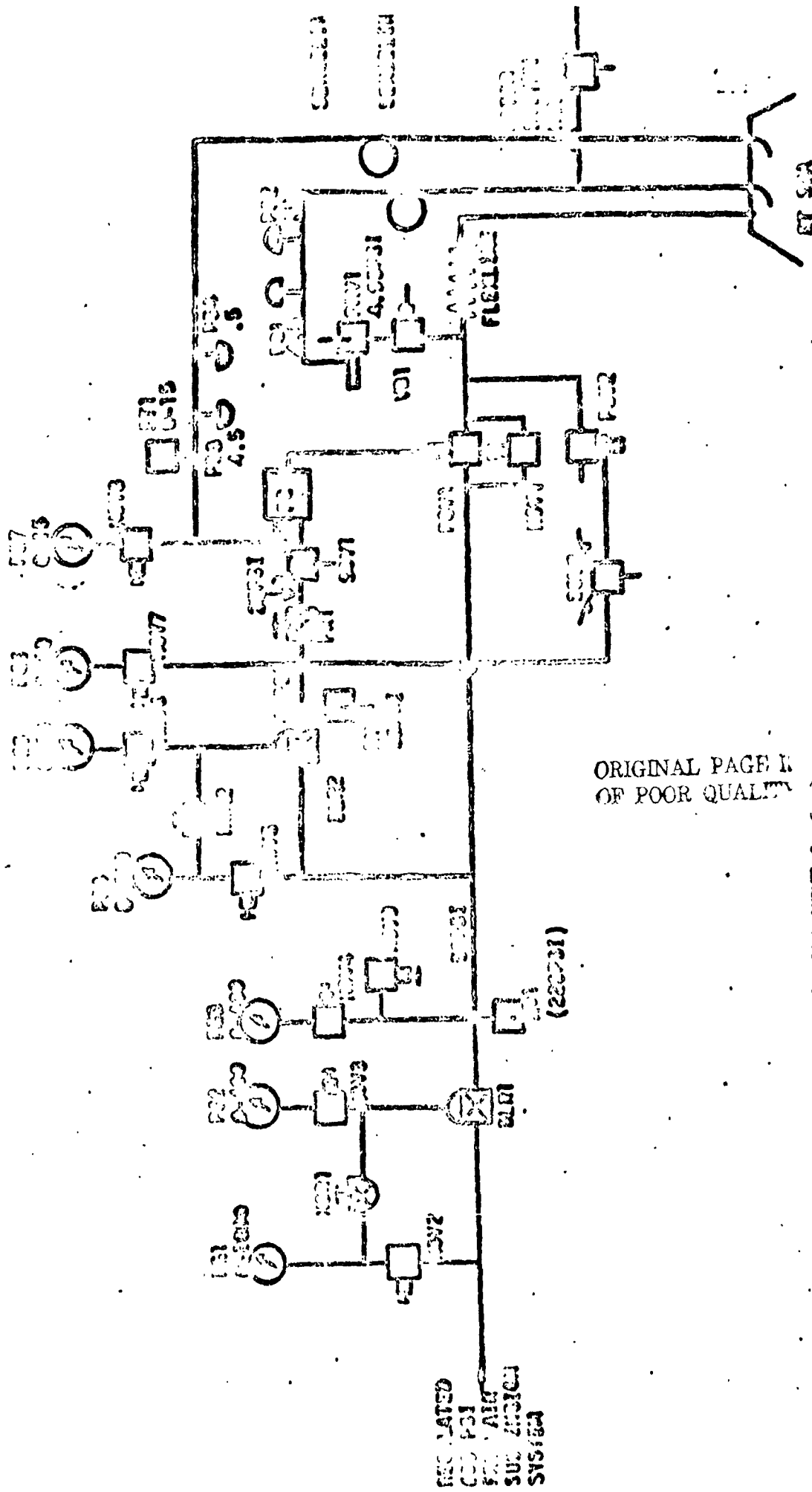
FIGURE 1



Figure 2



NAV SUBSISTEM...
FIGURE 3



ORIGINAL PAGE IS
OF POOR QUALITY

FUEL SYSTEM, POWER, AND VENT SYSTEM

FIGURE 5

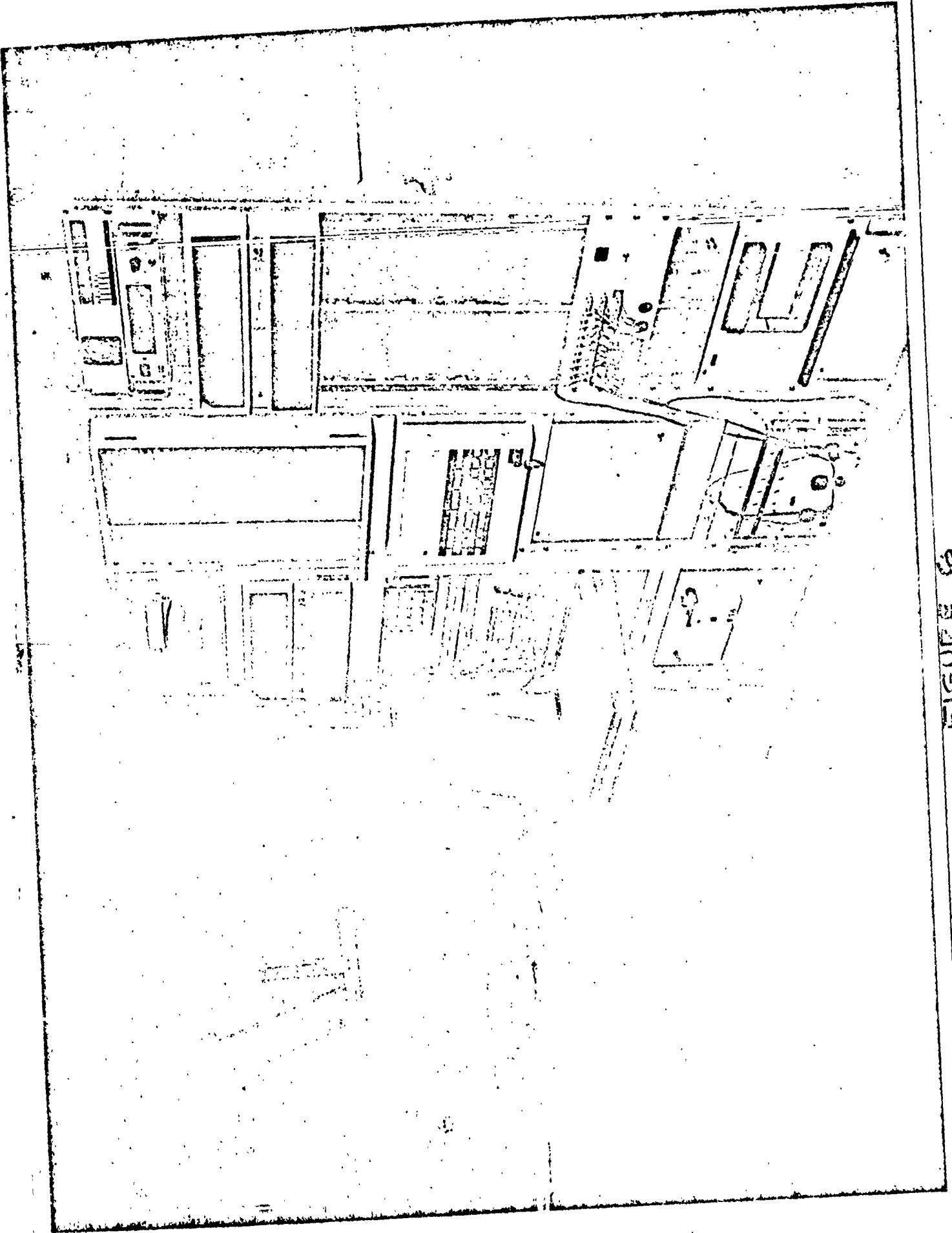
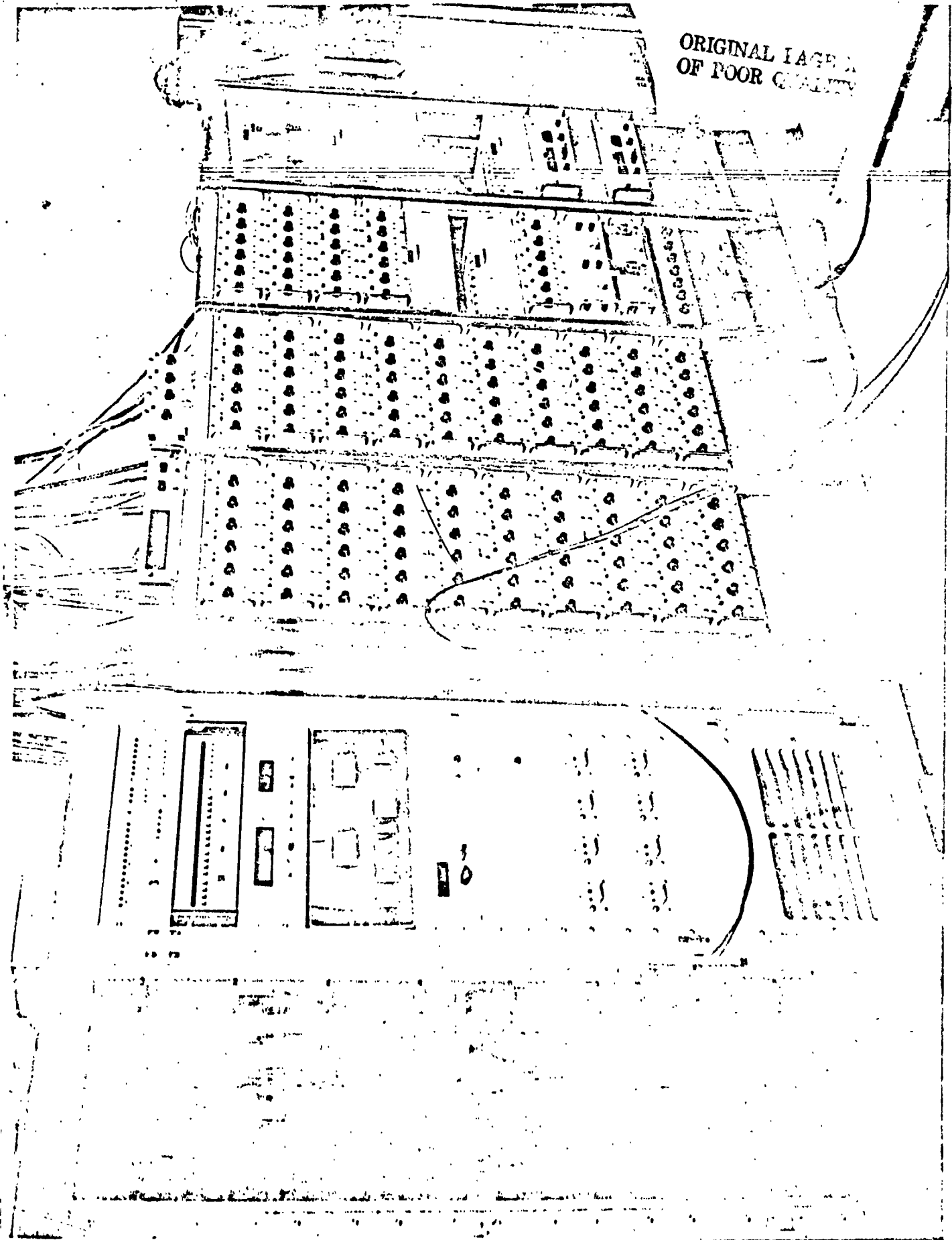


FIGURE 6



ORIGINAL LAYER
OF POOR QUALITY

FIGURE 7

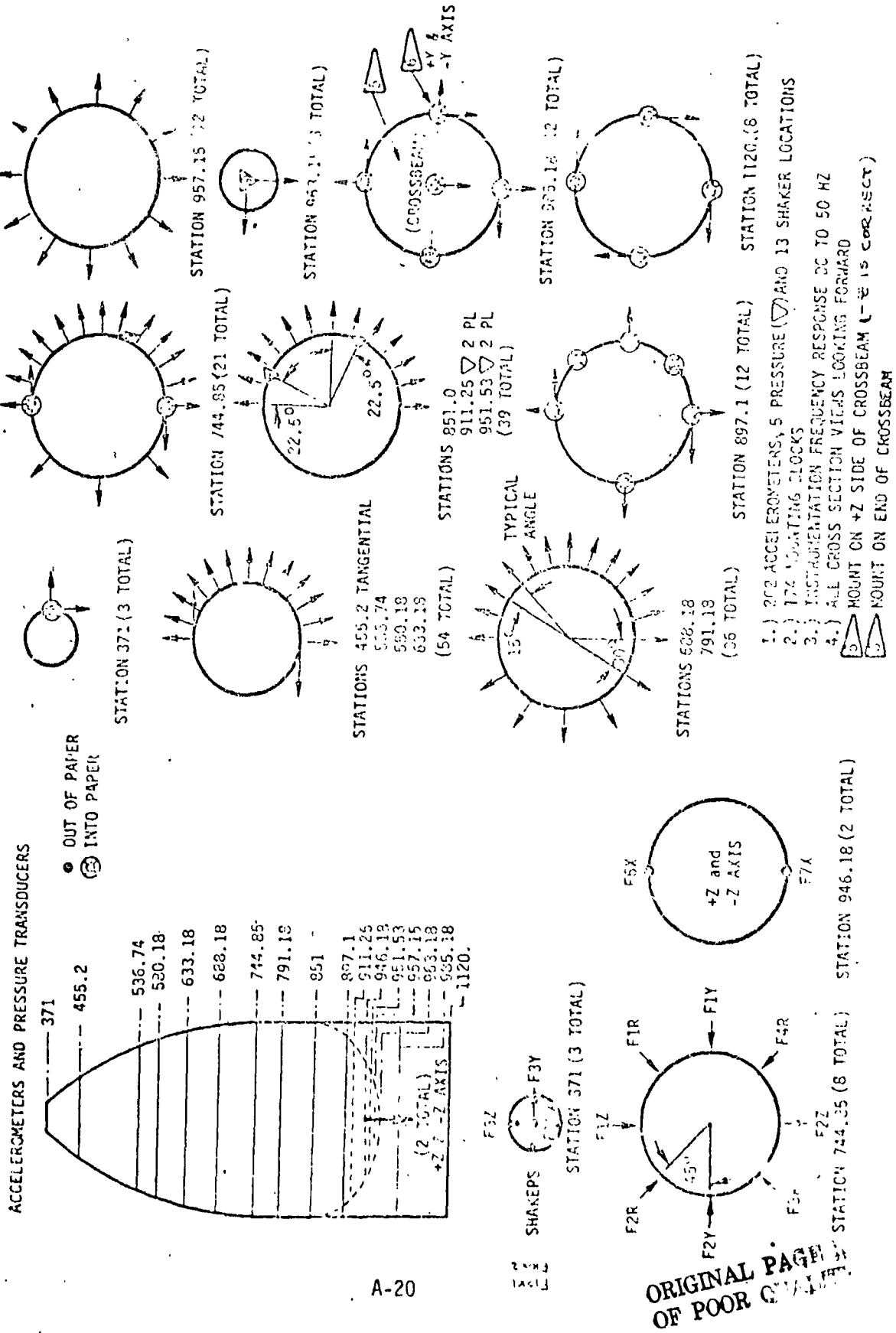


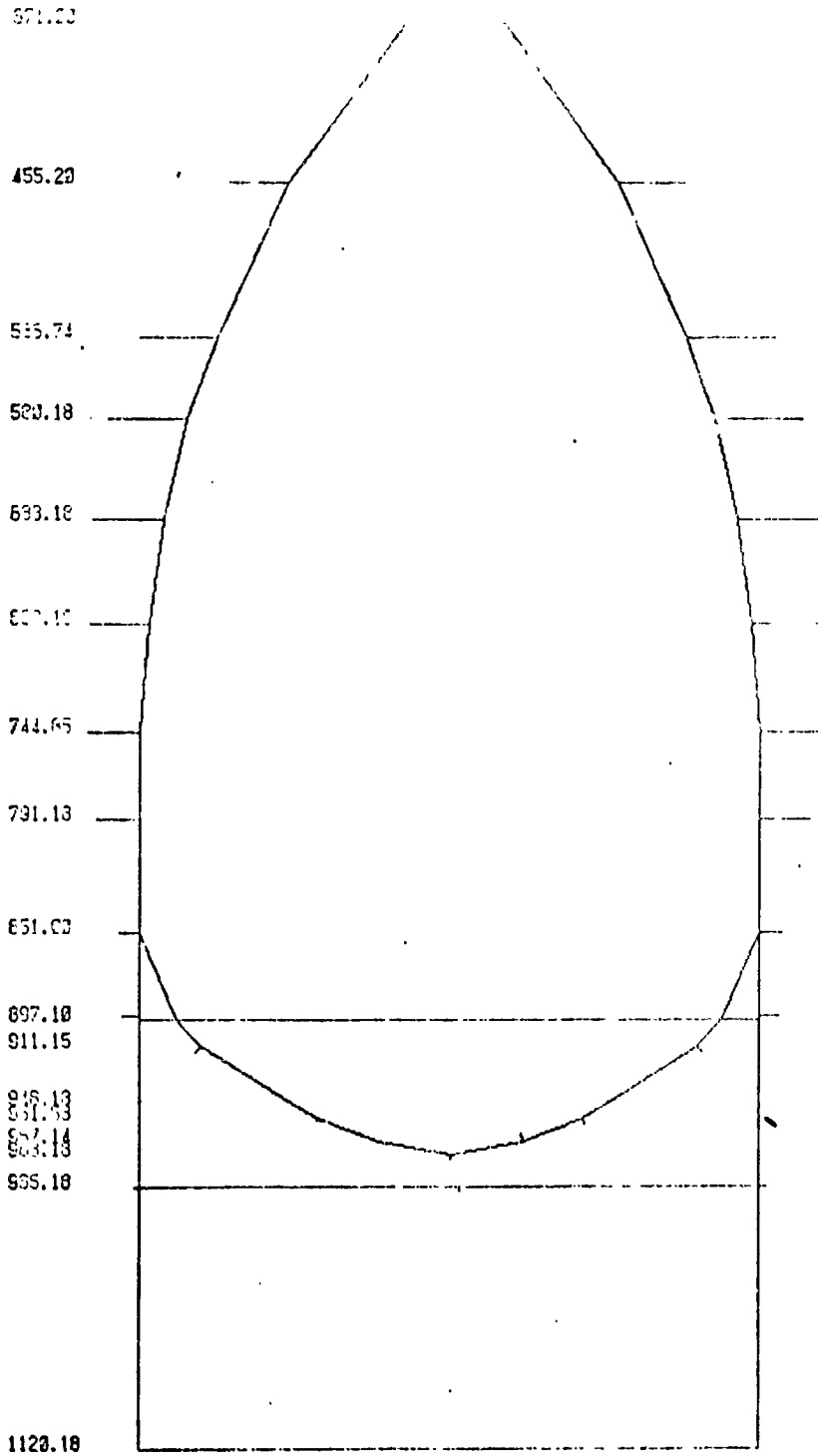
FIGURE 8

ORIGINAL PAGE
OF POOR QUALITY

A COMPARISON OF TEST TECHNIQUES
USED DURING MODAL TESTING OF
RET LOX TANK

PRECEDING PAGE BLANK NOT FILMED

APPENDIX A



SECTION A-A

311.00

455.20

576.74

583.16

633.18

672.16

744.05

791.19

851.60

877.18

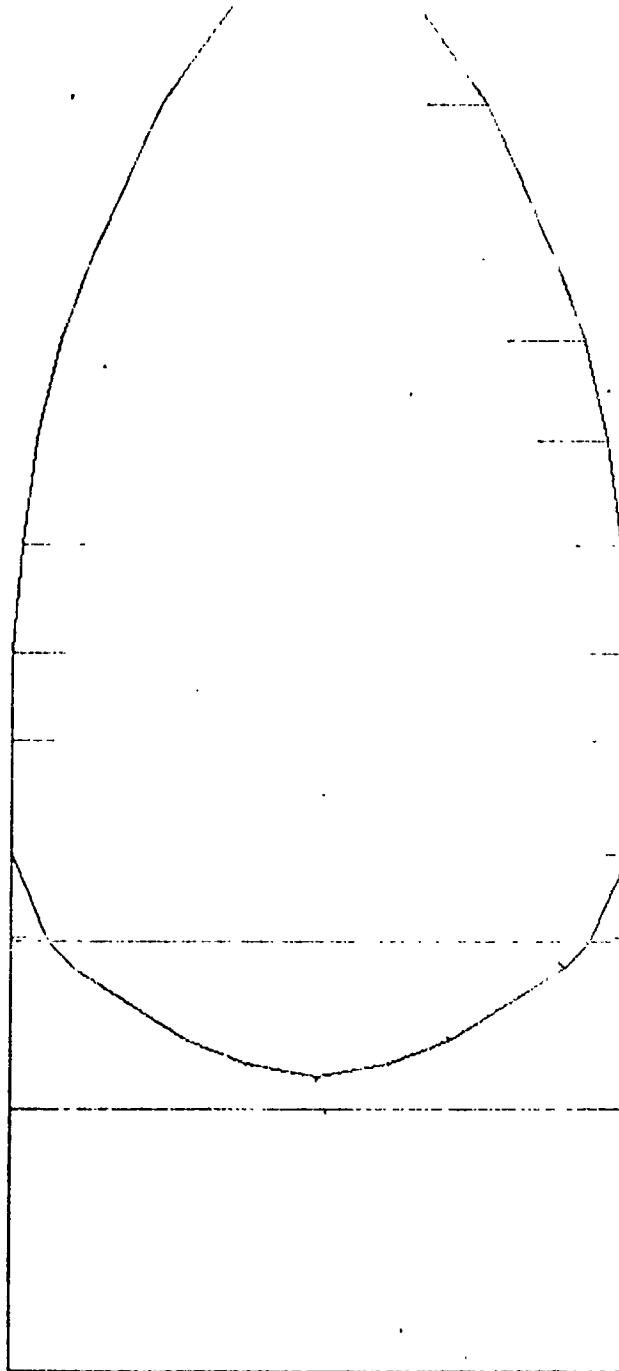
911.15

916.18

933.18

935.18

1129.18



SECTION 3

XCT65

TEST ID 15

48

D -1

3 1 6 4.9764 HERTZ

31

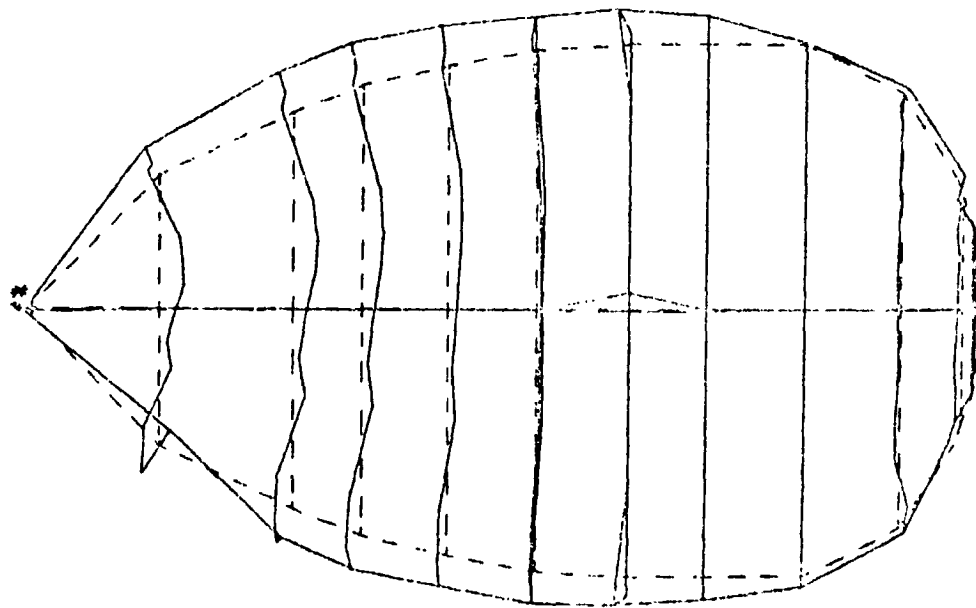
X 0 0 1

4.9764 HERTZ

31

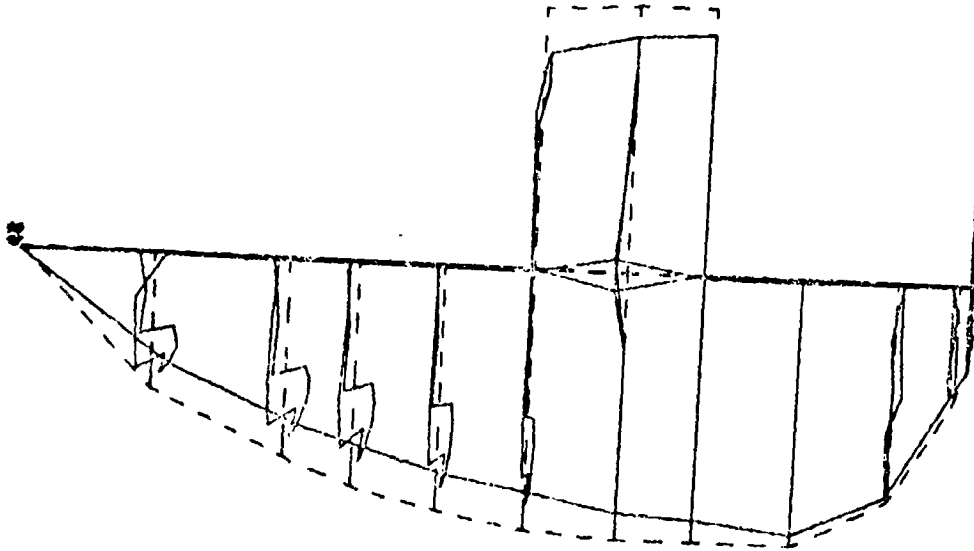
B 0 6

LM069-L1X



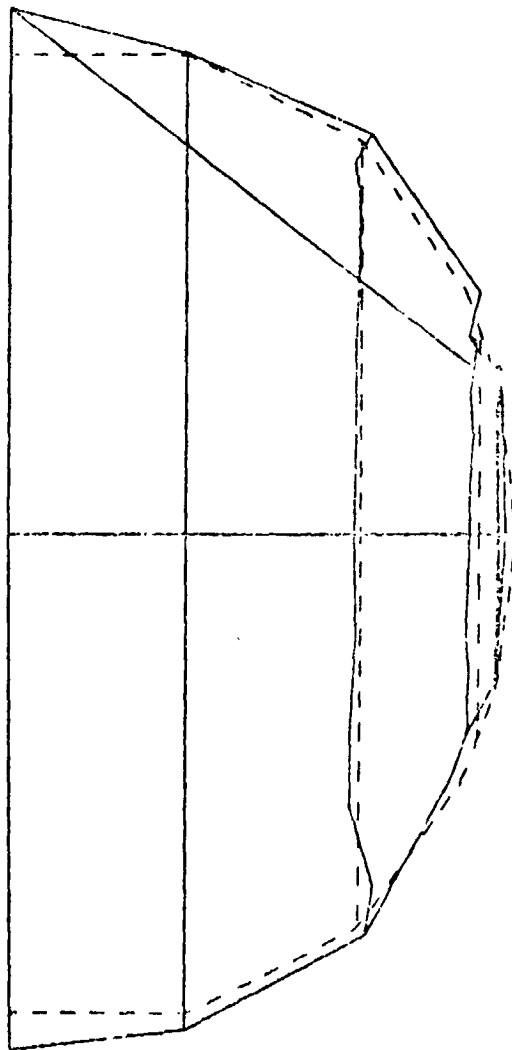
ORIGINAL PAGE IS
OF POOR QUALITY

ORIGINAL PAGE IS
OF POOR QUALITY



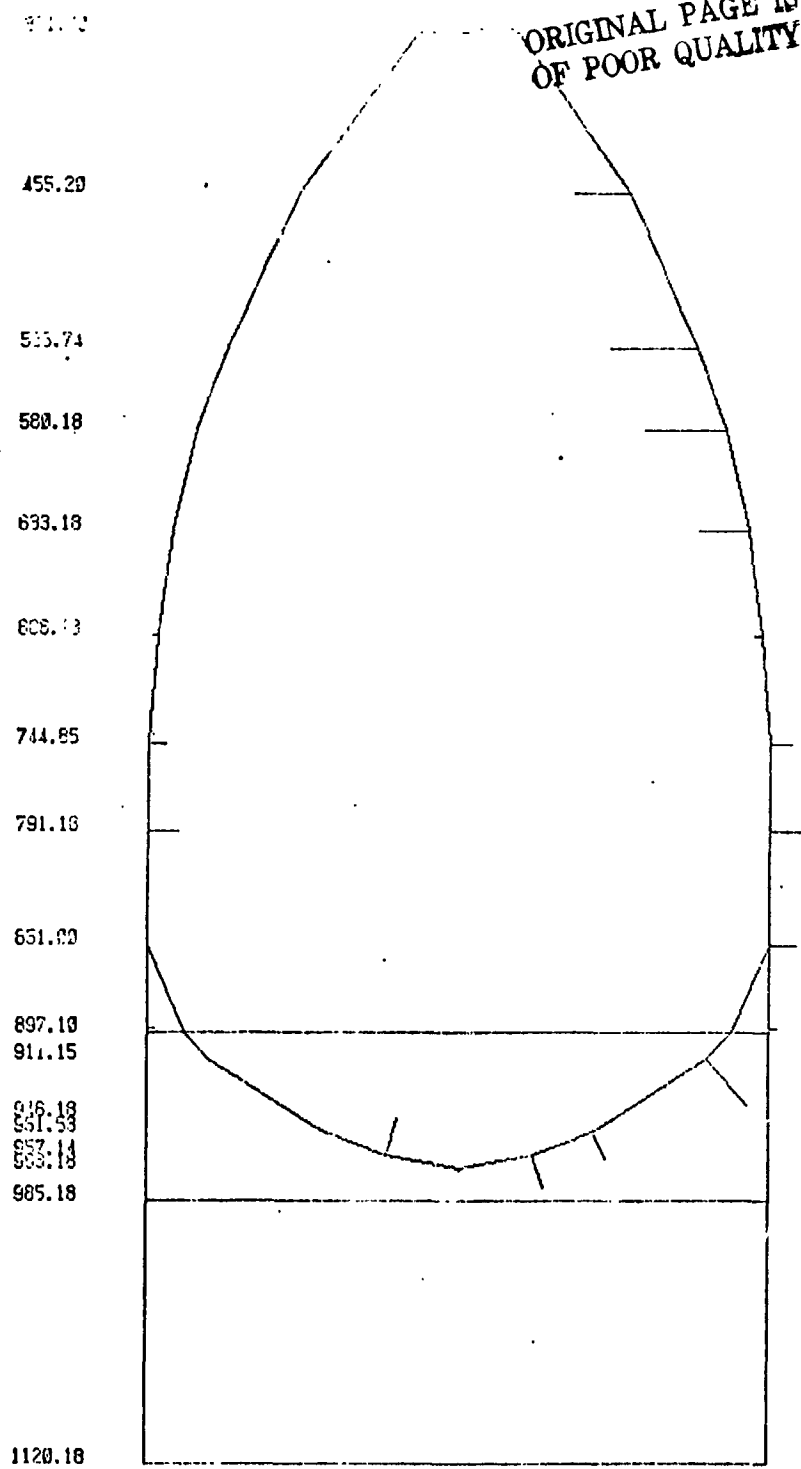
D
3x
D -1
4.9764 HERTZ
8x
X 1 5 ●
4.9764 HERTZ
3x
B 6 6

D-1234
4.9764 HERTZ
33
806

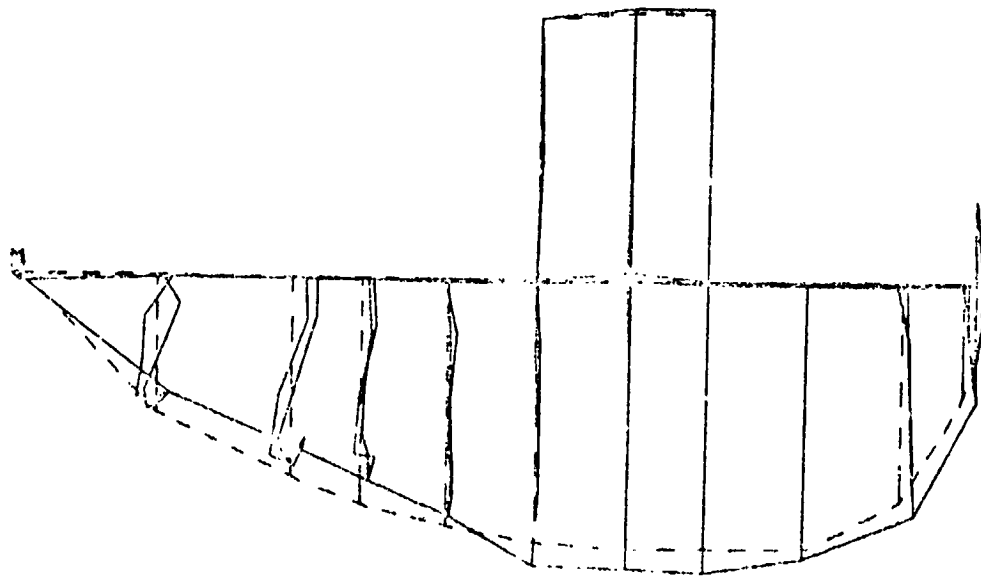


916

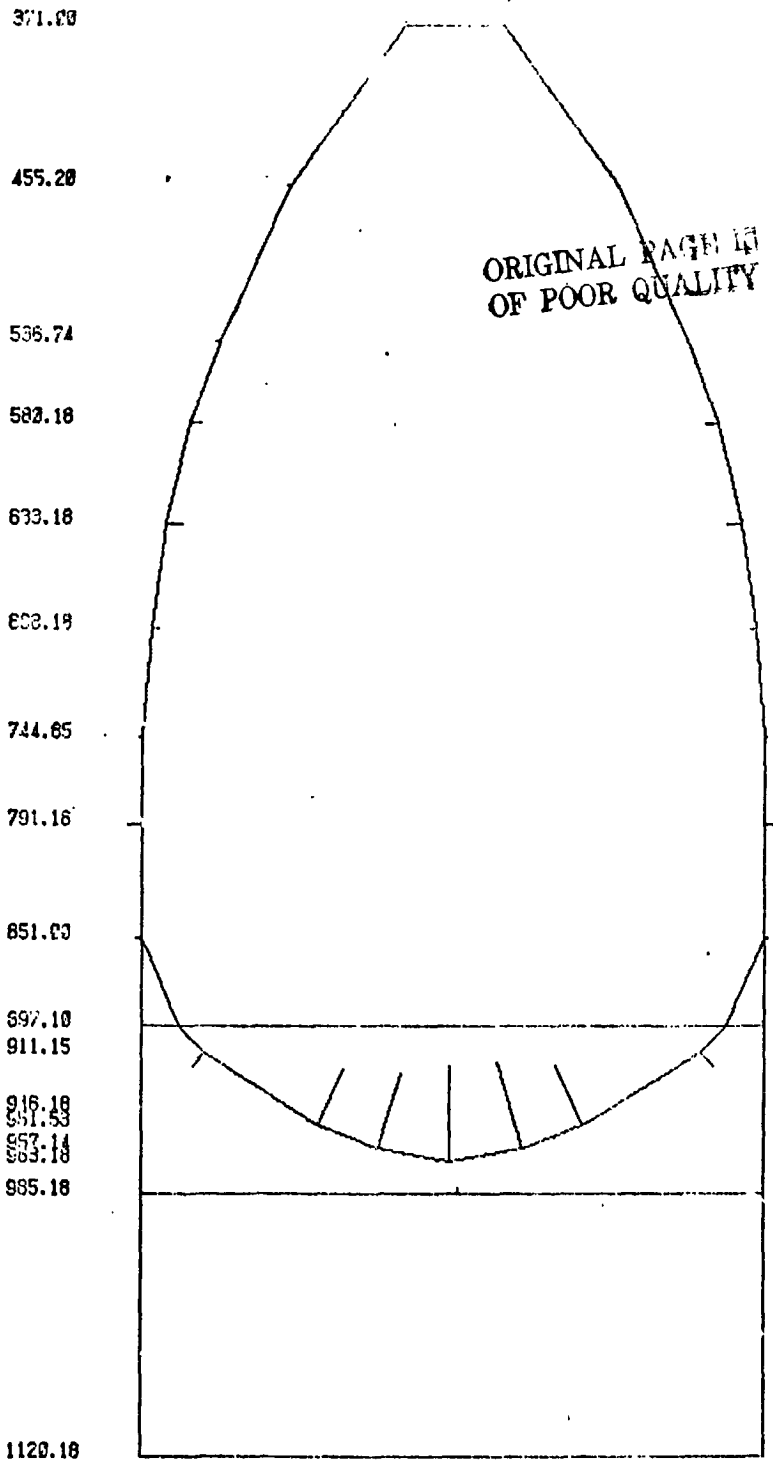
ORIGINAL PAGE IS
OF POOR QUALITY



SECTION-G-S



D -3
9.4053 HERTZ
3x
X 1 0 6
B 1 6
9.4268 HERTZ
3x
B 0 6



SECTION-A-M

11.00

475.20

535.74

583.18

633.18

683.18

744.65

791.18

851.03

897.12

911.15

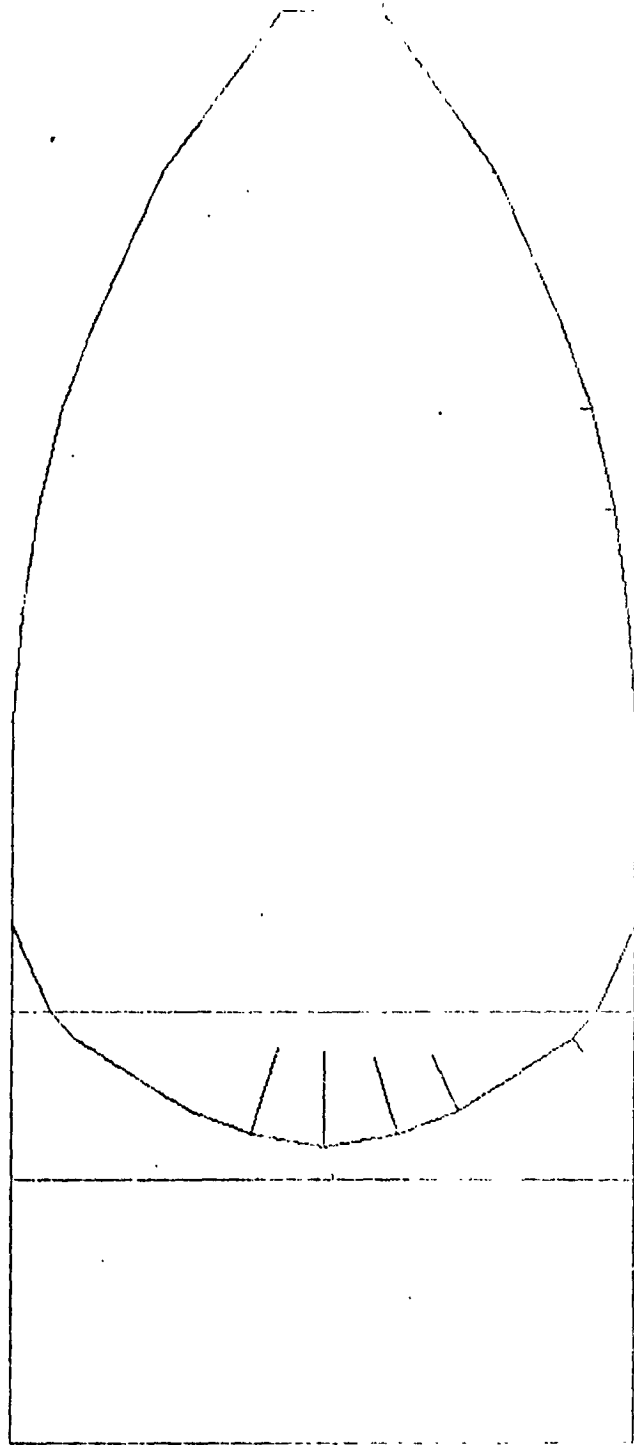
916.18

911.53

853.18

935.18

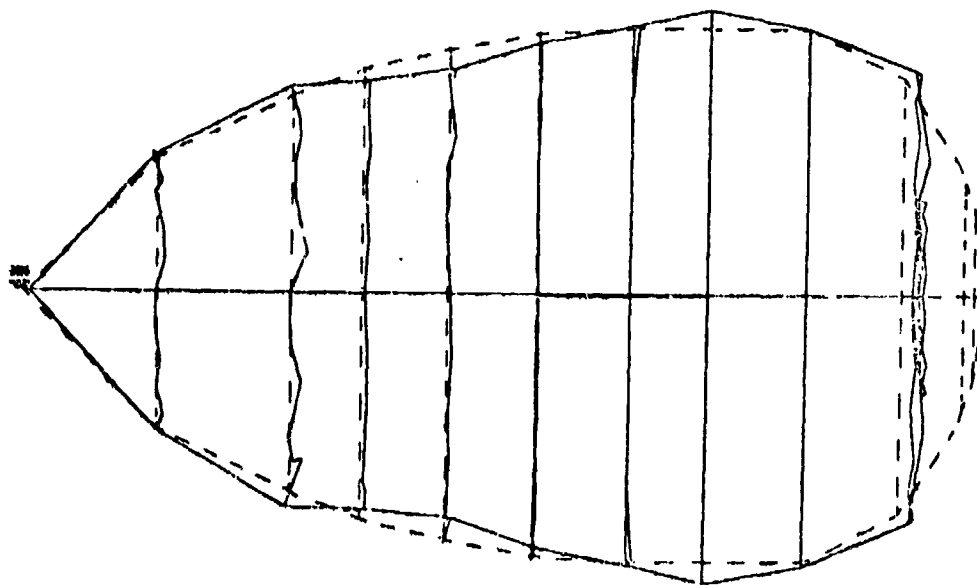
1120.19



SECTION G-5

VC-11a

ORIGINAL PAGE IS
OF POOR QUALITY

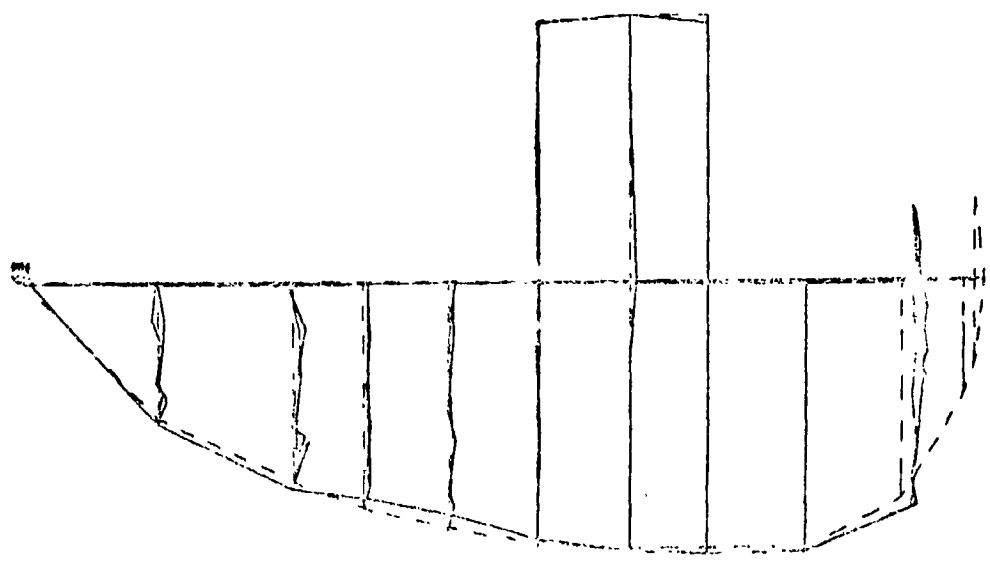


12.7475 HERTZ

34
P 0 6
2 1 6

10-11

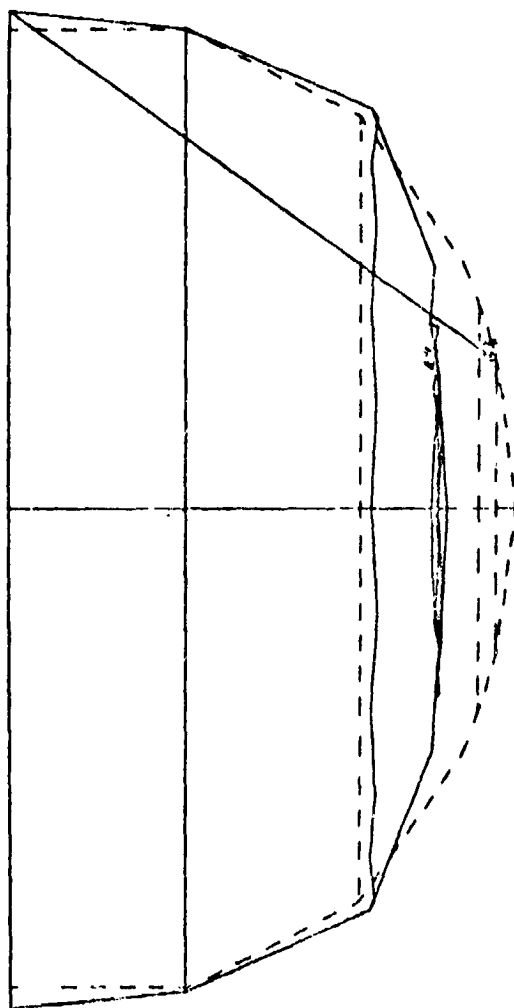
0 1 12.7475 HERTZ
3 1 0 0
3 1 6 12.7475 HERTZ
3 1 8 0 6



MC-II

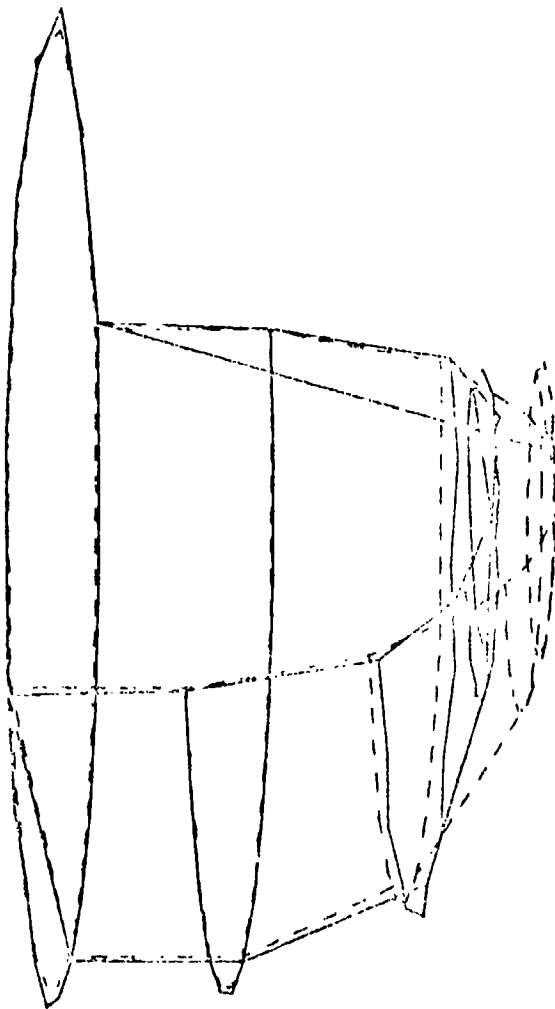
ORIGINAL PAGE IS
OF POOR QUALITY

D 1 2 3 4
12.7475 HERTZ
32
B 0 6



B 1 6

D 1 2 3 4
12.7475 HERTZ
3x
8 10 1 4
12.7475 HERTZ
3x
8 0 6



8 1 C

111.00

455.00

500.74

500.18

633.18

744.00

751.10

831.00

897.10

911.10

910.10

931.10

933.10

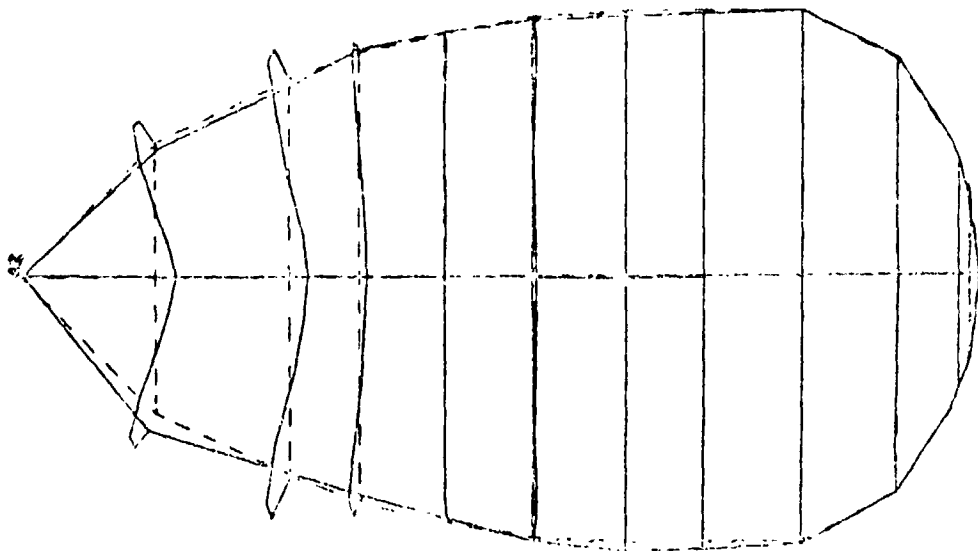
955.18

1150.10

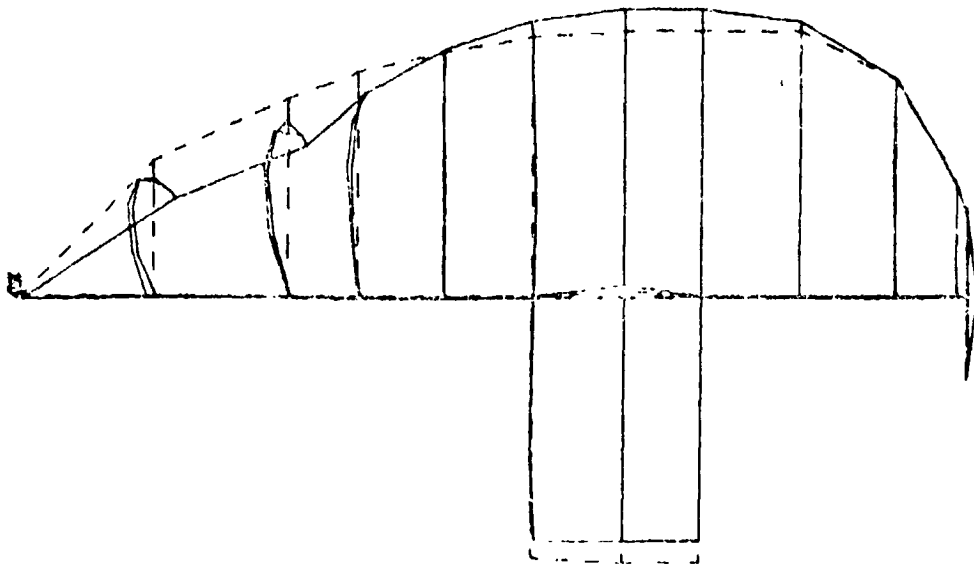
ORIGINAL PAGE IS
OF POOR QUALITY

SECTION-N-11

D 2 9.1912 HERTZ
38 2001
816 9.1018 HERTZ
52 306

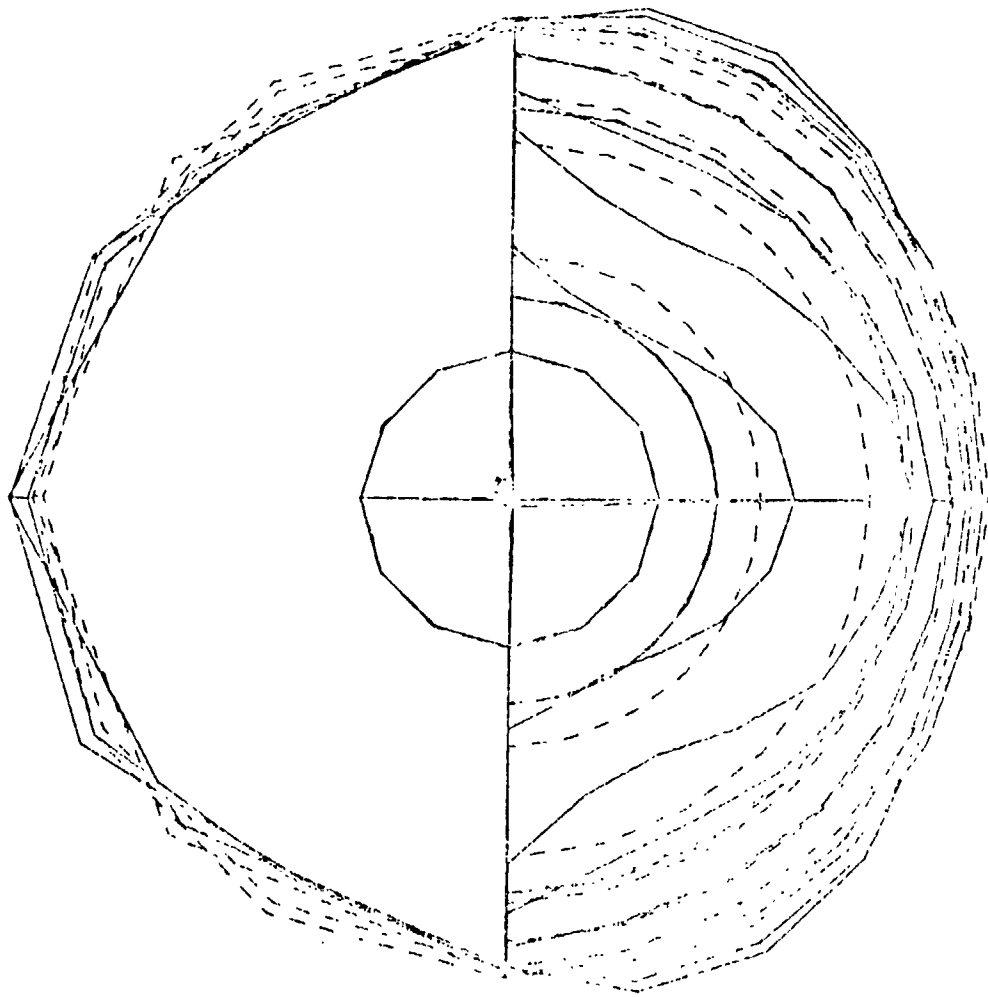


ORIGINAL PAGE IS
OF POOR QUALITY



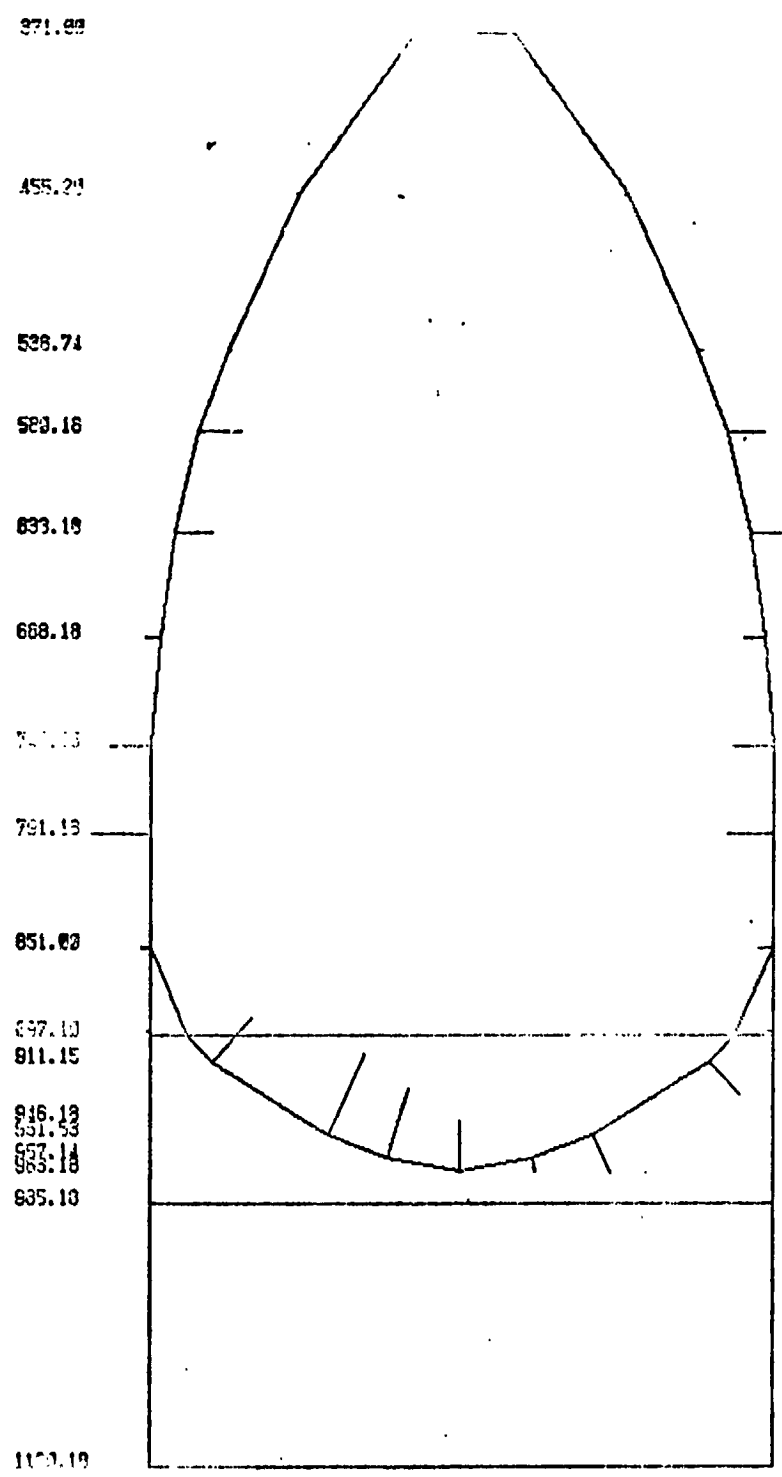
D -2
3x
9.1918 HERTZ
805
815

D 2
9.1836 HERTZ
21
8 11 6



206

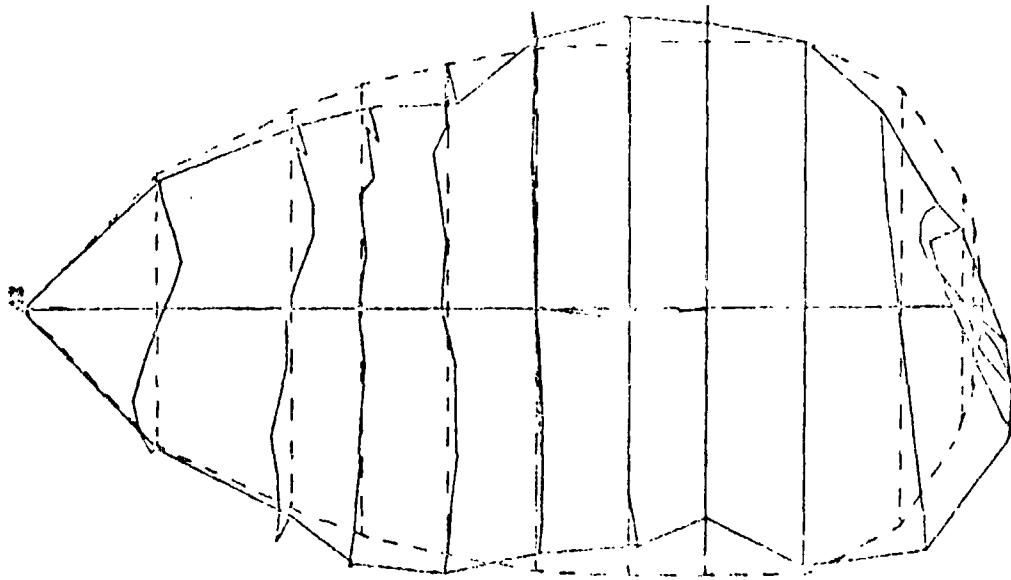
ORIGINAL PAGE IS
OF POOR QUALITY



SECTION-R-H

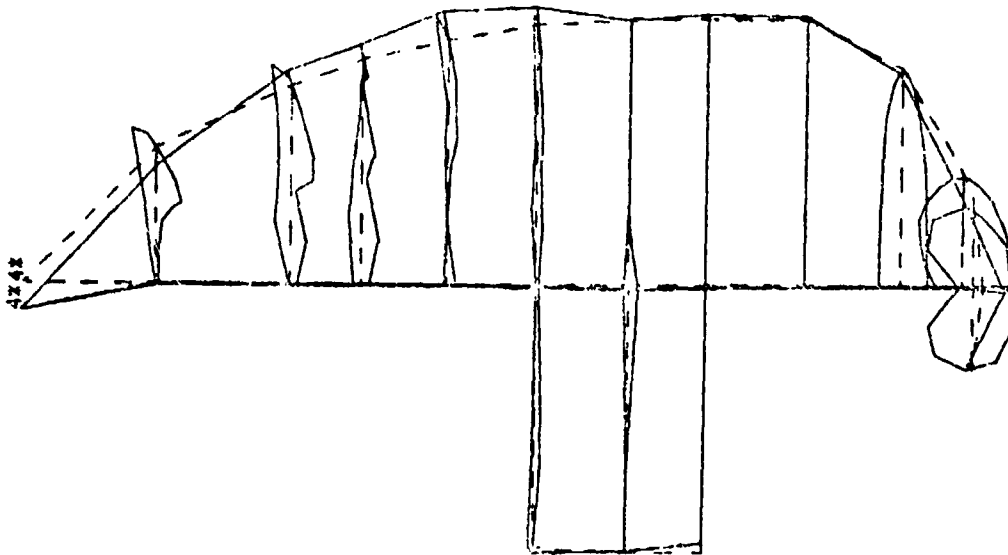
VC-15a

D 2 14.0566 HERTZ
33 X 0 0 1
B 1 6 14.0566 HERTZ
32 B 0 5
B 0 5

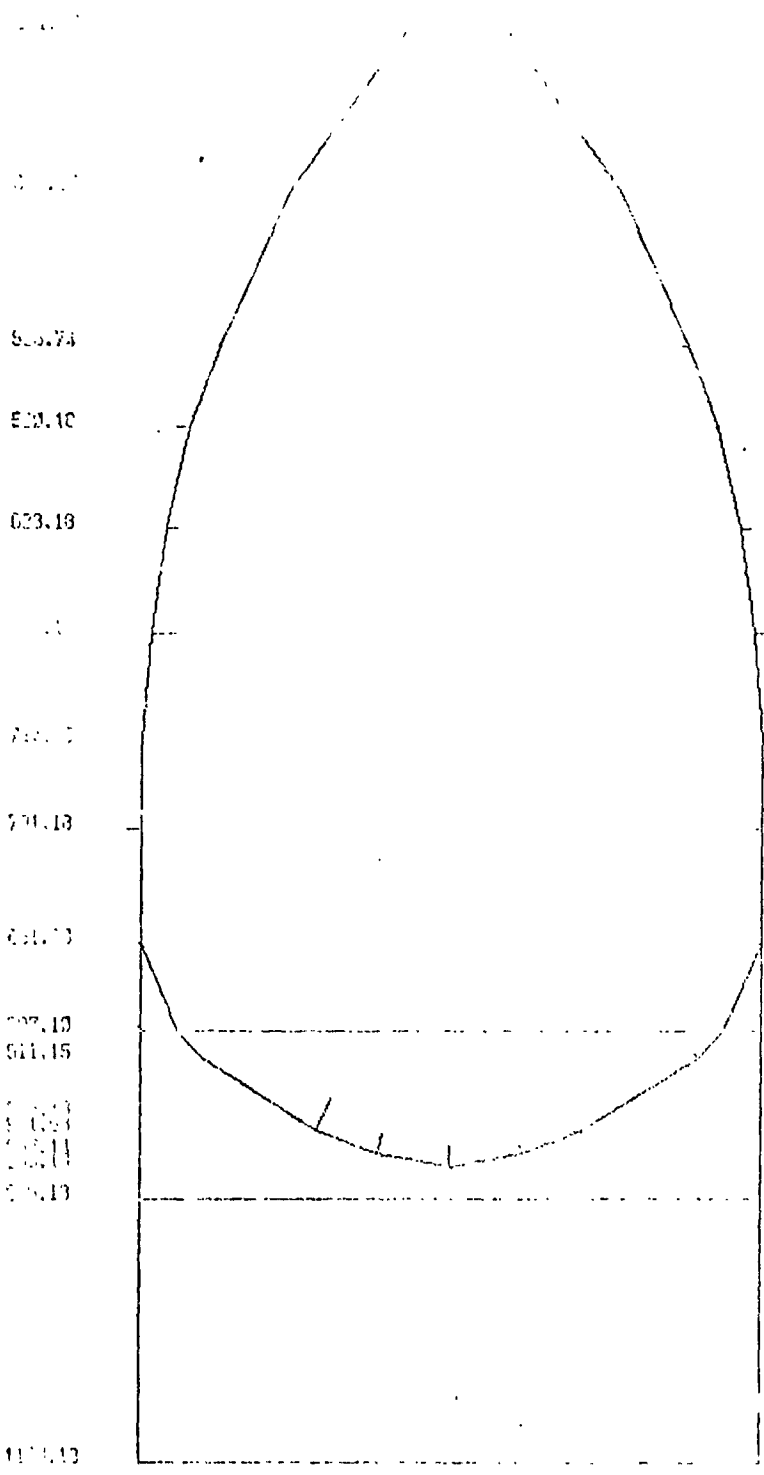


ORIGINAL PAGE IS
OF POOR QUALITY

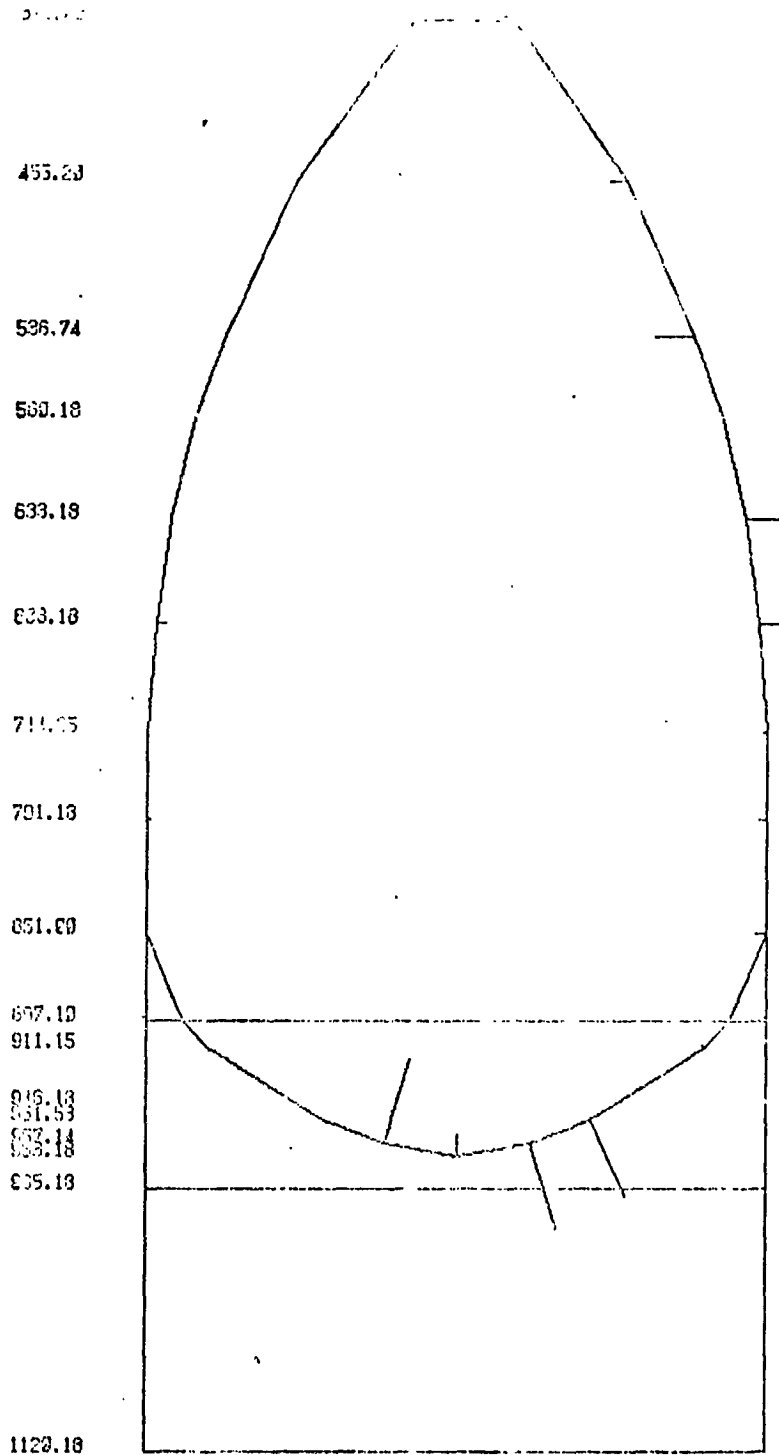
Y6-15.0



D -2
14.0586 HERTZ
38
506
B 16

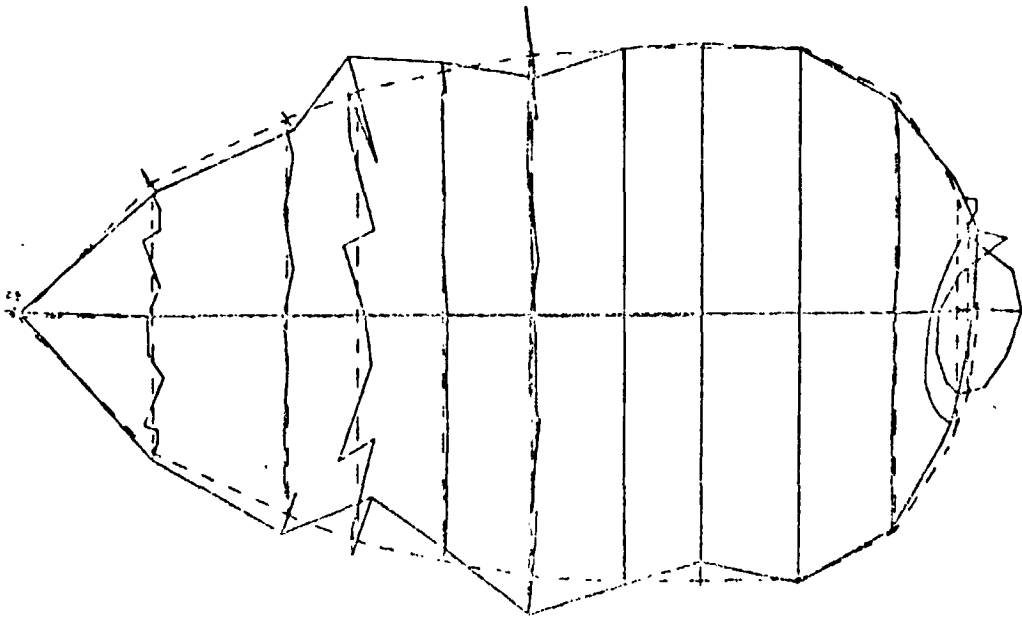


SECTION



SECTION G-3

VC-17.



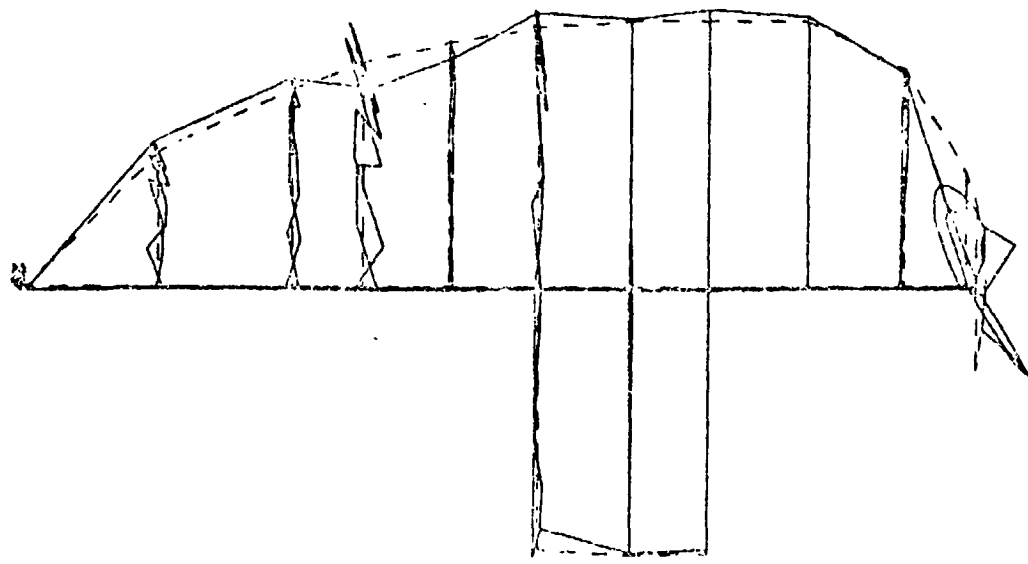
D-3

16.4531 HE-72

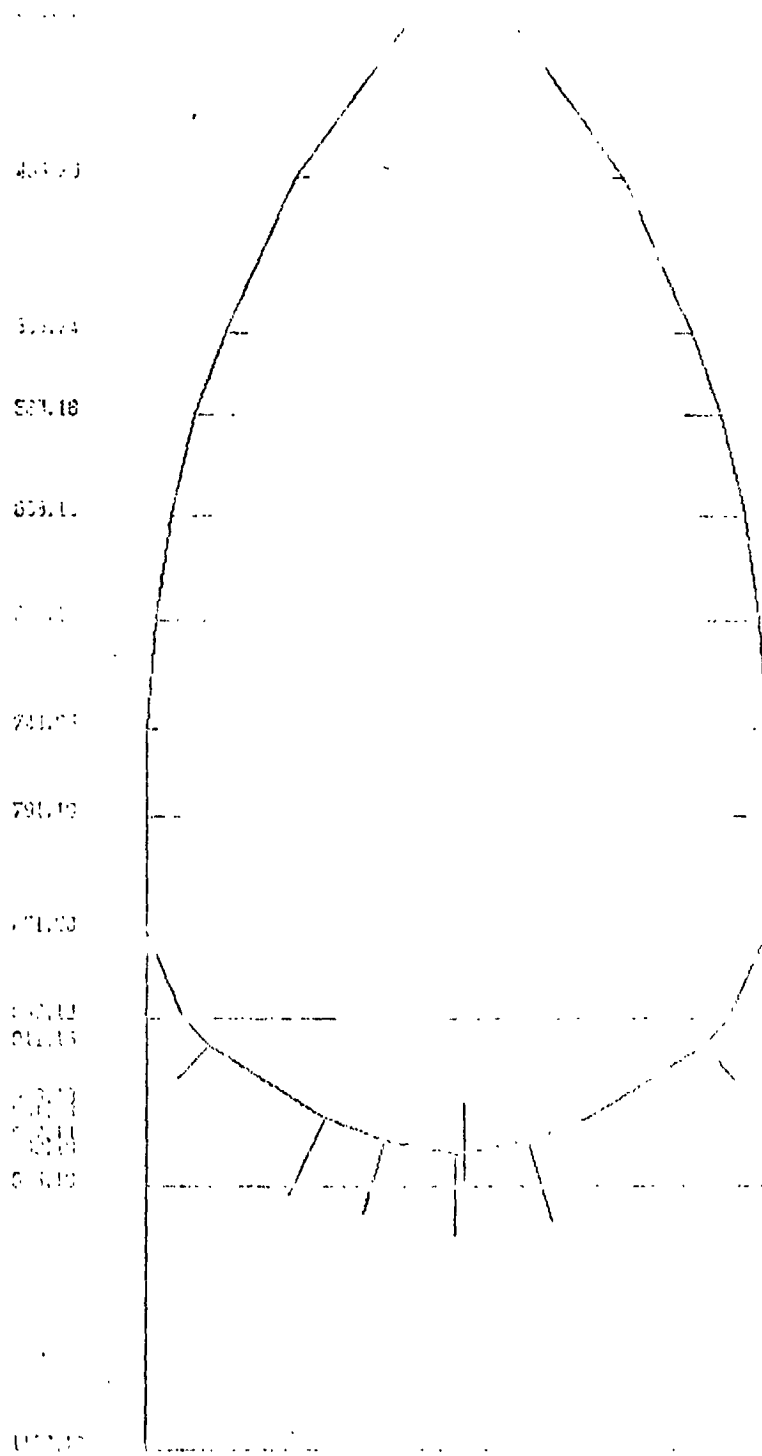
31
305
316

10-17-63

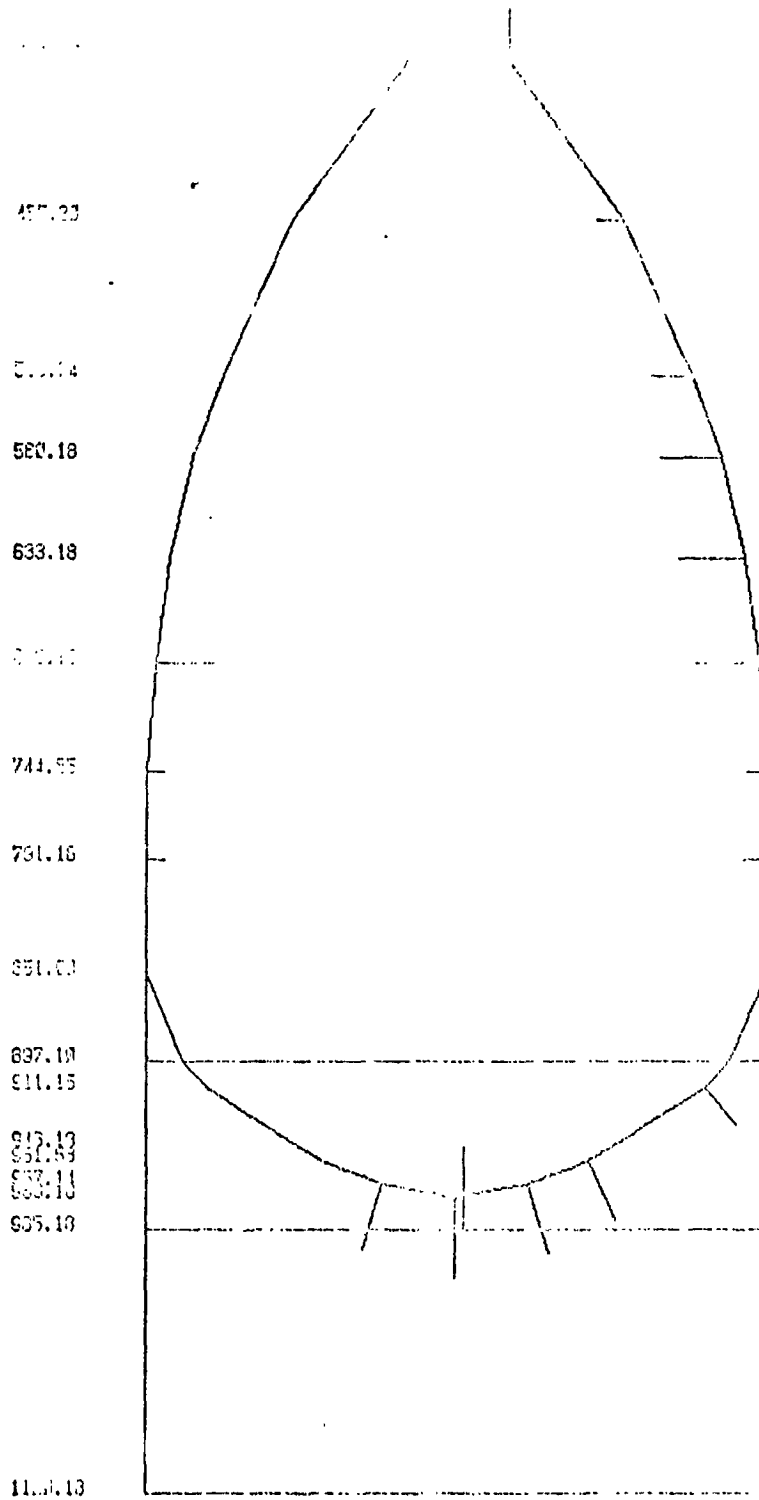
ORIGINAL PAGE IS
OF POOR QUALITY



D 3 16.4601 HERTZ
3x X -1.0 6
D 1 6 16.4601 HERTZ
3x B 0 6



ORIGINAL PAGE IS
OF POOR QUALITY

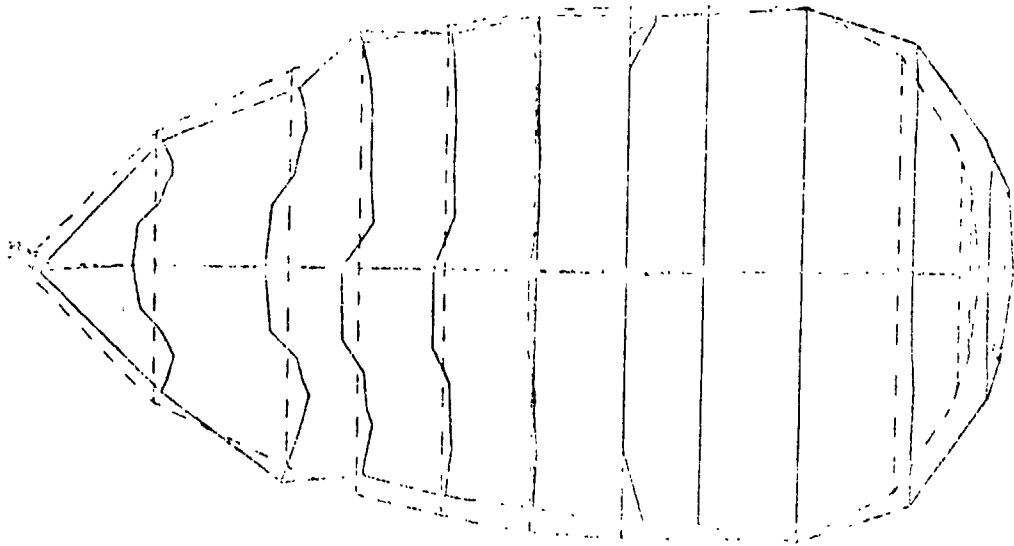


SECTION G-S

D-5

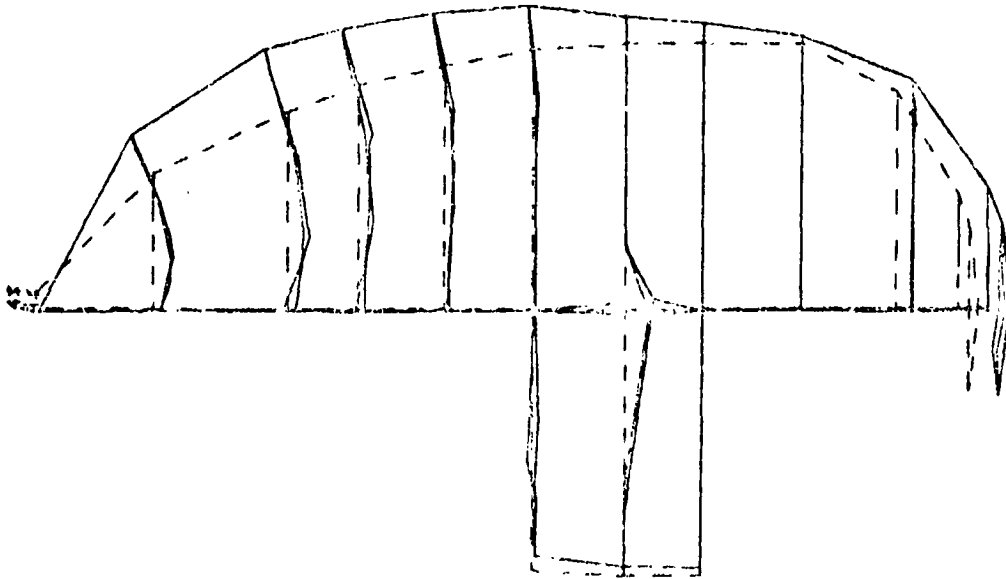
5.0000 HERTZ

339
310



001010

ORIGINAL PAGE IS
OF POOR QUALITY



D 5
5.8528 HERTZ
3x
x-1 0
B 1 5
5.8528 HERTZ
3x
B 0 6

MODELING OF SHUTTLE PAYLOAD BAY ACOUSTIC ENVIRONMENT

J. YOUNG

NASA - GODDARD SPACE FLIGHT CENTER

PRECEDING PAGE BLANK NOT FILMED

PRESENTED AT

PAYLOAD FLIGHT LOADS PREDICTION METHODOLOGY WORKSHOP

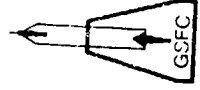
MARSHALL SPACE FLIGHT CENTER

NOVEMBER 14-16, 1978

SHUTTLE P/L BAY ACOUSTIC ENVIRONMENT PREDICTION ACTIVITY

BACKGROUND

- SUPPORTED BY NASA HEADQUARTERS/PAYLOAD PLANNING - OSTA
- EFFORT BEGAN DECEMBER 1975 WITH CONTRACT TO BOLT BERANEK & NEWMAN
- PRIMARY OBJECTIVE IS TO PRODUCE THE CAPABILITY TO PREDICT P/L BAY ACOUSTIC ENVIRONMENT ACCOUNTING FOR PRESENCE OF ARBITRARY PAYLOAD COMPLEMENT
- WORK HAS CONSISTED OF THREE PARTS
 - ANALYTICAL TO CREATE MATH MODEL
 - WRITING OF COMPUTER PROGRAM - PACES (PAYLOAD ACOUSTIC ENVIRONMENT FOR SHUTTLE)
 - TEST PROGRAMS TO SUPPORT DEVELOPMENT AND VALIDATION OF MATH MODEL/COMPUTER PROGRAM



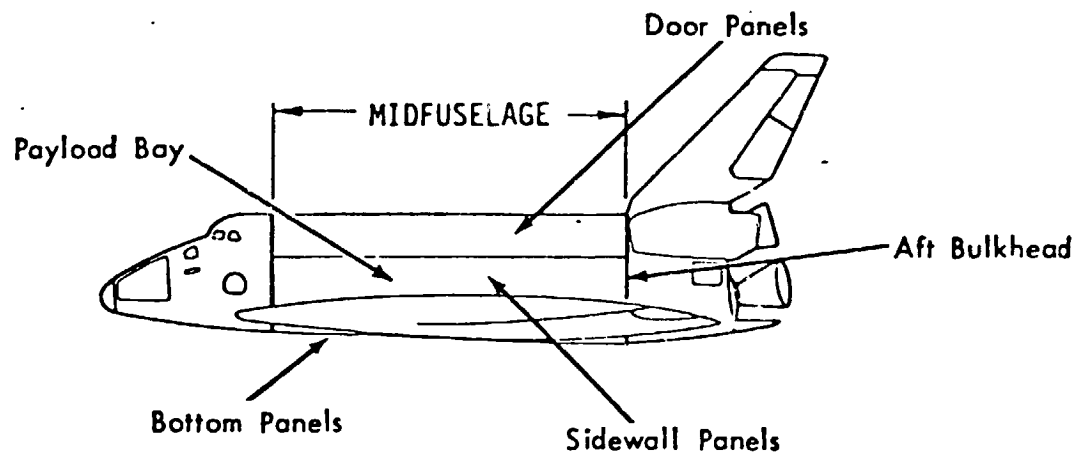
SHUTTLE P/L BAY ACOUSTIC ENVIRONMENT PREDICTION ACTIVITY

DEVELOPMENT OF MAT-4 MODEL/COMPUTER PROGRAM

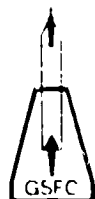
ACTIVITY	CY76	CY77	CY78	CY79
<ul style="list-style-type: none"> ● INITIAL FORMULATION ● OV101 LOUDSPEAKER TEST (EMPTY BAY) ● OV101 JET NOISE TEST (EMPTY BAY) ● PROGRAM VALIDATION ● PROGRAM RELEASE - PACES (VER. 1) ● UPGRADE LOW FREQUENCY ACCURACY <ul style="list-style-type: none"> ○ EXTEND TO 12 Hz ○ ADD SIDEWALL DYNAMICS ● 1/4 SCALE MODEL TEST & VALIDATION ● FINAL PRE-FLIGHT VALIDATION ● PROGRAM RELEASE - PACES (VER. 2) ● VALIDATION USING SHUTTLE FLIGHT DATA (SS-1 THRU SS-4) - FY80 				



SHUTTLE P/L BAY ACOUSTIC ENVIRONMENT PREDICTION ACTIVITY

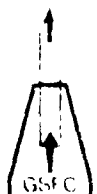
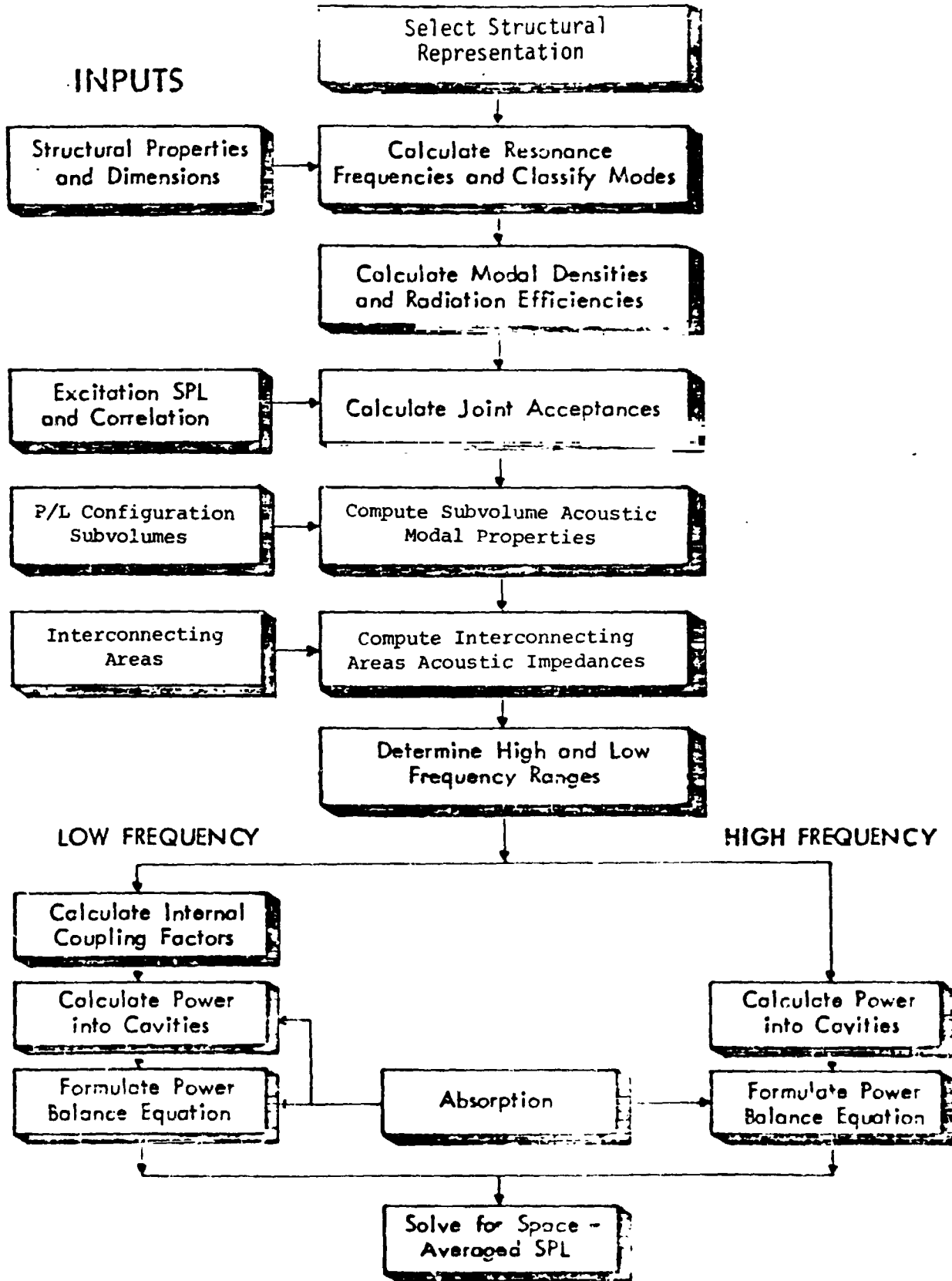


SPACE SHUTTLE ORBITER VEHICLE

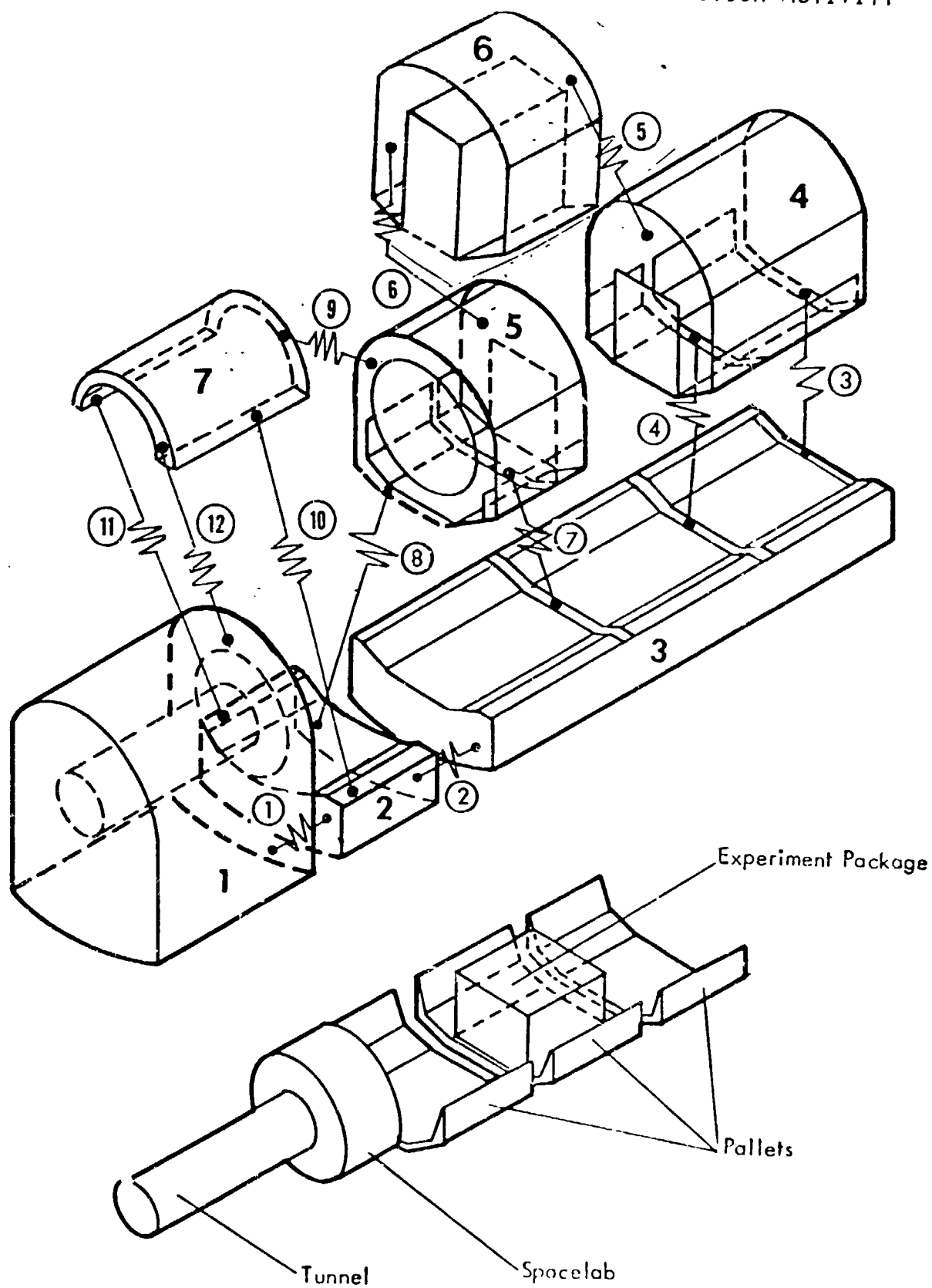


SHUTTLE P/L BAY ACOUSTIC ENVIRONMENT PREDICTION ACTIVITY

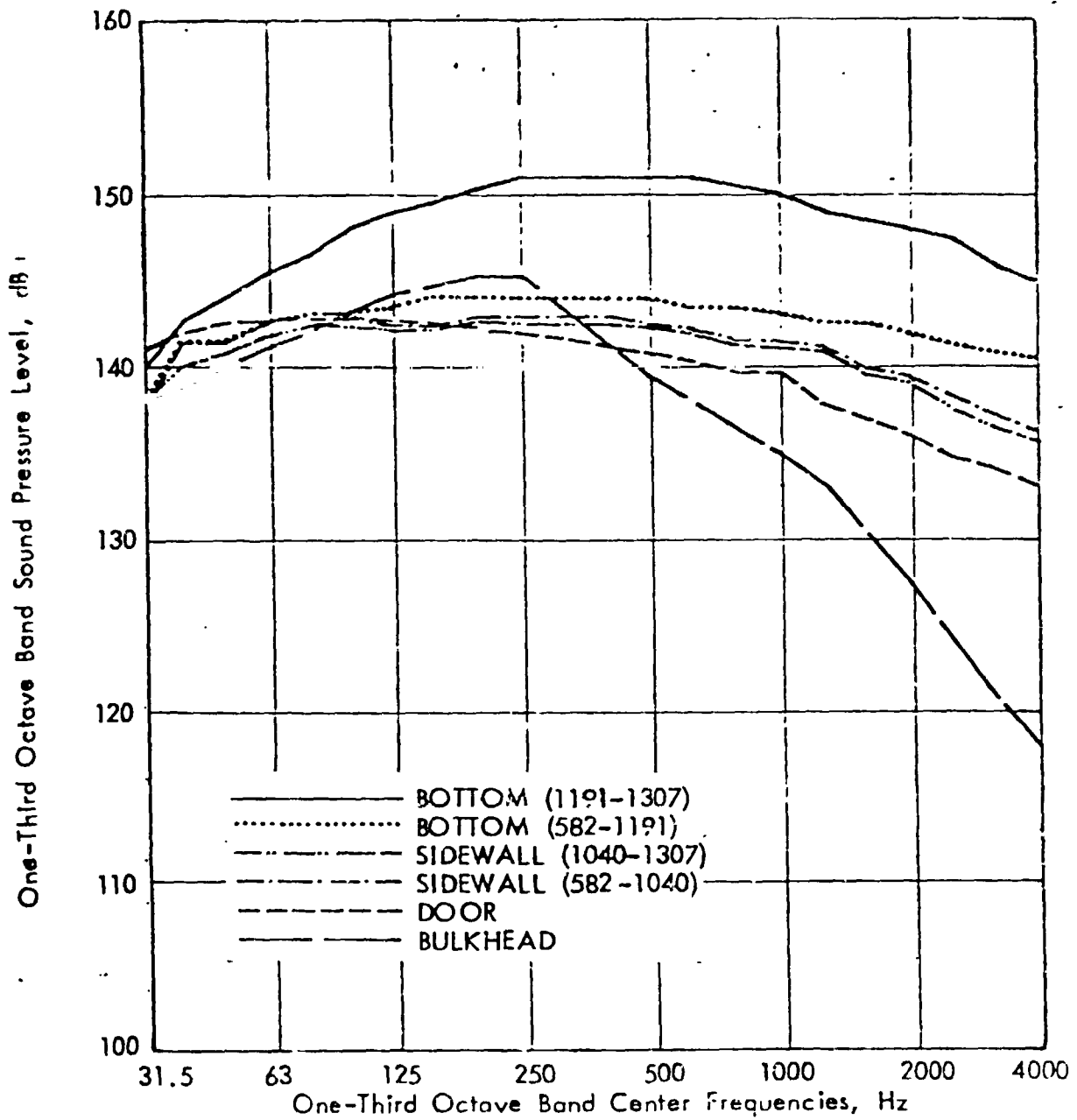
OPERATION



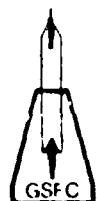
SHUTTLE P/L BAY ACOUSTIC ENVIRONMENT PREDICTION ACTIVITY



SHUTTLE P/L BAY ACOUSTIC ENVIRONMENT PREDICTION ACTIVITY

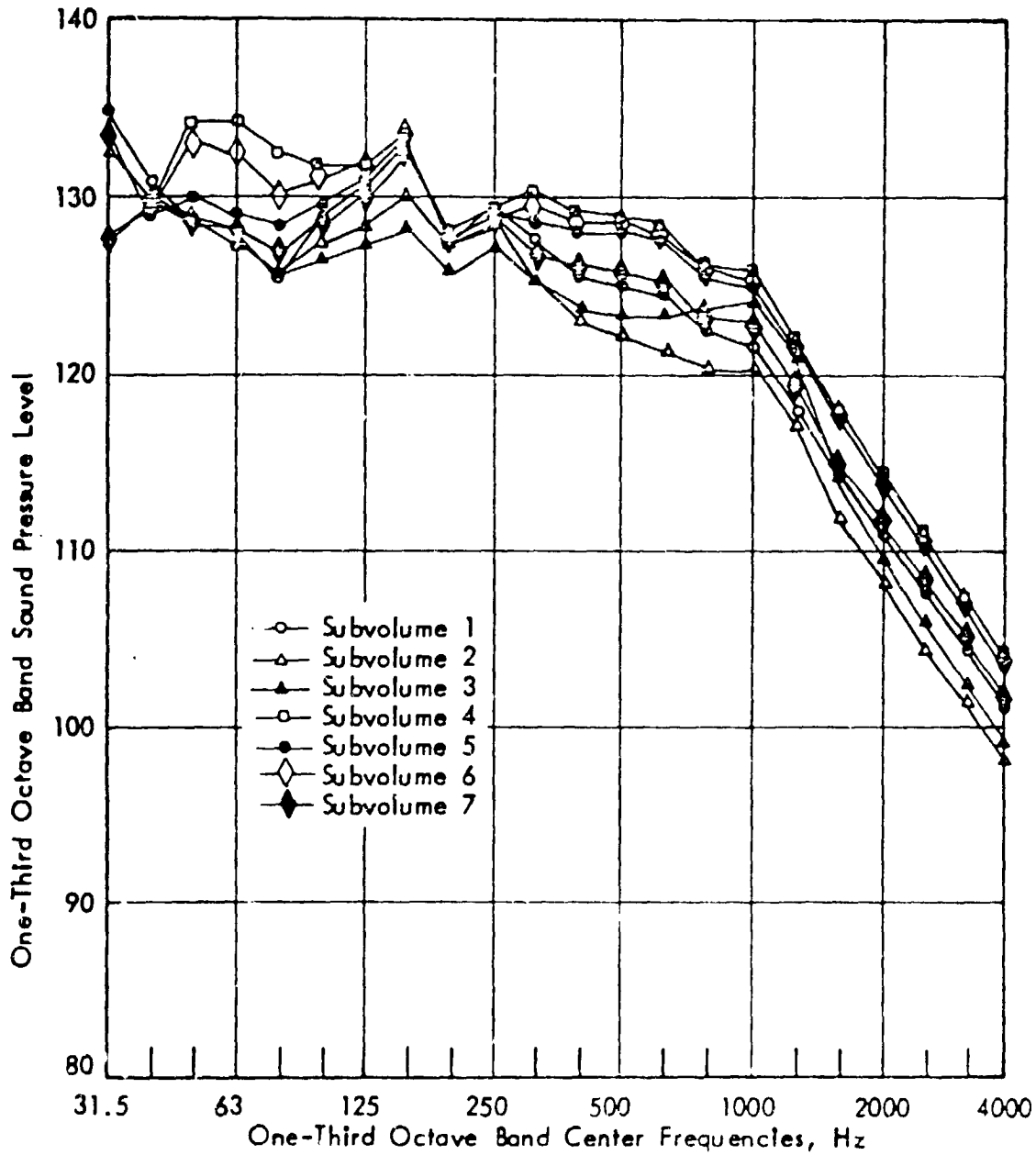


EXTERNAL ACOUSTIC FIELD ON DIFFERENT STRUCTURAL REGIONS



SHUTTLE P/L BAY ACOUSTIC ENVIRONMENT PREDICTION ACTIVITY

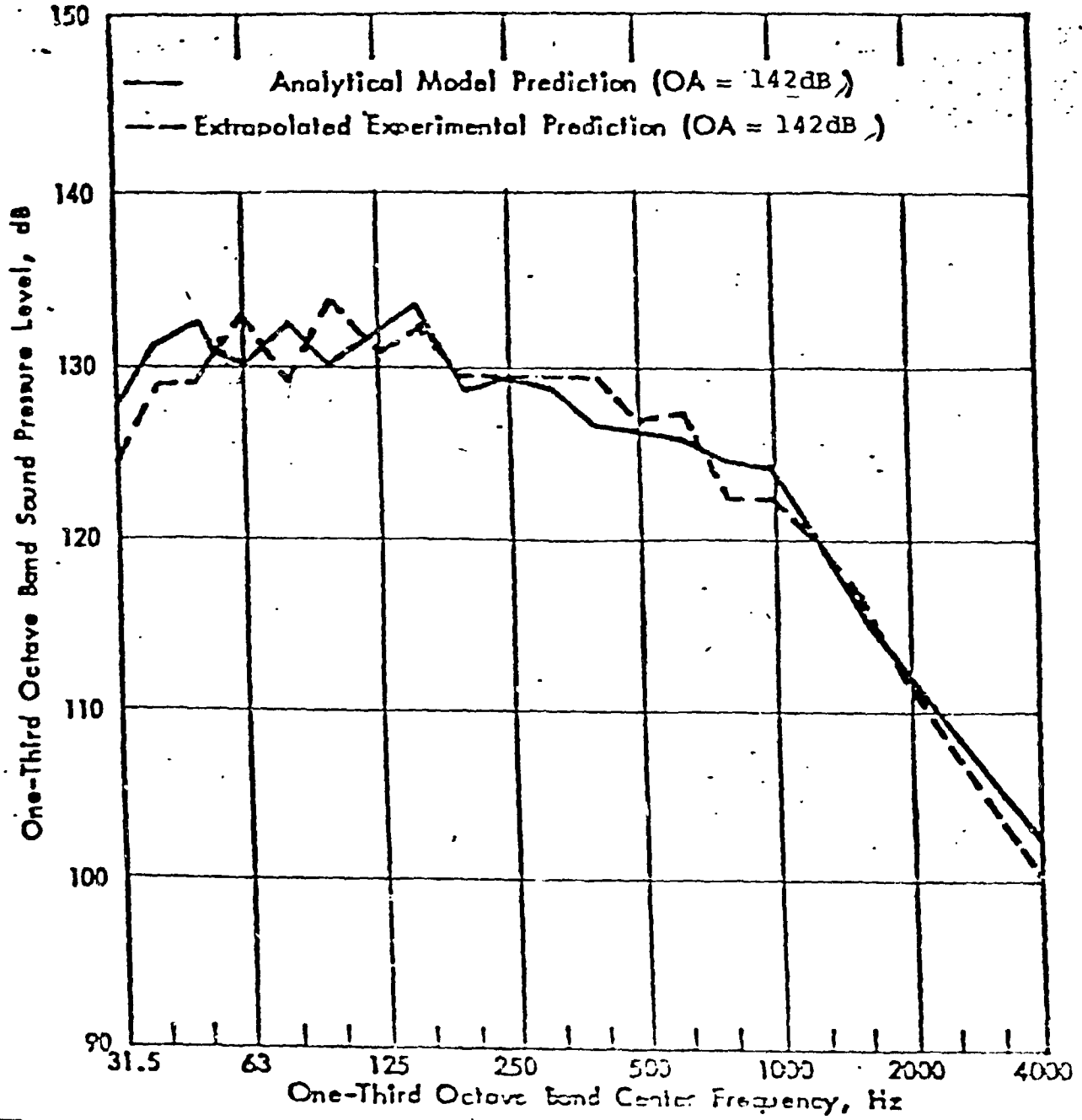
TYPICAL PROGRAM OUTPUT



PREDICTED SPACE AVERAGED SOUND PRESSURE LEVELS IN PAYLOAD BAY WITH SPACELAB CONFIGURATION 2



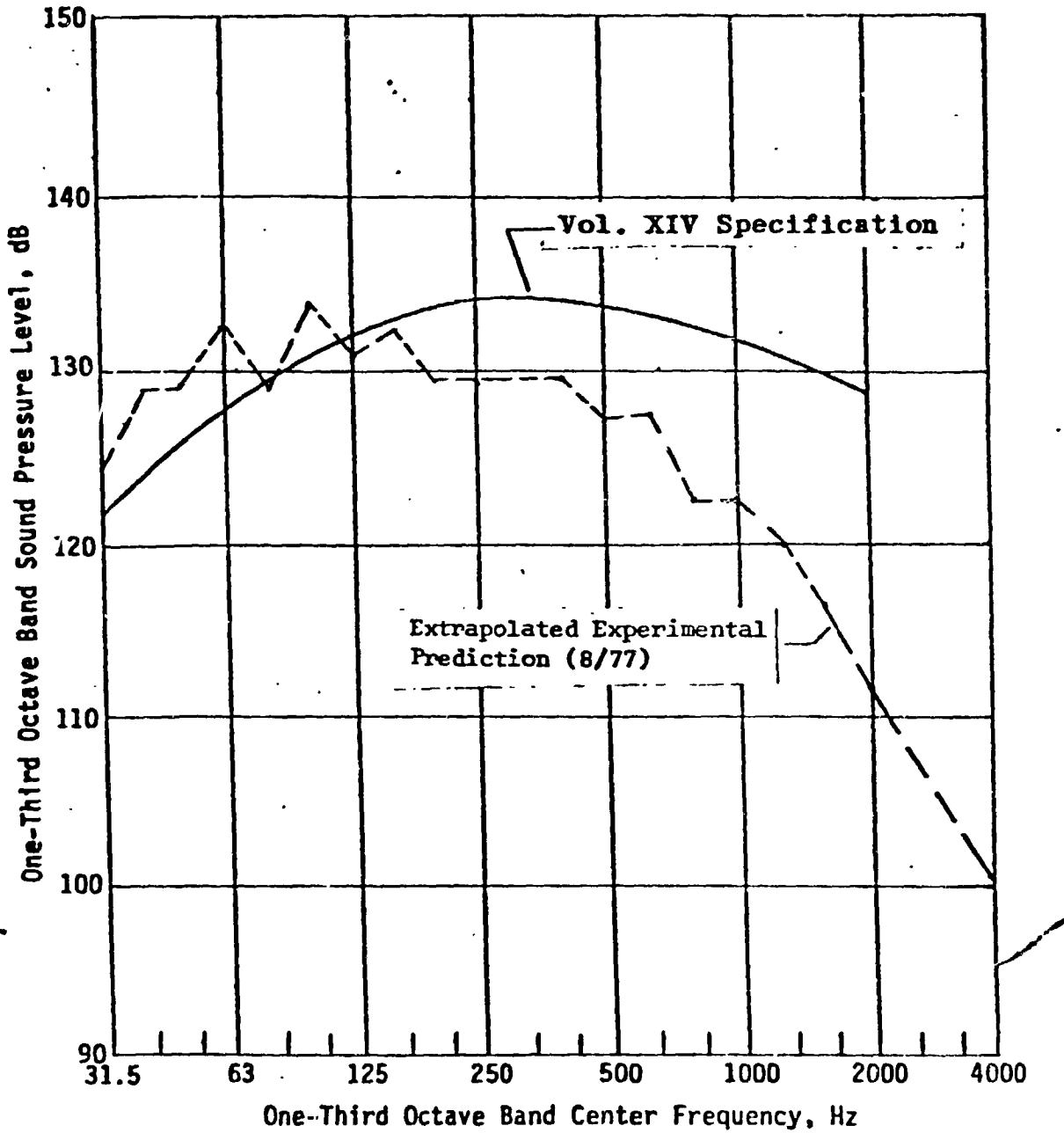
SHUTTLE P/L BAY ACOUSTIC ENVIRONMENT PREDICTION ACTIVITY



PREDICTION OF SPACE AVERAGED SPL IN OV102 EMPTY PAYLOAD 1A



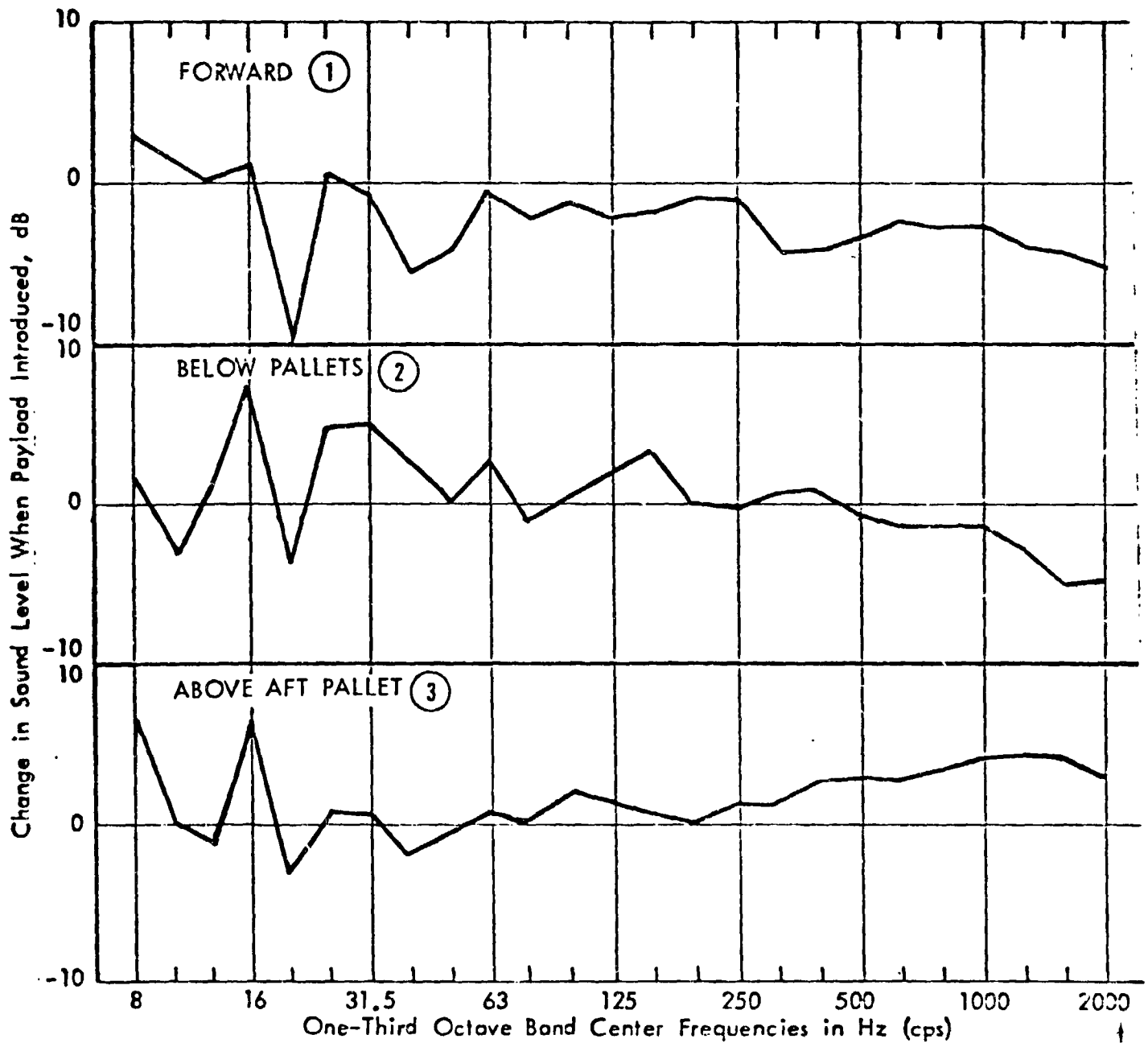
SHUTTLE P/L BAY ACOUSTIC ENVIRONMENT PREDICTION ACTIVITY



COMPARISON OF EMPTY P/L BAY EXTRAPOLATED EXPERIMENTAL PREDICTION
AND VOL. XIV SPECIFICATION

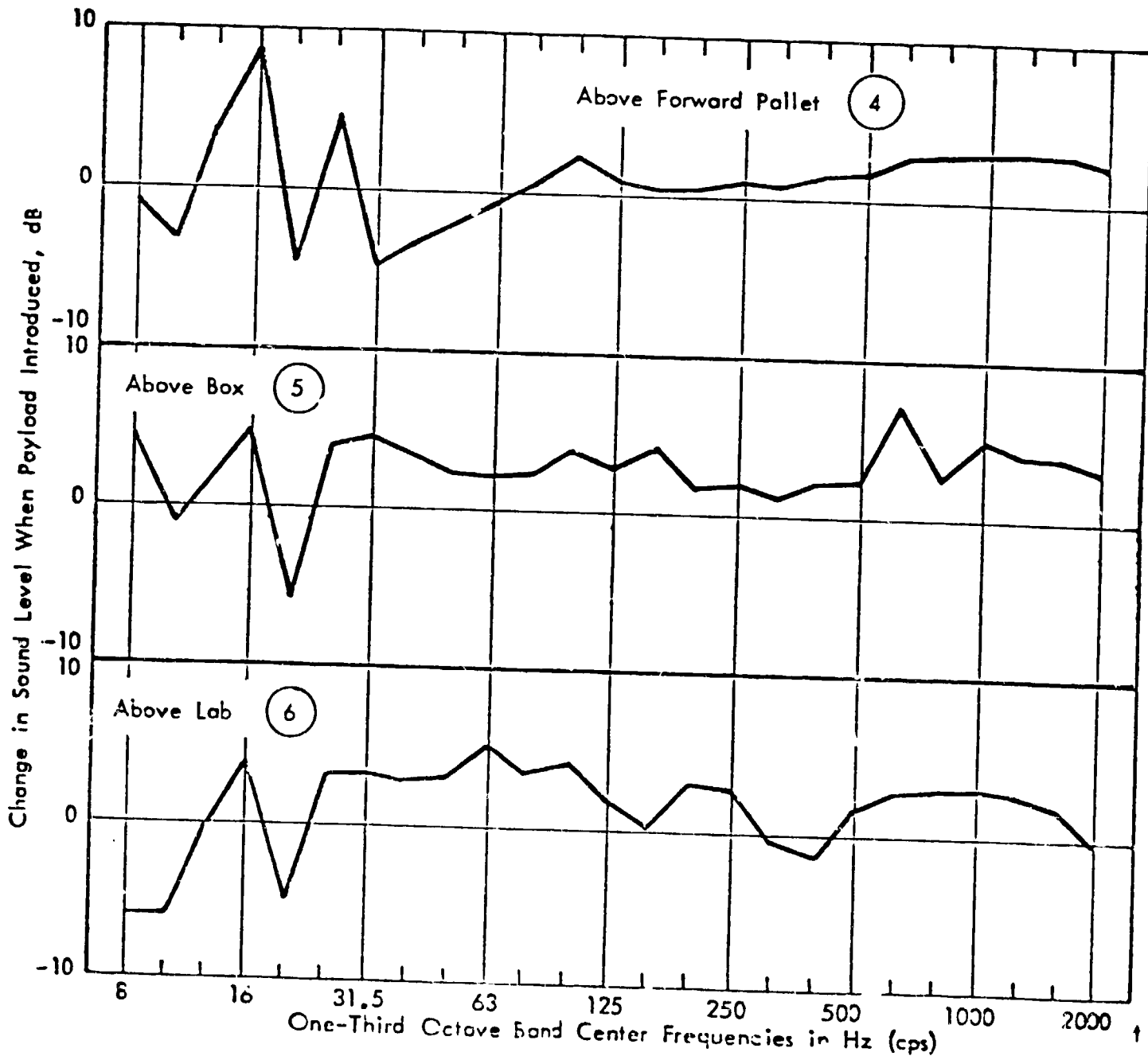
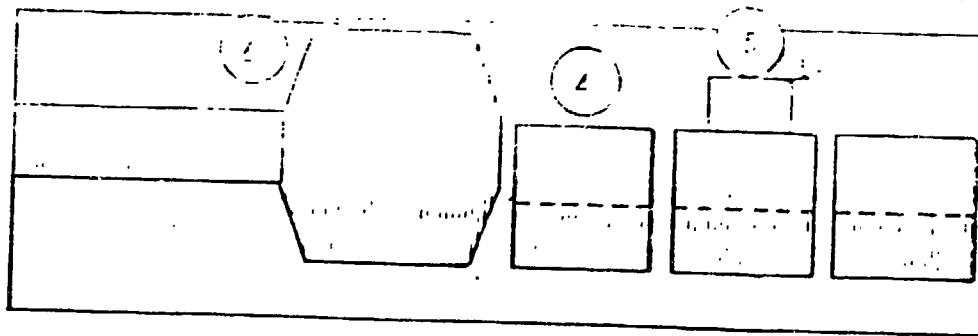


SHUTTLE P/L BAY ACOUSTIC ENVIRONMENT PREDICTION ACTIVITY



EFFECT OF SPACELAB 2 PAYLOAD ON SUBVOLUME SPACE-AVERAGED SOUND PRESSURE LEVELS

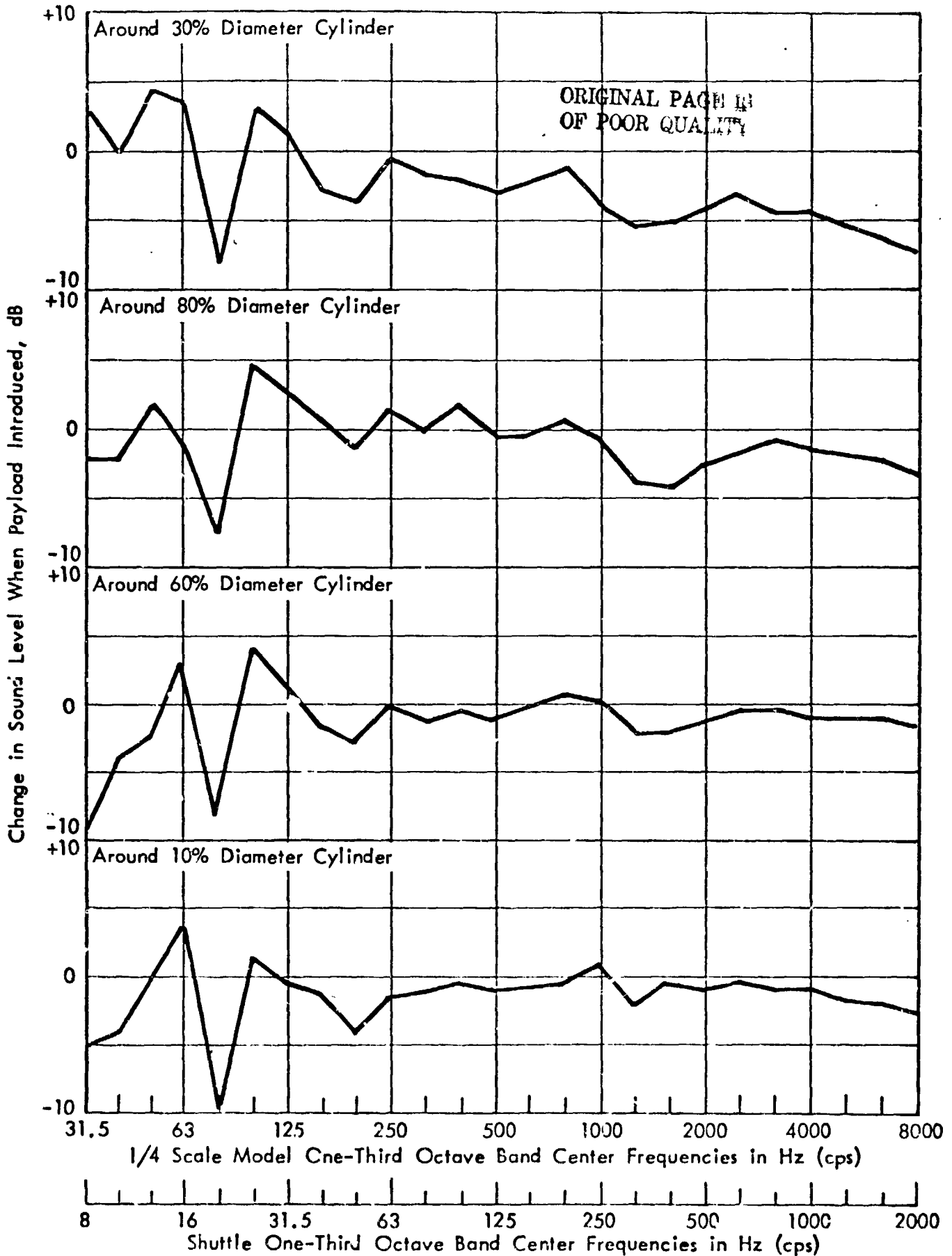




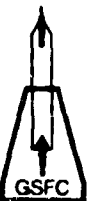
EFFECT OF SPACELAB 2 PAYLOAD ON SUBVOLUME SPACE-AVERAGED SOUND PRESSURE LEVELS



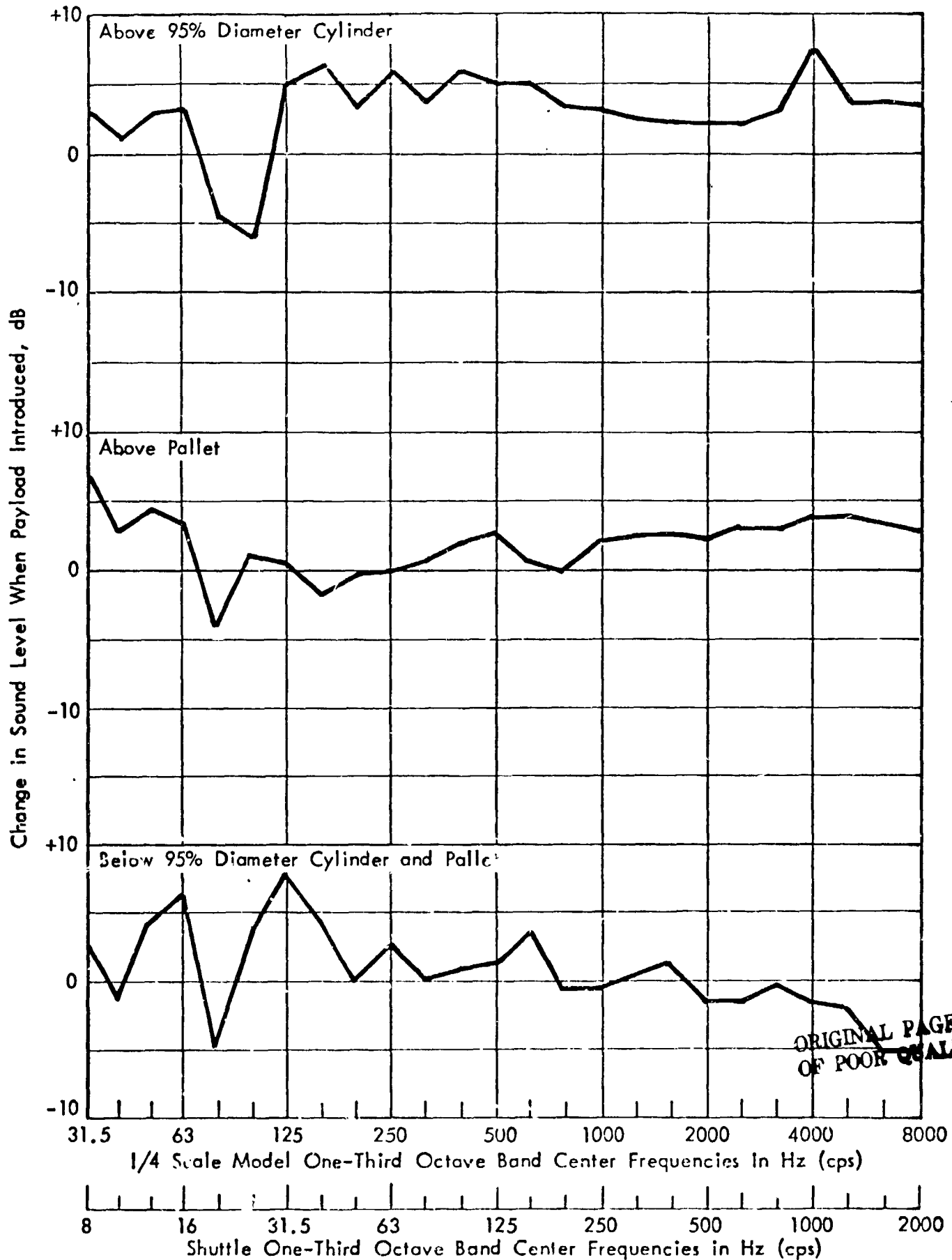
SHUTTLE PAYLOAD ACOUSTIC ENVIRONMENT PREDICTION ACTIVITY



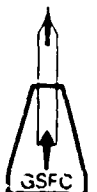
EFFECT OF DELTA D PAYLOAD ON SUBVOLUME SPACE-AVERAGED SOUND PRESSURE LEVELS 295



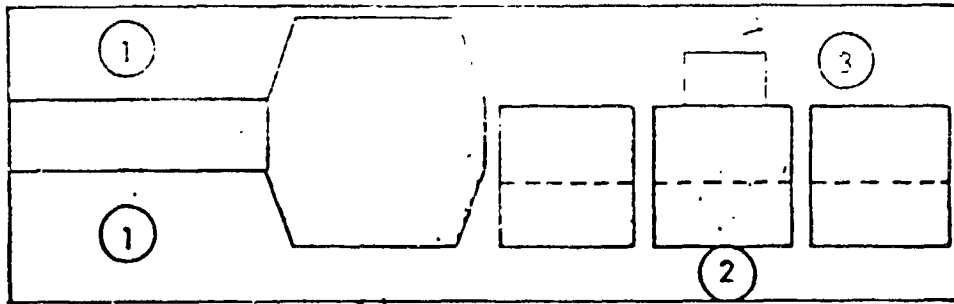
SHUTTLE P/L BAY ACOUSTIC ENVIRONMENT PREDICTION ACTIVITY



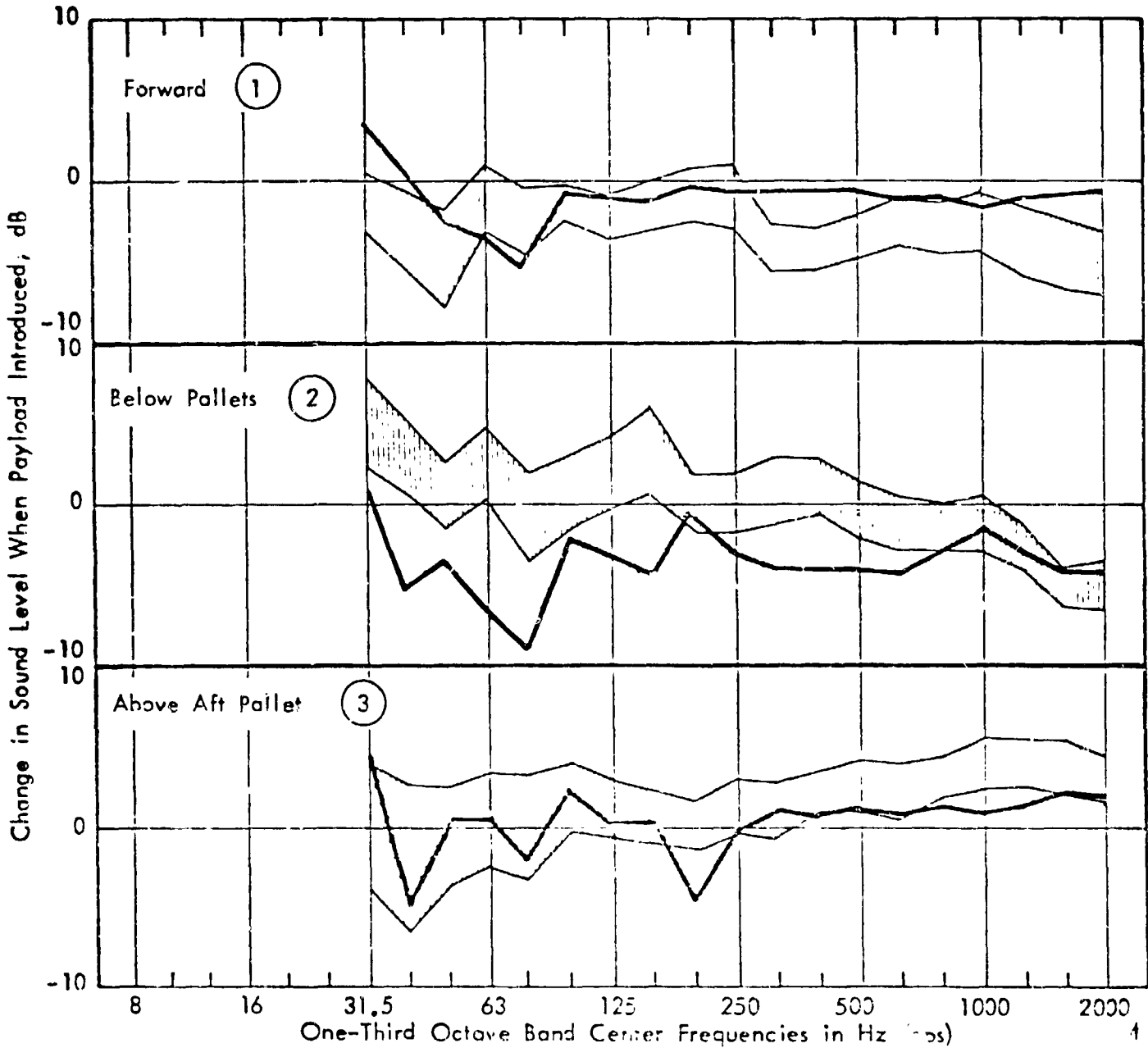
EFFECT OF DELTA D PAYLOAD ON SUBVOLUME SPACE-AVERAGED SOUND PRESSURE LEVELS



SHUTTLE P/L BAY ACOUSTIC ENVIRONMENT PREDICTION ACTIVITY



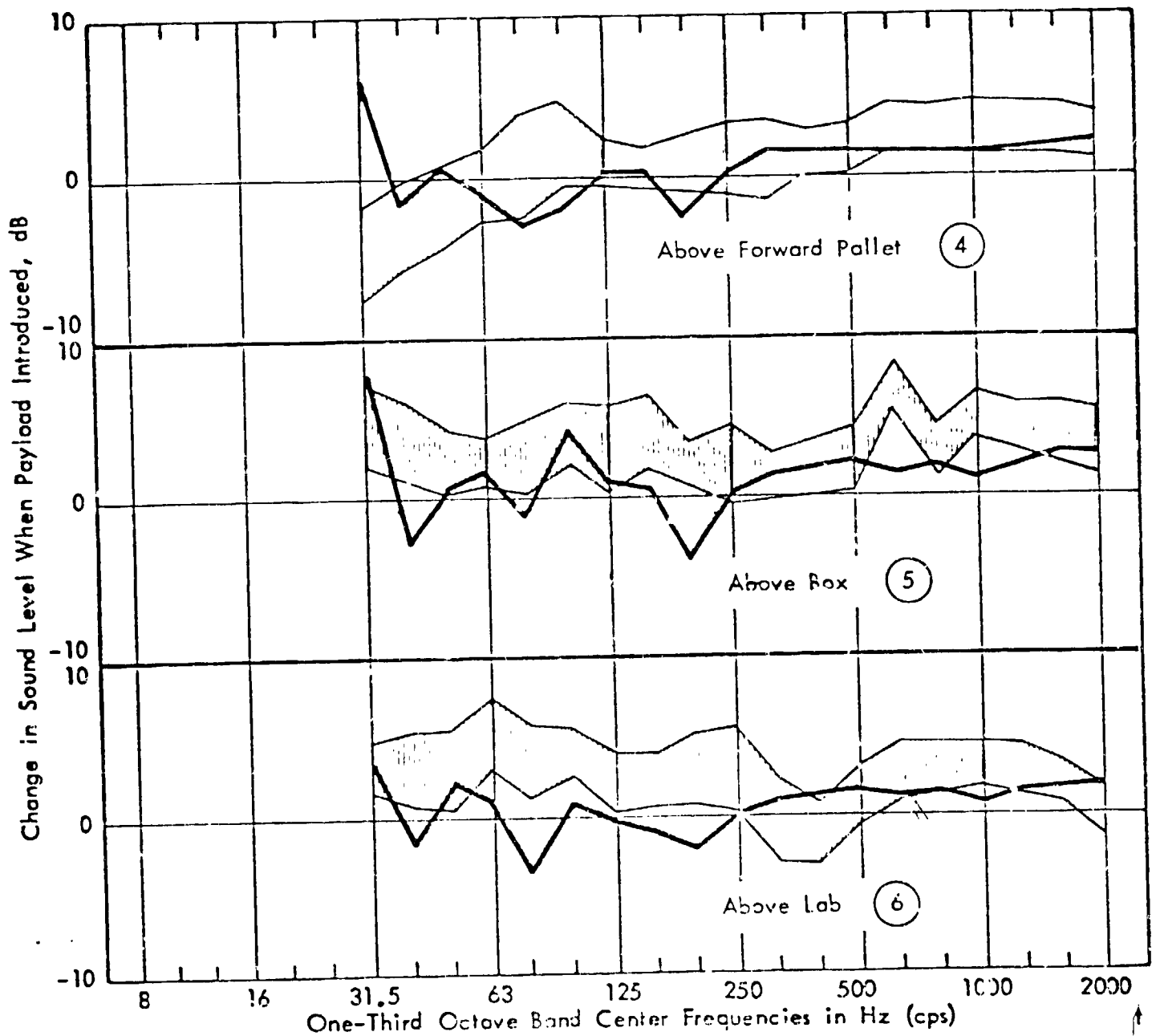
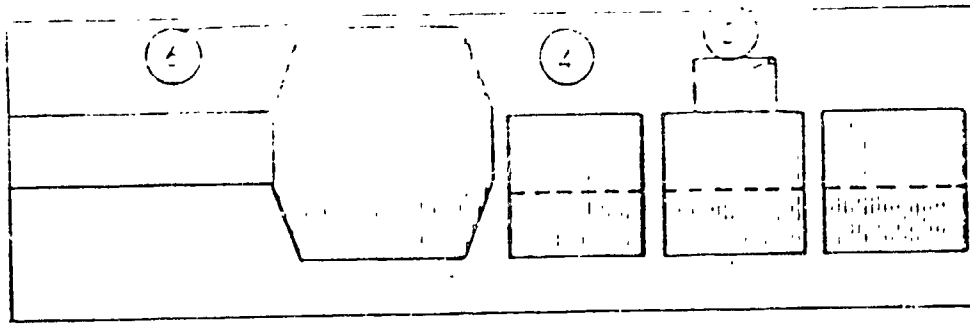
ORIGINAL PAGE IS
OF POOR QUALITY



COMPARISON OF PREDICTED AND MEASURED CHANGES IN SOUND LEVELS (SPACELAB CONFIGURATION 2)

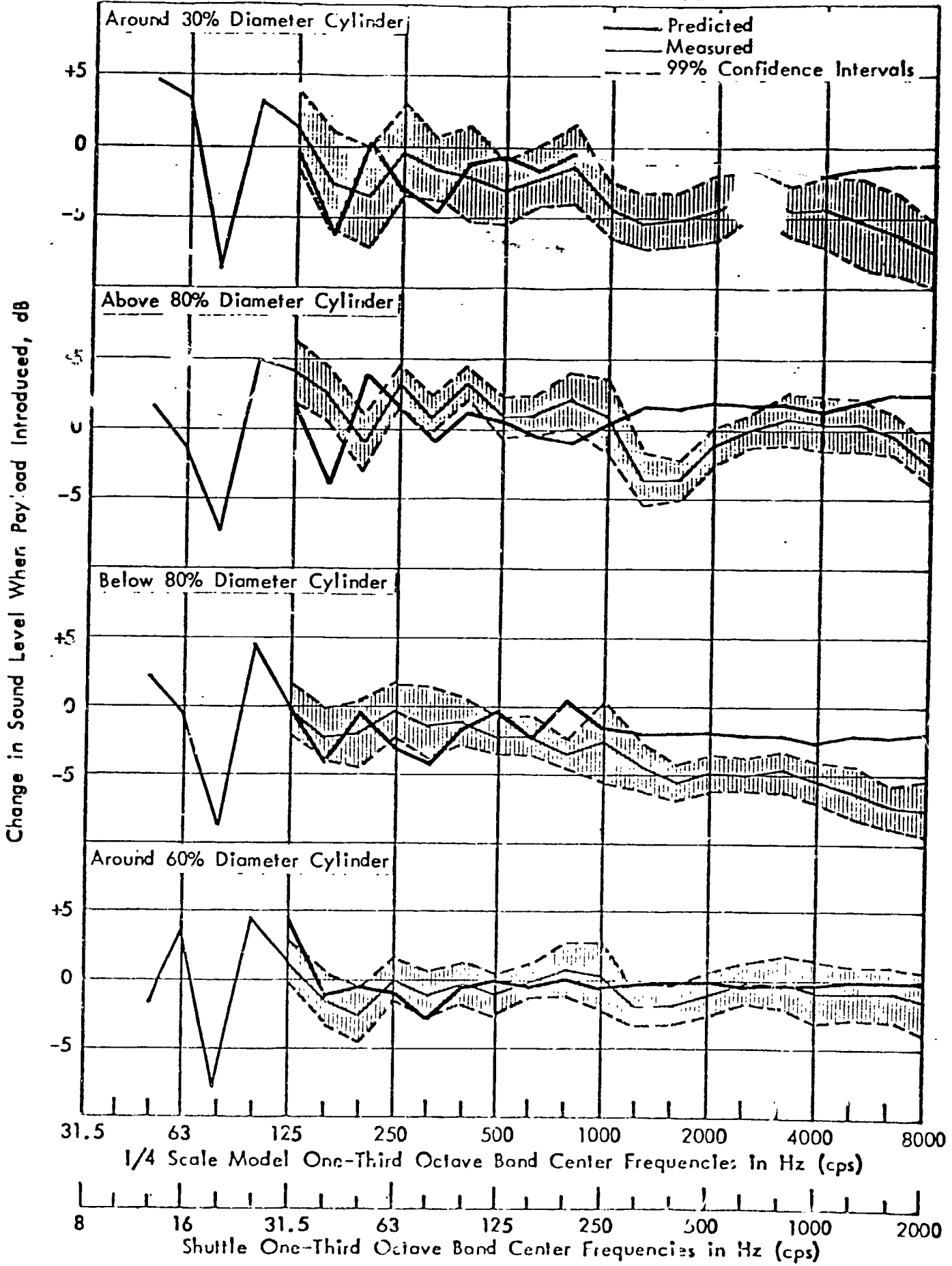


CRUTLER P/L ENVIRONMENTAL PREDICTION ACTIVITY



COMPARISON OF PREDICTED AND MEASURED CHANGES IN SOUND LEVELS (SPACELAB CONFIGURATION 2)

SHUTTLE PAYLOAD MODEL SOUND LEVEL PREDICTION ACTIVITY

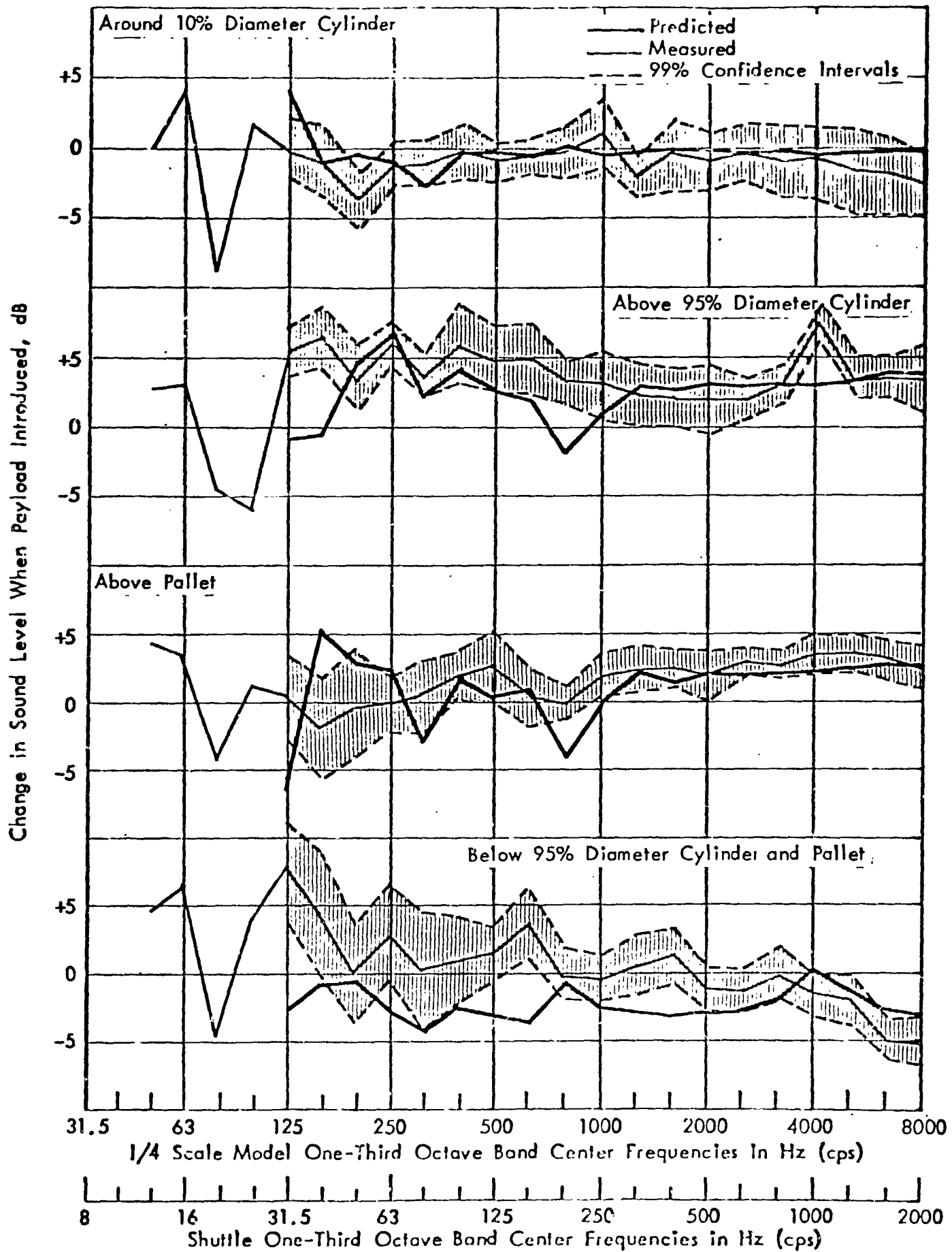


C-4

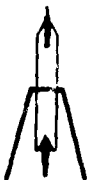
FINAL COMPARISON OF PREDICTED AND MEASURED CHANGES IN SOUND LEVELS, DELTA D PAYLOAD MODEL



SHUTTLE PAYLOAD ACOUSTIC ENVIRONMENT PREDICTION ACTIVITY



FINAL COMPARISON OF PREDICTED AND MEASURED CHANGES IN SOUND LEVELS, DELTA D PAYLOAD MODEL



SHUTTLE P/L BAY ACOUSTIC ENVIRONMENT PREDICTION ACTIVITY

MAJOR MILESTONES

- UPDATE PREDICTION MATH MODEL TO EXTEND COMPUTATION RANGE DOWN TO 12 Hz 1/3 OCTAVE BAND. 1/79
- UPDATE MATH MODEL TO INCLUDE LOW FREQUENCY DYNAMIC PROPERTIES OF SIDEWALL STRUCTURE. 3/79
- FINAL VALIDATION OF MATH MODEL PRIOR TO SS-1 FLIGHT USING ALL AVAILABLE GROUND TEST DATA. 5/79
- COMPUTER PROGRAM RELEASE - PACES (VER. 2) 6/79
- VALIDATION OF MATH MODEL USING SHUTTLE FLIGHT DATA (SS-1 THRU SS-4) 1/80 - 9/80

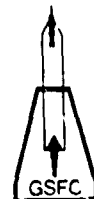


SHUTTLE P/L BAY ACOUSTIC ENVIRONMENT PREDICTION ACTIVITY

CURRENT STATUS

(11/78)

- COMBINATION OF OV 101 AND 1/4 SCALE MODEL TEST RESULTS HAVE VALIDATED THE BASIC FORMULATION OF THE PREDICTION MATH MODEL FOR BOTH THE EMPTY AND PAYLOAD OCCUPIED BAY CONDITIONS
- 1/4 SCALE MODEL TEST HAS VALIDATED AND GIVEN QUANTITATIVE EVIDENCE TO THE NOTION THAT SOME P/L CONFIGURATIONS CAN PRODUCE SIGNIFICANT INCREASES OVER THE EMPTY BAY ACOUSTIC LEVELS
- THE OV 101 AND 1/4 SCALE TEST RESULTS ARE CONSISTENT IN IDENTIFYING SOME SIGNIFICANT MATH MODEL DEFICIENCIES IN PORTIONS OF THE LOW FREQUENCY REGION BELOW 200 HZ. THE LARGE MAJORITY OF THESE DEFICIENCIES ARE IN THE UNCONSERVATIVE DIRECTION.
- ALL TESTS TO DATE HAVE BEEN CONDUCTED WITHOUT P/L DOOR RADIATORS PRESENT. THEREFORE THERE HAS BEEN NO VALIDATION OF THEIR EFFECT.

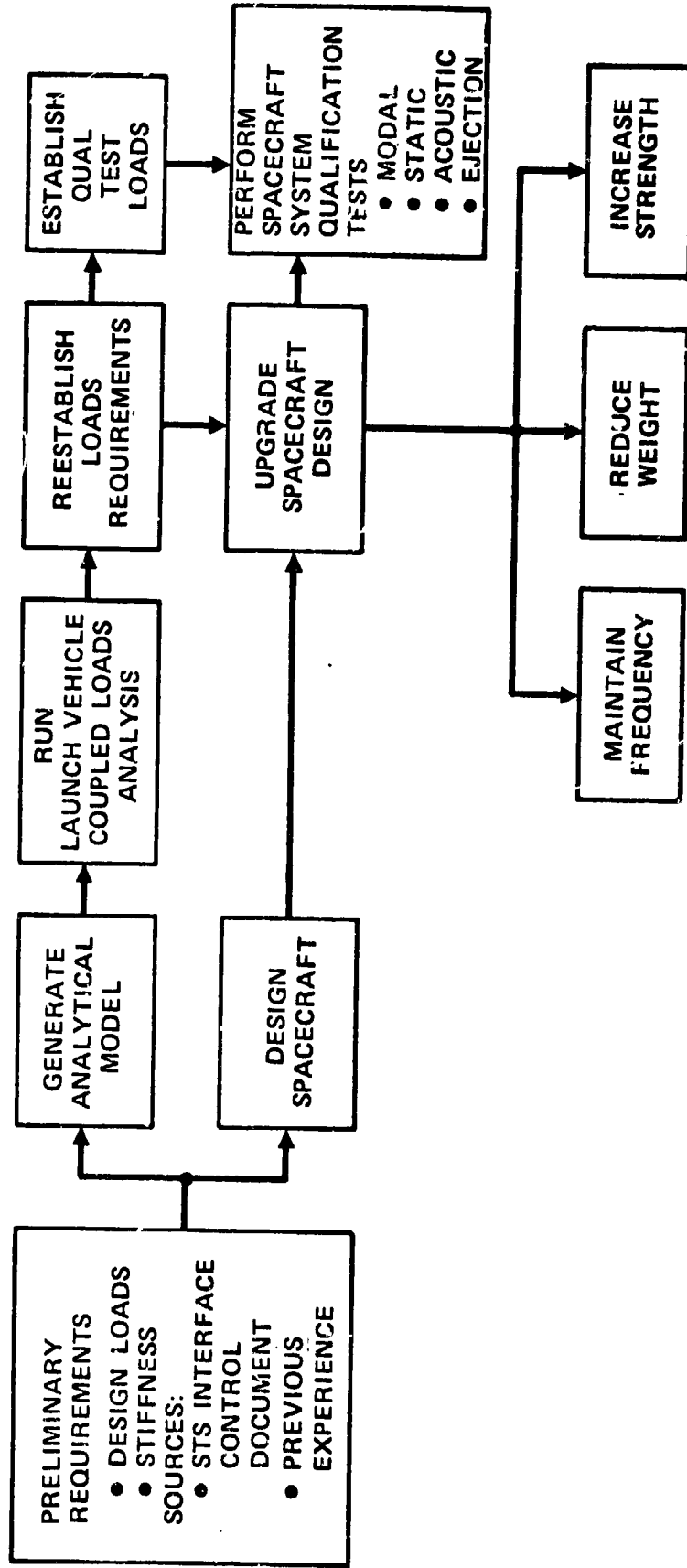


**STS LOADS IMPACT ON
SYNCOM IV**

HUGHES

TYPICAL STRUCTURAL DESIGN AND QUALIFICATION SEQUENCE

HUGHES



SYNCOM IV DESIGN PHILOSOPHY

HUGHES

DESIGN OBJECTIVES

- OPTIMIZE SPACECRAFT FOR SHUTTLE LAUNCH
- MINIMIZE REQUIRED SHUTTLE LIFTOFF VOLUME
- MINIMIZE WEIGHT FOR FUTURE GROWTH
- USE COST EFFECTIVE DESIGN APPROACH

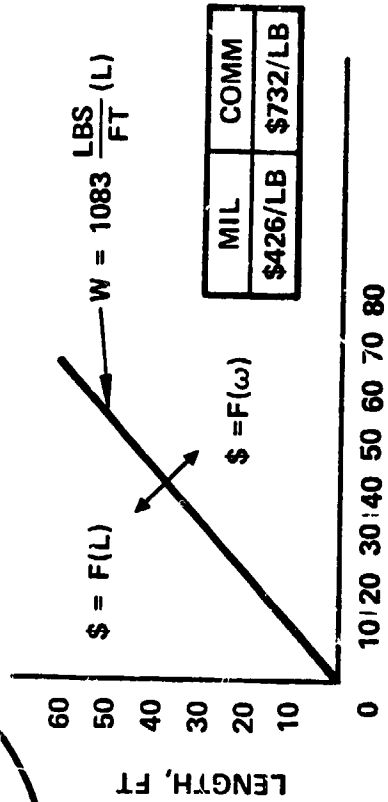
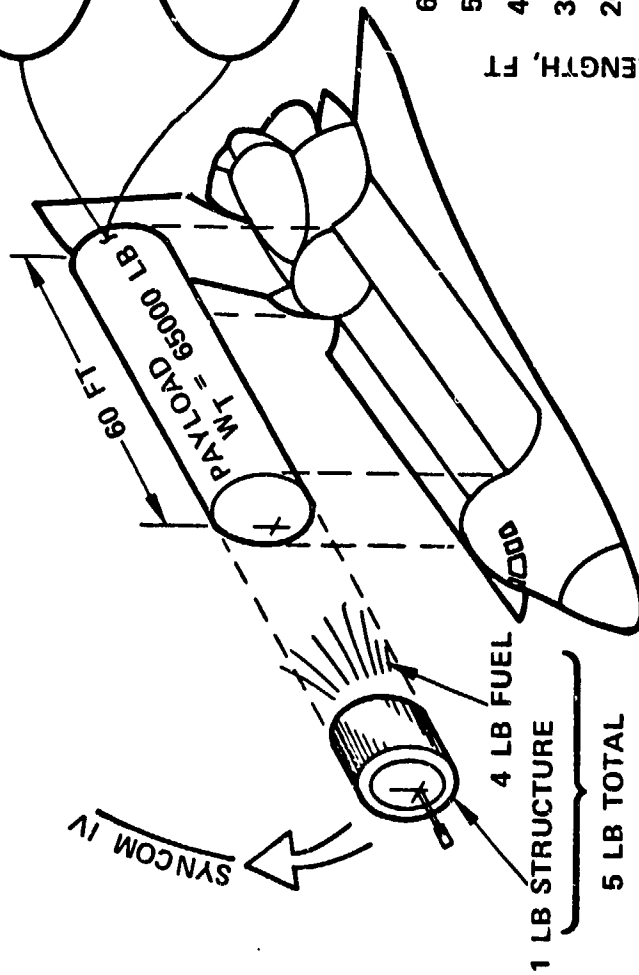
APPROACH

- INTEGRATE PROPULSION COMPONENTS
- PERFORM SELECTIVE DIAMETRAL PACKAGING
- CLOSE COUPLE SPACECRAFT WITH SHUTTLE
- INTEGRATE SPACECRAFT WITH CRADLE
- EVALUATE MULTIPLE STS LOCATIONS FOR FLIGHT AND GROWTH VERSIONS

STS LAUNCH PARAMETERS, 1982

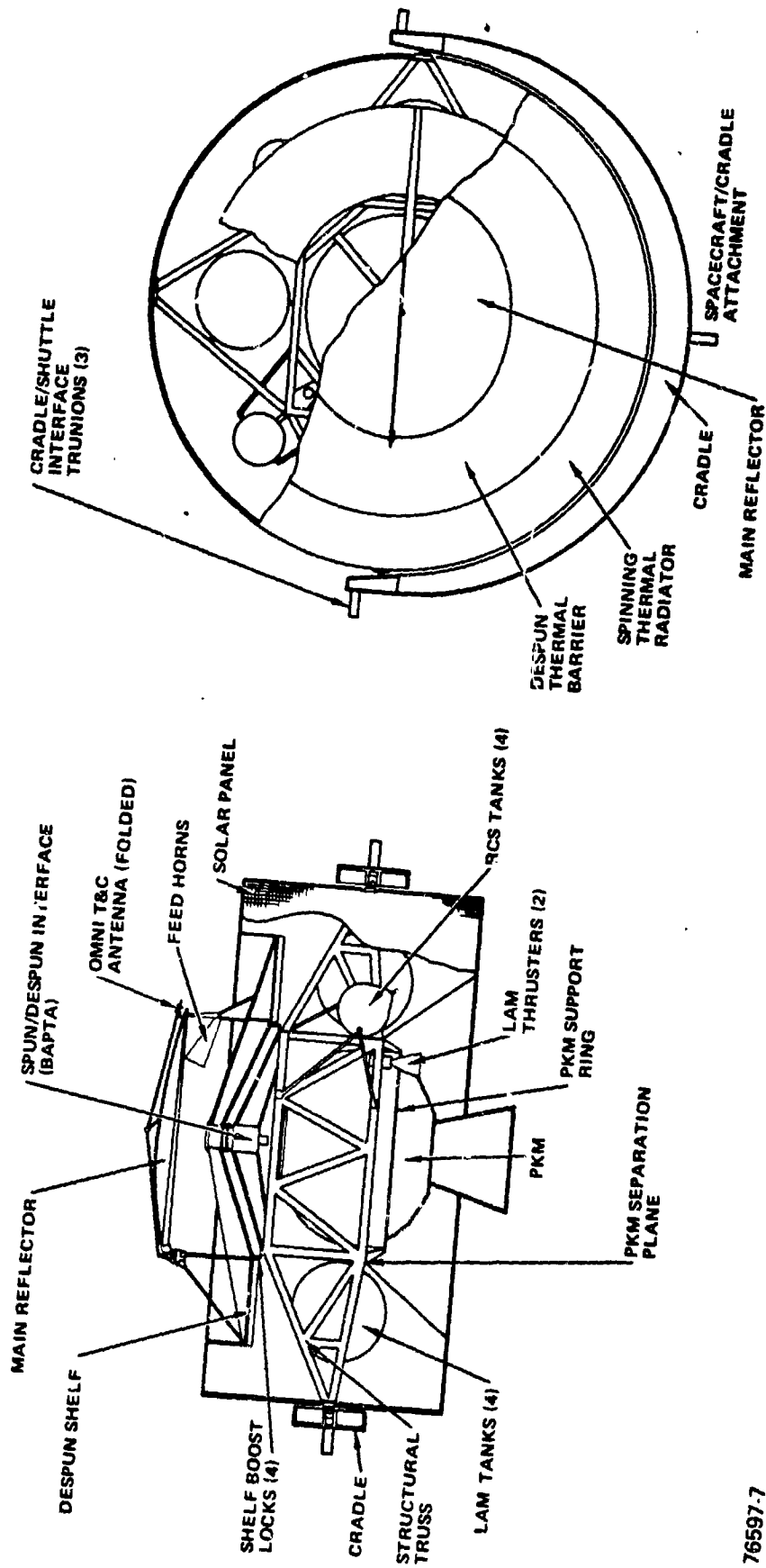
HUGHES

A L O N E		S H A R E	
MIL	COMM	MIL	COMM
\$20.8M	35.7M	\$27.7M	\$47.6



SYNCOM IV SPACECRAFT CONFIGURATION

HUGHES



76597-7

SYNCOM IV SPACECRAFT PHYSICAL AND DYNAMIC PROPERTIES

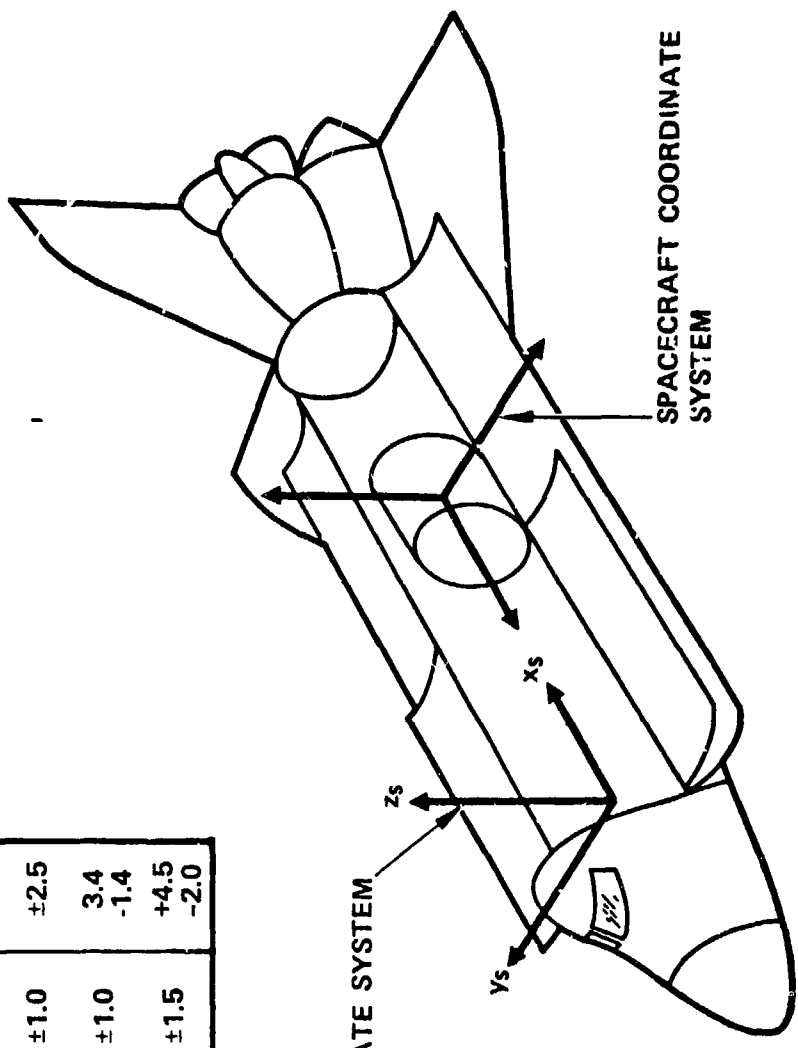
HUGHES

	SYNCOM IV - 10000	SYNCOM - 6000
COUPLED SPACECRAFT/CRADLE	18165	12350
WEIGHT (LB)		
I_{xx}	31.6×10^6	25.6×10^6
I_{yy}	24.6×10^6	14.7×10^6
MASS PROPERTIES		
I_{zz} (LB IN ²)	26.7×10^6	16.9×10^6
I_{xy}	-	-
I_{xz}	$-.08 \times 10^6$	$-.08 \times 10^6$
I_{yz}	$-.08 \times 10^6$	$-.08 \times 10^6$
S/C CG LOCATION	0.50 IN. FORWARD OF SEPARATION PLANE	0.50 IN. FORWARD OF SEPARATION PLANE
SPACECRAFT MODES		
f_{n1}	7.66 CPS (S/C-X)	9.93 CPS (S/C-X)
f_{n2}	8.51 CPS (S/C-Y)	10.64 CPS (S/C-Y)
f_{n3}	11.28 CPS (S/C-Z)	14.94 CPS (S/C-Z)
f_{n4}	13.42 CPS (PKM-X,Z)	16.51 CPS (PKM-X,Z)
f_{n5}	15.8 CPS (PKM- θ -Z)	22.83 CPS (PKM- θ -Z)

SYNCOM IV DESIGN LOAD FACTORS

SELECTED LIMIT ACCELERATION FACTORS (G'S)

FLIGHT EVENT	A_{x_s}	A_{y_s}	A_{z_s}
LIFTOFF	-0.2 -3.2	±1.0	±2.5
LANDING (6.0 FPS)	±1.5	±1.0	3.4 -1.4
EMERGENCY LANDING	+4.5 -1.5	±1.5	+4.5 -2.0

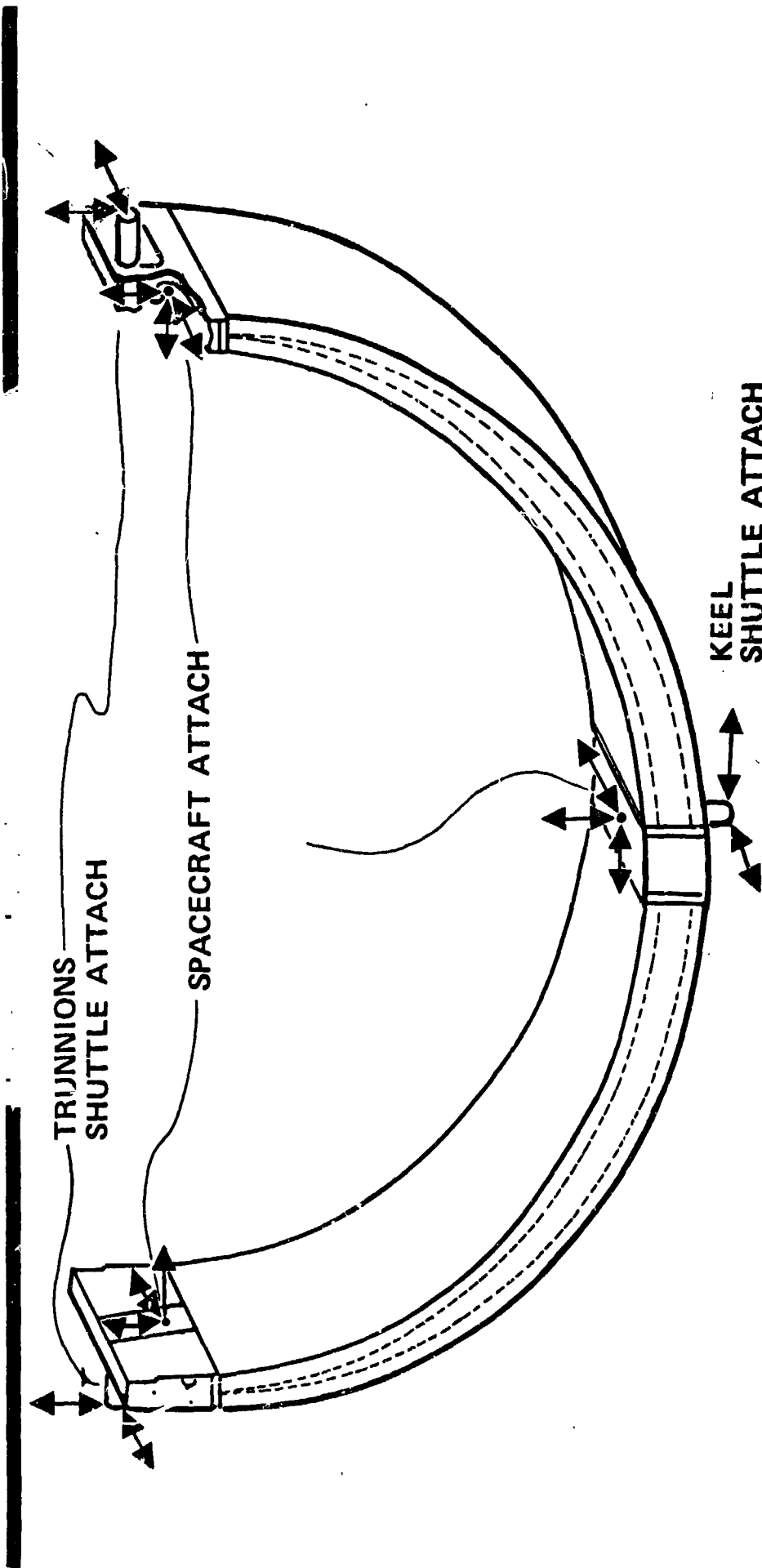


SHUTTLE COORDINATE SYSTEM

SPACECRAFT COORDINATE SYSTEM

SYNCOM IV CRADLE

HUGHES



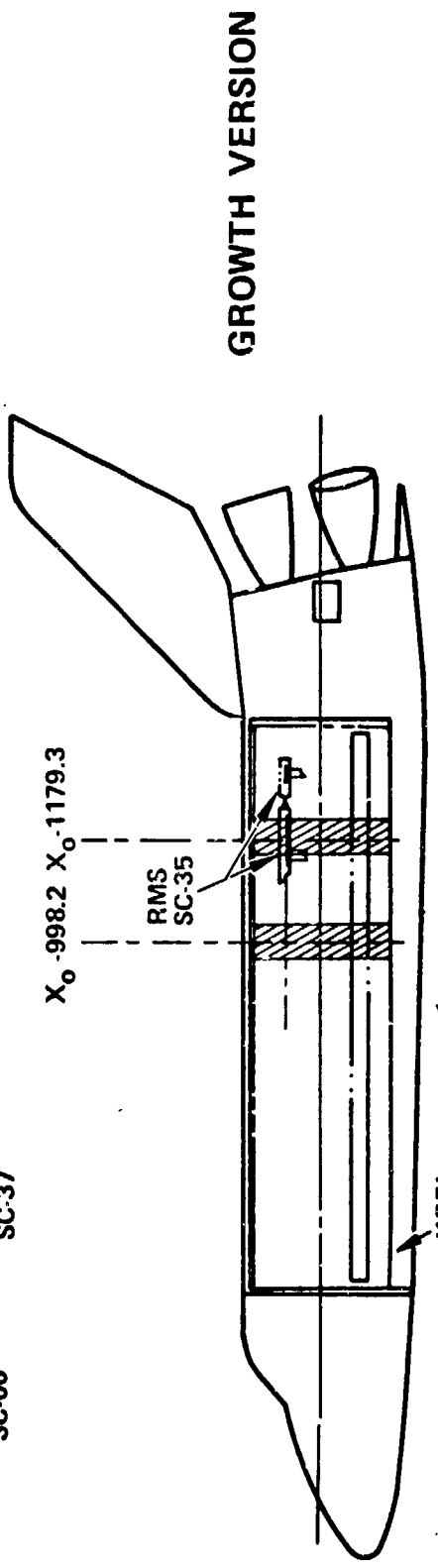
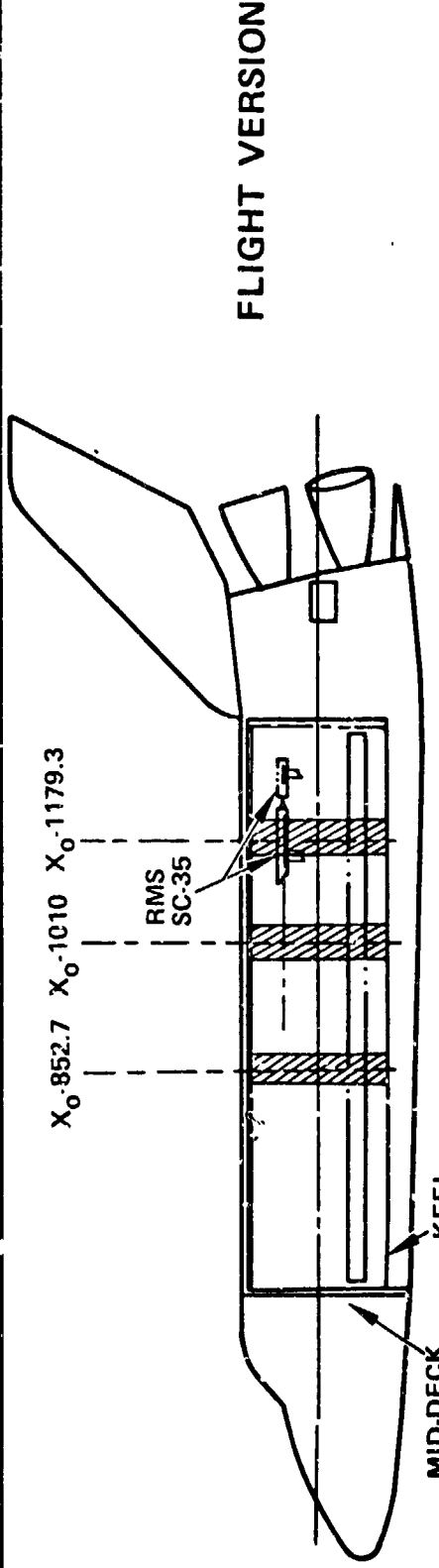
COUPLED LOADS ANALYSIS PHILOSOPHY

HUGHES

- ESTABLISH LOADS FOR THE IDENTICAL SPACECRAFT WITH TWO DIFFERENT MASS DISTRIBUTIONS, (FLIGHT VERSION AND GROWTH VERSION)
- SELECT VARIED LOCATIONS ON SHUTTLE FOR POSITION EFFECTS
- EVALUATE WORST CASE CONDITIONS BOTH IN LIFTOFF AND LANDING

SHUTTLE PAYLOAD LOCATION FOR SYNCOM IV

HUGHES



**COUPLED ANALYSIS CONDITIONS
COUPLED ANALYSIS CASE (LANDING)**

HUGHES

SYNCOM IV 10,000	SYNCOM IV 6,000	SINK SPEED, FPS	CROSSWIND, KNOT	ANGLE OF ATTACK, DEG	HORIZONTAL VELOCITY, KNOT
LN980	LN976	6.0	NO CROSSWIND NOSE GEAR SLAPDOWN	15.84/13.93, HIGH	150/152
LM981	LM977	6.0	NO CROSSWIND	7.17.81, LOW	206/205
LM982	LM978	5.0	20.0	15.84/16.93, HIGH	143/143
LM923	LM979	5.0	20.0	7.08/7.79, LOW	208/205

86764-10X

**COUPLED ANALYSIS CONDITIONS
COUPLED ANALYSIS CASE (LIFT-OFF)**

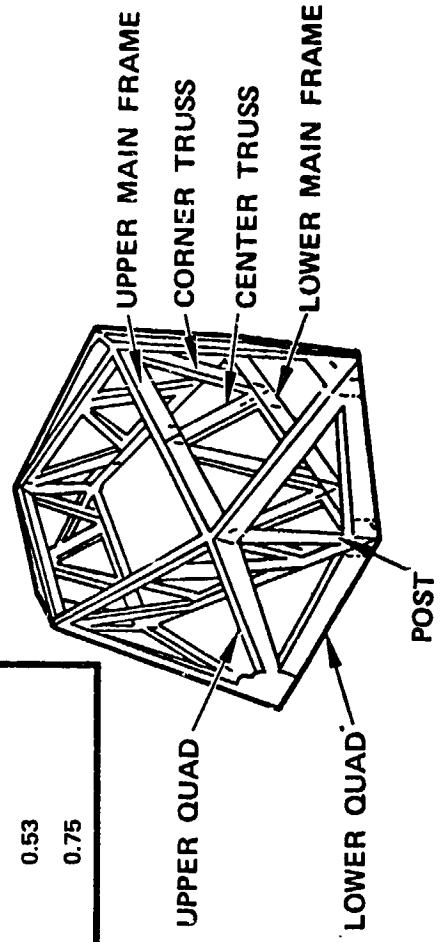
HUGHES

SYNCOM IV- 10,000	SYNCOM IV- 6,000	SRB STIFFNESS		SRB THRUST AND TIMING	SRB MISMATCH	SRB LAG, SEC
		0.8	1.2			
LP510	LP510	0.8		HIGH PERFORMANCE, FAST	200 K	0.333
			1.2			
LP512	LP512	0.8		LOW PERFORMANCE, FAST	200 K	0
			1.2			
LO549	LO549	0.8		HIGH PERFORMANCE, SLOW	200 K	0.333
			1.2			
-	LP519	1.2		LOW PERFORMANCE, SLOW	200 K	0.333
			-			

COUPLED LOADS ANALYSIS INTERNAL LOADS RESULTS

HUGHES

ITEM	ULT DESIGN LOAD LBS.	1.65 x COUPLED ANALYSIS LOADS LBS.	COUPLED LOADS ANALYSIS DESIGN LOADS
LOWER MAIN QUAD	89400	44600	0.50
UPPER MAIN QUAD	59200	34500	0.58
LOWER KEEL QUAD	26700	13000	0.49
UPPER KEEL QUAD	16000	13700	0.86
LOWER MAIN FRAME	59400	30700	0.52
LOWER KICK FRAME	50700	33500	0.66
UPPER MAIN FRAME	35400	29000	0.82
UPPER KICK FRAME	30100	25800	0.86
POST	24700	12500	0.51
CORNER TRUSS	18600	9900	0.53
CENTER TRUSS	6500	4900	0.75



86764-11

NEW DESIGN LOAD FACTORS FROM COUPLED ANALYSIS INVESTIGATION

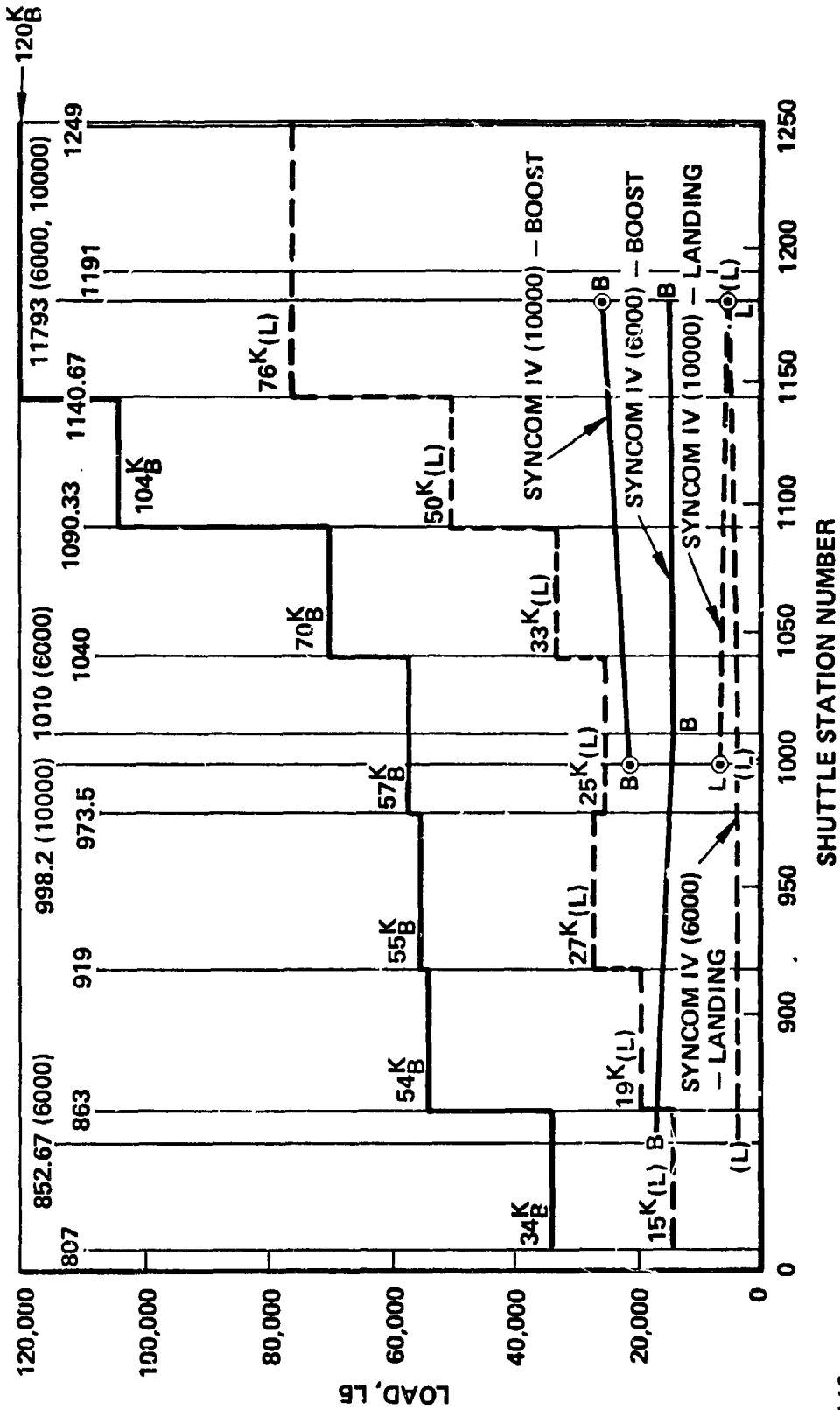
HUGHES

		COND	X, G'S	Y, G'S	Z, G'S	θy, G'S/IN.
LIFTOFF	MAX X	LP5101P2	-3.03	—	-0.4	-0.026
	MAX Y	LO549P8	-1.09	±0.98	—	+0.016
	MAX θy	LP512P8	-2.40	±0.20	+0.69	-0.023
LANDING (6.0 FPS)	MAX Z	LM981	—	—	+2.57	-0.053
	EMERGENCY* LANDING		+4.5 -1.5	±1.0	+4.5 -2.0	

* ULTIMATE LOADS INCLUDES 1.4 FACTOR REQUIREMENT

SHUTTLE INTERFACE LONGERON X LOADS VS ALLOWABLES

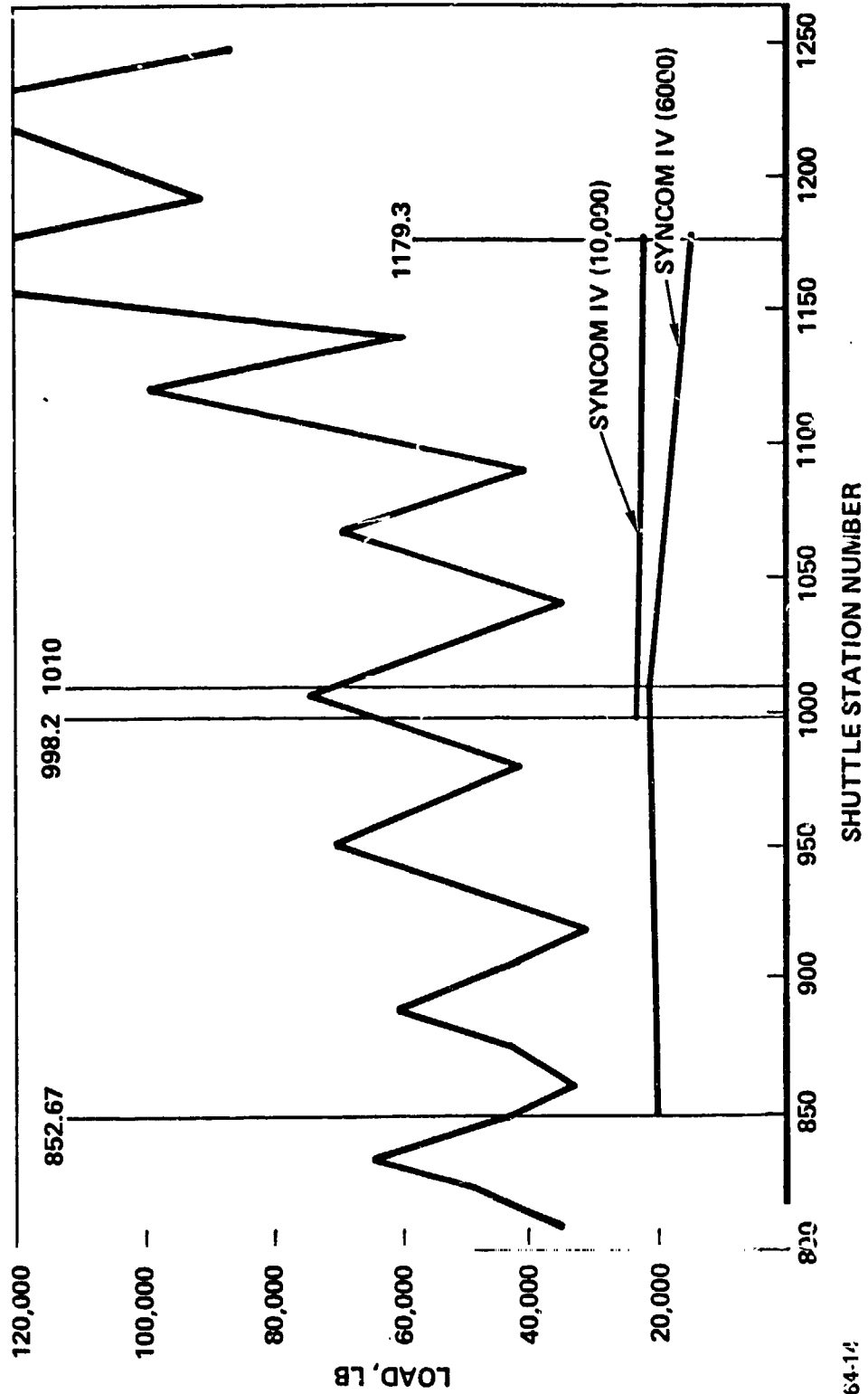
HUGHES



86764-13

SHUTTLE INTERFACE LONGERON Z LOADS VS ALLOWABLES

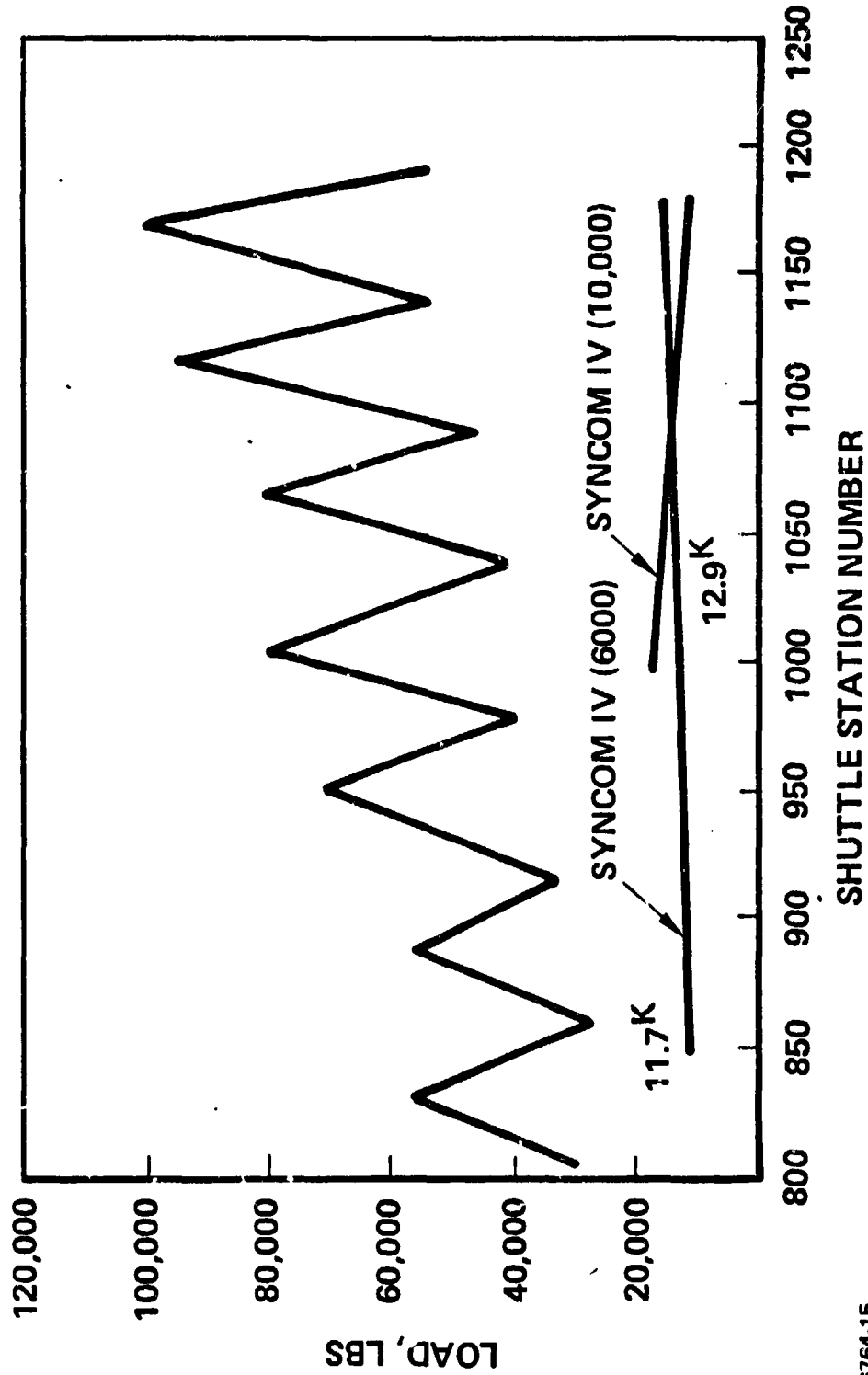
HUGHES



86764-14

SHUTTLE INTERFACE KEEL Y LOADS VS ALLOWABLES

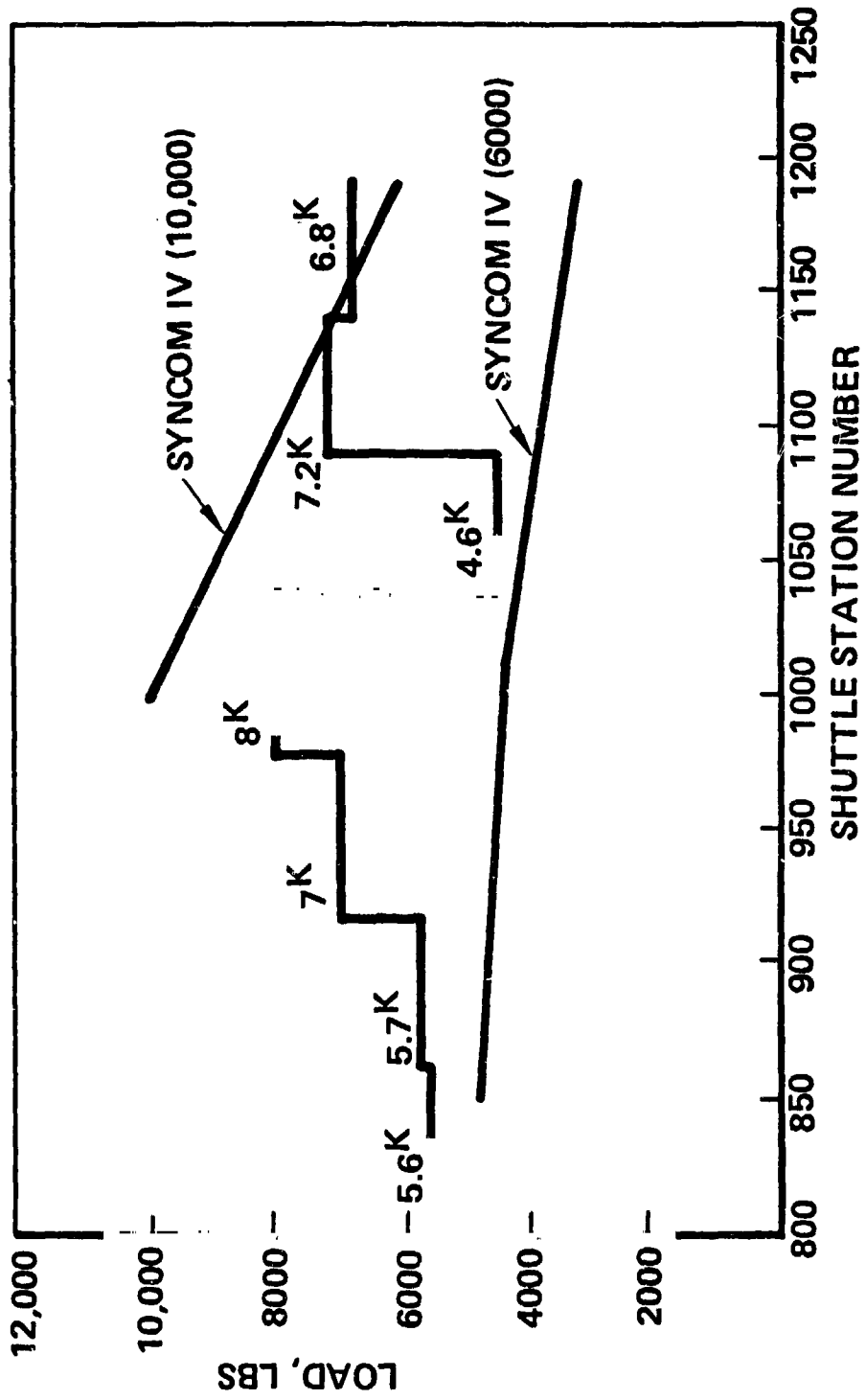
HUGHES



86764-15

SHUTTLE INTERFACE KEEL X LOADS VS ALLOWABLES

HUGHES



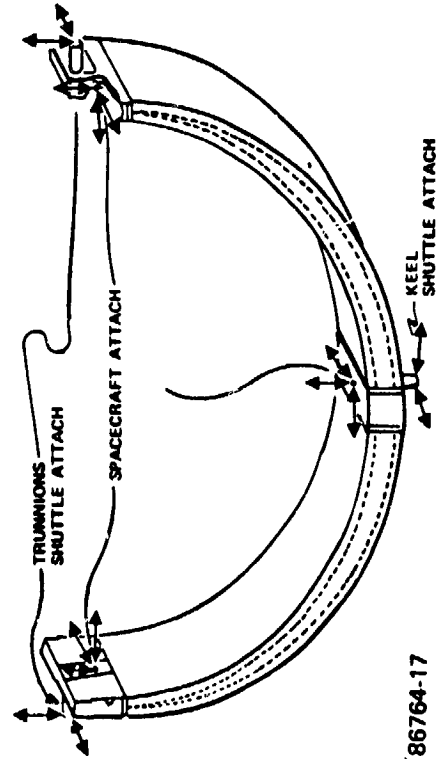
SOLUTION TO KEEL OVERLOAD

HUGHES

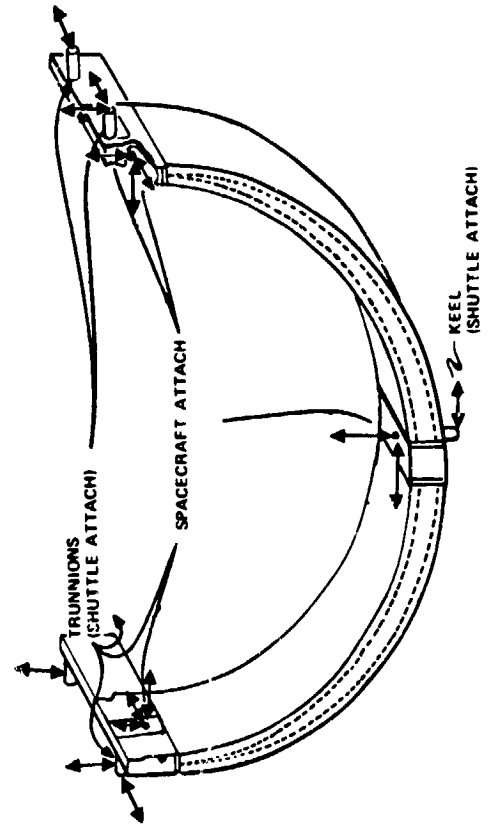
- ADD OUTRIGGERS TO EXISTING CRADLE
- REMOVE X CONSTRAINT AT KEEL
- ADD STRUCTURE TO SPACECRAFT FOR NEW LOAD PATH
- REQUIRES 2 MORE BRIDGE FITTINGS

WEIGHT IMPACT \approx 300 LB

3 POINT CRADLE, ORIGINAL



5 POINT CRADLE, NEW



86764-17

HUGHES

CONCLUSIONS

- PRELIMINARY QUASI-STATIC (ICD) RECOMMENDED LOAD VECTORS ARE CLOSE
- SIGNIFICANT SEPARATION OF LOAD VECTORS EXIST FOR PAYLOADS OF SYNCOM IV TYPE
- PITCH VECTOR SHOULD BE RECOMMENDED
- KEEL CAPABILITY SHOULD BE UPGRADED FOR MORE EFFICIENT PAYLOAD TRANSFER
- STIFFNESSES OF STS PAYLOAD INTERFACE POINTS WOULD BE VALUABLE FOR MODAL COUPLING INVESTIGATION

EMPLOYMENT OF RESIDUAL MODE EFFECTS
IN
VEHICLE / PAYLOAD DYNAMIC LOADS ANALYSIS

R. N. COPPOLINO
AEROSPACE CORPORATION

Component mode truncation and modal synthesis are commonly employed in formulation of launch vehicle/payload dynamic models. The advantages of this approach are (1) computational economy and (2) accommodation for employment of component mode test data. Typically, payload component test data is in the form of fixed interface modes. In addition, the launch vehicle test data (for Space Shuttle*) is in terms of unconstrained modes.

It is well established that proper characterization of component interfaces is crucial to convergence of the modal synthesis procedure. In the present discussion, the augmentation of a truncated set of unconstrained vehicle modes with residual vectors is employed for complete static characterization of the payload interface.

* Also referred to herein as STS (Space Transportation System)

CONTENTS

- RESIDUAL VECTOR DEFINITION
- RAYLEIGH-RITZ COMPONENT FORMULATION
- DEMONSTRATION PROBLEM: STS/IUS/DSP LIFT-OFF
- MODAL SYNTHESIS ERROR SPECTRA AND SELECTED DYNAMIC
RESPONSE COMPARISONS
- CONCLUDING REMARKS

The present discussion includes definition of a "residual" vector set associated with unconstrained component interface static behavior not fully described by a truncated set of unconstrained component modes. The truncated modal set augmented by residuals comprises the trial vector set for a Rayleigh-Ritz component approximation. The resulting equation set is readily expressed in a form identical to a simple unconstrained mode truncation; moreover, it is equivalent to the Rubin component approximation.*

A demonstration problem consisting of Space Transportation System/Inertial Upper Stage/DSP lift-off configuration modal synthesis and dynamic response is employed. Truncation error analysis demonstrates the qualities of the subject procedure. Employment of truncated unconstrained mode/residual approximations may provide a means for efficient and predictably convergent analysis for a variety of structural dynamic analysis tasks as well as the application presented herein.

*"Improved Component - Mode Representation for Structural Dynamic Analysis", S. Rubin, AIAA Journal, Vol. 13, No. 8, August 1975, pp 995-1006

UNCONSTRAINED COMPONENT

DYNAMIC EQUATION SET

$$M\ddot{x} + Kx = \Gamma_a f_a + \Gamma_e f_e$$

SYSTEM MODES

$$X = \underbrace{\Phi_r q_r}_{\text{"Rigid Body"}} + \underbrace{\Phi_l \eta_l}_{\text{"Low" Frequency}} + \underbrace{\Phi_h q_h}_{\text{"High" Frequency}}$$

TRANSFORMATION TO RIGID BODY AND FLEXIBLE DOF'S

$$X = \underbrace{\Gamma_r X_r}_{\text{Rigid Body Shapes}} + \underbrace{\Gamma_f X_f}_{\text{Flexible Body Orthogonal to Rigid Body}}$$

The free-free component dynamic equation set is expressed in terms of system physical dof's X , with applied dynamic loads consisting of attachment (or interface) loads, f_a , and external loads, f_e , such as thrust, aerodynamic loads and stand forces. The matrices Γ_a and Γ_e serve as allocation matrices for the respective applied load classes. The system modes of the component are grouped into rigid body, "low" frequency and "high" frequency categories. The latter category comprises the modes truncated out of the complete description. For the purpose of calculation of static flexible displacement distributions, the system physical degrees of freedom are expressed in terms of rigid body shapes, T_r , based upon selected ignorable dof's (X_r), and in terms of flexible body shapes, T_f , orthogonal to the rigid body shapes (i. e. $T_r^T M T_f = 0$).

RESIDUAL VECTOR DEFINITION

CHOOSE TRUNCATED MODE SET $(\phi_r | \phi_l)$ WITH FREQUENCY CUT-OFF BASED ON EXTERNAL LOAD CHARACTERISTICS

RESIDUAL VECTORS = EXACT STATIC FLEXIBLE DISPLACEMENT MINUS APPROXIMATE TRUNCATED STATIC FLEXIBLE DISPLACEMENT (DUE TO UNIT ATTACHMENT DOF FORCES, f_a)

FORM 1 - EMPLOYING STATIC SOLUTION AND LOW FREQUENCY MODES

$$G\rho = K^{-1}\Gamma_a - \phi_l \omega_l^{-2} \phi_l^T \Gamma_a$$

with $K^{-1} = T_f (T_f^T K T_f)^{-1} T_f^T$

FORM 2 - EMPLOYING HIGH FREQUENCY MODES

$$G\rho = \phi_h \omega_h^{-2} \phi_h^T \Gamma_a$$

The truncated modal set ($\phi_r | \phi_l$) is selected on the basis of frequency content of the external loads and possibly modal external load distribution character, $\phi^T T_e$. Recognizing the fact that the selected modal truncation cannot generally describe the complete static behavior of the component interface, a set of residual vectors corresponding to the difference between total flexible body displacements and those associated with the truncated mode set (due to unit attachment d. o. f. forces) are defined.* The symbol C_p is deliberately used for this vector set since it corresponds exactly to the residual flexibility matrix employed by Rubin. Two forms of residual vectors are noted: (1) based directly on the above stated definition** and (2) a description in terms of the high frequency modes which are truncated from the full set. The latter form is of practical interest where truncation of a large set of modes is warranted. It should be noted that a mix of (1) and (2) may also be employed.

* The Residual/Vectors differ from Hintz's attachment modes since contribution of lower modes is presently removed; see "Analytical Methods in Component Mode Synthesis", R. M. Hintz, AIAA Journal, Vol. 13, No. 8, Aug. 1975, pp 1007 - 1016.

** The inverse of the singular stiffness matrix, K , is defined here in terms of the flexible body transformation. The Inertia relief transformation is equally appropriate.

RAYLEIGH-RITZ COMPONENT DESCRIPTION

MacNEAL AND RUBIN VERSUS RAYLEIGH-RITZ VIEWPOINT

- RUBIN: $X = \phi_t q_t + (G_p + \omega^2 H_p) f_a$
 G_p INTERPRETED AS RESIDUAL FLEXIBILITY, DYNAMIC EQUATIONS
BASED ON PHYSICAL APPROXIMATION

- R-R : $X = \phi_t q_t + G_p q_p$

G_p INTERPRETED AS RESIDUAL DISPLACEMENT SHAPES, DYNAMIC EQUATIONS BASED ON ENERGY CONSIDERATIONS

QUALITIES -

- ORTHOGONALITY OF TRUNCATED MODES, RESIDUAL DISPLACEMENT SHAPES

$$\phi_t^T M G_p = \phi_t^T K G_p = 0$$

- EQUIVALENCE OF RUBIN AND R-R EQUATION SETS VIA TRANSFORMATION

$$X_a = \Gamma_a^T \phi_t q_t + \Gamma_a^T G_p q_p$$

It is of interest to note two equally valid interpretations of the significance of the residual vector set, C_p , namely (1) the MacNeal*/Rubin viewpoint which considers C_p a residual flexibility matrix and (2) the present Rayleigh-Ritz viewpoint which considers C_p a set of auxiliary trial vectors added to the truncated modal set $\Phi_t = (\Phi_r | \Phi_l)$. The MacNeal/Rubin viewpoint requires physical approximations to achieve the component formulation while the Rayleigh-Ritz viewpoint considers the approximating process complete with the choice of trial vectors.**

The Rayleigh-Ritz procedure necessarily results in generalized mass and stiffness matrix partitions which are orthogonal to those partitions associated with the truncated modal set. Noting the equivalence of forms (1) and (2) on the previous page, the orthogonality condition is readily proven; e. g.

$$\begin{aligned}\Phi_t^T M C_p &= (\Phi_t^T M \Phi_h) \omega_h^{-2} \Phi_h^T \Gamma_a = (0) \omega_h^{-2} \Phi_h^T \Gamma_a = 0 \\ \Phi_t^T K C_p &= (\Phi_t^T K \Phi_h) \omega_h^{-2} \Phi_h^T \Gamma_a = (0) \omega_h^{-2} \Phi_h^T \Gamma_a = 0\end{aligned}$$

Equivalence of the Rubin and Rayleigh-Ritz equation sets is noted upon application of the attachment d. o. f. transformation given below to the Rayleigh-Ritz equations

$$X_a = \Gamma_a^T X = \Gamma_a^T \Phi_t q_t + \Gamma_a^T C_p q_p$$

* "A Hybrid Method of Component Mode Synthesis", R. H. MacNeal, Computers and Structures, Vol. 1, Dec. 1971, pp 581-601.

** A slightly different viewpoint was taken by Craig and Chang who employed a dual identification of the generalized coordinate, q_p , as both displacement and force requiring the use of Lagrange multipliers: "On the Use of Attachment Modes in Substructure Coupling for Dynamic Analysis", R. R. Craig and C. Chang, AIAA 18th SDM Conf., March 1977, pp 89-99

RAYLEIGH-RITZ COMPONENT EQUATION SET

DYNAMIC EQUATIONS

$$\begin{pmatrix} I_t & 0 \\ 0 & H_{pa} \end{pmatrix} \begin{Bmatrix} \ddot{q}_t \\ \ddot{q}_p \end{Bmatrix} + \begin{pmatrix} \omega_t^2 & 0 \\ 0 & G_{pa} \end{pmatrix} \begin{Bmatrix} q_t \\ q_p \end{Bmatrix} = \begin{pmatrix} \phi_t^T \Gamma_a \\ G_{pa} \end{pmatrix} \{f_a\} + \begin{pmatrix} \phi_t^T \Gamma_e \\ G_{pe} \Gamma_e \end{pmatrix} \{f_e\}$$

- Where $H_{pa} = G_p^T M G_p$, $G_{pa} = G_p^T \Gamma_a = \Gamma_a^T G_p$

ORTHOGONALIZATION OF RESIDUALS

$$q_p = \psi_p q'_p : \psi_p^T H_{pa} \psi_p = I_p, \psi_p^T G_{pa} \psi_p = \omega_p^2$$

- Property: lowest $\omega_p >$ highest ω_t
- Resulting Dynamic Equations Identical to Free-Free Modal Form

$$\begin{pmatrix} I_t & \\ & I_p \end{pmatrix} \begin{Bmatrix} \ddot{q}_t \\ \ddot{q}'_p \end{Bmatrix} + \begin{pmatrix} \omega_t^2 & \\ & \omega_p^2 \end{pmatrix} \begin{Bmatrix} q_t \\ q'_p \end{Bmatrix} = \begin{pmatrix} \phi_t^T \Gamma_a \\ \psi_p^T G_{pa} \end{pmatrix} \{f_a\} + \begin{pmatrix} \phi_t^T \Gamma_e \\ \psi_p^T G_{pe} \Gamma_e \end{pmatrix} \{f_e\}$$

The set of dynamic equations in terms of truncated modal q_t and residual, q_p , generalized dof's are illustrated with partitions H_{pa} and C_{pa} denoted by the same symbols as the corresponding terms in Rubin's work. The coefficient matrices employed in definition of generalized forcing functions are obtained on the basis of virtual work considerations.

A set of pseudo-residual modes, defined as the modes of the lower partition ($H_{pa} \ddot{q}_p + C_{pa} \dot{q}_p = 0$), orthogonalize the residuals with respect to one another. The final result is an uncoupled set of dynamic equations with pseudo-residual eigenvalues greater in value than the highest valued member of the truncated set of eigenvalues.

DEMONSTRATION PROBLEM: SPACE SHUTTLE/IUS/DSP LIFT-OFF LOADS

SYSTEM COMPONENTS

- STS: 300 FREE-FREE MODES TO 67 HZ
- IUS: 84 DOF MASS AND STIFFNESS MATRICES
10 DOF STATICALLY DETERMINATE CRADLE/ORBITER INTERFACE
- DSP: 19 BASE FIXED MODES TO 50 HZ
24 BASE (DSP/IUS INTERFACE) CONSTRAINT MODES

REFERENCE "EXACT" ANALYSIS -

- 393 DOF SYSTEM MODEL
- 200 MODE, 32 HZ CUT-OFF DYNAMIC RESPONSE AND LOADS CALCULATION
- SYSTEM DAMPING RATIO $\xi = .01$ ASSUMED FOR ALL MODES

The Space Shuttle/IUS/DSP lift-off configuration, which along with the corresponding abort landing configuration, has recently been studied at the Aerospace Corporation, is chosen as a demonstration problem. A mix of system component descriptions was supplied by the responsible contractors; the space shuttle is the component to be reduced to a truncated unconstrained mode/residual description. The availability of unconstrained modal test data for the shuttle, while not currently employed, gives additional motivation for practical use of the proposed technique.

An "exact" modal synthesis using a 393 DOF system model and 200 mode response analysis (employing the resulting system modes) serve as the baseline reference for evaluation of truncated models.

DEMONSTRATION PROBLEM: TRUNCATED SYSTEM ANALYSES

SUBSYSTEMS

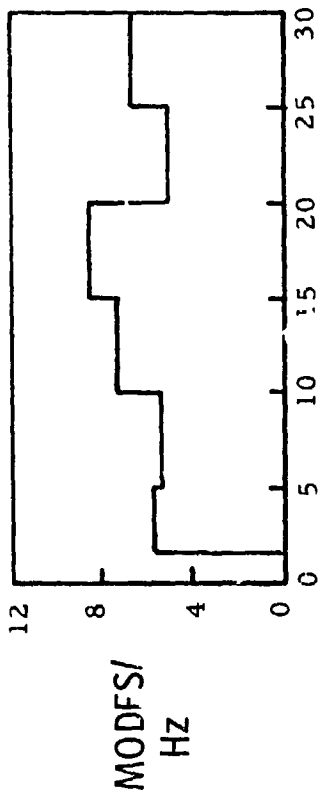
- A: 30 DSP/IUS MODES FIXED AT ORBITER INTERFACE TO 30 HZ
10 CONSTRAINT MODES ASSOCIATED WITH ORBITER INTERFACE MOTION
- B: 170 DOF SHUTTLE SYSTEM TRUNCATIONS
 - (1) SIMPLE 170 MODE TRUNCATION TO 31 HZ
 - (2) 160 MODE TRUNCATION TO 30 HZ PLUS 10 ORTHOGONALIZED RESIDUAL MODES

FORM OF SYSTEM MATRICES -

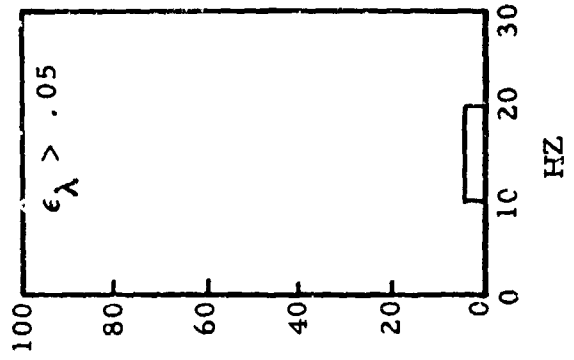
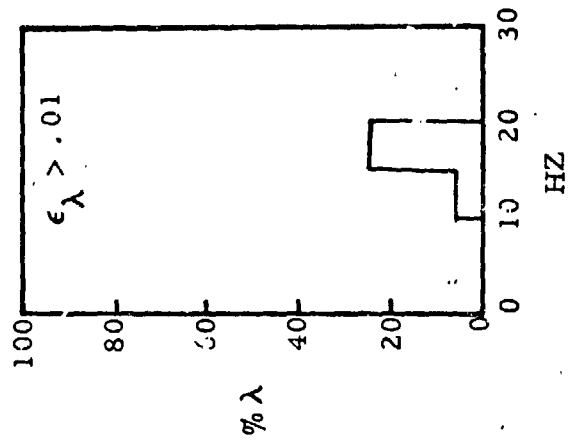
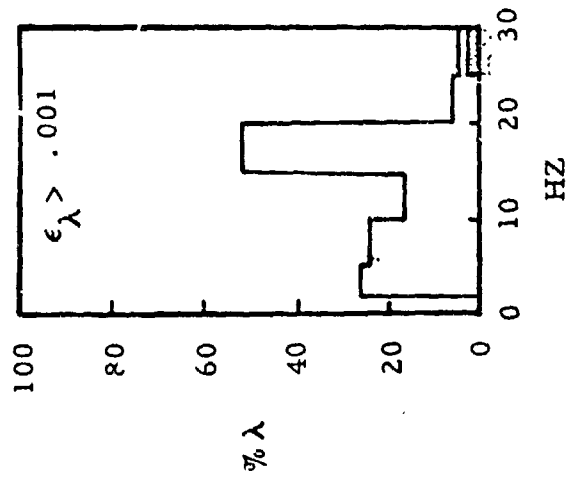
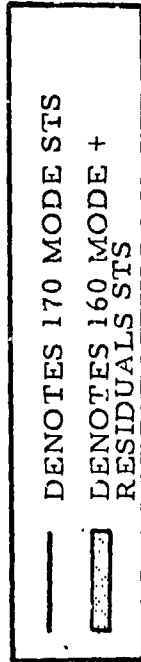
- FULLY COUPLED MASS MATRIX
- DIAGONAL GENERALIZED STIFFNESS CONSISTING OF ω^2 DSP/IUS and ω^2 STS
- NOTE: REDUNDANT STS/PAYLOAD INTERFACE WOULD HAVE RESULTED IN STIFFNESS COUPLING UNLESS HRUDA-BENFIELD METHOD WERE EMPLOYED.

EIGENVALUE ERROR SPECTRA ($\epsilon_\lambda = |1 - \omega^2_{\text{approx}}/\omega^2_{\text{exact}}|$)

- MODAL DENSITY SPECTRUM



- PERCENTAGE OF EIGENVALUES ABOVE ERROR THRESHOLDS IN 5 HZ BANDS

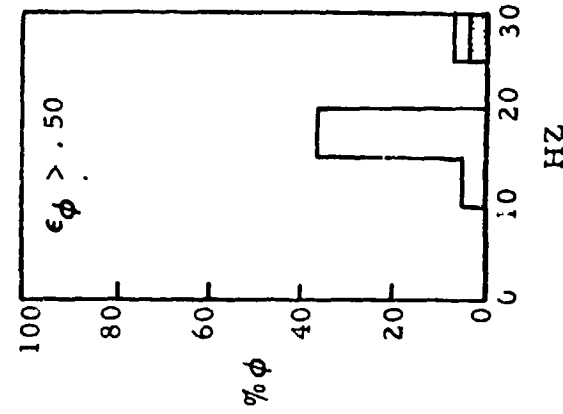
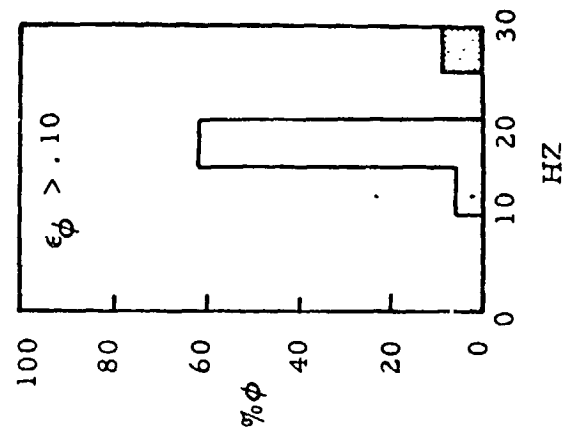
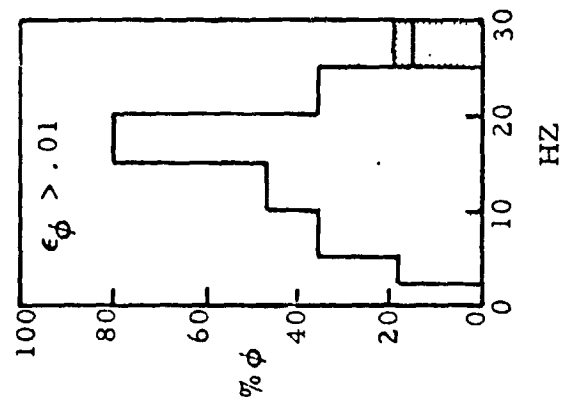
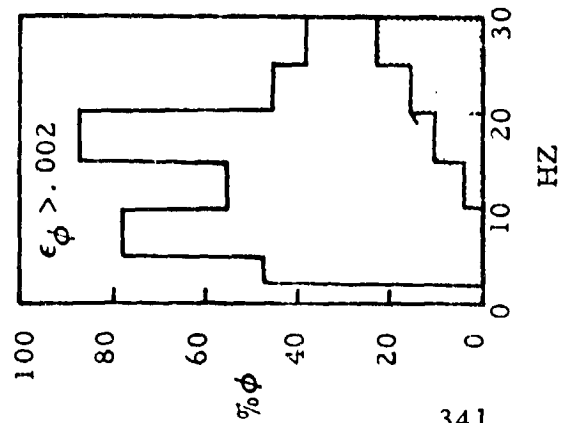


System mode truncation errors associated with the two STS/IU: DSP approximations relative to the baseline 393 DOF system model are illustrated; 187 system modes (to 30 Hz) are considered. Modal density, illustrated in 5 Hz bands is fairly high, averaging 6.4 modes per Hz in the 2 - 30 Hz range. Eigenvalue errors for corresponding modes calculated with the 170 mode STS and 160 mode/10 residual STS are exhibited as percentage of modes in 5 Hz bands exceeding the error thresholds = .001, .01, .05, respectively. Superior accuracy associated with the 160 mode/10 residual STS is apparent. The largest eigenvalue errors for the 170 mode STS case occur in the 10 - 20 Hz range. In the 160 mode/10 residual STS case only four modes in the 25 - 30 Hz range, have errors of value $.001 < \epsilon_{\lambda} < .01$.

MODE SHAPE ERROR SPECTRA, ϵ_ϕ , FOR VARIOUS ERROR THRESHOLDS IN 5 HZ BANDS

$$(\epsilon_\phi = \sqrt{\frac{(\phi_a - \phi_e)_T^T (\phi_a - \phi_e)_i}{\phi_e^T \phi_e}})$$

— DENOTES 170 MODE STS
 ▨ DENOTES 160 MODE + RESIDUALS STS



Evaluation of the two STS truncations with respect to mode shape accuracy is presented in terms of modal error norms, ϵ_{ϕ} . As in the case of eigenvalue errors, the mode shape error spectrum is present in terms of percentage of modes exceeding error norm thresholds, $\epsilon_{\phi} = .002, .01, .10, .50$, in 5 Hz bands. The overall performance of the 160 mode/10 residual STS truncation is superior to the 170 mode STS truncation; mode shape accuracy degrades monotonically with frequency for the 160 mode/10 residual STS case. The major region of mode shape error in the 170 mode STS case is in the 15 - 20 Hz range.

On the basis of eigenvalue and mode shape error spectra it appears that employment of residual trial vectors in a component mode truncation produces superior convergence quality relative to a simple mode truncation.

The effect of truncation error on lift-off peak response quantities is next examined.

SELECTED PEAK RESPONSES AND LOADS FOR LIFT-OFF ILLUSTRATING TRUNCATION ERRORS

DSP TIP RESPONSE

<u>DOF</u>	<u>"Exact" (g)</u>	<u>% Error, 170 Mode STS</u>	<u>% Error, 160 Mode/10 Res. STS</u>
T	5.55, -5.34	-6.1, -2.8	* , *
S	4.32, -4.83	-4.7, +1.3	* , -0.1
Z	3.92, -1.07	-0.9, -0.3	-0.1, -0.3

CONTRACTOR INTERFACE

<u>Load</u>	<u>"Exact" (in. -lb)</u>	<u>% Error, 170 Mode STS</u>	<u>% Error, 160 Mode/10 Res. STS</u>
MX	48445, -57115	2.4, -1.0	0.4, 0.2
MY	118380, -111990	0.8, 0.7	* , *
MZ	8635, -8929	-5.7, -2.0	0.2, 0.5

IUS INTERFACE

<u>Load</u>	<u>"Exact" (in. -lb)</u>	<u>% Error, 170 Mode STS</u>	<u>% Error, 160 Mode/10 Res. STS</u>
MX	398710, -373330	1.4, -0.5	-0.1, -0.2
MY	786190, -795630	1.1, 1.3	* , *
MZ	24368, -23794	-5.7, -4.6	* , 0.1

* error < 0.05%

Response of the STS/IUS/DSP lift-off configuration to a set of theoretical forcing functions was computed for the "exact" set of system modes (first 200 modes) and for the two approximate sets of system modes based on truncated component representation (187 modes each). Selected peak responses are presented illustrating, as expected, superior accuracy of the 160 mode/10 residual STS truncation. While peak response errors for the 170 mode case are not excessive, one should be cautioned that the frequency content of the presently employed lift-off forcing functions is generally below 10 Hz; thus the least accurate modes in the 15 - 20 Hz range were not excited to high levels. Forcing functions based on engine start transient data may possibly contain significant components in the higher frequency range.

It should be noted that for the STS/IUS/DSP abort landing case (not presently discussed) significant 15 - 17 Hz landing gear input forces are experienced. While a thorough evaluation of truncation errors was not conducted, an exercise comparing results of a 100 mode/10 residual STS representation to a 200 mode STS representation was performed. Excellent accuracy of the truncated mode/residual approximation with respect to both system modes and peak response were noted in that series of calculations.

CONCLUDING REMARKS :

ADVANTAGE OF TRUNCATED COMPONENT MODE/RESIDUAL DESCRIPTION
DEMONSTRATED

MIX OF TRUNCATED COMPONENT REPRESENTATIONS CONSISTENT WITH ANTI-
CIPATED GROUND VIBRATION TEST DATA UTILIZED

POTENTIAL ADVANTAGE OF TRUNCATED MODE/RESIDUAL MODELS FOR VEHICLE/
STAND LIFT-OFF ANALYSES, STRUCTURE/CONTROL SYSTEM INTERACTION
ANALYSIS, EFFICIENT STRUCTURE ALTERATION ANALYSIS, ETC.

The advantage of a truncated component mode/residual description over a simple component mode truncation has been demonstrated with a problem of current interest, namely, the space shuttle with payload. In view of standard forms of payload dynamic test data (cantilevered/constraint modes) and unconstrained space shuttle modal test data, a mix of subsystems was employed in the demonstration pointing to use of the methodology as a practical analysis tool.

While the current demonstration of a lift-off dynamic response calculation made use of a set of reference applied transient loads (including launch stand forces) a more complete and consistent simulation should encompass non-linear vehicle system/stand interaction. For such an analysis it is anticipated that the use of residual effects, augmenting a vehicle system truncated set of modes, would provide an efficient and rational approach to non-linear lift-off analysis. In general, it is thought that employment of residual effects in structural system/interacting media dynamic analysis will provide rationale for system approximations (e. g. vehicle/control, structure/fluid, pogo). It is finally noted that a closely related residual concept (recently demonstrated on elementary structures) is being employed for use in offshore oil platform structural damage identification studies at the Aerospace Corporation.



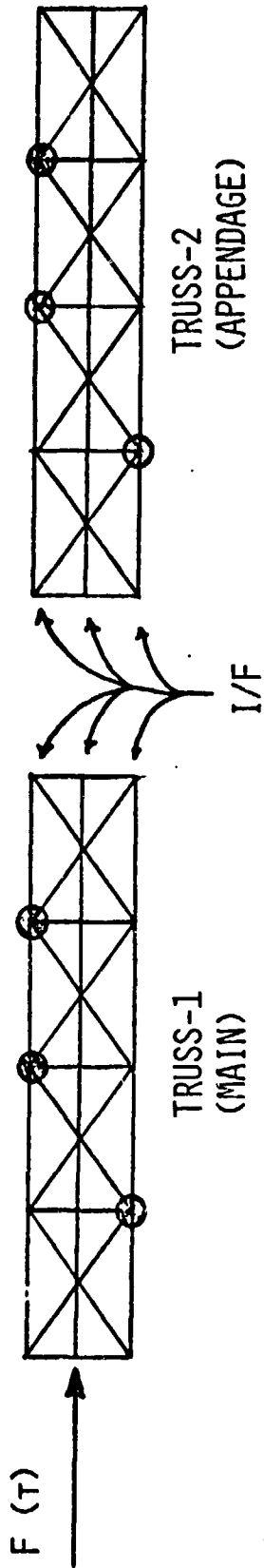
COMPARISON OF
MODAL SYNTHESIS TECHNIQUES
EFFECTS ON MODES, FREQUENCIES, LOADS

R. HRUDA
MARTIN MARIETTA

MARTIN MARIETTA



STRUCTURE USED FOR COMPARISONS



- o PLANKER PROBLEM (3 RIGID BODY DOFS)
- o 2 TRANSLATION DOFS AT EACH PINNED JOINT
- o REDUNDANT INTERFACE (3 JOINTS AT 2 DOFS)
- o HEAVY ASYMMETRIC MASS TO CAUSE I/F DISTORTION
- o RAMP FORCING FUNCTION

TECHNIQUES CONSIDERED FOR COMPARISONS:

- IMSL - Inertial coupling of truss-2 constrained modes onto free-free modes of truss-1 which was mass and stiffness "loaded" at its truss-2 interface dofs by the interface properties from truss-2. (Benfield/Hruda technique)
- I/F - Inertial coupling of truss-1 and truss-2 constrained modes onto a free-free modal representation of the interface dofs which derives its mass and stiffness properties from the sum of the two trusses interface masses and interface stiffnesses. (Craig/Bampton technique)
- RFSWOM - Residual flexibility approach of coupling truss-2 constrained modes onto free-free modes of truss-1 which creates stiffness coupling: residual mass was not included. (MacNeal technique)
- RFIWM - R. Coppolino's adaptation of the residual flex approach, coupling truss-2 constrained modes onto free-free modes of truss-1 which yields only inertial coupling, and, by consistent application to the mass and stiffness terms in the equations of motion, yields both residual stiffness and residual mass terms.
- RFIWOM - Same as RFIWM except without the residual mass contribution for truss-1.



TECHNIQUES CONSIDERED FOR COMPARISONS

- o IMSL - INERTIAL COUPLING WITH M AND K LOADING
- o I/F - INTERFACE TECHNIQUE OF INERTIAL COUPLING
- o RFSWOM - RESIDUAL FLEX: STIFFNESS COUPLING, W/O RESIDUAL MASS
- o RFIWM - RESIDUAL FLEX: INERTIAL COUPLING WITH RESIDUAL MASS
- o RFIWOM - RESIDUAL FLEX: INERTIAL COUPLING W/O RESIDUAL MASS

NOTE: RESIDUAL FLEX IS BASED ON FREQUENCY CUTOFF AND
ALL REMAINING HIGH FREQUENCY MODES.

CASES CONSIDERED FOR COMPARISONS:

The "exact" results, against which all comparisons were made, were obtained by extracting eigenvalues, eigenvectors, and loads directly from a finite element discrete/physical model using no modes at all.

The total number of modes retained for modal synthesis in cases A, B, C, and F are shown on the facing page. It should be noted that, for the transient analyses for loads, several highest frequency coupled system modes were discarded due to their inherent numerical inaccuracies (e.g. not all 50 coupled system modes were used for the transient analysis of case B).

CASES CONSIDERED FOR COMPARISONS



- o EXACT - DISCRETE/PHYSICAL MODEL, 70 DOF
- o CASE A - MODALLY COUPLED, 70 MODES RETAINED (100%)
- o CASE B - MODALLY COUPLED, 50 MODES RETAINED (71%)
- o CASE C - MODALLY COUPLED, 32 MODES RETAINED (46%)
- o CASE F - MODALLY COUPLED, 19 MODES RETAINED (27%)

MARLIN MARLETTA

DEFINITION OF COMPARISON VALUES:

- Frequency: Simply the percent error against the "exact" (see previous page) solution
- Modes: An error vector is formed ($\Phi_N - \Phi_R$) and its norm is calculated (which is defined as the RSS of the elements in the vector); the value is then defined as the norm of the error divided by the norm of the base/exact mode. Note, the norms are based on the modal amplitudes of all the dofs from the composite structure.
- Loads: Loads were calculated at the truss interface on both the truss-1 and truss-2 joints.
A percent error of the absolute value of the largest (either max or min) value from a given case against the absolute value of the largest (either max or min) value from the exact solution.

DEFINITION OF COMPARISON VALUES



FREQUENCY:
 VALUE = $\frac{F_N - F_E}{F_E} * 100$

MODES:
 VALUE = $\frac{RSS(\{\emptyset_N\} - \{\emptyset_E\})}{RSS\{\emptyset_E\}} * 100$

LOADS:
 VALUE = $\frac{|L_N| - |L_E|}{|L_E|} * 100$

WHERE: E = EXACT SOLUTION

N = CASE BEING COMPARED

MARTIN MARIETTA

NOTES ON FREQUENCY COMPARISONS:

- For the 100% case-A, the "RFSWOM" technique requires the inversion of the residual flexibility matrix to obtain a "residual stiffness." When attempting to retain all (100%) of the modes, this residual flex matrix is a function of the interface highest frequency modal amplitudes which can (as it did in this case) cause an ill-conditioned matrix. Since this is an unrepresentative case, it should not be deduced that this is an unacceptable technique. As can be seen in succeeding cases, where more residual modes are available, the RFSWOM column falls into line with other techniques.

- Note that in cases B, C, and F, in both the frequency and mode shape comparisons, that the RFSWOM and RFIWOM columns are identical, thereby numerically supporting R. Coppelino's (Aerospace) contention that these two techniques are equivalent for modal synthesis.

FREQUENCY COMPARISON
CASE A - 100% OF AVAILABLE MODES.
% DIFF FOR VARIOUS MODAL COUPLING TECH.

MODE NO	EXACT FREQ (HZ)	IMSL 38/32	I/F 38/32	RFSWOM 32+6/32	RFIMM 32+6/32	RFIMOM 32+6/32
4	.76	-.00	-.00	-49.17	-.00	-.00
5	1.75	-.00	-.00	6.75	-.00	-.00
6	2.84	-.00	-.00	-21.81	-.00	-.00
7	3.08	-.00	-.00	-3.63	-.00	.01
8	3.80	-.00	-.00	-9.24	-.00	-.00
9	4.62	-.00	-.00	-16.35	-.00	-.00
10	5.11	-.00	-.00	-24.08	-.00	.03
11	5.50	-.00	-.00	-6.62	-.00	.01
12	5.81	-.00	-.00	-3.31	-.00	-.00
13	7.69	-.00	-.00	-6.08	-.00	.01
14	8.69	-.00	-.00	-.60	-.00	-.00
15	9.14	-.00	-.00	-3.32	-.00	-.00
16	9.42	-.00	-.00	-1.78	-.00	-.00
17	9.73	-.00	-.00	-.92	-.00	-.00
18	9.85	-.00	-.00	-.98	-.00	-.00
19	10.36	-.00	-.00	-1.36	-.00	-.00
20	10.43	-.00	-.00	-.33	-.00	-.00
21	10.79	-.00	-.00	-2.99	-.00	-.00
22	10.90	-.00	-.00	-2.55	-.00	-.00
23	11.37	-.00	-.00	-1.89	-.00	-.00
24	11.49	-.00	-.00	.80	-.00	-.00
25	11.78	-.00	-.00	.39	-.00	-.00
26	11.96	-.00	-.00	-.12	-.00	-.00
27	12.03	-.00	-.00	.19	-.00	-.00
28	12.20	-.00	-.00	.40	-.00	-.00
29	12.43	-.00	-.00	.12	-.00	-.00
30	12.50	-.00	-.00	5.58	-.00	-.00
31	12.75	-.00	-.00	4.00	-.00	-.00
32	13.29	-.00	-.00	2.54	-.00	-.00
33	13.51	-.00	-.00	3.12	-.00	-.00
34	14.22	-.00	-.00	-.19	-.00	.02
35	14.53	-.00	-.00	.31	-.00	-.00
36	14.86	-.00	-.00	-.11	-.00	-.00
37	15.19	-.00	-.00	1.59	-.00	-.00
38	15.54	-.00	-.00	1.23	-.00	.03
39	15.69	-.00	-.00	2.50	-.00	.01
40	16.16	-.00	-.00	.55	-.00	-.00
41	16.17	-.00	-.00	.60	-.00	-.00
42	16.28	-.00	-.00	3.34	-.00	.01
43	16.86	-.00	-.00	.46	-.00	.02
44	17.07	-.00	-.00	.21	-.00	-.00
45	17.17	-.00	-.00	1.12	-.00	.01
46	18.17	-.00	-.00	.03	-.00	-.00
47	18.17	-.00	-.00	10.37	-.00	-.00
48	20.11	-.00	-.00	.81	-.00	.02
49	20.27	-.00	-.00	3.02	-.00	-.00
50	21.11	-.00	-.00	.14	-.00	.01
51	21.15	-.00	-.00	.08	-.00	-.00
52	21.26	-.00	-.00	.07	-.00	-.00
53	21.29	-.00	-.00	.53	-.00	.02
54	21.45	-.00	-.00	.02	-.00	-.00
55	21.47	-.00	-.00	2.91	-.00	.01
56	22.06	-.00	-.00	.45	-.00	-.00
57	22.15	-.00	-.00	2.18	-.00	-.00
58	22.63	-.00	-.00	5.09	-.00	-.00

ORIGINAL PAGE IS
OF POOR QUALITY

ORIGINAL PAGE IS
OF POOR QUALITY

FREQUENCY COMPARISON
CASE B = 71% OF AVAILABLE MODES.
% DIFF FOR VARIOUS MODAL COUPLING TECH.

MODE NO	EXACT FREQ (HZ)	IMSL 28/22	I/F 28/22	HFSWOM 22+6/22	RFIWM 22+6/22	RFIWM 22+6/22
4	.76	.00	.00	.00	.00	.00
5	1.75	.00	.00	.00	.00	.00
6	2.84	.00	.00	.02	.00	.00
7	3.08	.00	.00	.06	.00	.06
8	3.80	.00	.00	.00	.00	.00
9	4.62	.00	.00	.04	.00	.04
10	5.11	.00	.00	.00	.00	.00
11	5.50	.00	.00	.05	.00	.05
12	5.81	.04	.05	.03	.03	.03
13	7.69	.00	.00	.21	.00	.21
14	8.69	.02	.02	.03	.01	.03
15	9.14	.04	.06	.12	.04	.12
16	9.42	.01	.01	.01	.00	.01
17	9.73	.01	.02	.02	.01	.02
18	9.85	.03	.04	.03	.03	.03
19	10.36	.01	.01	.06	.01	.06
20	10.43	.00	.00	.01	.00	.01
21	10.79	.03	.05	.04	.02	.04
22	10.90	.03	.03	.04	.02	.04
23	11.37	.00	.00	.03	.00	.03
24	11.49	.00	.01	.05	.00	.05
25	11.78	.03	.03	.08	.03	.08
26	11.96	.08	.09	.08	.07	.08
27	12.03	.02	.03	.04	.02	.04
28	12.20	.13	.13	.10	.10	.10
29	12.43	.01	.01	.02	.00	.02
30	12.50	.03	.09	.07	.03	.07
31	12.75	.07	.07	.08	.06	.08
32	13.29	.04	.05	.06	.02	.06
33	13.51	.08	.07	.07	.05	.07
34	14.22	.13	.13	.09	.07	.09
35	14.53	.09	.13	.29	.07	.29
36	14.86	.01	.01	.17	.01	.17
37	15.19	.06	.07	.11	.05	.11
38	15.54	.01	.03	1.17	.04	1.17
39	15.69	.02	.02	1.51	.03	1.51
40	16.16	.01	.02	.13	.09	.13
41	16.17	.07	.08	2.68	.12	2.68
42	16.28	.37	.44	3.88	.34	3.88
43	16.86	.13	.12	7.73	.25	7.73
44	17.07	.06	.10	18.51	1.52	18.51
45	17.17	1.00	1.00	66.94	5.86	66.94
46	18.17	.02	.02	72.29	9.54	72.29
47	18.17	.03	.04	122.22	11.51	122.22
48	20.11	.57	.60	473.05	7.55	473.05
49	20.27	.31	.38	962.70	8.65	962.70
50	21.11	4.07	4.20	*536.67	19.40	*536.67

FREQUENCY COMPARISON
CASE C - 46% OF AVAILABLE MODES.
% DIFF FOR VARIOUS MODAL COUPLING TECH.

MODE NO	EXACT FREQ (HZ)	INSL 18/14	I/F 18/14	RFSWOM 12+6/14	RFIMM 12+6/14	RFIWM 12+6/14
4	.76	.00	.00	.02	.00	.02
5	1.75	.02	.00	.00	.00	.00
6	2.84	.04	.02	.12	.01	.12
7	3.08	.01	.00	.28	.00	.28
8	3.80	.02	.00	.00	.00	.00
9	4.62	.12	.05	.26	.02	.26
10	5.11	.02	.01	.01	.00	.01
11	5.50	.26	.10	.35	.05	.35
12	5.81	.16	.24	.12	.08	.12
13	7.69	.03	.04	1.55	.06	1.55
14	8.69	.14	.22	.17	.08	.17
15	9.14	.32	.33	.41	.17	.41
16	9.42	.05	.07	.07	.01	.07
17	9.73	.13	.18	.34	.08	.34
18	9.85	.30	.27	.31	.18	.31
19	10.36	.11	.11	.51	.12	.51
20	10.43	.09	.04	.45	.42	.45
21	10.79	.17	.33	.73	.11	.73
22	10.90	.41	.42	3.43	.55	3.43
23	11.37	.06	.04	3.23	1.49	3.23
24	11.49	.04	.11	5.14	3.66	5.14
25	11.78	.17	.17	5.52	2.76	5.52
26	11.96	.40	.90	4.79	3.70	4.79
27	12.03	.30	3.16	53.65	4.71	53.65
28	12.20	1.73	2.35	77.63	3.91	77.63
29	12.43	.41	4.68	80.30	14.58	80.30
30	12.50	1.94	12.32	143.04	22.38	143.04
31	12.75	3.52	14.90	167.76	29.91	167.76
32	13.29	11.88	61.19	630.91	63.27	630.91

ORIGINAL PAGE IS
OF POOR QUALITY

FREQUENCY COMPARISON
CASE F = 27% OF AVAILABLE MODES.
% DIFF FOR VARIOUS MODAL COUPLING TECH.

MODE NO	EXACT FREQ (HZ)	IMSL 12/7	I/F 12/7	RFSWOM 6+6/7	RFIMW 6+6/7	RFIWM 6+6/7
4	.76	.00	.00	.05	.00	.05
5	1.75	.02	.00	.02	.00	.02
6	2.84	.06	.06	.31	.03	.31
7	3.08	.07	.00	4.32	.19	4.32
8	3.80	.03	.01	.03	.00	.03
9	4.02	.18	.14	.71	.08	.71
10	5.11	.05	.03	.03	.01	.03
11	5.50	.46	.34	1.64	.49	1.64
12	5.81	1.03	1.13	23.29	4.70	23.29
13	7.69	.14	.16	15.39	8.20	15.39
14	8.69	1.05	1.14	45.28	1.30	45.28
15	9.14	1.20	6.85	84.48	8.49	84.48
16	9.42	.37	27.17	98.00	27.57	98.00
17	9.73	2.23	36.67	97.08	36.41	97.08
18	9.85	18.25	37.17	203.74	37.43	203.74
19	10.36	22.07	103.62	279.52	105.23	279.52

ORIGINAL PAGE IS
OF POOR QUALITY

10 PAGE

NOTES ON MODE SHAPE COMPARISONS:

- Same as those for frequency comparisons.

ORIGINAL PAGE IS
OF POOR QUALITY

MODE SHAPE COMPARISON
CASE A = 100% OF AVAILABLE MODES.
% DIFF FOR VARIOUS MODAL COUPLING TECH.

MODE NO	EXACT NORM (---)	IMSL 38/32	I/F 38/32	RFSWOM 32+6/32	RFIWM 32+6/32	RFIWM 32+6/32
4	14.84	.00	.00	104.09	.00	.00
5	13.95	.00	.00	92.76	.00	.01
6	13.45	.00	.00	104.91	.00	.01
7	13.70	.00	.00	94.49	.00	.02
8	12.23	.00	.00	132.95	.00	.02
9	11.21	.00	.00	100.73	.00	.03
10	9.54	.00	.00	152.35	.00	.05
11	8.75	.00	.00	104.39	.00	.12
12	13.25	.00	.00	129.05	.00	.08
13	10.51	.00	.00	186.06	.00	.18
14	11.49	.00	.00	96.78	.00	.04
15	11.24	.00	.00	102.21	.00	.16
16	14.55	.00	.00	71.19	.00	.07
17	13.16	.00	.00	141.80	.00	.09
18	13.99	.00	.00	90.01	.00	.02
19	15.47	.00	.00	81.01	.00	.12
20	13.49	.00	.00	99.38	.00	.05
21	12.74	.00	.00	136.40	.00	.13
22	15.25	.00	.00	138.19	.00	.15
23	16.56	.00	.00	132.20	.00	.15
24	18.06	.00	.00	100.18	.00	.75
25	17.70	.00	.00	132.72	.00	.18
26	17.29	.00	.00	142.58	.00	.17
27	16.94	.00	.00	68.01	.00	.09
28	17.58	.00	.00	69.89	.00	.03
29	17.06	.00	.00	41.89	.00	.19
30	16.31	.00	.00	138.22	.00	.28
31	15.86	.00	.00	149.30	.00	.01
32	18.16	.00	.00	138.85	.00	.08
33	16.92	.00	.00	148.49	.00	.11
34	15.21	.00	.00	91.84	.00	.84
35	18.67	.00	.00	75.41	.00	.52
36	18.48	.00	.00	49.75	.00	.38
37	17.23	.00	.00	89.32	.00	.18
38	18.14	.00	.00	145.84	.00	1.36
39	18.12	.00	.00	146.47	.00	.72
40	16.82	.00	.00	160.19	.00	.51
41	19.22	.00	.00	126.88	.00	.56
42	15.63	.00	.00	162.42	.00	.90
43	18.47	.00	.00	124.22	.00	1.12
44	19.44	.00	.00	61.05	.00	.45
45	16.54	.00	.00	135.41	.00	.84
48	18.17	.00	.00	54.79	.00	.32
47	18.33	.00	.00	142.35	.00	.30
48	18.25	.00	.00	145.79	.00	2.22
49	19.16	.00	.00	139.28	.00	.27
50	19.29	.00	.00	65.32	.00	2.16
51	19.51	.00	.00	62.72	.00	1.22
52	19.17	.00	.00	52.42	.00	3.43
53	18.89	.00	.00	105.50	.00	4.69
54	19.52	.00	.00	38.21	.00	1.48
55	19.13	.00	.00	103.39	.00	2.35
56	11.17	.00	.00	161.11	.00	5.68
57	19.83	.00	.00	141.29	.00	.17
59	19.81	.00	.00	135.33	.00	.00

MODE SHAPE COMPARISON
CASE B - 71% OF AVAILABLE MODES.
% DIFF FOR VARIOUS MODAL COUPLING TECH.

MODE NO	EXACT NORM (--)	IMSL 28/22	I/F 28/22	RFSWOM 22+6/22	RFIMM 22+6/22	RFINOM 22+6/22
4	14.84	.00	.00	.00	.00	.00
5	13.95	.02	.01	.01	.01	.01
6	13.45	.04	.03	.18	.02	.18
7	13.70	.07	.01	.23	.01	.23
8	12.23	.08	.06	.06	.05	.06
9	11.21	.12	.08	.33	.06	.33
10	9.54	.16	.18	.16	.15	.16
11	8.75	.22	.22	.66	.14	.66
12	13.25	.80	.89	.76	.70	.76
13	10.51	.30	.41	1.78	.27	1.78
14	11.49	.91	1.21	.88	.57	.88
15	11.24	1.75	2.05	2.53	1.67	2.53
16	14.55	.61	.71	.95	.34	.95
17	13.16	1.02	1.10	1.02	.70	1.02
18	13.99	1.52	1.67	1.63	1.50	1.63
19	15.47	1.28	1.03	1.85	.77	1.86
20	13.49	1.30	1.03	1.21	.75	1.21
21	12.74	1.54	2.02	2.20	1.23	2.20
22	15.25	1.93	1.84	1.98	1.50	1.98
23	16.56	.38	1.62	3.31	.12	3.31
24	18.06	.32	.81	3.56	.31	3.56
25	17.70	3.44	3.63	4.94	3.43	4.94
26	17.29	9.71	9.84	8.91	8.36	8.91
27	16.94	8.77	8.24	7.18	7.04	7.18
28	17.58	7.18	7.5	6.09	5.94	6.09
29	17.06	1.11	2.22	3.50	.79	3.50
30	16.31	3.83	5.48	5.80	3.52	5.80
31	15.86	3.90	3.85	4.95	3.86	4.95
32	18.16	2.81	2.72	4.45	2.02	4.45
33	16.92	4.06	3.29	3.91	2.92	3.91
34	15.21	6.36	4.34	25.34	4.43	25.34
35	18.67	5.53	5.12	22.71	4.42	22.71
36	18.48	1.64	1.62	16.67	1.79	16.67
37	17.23	4.65	5.05	12.42	3.98	12.42
38	18.14	1.43	2.71	71.43	6.38	71.43
39	18.12	2.45	2.06	189.04	4.32	189.04
40	18.82	35.58	19.60	164.85	60.42	164.85
41	19.22	39.52	27.35	128.81	60.10	128.81
42	15.63	26.78	27.93	126.75	28.17	126.75
43	18.47	9.51	9.90	140.52	38.29	140.52
44	18.44	14.36	15.85	144.04	126.68	144.04
45	16.54	24.08	24.65	213.55	142.78	213.55
46	18.17	3.25	4.86	150.22	123.17	150.22
47	18.33	4.54	5.77	250.51	144.13	250.51
48	18.25	62.46	70.59	553.15	77.72	553.15
49	19.16	57.97	66.55	965.90	130.07	965.90
50	19.20	114.23	116.94	930.68	128.01	930.68

ORIGINAL PAGE IS
OF POOR QUALITY

MODE SHAPE COMPARISON
CASE C = 46% OF AVAILABLE MODES.
% DIFF FOR VARIOUS MODAL COUPLING TECH.

MODE NO	EXACT NORM (--)	IMSL 18/14	I/F 18/14	RFSWOM 12+6/14	RFIWM 12+6/14	RFIWM 12+6/14
4	14.84	.02	.02	.03	.02	.03
5	13.95	.18	.04	.03	.03	.03
6	13.45	.47	.45	.49	.31	.49
7	13.70	.31	.10	.55	.13	.55
8	12.23	.54	.23	.18	.16	.18
9	11.21	1.59	1.30	2.00	.90	2.00
10	9.54	1.10	.74	.41	.36	.41
11	8.75	2.79	3.01	3.61	1.79	3.61
12	13.25	2.50	3.48	2.42	1.79	2.42
13	10.51	1.92	2.35	9.62	1.83	9.62
14	11.49	4.84	7.14	5.19	3.88	5.19
15	11.24	8.72	9.37	8.63	5.92	8.63
16	14.55	3.33	4.77	3.71	1.62	3.71
17	13.16	9.03	9.46	13.85	5.90	13.85
18	13.99	11.17	10.37	13.28	7.67	13.28
19	15.47	12.62	11.13	68.73	9.12	68.73
20	13.49	13.23	10.81	81.34	7.48	81.34
21	12.74	7.56	16.01	46.68	10.40	46.68
22	15.25	16.60	19.11	54.62	20.68	54.62
23	16.56	6.01	5.57	123.28	97.95	123.28
24	18.06	4.87	9.79	129.15	145.42	129.15
25	17.70	17.82	16.45	135.79	155.65	135.79
26	17.29	68.71	127.43	150.09	124.74	150.09
27	16.94	72.98	144.11	134.45	120.45	134.45
28	17.58	103.74	98.65	152.44	150.49	152.44
29	17.06	81.82	139.33	166.49	128.91	166.49
30	16.31	110.88	130.70	145.30	111.59	145.30
31	15.88	95.31	153.24	243.62	141.77	243.62
32	18.16	101.15	122.19	695.80	128.54	695.80

13

MODE SHAPE COMPARISON
CASE F = 27% OF AVAILABLE MODES.
% DIFF FOR VARIOUS MODAL COUPLING TECH.

MODE NO	EXACT NDRM (---)	IMSL 12/7	I/F 12/7	RFSWOM 6+6/7	RFIWM 6+6/7	RFIWM 6+6/7
4	14.34	.04	.05	.06	.03	.06
5	13.95	.24	.07	1.26	.06	.26
6	13.45	1.71	.89	2.63	.71	2.63
7	13.70	1.02	.20	8.59	2.36	8.69
8	12.23	.74	.39	1.48	.42	1.48
9	11.21	2.58	2.75	4.62	1.96	4.62
10	9.54	2.84	2.19	1.40	.98	1.40
11	8.75	10.05	9.34	38.19	23.43	38.19
12	13.25	10.96	11.05	65.52	28.35	65.52
13	10.51	7.03	7.59	128.49	53.35	128.49
14	11.49	29.41	33.79	159.45	43.11	159.45
15	11.24	33.59	66.95	167.22	68.27	167.22
16	14.55	30.24	113.08	161.12	119.44	161.12
17	13.16	111.59	138.72	161.33	140.08	161.33
18	13.99	123.87	130.93	148.55	132.90	148.55
19	15.47	148.78	127.29	379.09	127.01	379.09

NOTES ON LOADS COMPARISONS:

- Huge discrepancy in RFSWOM column for case-A (100%) reflects propagation of ill-conditioning mentioned earlier.
- Loads were calculated by the modal acceleration technique for all methods except the RFSWOM. Due to the stiffness coupling involved in the RFSWOM method of modal synthesis, a complete modal acceleration technique of calculating loads could not be used, therefore, the modal displacement technique of calculating loads was used. Because of this, I contribute the larger loads inaccuracies in the RFSWOM column more to the technique of loads calculations than to the method of modal coupling.

ORIGINAL PAGE IS
OF POOR QUALITY

COMPARISONS OF MAXIMUM ABSOLUTE VALUES OF INTERFACE LOADS

CASE A = 100% OF AVAILABLE MODES

LOAD NO.	LOAD NAME	EXACT LOAD (LBS)	IMSL	PERCENT DIFFERENCES I/F	ABS. RFSWOM	MAX. LOADS RFIWM	RFIWM
1	1 17 X	-481.999	0.	-.00	3419.56	.00	-.05
3	1 18 X	-202.138	0.	-.00	10154.67	.00	-.08
5	1 19 X	-498.819	0.	-.00	3957.31	-.00	.11
7	2 17 X	474.713	0.	-.00	2208.71	.00	-.03
9	2 18 X	191.901	0.	-.00	22733.86	.00	-.02
11	2 19 X	486.870	0.	.00	17322.92	.00	.03

IMSL = INERTIAL COUPLING W/ MASS AND STIFFNESS LOADING

I/F = INTERFACE METHOD OF INERTIAL COUPLING

RFSWOM = RESIDUAL FLEXIBILITY WITH STIFFNESS COUPLING, WITHOUT RESIDUAL MASS

RFIWM = RESIDUAL FLEXIBILITY WITH INERTIAL COUPLING, WITH RESIDUAL MASS

RFIWM = RESIDUAL FLEXIBILITY WITH INERTIAL COUPLING, WITHOUT RESIDUAL MASS

COMPARISONS OF MAXIMUM ABSOLUTE VALUES OF INTERFACE LOADS
CASE B - 71% OF AVAILABLE MODES

LOAD NO.	LOAD NAME	EXACT LOAD (LBS)	IMSL	I/F	APX. RFSWOM	MAX. RFIWM	RFINOM
1	1 17 X	-481.999	.10	.00	2.08	.10	-.38
3	1 18 X	-202.138	.26	.27	2.62	.27	.26
5	1 19 X	-498.819	.12	.13	.13	.14	-.20
7	2 17 X	474.713	.17	.15	-1.36	.18	.22
9	2 18 X	191.901	.15	.18	.26	.15	-.24
11	2 19 X	486.870	.19	.19	2.00	.24	-.10

IMSL = INERTIAL COUPLING W/ MASS AND STIFFNESS LOADING
I/F = INTERFACE METHOD OF INERTIAL COUPLING
RFSWOM = RESIDUAL FLEXIBILITY WITH STIFFNESS LOADING
RFIWM = RESIDUAL FLEXIBILITY WITH STIFFNESS COUPLING, WITHOUT RESIDUAL MASS
RFINOM = RESIDUAL FLEXIBILITY WITH INERTIAL COUPLING, WITH RESIDUAL MASS
RFINOM = RESIDUAL FLEXIBILITY WITH INERTIAL COUPLING, WITHOUT RESIDUAL MASS

ORIGINAL PAGE IS
OF POOR QUALITY

COMPARISONS OF MAXIMUM ABSOLUTE VALUES OF INTERFACE LOADS

CASE C = 46% OF AVAILABLE MODES

LOAD NO.	LOAD NAME	EXACT LOAD (LBS)	IMSL	PERCENT DIFFERENCES I/F	ABS. RFSWOM	MAX. RFIWM	LOADS RFIWM	RFIWM
1	1 17 X	-481.999	-1.32	-1.29	-4.07	-1.09	-1.09	.29
3	1 18 X	-202.138	2.34	2.32	3.10	2.43	2.43	3.19
5	1 19 X	-498.819	.25	.39	-7.33	.45	.45	.17
7	2 17 X	474.713	-1.48	-1.43	2.93	-1.36	-1.36	-.34
9	2 18 X	191.901	.00	-.12	-25.44	-.07	-.07	-1.48
11	2 19 X	486.870	-.85	-.77	-3.88	-.78	-.78	-.73

IMSL = INERTIAL COUPLING W/ MASS AND STIFFNESS LOADING

I/F = INTERFACE METHOD OF INERTIAL COUPLING

RFSWOM = RESIDUAL FLEXIBILITY WITH STIFFNESS COUPLING, WITHOUT RESIDUAL MASS

RFIWM = RESIDUAL FLEXIBILITY WITH INERTIAL COUPLING, WITH RESIDUAL MASS

RFIWM = RESIDUAL FLEXIBILITY WITH INERTIAL COUPLING, WITHOUT RESIDUAL MASS

17

COMPARISONS OF MAXIMUM ABSOLUTE VALUES OF INTERFACE LOADS

CASE F = 27% OF AVAILABLE MODES

LOAD NO.	LOAD NAME	EXACT LOAD (LBS)	IMSL	PERCENT DIFFERENCES I/F	ABS. RFSWOM	MAX. LOADS RFIWM	RFIWM
1	1 17 X	-481.999	-2.45	-2.88	6.36	-6.68	-2.60
3	1 18 X	-202.138	-3.04	-2.85	9.69	-10.99	.27
5	1 19 X	-498.819	-2.24	-2.61	8.02	-4.49	-1.85
7	2 17 X	474.713	-3.82	-4.44	10.81	-8.79	-10.31
9	2 18 X	191.901	-2.79	-.54	21.52	-7.54	-14.76
11	2 19 X	486.670	.08	-.48	17.06	-4.28	-7.60

IMSL = INERTIAL COUPLING W/ MASS AND STIFFNESS LOADING

I/F = INTERFACE METHOD OF INERTIAL COUPLING

RFSWOM = RESIDUAL FLEXIBILITY WITH STIFFNESS COUPLING, WITHOUT RESIDUAL MASS

RFIWM = RESIDUAL FLEXIBILITY WITH INERTIAL COUPLING, WITH RESIDUAL MASS

RFIWM = RESIDUAL FLEXIBILITY WITH INERTIAL COUPLING, WITHOUT RESIDUAL MASS

ORIGINAL PAGE IS OF POOR QUALITY



SUMMARY

- o ALL METHODS SHOWN WOULD BE ACCEPTABLE
- o RESIDUAL FLEX NOT QUITE AS ACCURATE FOR SAME NUMBER MODES
- o OTHER TECHNIQUES REQUIRE RE-CALCULATION OF SSV MODES FOR EACH PAYLOAD AND/OR ATTACH LOCATIONS
- o RESIDUAL FLEX TECHNIQUE REQUIRES NO KNOWLEDGE OF PAYLOAD PROPERTIES
- o COST SAVINGS AND CONVENIENCE OF RESIDUAL FLEX FAR OUTWEIGH SLIGHTLY LESS NUMERICAL ACCURACY

MARTIN MARIETTA



SENSITIVITY OF PAYLOAD TO LIFTOFF AND LANDING LOADS STUDY

E. A. COATES
C. R. LARSON
S. S. LI
S. YAHATA



372

CHART 1

OBJECTIVE:

- 0 STUDY RESULTS OF PAYLOAD STIFFNESS, MASS, SUSPENSION SYSTEM, MODAL CHARACTERISTIC, LOCATION IN CARGO BAY, AND PAYLOAD MIX VERSUS RESPONSE PAYLOAD LOADS.

- 0 ALL EXISTING PAYLOAD RESPONSE ANALYSES RESULTS WILL BE USED TO DETERMINE TREND.

Space Transportation System
Integration & Operations Division
Space Systems Group



Rockwell
International



SHUTTLE PAYLOAD FLIGHT LOADS SURVEY INDICATES THAT SIGNIFICANT DYNAMIC RESPONSES ARE RESULTING FROM LIFTOFF AND LANDING CONDITIONS. THE PURPOSE OF THIS STUDY IS TO SURVEY THE DATA GENERATED FROM EXISTING LIFTOFF AND LANDING DYNAMIC ANALYSES, AND TO DETERMINE IF PAYLOAD RESPONSES EXHIBIT TRENDS WHICH MAY BE USEFUL IN ASSISTING PAYLOAD RETENTION DESIGN. THE SENSITIVITY OF THE PAYLOAD RESPONSE RELATIVE TO CERTAIN CHOSEN PARAMETERS IS INVESTIGATED IN THE STUDY.

ORIGINAL PAGE IS
OF POOR QUALITY



EXISTING PAYLOAD RESPONSE TO BE INVESTIGATED:

- o MMS + DFI + SP
- o LDEF + DFI + SP
- o SPACELAB - 3P + 2P
- o SPACELAB - LM + SP
- o 3 TRS (LANDING ONLY)
- o 1 TRS (LIFTOFF ONLY)
- o OFT-2 + DFI
- o 3 SYNCOM IV IN BAY
- o 2 SYNCOM IV IN BAY
- o OSTA-1 + DFI
- o PFTA + DFI + OSS-1
- o OSS-1 + DFI
- o 3 P-80-1
- o 2-STAGE IUS/DOF-1
- o 2-STAGE IUS-F/DOD-1
- o 2-STAGE IUS-F/TDRS
- o 2-STAGE IUS-F/DSP
- o 3-STAGE IUS/PL13



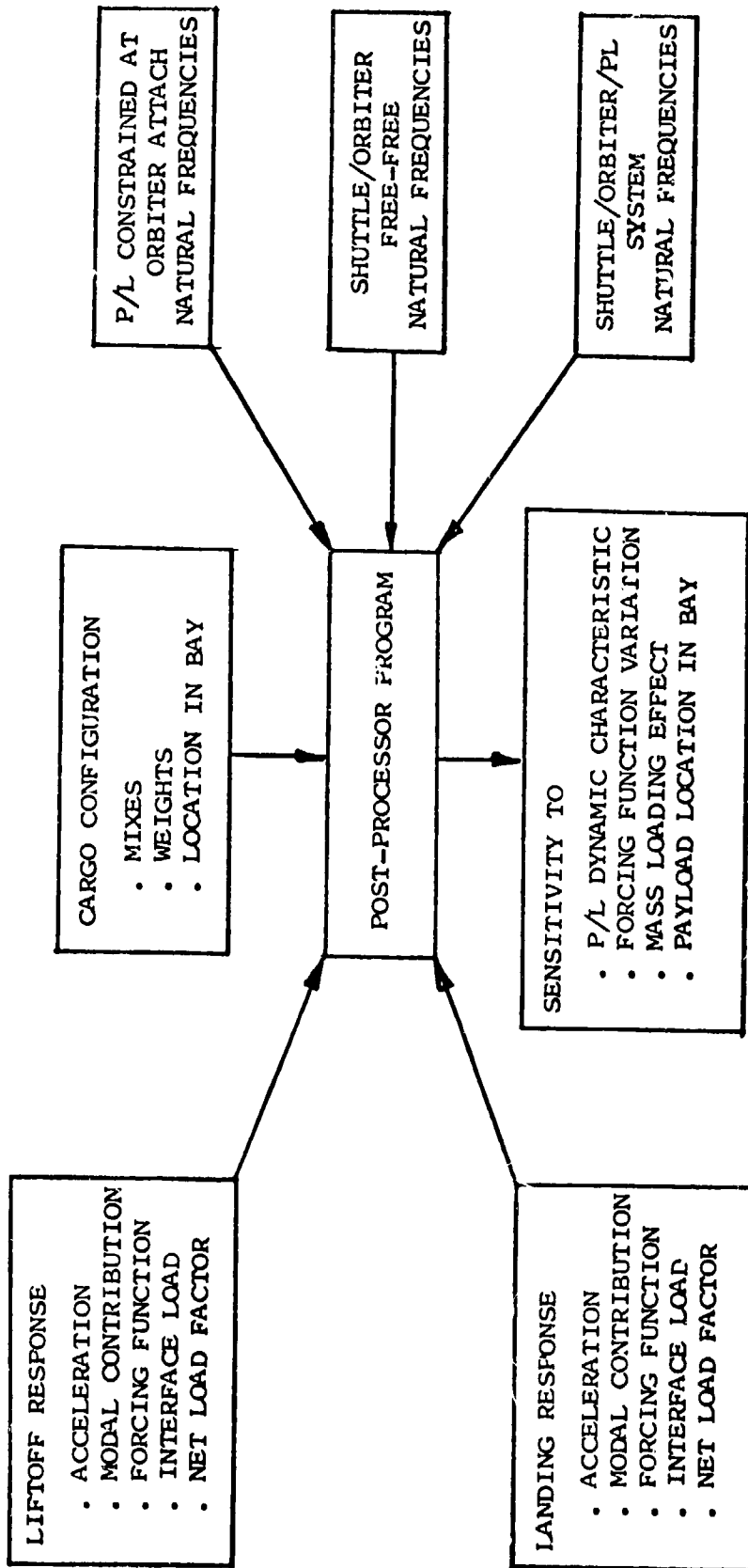
TO DATE, 14 PAYLOAD CONFIGURATIONS ARE LISTED FOR WHICH COUPLED DYNAMIC ANALYSES WERE PERFORMED. DATA ACCUMULATED FROM THESE ANALYSES ARE BEING USED TO CONDUCT THE STUDY. THE VOLUMINOUS AMOUNT OF DATA TO BE SURVEYED PRESENTS A NEED FOR AN AUTOMATED DATA PROCESSOR IN THE METHODOLOGY. IN ADDITION, A GRAPHICAL PRESENTATION OF ALL THE IMPORTANT DYNAMIC PARAMETERS IN A CONCISE MANNER IS REQUIRED.





METHOD OF INVESTIGATION

CHART 3





THE METHOD OF INVESTIGATION IS TO UTILIZE A POST-PROCESSOR PROGRAM WHICH RETRIEVES NATURAL FREQUENCIES AND MODE SHAPES AT THE PAYLOAD AND SYSTEM LEVELS, AND SORTS RESPONSE VERSUS FREQUENCIES. DOING THIS FOR EVERY PAYLOAD, HOPEFULLY CERTAIN TRENDS WILL BE ESTABLISHED REGARDING PAYLOAD SENSIVITY PARAMETERS.



POST-PROCESSOR PROGRAM

CHART 4

- OBJECTIVE - TO PROVIDE SPECTRAL PLOTS WHICH WILL SHOW
 - COUPLING OF P/L TO ORBITER MODES
 - CRITICALITY OF FORCING FUNCTION
 - MECHANISM OF THE NET PAYLOAD RESPONSE

- THIS AUTOMATED PROGRAM IS CURRENTLY UNDER DEVELOPMENT

- ALL COMPONENT DATA FOR THE EXISTING ANALYSES ARE SAVED ON TAPES. NO MAJOR PROBLEM IN RESTART OR RETRIEVE TO IMPLEMENT THE POST-PROCESSING.

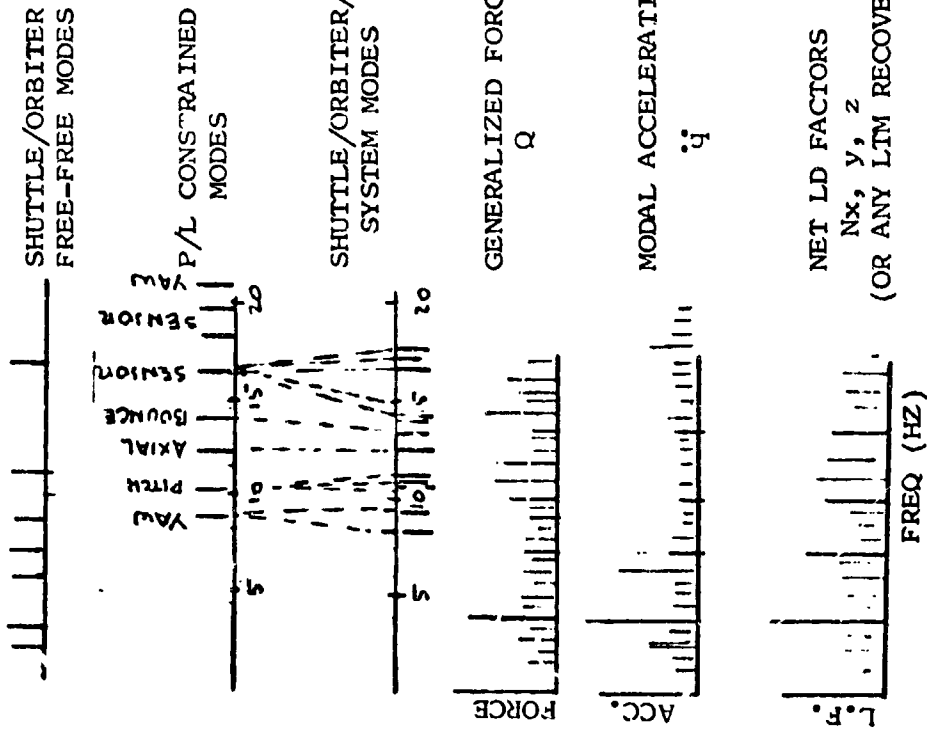


THE DATA NEEDED FOR THE SPECTRAL PLOTS ARE ALL AVAILABLE. THE POST-PROCESSOR PROGRAM BEING DEVELOPED WILL BE FULLY AUTOMATED AND SHOULD RESULT IN SIGNIFICANT LABOR SAVING.



POST-PROCESSING DATA

CHART 5



• TO BE PLOTTED FOR ALL AVAILABLE PAYLOAD DYNAMIC ANALYSES



RESULTS OF THE POST-PROCESSING INCLUDE SPECTRAL PLOTS OF KEY DATA SHOWN. THESE PLOTS WILL BE GENERATED FOR ALL THE PAYLOADS BEING INVESTIGATED. AS NEW PAYLOADS ARE ASSIGNED, THESE PLOTS WILL FACILITATE EXPEDIENT EVALUATIONS OF THE DYNAMIC CHARACTERISTICS OF THE PROPOSED INSTALLATIONS AND RECOMMEND DESIGN CHANGES AS NECESSARY.



RECOMMENDATIONS

CHART 6

382

- FOR UNIQUE PAYLOAD CONFIGURATIONS, PERFORM DYNAMIC ANALYSIS WITH THREE OF THE SAME PAYLOADS IN THE CARGO BAY TO GET THE MOST DATA FROM THE ANALYSIS.
- AVOID COUPLING WITH FUNDAMENTAL SHUTTLE BENDING FREQUENCIES AT 3, 5, 11, 15, AND 20 HZ IN PAYLOAD RETENTION DESIGN. HOWEVER, LOW FREQUENCY SUSPENSION CREATES:
 - SHUTTLE/ORBITER CONTROL AND STABILITY PROBLEM
 - LARGE PAYLOAD DEFLECTION WHICH MAY INTERFERE WITH ORBITER
 - LARGE ROTATION AT ORBITER/PAYLOAD TRUNNIONS
- AVOID LANDING SPRING-BACK FORCING FREQUENCY (APPROXIMATELY 17 HZ)

VOYAGER SPACECRAFT FLIGHT LOADS

BY

Jay C. Chen

John A. Garba

Fred D. Day III



**APPLIED MECHANICS TECHNOLOGY SECTION
JET PROPULSION LABORATORY**

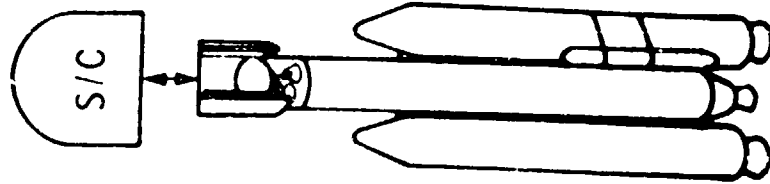
**Sponsored by
OAST - NASA**



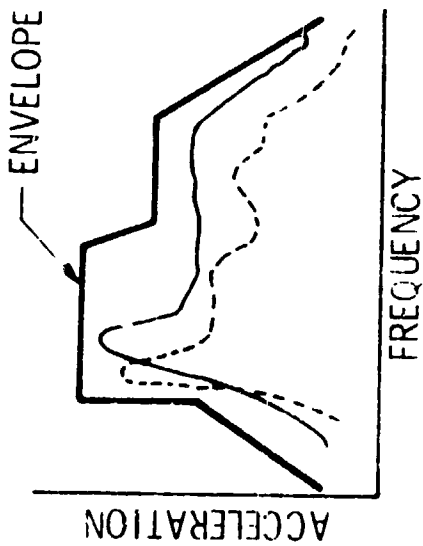
OBJECTIVES

- VERIFY THE DESIGN ASSUMPTIONS
- LAUNCH AND STAGE I BURN OUT ARE THE CRITICAL EVENTS
- SHOCK SPECTRA/IMPEDANCE METHOD PROVIDES CONSERVATIVE LOADS
- COMPARE THE FLIGHT LOADS WITH THE PREDICTED LOADS
- VERIFY THE SPACECRAFT STRUCTURE INTEGRITY

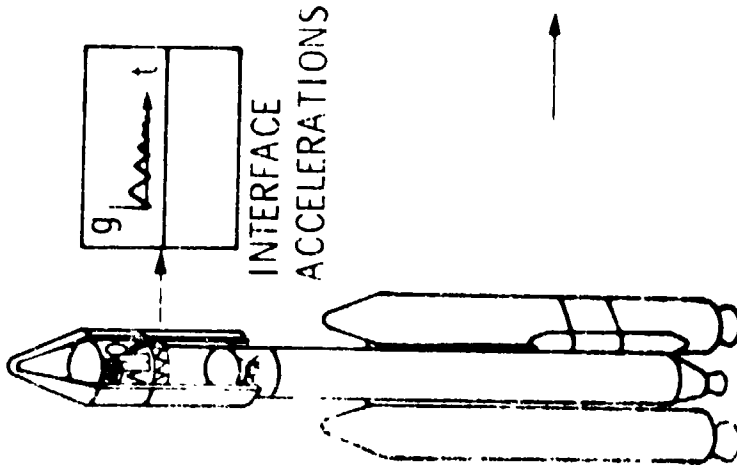
LOADS ANALYSIS BY SHOCK SPECTRA



NEW S/C LOADS OBTAINED FROM SHOCK SPECTRA ENVELOPE



CONSTRUCTION OF SHOCK SPECTRA ENVELOPE



INTERFACE ACCELERATIONS FROM PREVIOUS FLIGHTS AND/OR LAUNCH VEHICLE/PAYLOAD SYSTEM ANALYSIS

DETERMINATION OF DYNAMIC ENVIRONMENTS FOR DESIGN

● PREVIOUS TITAN III/CENTAUR FLIGHTS

1. VIKING DYNAMIC SIMULATOR, FEBRUARY 1974
2. HELIOS A, DECEMBER 1974
3. VIKING A, AUGUST 1975
4. VIKING B, SEPTEMBER 1975

● CRITICAL DYNAMIC EVENTS

1. TITAN STAGE 0 IGNITION (LAUNCH OR LIFT-OFF)
2. MAXIMUM AERODYNAMIC PRESSURE (MAX α_q)
3. TITAN STAGE I IGNITION (STG I IG)
4. TITAN STAGE I BURNOUT (STG I B0)
5. TITAN STAGE II BURNOUT (STG II B0)
6. FIRST CENTAUR MAIN ENGINE CUTOFF (MECO I)
7. SECOND CENTAUR MAIN ENGINE CUTOFF (MECO II)

ORIGINAL PAGE IS
OF POOR QUALITY

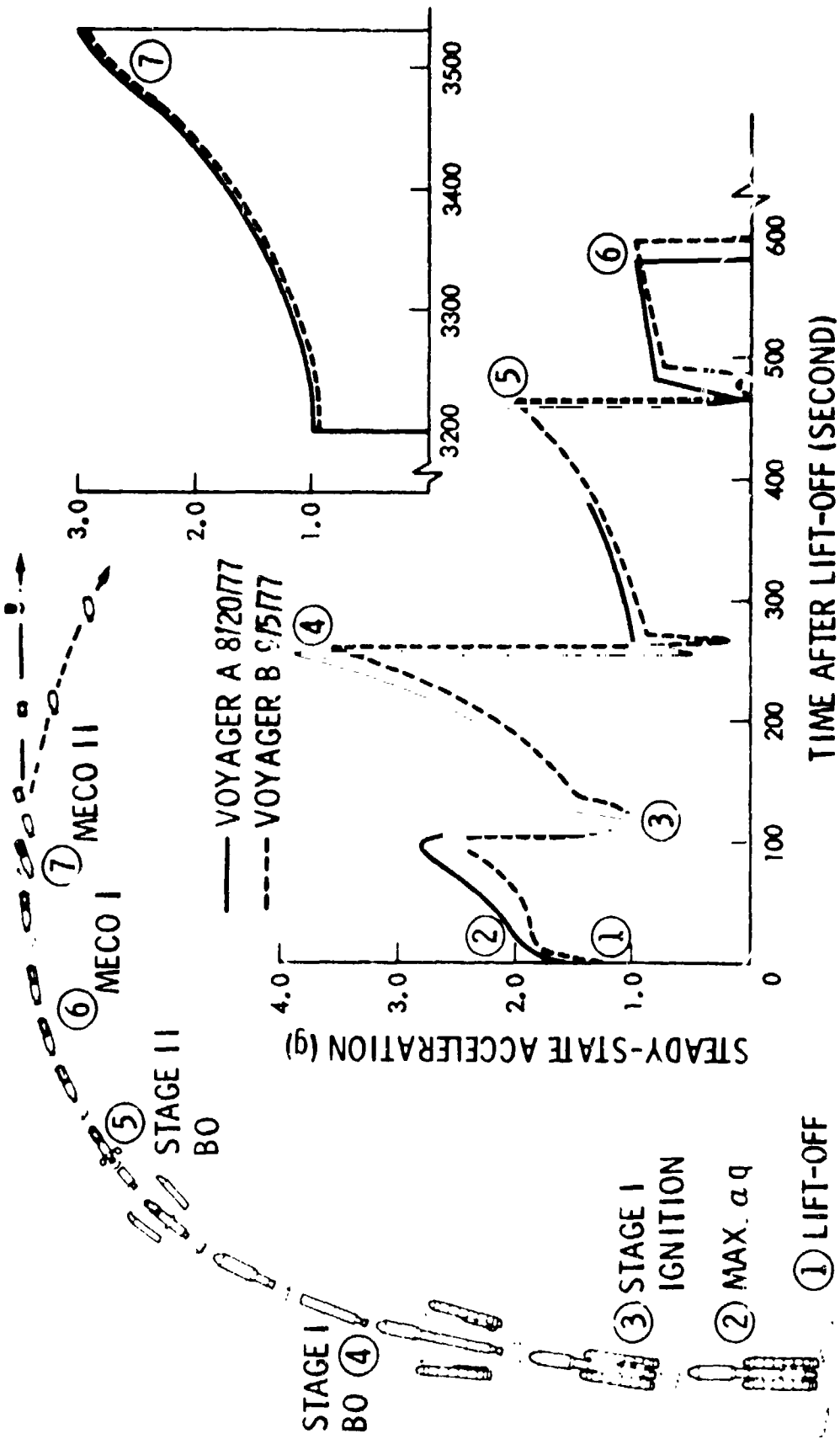
HIGH GAIN
ANTENNA
TRUSS

SCIENCE
BOOM

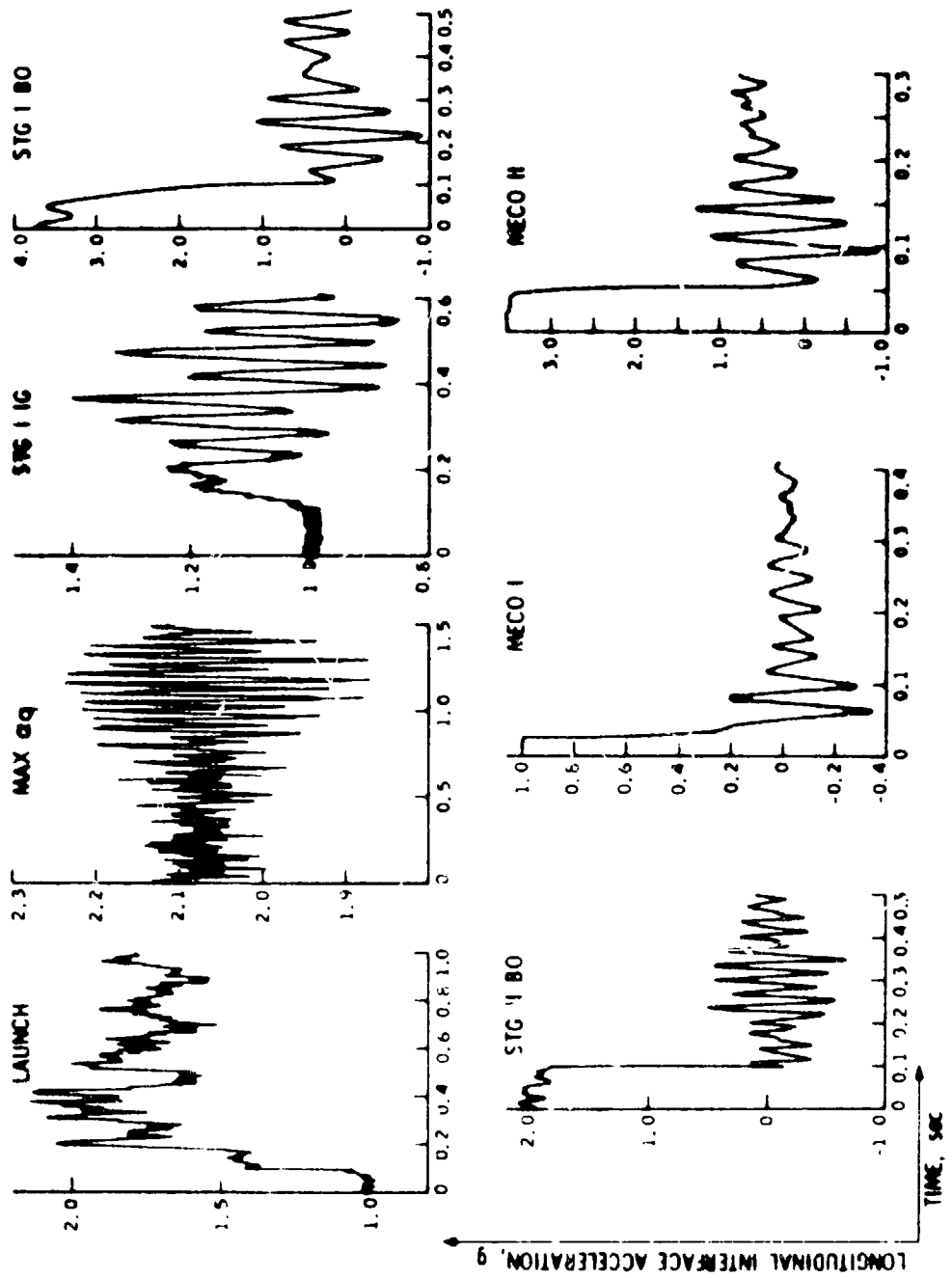




STEADY STATE ACCELERATION OF LAUNCH VEHICLE/VOYAGER INTERFACE

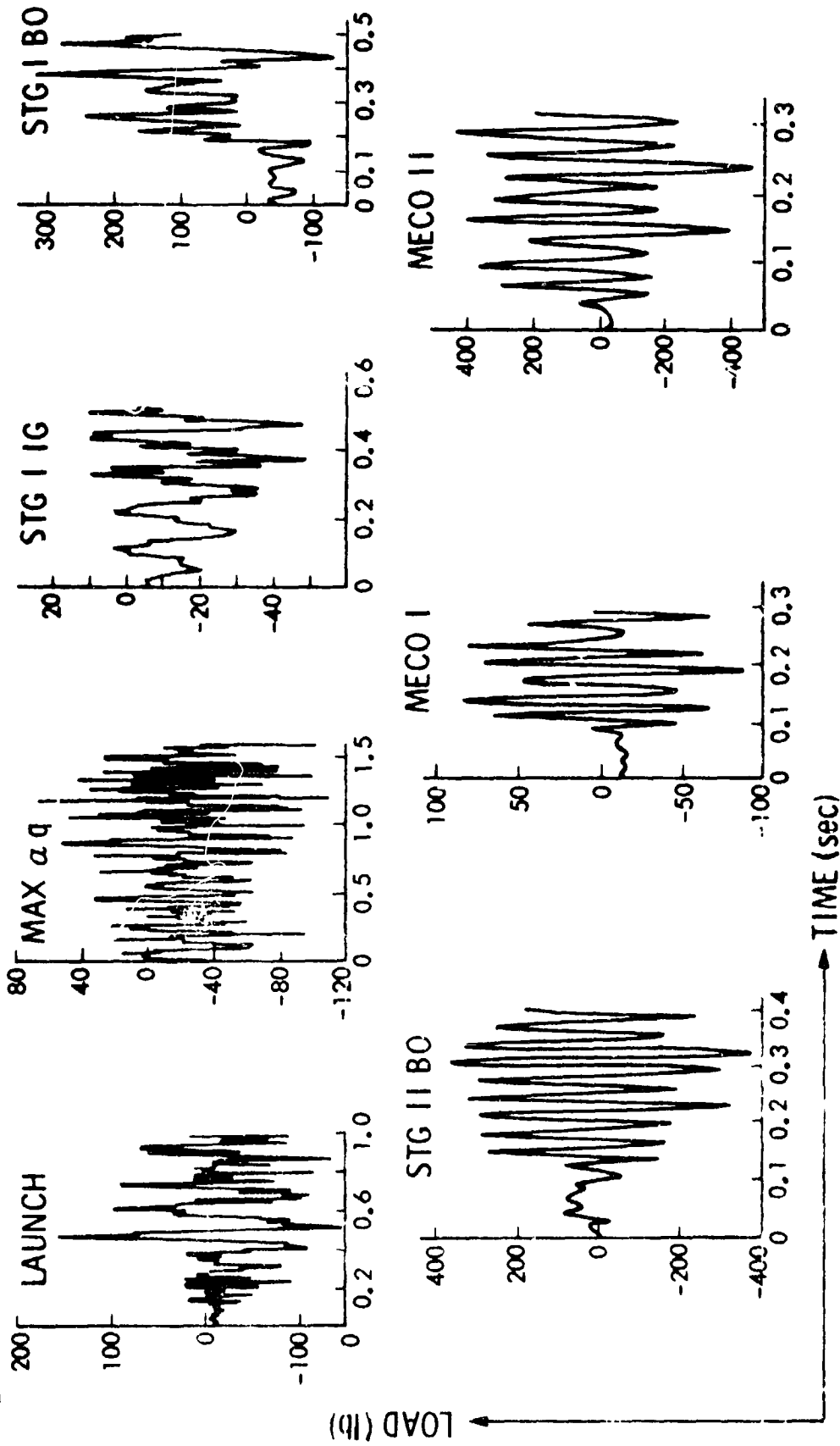


FLIGHT MEASURED VOYAGER SPACECRAFT INTERFACE ACCELERATION



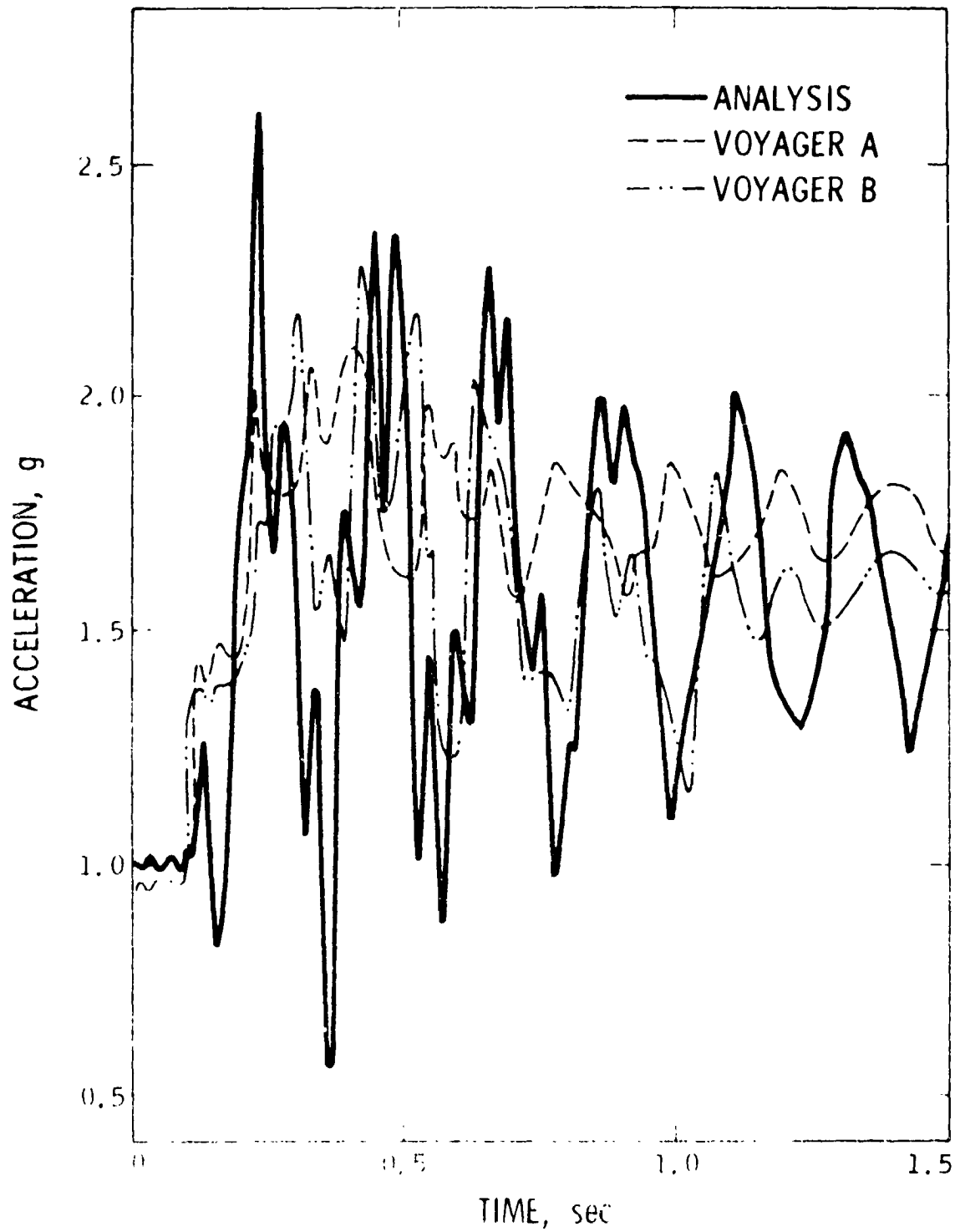


FLIGHT LOAD HISTORY OF MEMBER 71937



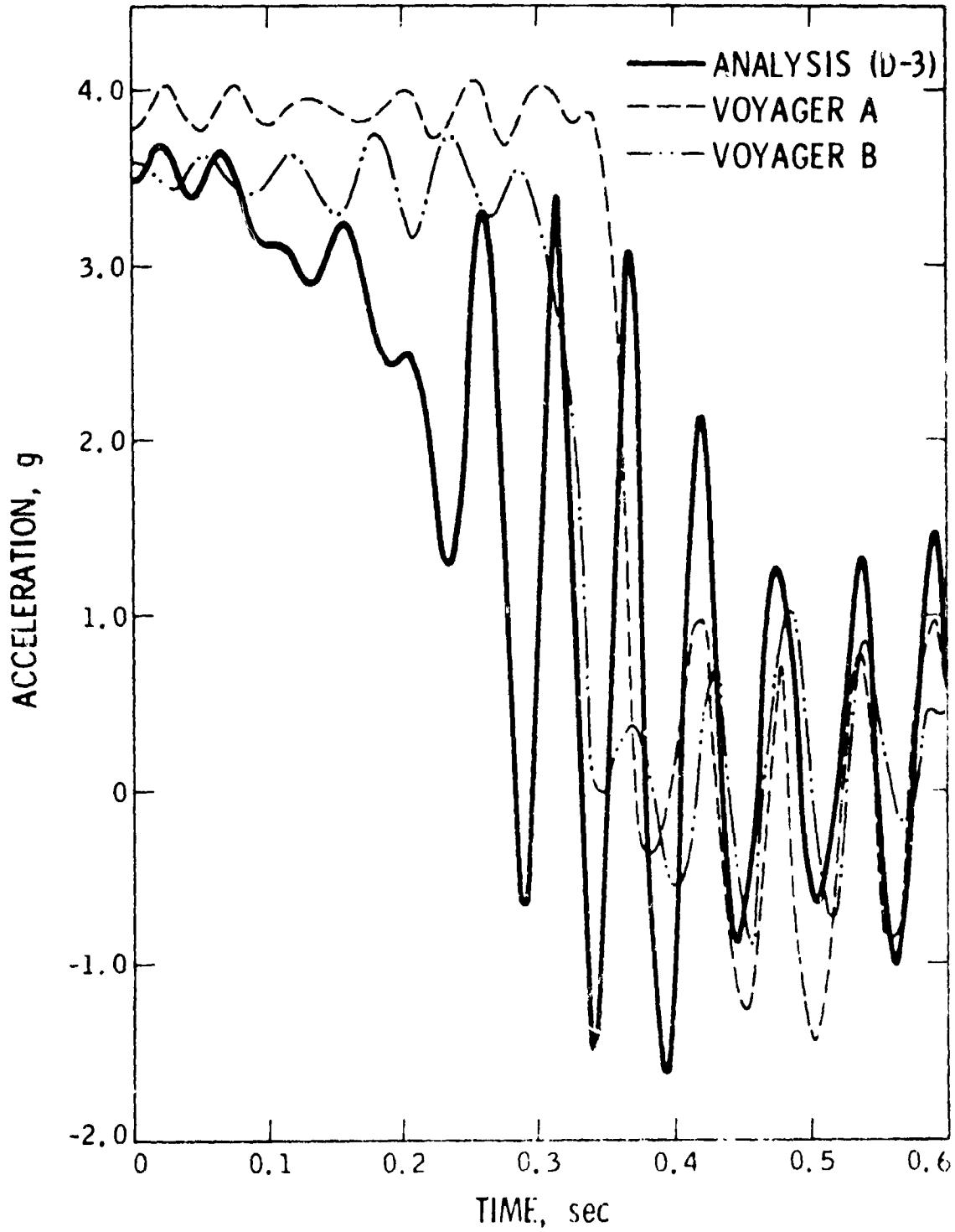


INTERFACE ACCELERATIONS FOR LAUNCH





INTERFACE ACCELERATIONS FOR STAGE I BURN OUT



MAX/MIN FLIGHT AND PREDICTED LOADS COMPARISON FOR MISSION MODULE TRUSS

ORIGINAL PAGE IS
OF POOR QUALITY

MEMBER	LAUNCH						STAGE I BURN OUT					
	FLIGHT			PREDICTED			FLIGHT			PREDICTED		
	A	B	S.S.	TRANSIENT	S.S.		A	B	S.S.	TRANSIENT	S.S.	
68011	412.9 -1130.7	1604.5 -2370.1	5900.0	2369.9 -3134.0	5900.0		225.9 -1316.0	282.7 -761.0		2667.1 -2784.8	4320.0	
68021	919.4 -1104.1	2804.3 -2102.2	7060.0	3174.0 -3753.0	7060.0		1179.4 -1039.6	612.5 -827.1		2702.0 -3432.7	4910.0	
68031	61.5 -635.1	195.7 -1039.4	7120.0	1676.0 -2507.0	7120.0		132.6 -1312.0	735.3 -1631.5		1381.6 -1543.0	4520.0	
68041	111.0 -643.9	788.0 -1720.3	6870.0	1733.0 -2143.0	6870.0		1237.4 -802.3	1850.9 -753.0		1034.2 -1393.0	4050.0	
68051	959.8 -1145.6	2737.4 -2611.7	6770.0	3149.0 -3398.0	6770.0		1571.3 -904.2	580.5 -710.5		2797.1 -3321.9	4880.0	
68061	638.0 -1404.2	2057.0 -3597.9	7110.0	3287.0 -3774.0	7110.0		775.2 -1597.2	1036.2 -823.9		3021.9 -3434.0	4320.0	
68071	221.9 -580.8	790.4 -1493.1	6990.0	1872.0 -2056.0	6990.0		1263.1 -754.5	1725.0 -591.8		736.0 -864.3	4890.0	
68081	181.3 -724.5	1044.3 -1204.5	5800.0	1390.0 -2038.0	5800.0		167.5 -1385.6	493.5 -1474.6		1020.5 -1320.0	4320.0	



MAX FLIGHT LOADS AND LIMIT CAPABILITY COMPARISON FOR MISSION MODULE TRUSS

MEMBER	MAX. FLIGHT LOAD(a)	MAX DESIGN LOAD		LIMIT CAPABILITY(d)	S. S. DESIGN MAX. FLIGHT	MARGIN OF SAFETY(e)
		TRANSIENT(b)	S. S. (c)			
68011	2370.1	3234.0	5900.0	13700	2.489	4.780
68021	5312.1	3753.0	7060.0	12500	1.329	1.353
68031	9446.1	2922.0	7120.0	12000	0.754	0.270
68041	7828.2	2798.0	6870.0	13600	0.878	0.737
68051	3667.5	3398.0	6770.0	13600	1.846	2.708
68061	5651.8	3774.0	7110.0	12000	1.258	1.123
68071	8526.7	2944.0	6990.0	12500	0.820	0.466
68081	5902.1	-2335.0	5800.0	13700	0.983	1.321

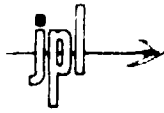
(a) ALL LOADS ARE FROM THE MECO II EVENT EXCEPT MEMBER 68011 WHICH IS FROM THE LAUNCH EVENT

(b) LOADS FOR 68011, 68021, 68051, 68061 ARE FROM THE LAUNCH EVENT, OTHERS ARE FROM THE MAX. aq EVENT.

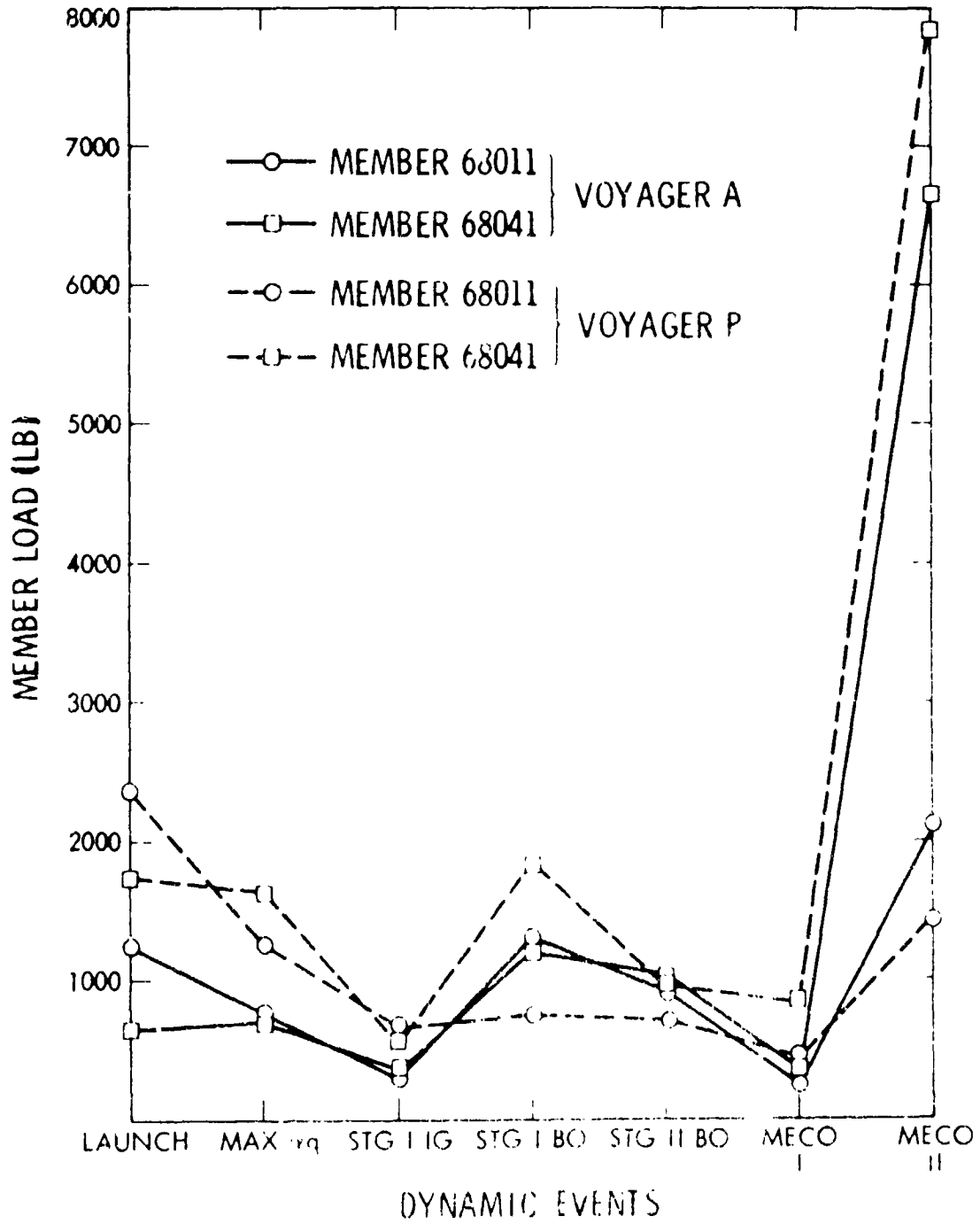
(c) ALL LOADS ARE FROM THE LAUNCH EVENT

(d) LIMIT CAPABILITY = ULTIMATE CAPABILITY ÷ 1.25

(e) MARGIN OF SAFETY = $\frac{\text{LIMIT CAPABILITY}}{\text{MAX. FLIGHT LOAD}} - 1$

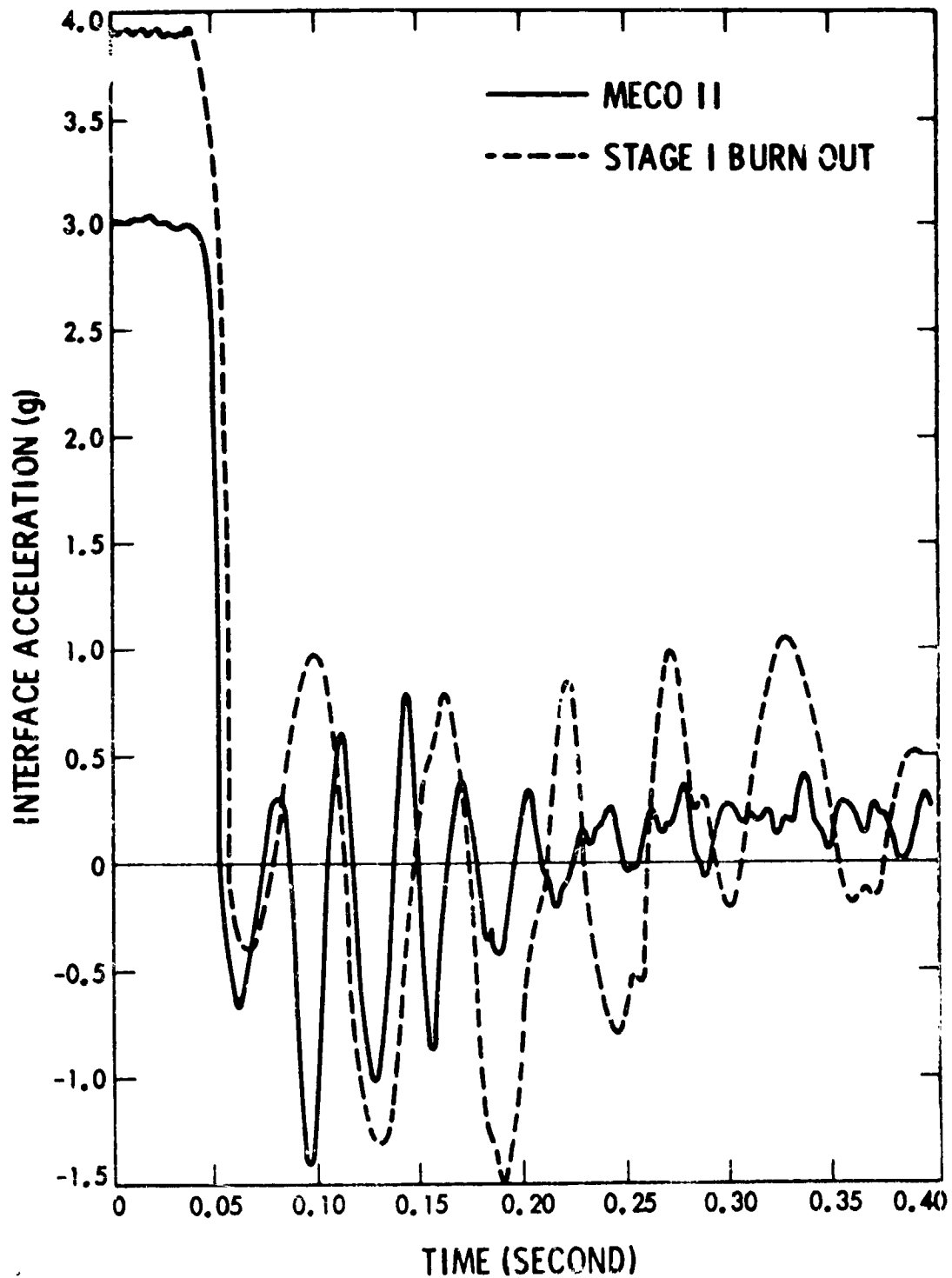


MAXIMUM MEMBER LOAD FOR VARIOUS EVENTS





VOYAGER A INTERFACE ACCELERATIONS FOR TITAN STAGE I BURNOUT AND CENTAUR MAIN ENGINE CUTOFF



05



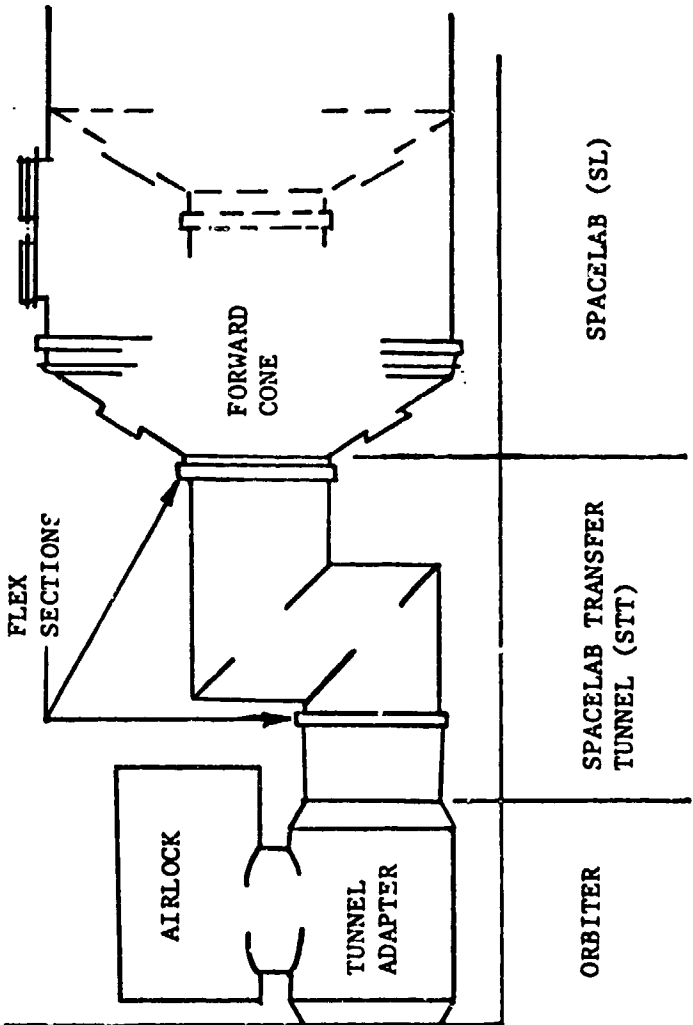
CONCLUSIONS

- NEGLECTING MECO II EVENT IS A SERIOUS OMISSION
- EXCEPT MECO II, LAUNCH AND STAGE I BURN OUT DO PROVIDE THE MAXIMUM LOADS
- LOADS OBTAINED BY THE SHOCK SPECTRA/IMPEDANCE METHOD ARE GREATER THAN THE FLIGHT LOADS FROM THE CORRESPONDING EVENTS
- POSITIVE MARGIN OF SAFETY HAS BEEN ACHIEVED FOR BOTH SPACECRAFTS

ORGANIZATION: STRUCTURES AND PROPULSION LABORATORY/EP42	MARSHALL SPACE FLIGHT CENTER PAYLOAD FLIGHT LOADS PREDICTION METHODOLOGY WORKSHOP	NAME: J. S. MOORE DATE: NOVEMBER 1978
---	---	--

LOADS METHODOLOGY FOR THE SPACELAB TRANSFER TUNNEL

PRECEDING PAGE BLANK NOT FILMED



LOADS METHODOLOGY FOR THE SPACELAB TRANSFER TUNNEL

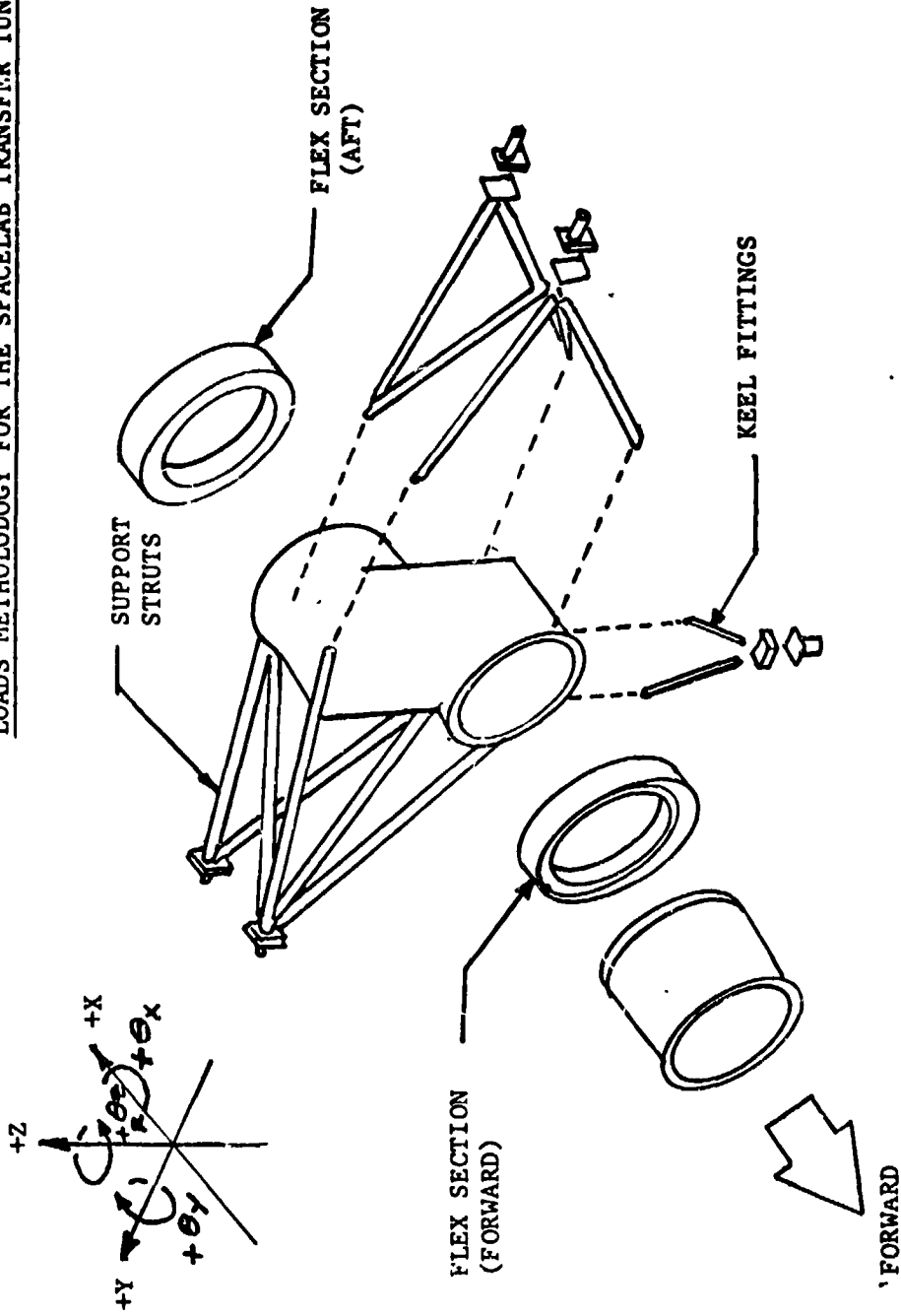
The Spacelab Transfer Tunnel (STT), located within the orbiter payload bay, provides access from the orbiter cabin to the Spacelab (SL) experimental area. At the forward end, the tunnel adapter connects the STT with the orbiter cabin. At the aft end the STT attaches to the forward cone of the SL.

The configuration shown is known as the short tunnel. The long tunnel configuration, indicated by dashed lines for the SL forward cone, has an additional cylindrical section added at the front keeping the joggle section next to the SL.

Design and construction of the STT has been contracted to the McDonnell Douglas Technical Services Company (MDTSCO) by MSFC with MDTSCO subcontracting the flex sections to Goodyear Aerospace Corporation (GAC).

ORGANIZATION: STRUCTURES AND PROPULSION LABORATORY/EP42	MARSHALL SPACE FLIGHT CENTER PAYLOAD FLIGHT LOADS PREDICTION METHODOLOGY WORKSHOP	NAME: J. S. MOORE	DATE: NOVEMBER 1978
---	---	----------------------	------------------------

LOADS METHODOLOGY FOR THE SPACELAB TRANSFER TUNNEL



LOADS METHODOLOGY FOR THE SPACELAB TRANSFER TUNNEL (STT)

The support struts and keel fittings are designed by the STT inertia loads during the various phases of flight. The forward and aft flex sections are designed by loads due to pressurization and deflections. The flex sections are interchangeable and are designed by the envelope of loading conditions.

Positive forces and moments are as indicated.

<p>ORGANIZATION:</p> <p>STRUCTURES AND PROPULSION LABORATORY/EP42</p>	<p>MARSHALL SPACE FLIGHT CENTER</p> <p>PAYLOAD FLIGHT LOADS PREDICTION METHODOLOGY WORKSHOP</p>	<p>NAME:</p> <p>J. S. MOORE</p> <p>DATE:</p> <p>NOVEMBER 1978</p>
<p><u>LOADS METHODOLOGY FOR THE SPACELAB TRANSFER TUNNEL (STT)</u></p> <p>STT DESIGN CRITERIA</p> <ul style="list-style-type: none"> ● STT DESIGNED TO WITHSTAND ITS OWN INERTIA LOADS DEVELOPED DURING PRELAUNCH, ASCENT, FLIGHT, LANDING AND CRASH CONDITIONS AND TO TRANSMIT THESE LOADS INTO THE ORBITER THRU SUPPORT STRUTS AND KEEL FITTINGS. ● LOADS AT TUNNEL/TUNNEL ADAPTER AND TUNNEL/SPACELAB INTERFACE MINIMIZED TO INCLUDE ONLY LOADS RESULTING FROM PRESSURE AND THE RESISTENCE OF THE FLEX SECTIONS TO INDUCED DEFLECTIONS. 		

LOADS METHODOLOGY FOR THE SPACELAB TRANSFER TUNNEL

The basic STT design consist of having the STT response to its environments taken out through the STT support struts and the keel fittings. At the Orbiter/STT and Spacelab/STT interfaces the only loads will be those due to pressure and the resistance of the flex sections to induced deflections.

ORGANIZATION: STRUCTURES AND PROPULSION LABORATORY/EP42	MARSHALL SPACE FLIGHT CENTER		NAME:
	PAYLOAD FLIGHT LOADS PREDICTION METHODOLOGY WORKSHOP		J. S. MOORE
			DATE: NOVEMBER 1978

LOADS METHODOLOGY FOR THE SPACELAB TRANSFER TUNNEL (STT)

STT FLEX SECTION DISPLACEMENT REQUIREMENTS

CONDITION	AXIAL X (IN.)	DISPLACEMENT			PRESSURE (PSI)	
		LATERAL Y&Z (IN.)	TORSIONAL θ_x (DEG.)	ROTATIONAL θ_y & θ_z (DEG.)	MINIMUM	MAXIMUM
LIFTOFF	.91	1.76	.27	.48	-0.5	+0.5
	-.96	1.76	.27	.48		
HIGH Q BOOST	1.52	2.45	.67	1.20	7.5	13.4
	-.77	2.45	.67	1.20		
ORBITER MAX. LOAD	1.00	2.13	.24	1.33	11.7	15.9
	-.59	2.13	.24	1.33		
PITCH	2.33	2.43	.30	1.25	0	15.9
	-.72	2.43	.30	1.25		
YAW	1.68	2.69	.30	1.26	0	15.9
	-.92	2.69	.40	1.26		
LANDING	.98	1.47	.35	.58	-0.5	+1.4
	-1.81	1.47	.35	.58		

LOADS METHODOLOGY FOR THE SPACELAB TRANSFER TUNNEL

Displacements and pressure requirements for designing the forward
and aft flex sections.

<p>ORGANIZATION: STRUCTURES AND PROPULSION LABORATORY/EP42</p>	<p>MARSHALL SPACE FLIGHT CENTER PAYLOAD FLIGHT LOADS PREDICTION METHODOLOGY WORKSHOP</p>	<p>NAME: J. S. MOORE DATE: NOVEMBER 1978</p>
<p style="text-align: center;"><u>LOADS METHODOLOGY FOR THE SPACELAB TRANSFER TUNNEL</u></p> <p>MATERIAL</p> <ul style="list-style-type: none"> - FABRIC CONSISTS OF TWO PLYS OF CLOTH COATED WITH VITON AND PLACED AT A BIAS ANGLE OF 15°. - CONSTRUCTION OF SINGLE PLY IS IDENTIFIED AS TO YARN, WEAVE, DENIER (WARP), THREAD COUNT, WEIGHT AND TENSILE STRENGTH. - WEIGHT OF COATED FABRIC IS MEASURED. - MINIMUM STRENGTH OF SINGLE PLY DETERMINED BY PULL TESTS. - INITIAL MODULUS OF ELASTICITY IS FOUND BY MULTIPLYING INITIAL SLOPE OF STRESS STRAIN CURVE BY MINIMUM STRENGTH. 		

ORGANIZATION: STRUCTURES AND PROPULSION LABORATORY/EP42	MARSHALL SPACE FLIGHT CENTER PAYLOAD FLIGHT LOADS PREDICTION METHODOLOGY WORKSHOP	NAME: J. S. MOORE DATE: NOVEMBER 1978
--	--	--

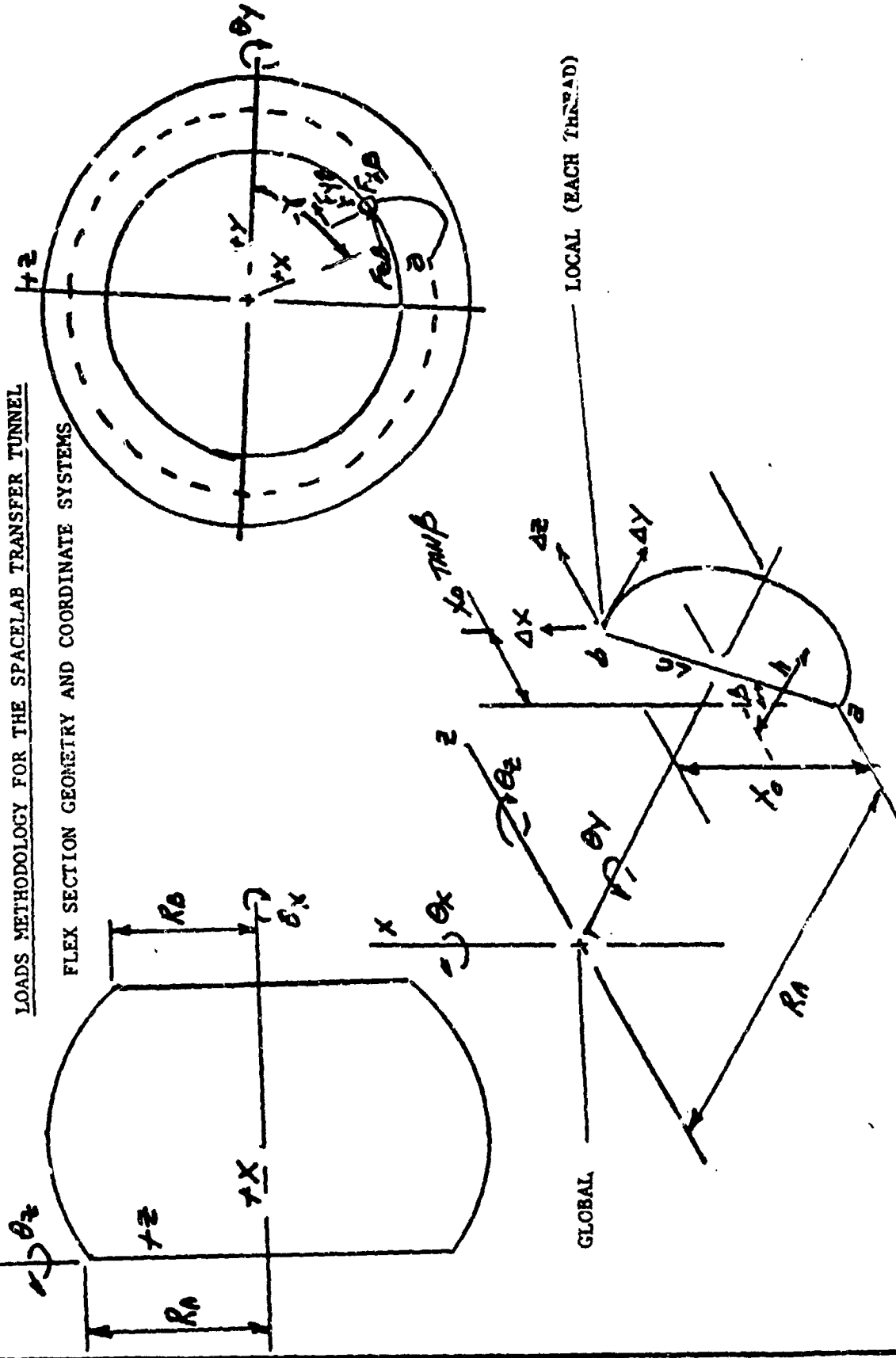
LOADS METHODOLOGY FOR THE SPACELAB TRANSFER TUNNEL (STT)

LOADS CALCULATIONS

• ASSUMPTIONS

1. CANTED STRING LIES IN A PLANE. ACTUALLY, INTERNAL PRESSURE CAUSES THREE DIMENSIONAL CURVATURE.
 2. TREAT STRING AS HAVING CONSTANT RADIUS. ACTUALLY, TAPEDED LOADING FROM CURVATURE PRODUCES ELLIPTICAL CURVE.
- PRESSURE LOADS CARRIED BY TENSION IN THE DIRECTION OF THE PLYS. (TWO PLYS AT A BIAS ANGLE OF 15°).
 - RING LOADINGS DEFINED BY DISPLACEMENT OF ONE END OF THE THREADS RELATIVE TO THE OTHER END OF THE SAME THREAD.
 - LOADS INTEGRATED AROUND THE RINGS TO DETERMINE TOTAL LOADS.

ORGANIZATION: STRUCTURES AND PROPULSION LABORATORY/EP42	MARSHALL SPACE FLIGHT CENTER PAYLOAD FLIGHT LOADS PREDICTION METHODOLOGY WORKSHOP	NAME: J. S. MOORE DATE: NOVEMBER 1978
---	---	--



ORGANIZATION:

STRUCTURES AND PROPULSION
LABORATORY/EP42

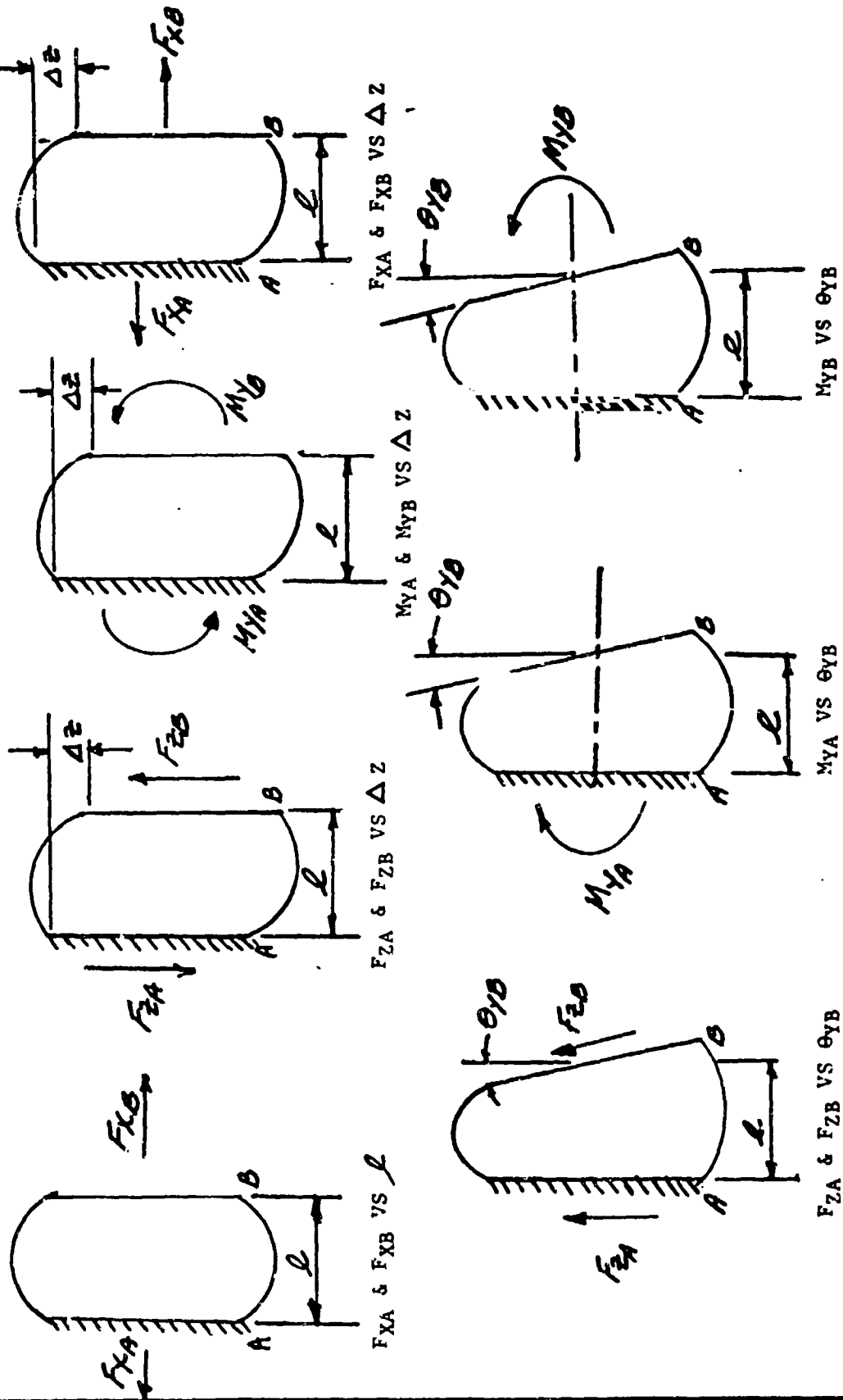
MARSHALL SPACE FLIGHT CENTER

NAME:
J. S. MOORE

DATE:
NOVEMBER 1978

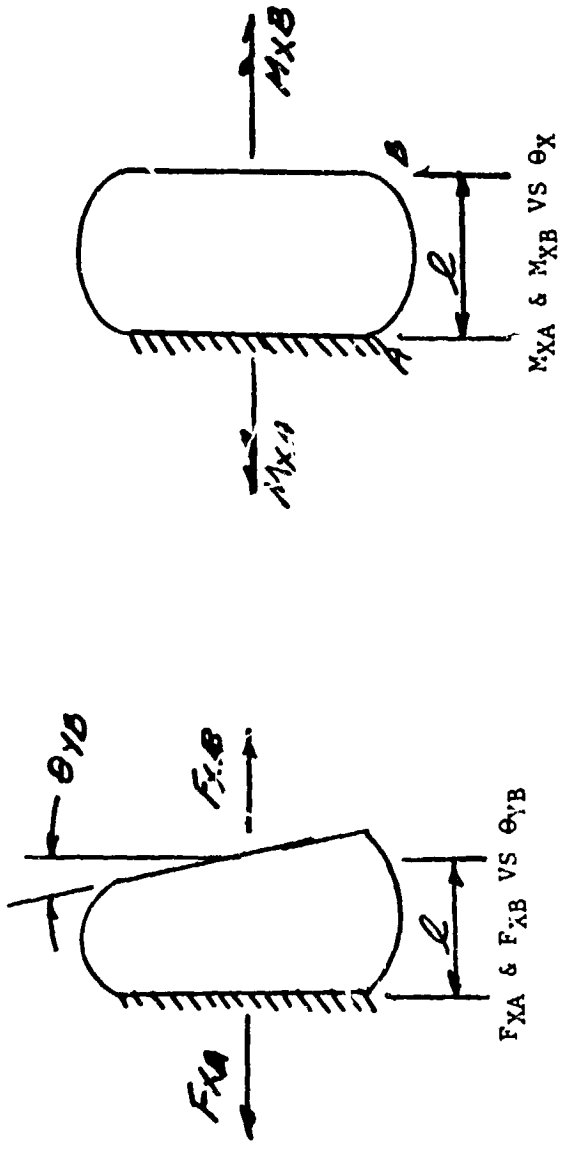
PAYLOAD FLIGHT LOADS PREDICTION
METHODOLOGY WORKSHOP

LOADS METHODOLOGY FOR THE SPACELAB TRANSFER TUNNEL



ORGANIZATION: STRUCTURES AND PROPULSION LABORATORY/EP42	MARSHALL SPACE FLIGHT CENTER		NAME: J. S. MOORE
	PAYLOAD FLIGHT LOADS PREDICTION METHODODOLOGY WORKSHOP		DATE: NOVEMBER 1978

LOADS METHODOLOGY FOR THE SPACELAB TRANSFER TUNNEL



CONCLUSION

- COMPUTER OUTPUT OF GAC'S "FLEXSET" PROGRAM PRESENTS THE LOADS RESULTING FROM THE MOST CRITICAL DISPLACEMENT CONDITIONS AND THE LOADS WHICH RESULT FROM BENDING, TORSIONAL, AXIAL AND TRANSVERSE DEFLECTIONS AT ONE END OF THE FLEX SECTION WHILE THE OTHER END IS HELD FIXED.
- AS EACH LOAD PARAMETER IS EXPRESSED AS A FUNCTION OF PRESSURE AND FLEX SECTION WIDTH, THE MOST EFFICIENT WIDTH FOR MINIMIZING LOADS CAN BE SELECTED.



SPACECRAFT LOADS ANALYSES

FOR

THE TITAN/CENTAUR LAUNCH VEHICLE

A CASE HISTORY

B. K. WADA

J. A. GARBA

JET PROPULSION LABORATORY

PRECEDING PAGE BLANK NOT FILMED

jpj →

2

OUTLINE

OBJECTIVE

DEFINITION

LOAD ANALYSIS APPROACH

FLIGHTS

- VDS/VIKING
- HELIOS
- VOYAGER

SUMMARY

CONCLUSION



3

OBJECTIVES

- DESCRIBE LOADS/FLIGHT DATA
- SUMMARIZE-LOAD PREDICTION/FLIGHT DATA
- STATUS-LOADS TECHNOLOGY
- CONCLUDE



DEFINITION

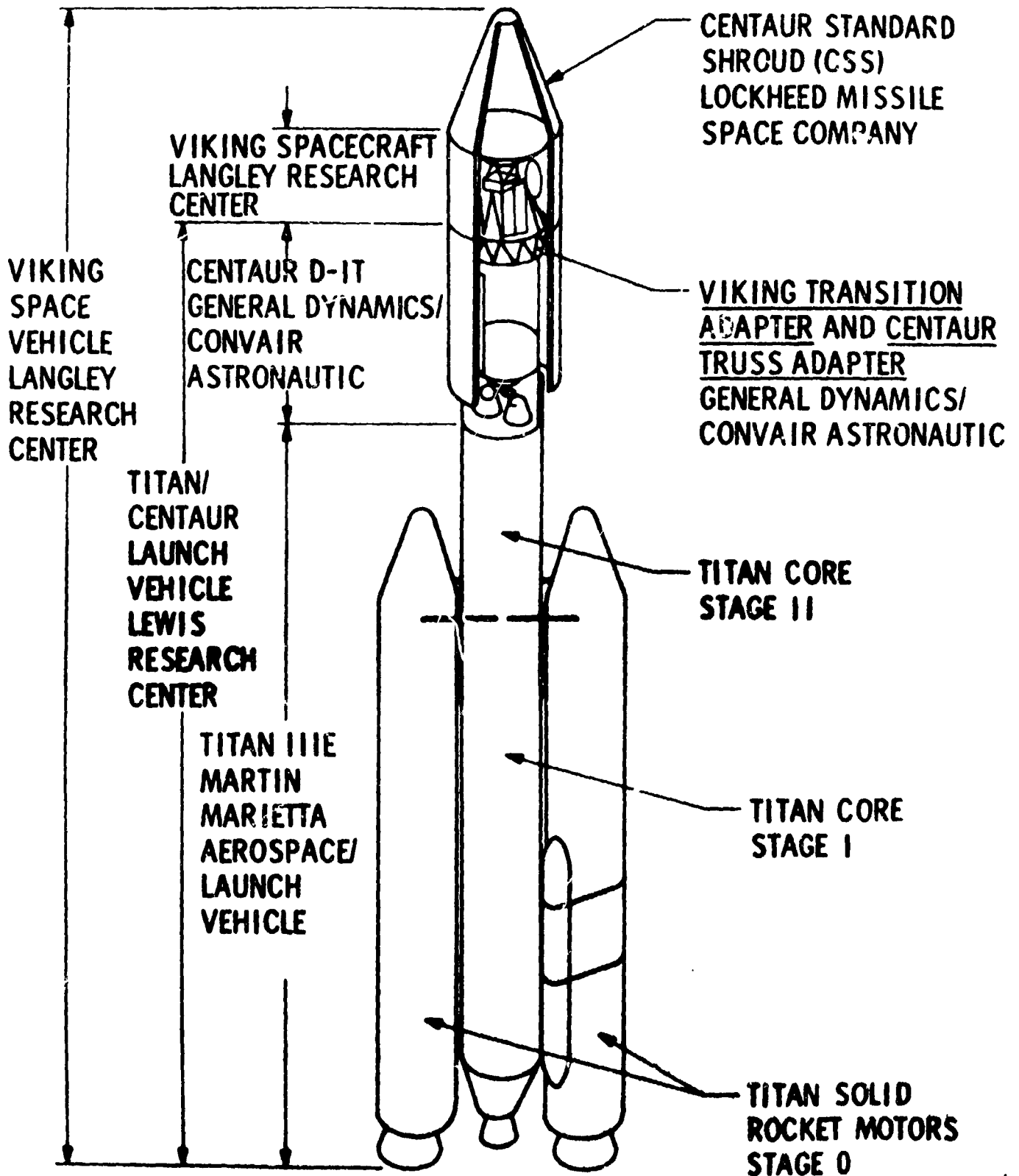
- LAUNCH VEHICLE
 - NEW TITAN/CENTAUR
 - NEW FAIRING
 - AVAILABLE DATA
 - 80 TITAN FLIGHTS / 25-35 CENTAUR
 - ~10 WITH P/L INSTRUMENTATION
 - FORCING FUNCTIONS
 - P/L LOAD PREDICTION
 - CRITICAL EVENTS
 - MATH MODELS
 - ANALYSIS PROCEDURES

↑
jpl

6

DEFINITION (CON'T)

- COMPLEX INTERACTION
- FLIGHT INSTRUMENTATION (?)





7

AVAILABLE FORCING FUNCTIONS
AT THE INCEPTION OF THE TITAN/CENTAUR
LAUNCH VEHICLE DEVELOPMENT

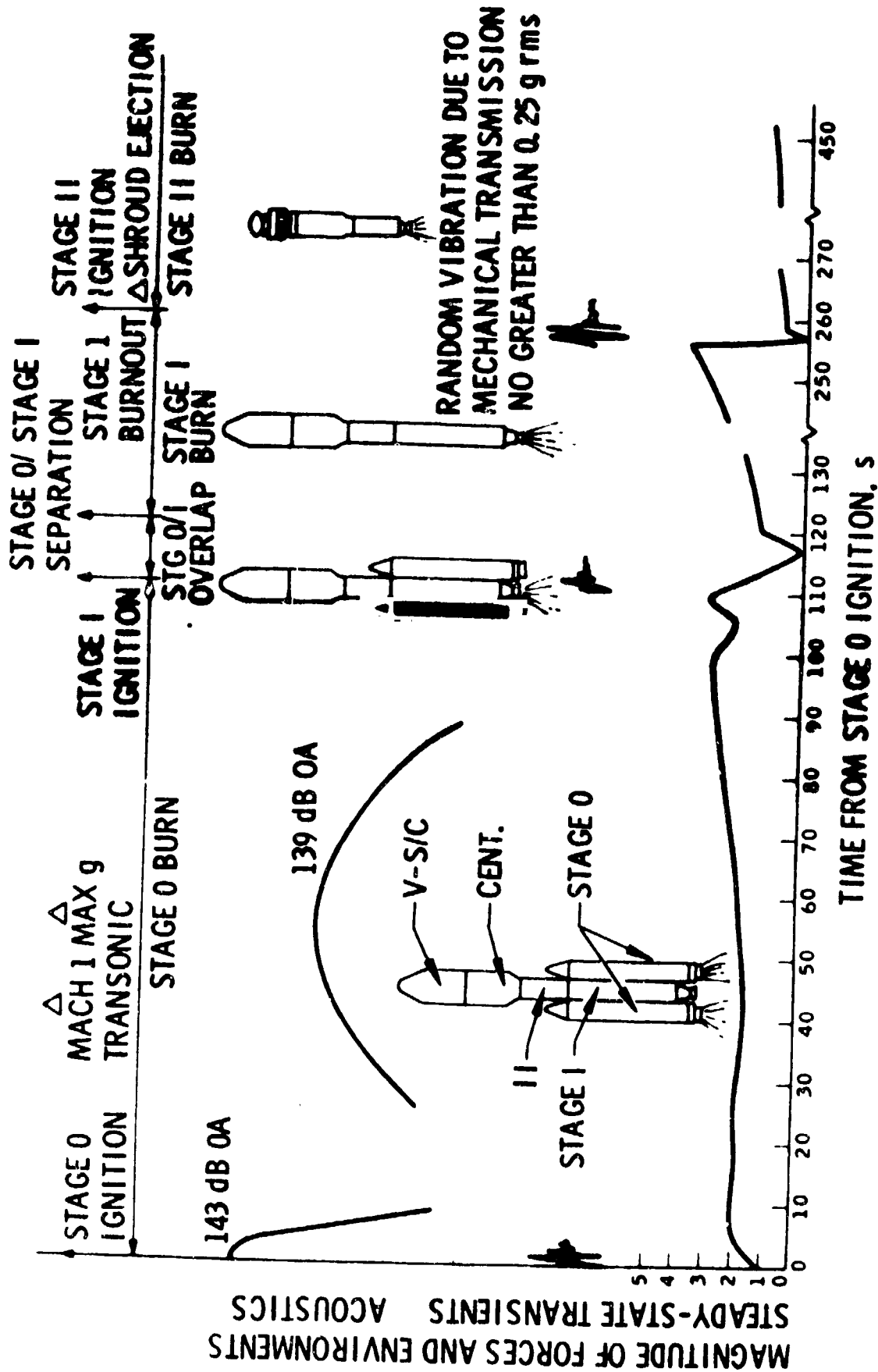
EVENTS	NO. OF FORCING FUNCTIONS OR CONDITIONS	SOURCE
GROUND CONDITIONS	6	SPECIFICATION
STAGE 0 IGNITION	21	FLIGHT DATA
AIRLOADS	5	SYNTHESIZED
STAGE 0 MAX. ACCELERATION	1	SYNTHESIZED
STAGE I IGNITION	12	FLIGHT DATA
SRM SEPARATION	1	SYNTHESIZED
STAGE I BURNOUT	29	FLIGHT DATA
STAGE II IGNITION	3	SYNTHESIZED
STAGE II BURNOUT	19	FLIGHT DATA
CENTAUR MAIN ENGINE START I (MES I)	1	SPECIFICATION
CENTAUR MAIN ENGINE CUTOFF I (MECO I)	1	SPECIFICATION
CENTAUR MAIN ENGINE START II	1	SPECIFICATION
CENTAUR MAIN ENGINE CUTOFF II (MECO II)	1	SPECIFICATION

8

LOAD ANALYSIS APPROACH

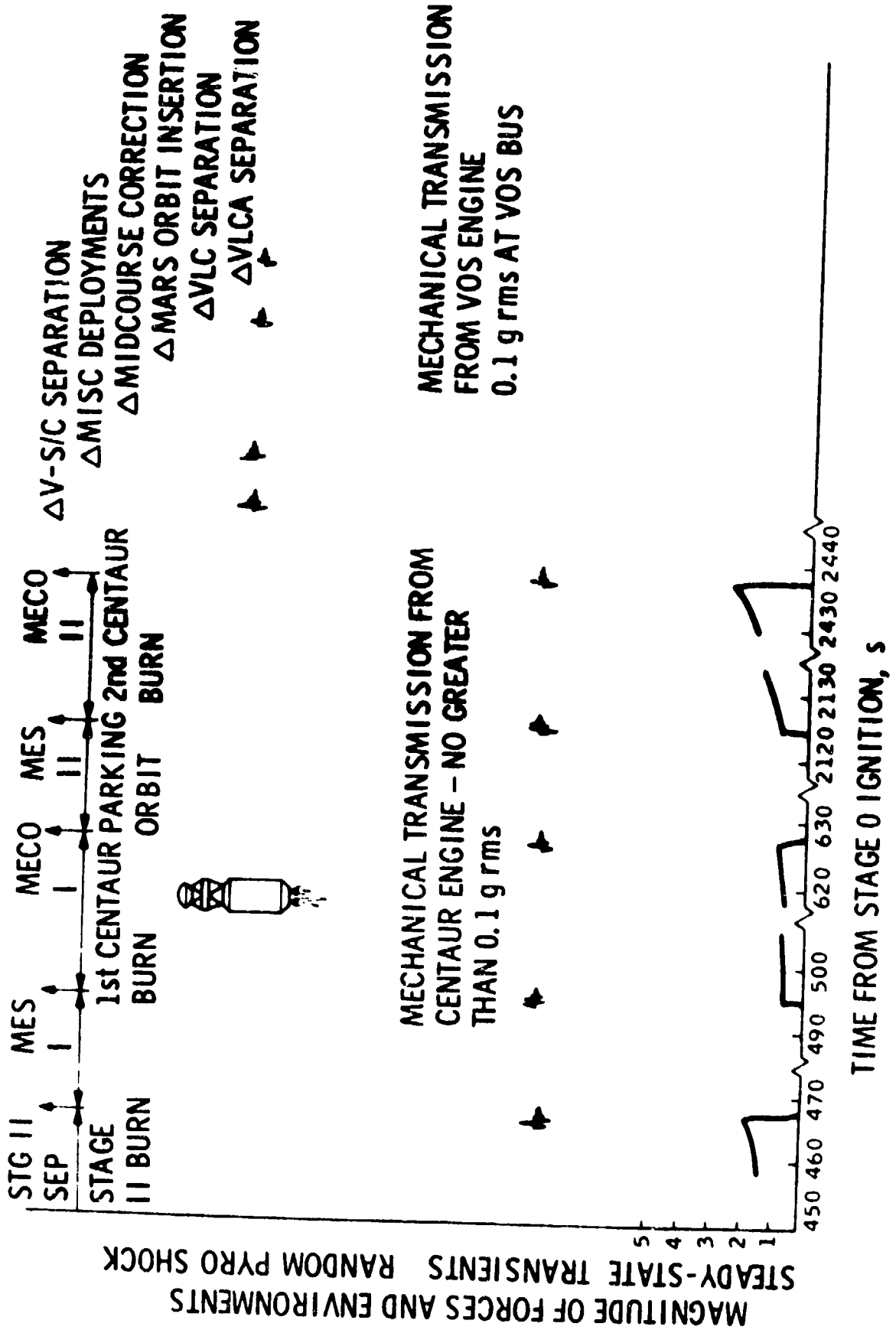


FLIGHT EVENTS

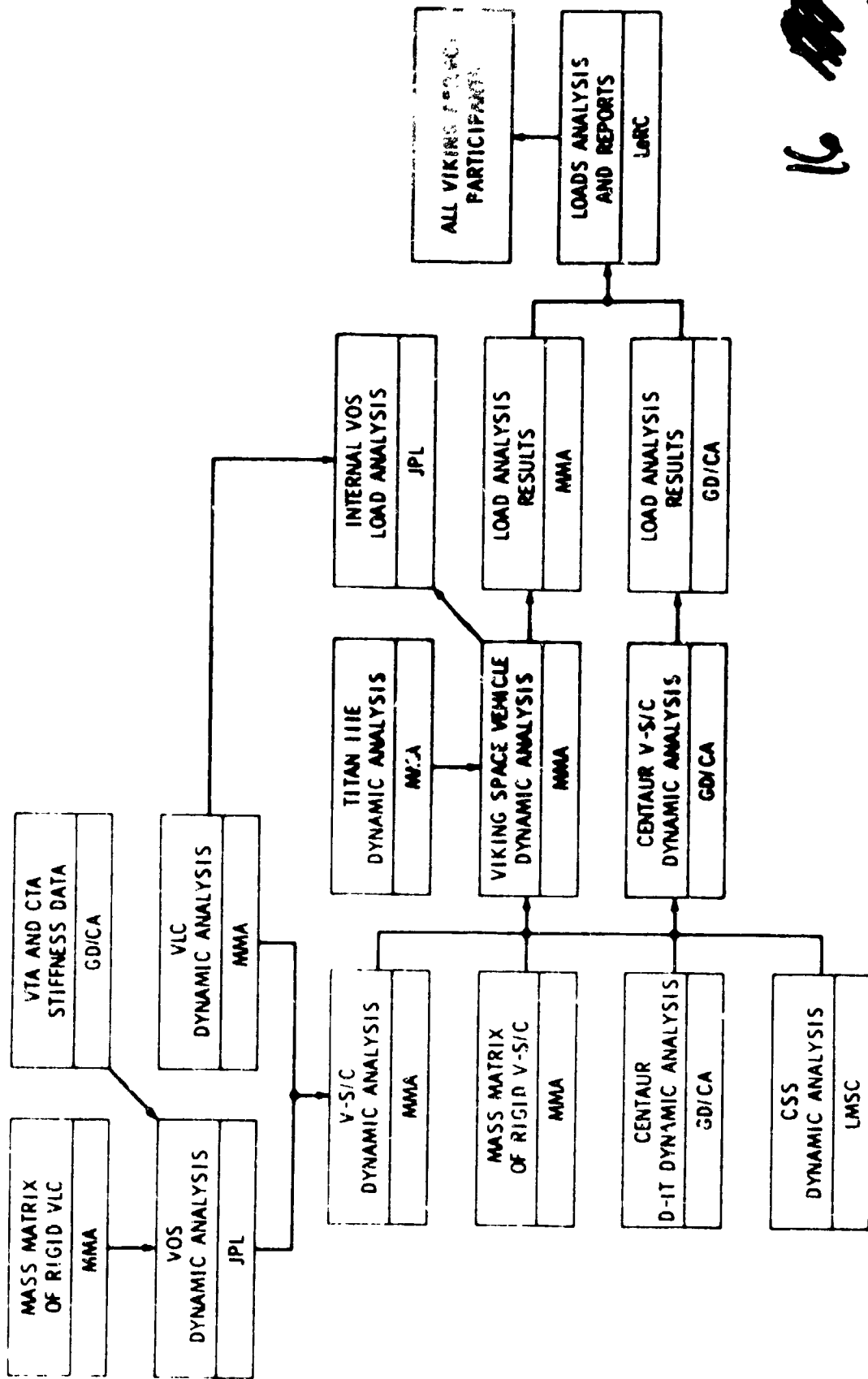


FLIGHT EVENTS, CONTINUED

7



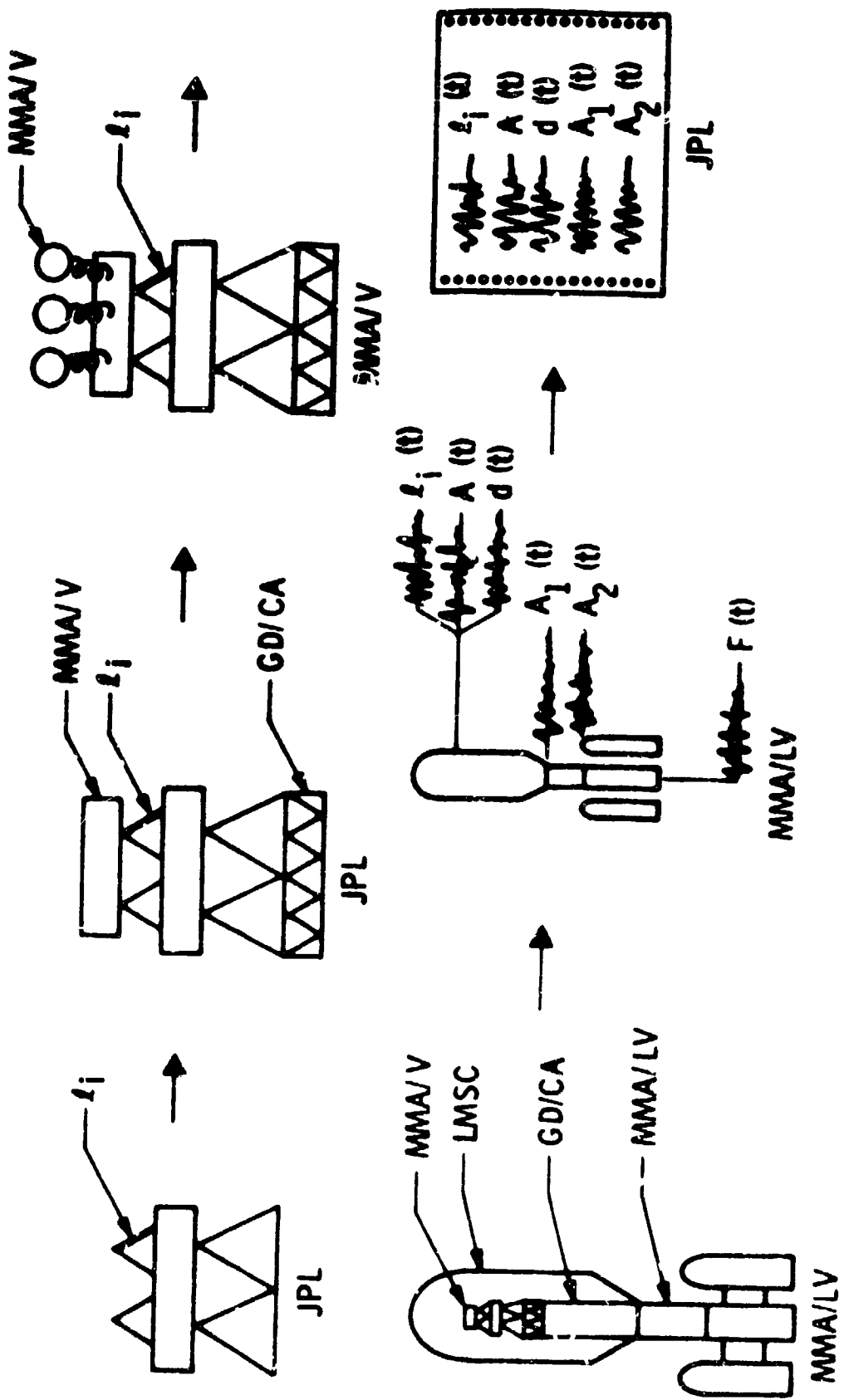
7



16

NOTED: *Guth et al*
 FIG. NO. 6
 LOG NO. 45703
 REDUCE TO *16*

LOAD ANALYSIS PROCESS



15



LOAD ANALYSIS APPROACH

ESTABLISH DESIGN LOADS	VERIFICATION
LOAD ANALYSIS - - - - - • MINI ANALYSIS APPROX. METHOD - - - - - • SHOCK SPECTRUM QUASI-STATIC - - - - - QUALIFICATION TEST - - - - -	- - - - - LOAD ANALYSIS - - - - - LOAD ANALYSIS - - - - - LOAD ANALYSIS - - - - - LOAD ANALYSIS

14
11

FLIGHTS





TITAN/CENTAUR FLIGHTS

- PROOF TEST FLIGHT

VIKING DYNAMIC SIMULATOR -- GENERAL DYNAMICS/CONVAIR

- HELIOS (2)

FEDERAL REPUBLIC OF GERMANY

- VIKING (2)

ORBITER --- JET PROPULSION LABORATORY

LANDER -- MARTIN MARITTA AEROSPACE

PROJECT MANAGEMENT -- LANGLEY RESEARCH CENTER

- VOYAGER (2)

JET PROPULSION LABORATORY



- LOAD ANALYSIS APPROACH
- ANALYSIS FACTOR
 - L.V. MODELS
 - P/L MODELS
 - FORCING FUNCTION
 - TRANSIENT ANALYSIS
 - FLIGHT DATA
 - ANALYSIS VS FLIGHT
 - SENSITIVITY
 - COMMITMENTS, SCHEDULE
 - 1.30
- FLIGHT INSTRUMENTATION
- TEST PHILOSOPHY



CRITICAL FLIGHT EVENTS

- BASED ON PAST EXPERIENCE WITH TITAN AND CENTAUR IN ORDER OF IMPORTANCE
 - STAGE I BURNOUT
 - CENTAUR MAIN ENGINE START AND MAIN ENGINE CUTOFF
 - AIRLOADS
- PRELIMINARY TITAN/CENTAUR ANALYSES IDENTIFIED ADDITIONAL EVENTS AS POTENTIALLY CRITICAL
 - STAGE 0 IGNITION (LAUNCH)
 - STAGE II IGNITION
- ADDITIONAL FORCING FUNCTIONS REQUIRED DUE TO:
 - DIFFERENT LAUNCH VEHICLE CONFIGURATION
 - INTEGRATED ANALYSIS APPROACH

jjd →

15

VIKING DYNAMIC SIMULATOR

- OBJECTIVE TO DYNAMICALLY SIMULATE THE VIKING SPACECRAFT FREQUENCY, MODE SHAPE, EFFECTIVE MASS
- SIMULATOR THOROUGHLY TESTED AND ANALYZED -- LOWLY DAMPED SYSTEM
- INSTRUMENTATION

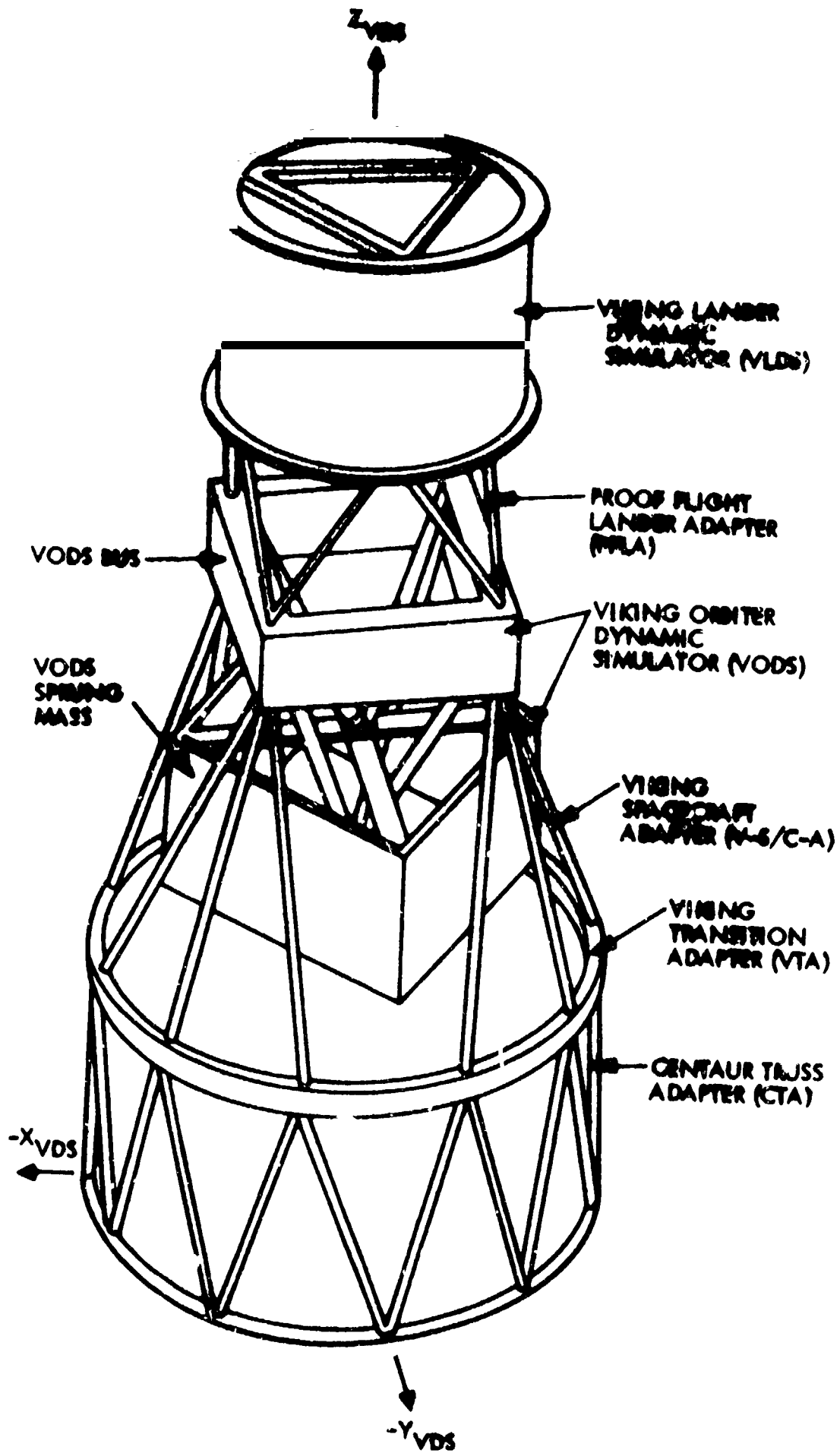
ALL INSTRUMENTATION PHASE CORRELATED STRAIN GAUGES

- 6 DEFINING FORCE ACROSS STATICALLY DETERMINATE INTER-FACE
- 2 CHECKPOINT ON MAJOR STRUCTURAL MEMBERS

ACCELEROMETERS

- 7 LOW FREQUENCY ON MAJOR MASSES 0 - 50 Hz
- 1 HIGH FREQUENCY

MICROPHONE





TEST PHILOSOPHY

- LOADS IN PRIMARY STRUCTURE DURING TESTING NOT TO EXCEED FLIGHT LOADS
- STATIC TEST USED FOR VERIFICATION OF PRIMARY STRUCTURE
- SECONDARY STRUCTURE QUALIFIED BY VIBRATION, PYRO-SHOCK, AND ACOUSTIC TEST



FLIGHT INSTRUMENTATION

- DUAL PURPOSE
DIAGNOSTIC
ENGINEERING DATA
- TRANSDUCERS
 - 6 STRAIN GAUGES ACROSS STATICALLY
DETERMINE INTERFACE
 - 4 CRYSTAL ACCELEROMETERS
- STRAIN GAUGED STRUTS CALIBRATED -- DIRECT LOAD MEASUREMENT
- PHASE CORRELATION ON ALL CHANNELS
- DATA REDUCTION TO AID IN CONSENT TO LAUNCH SECOND SPACECRAFT
- LOADS ESTIMATION BY INVERSE SOLUTION IN FREQUENCY DOMAIN

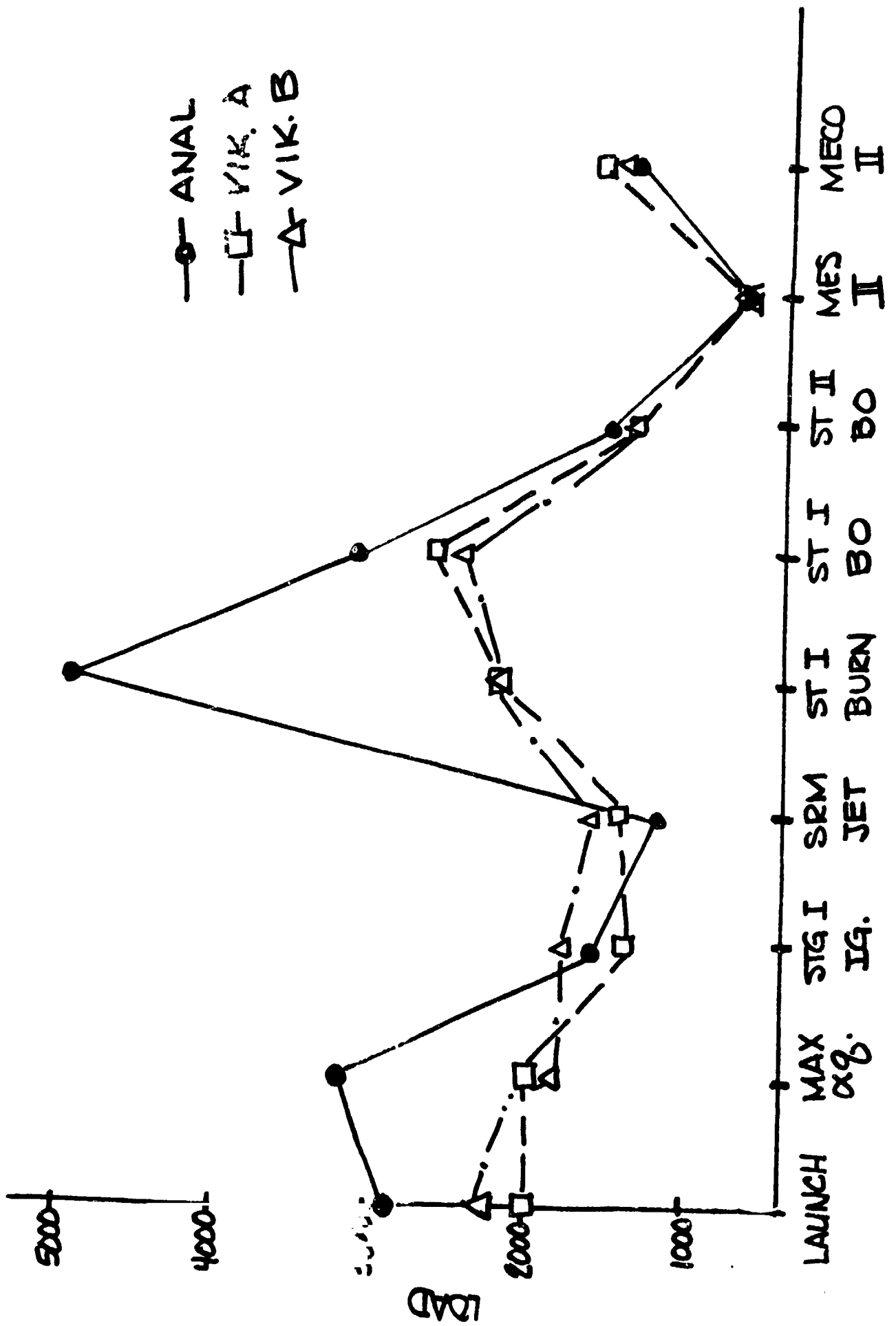
VIKING LOADS.

EVENT	1970	1971	1972	1973	1974
PROGRAM START ▲					
VIKING LOADS CYCLE ▲	▲	▲	▲	▲	
JPL IN-HOUSE LOADS ▲	▲	▲ ▲	▲ ▲		
SUBSTRUCTURE TESTS				■	
SYSTEM MODAL TEST				■	
FLIGHT LOADS FOR QUAL.					▲
STATIC QUAL.					▲

61

VIKING -- ANALYSIS VS FLIGHT

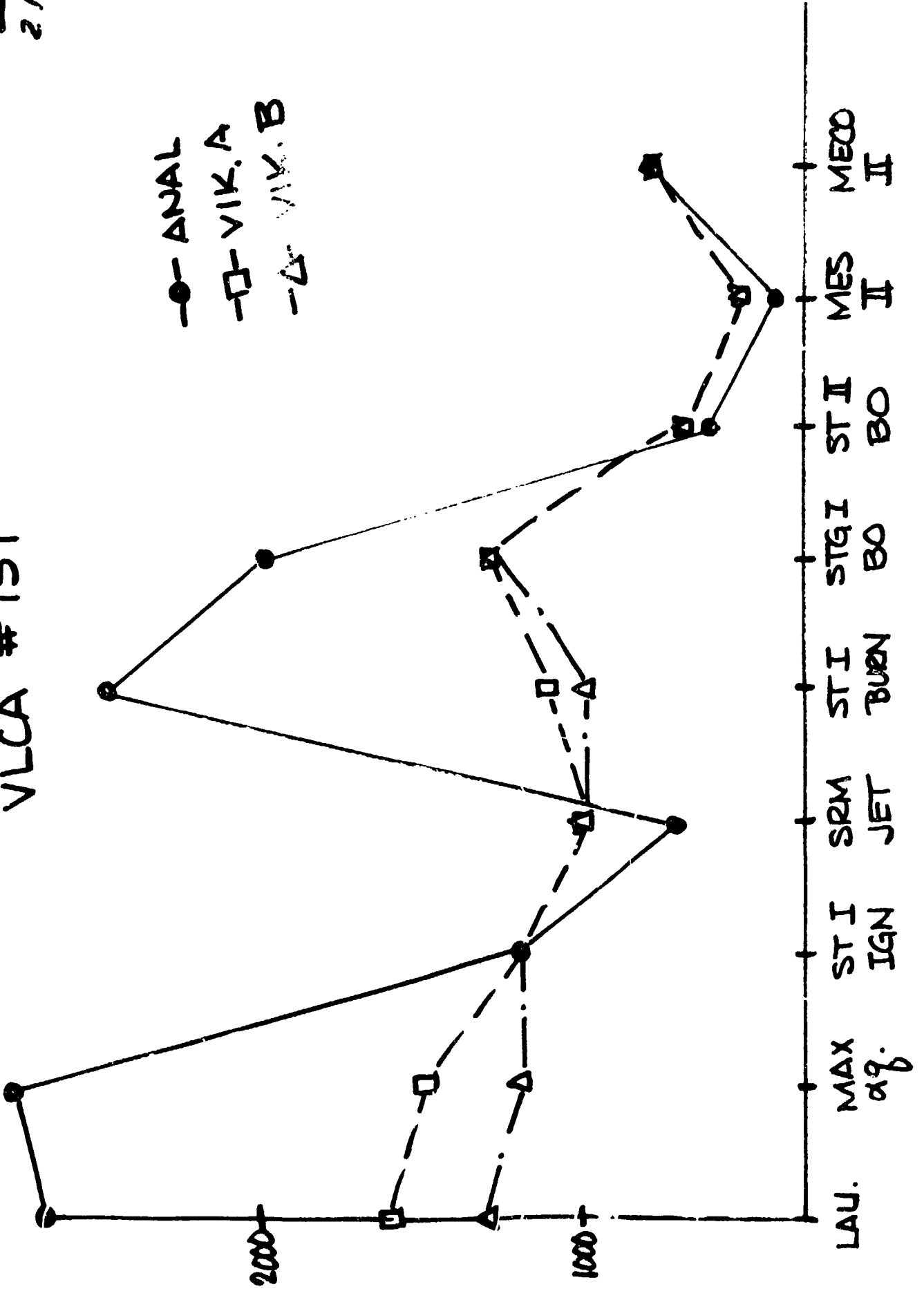
VLCA - # 750



21

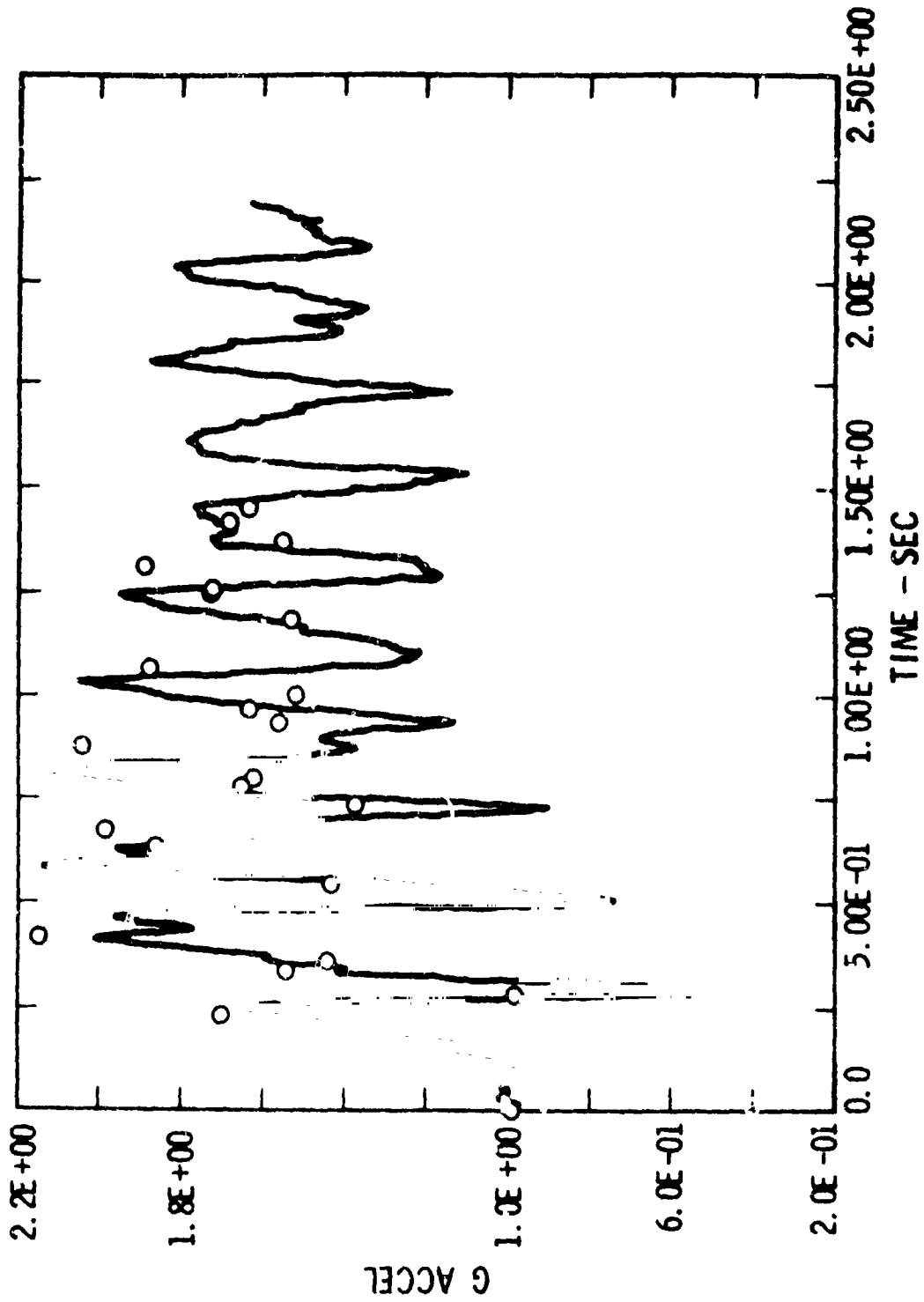
VLCA #751

● ANAL
 □ VIK. A
 △ VIK. B



TC-3 LANDER Z CG ACCEL - CASE 21 (X1.0)

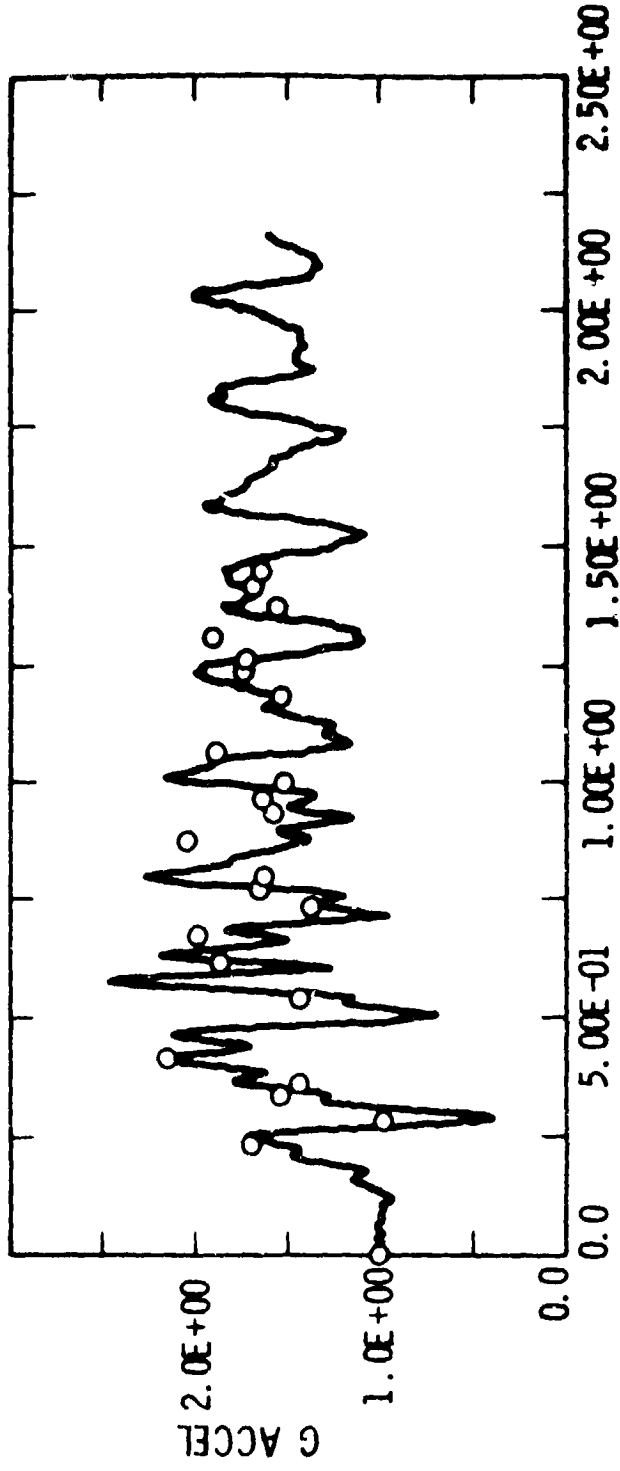
22



LINE PLOT - TEST DATA

POINT PLOT - ANALYTICAL DATA

IC-4 LANDER Z CG ACCEL -- CASE 21 (X1.0)

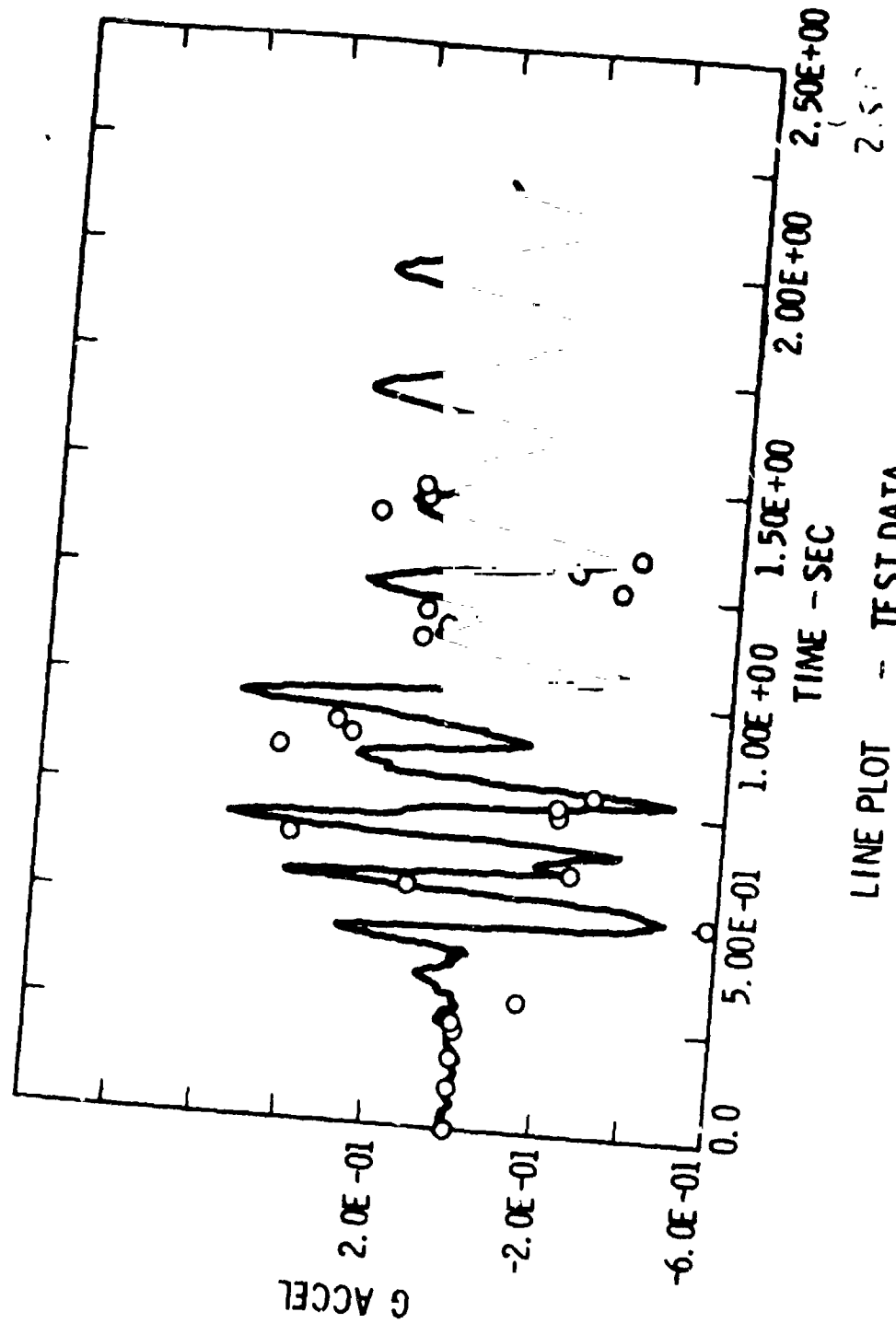


TIME - SEC

LINE PLOT - TEST DATA

POINT PLOT - ANALYTICAL DATA

TC-3 LANDER Y CG ACCEL -- CASE 21 (X1.25)



LINE PLOT -- TEST DATA
 POINT PLOT -- ANALYTICAL DATA



THE INVERSE SOLUTION PROBLEM

- THEORY
- SAMPLE SOLUTION
- RESPONSE
- CONCLUSION

$j\omega$ →

THEORY (CONT)

- $a_A(t) \rightarrow a_A(\omega)$
- $a_B(\omega) = H^{-1}(\omega) a_A(\omega)$
- $a_B(\omega) \rightarrow a_B(t)$
- $m\ddot{q} + c\dot{q} + kq = a_B(t)$

$$a = [\varphi] \ddot{q}$$

$$f = [s] q$$

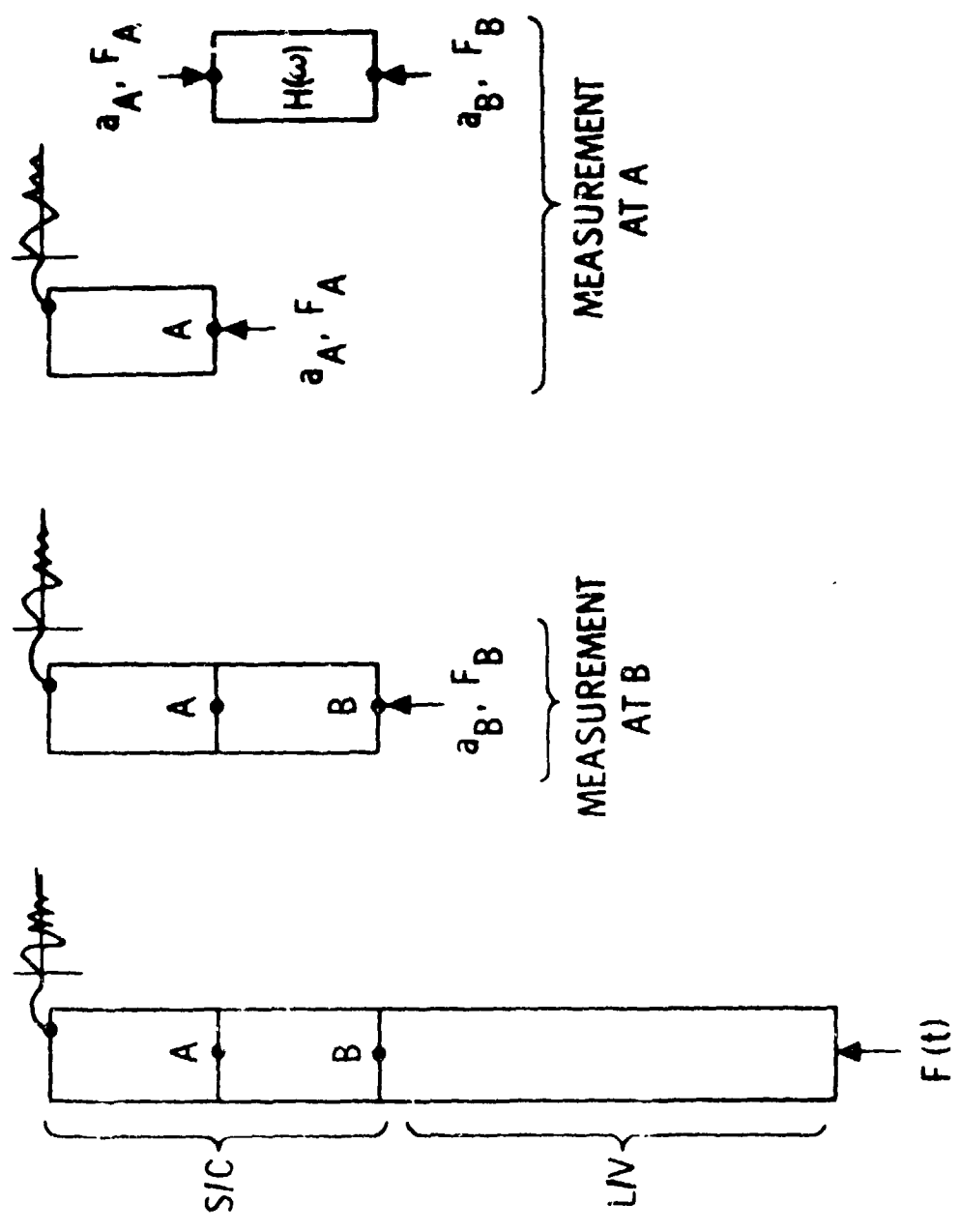


2.3

38

$j\omega$ →

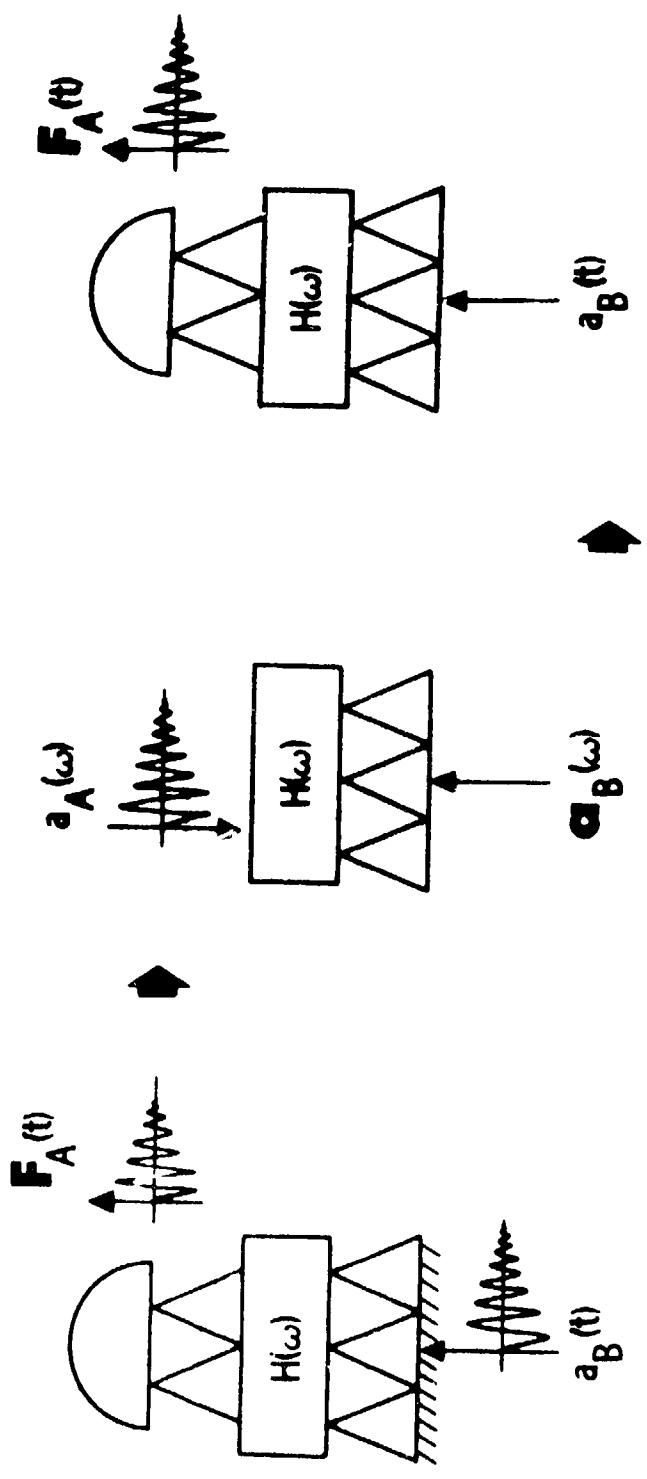
THEORY



13
33



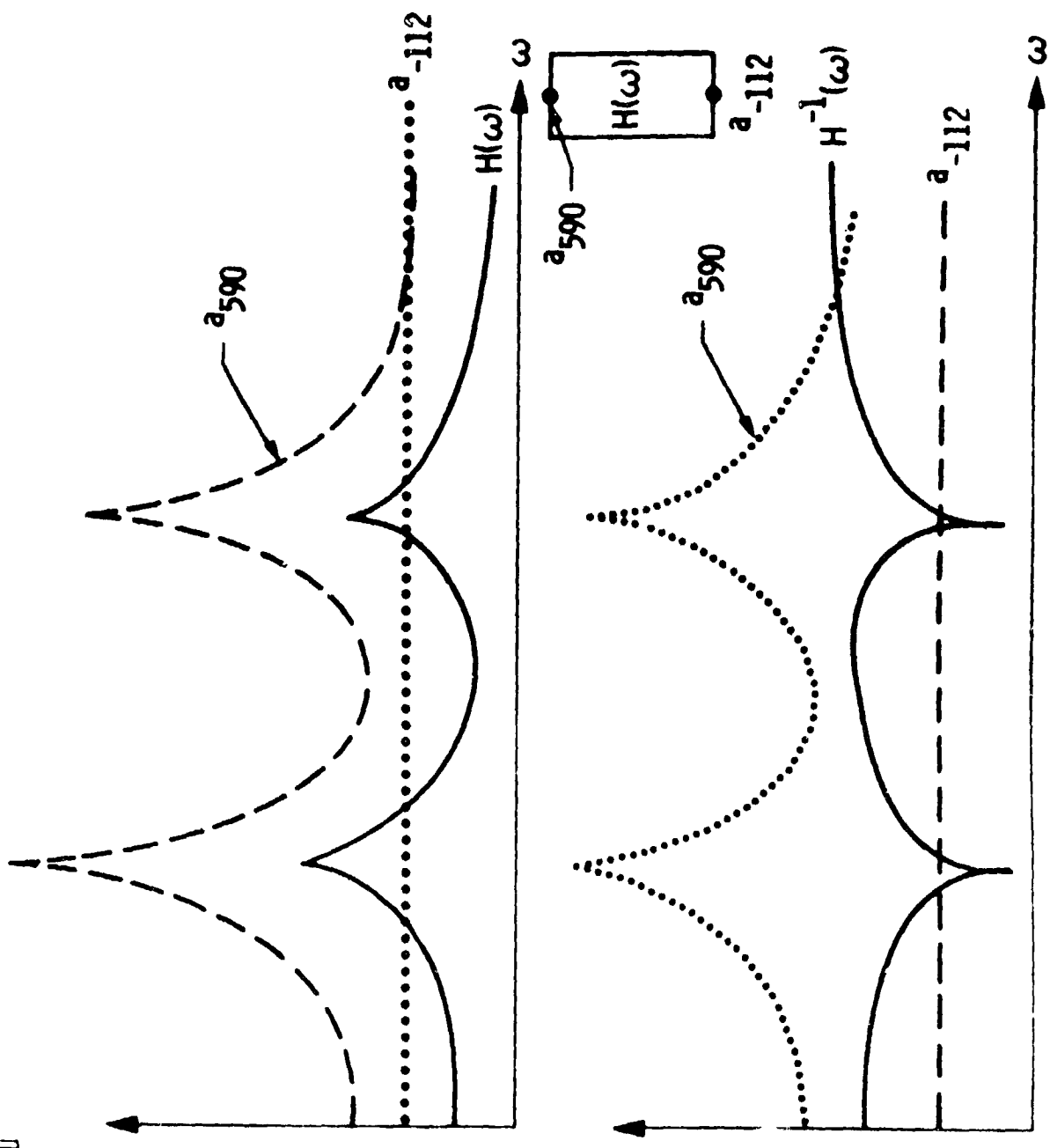
SAMPLE SOLUTION



- MODAL TEST VER MATH MODEL
- FLIGHT TYPE DATA

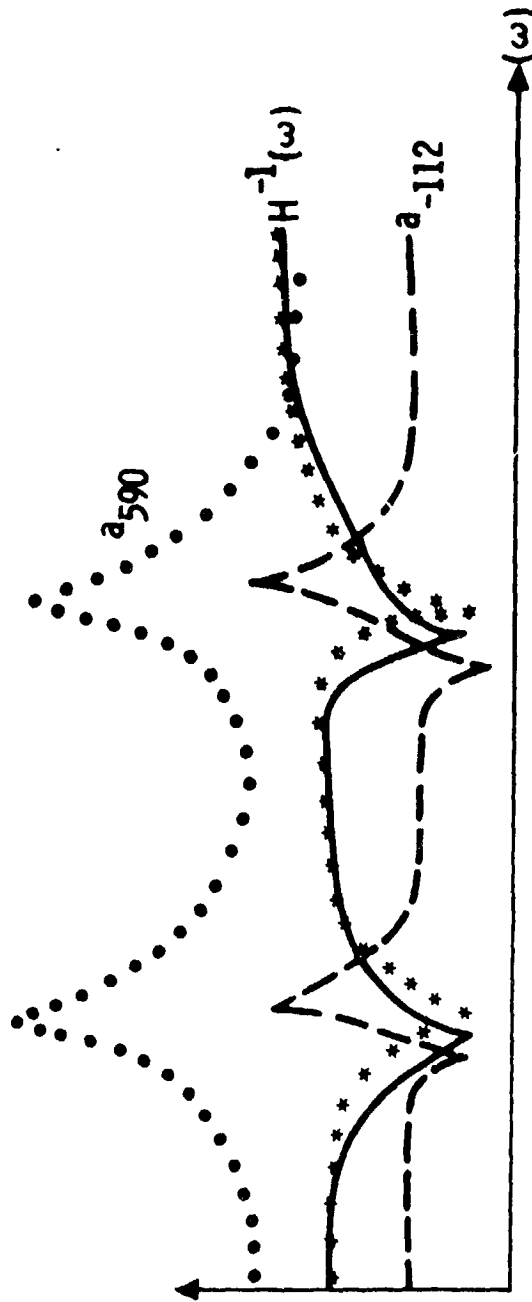
j ω

RESPONSE





RESPONSE -- FREQUENCY MISMATCH



- MATCH ω OF $H^{-1}(\omega)$
- MATCH ω OF a_{590}

34
35

42

— jpl —→

CONCLUSION

- INCORRECT RESULTS
- SENSITIVE ω
- FORWARD SOLUTION - REASONABLE
- STRAIN GAGE
 - LIMITS
 - GOOD DATA

42



HELICS

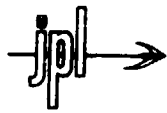
- QUASI STATIC APPROACH
- FLIGHT INSTRUMENTATION --- BASE
(1 AXIAL, 2 LATERAL)



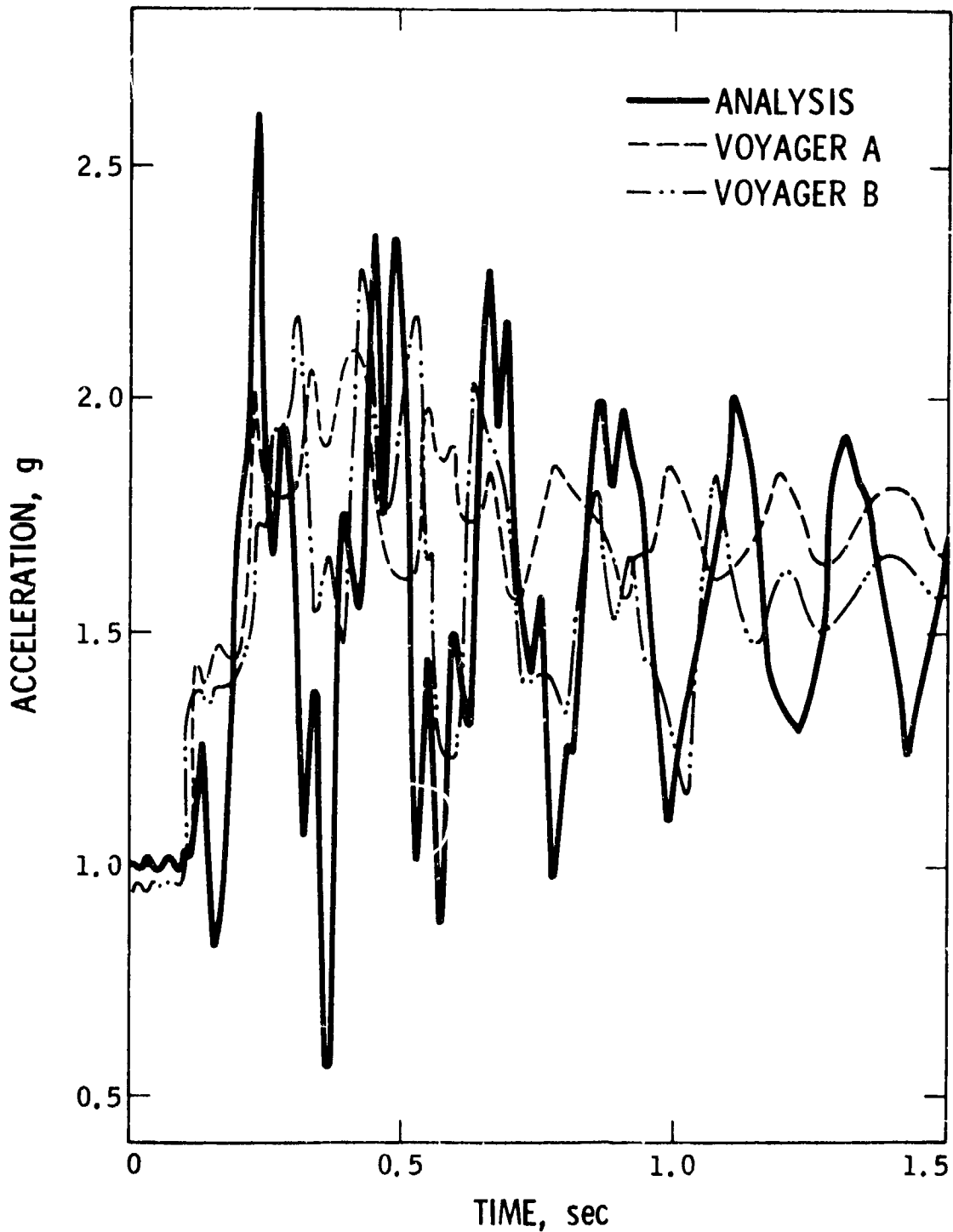
52

VOYAGER

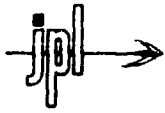
- SHOCK SPECTRA
- DEPENDENT ON PAST FLIGHT & ANALYSIS
- FLIGHT INSTRUMENT -- BASE
- MODERATELY CONSERVATIVE LOADS --
COST AND SCHEDULE SAVINGS



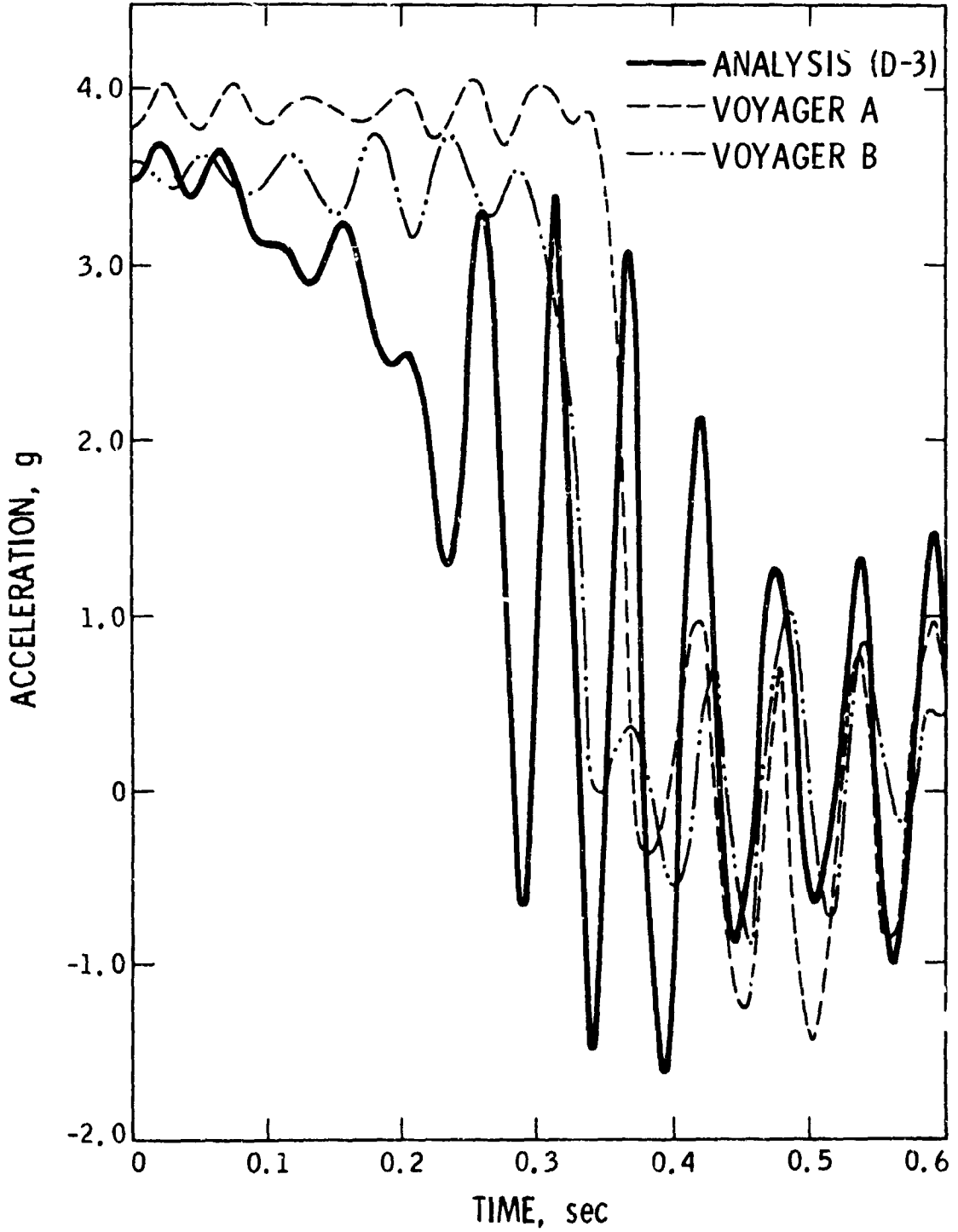
INTERFACE ACCELERATIONS FOR LAUNCH

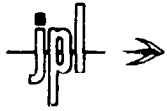


27

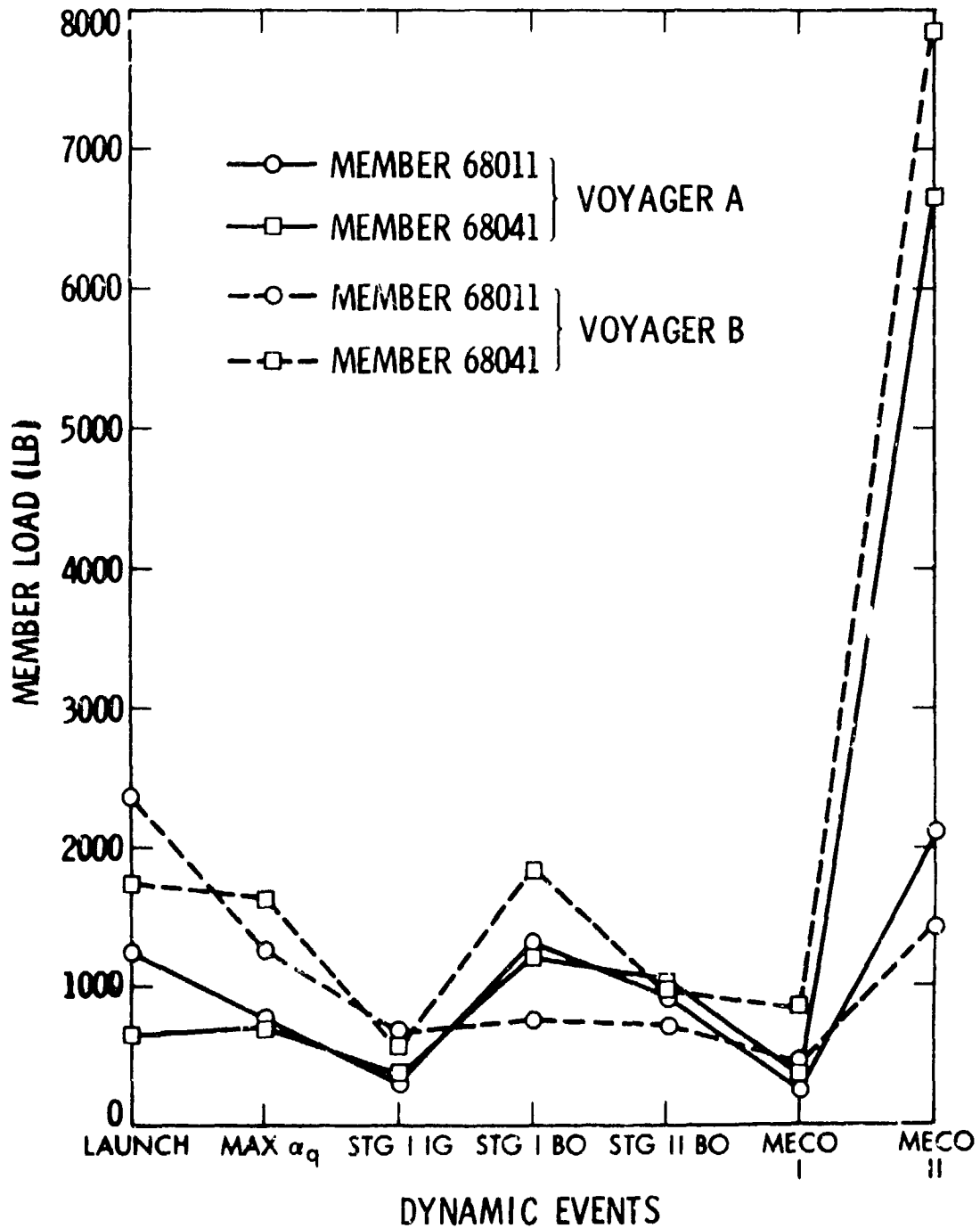


INTERFACE ACCELERATIONS FOR STAGE I BURN OUT





MAXIMUM MEMBER LOAD FOR VARIOUS EVENTS



6.2

SUMMARY



SPACECRAFT LOADS EXPERIENCE SUMMARY

<u>EVENT</u>	<u>EFFECT</u>	<u>CORRECTIVE ACTION</u>
PRELIMINARY LOADS ANALYSIS	CENTAUR SKIRT OVERSTRESSED	INCORPORATE FORWARD BEARING REACTION (FBR) STRUT
INTERMEDIATE LOADS ANALYSIS WITH SEVERAL SPACECRAFT MODELS	(1) MEMBER LOADS SENSITIVE TO MODEL CHANGES	(1) USE LOADS ANALYSIS FACTOR OF 1.3 ON ALL SUBSEQUENT DATA. INITIATE SEARCH FOR METHOD NOT SENSITIVE TO MODEL CHANGES.
	(2) ANALYSIS DEFICIENT IN PREDICTING STAGE I BURNOUT/STAGE II IGNITION LOADS	(2) CONSERVATIVELY ESTIMATE MEMBER LOADS BY ADDITIONAL ANALYTICAL MEANS
VIKING DYNAMIC SIMULATOR PRE-FLIGHT ANALYSES	(1) LAUNCH VEHICLE STABILITY MARGINAL	(1) ACCERT ANALYSIS AS CONSERVATIVE AND FLY
	(2) MAX _q LOADS HIGHER THAN ORIGINALLY PREDICTED MAY BE DESIGN CONDITION	(2) CHECK VIKING SPACECRAFT LOADS FOR MAX _q INITIATE MAJOR ANALYSIS EFFORT FOR VIKING



SPACECRAFT LOADS EXPERIENCE SUMMARY, CONTINUED

<u>EVENT</u>	<u>EFFECT</u>	<u>CORRECTIVE ACTION</u>
VIKING DYNAMIC SIMULATOR FLIGHT DATA EVALUATION	(1) LAUNCH VEHICLE MARGIN- ALLY STABLE -- POGO	(1) MAJOR ANALYTICAL EFFORT TO REEVALUATE STABILITY ANALYSIS INCORPORATE SUPERHEATER ON FUEL LINES
	(2) LAUNCH (STAGED IGNITION) LOADS MUCH HIGHER THAN PREDICTED -- 30 LAUNCH BASED ON ANALYSIS	(2) REEVALUATE LAUNCH EVENT FORCING FUNCTION. INITIATE MAJOR ANALYSIS EFFORT TO FIND DISCREPANCY--HELIOS ANTENNA RETEST
	(3) MEMBER LOADS ARE HIGH	(3) INITIATE DATA REDUCTION PROGRAM TO EVALUATE VIKING LIGHT DATA BEFORE LAUNCHING SECOND SPACECRAFT
	(4) MAX σ_9 LOADS HIGHER THAN PREDICTED. SOME VIKING LOADS HIGHER THAN QUALI- FICATION LOADS	(4) REEVALUATE VIKING ANALYSIS FOR GUST AND BUFFET. RE- TEST SELECTED VIKING MEM- BERS.



SPACECRAFT LOADS EXPERIENCE SUMMARY CONTINUED

<u>EVENT</u>	<u>EFFECT</u>	<u>CORRECTIVE ACTION</u>
HELIOS A FLIGHT DATA EVALUATION	(1) VEHICLE marginally stable effect of superheaters questionable (2) LAUNCH (STAGED IGNITION) LOADS NOT FULLY UNDERSTOOD	(1) INITIATE MAJOR HARDWARE PROGRAM FOR THE INCORPORATION OF TITAN ACCUMULATORS (2) CONTINUE INVESTIGATION INTO LAUNCH FORCING FUNCTION-RECONSTRUCT FORCING FUNCTION
VIKING A FLIGHT DATA EVALUATION	FLIGHT LOADS ACCEPTABLE BUT SYSTEMATIC EVALUATION OF MEMBER LOAD FAILS DUE TO ANALYSIS/FLIGHT DATA MISMATCH. INVERSE SOLUTION IF FREQUENCY DOMAIN FAILS	USE APPROXIMATE METHODS FOR FLIGHT LOAD EVALUATION



SPACECRAFT LOADS EXPERIENCE SUMMARY, CONTINUED

<u>EVENT</u>	<u>EFFECT</u>	<u>CORRECTIVE ACTION</u>
VIKING B FLIGHT DATA EVALUATION	FLIGHT LOADS ACCEPTABLE. STAGE 0 IGNITION LOADS REASONABLE IN LEVEL BUT NOT WELL UNDERSTOOD IN FREQUENCY CONTENT	CONTINUE WORK ON DEFINITION OF LAUNCH FORCING FUNCTION. SYNTHESIZE FORCING FUNCTION FOR VOYAGER USING HELIOS A DATA. USE OBTAINED FLIGHT DATA FOR VOYAGER DESIGN LOADS.
VOYAGER	MECO 11 LOADS LARGER THAN PREDICTED.	

TITAN / CENTAUR LOADS.

EVENT	1974	1975	1976	1977
MAX. α g. ANALYSIS	██████████	██████████	██████████	██████████
POGO / FLMN ANALYSIS	██████████	██████████	██████████	██████████
LAUNCH F.F. SYNTHESIS	██████████	██████████	██████████	██████████
DEVELOP S.S. / IMPEDANCE	██████████	██████████	██████████	██████████
LAUNCHES	▲ DS ▲ HEL. A. ▲ VIK	▲ HEL. A. ▲ VIK	▲ HEL. B	▲ VOY.
FLIGHT DATA ANALYSES	██████████	██████████	██████████	██████████



31

COMPARISON OF ANALYTICAL PREDICTIONS TO FLIGHT DATA

- VIKING

MEASURED LOADS DIRECTLY FROM FLIGHT STRAIN GAUGES

- VOYAGER

RECONSTRUCTED INTERFACE ACCELERATIONS FROM FLIGHT ACCELEROMETERS



USE OF TITAN/CENTAUR FLIGHT DATA

- DEVELOPED SHOCK SPECTRA/IMPEDANCE METHOD FOR OBTAINING MODERATELY CONSERVATIVE SPACECRAFT DESIGN DATA
 - REQUIRES INTERFACE ACCELERATION DATA FROM ANALYSIS AND FLIGHT
- UNCOVERED ANALYSIS DEFICIENCIES
 - SYNTHESIZED FORCING FUNCTIONS
- INCREASED RELIABILITY OF LOADS ANALYSIS FOR FUTURE FLIGHTS
- REDUCED COST OF LOADS ANALYSIS PROCESS
- HELP AVOID POTENTIAL PROBLEMS



LOAD ANALYSIS PROCEDURE

- REQUIRES CONTINUAL CORRELATION OF MATH MODEL → FLIGHT DATA
- AS P/L DYNAMICS CHANGE LESS SIG. CHARACTERISTIC → MORE DOMINANT
- DEPENDENT ON:
 - * L/V MODEL (?)
 - * FORCING FUNCTION (?)
 - * SIGNIFICANT EVENTS (?)
 - * ESTABLISH BOUNDS (?)
 - * ACCURACY S/C MODEL (?)
- EXPENSIVE, SCHEDULE, ERRORS
 - * APPROXIMATE METHODS



CONCLUSIONS

- FLIGHT DATA PROVED INVALUABLE FOR
 - UNDERSTANDING PHYSICAL PHENOMENA OF FORCING FUNCTIONS, MODEL, DYNAMICS
 - DIAGNOSTIC TOOL
 - COST EFFECTIVENESS FOR FUTURE LOADS
- PREDICTION AND DEVELOPMENT OF ANALYTICAL TOOLS
- LOAD ANALYSIS
 - UPDATE LOAD ANALYSIS PROCEDURE (MATH VS. FLIGHT)
 - APPROXIMATE METHODS REQUIRED
- INSURANCE



RECOMMENDATIONS

- INSTRUMENT LAUNCH VEHICLE TO OBTAIN IMPEDANCE AND FORCING FUNCTION MEASUREMENTS FOR DATA EXTRAPOLATION FOR FUTURE FLIGHTS
- PROPERLY INSTRUMENTED LAUNCH VEHICLES CAN BE USED TO ESTIMATE THE FOLLOWING:
 - LAUNCH VEHICLE DAMPING
 - EXCITATIONS
 - MODAL PARAMETERS
 - UPPER BOUNDS OF RESPONSES FOR FUTURE FLIGHTS

PRECEDING PAGE BLANK NOT FILMED



PAM DYNAMIC LOADS ANALYSIS
MODEL INTERFACES AND LOAD CYCLE PROCESS

M. MARKOWITZ
MCDONNELL DOUGLAS AERONAUTICS CO.
HUNTINGTON BEACH, CALIFORNIA



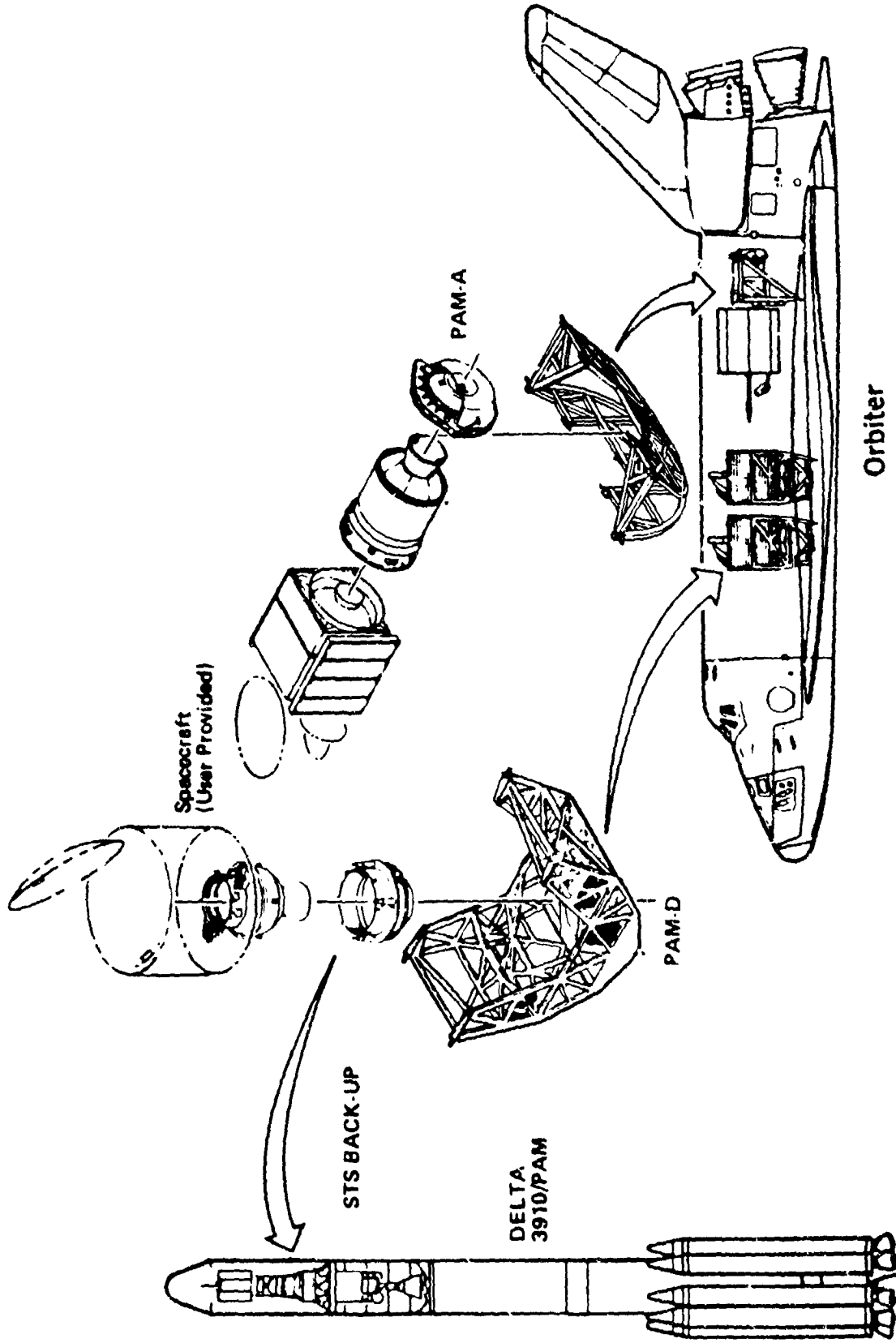
MDAC PAYLOAD ASSIST MODULE (PAM) PROGRAMS

MDAC offers to the spacecraft community Payload Assist Module (PAM) programs which provide launch capability for both Delta weight class (PAM-D) and Atlas weight class (PAM-A) payloads. The PAM concept was formulated by MDAC to meet the needs of the satellite system users for increased launch vehicle performance and to provide a system, for the PAM-D class of payloads, that can be used with either the NASA STS Orbiter or the Delta Expendable Launch Vehicle as an ascent vehicle.

The PAM systems provide the necessary injection velocities to place their respective payloads (spacecraft) into their required orbits above the low altitude parking orbit attainable from the STS Orbiter. The PAM system includes the vehicle expendable hardware consisting of spinning solid rocket motor (SSRM) and the payload attach fitting (PAF). The reusable Airborne Support Equipment (ASE) includes the cradle for structurally mounting the PAM and spacecraft in the Orbiter, the spin system, and all functional power, control, and monitoring subsystems required to interface with the Orbiter.



MDAC PAYLOAD ASSIST MODULE (PAM) PROGRAMS





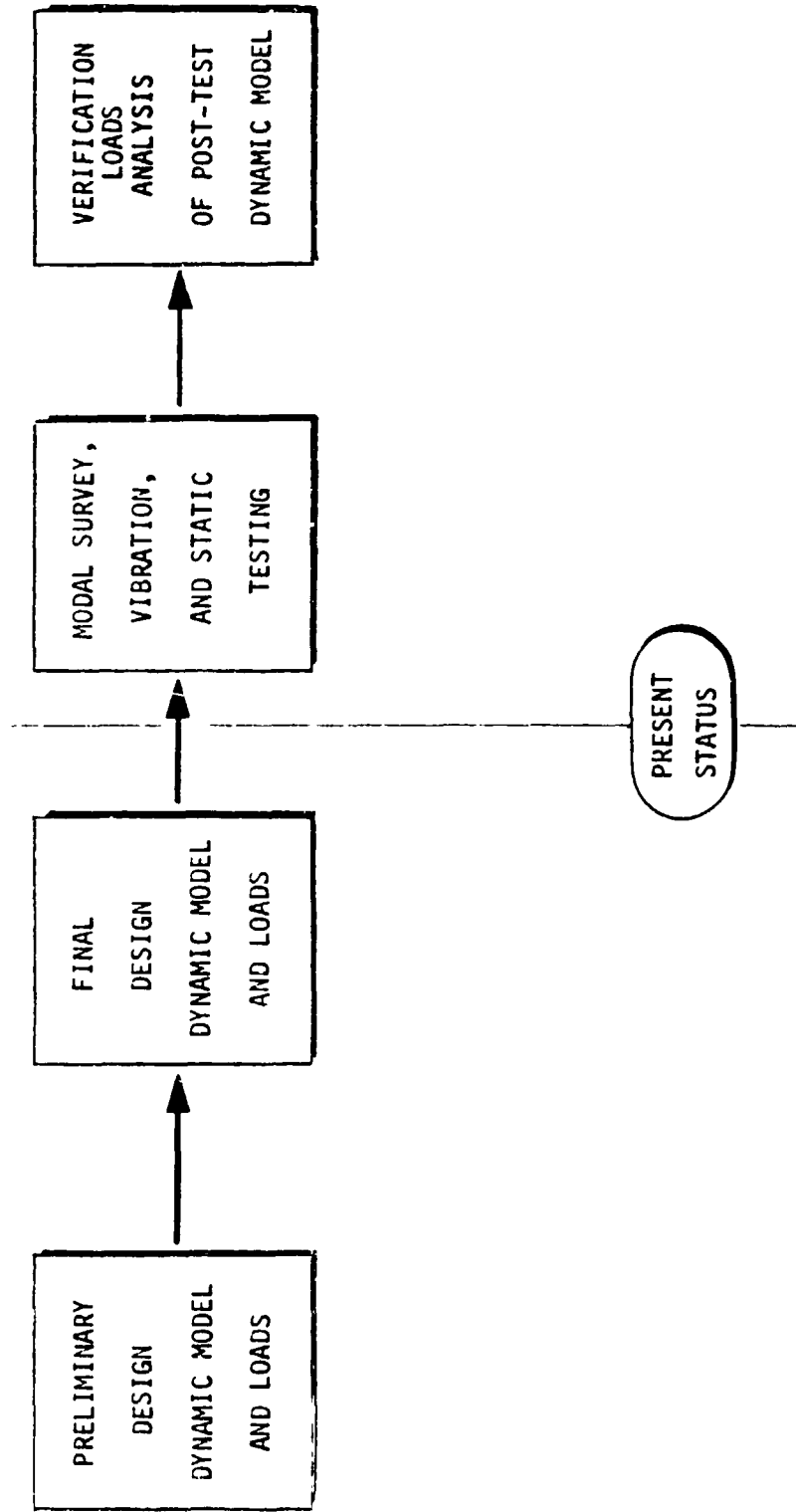
PAM DYNAMIC MODEL AND LOADS VERIFICATION PROCESS

The MDAC verification process to validate design of the PAM system employs the same philosophy used for spacecraft design. Preliminary loads and models are used for initial design effort which, after a period of refined design and analysis effort, results in the final system design. PAM systems were designed to not only satisfy the critical NASA interface requirements, but also incorporate frequency response characteristics which minimize Orbiter induced loading on spacecraft.

Modal, vibration, and static testing of the PAM system will be performed in the near future to verify that the dynamic model reflects the true structural dynamic response characteristics. Using the post-test dynamic model, MDAC will perform a verification loads analysis to validate the integrity of the established spacecraft and Orbiter interface dynamic environments.



PAM DYNAMIC MODEL AND LOADS VERIFICATION PROCESS





STS PAM DYNAMIC LOADS ANALYSIS CYCLE

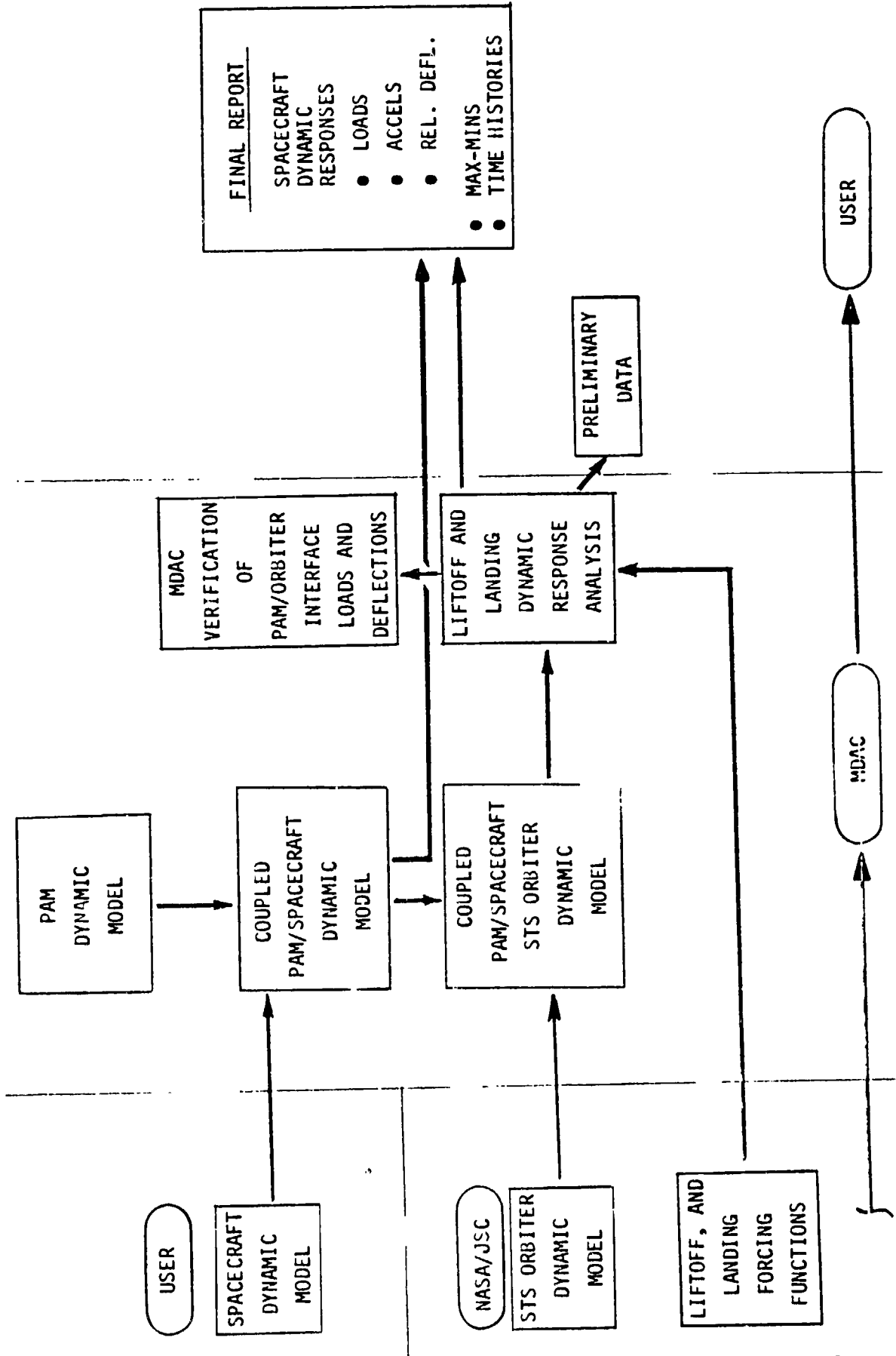
Spacecraft structural dynamic models are provided by the spacecraft manufacturer (user) to MDAC in one of three acceptable formats: (1) discrete mass and stiffness matrices, (2) constrained modal mass, stiffness, and load, acceleration, and deflection transformation matrices, and (3) NASTRAN bulk data decks.

Two dynamic load cycles are performed to calculate maximum expected dynamic responses of spacecraft structure for the STS Orbiter liftoff and abort landing conditions. The first load cycle is performed to provide dynamic loads used in final spacecraft design evaluation. The second load cycle is performed to verify prior to Orbiter launch that, after the spacecraft model has been modified to agree with modal and vibration testing results, the spacecraft structure dynamic responses still satisfy all spacecraft, PAM, and STS Orbiter design requirements.

Each load cycle involves MDAC coupling the spacecraft model to the appropriate PAM system dynamic model and then coupling this payload assembly to the cargo bay interfaces of the STS Orbiter vehicle model, supplied by NASA/JSC. Coupled payload/Orbiter transient response analyses are performed using sixteen liftoff and five landing forcing functions also supplied by NASA/JSC.

Preliminary transmittal of response data are made available to the PAM user after completion of all liftoff and landing dynamic analyses. Time histories of spacecraft generalized coordinate accelerations and deflections are provided to the user in computer tape format. In addition to the final report documenting the complete analysis, MDAC also provides the user with the spacecraft/PAM system coupled dynamic model. This model is required by NASA/JSC of all STS users for a special NASA verification analysis performed prior to launch for all payloads constituting the STS launch mission specific cargo bay manifest.

STS PAM DYNAMIC LOADS ANALYSIS CYCLE





PAM-D DYNAMIC MODEL SCHEMATIC

The PAM-D system structural dynamic model was generated using NASTRAN finite-element modeling and MDAC computer codes SA48 and SA49 to assemble various substructure assemblies via constrained normal mode coupling techniques.

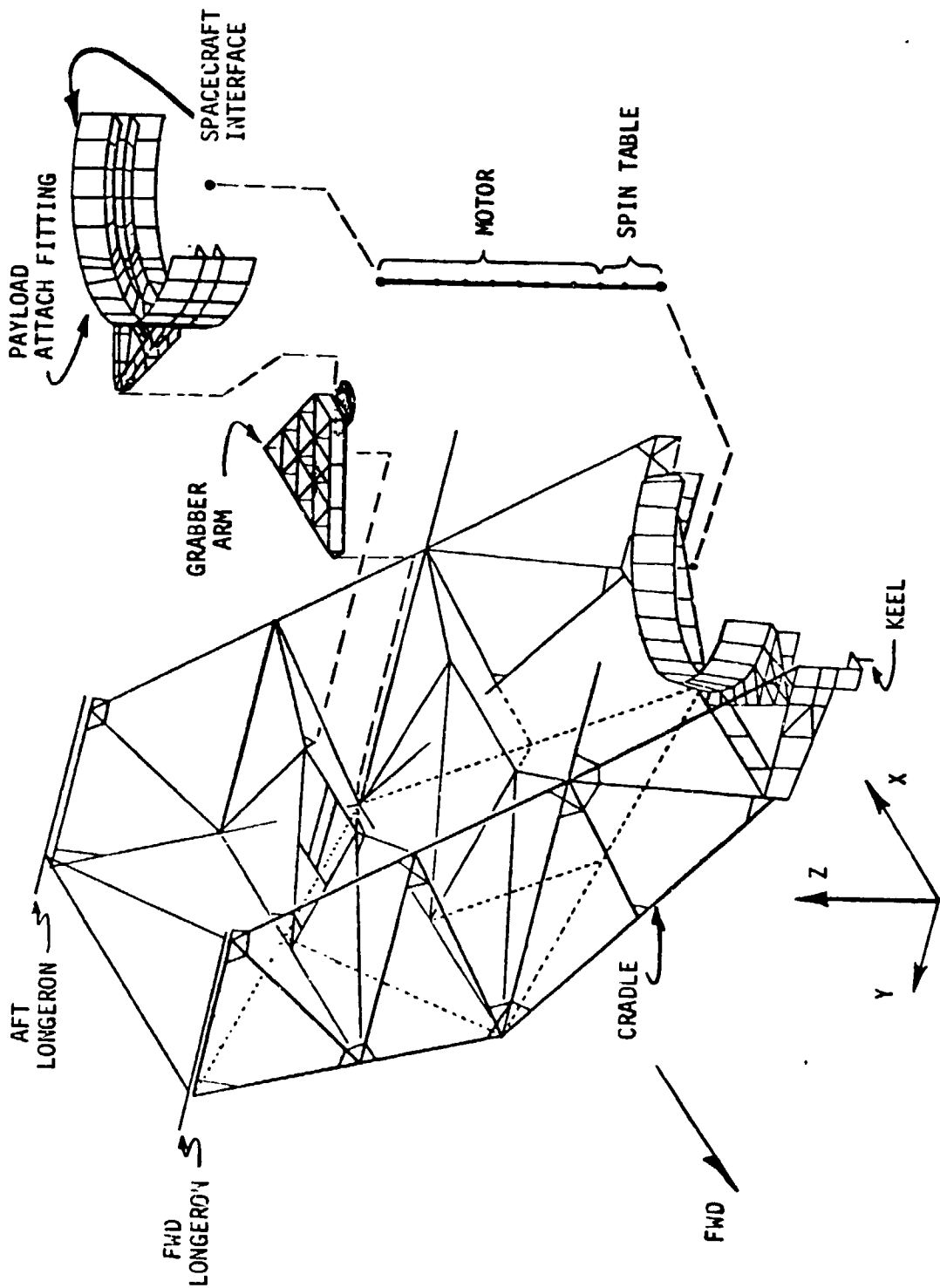
Half-models about the X-Z plane were constructed for the symmetric cradle and payload attach fitting structural assemblies. Full models of these two assemblies and of the two grabber arms were generated using the technique of image modeling, defining the X-Z plane as the "mirror": $X=X, Y=-Y, Z=Z, \theta_x = -\theta_x, \theta_y = \theta_y, \theta_z = -\theta_z$.

The PAM structure is designed so as to possess stiffness characteristics that will allow its fundamental frequencies to avoid adverse coupling with STS Orbiter vehicle high gain modes. The use of substructure modeling for PAM allowed MDAC, during the design process, ease in modifying structural component design to obtain desired stiffness characteristics.

The keel and four longeron fittings which define the structural interfaces with the Orbiter bay are maintained in the model as discrete degrees of freedom. Similarly, the forward end of the payload attach fitting is maintained as discrete degrees of freedom for coupling to the spacecraft structural model.



PAM-D DYNAMIC MODEL SCHEMATIC





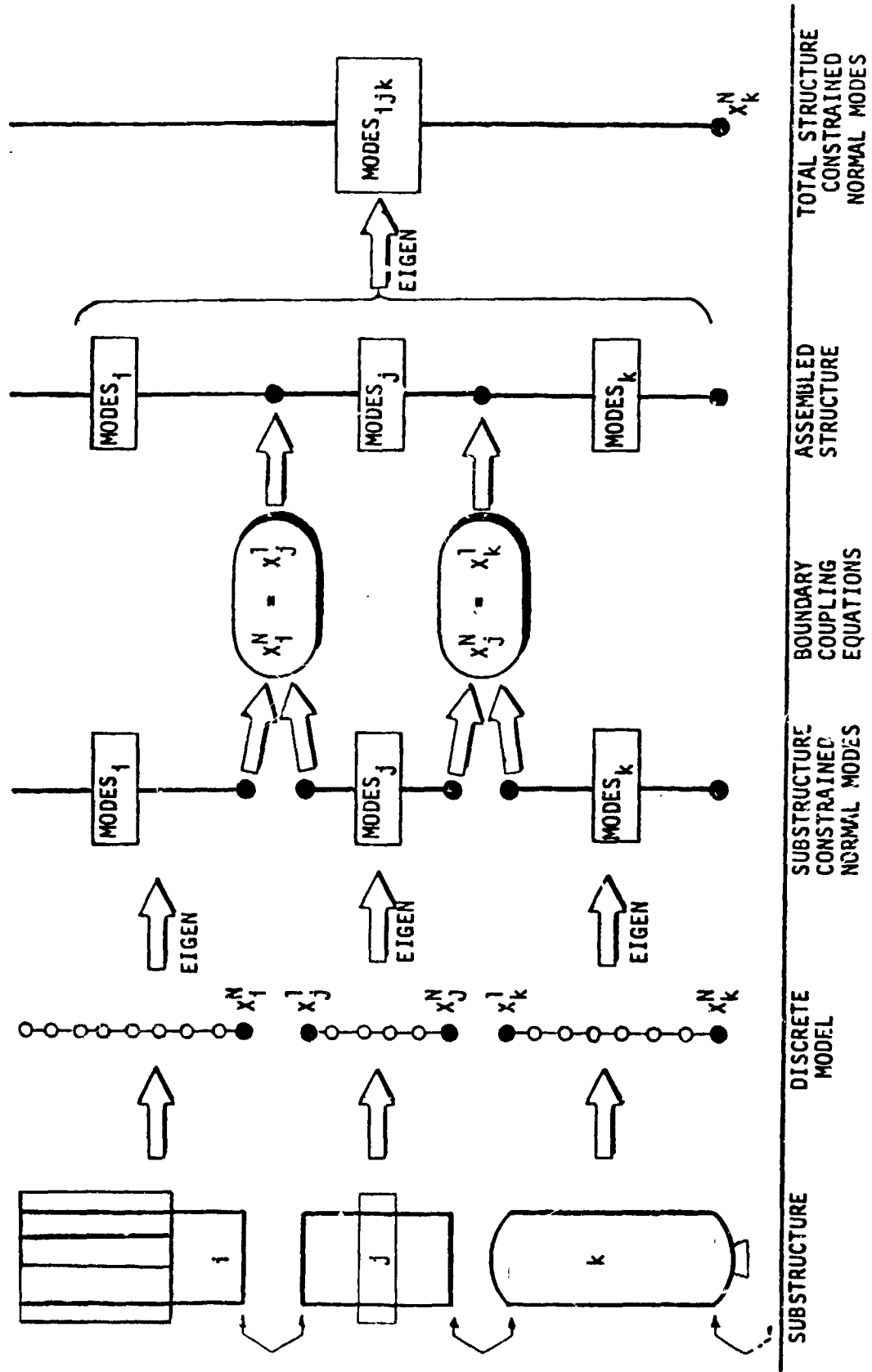
PAM SYSTEM SUBSTRUCTURE MODELING AND ASSEMBLY TECHNIQUE

The PAM system structural dynamic model is generated from an assemblage of substructure models using Hurty's method of component mode synthesis and the method of image modeling. Discrete models of the various substructures are generated. Fixed constraint normal modes and constraint shapes are calculated as are any necessary internal load and displacement transformations. Boundary coupling equations are used to assemble the various models at their discrete degree of freedom interfaces. These common internal interfaces are included with the i, j and k modal coordinates as the new set of generalized coordinates. Generally, an additional solution of this set of equations is used to calculate a reduced number of generalized coordinates which can be back-transformed to recover discrete internal loads and displacements.

The method of component mode synthesis is used in conjunction with the method of image modeling in the development of the PAM model because they provide a rationale for reducing the total number of equations to be solved while, at the same time, maintaining a high degree of fidelity in the desired frequency range of interest.



PAM SYSTEM SUBSTRUCTURE MODELING AND ASSEMBLY TECHNIQUE





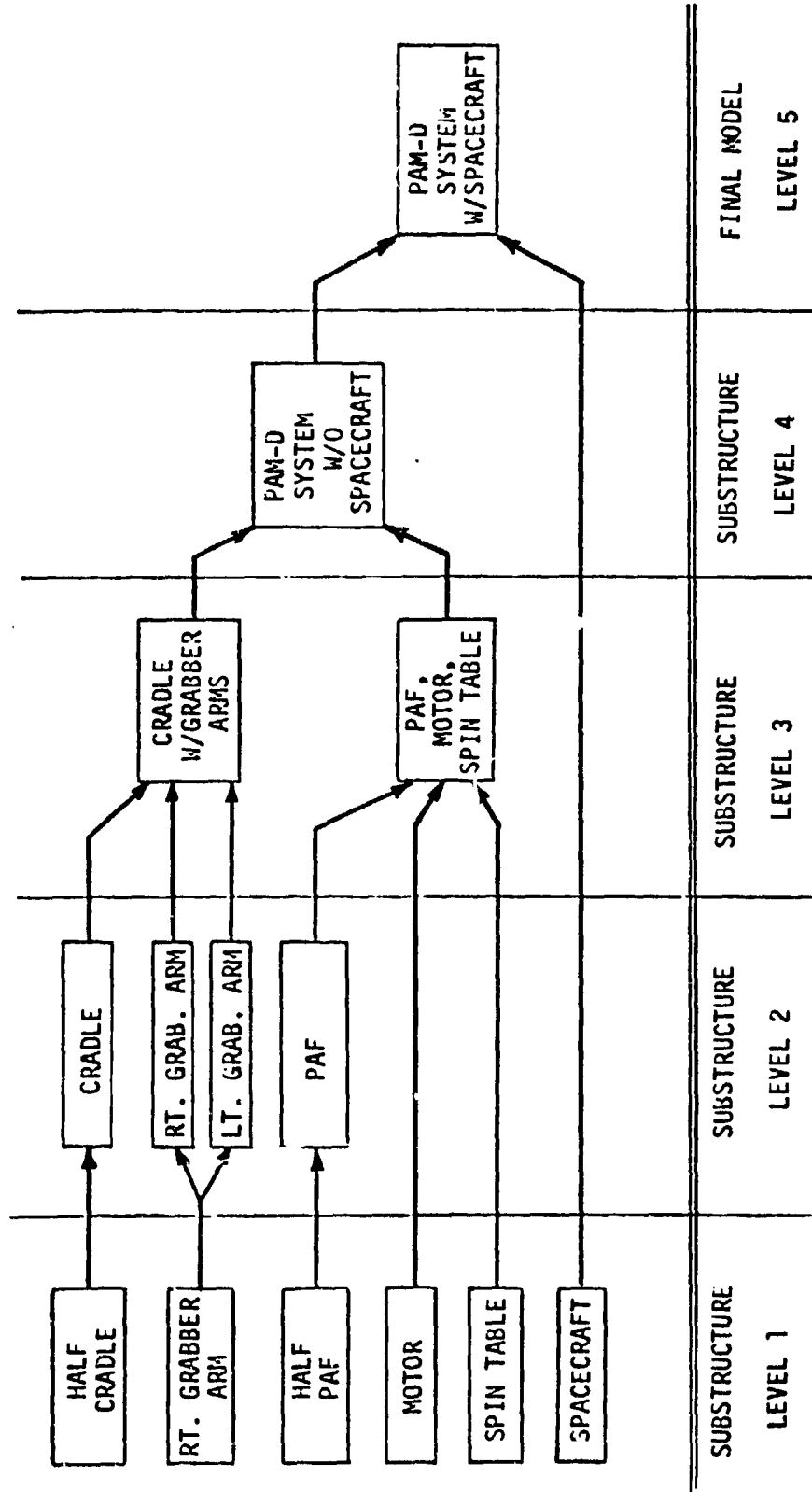
PAM-D DYNAMIC MODEL - ASSEMBLY FLOWCHART

Five levels of model assembly are used to generate a coupled PAM/spacecraft structural dynamic model. The components that define a complete substructure assembly are combined and retained for coupling to other complete substructure assemblies. This allows for future modification or implementation of new components (i.e., motor with more propellant for heavier payloads) to be easily introduced to the system for a specific design or mission requirement.

Before the spacecraft model is coupled to the PAM system, MDAC performs standard analytical checks on the spacecraft model to verify that its model properties are in agreement with those as documented by the spacecraft manufacturer. Included in the checks are simple base response analyses for identifying any unusual spacecraft dynamic response qualities that would result in abnormal dynamic responses in the coupled Orbiter/PAM/spacecraft analysis.



PAM-D DYNAMIC MODEL - ASSEMBLY FLOWCHART





PAM-D DYNAMIC MODEL - SUBSTRUCTURE MODEL SIZE DESCRIPTION

By utilizing the methods of component modal synthesis and image modeling, detailed NASTRAN discrete finite element models are reduced to sets of generalized coordinates. The reduction of the number of equations of motion describing the structure facilitates computational procedures in generating total coupled system dynamic models.

Frequency content of the constrained normal modes for each component is selected so as to provide accurate definition of the total PAM system dynamic model. For liftoff and landing transient analysis, the Orbiter vehicle model and forcing functions require a payload model to be accurately defined for frequencies \leq 45 Hz.



PAM-D DYNAMIC MODEL - SUBSTRUCTURE MODEL SIZE DESCRIPTION

LEVEL	MODEL DESIGNATION	DISCRETE MODEL		MODAL MODEL	
		NO. GRIDS	NO. DOF	TOTAL MODES	FREQUENCY (HZ)
LEVEL 1	HALF CRADLE	302	304	25 NORMAL, 133 CONSTRAINT	38.9 TO 409.3
	RT. GRABBER ARM	87	126	7 NORMAL, 16 CONSTRAINT	111.9 TO 737.8
	HALF PAF	217	200	15 NORMAL, 83 CONSTRAINT	532.7 TO 1518.3
	MOTOR	23	126	17 NORMAL, 12 CONSTRAINT	152.5 TO 960.5
	SPIN TABLE	57	74	4 NORMAL, 18 CONSTRAINT	231.3 TO 240.6
	SPACECRAFT	-	-	20 NORMAL, 6 CONSTRAINT	15.8 TO 111.0
LEVEL 2	CRADLE	-	-	51 NORMAL, 39 CONSTRAINT	37.7 TO 298.5
	RT. GRABBER ARM	-	-	7 NORMAL, 16 CONSTRAINT	111.9 TO 737.8
	LT. GRABBER ARM	-	-	7 NORMAL, 16 CONSTRAINT	111.9 TO 737.8
	PAF	-	-	41 NORMAL, 18 CONSTRAINT	139.9 TO 993.0
LEVEL 3	CRADLE W/GRABBER ARMS	-	-	68 NORMAL, 17 CONSTRAINT	18.2 TO 296.9
	PAF, MOTOR, SPIN TABLE	-	-	22 NORMAL, 16 CONSTRAINT	80.9 TO 269.9
LEVEL 4	PAM-D SYSTEM W/O SPACECRAFT	-	-	91 NORMAL, 13 CONSTRAINT	18.2 TO 296.6
LEVEL 5 (FINAL)	PAM-D SYSTEM W/SPACECRAFT	-	-	30 NORMAL, 7 CONSTRAINT	7.2 TO 66.1



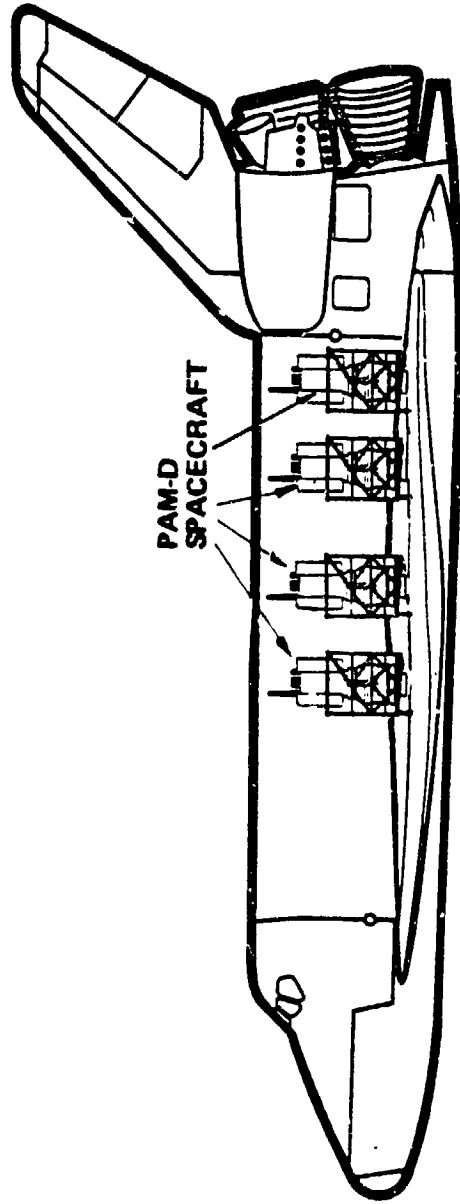
TYPICAL ORBITER/PAM CARGO MANIFEST FOR DYNAMIC ANALYSIS

Spacecraft dynamic response analysis is performed with the Orbiter bay manifested with cargo that possesses weight and c.g. definition consistent with STS requirements. When possible, payloads are analytically manifested in the cargo bay in such a manner that spacecraft responses can be calculated at various locations to determine the effect of position in the bay.

A typical PAM-D dynamic analysis uses four identical models of the specific payload located at various positions in the bay. Responses are used to determine the worst loading the spacecraft can anticipate and also to determine what location, if any, would produce the lowest and most favorable environment for the spacecraft.



TYPICAL ORBITER/PAM-D CARGO MANIFEST
FOR DYNAMIC ANALYSIS





STS ORBITER DYNAMIC MODEL SUPPLIED BY NASA/JSC

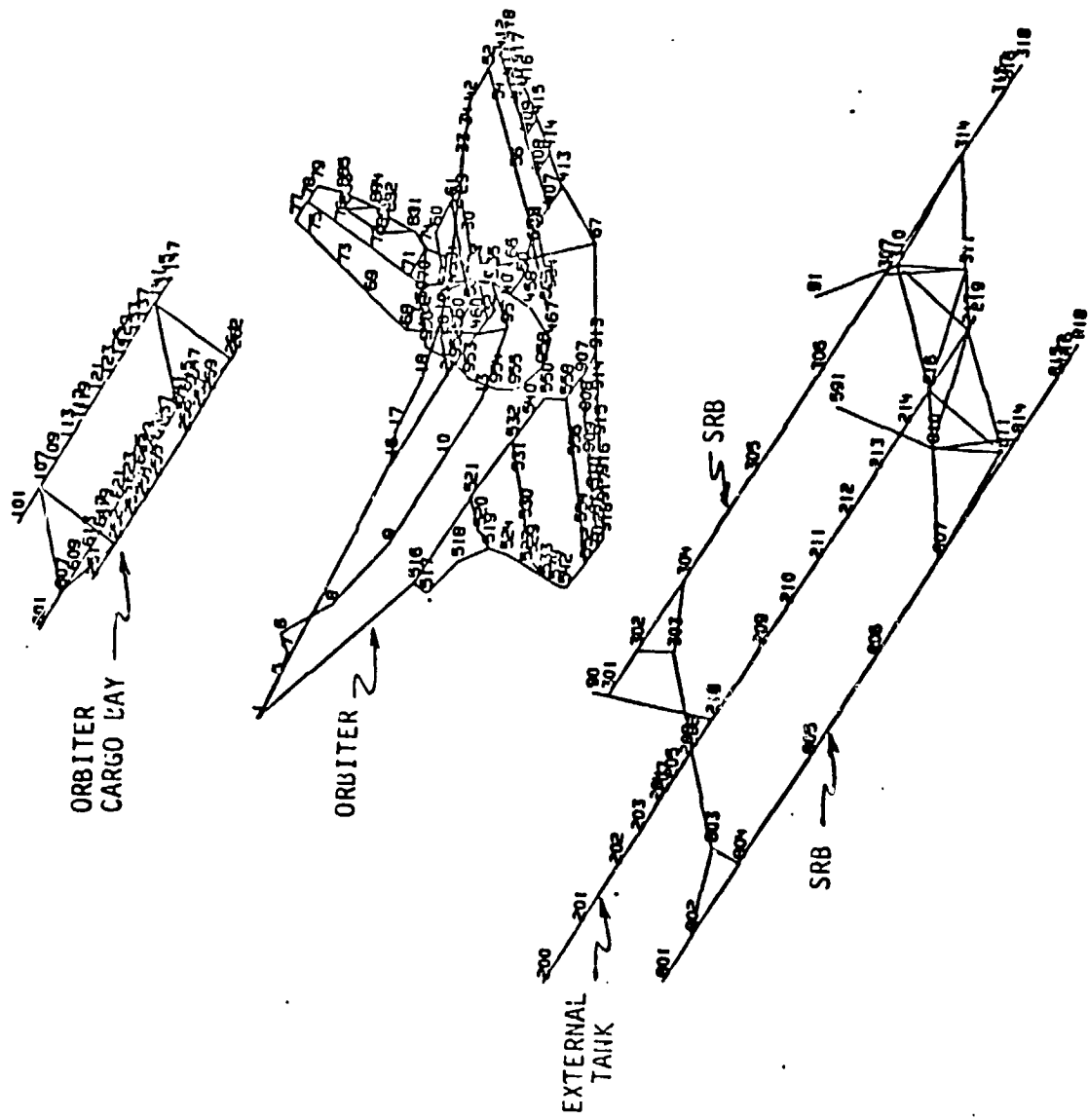
The Orbiter vehicle dynamic models were provided to MDAC by NASA/JSC. These models were generated by Rockwell International, Space Division, Downey, California.

The Orbiter dynamic models provided to MDAC are the version defined as Model M5.4D05. Two liftoff models and one landing model were developed by Rockwell. For liftoff, one model designated as M5.4D05 LOH includes the two SRBs modeled with 90 degree propellant temperature. This model is referred to as the HOT liftoff model. The liftoff model designated as M5.4D05 LOC includes the two SRBs modeled with 40 degree propellant temperature. This model is referred to as the COLD liftoff model. The one landing model is designated as M5.4D05.

The liftoff and landing Orbiter vehicle dynamic models were provided as 300 free-free modal coordinates. Modal data for each model consist of diagonal modal mass (equal to unity), modal stiffness, and a modal displacement transform which recovers deflections at payload attachment locations in the cargo bay and at all vehicle locations required for external load application.



STS ORBITER DYNAMIC MODEL SUPPLIED BY NASA/JSC



300
FREE-FREE
MODES

$M = [I]$
 $K = [w^2]$
 $X_{BAY} = \phi_{BAY} \cdot q_0$
 $X_{FORCE} = \phi_{FORCE} \cdot q_0$

ORIGINAL PAGE IS OF POOR QUALITY



PAM-D, ORBITER VEHICLE, AND COUPLED ORBITER/PAM-D MODEL SIZE DESCRIPTION

In general, the total number of PAM payload model normal modes required to accurately define response in the lower frequency range is much less than the number of Orbiter free-free modes. For liftoff, 212 normal Orbiter modes are required to define frequencies up to 45 Hz, while for landing 158 modes are required for frequencies up to 65 Hz.

The PAM payload models are coupled to the Orbiter cargo bay model at their longeron and keel interfaces by writing the relationships which equate the deflections of the PAM interfaces (discrete degrees of freedom) to the deflection of the Orbiter interfaces (modal representation), i.e. $X_{PAM} = \phi_{BAY} \cdot q_0$.

The total Orbiter/PAM-D coupled model, with four PAM-D payloads manifested in the cargo bay, requires approximately 280 normal modes to define frequencies up to 45 Hz and 65 Hz for liftoff and landing, respectively. All modes are used in the transient response analysis in conjunction with a constant value for modal damping of 0.01 of critical for all modes.



PAM-D, ORBITER VEHICLE, AND COUPLED ORBITER/PAM-D
MODEL SIZE DESCRIPTION

COUPLED MODEL DESIGNATION	COMPONENT MODELS			ORBITER/PAM-D COUPLED MODEL	
	TYPICAL PAM-D PAYLOAD MODEL* TOTAL MODES FREQUENCY (HZ)	ORBITER VEHICLE MODEL TOTAL MODES FREQUENCY (HZ)	TOTAL MODES FREQUENCY (HZ)	TOTAL MODES FREQUENCY (HZ)	
LIFTOFF (HOT)	17 NORMAL 7 CONSTRAINT 7.20-45.53	212 NORMAL 6 RIGID BODY 2.12-45.58	280 NORMAL 6 RIGID BODY 2.11-45.83		
LIFTOFF (COLD)	17 NORMAL 7 CONSTRAINT 7.20-45.53	212 NORMAL 6 RIGID BODY 2.16-45.56	280 NORMAL 6 RIGID BODY 2.16-45.83		
LANDING	30 NORMAL 7 CONSTRAINT 7.20-66.06	158 NORMAL 6 RIGID BODY 3.98-65.43	273 NORMAL 6 RIGID BODY 3.96-65.43		

*ONE OF FOUR IDENTICAL PAYLOADS IN ORBITER CARGO BAY.



STS ORBITER FORCING FUNCTIONS SUPPLIED BY NASA/JSC

The liftoff and landing STS Orbiter forcing functions used for transient response analyses of PAM/spacecraft payloads are supplied to MDAC by NASA/JSC. These forcing functions are developed by Rockwell International, Space Division, Downey, California, and represent force conditions expected to produce limit loads, accelerations, and deflections of Orbiter payloads.

Eight separate forcing functions defining variations in expected liftoff effects are applied to both the HOT and COLD versions of the STS Orbiter liftoff dynamic model for a total of sixteen response cases. Each forcing function contains 101 transient forces externally applied to the STS Orbiter vehicle.

Four separate forcing functions defining the 6.0 fps descent rate abort landing conditions are described by five distinct response cases. Each forcing function contains 286 transient and aerodynamic forces externally applied to the Orbiter vehicle.

The force time history data for all liftoff and landing forcing functions are provided to MDAC in NASTRAN "TABLED1" format, consisting of data pairs (t_i , f_i). These data are linearly interpolated to a constant sampling rate, 160 samples/second for liftoff forces and 200 samples/second for landing forces. This procedure is consistent with NASTRAN processing of "TABLED1" data.



STS ORBITER FORCING FUNCTIONS SUPPLIED BY NASA/JSC

- FORCING FUNCTIONS DEFINING LIFTOFF EVENT PROVIDED BY NASA/JSC
 - 16 CASES RESULTING FROM 8 FORCE CONDITIONS APPLIED TO BOTH HOT AND COLD ORBITER SRB LIFTOFF MODELS
 - 8 FORCE CONDITIONS DEVELOPED BY ROCKWELL INCLUDE VARIATIONS IN EXPECTED ORBITER PROPULSION, THERMAL, AND LAUNCH EFFECTS

(1)	LO518AR	(5)	LP516
(2)	LP510	(6)	LP519
(3)	LP512	(7)	LP521
(4)	LP549	(8)	LP522
 - EACH FORCE CONDITION CONTAINS 101 TRANSIENT FORCES APPLIED TO ORBITER VEHICLE
- FORCING FUNCTIONS DEFINING LANDING EVENT PROVIDED BY NASA/JSC
 - 6.0 fps DESCENT RATE CRITERIA
 - 5 CASES RESULTING FROM 4 FORCE CONDITIONS DEVELOPED BY ROCKWELL

(1)	LN896	-	MAX NOSE SLAP (6.0 fps, NO CROSSWIND)
(2)	LM896	-	6.0 fps, NO CROSSWIND, HIGH α
(3)	LM897	-	6.0 fps, NO CROSSWIND, LOW α
(4)	LM898	-	5.0 fps, 20 KT CROSSWIND, HIGH α
(5)	LM899	-	5.0 fps, 20 KT CROSSWIND, LOW α
- EACH FORCE CONDITION CONTAINS 286 TRANSIENT AND AERODYNAMIC FORCES APPLIED TO ORBITER VEHICLE



ORBITER/PAM-D LIFTOFF DYNAMIC RESPONSE ANALYSIS

For each of the sixteen liftoff force cases, coupled Orbiter/PAM/spacecraft modal accelerations $[\ddot{q}(t)]$ and displacements $[q(t)]$ are calculated for all modes at a constant output sampling rate of 160 samples per second for a period of 7.0 seconds. Payload responses are calculated by utilizing specific transformation matrices applied to the payload model generalized coordinate acceleration and displacement vectors, $[\ddot{q}_p(t)]$ and $[q_p(t)]$, which are recovered from $[\ddot{q}(t)]$ and $[q(t)]$.

For each PAM and spacecraft manifested in the Orbiter for the response analysis, all acceleration, load, deflection, and appropriate relative deflection responses, both requested by the spacecraft manufacturer (user) and required for Orbiter/payload interface requirement verification, are recovered. Time histories and maximum-minimum summary tables of responses for all liftoff cases are presented to the user. Spacecraft generalized coordinate acceleration and deflection time histories for all cases are supplied to the user in computer tape format for their use in performing any further detailed evaluation of spacecraft responses.

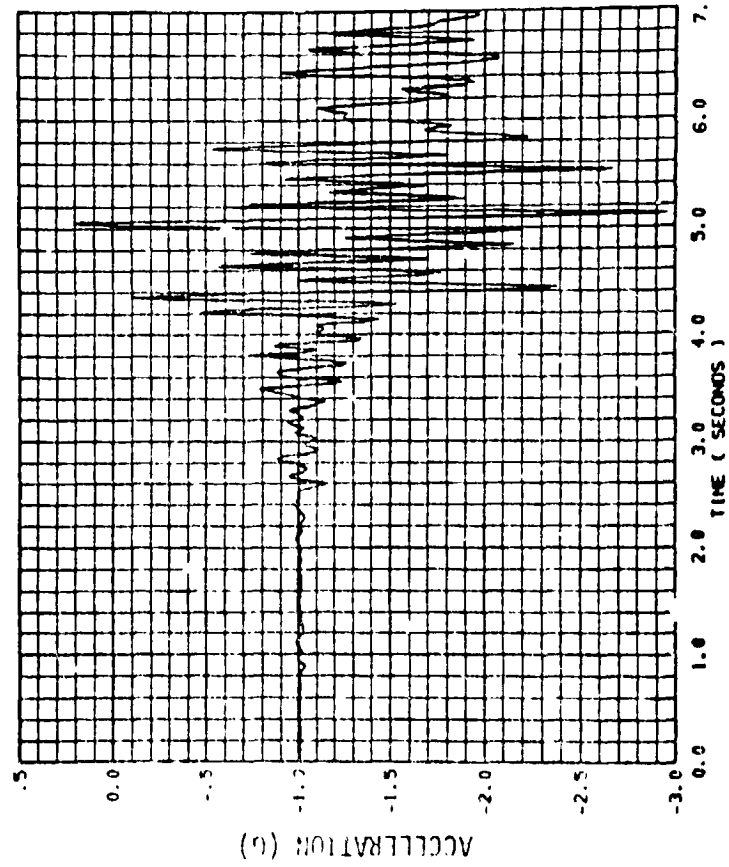


ORBITER/PAM-D LIFTOFF DYNAMIC RESPONSE ANALYSIS

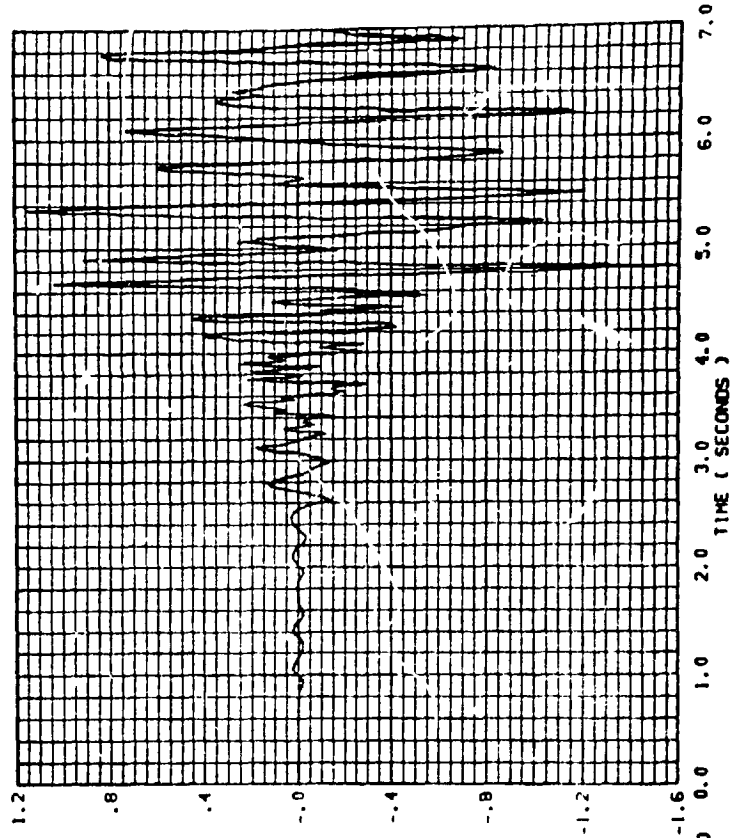
- SAMPLE CASE, 1 OF 16 -

SPACECRAFT C.G. ACCELERATIONS

$\ddot{X}(\text{ORB})$ - 2320 LB BASELINE SPACECRAFT C-G



$\ddot{Z}(\text{ORB})$ - 2320 LB BASELINE SPACECRAFT C-G





ORBITER/PAM-D LANDING DYNAMIC RESPONSE ANALYSIS

For each of the five landing force cases, coupled Orbiter/PAM/spacecraft modal accelerations $[\ddot{q}(t)]$ and displacements $[q(t)]$ are calculated for all modes at a constant output sampling rate of 200 samples per second for a period of 2.0 seconds. Payload responses are calculated by utilizing specific transformation matrices applied to the payload model generalized coordinate acceleration and displacement vectors, $[\ddot{q}_p(t)]$ and $[q_p(t)]$, which are recovered from $[\ddot{q}(t)]$ and $[q(t)]$.

For each PAM and spacecraft manifested in the Orbiter for the response analysis, all acceleration, load, deflection, and appropriate relative deflection responses, both requested by the spacecraft manufacturer (user) and required for Orbiter/payload interface requirement verification, are recovered. Time histories and maximum-minimum summary tables of responses for all landing cases are presented to the user. Spacecraft generalized coordinate acceleration and deflection time histories for all cases are supplied to the user in computer tape format for their use in performing any further detailed evaluation of spacecraft responses.

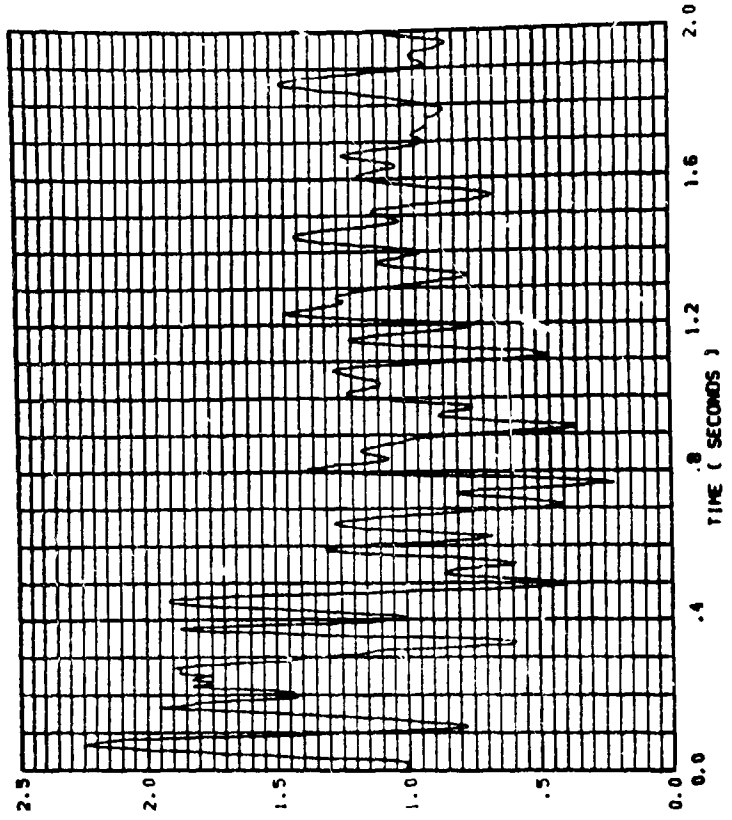


ORBITER/PAM-D LANDING DYNAMIC RESPONSE ANALYSIS

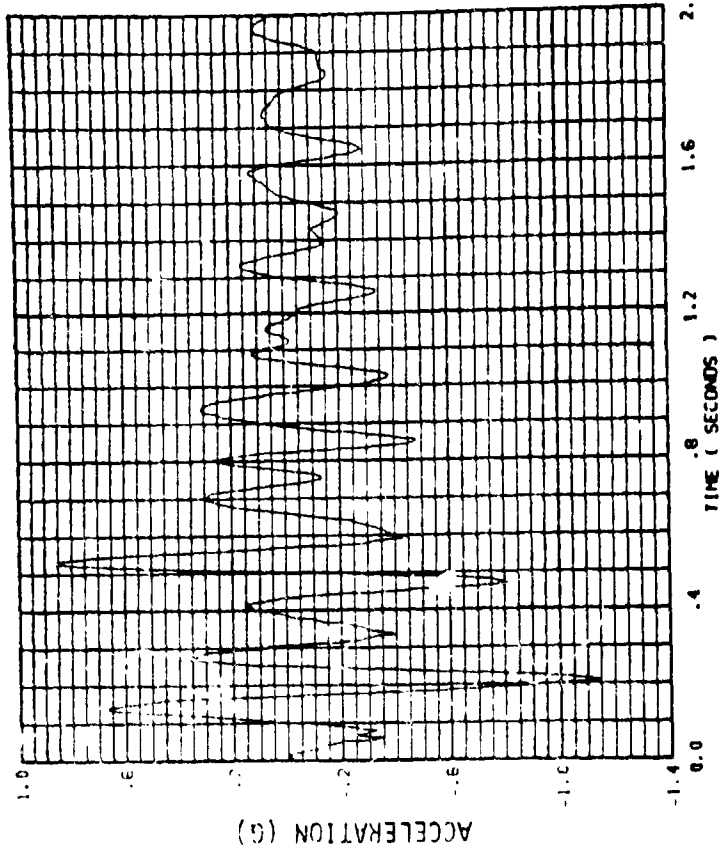
- SAMPLE CASE, 1 OF 5 -

SPACECRAFT C.G. ACCELERATIONS

$\ddot{z}(\text{ORB}) - 2320 \text{ LB BASELINE SPACECRAFT C-G}$



$\ddot{x}(\text{ORB}) - 2320 \text{ LB BASELINE SPACECRAFT C-G}$





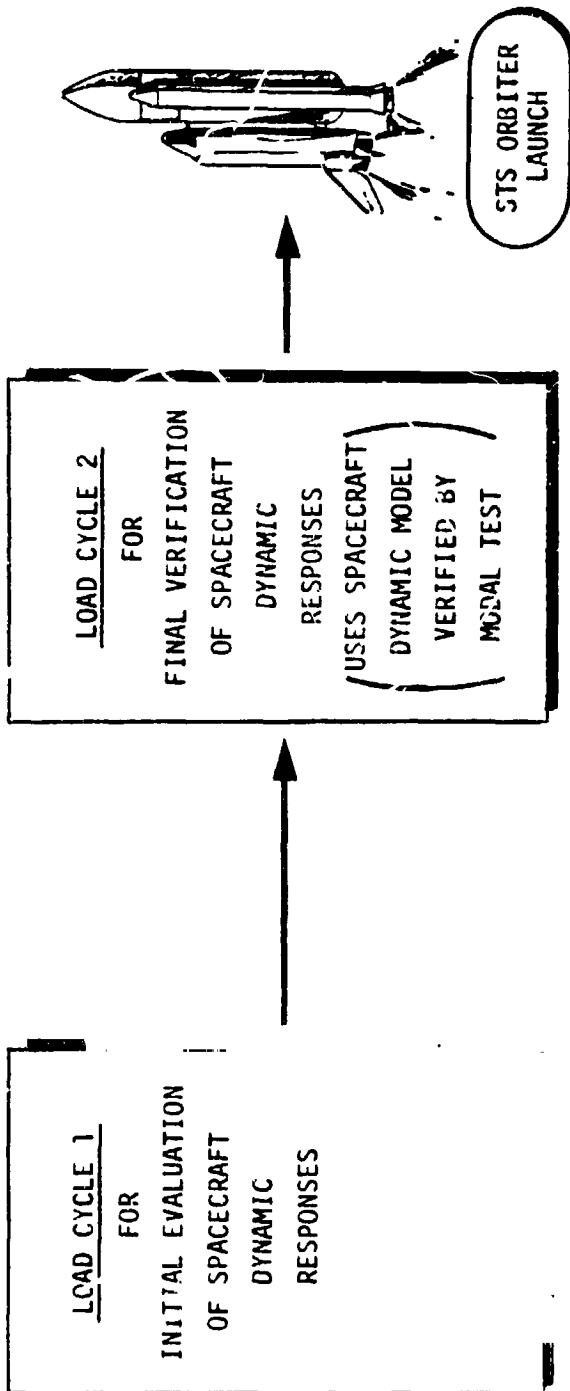
MDAC PAM/SPACECRAFT DYNAMIC LOADS ANALYSIS SCHEDULE

It is recommended that two distinct dynamic loads analyses be performed for spacecraft launched in the NASA STS Orbiter. Initial evaluation of spacecraft dynamic loads and deflections is performed for payloads in Load Cycle 1. Results from this dynamic analysis are used by the spacecraft manufacturer to ensure that the spacecraft meets design criteria and NASA interface requirements.

Since it is important to verify that the spacecraft meet the critical design and interface requirements for STS Orbiter flight, Load Cycle 2 dynamic analysis is performed after the spacecraft model has been verified and/or modified by modal test. The spacecraft model used in Load Cycle 2 also reflects any design modifications implemented by the spacecraft manufacturer since the initial Load Cycle 1 analysis evaluation.



MDAC PAM/SPACECRAFT DYNAMIC RESPONSE ANALYSIS SCHEDULE



PRECEDING PAGE BLANK NOT FILMED

DATE PROGRAM OVERVIEW

by

**W. Brian Keegan/William F. Bangs
NASA/Goddard Space Flight Center**

(Figure 1)

The Dynamic, Acoustic, and Thermal Environments (DATE) Program is an effort to provide comprehensive measurements of three potentially critical environments for payloads contained in the STS cargo bay, and to coordinate the utilization of this information such that all STS payload developers will benefit from it to the fullest possible extent.

The DATE program was conceived because of a perceived void in the attention being given to payload environments by the STS developer. While this lack of attention to payloads was understandable (given the problems associated with the development of such a complex vehicle as the STS), it was nonetheless apparent that the payload community itself would have to initiate the effort to obtain the data it felt it needed if the cost benefits associated with the use of STS were to be fully realized.

Thus, the DATE program was formulated and a proposal was made to NASA Headquarters in October 1977, that the DATE experiment constitute a portion of the OEX Program whose primary objective is "to augment the research and technology base for future aerospace vehicle design by utilizing the Space Shuttle as a research vehicle to collect data in all related technology disciplines."

(Figure 2)

In line with this OEX Program objective therefore, the principle objective of DATE is to develop accurate prediction techniques for payload environments in each of the three critical areas through an iterative process of payload response prediction, followed by the actual measurement of the environments, followed in turn by refinement of the prediction techniques until the process of response prediction has been verified to be accurate through flight measurement.

While the STS is being used to accomplish this objective, the prediction techniques so developed would obviously not be restricted to STS payloads.

(Figure 3)

The approach to be followed in meeting this objective is to first acquire a set of baseline measurements that consider the effects of several potentially significant parameters. These include payload mass and size, particularly as the size affects the clearance with the cargo bay walls. Studies performed by Bolt, Beranek and Newman on the STS cargo bay acoustic environment have predicted that, in certain cases, reduced clearances may have an adverse effect on the acoustic noise environment encountered by payloads.

Meanwhile, the variation in dynamic loads must be assessed because they will be influenced by the payload location within the bay and by its mounting configuration, that is, method of attachment to the STS payload support structure.

And finally, the flight-to-flight variations brought about by trajectory dispersions, winds, and the like must also be measured.

Simultaneous with these baseline measurements, potential improved methods for payload environmental prediction could be developed, the effectiveness of which could be evaluated by comparing the measured responses with the predicted ones. These analytic methods could thus be refined and re-evaluated until their accuracy has been verified, at which time these methods could be utilized by all payload developers.

The DATE program is being managed by the Goddard Space Flight Center (GSFC). However, because this principle objective of DATE has such broad technology implications, a NASA-wide panel of experts has been established, known as the DATE Working Group. It provides guidance and direction for the technology development permitted by the DATE measurements and their subsequent application.

(Figure 4)

Of necessity, this objective of improved technology is a long term one. There are, additionally, some near term benefits of the data acquisition sought by DATE and these are best summarized by the secondary objectives of characterizing the STS payload dynamic, acoustic and thermal environments and of developing a set of design and test criteria, directly applicable to STS payloads in order to permit design optimization so as to better utilize the full capabilities of the STS.

(Figure 5)

Because of practical considerations necessitated by the STS launch schedule, the DATE measurement program has been subdivided into two phases. Phase I, while containing fewer instrumentation channels than is truly desirable, will permit some data to be obtained during the STS orbital flight test sequences, namely on mission 4, on which the payload will be the Geostationary Operational Environmental Satellite-D (GOES-D), a free-flier that will be boosted to synchronous altitude by the Solid Spinning Upper Stage (SSUS) and on mission 5 on which the payload will be a single pallet that will remain attached to the STS for landing as well. Thus Phase I data will indeed begin to characterize the STS payload environments for the two basic types of payloads, and will serve as a basis from which to refine the instrumentation plans for specific follow-on missions.

Permission has been received from the STS Project Office at Johnson Space Center (JSC) to utilize the development flight instrumentation system to record this Phase I data, barring any undue complications resulting from the earlier STS orbital flights.

(Figure 6)

The DATE Phase II program will consist of a far more extensive set of measurements on approximately 9 missions during an 18-24 month period after the STS becomes operational. For this phase, the measurement complement would be expanded to include force gages and thermal measurements. Recording of this data would utilize the Technology Flight Instrumentation System, which will be developed by the OEX Project Office for joint use by all OEX funded experiments. The Phase II instrumentation plan shown here is intended to conceptualize the program. Specific payloads have not yet been assigned to all these missions and the actual missions which are instrumented and the precise number of transducers used on each will undoubtedly vary as the program develops.

(Figure 7)

While the payload shown here is only conceptual, it can be used to illustrate typical locations that may be selected for making measurements during the DATE program. Microphone locations would be selected to measure the spatial variation

throughout the cargo bay, particularly as influenced by the affects of the payload configuration. High frequency accelerometers would emphasize component responses, induced by both payload bay acoustics as well as structure borne random vibration. Additionally, an attempt would be made to determine the magnitude of the random vibration directly transmitted to the payload by the STS. Low frequency accelerometers would attempt to measure the forcing functions at the payload/STS interface, as well as responses at critical structural locations throughout the payload. The force gages will be used principally to measure the forces transmitted across the payload/STS interface. Finally, the thermal measurements would be used to measure temperatures at critical locations on the structure and to measure thermal fluxes incident at various locations on the payload as a result of the sun, as well as from other payloads and the STS itself.

(Figure 8)

Problems currently being encountered by DATE are outlined here. The problem of payload manifesting, that is, which payload will be launched on which mission, impacts our program because for any particular mission, the STS data recording system must be properly configured for the instrumentation complement that is contained on a specific payload. Changing the payload to a different mission creates obvious problems of coordination. As an example of the problems, the payload planned for mission number 4 has changed three times in the last two months. While obviously not an insurmountable problem, it does create headaches.

The schedule is rapidly becoming a problem. Despite the fact that the STS launch schedule has slipped somewhat, our ability to start the necessary preliminary activities has also been delayed because of delays in funding authority. This is creating a schedule compression, which, while not yet a serious problem, will rapidly become one if funding commitments are not soon forthcoming.

(Figure 9)

The DATE funding requirements are outlined here, and include funds for the acquisition, preparation and calibration of the flight measurement system including the transducers, cabling, and signal conditioning equipment. Additionally, funds are included for reduction, analysis, and reporting of all data obtained by the DATE program.

Expenses associated with the integration of DATE hardware onto the payloads, a relatively modest expense, would be borne by the payloads themselves. The expenses of integrating DATE hardware into the STS itself would be borne by the STS program office.

It must be emphasized that the funding outlined here does not include the development of a data recording system and, in fact, assumes essentially free usage of an existing system. Additionally, the costs associated with the development of the associated new technology are not included and would, therefore, have to be funded through the NASA Research and Technology Operating Plan (RTOP) process.

Some continuing measurement program beyond Phase II would probably be desired at a significantly reduced scope in order to evaluate vehicle modifications and the like. Funding for such an effort is not included in the currently requested resources, however.

(Figure 10)

DATE is certainly not the only program in existence that has as one of its objectives the measurement of STS payload environments. In closing, then, a brief review of the status of such programs was felt to be in order.

First, DATE is officially unfunded for FY 79 and beyond. While some indications of potential FY 79 funding have been received, no dollars have thus far been received.

The Payload Wideband Data System (PWDS) is an effort by the Shuttle Payload Integration and Development Project Office at NASA/JSC, to provide payload associated environmental measurements after the STS becomes operational. To the best of our knowledge, this effort remains unfunded at this time.

Similarly, Martin-Marietta has proposed development of the Environmental Response Instrumentation System (ERIS) to the Air Force for the measurement of STS payload environments, but again, to the best of our knowledge the effort remains unfunded.

Two programs that will make STS payload environmental measurements, at least on a limited basis, are LDEF/SBEM and VFI.

The Shuttle Bay Environment Monitor (SBEM) will make reasonably extensive acoustic and vibration measurements during the flight of the NASA-Langley Long Duration Exposure Facility (LDEF). This will be limited, however, to a single mission on what is probably a not-too-typical STS payload, thereby limiting the application of the acquired data.

Meanwhile, the Verification Flight Instrumentation (VFI) is being developed by NASA/Marshall Space Flight Center for use on the first two STS spacelab missions. While here also the dynamic and acoustic instrumentation is extensive, it must be noted that its use will be limited to two missions and much of the data acquired will apply to rather specialized Spacelab hardware.

In conclusion, therefore, it must be emphasized that there are no funded programs which have as their objectives the general characterizations of environments for the various classes of typical STS payloads. It is felt that this situation should be remedied quickly, if the somewhat haphazard and after-the-fact methods that sometimes accompanied the characterization of payload environments on conventional launch vehicles is to be avoided.

FIGURE 1

DATE PROGRAM

D Y N A M I C

A C O U S T I C

T H E R M A L

E N V I R O N M E N T S

FIGURE 2

PRINCIPLE OBJECTIVE

TO DEVELOP ACCURATE PREDICTION TECHNIQUES
FOR PAYLOAD ENVIRONMENTS THROUGH THE
ITERATIVE PROCESS OF PREDICTION, MEASUREMENT,
AND REFINEMENT

FIGURE 3

APPROACH

- 0 ACQUIRE BASELINE MEASUREMENTS ON STS PAYLOADS
CONSIDERING:
 - PAYLOAD MASS AND CONFIGURATION EFFECTS
 - BAY LOCATION AND ATTACHMENT METHOD EFFECTS
 - FLIGHT-TO-FLIGHT VARIATIONS

- 0 DEVELOP IMPROVED ANALYTIC METHOD FOR PAYLOAD
ENVIRONMENTAL PREDICTION

- 0 TEST IMPROVED METHODS AGAINST MEASURED DATA

- 0 REFINE AND ITERATE METHODS AS APPROPRIATE

- 0 DISSEMINATE PREDICTION METHODS AND DATA FOR APPLICATION

FIGURE 4

SECONDARY OBJECTIVE

- O TO CHARACTERIZE THE STS PAYLOAD DYNAMIC, ACOUSTIC AND THERMAL ENVIRONMENTS

- O TO DEVELOP INTERIM DESIGN AND TEST CRITERIA FOR STS PAYLOADS

FIGURE 5

PHASE I INSTRUMENTATION PLAN

<u>MISSION</u>	<u>MIKES</u>	<u>ACCELEROMETERS</u>	
		<u>HIGH FREQ.</u>	<u>LOW FREQ.</u>
SS-4	5	10	12
SS-5	5	10	12

FIGURE 6

PHASE II INSTRUMENTATION PLAN

<u>MISSION</u>	<u>MIKES</u>	<u>ACCELEROMETERS</u>		<u>FORCE GAGES</u>	<u>THERMAL</u>
		<u>HIGH FREQ.</u>	<u>LOW FREQ.</u>		
8	30	36	30	12	100
10	30	30	-	-	100
11	30	12	12	-	-
14	30	36	30	12	100
16	30	36	30	12	100
20	30	12	12	-	-
22	30	36	30	12	100
25	30	-	30	6	-
28	30	36	30	12	100

FIGURE 7

TYPICAL DATE INSTRUMENTATION LOCATIONS

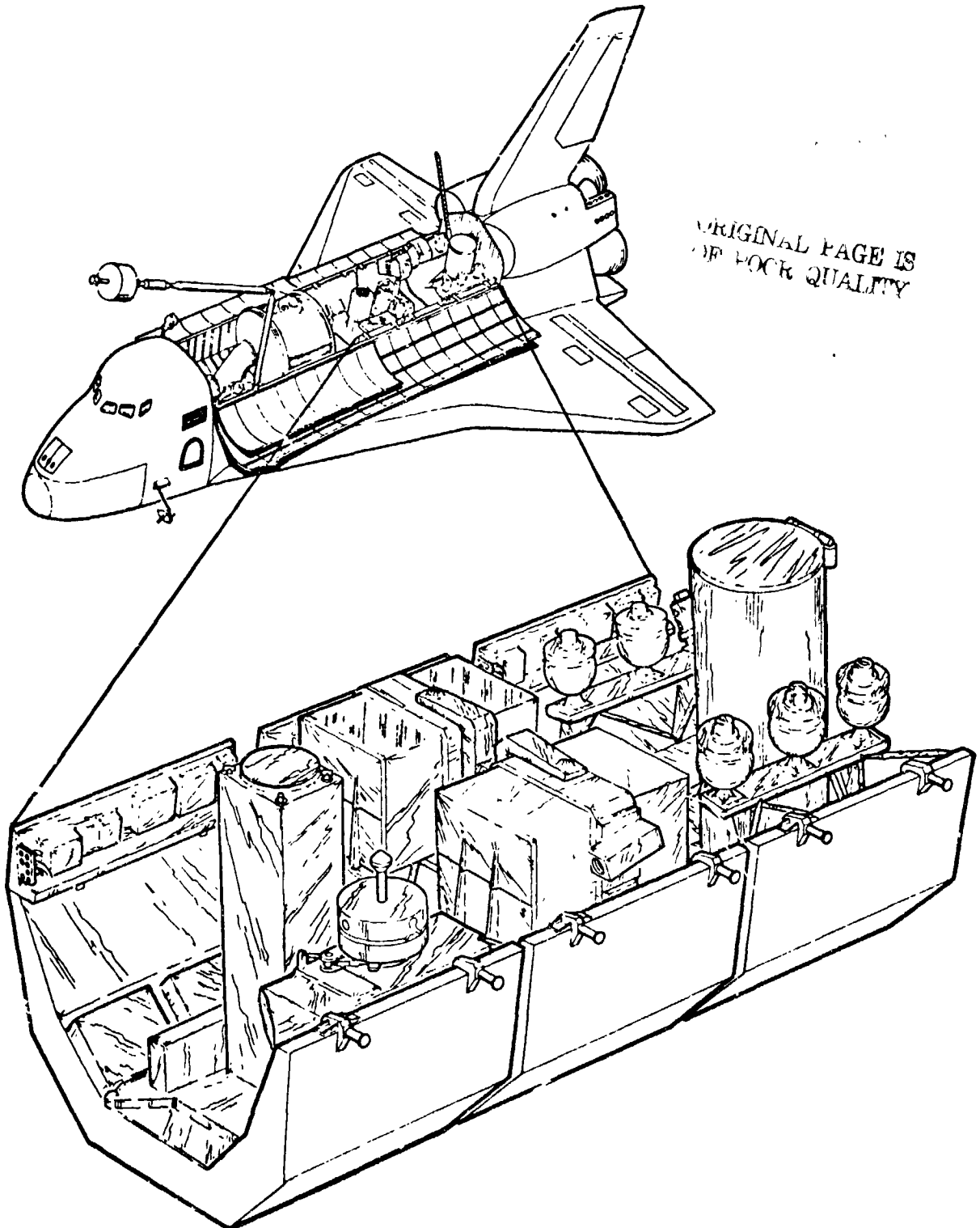


FIGURE 8

PROBLEMS

- 0 PAYLOAD MANIFESTING
- 0 SCHEDULE
- 0 FUNDING

FIGURE 9

DATE FUNDING

FY 78	55K	RECEIVED
FY 79	220K	REQUEST SUBMITTED
FY 80	850K	
FY 81	700K	
FY 82	450K	
FY 83	100K	
FY 84	90K	
FY 85	<u>60K</u>	
	\$2.5M	

FIGURE 10

STATUS OF STS PAYLOAD MEASUREMENT PROGRAMS

o	DATE	(GSFC/OAST)	UNFUNDED AFTER FY 78
o	PWDS	(SPIDPO)	UNFUNDED
o	ERIS	(DoD/MMC)	UNFUNDED
o	LDEF/SBEM	(LRC)	FUNDED AT REDUCED SCOPE
o	VFI	(MSFC)	FUNDED

AN IMPEDANCE TECHNIQUE
FOR
DETERMINING LOW FREQUENCY
PAYLOAD ENVIRONMENTS

Kenneth R. Payne
Martin Marietta Corporation
Denver Division

SUMMARY

Analysis of various payload configurations is a very lengthy and expensive task. Individual extensive models of the payload and booster must be mathematically coupled for the final system models and then elaborate time domain response analyses conducted. The task of the analysis integration for all the organizations involved as well as the manpower involved in model coupling and loads computations drive these costs skyward. With the expected payloads exhibiting numerous variations in configurations and experiments, the detailed approach of the past will not be a viable cost-effective technique.

A preferable technique would eliminate the necessity of creating detailed coupled models as well as eliminating the need of an integration task. If possible, the technique would allow the payload organization of designers and dynamicists to generate with model information from the booster organization, their own payload response and loads predictions.

This study reported in this paper was conducted to determine the feasibility of a new impedance technique for determining payload low frequency environments. By accounting for the dynamic coupling of the payload and booster in the equation of motion in the frequency domain, the analytical effort is diminished by eliminating the final eigensolutions as well as reducing the equations to simple complex transfer function multiplications. In addition, the model requirements of the booster consist of free-free unloaded interface modal characteristics. Therefore, the task of integrating the loads analysis can be accomplished by obtaining a set of "standard" booster

model data and the payload organizations computing their own loads analysis cycles.

The information presented in this paper includes results of the use of the impedance technique on Titan flight data as well as predictions of the low frequency environments for a proposed Shuttle payload. The requirements for implementing the impedance techniques and it's feasibility are discussed.

AN IMPEDANCE TECHNIQUE
FOR
DETERMINING LOW FREQUENCY
PAYLOAD ENVIRONMENTS

BY
KENNETH R. PAYNE

PRESENTED AT THE
49TH SHOCK & VIBRATION SYMPOSIUM
WASHINGTON, D.C.
OCTOBER 1978

MARTIN MARIETTA

AN IMPEDANCE TECHNIQUE FOR DETERMINING LOW FREQUENCY
PAYLOAD ENVIRONMENTS

Kenneth R. Payne
Senior Engineer
Analytical Mechanics
Martin Marietta Corporation

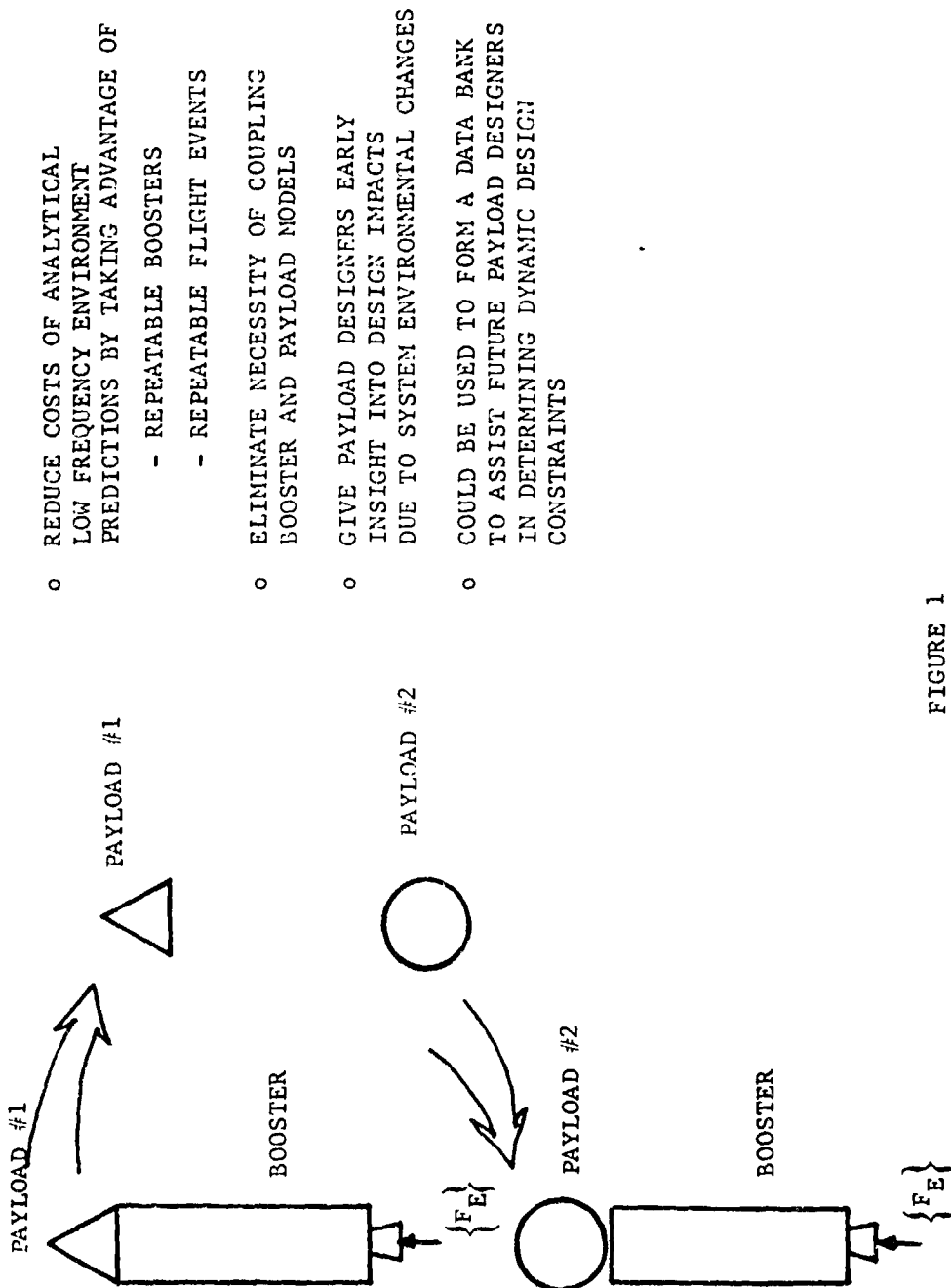
This brief paper discusses the results of a study contract, (MAS1-14370)*, with NASA Langley Research Center to investigate a new approach for determining payload low frequency (below 50Hz) environments.

Work in this area began at the end of the Viking Project when the massive expense of model generation, coupling, and time domain payload design loads analyses were realized. Initial ideas for the impedance technique were based on taking advantage of both repeatable boosters and repeatable flight events as well as inexpensive frequency domain analysis.

Results of the impedance technique applications with Titan/Centaur data and its use on a future STS payload are presented.

*Brantley Hanks - Technical Monitor

DESIRED FEATURES OF AN ANALYTICAL TECHNIQUE



- REDUCE COSTS OF ANALYTICAL LOW FREQUENCY ENVIRONMENT PREDICTIONS BY TAKING ADVANTAGE OF
 - REPEATABLE BOOSTERS
 - REPEATABLE FLIGHT EVENTS
- ELIMINATE NECESSITY OF COUPLING BOOSTER AND PAYLOAD MODELS
- GIVE PAYLOAD DESIGNERS EARLY INSIGHT INTO DESIGN IMPACTS DUE TO SYSTEM ENVIRONMENTAL CHANGES
- COULD BE USED TO FORM A DATA BANK TO ASSIST FUTURE PAYLOAD DESIGNERS IN DETERMINING DYNAMIC DESIGN CONSTRAINTS

FIGURE 1

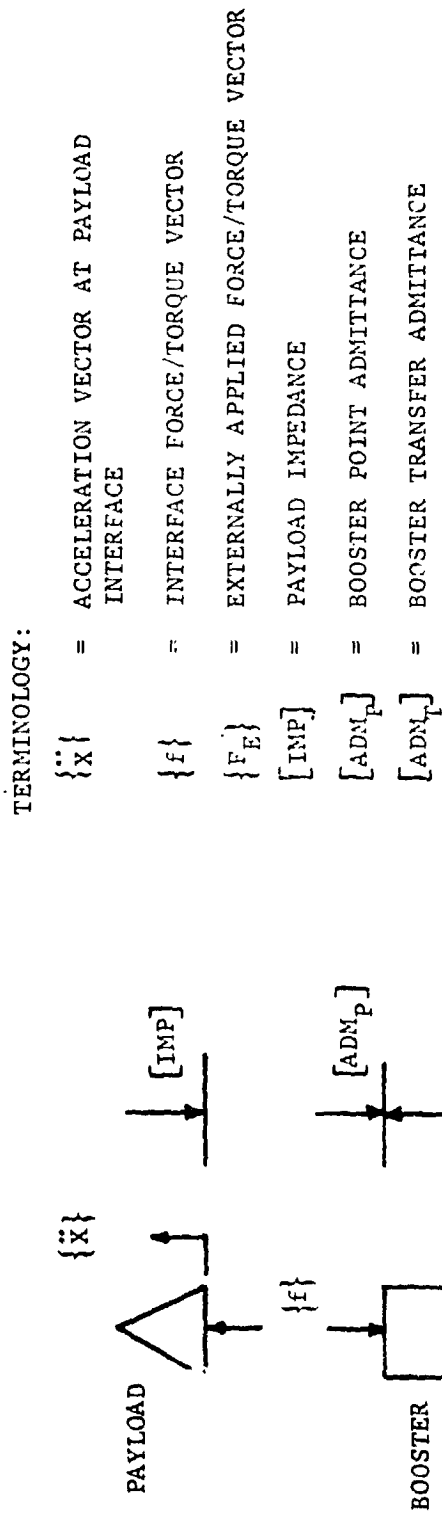
MARTIN MARIETTA

THE IMPEDANCE APPROACH (FIGURE 2)

The impedance approach is based on deriving the equations of motion for the free (unloaded) booster and payload separately, then coupling the equations by substitutions for the interface force/torque vectors. Each set of responses, applied forces and vehicle dynamic characteristics are defined as a function of input frequency, reducing the coupling of the structures to simple complex matrix multiplication.

If the external forces remain the same for both coupled structures, then the low frequency environment for a second difference payload can be "ratioed" from the acceleration spectra of the first payload.

IMPEDANCE APPROACH



TERMINOLOGY:

- $\{\ddot{x}\}$ = ACCELERATION VECTOR AT PAYLOAD INTERFACE
- $\{f\}$ = INTERFACE FORCE/TORQUE VECTOR
- $\{F_E\}$ = EXTERNALLY APPLIED FORCE/TORQUE VECTOR
- $[IMP]$ = PAYLOAD IMPEDANCE
- $[ADM_P]$ = BOOSTER POINT ADMITTANCE
- $[ADM_T]$ = BOOSTER TRANSFER ADMITTANCE

EQUATIONS OF MOTION:

$$\left([I] - [ADM_P] [IMP] \right) \{\ddot{x}\}_i = [ADM_T] \{F_E\}_i$$

AND

$$\{\ddot{x}_2\} = \left([I] - [ADM_P] [IMP] \right)^{-1} \left([I] - [ADM_P] [IMP] \right) \{\ddot{x}_1\}$$

$i = 1, 2, \dots$
NO. OF INPUT
FREQUENCIES

FIGURE 2

MARTIN MARIETTA

USE OF THE IMPEDANCE TECHNIQUE (FIGURE 3)

To investigate the feasibility of this technique and the pitfalls of frequency domain analysis, flight data from the first four Titan/Centaur flights were used as a demonstration of a practical application.

Unfortunately, the data available did not contain sufficient information to truly define the characteristics at the payload interfaces.

USE OF THE IMPEDANCE TECHNIQUE WITH TITAN FLIGHT DATA

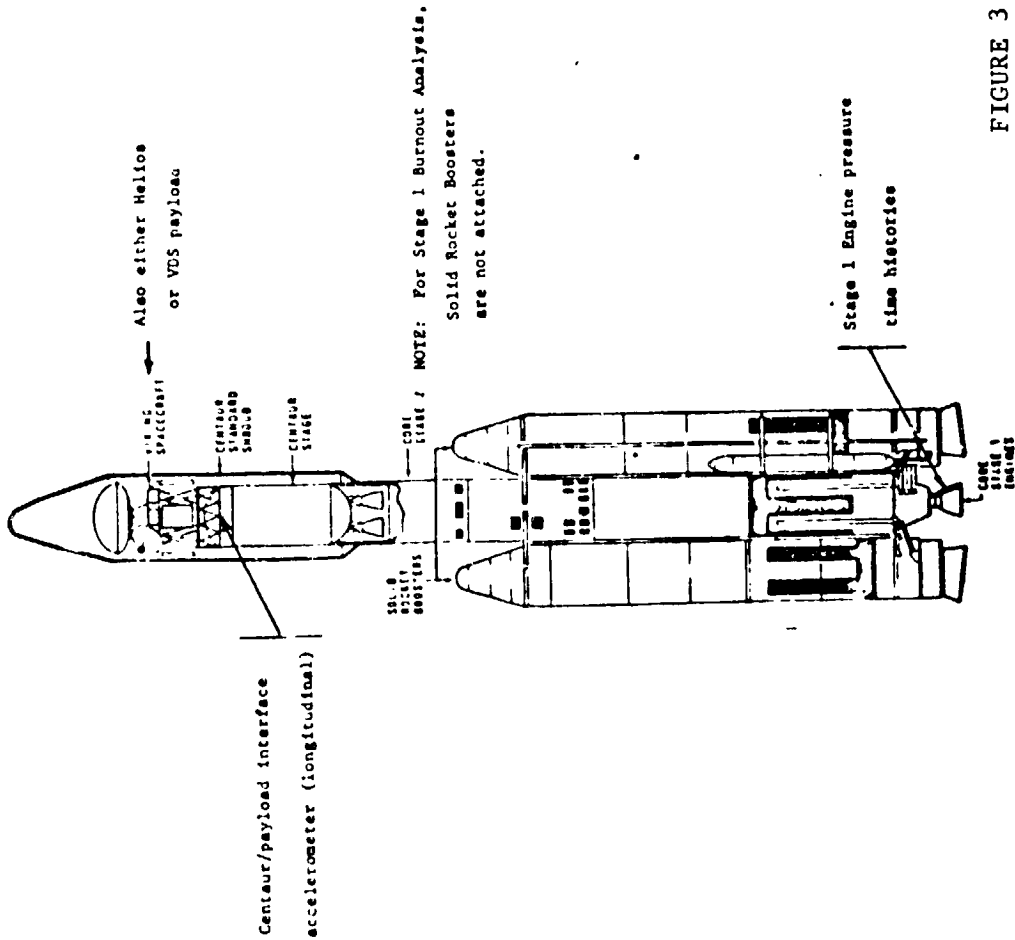


FIGURE 3

FLIGHT DATA ANALYSIS:

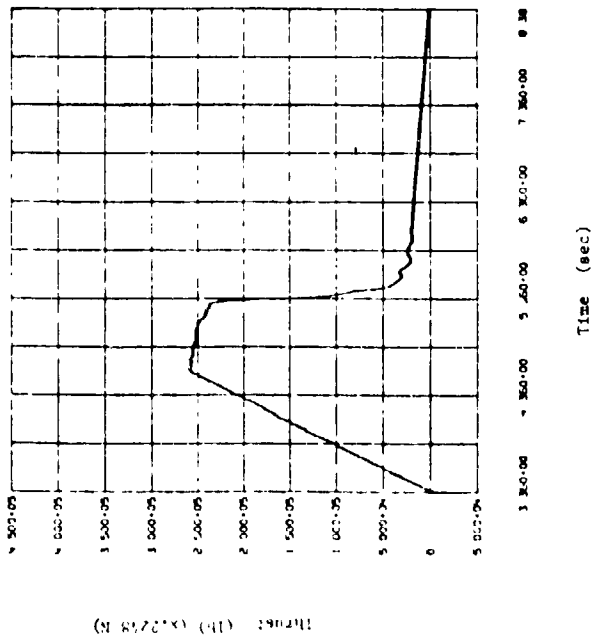
- o TIME PHASED FM/FM AND PCM FLIGHT DATA FROM E-1, E-2, E-3, AND E-4 FLIGHTS
- o DIGITIZED DATA AT 1024 SPS
- o 50 HZ LOW PASS FILTER
- o FAST FOURIER TRANSFORMS (FFT) CALCULATED FOR CMIOLA AND ENGINE PRESSURE TIME HISTORIES FOR FOUR SECONDS DURING STAGE I BURNOUT
- o IMPEDANCE TECHNIQUE USED TO PREDICT INTERFACE ACCELERATIONS WITH ANALYTICAL MODELS, THEN COMPARED TO FOURIER SPECTRA FROM FLIGHT DATA TAPES

MARTIN MARIETTA

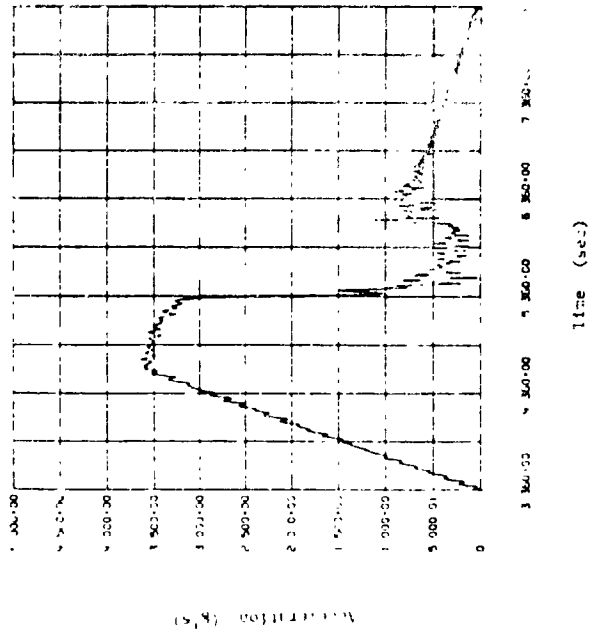
TYPICAL STAGE I BURNOUT DATA (FIGURE 4)

The troublesome characteristic of a steady-state shift in the engine pressures and CNIOIA acceleration time histories required some initial attempts at signal conditioning. The technique used in the early going was a simple "ramp." The data was forced to ramp from zero level to the steady-state level in a set interval of time. The reverse process was used at the very last of the signal to "ramp" down to zero level. Each signal from each flight was treated in the same manner to achieve commonality.

TYPICAL STAGE I BURNOUT DATA



Pressure Time History for IP315 From E-3 Stage I Burnout With Front and End Ramps



Acceleration Time History for CM101A From E-3 Stage I Burnout With Front and End Ramps

FIGURE 4



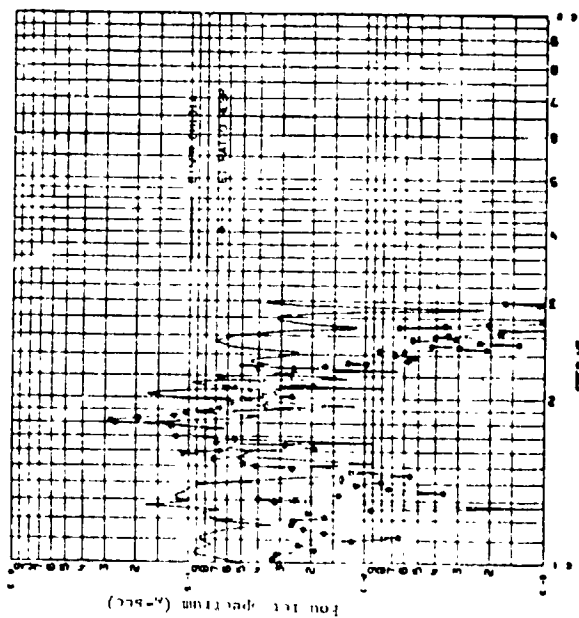
ORIGINAL PAGE IS OF POOR QUALITY

IMPEDANCE RESULTS WITH FLIGHT DATA (FIGURE 5)

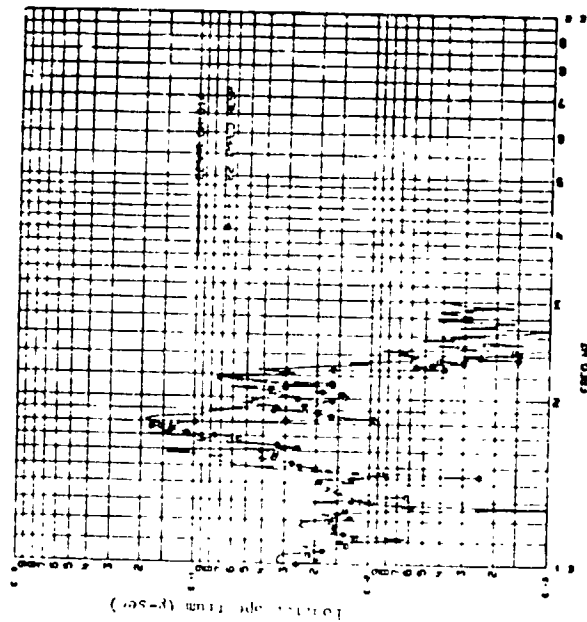
The Titan/Centaur Stage I Burnout is usually depicted by an 18 Hz longitudinal excitation at the payload/Centaur interface. The impedance technique seems to predict this response reasonably well. However, the predicted and the recorded flight data are even more different for some other frequencies.

A large portion of the discrepancy is due to the unfortunate location of CMIOIA on the circumferential position of the interface, allowing not only addition of vehicle bending modes but local dynamic characteristics as well. Another source of difference lies in the Stage I Burnout phenomena itself. The pressure time histories go through a steady-state change to an almost zero level at the shutdown. This forcing function is used to excite the structural analytical model. However, at the shutdown, Stage II ignition begins as well as the separation excitation. Therefore, accelerometer CMIOIA naturally has other content than can be generated from the Stage I engine histories.

IMPEDANCE RESULTS WITH FLIGHT DATA



Comparison of CMI01A E-1 Spectrum With
Impedance Ratio Response From E-2



Comparison of CMI01A F11-17 Data
Spectrum With Impedance Analytical
Predictions for F-2 Stead I Burnout

FIGURE 5

MARTIN MARIETTA

ORIGINAL PAGE IS
OF POOR QUALITY

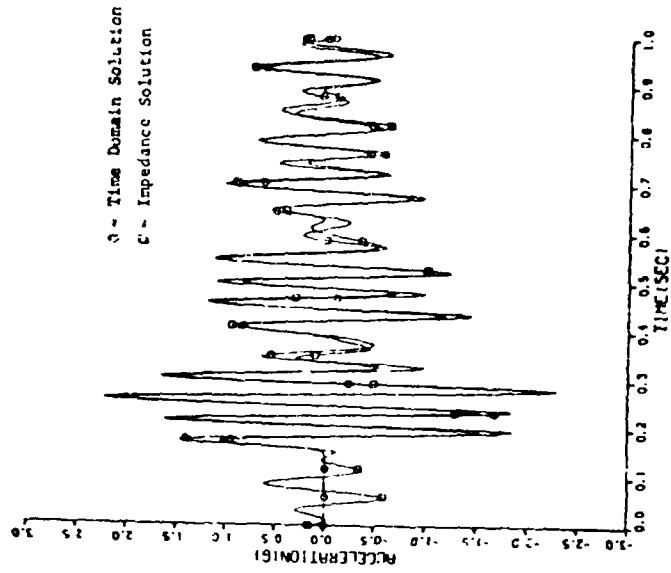
THREE MASS MODEL ANALYSIS (FIGURE 6)

The results of the Titan data analysis indicated that the Fourier spectrum form of results presentation does not relate all the insight necessary for the designer to evaluate the design limit loads. The three mass model analysis was initiated to directly compare time domain loads analysis and the frequency domain impedance technique results and evaluate the results presented as an inverse FFT.

Direct comparisons of the transfer functions of a coupled system versus the impedance transfer functions showed a resultant difference in system modal damping. However, for small values of damping this discrepancy should be negligible.

Two general types of forcing function were used: with and without a steady state value. These forcing functions were classified as damped sine waves representing engine transients.

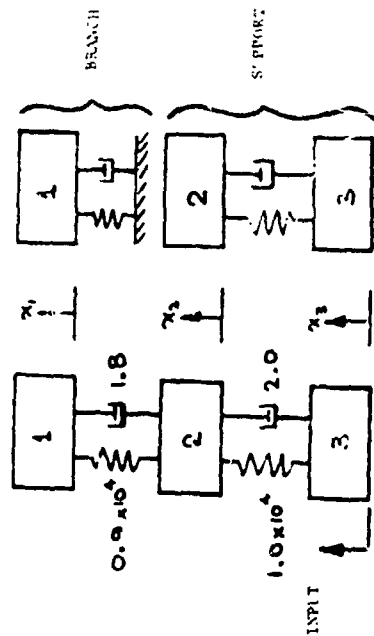
THREE MASS MODEL ANALYSIS



ORIGINAL PAGE IS OF POOR QUALITY

Time Domain Comparison of Impedance Technique Responses and Time Domain Responses to Decaying Sine With No Steady State.

FIGURE 6

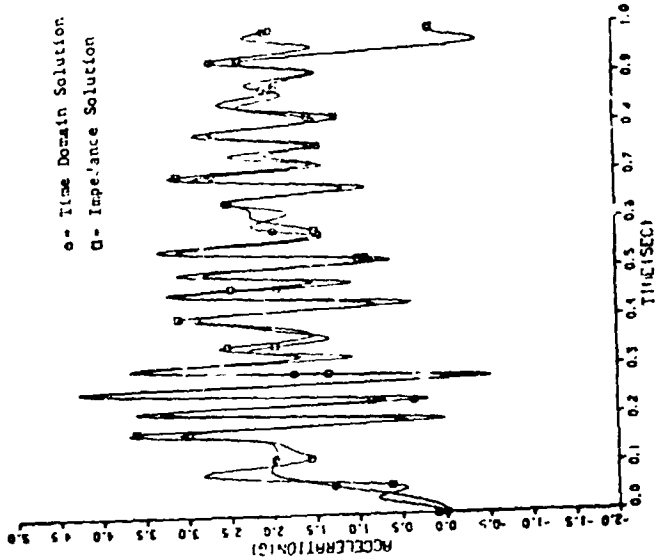


MARTIN MARIETTA

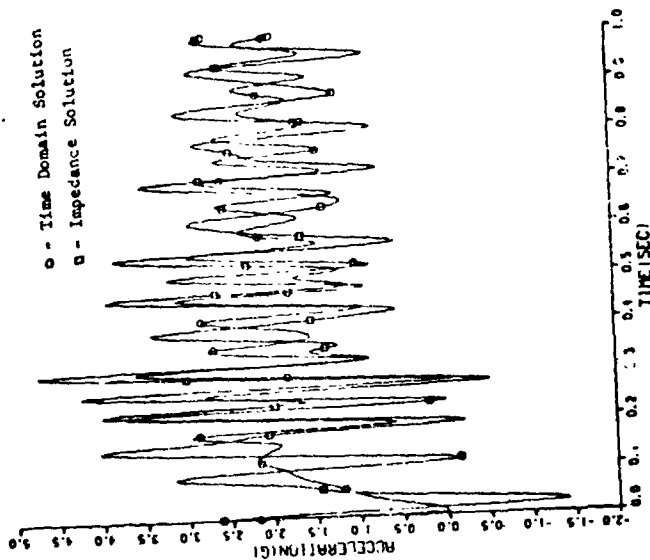
THREE MASS MODEL RESULTS (FIGURE 7)

Using the Tukey Windowing technique (usually applied to random data) excellent results were obtained with the impedance technique when applied to the forcing function with a steady-state value.

THREE MASS MODEL RESULTS



Time Domain Comparisons of Impedance
And Time Domain Solutions With A
Tukey Window.



Time Domain Comparisons of Impedance
And Time Domain Solutions Without A
Tukey Window.

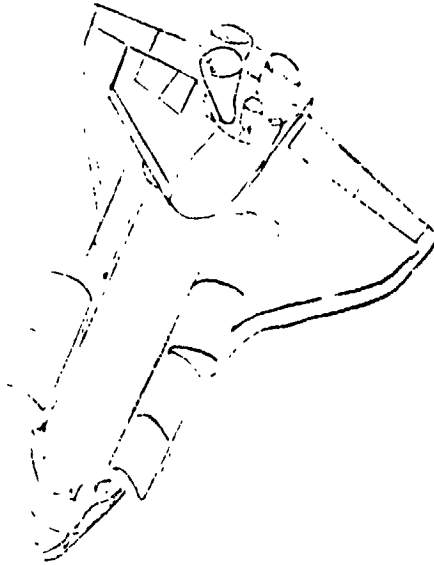
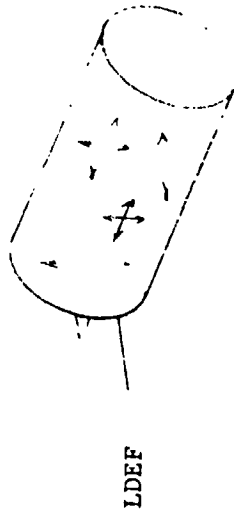
FIGURE 7

MARTIN MARIETTA

LDEF/STS PREDICTION ANALYSIS (FIGURE 8)

To further demonstrate the technique, evaluate its salient features and to form data for future flight data comparisons, the technique was used to predict the interface accelerations for the Long Duration Exposure Facility (LDEF) during two STS events: Lift-off and landing. (See Reference 1 for LP50R and LM550.)

LDEF/STS PREDICTION ANALYSIS



- o LRC PROVIDED STS MODEL
200 EIGENVECTORS
1% DAMPING FOR ALL MODES
- o LRC PROVIDED LDEF MODEL
40 EIGENVECTORS
1% DAMPING FOR ALL MODES
- o TWO EVENTS WERE ANALYZED
LIFT-OFF (62 FORCING FUNCTIONS) LP50IR
LANDING (266 FORCING FUNCTIONS) LM550

MARTIN MARIETTA

ORIGINAL PAGE IS
OF POOR QUALITY

LDEF/STS ANALYSIS RESULTS (FIGURE 9)

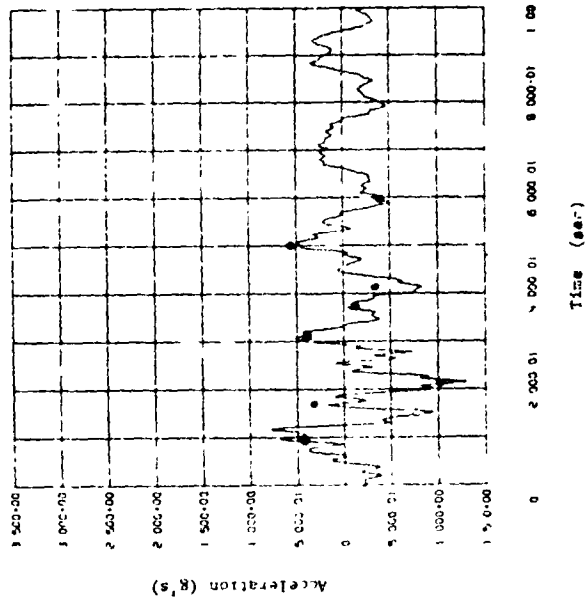
These comparisons cannot be called a "controlled" comparison. Corresponding peak amplitudes from the Rockwell report were transcribed to show relative results.

The lift-off results show by far the best comparison. Where compared to the time histories in Reference 2, the time histories of the interface accelerations are the same.

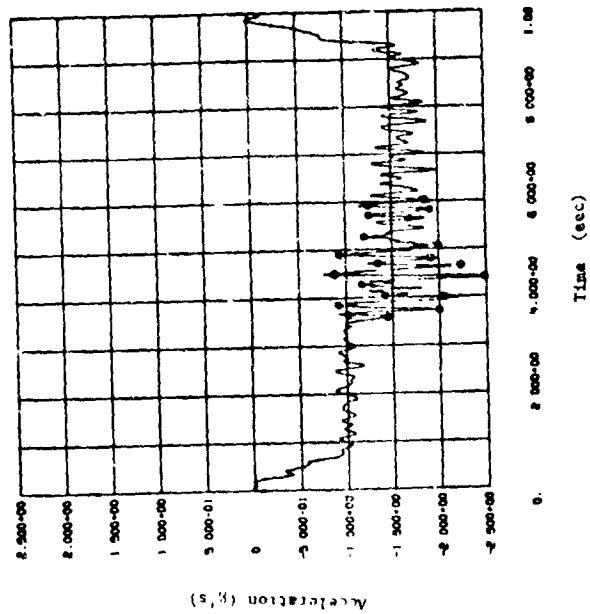
The landing results became the most significant because they pointed out the importance of frequency resolution. Two different lengths of forcing functions time histories were applied for landing. The landing strut time histories were approximately 10 seconds (while the aerodynamic forces were only 0.8 seconds in length. As a result of not having enough frequency resolution, the landing analysis was finally run with strut loads only.

IDEF/STS ANALYSIS RESULTS

532



Response X Forward Attach Right Hand Side For Landing Due To Strut Forces Only.



Response X Forward Attach Right Hand Side For Lift-Off.

FIGURE 9

MARTIN MARIETTA

ORIGINAL PAGE IS OF POOR QUALITY

CONCLUSIONS

- o TECHNIQUE REDUCES ANALYTICAL COSTS
 - ELIMINATES MODAL COUPLING
 - FREQUENCY DOMAIN COMPLEX ALGEBRA
- o DATA SYNTHESIS AND SIGNAL CONDITIONING TECHNIQUES ARE KEY ITEMS IN THE USE OF THIS TECHNIQUE
- o COMBINATION OF SPECTRAL AND TIME DOMAIN RESULTS GIVE BEST INSIGHT INTO PAYLOAD ENVIRONMENTS

MARTIN MARIETTA

REFERENCES

1. Martens, M. A., D. Artilo, D. O., and Metan, R.: Shuttle Static and Dynamic Models with Forcing Functions for MMS and LDEF Payloads. SK77-SH-0083, Rockwell International Space Division, July 1977, NAS9-14000.
2. Martens, M. A., Henkel, E. E., and Metsa, R.: Load Data Book for Long Duration Exposure Facility, Development Flight Instrumentation and Spacelab Single Pallet Cargo System. S079-SH-0116, Rockwell International Space Division, April 1977, NAS9-14000.

IMPEDANCE TECHNIQUE FUTURE USES

- o DERIVATION OF PAYLOAD LOW FREQUENCY ENVIRONMENTS WITHOUT MODAL COUPLING
- o INEXPENSIVE APPROACH TO EVALUATING PAYLOAD STRUCTURAL CHANGES
- o CREATING A DATA BANK OF LOW FREQUENCY ENVIRONMENTS FOR EARLY IMPACT ON PAYLOAD DESIGN CONSTRAINTS (ESP. PALLET MOUNTED EXPERIMENTS)

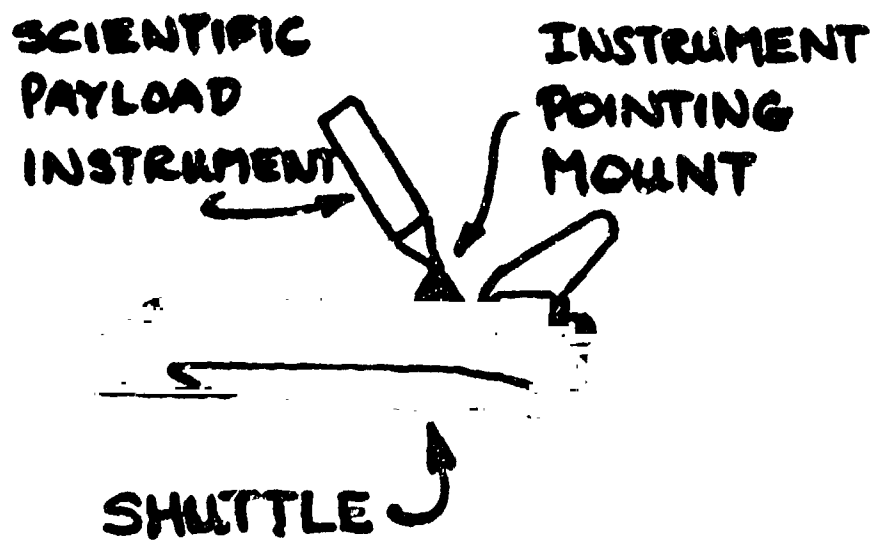
MARTIN MARIETTA

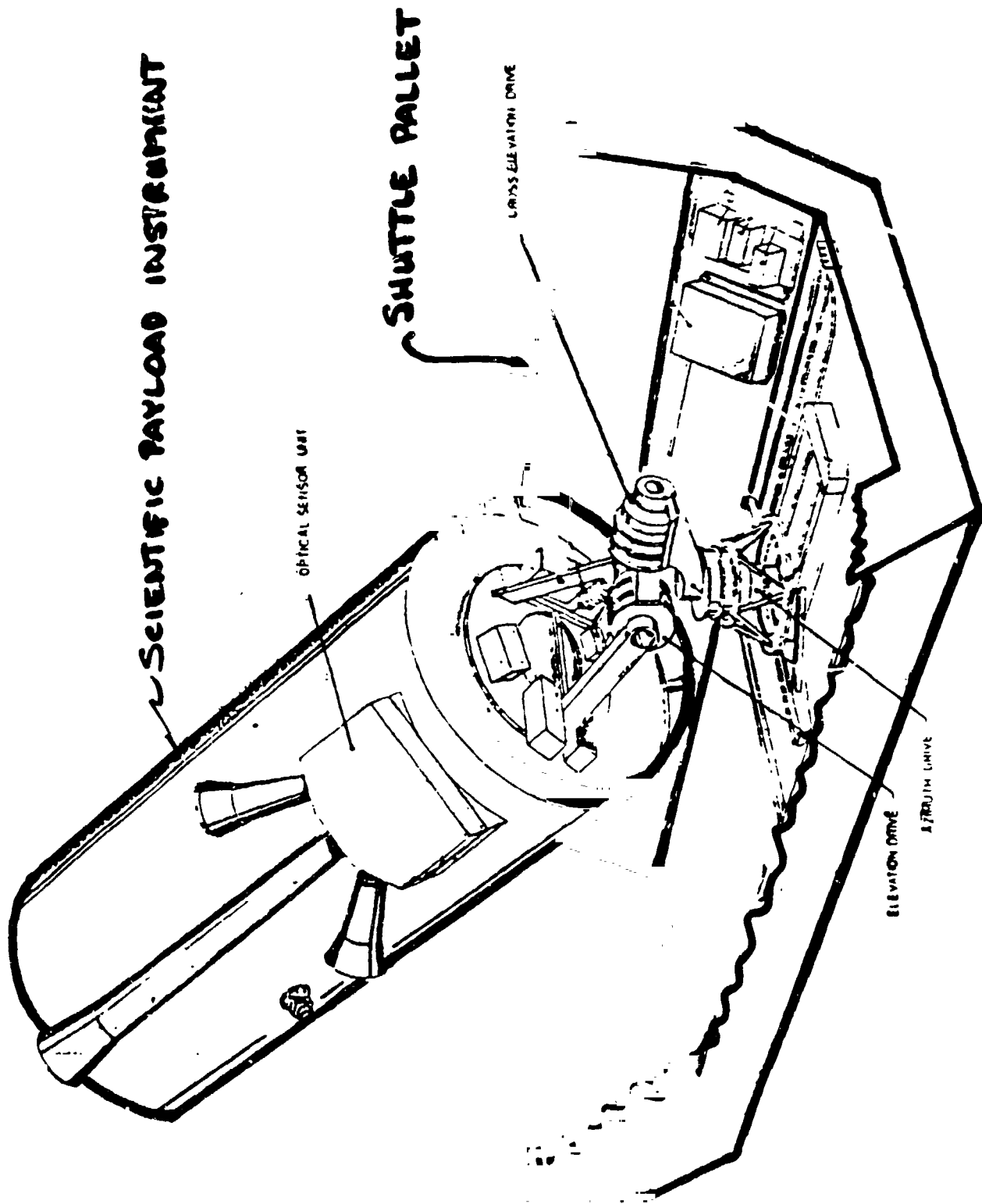
SATELLITE INSTRUMENT FLEXIBILITY
SPECIFICATION USING PARAMETER PLANE
STABILITY ANALYSIS*

PRECEDING PAGE BLANK NOT FILMED

Chittur Viswanathan
Sherman Seltzer
and
Peter Likins

* Research supported by NASA
Marshall Space Flight Center





SCIENTIFIC PAYLOAD INSTRUMENT

SHUTTLE PALLET

OPTICAL SENSOR UNIT

CROSS ELEVATION DRIVE

ELEVATION DRIVE

AZIMUTH DRIVE

INSTRUMENT POINTING SUBSYSTEM

TRADITIONAL DESIGN SEQUENCE

1. Specify structural design constraints.

- Loads
- Base accelerations
- Frequency limits
- Weight limits

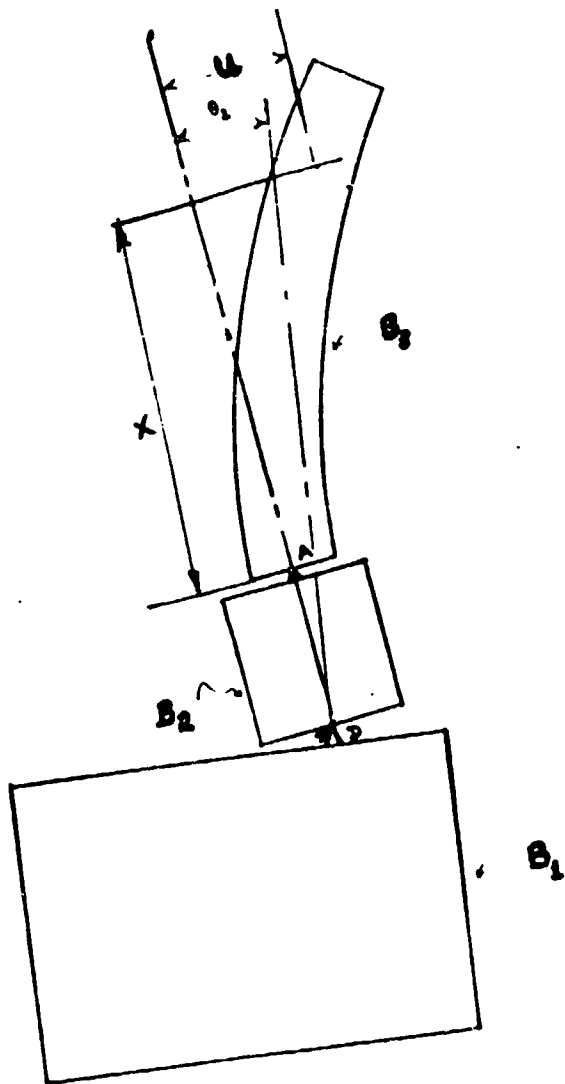
2. Design structure to meet strength, stiffness, and mass distribution requirements.

3. Design control system to meet mission performance requirements for given structure.

SHUTTLE IPS INSTRUMENT DESIGN SEQUENCE:

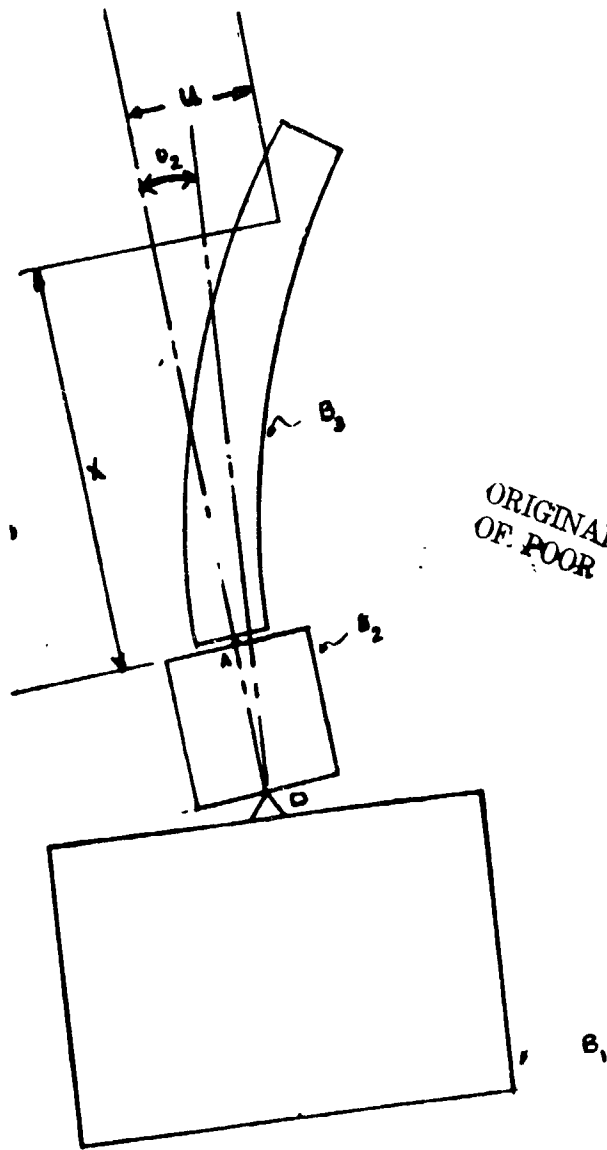
1. Specify current instrument structural design constraints.
2. Design current instrument structure.
3. Design gimbal control system for current instrument structure to meet mission performance requirements.
4. Design structure for future instruments to perform missions with given control system.

STEP #4 is new, and new methods are required to deal with this inversion of the traditional design problem.



THREE-BODY SYSTEM (A GENERAL CASE)

ORIGINAL PAGE IS
OF POOR QUALITY



ORIGINAL PAGE IS
OF POOR QUALITY

THREE-BODY SYSTEM (A SYMMETRIC CASE)

- Equations of motion.
- Linearization.
- Characteristic equation in s .
- Algebraic equations in design parameters α and β , with $s = -\zeta\omega_n + i\omega_n\sqrt{1-\zeta^2}$.
- Solution loci in α, β parameter plane, for given ζ and ascending ω_n .
- Stability boundaries in α, β parameter plane, established by $\zeta = 0$ loci.

EXAMPLE

Special Case

$\theta_2 \equiv 0$ (Gimbal locked)

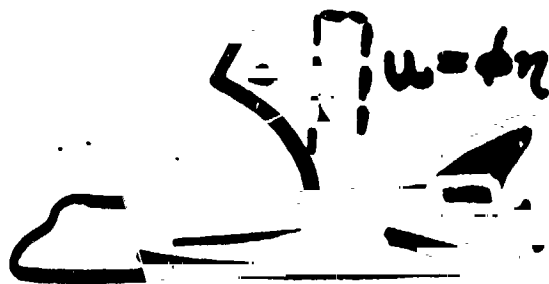
$$\tau_1 = -[k_p \theta_1 + k_d \dot{\theta}_1 + k_i \int_0^t \theta_1 dt] \quad (\text{P.D.I. control})$$

where τ_1 = vehicle control torque magnitude
and deformation $u = \phi \eta$ (single mode).

Linearized equations of motion

$$I^* \ddot{\theta}_1 - \delta \ddot{\eta} = \tau_1$$

$$\ddot{\eta} + 2\zeta_n \sigma \dot{\eta} + \sigma^2 \eta - \delta \ddot{\theta}_1 = 0$$



Characteristic equation

$$\sum_{j=0}^5 f_j s^j = 0$$

$$f_0 = a_I \sigma^2$$

$$f_1 = a_P \sigma^2 + 2s_A a_I \sigma$$

$$f_2 = a_0 \sigma^2 + 2s_A a_P \sigma + a_I$$

$$f_3 = \sigma^2 + 2s_A a_0 \sigma + a_P$$

$$f_4 = 2s_A \sigma + a_0$$

$$f_5 = 1 - \frac{\delta^2}{I^*}$$

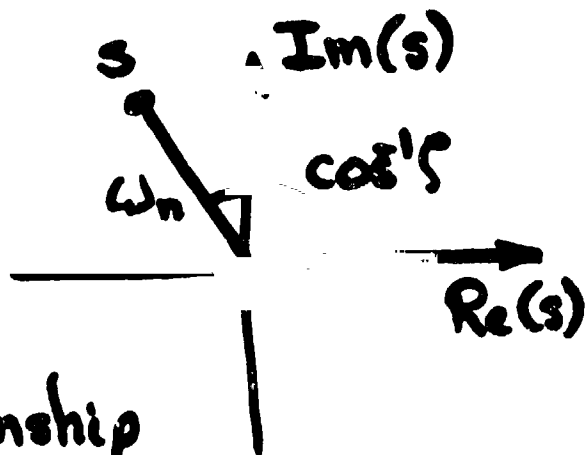
where $a_P = \frac{k_P}{I^*}$

$$a_0 = \frac{k_0}{I^*}$$

$$a_I = \frac{k_I}{I^*}$$

Let $s \triangleq -\zeta\omega_n + i\omega_n\sqrt{1-\zeta^2}$
for complex roots

Let $s^j \triangleq X_j + iY_j$



Note recursive relationship

$$Z_j = -2\zeta\omega_n Z_{j-1} - \omega_n^2 Z_{j-2}$$

for $Z_j = X_j$ and $Z_j = Y_j$

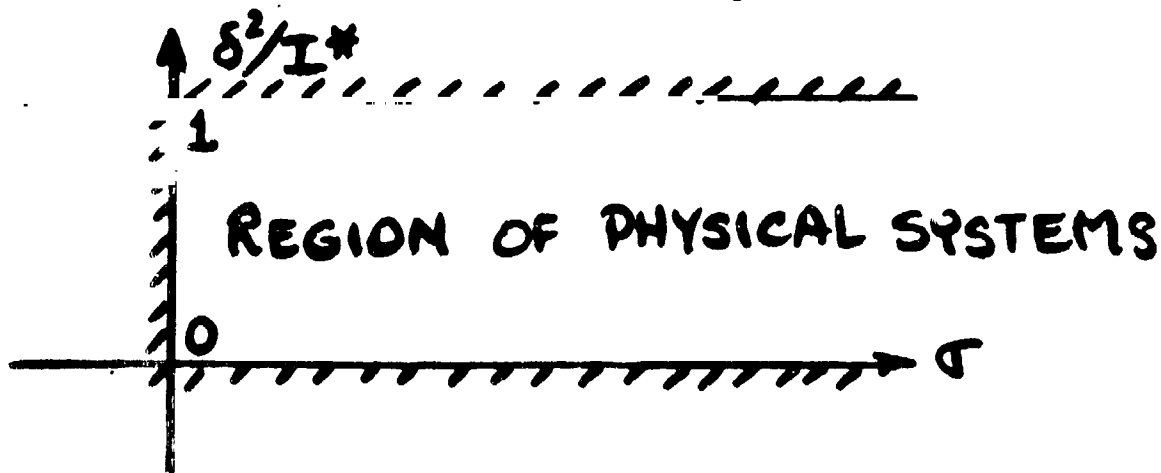
Characteristic equations (real & imaginary)

$$\sum_{j=0}^5 f_j X_j = 0 \Rightarrow A_1 \sigma^2 + A_2 \sigma + A_3 (\delta^2 / I^*) + A_4 = 0$$

$$\sum_{j=0}^5 f_j Y_j = 0 \Rightarrow B_1 \sigma^2 + B_2 \sigma + B_3 (\delta^2 / I^*) + B_4 = 0$$

Given A_k and B_k ($k=1, \dots, 4$)

can solve for σ (2 values) and δ^2 / I^*



Let $s = \sigma \pm j\omega$ for real roots

$$\sum_{j=0}^5 f_j U^j = 0 \Rightarrow C_1 \sigma^2 + C_2 \sigma + C_3 (\delta^2 / I^*) + C_4 = 0$$

Given C_k ($k=1, \dots, 4$) can solve for $\sigma = \sigma(\delta^2 / I^*)$.

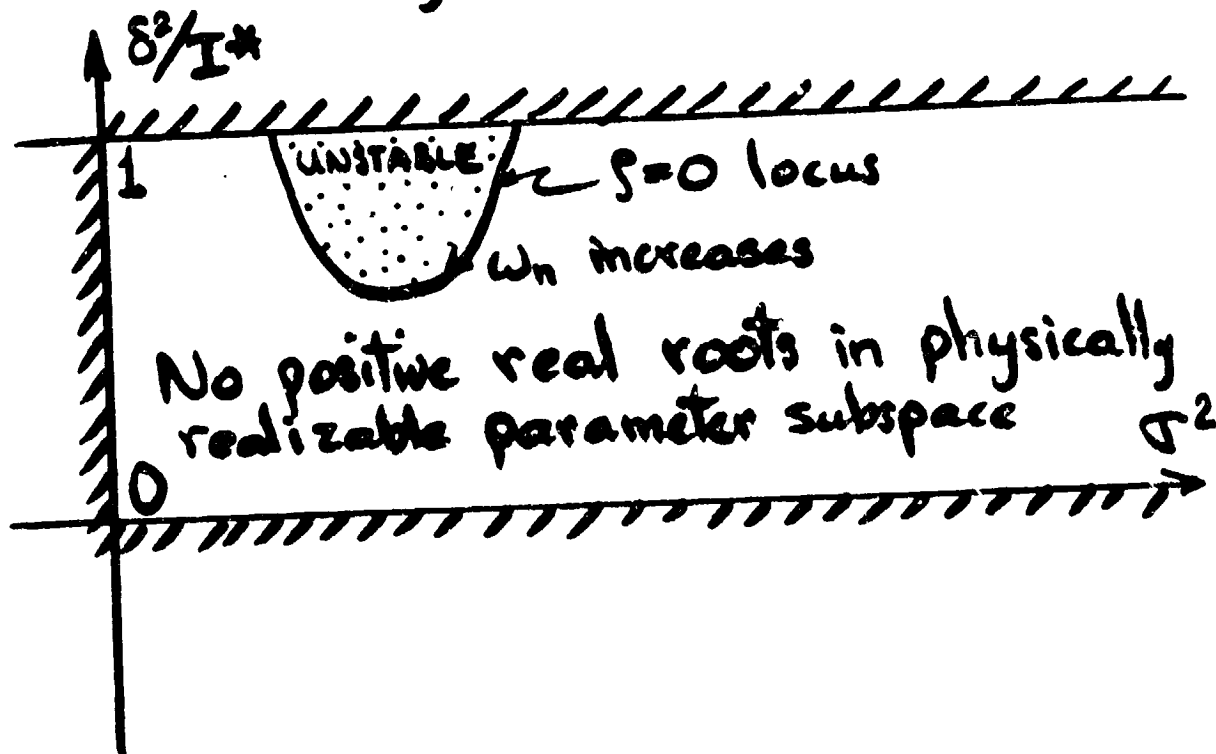
STABILITY ANALYSIS

(1) Find regions with positive real roots ($\sigma > 0$)

(2) Find loci of imaginary roots ($\sigma = 0$)

(3) Apply conformal mapping rules

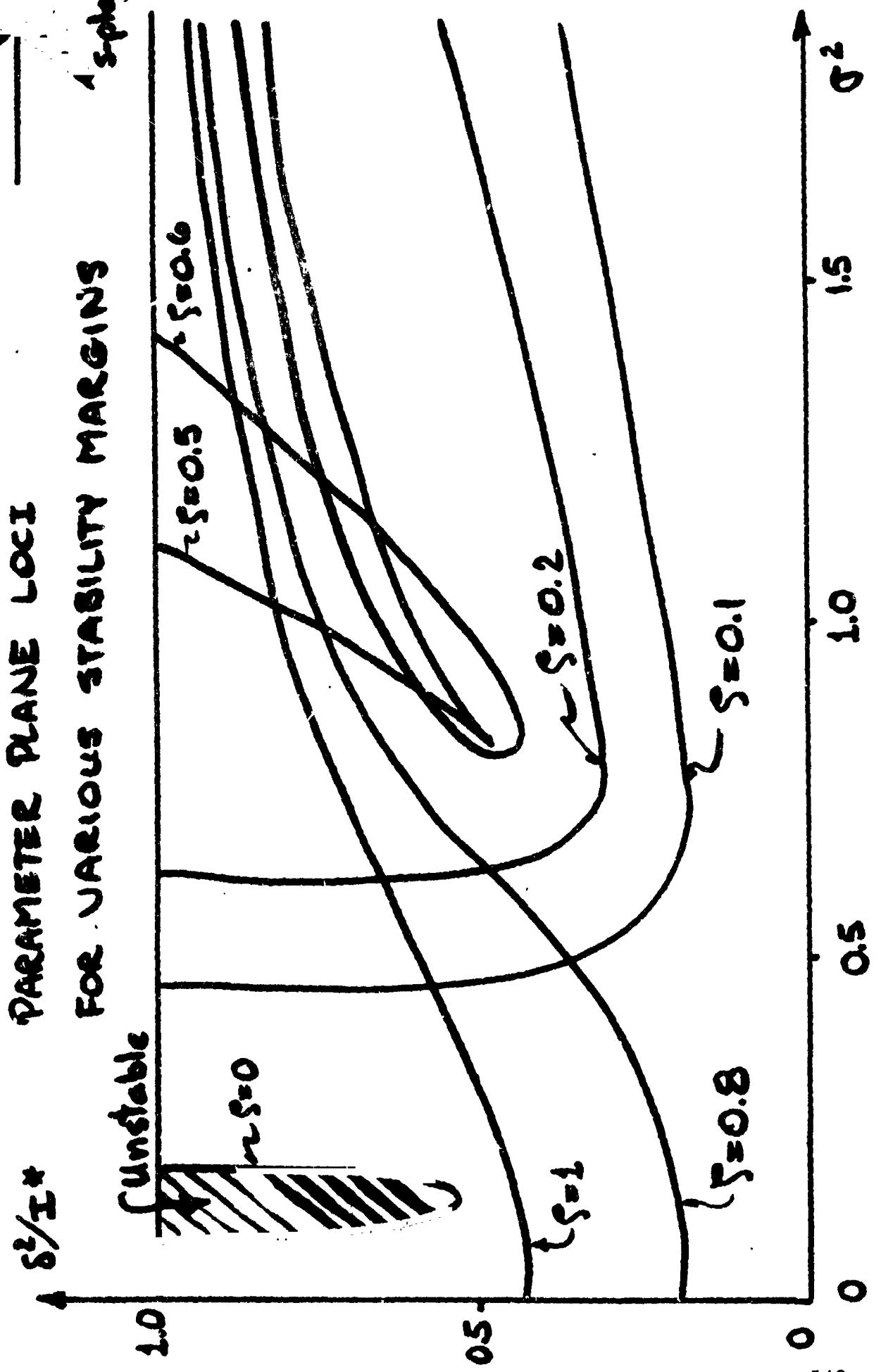
or parameter point stability analyses to identify parameter regions of stability

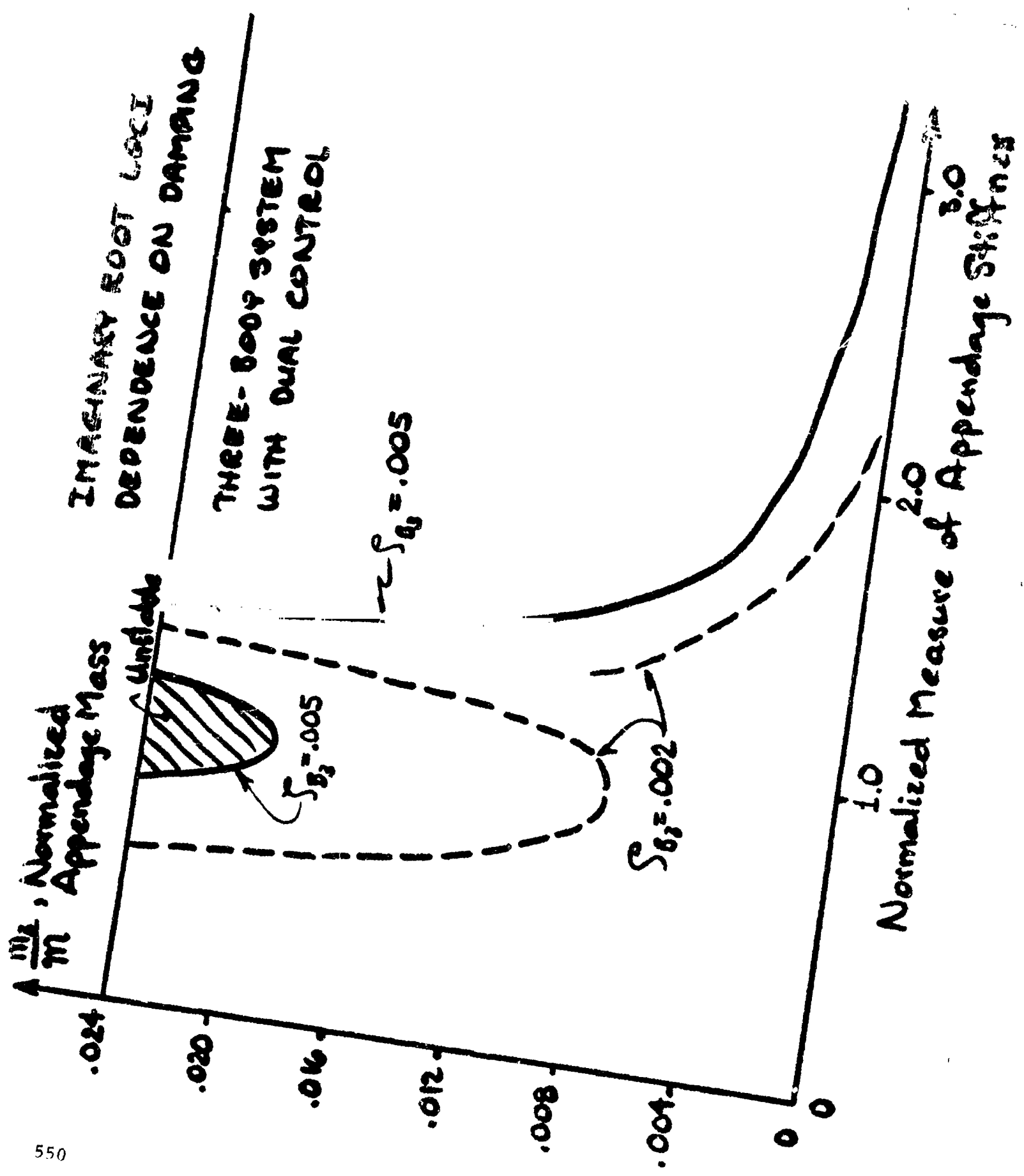




PARAMETER PLANE LOCI FOR VARIOUS STABILITY MARGINS

s -plane







PAYLOAD Z-LOAD ALLEVIATION STUDY

J. DAWSON
R. GARDNER
H. WING
S. YAHATA



PAYLOADS GENERALLY EXPERIENCE LARGE DYNAMIC RESPONSE DURING LIFTOFF AND LANDING. AN EXAMPLE OF THIS IS ILLUSTRATED BY THE FOLLOWING PLOT SHOWING THE ACCELERATION AS A FUNCTION OF THE ORBITER STATION FOR THE IUS PAYLOAD. THE LARGE ACCELERATIONS INDICATE A NEED FOR LOAD ALLEVIATING DEVICES. THIS STUDY IS AN ATTEMPT TO INVESTIGATE VARIOUS DESIGN CONCEPTS TO ALLEVIATE THE HIGH Z LOADS DUE TO THESE LARGE ACCELERATIONS. ONE DEVICE CONCEPT (VISCIOUS DAMPER) WAS SELECTED FOR STUDY. THE ADVANTAGE OF USING THIS CONCEPT IS THAT IT CAN BE READILY EMPLOYED FOR ALMOST ANY PAYLOAD THAT EXCEEDS THE ALLOWABLE ACCELERATION WITHOUT ANY MAJOR REDESIGN EFFORT INVOLVED.

UNFORTUNATELY THE ANALYSIS WAS NOT COMPLETED TO PROVE THAT SUCH A SYSTEM DOES ALLEVIATE THE PAYLOAD Z LOAD. DUE TO MANPOWER PRIORITY, THE DYNAMIC ANALYSIS COULD NOT BE COMPLETED. THE STUDY WAS DISCONTINUED. THE DEVICES RECOMMENDED SHOW SOME PROMISE, AND THAT THIS STUDY SHOULD BE COMPLETED.





Z AXIS PAYLOAD LOAD ALLEVIATION FEASIBILITY STUDY

CHART 1

PROBLEM

- o LARGE ACCELERATIONS FOR CANTILEVERED AND SOME NON-CANTILEVERED PAYLOADS DURING LIFTOFF AND LANDING.
- o Z LOADS DUE TO ACCELERATION MAY EXCEED PAYLOAD ALLOWABLE.

APPROACH TO PROBLEM

- o REDESIGN OF PAYLOAD OR CARRIER MAY NOT BE FEASIBLE.
- o ALTERNATIVE - LOAD ALLEVIATING DEVICES.

TASK DESCRIPTION

- o IDENTIFY AND MAKE CONCEPTUAL DESIGN OF TWO CONCEPTS OF PROVIDING FORWARD IUS PAYLOAD AND TIE SUPPORTS.
- o CONCEPTS TO BE SUCH THAT THEY CAN BE MODELED FOR DYNAMIC ANALYSIS.

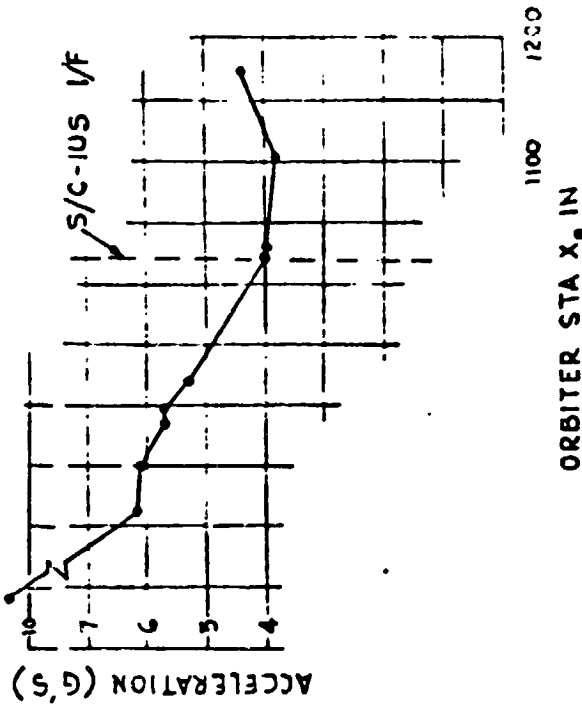
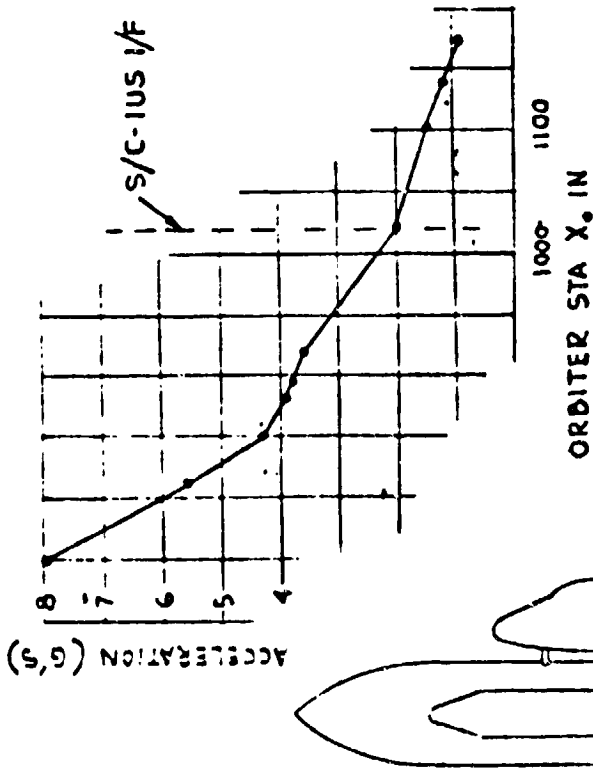
STATUS

- o CONCEPTUAL DESIGN COMPLETED.
- o DYNAMIC ANALYSIS NOT COMPLETED (MANPOWER NOT AVAILABLE).
- o STUDY DISCONTINUED.

PAYLOAD Z-LOAD ALLEVIATION STUDY

CHART 2

554





PAYLOAD CANTILEVERED FROM A CARRIER SUCH AS AN IUS MOUNTED ON A HARD CRADLE EXPERIENCE HIGH ACCELERATIONS DURING LIFTOFF AND LANDING LOAD EVENTS. THE ACCELERATIONS COMPUTED FOR ONE PAYLOAD ARE ILLUSTRATED ON CHART NO. 2. THIS STUDY IS AN ATTEMPT TO INVESTIGATE VARIOUS ALTERNATE DESIGN DEVICE CONCEPTS TO ALLEVIATE THE HIGH Z LOADS. ONE DEVICE CONCEPT WAS SELECTED AND ANALYZED. THE RESULTS OF THIS STUDY ARE BEING PRESENTED.

THE ADVANTAGE OF USING THIS CONCEPT IS THAT IT CAN BE READILY EMPLOYED FOR PAYLOADS WHICH EXCEED THE ALLOWABLE ACCELERATION WITHOUT ANY MAJOR REDESIGN EFFORT INVOLVED.



GUIDELINES

- USE BOEING TWIN-STAGE CRADLE
- ALLOW P/L TO MOVE AT LOW VELOCITIES
 - ✓ THERMAL DEFORMATIONS
 - ✓ STATIC DISPLACEMENT-RETAIN DETERMINATE SUSPENSION
- ATTENUATION MUST BE SOFTER THAN CRADLE
 - ✓ BENDING MOMENT AT S/C-IUS I/F
- REDUCE S/C VERTICAL ACCELERATIONS TO ACCEPTABLE LEVEL
 - ✓ REDUCE VERTICAL DISPLACEMENT VELOCITIES
- ATTENUATION LOADS MUST NOT CREATE BENDING MOMENTS ON S/C BEYOND ALLOWABLE LIMIT
 - ✓ LOADS MUST BE WITHIN ORBITER STRUCTURAL ALLOWABLES AT DEVICE ATTACH POINT





THE GUIDELINES AGREED UPON FOR THIS STUDY ARE THE FOLLOWING:

WE WILL USE THE CRADLE USED ON THE BOEING TWIN-STAGE IUS. THE DEVICE SHOULD BE SELF-LEVELING AND ADJUSTABLE SO THAT IT CAN ACCOMMODATE ANY THERMAL DEFORMATION OR STATIC DEFLECTION AND STILL MAINTAIN A DETERMINATE SUSPENSION SYSTEM.

THE ATTENUATION PROVIDED MUST BE SUCH THAT THE BENDING MOMENT AT THE S/C-IUS INTERFACE IS MINIMAL. ALSO, THE DEVICE SHOULD REDUCE THE "VERTICAL" (Z) DISPLACEMENTS AND ACCELERATIONS TO ACCEPTABLE LEVEL.

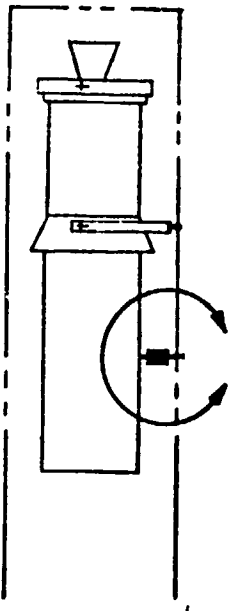
IN ADDITION, THE ATTENUATOR LOADS MUST NOT CREATE BENDING MOMENTS ON THE SPACECRAFT THAT EXCEEDS THE ALLOWABLE NOR LOADS EXCEEDING THE KEEL ALLOWABLE.





DEVICE CONCEPTS

- HONEYCOMB
- TOR-SHOK/ROTO-SHOK
- VISCOUS DAMPER
- FRICITION DAMPER
- AIR BAG
- ATTENUATOR STRAP
- SECONDARY CRADLE



✓ NO IMPACT ON BAC CRADLE



SOME OF THE DEVICES SELECTED FOR STUDY ARE SHOWN ON THE CHART "DEVICE CONCEPT". SOME OF THESE DEVICES, SUCH AS HONEYCOMB AND AIR BAG, ARE "SINGLE" ACTION DEVICES WHICH WILL BE EFFECTIVE ONLY IN ALLEVIATING LANDING LOADS AND, HENCE, ARE ADAPTABLE TO RETRIEVABLE NON-DEPLOYED PAYLOADS. OTHER DEVICES WERE DOUBLE-ACTION. HENCE, THIS SUGGESTS THAT THE STUDY OF THE VARIOUS DEVICES SHOULD CONSIDER THEIR ADAPTABILITY TO DIFFERENT TYPES OF PAYLOADS.



CONCEPT COMPARISONS

CHART 5

560

System	Adaptable To P/L GP*	Tech Feasibility	Producibility	Est. Wt. Incl I/F Attach	Double Action	Impact On Interface	Comments
Contained Honeycomb	Retrieved	Ldg Only	State of the Art	40	No	Attach Pts at S/C	Consumed Stroke
	Non-Deployed						
Tor-Shok	Retrieved	Ldg Only	Exist Mfg. Item	50	Yes	Attach Pts at S/C	Hysteresis
	Non-Deployed			60			
Viscous Damper	All *	All Events Min Effect at Ldg	State of the Art Close Tol. Mach.	147	Yes	Attach Pts at S/C	Excellent Stroke
	All *	All Events Min Effect at Ldg	State of the Art Close Tol. Mach.	155	Yes	Attach Pts at S/C	Hysteresis
Air Bag	Retrieved Non-Deployed	Ldg Only	State of the Art	220	No	Struct Back-Up Req'd on Orbiter	Gas Syst. Req'd
Attenuator Strap	Retrieved Non-Deployed	Ldg. Only	State of the Art	45	No	None	
Secondary Cradle	All *	All Events	State of the Art	390 +440* *	Yes	Attach Pts at S/C	Thermal Issues, - Wt

*PAYLOAD GROUPS: NON-DEPLOYABLE
 DEPLOYABLE (ONLY)
 DEPLOYABLE AND RETRIEVABLE
 RETRIEVED (ONLY)

**LONG & KEEL BRIDGES, FTGS

VISCOUS DAMPER WAS SELECTED



Rockwell International



A COMPARISON STUDY WAS MADE OF THE VARIOUS LOAD ALLEVIATING DEVICES CONSIDERING THEIR ADAPTABILITY TO THE DIFFERENT PAYLOAD GROUPS, THEIR REPRODUCIBILITY, EVENTS IN WHICH THEY WILL BE EFFECTIVE, ETC. THE RESULTS OF THIS STUDY ARE SUMMARIZED IN THE TABLE THAT FOLLOWS.

FROM THIS STUDY, IT WAS DECIDED THAT THE VISCOUS DAMPER WAS THE MOST PROMISING SINCE IT CAN BE USED FOR ALL PAYLOAD GROUPS, AND WILL ALLEVIATE LOAD FOR ALL EVENTS.

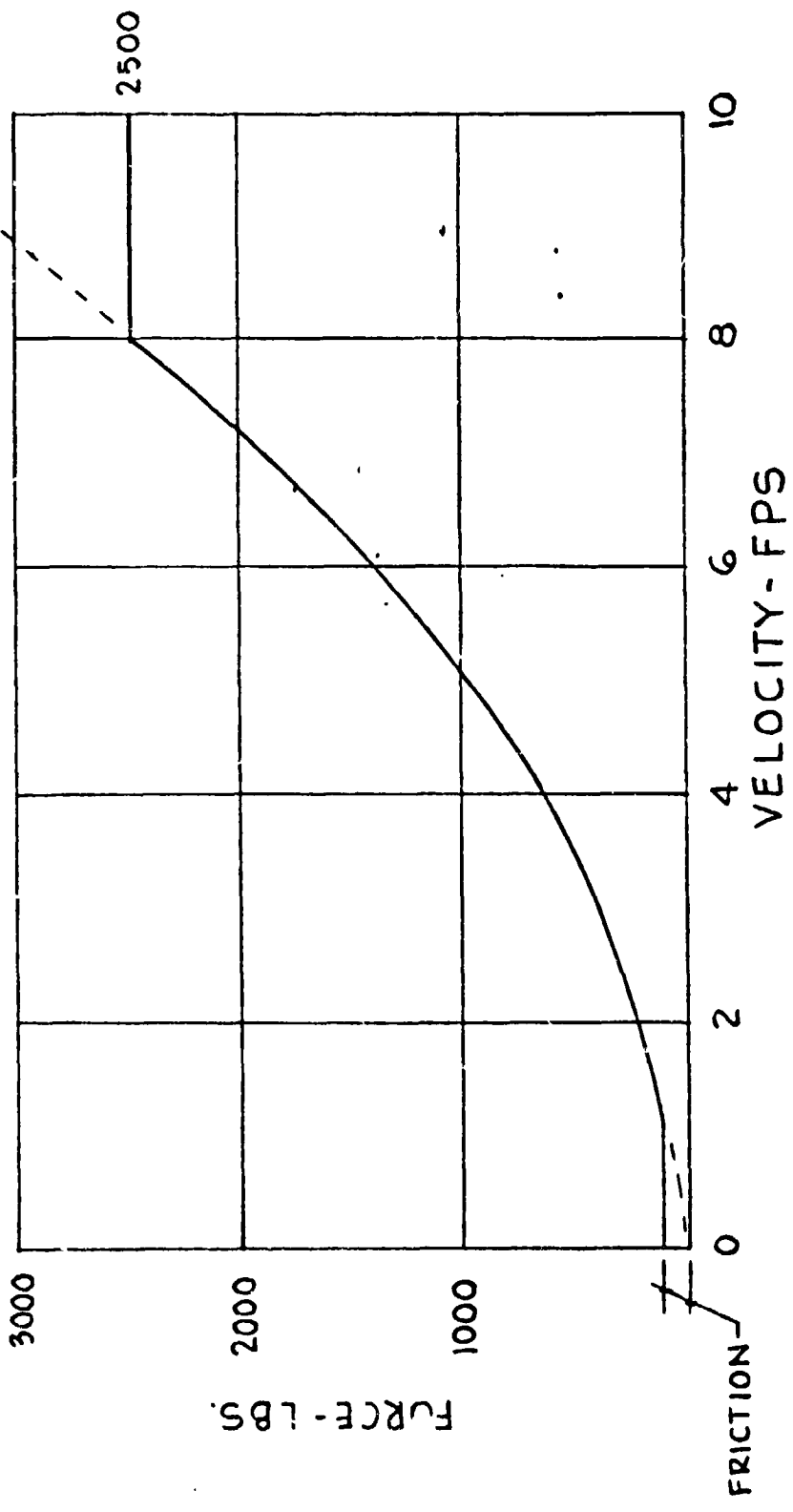


FORCE / VELOCITY CURVE FOR HYDRAULIC SHOCK ABSORBER SYSTEM

CHART 6

3" CYLINDER, 1" SHAFT
0.52" SMOOTH ORIFICE
LIGHT WEIGHT OIL (MIL 5606)

DAMPER A





DAMPER A IS A SIMPLE POSITION-ORIFICE TYPE VISCOUS DAMPER WHICH CAN ABSORB A MAXIMUM FORCE OF 2,500 LBS. AT 8 FPS AND ABOVE. THIS PARTICULAR DAMPER HAS A STROKE OF + 9". BELOW THE CUTOFF VELOCITY OF 8 FPS, THE FORCE VARIES AS THE SQUARE OF THE VELOCITY IN FPS.

$$F = 39V^2$$

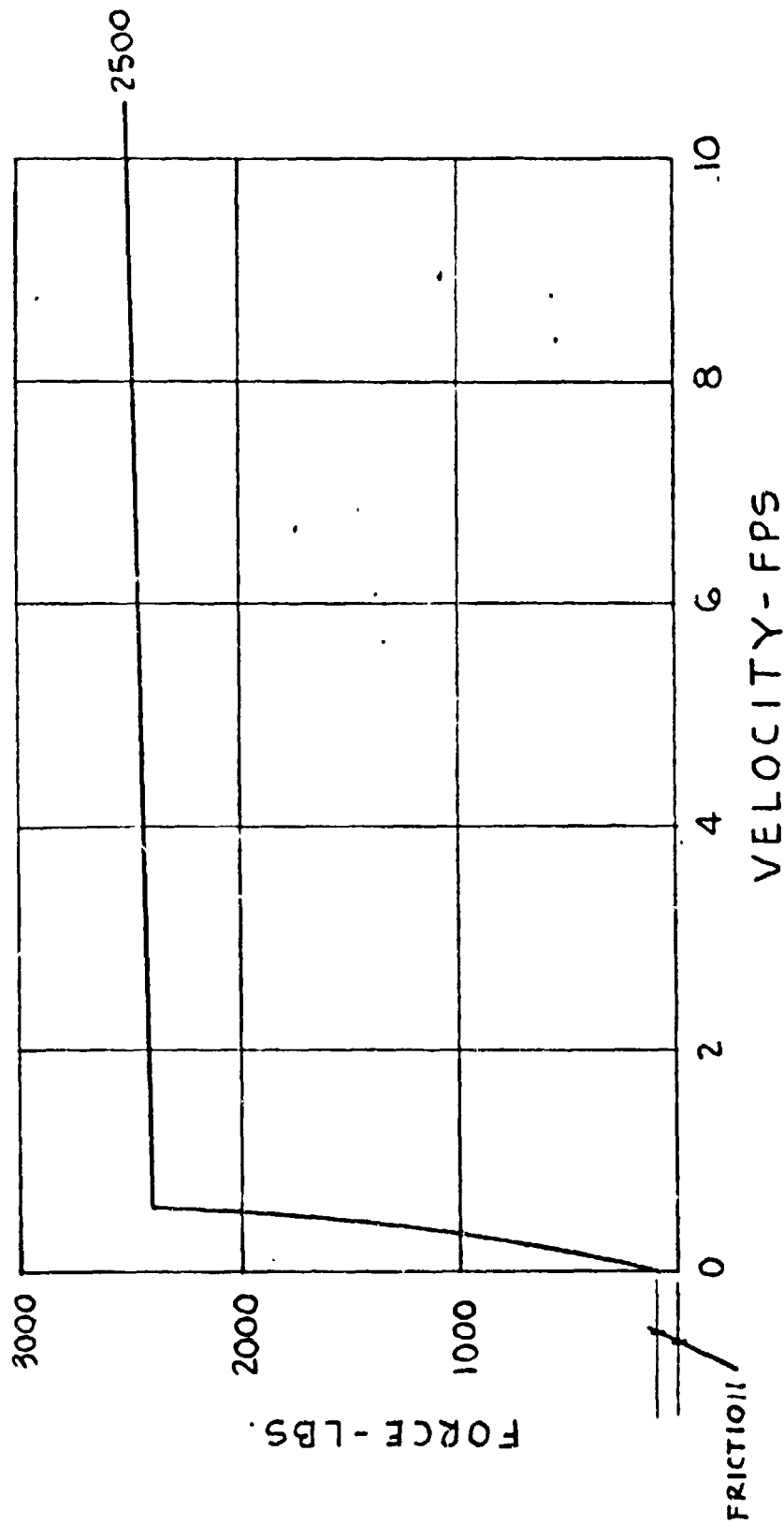


(ALTERNATE) FORCE/VELOCITY CURVE FOR HYDRAULIC SHOCK
ABSORBER SYSTEM

CHART 7

3" DIA CYLINDER, 1" SHAFT
.040 ORIFICE (4)
MIL 5606 OIL

DAMPER B





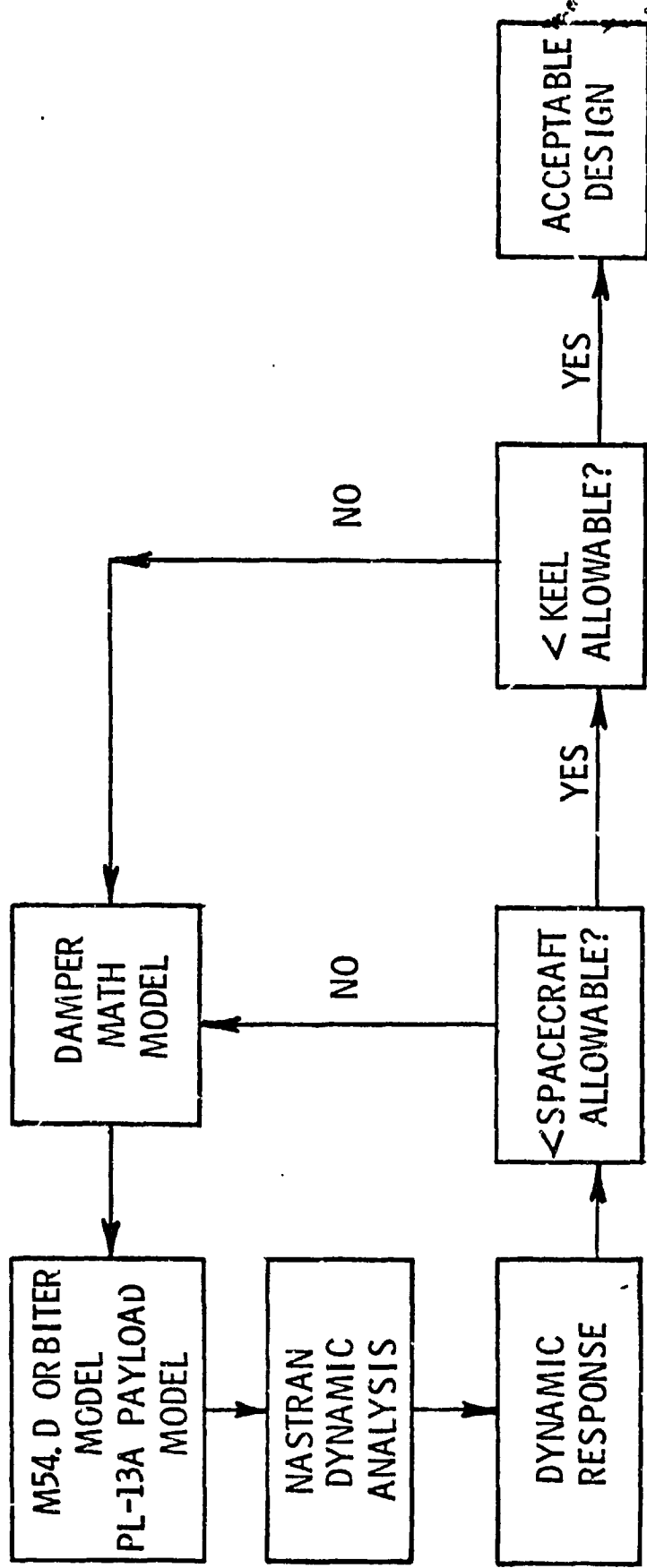
DAMPER B IS DAMPER A WITH FOUR SETS OF RELIEF VALVES (BALL WITH SPRING), TWO FOR "UP STROKE" AND TWO FOR "DOWN" STROKE. THE VALVES ARE SET FOR RELIEF AT 500 PSI AND WILL RESEAT AT 450 PSI. FULL FLOW IS ATTAINED AT 475 PSI.





566

DYNAMIC ANALYSIS FLOW CHART





DYNAMIC ANALYSIS

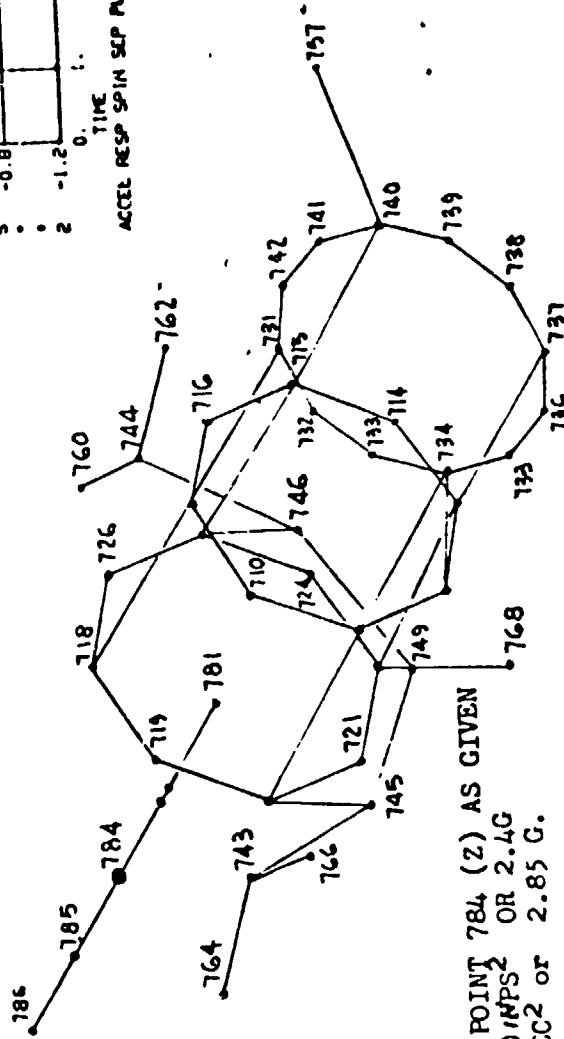
SINCE THE LOAD CHARACTERISTIC OF THE VISCOUS DAMPER IS NONLINEAR, IT WAS NECESSARY TO MODEL IT IN NASTRAN USING EXTRA POINTS. ONE OF THESE EXTRA POINTS IS DEFINED BY THE DIFFERENCE IN VELOCITIES OF THE DAMPER ATTACH POINTS. THE DAMPER FORCE IS EXPRESSED IN TERMS OF THIS EXTRA POINT.

THE USE OF THE EXTRA POINT APPROACH HAS ONE ADVANTAGE OVER USING A PHYSICAL ELEMENT FOR THE DAMPER. IT ALLOWS US TO USE BOTH ORBITER AND PAYLOAD MODES OBTAINED FROM OUR COMPUTER RUNS DIRECTLY WITHOUT ALTERATION IN OBTAINING THE SYSTEM RESPONSE.

THIS DAMPER MODEL IS INCORPORATED INTO THE M5.4D ORBITER MODEL WITH PL-13A ATTACHED. A NASTRAN ANALYSIS IS THEN MADE TO DETERMINE THE DYNAMIC RESPONSE OF THE SYSTEM. THESE RESULTS ARE COMPARED TO BOTH THE SPACECRAFT AND KEEL ALLOWABLES. IF BOTH CRITERIA ARE MET, THE DAMPER DESIGN IS SATISFACTORY. IF EITHER ONE OF THE ALLOWABLES IS EXCEEDED, THE PROCESS IS REPEATED WITH NEW DAMPER PARAMETERS.

THE ACCELERATIONS OF THE MAIN BODY OF THE ORBITER HAS NOT BEEN PLOTTED BUT CERTAIN MAXIMUM VALUES ARE AVAILABLE AS FOLLOWS:

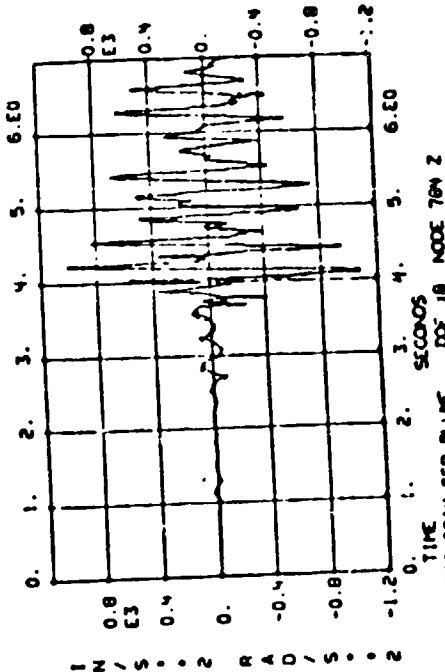
- POINT 784 Z - 1093.644 @ 4.100 Seconds.
- 1010.269 @ 4.229
- @ ABOUT 6 cps.
- POINT 744 Z - 591.255 @ 4.030
- 676.168 @ 3.93



ACCELERATION OF POINT 784 (Z) AS GIVEN IN THE PLOT IS + 900 IN/SEC² OR 2.4G AND - 1.1 x 10³ IN/SEC² OR 2.85 G.

ASSUMING linear MOTION,
 $S = \frac{1}{2} at^2$ with $a = 2.5 G$ and $t = 1/12 \text{ sec.}$
 then $S = 0.3 \text{ FT}$ or about 3.5 inches.
 $V = at$ Thus $V = 6.7 \text{ FPS.}$

TIME PHASING OF THE MOTION OF THE PAYLOAD AND MOTION OF THE ORBITER IS UNKNOWN THUS THEY MAY BE MOVING TOGETHER OR APART.





THIS GRAPH SHOWS A SCHEMATIC OF THE MATH MODEL OF PAYLOAD PL-13A. NODES 781 THROUGH 786 ARE MASS POINTS ON THE SPACECRAFT. THE DAMPER IS ATTACHED TO THE SPACECRAFT AT NODE 784. THE ACCELERATION OF THIS PARTICULAR NODE IS SHOWN ON THE PLOT AT THE UPPER RIGHT-HAND CORNER OF THE GRAPH. IT SHOWS THAT THE MINIMUM AND MAXIMUM ACCELERATIONS OF THE DAMPER ATTACH POINT ARE $-1,093 \text{ IN/SEC}^2$ AND 900 IN/SEC^2 , RESPECTIVELY. THESE TWO UNDAMPED ACCELERATIONS CORRESPOND TO 2.85 G'S AND 2.40 G'S. THE OBJECTIVE OF THE DYNAMIC ANALYSIS IS TO DETERMINE HOW EFFECTIVE A VISCOUS DAMPER WILL BE IN ATTENUATING THESE ACCELERATIONS.

PRECEDING PAGE BLANK NOT FILMED

SPACE SHUTTLE PAYLOAD LOAD ALLEVIATION USING BILINEAR LIQUID SPRINGS

R. G. Huntington,* R. E. Martin** and W. M. Dreyer†

General Dynamics Convair Division
San Diego, California

ORIGINAL PAGE IS
OF POOR QUALITY

ABSTRACT

A method has been developed for attenuating payload response to Space Shuttle Orbiter landing loads. The attenuation system consists of preloaded bilinear liquid springs acting between the payload and Orbiter. The springs provide high stiffness during liftoff when Shuttle input loads are of low frequency and moderate magnitude. During landing, when Orbiter-induced loads are high, the spring preload is exceeded, lowering the system frequency and attenuating payload response to the higher-frequency input. A nonlinear analysis procedure is employed and results are correlated with test data obtained from a one-third scale dynamic model.

INTRODUCTION

Two important goals of the Space Shuttle program are to:

1. Provide the simplest possible interface with a multiplicity of payloads.
2. Accept existing space payloads with little or no redesign.

From the standpoint of structural loads, these goals have been found to conflict, particularly for the larger payloads to be carried beyond low-earth orbit by the Interim Upper Stage (IUS). It is desired that the IUS be designed to be compact (allowing maximum payload size) and that all payloads attach only to a standard interface on the IUS (not directly to the Orbiter).

Dynamic studies have shown that critical design loads for most spacecraft will result from either the Space Shuttle liftoff transient or from landing of the Orbiter after an aborted mission. Further, normal (pitch-plane) load factors on the payload substantially exceed the 2 to 5g typical of current launch vehicles and, in some cases, the allowable attachment loads on the Orbiter are exceeded.

This paper describes a bilinear liquid spring for attaching the IUS to the Orbiter that provides the proper dynamic characteristics to attenuate both liftoff and landing loads to levels consistent with current expendable launch vehicles. The nonlinear dynamic analysis approach and its validation through dynamic model tests are also presented.

DYNAMIC ENVIRONMENT

Figure 1 illustrates a hypothetical spacecraft 10 feet in diameter, 40 feet long, and weighing 5 000 lb that is typical of one class of payloads requiring an IUS for boost to higher orbit. The potential for high normal accelerations of the spacecraft and high local loads at the IUS attachment points is obvious from the geometry.

Both critical design conditions for payload major structure and the attachments are transient loading conditions. Liftoff loads result from worst-case thrust buildup rates and thrust differentials among the three Orbiter liquid rockets

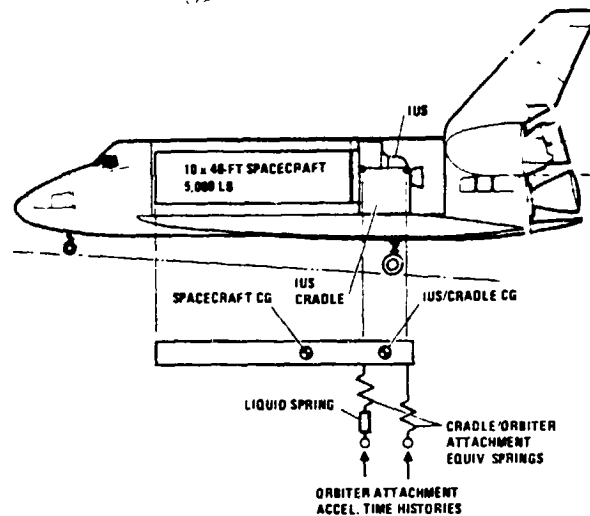


Figure 1. Trend model.

and the two large solid-propellant booster rockets as the complete Shuttle vehicle lifts off the launch pad. The second critical load condition results if the mission is aborted and the Orbiter lands with a complete payload at the design sink rate of 10 fps. The analytically predicted shock spectra at the IUS-to-Orbiter attach points for these conditions are shown in Figure 2. A shock spectrum is a plot of the peak response of a single-degree-of-freedom system to the load transient as a function of the system's natural frequency. Thus, payload mounting natural frequencies in the 4 to 5 Hz region will cause high dynamic responses for the liftoff condition, while the 17 Hz region is critical for abort landing.

Trend studies were performed using the simple model of Figure 1 to determine potential load levels as a function of the mounting stiffness. Due to the large overhang, most of the response comes from the fundamental pitching mode. Figure 3 shows the peak normal acceleration at the spacecraft center of gravity as a function of the fundamental pitching frequency.

It is seen that for liftoff a frequency greater than 7 Hz is required, but this frequency range produces unacceptably high accelerations at landing. Conversely, for landing, a frequency below 5 Hz is desired but gives unacceptable liftoff accelerations. A mounting frequency well below 5 Hz is ruled out due to large deflections at the tip of the spacecraft and the potential for coupling with Shuttle control system or propulsion system modes. Frequencies above the 17 Hz region are not practical due to the excess structural weight needed to achieve that degree of stiffness. Thus, the Shuttle dynamic environment requires different mounting stiffnesses at liftoff and abort landing to hold payload accelerations to the desired low levels.

* Chief of Structural Dynamics, Member AIAA

** Manager of Structures Technology, Associate Fellow AIAA

† Senior Dynamics Engineer

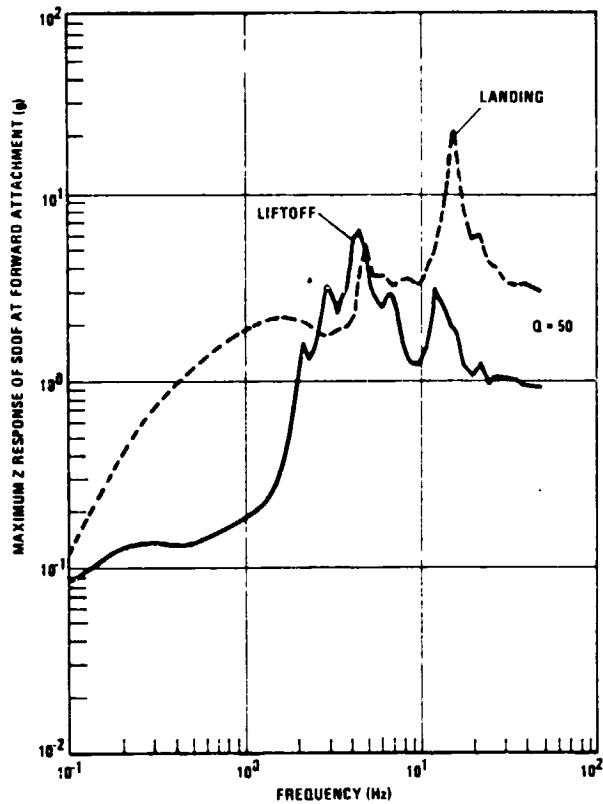


Figure 2. Orbiter forward attachment point shock spectra.

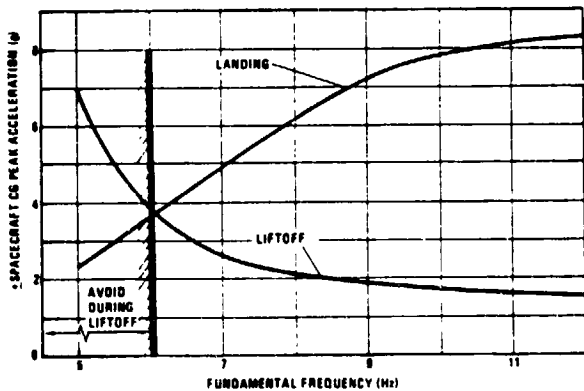


Figure 3. Spacecraft cg peak acceleration due to liftoff and landing versus fundamental pitch frequency.

LOAD ALLEVIATION CONCEPT

Several concepts were evaluated for providing the dual stiffness characteristics required to minimize payload response. The selected design consists of a stiff IUS structure mounted to the Orbiter by bilinear liquid springs. These springs provide high stiffness under the moderate liftoff loading condition and low stiffness during severe landings.

High structural stiffness is achieved through the support cradle system shown in Figure 4. The cradle acts as a "strongback" for the IUS and carries loads from the IUS to the Orbiter bay cargo attachment points. Figure 5 shows the six cradle-to-Orbiter support locations and the reaction force directions.

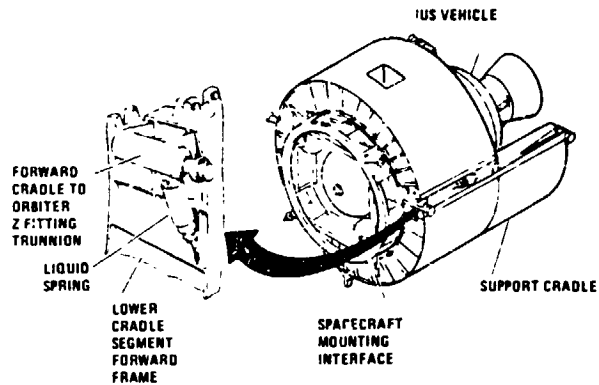


Figure 4. Bilinear liquid spring cradle-to-Orbiter attachment.

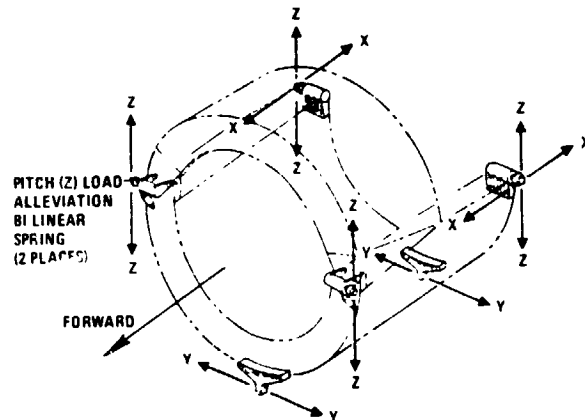


Figure 5. Cradle-to-Orbiter support reactions.

Since landing response is primarily in the Orbiter vertical (pitch) plane, liquid springs were considered only for the four cradle-to-Orbiter Z-attachments. Trend studies showed, however, that the aft springs contributed little to dynamic load reduction. Therefore, liquid springs were incorporated only at the two forward Z-attachments.

Liquid springs were selected for this application because they are light, compact, reliable, and have been space-qualified. A liquid spring stores energy by fluid compression and its piston orifices provide damping. Liquid spring double-action is achieved by mechanical caging, as shown in Figure 6. With this arrangement, the internal force due to differential piston area keeps the spring nulled until preload is exceeded. Preloading is achieved by silicone fluid pressurization at assembly. Until the preload is exceeded, no fluid compression takes place and only the structural stiffness of the IUS/cradle/Orbiter system is active. When the liquid spring preload is exceeded, fluid is compressed and the system stiffness drops to essentially that of the liquid spring. Reference 1 presents a detailed explanation of the liquid spring support system.

ANALYTICAL APPROACH

Dynamic analysis of the load alleviation system uses the method of normal modes calculated with an assumed linearized spring and incorporates the spring nonlinearity as part of the generalized force in the equations of motion. Figure 7 shows the bilinear force deflection curve characterizing the liquid spring. As pointed out in Reference 2, it is extremely important to account for this bilinear effect in the dynamic analysis (rather than use an average stiffness value) to determine the response accurately.

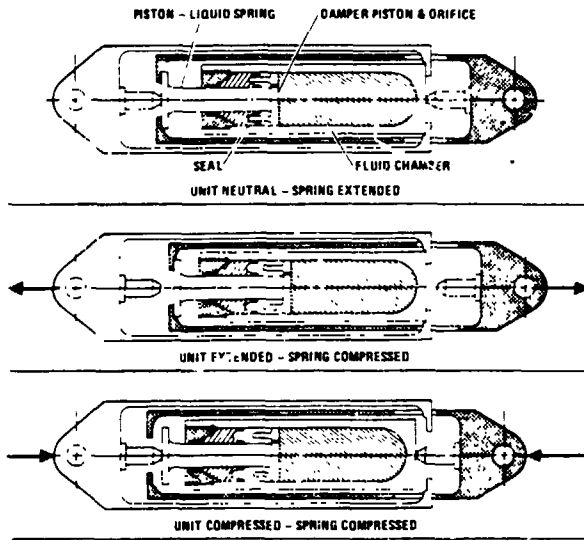


Figure 6. Liquid spring double-action capability.

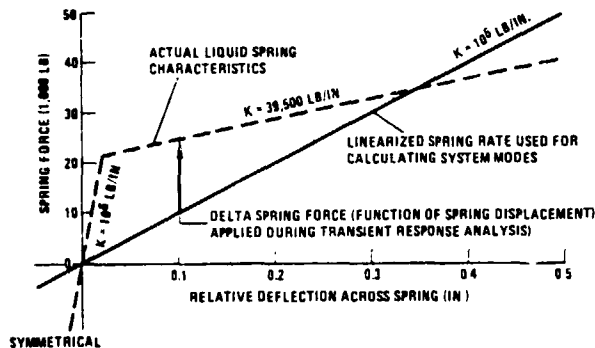


Figure 7. IUS liquid spring characteristics.

For a linear system, the equations of motion in matrix notation are given by:

$$[m] \{\ddot{x}\} + [c] \{\dot{x}\} + [k] \{x\} = \{F(t)\} \quad (1)$$

where $[m]$, $[c]$, and $[k]$ are the mass, damping, and stiffness matrices, respectively; while $\{F(t)\}$ is the time-dependent applied force vector. The variables x , \dot{x} , and \ddot{x} are displacement, velocity, and acceleration, respectively.

These equations are solved using normal (with respect to both the mass and stiffness matrices) modes as generalized coordinates by making the substitution:

$$\{x\} = [\Phi] \{q\} \quad (2)$$

where $[\Phi]$ is the matrix of modal vectors and $\{q\}$ is the vector of time-dependent generalized coordinates. This yields the equation of motion:

$$[\ddot{q}] + [2\zeta\omega] \{\dot{q}\} + [\omega^2] \{q\} = [M]^{-1} [\Phi]^T \{F(t)\} \quad (3)$$

where $[M]$ is the generalized mass matrix, ω is modal circular frequency, ζ is modal damping (c/c_{cr}) and the matrix superscripts -1 and T represent inverse and transpose, respectively.

Eq 3 is solved numerically by standard integration techniques for $\{q\}$, and its derivatives as a function of time. Displacements, velocities, and accelerations are obtained by substitution into Eq 2.

For a nonlinear system, the nonlinearities are treated as external forces and introduced into the right side of Eq 3 so that the right side becomes:

$$= [M]^{-1} [\Phi]^T \{F(t) + \bar{F}\} \quad (4)$$

where \bar{F} is the nonlinear force. The modal parameters $[\omega]$, $[M]^{-1}$ and $[\Phi]$ are based on the assumed linear spring represented by the solid line in Figure 7.

Nonlinear forces are described in terms of forces and damping coefficients whose magnitudes are functions of the relative displacement between two points on the structure. Specifically, at any two points on the structure, i and j , the total nonlinear forces are given by:

$$\bar{F}_i = \bar{P}(x_j - x_i) + \bar{C}(x_j - x_i) \cdot (\dot{x}_j - \dot{x}_i) \quad (5)$$

$$\bar{F}_j = -\bar{F}_i \quad (6)$$

where $\bar{P}(x_j - x_i)$ is the force as a function of relative displacement between i and j and $\bar{C}(x_j - x_i)$ is the damping coefficient as a function of relative displacement between i and j . Obviously, since the nonlinear forces are functions of displacement, a sufficient number of modes must be included in the analysis to describe the displacements adequately.

In this case, x_i and x_j represent the displacements of nodes in the finite-element model on either side of the liquid spring and are elements of $\{x\}$. The nonlinear spring force, \bar{P} , is obtained by table lookup of the force difference between the solid and dashed lines of Figure 7 for the given relative deflection, $x_j - x_i$. The liquid spring has a nearly constant damping coefficient so that $\bar{C}(x_j - x_i) \approx \bar{C}$ and the addition of the liquid spring damping to the generalized force is just $\bar{C}(\dot{x}_j - \dot{x}_i)$. Modal structural damping is estimated from experience and included in the left side of Eq 3. Eq 3 with the right-hand side modified by Eq 4 to include nonlinear forces, is solved incrementally in time by the same numerical integration techniques as in the linear case. At each time increment, the nonlinear forces are computed as a function of the appropriate relative deflections and added to the linear (time-dependent) forces.

The usual checks are made to determine that a small enough integration time increment is used to get acceptable accuracy. In addition, our experience has shown that better accuracy is obtained if the arbitrary linearized spring constant is closer to the lower of the bilinear spring constants. If it is too near the higher spring constant, too many modes are required to get accurate deflections.

Both liftoff and landing analyses considered only the symmetric (pitch plane) response. Liftoff forcing functions consisted of Orbiter engine and solid rocket motor thrust, stand reactions, and applied wind loads. Landing forcing functions included the longitudinal and vertical components of main landing loads at the fore and aft gear attachment points for a symmetrical landing condition.

The spacecraft analyzed was assumed to be rigid, 40 feet long, and to weigh 5,000 lb. It was cantilevered from the forward end of the IUS. The IUS/cradle system was 16 feet long and weighed 36,500 lb.

Modes for the spacecraft/IUS/cradle and Shuttle were obtained separately and then combined via mode synthesis. For the Shuttle, the lowest 48 free-free symmetric modes were employed without payload and unconstrained at the cradle attachment points. The spacecraft/IUS/cradle modes consisted of the lowest 13 symmetric modes with the system assumed fixed at the cradle/Orbiter attachment points. Each liquid spring was linearized to a value of 100 lb/in for mode computation, as shown in Figure 7. Total system modes were obtained by the component mode synthesis method described in References 3 and 4.

In the response analysis, the first 50 system normal modes were included. This covered the frequency range up to 24 Hz for liftoff and 38 Hz for landing. Liquid spring bilinear stiffness characteristics are shown in Figure 7. The damping coefficient for each liquid spring was assumed to be a constant 880 lb-sec/in.

ANALYSIS RESULTS

Typical time histories of spacecraft center of gravity (cg) transient accelerations during Orbiter landing are shown in Figures 8 and 9. As seen in Figure 8, maximum acceleration with no load alleviation is 5.6g and occurs 0.25 second after touchdown. Peak negative acceleration is -2.7g at $t = 0.74$ second. Figure 9 shows the corresponding response based on analysis using the liquid spring model. It can be seen that the nature of the response is quite different. Maximum positive acceleration still occurs at $t = 0.25$ second, but is reduced in magnitude to 3.4g. Peak negative acceleration is increased to -3.5g and occurs earlier at $t = 0.40$ second.

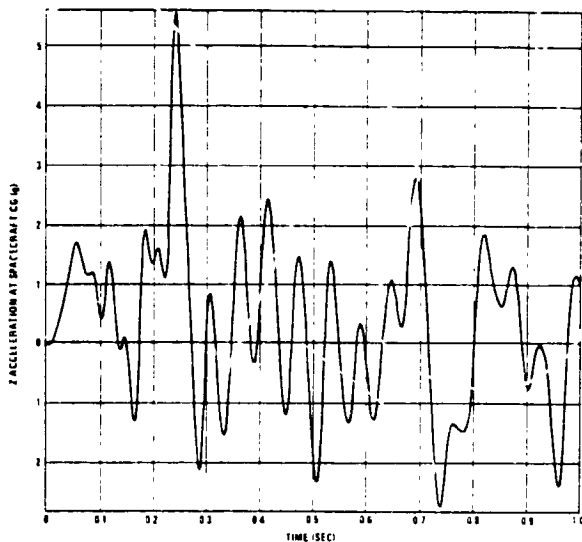


Figure 8. Landing response of spacecraft cg without load alleviation

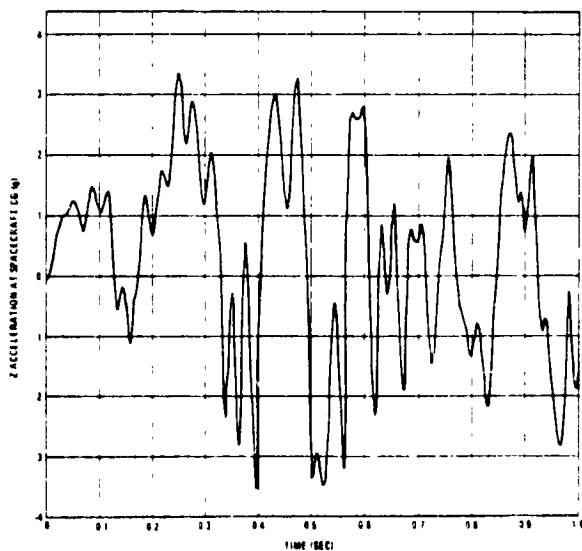


Figure 9 Landing response of spacecraft cg with load alleviation.

Figure 10 presents corresponding time histories of relative deflections between the IUS cradle and the Orbiter forward Z-attachment for the linear and nonlinear systems. For the linear system (no load alleviation), the peak relative deflection is about 0.072 inch (compression), producing a force on each Orbiter forward attachment of 72,000 lb. With the liquid spring connecting the cradle to the Orbiter at the forward supports, the peak relative deflection increases to -0.42 inch, but the maximum reaction force at each Orbiter forward Z-support is reduced to 37,100 lb. The liquid spring preload was set at 21,750 lb, corresponding to 0.022 inch relative deflection. This corresponds to approximately 2g load factor at the forward Z-attachments. The nonlinear analysis shows that a substantial portion of the total response time is spent on the soft portion of the stiffness curve during landing. Liftoff response calculations for this configuration predict that peak reactions never exceed the liquid spring preload.

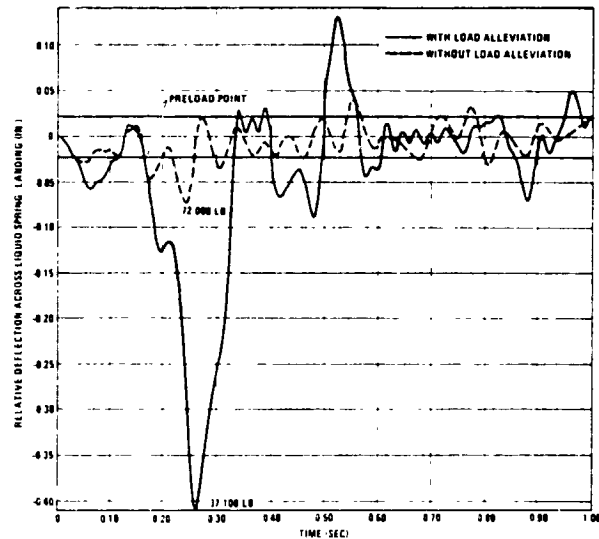


Figure 10 Liquid spring deflection during landing

Load and acceleration reductions due to the bilinear spring are summarized in Table 1 for the baseline system. Significant reductions in acceleration and attachment load can be seen when the liquid spring is incorporated in the landing analysis.

Table 1. Liquid spring effect on baseline system response.

Item	Condition	Results of Dynamic Analysis	
		Without Liquid Springs	With Liquid Springs
Spacecraft cg Peak Pitch (z) Acceleration	Liftoff	2.5g	4.0g
	Landing	5.6g	3.5g
Forward Z Reaction	Landing	72,000 lb	37,100 lb
Peak Elastic Z-Deflection at Spacecraft Tip (in.)	Liftoff	1.14	1.14
	Landing	0.58	1.44

Initial concern about increased spacecraft deflection due to liquid spring flexibility was found to be unwarranted. As shown in Table 1, spacecraft maximum tip deflection is only 1.44 inches. The relatively low deflection raises the question of reducing the liquid spring stiffness for greater attenuation of landing loads. A landing analysis assuming a 10,000 lb/in. spring rate instead of 39,500 lb/in., keeping the preload constant, increased the spacecraft tip deflection to 2.1 inches while

reducing spacecraft cg peak acceleration to 2.5g. Liftoff response is unaffected by reduction in spring constant since preload is not exceeded during liftoff.

While the 5,000-lb. rigid spacecraft was the basis for the trend studies and for sizing the liquid spring system, spacecraft flexibility was also considered. An existing Air Force spacecraft was analyzed by including the spacecraft cantilever modes in the mode synthesis and then performing the nonlinear dynamic response analysis in the same manner as for the rigid spacecraft. Results verified the effectiveness of the liquid spring system in reducing landing response.

The effect of spacecraft flexibility was also evaluated through trend studies in which the 5,000-lb., 40-foot-long spacecraft was assumed to be a uniform cantilever beam. Figure 11 shows the effect of spacecraft fundamental cantilever bending frequency on spacecraft cg peak acceleration due to landing when the liquid spring system is employed. It can be seen that peak landing response is relatively insensitive to spacecraft frequency.

NONLINEAR ANALYSIS VERIFICATION

To obtain better definition of the analytical uncertainties associated with the Shuttle-induced dynamic disturbances and to verify the nonlinear analysis procedure, a model test program was conducted. A one-third scale beam-type model (Figure 12) representing the spacecraft/IUS/cradle system was built and tested. Model-to-full scale ratios are listed below:

Length	1/3
Frequency	1.0
Mass and stiffness	0.056

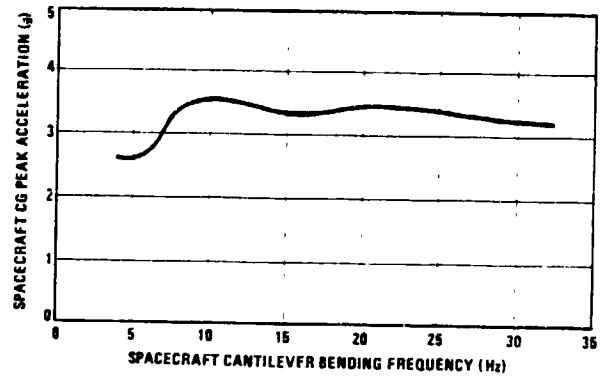


Figure 11. Effect of spacecraft fundamental cantilever bending frequency on cg peak acceleration.

The 0.056 stiffness ratio was based on an available liquid spring. IUS/cradle support stiffnesses were modeled with leaf springs. Two spacecraft were modeled, one stiff and one flexible, having interchangeable tip masses. This gave a spacecraft cantilever frequency range of 4 to 35 Hz.

The model was supported on two Ling Model B335 electromagnetic shakers to simulate Orbiter acceleration inputs at the forward and aft Orbiter-to-cradle Z-attachments. Three interchangeable forward support assemblies were tested:

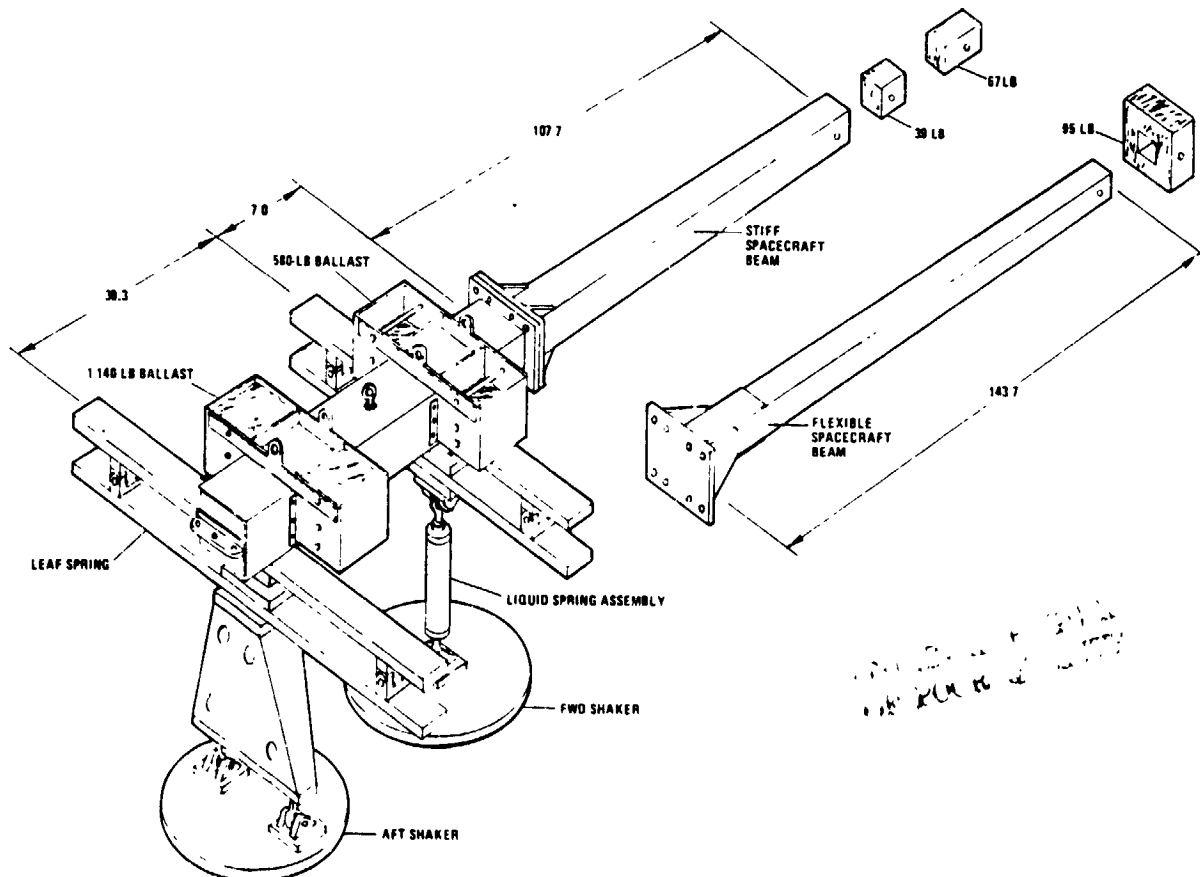


Figure 12. IUS dynamic test fixture

1. A rigid support link to act as a baseline for attenuation device comparison.
2. A liquid spring assembly with an average spring rate of 4,500 lb/in. having an adjustable preload range from 300 to 3,000 lb.
3. A dual parallel liquid spring assembly with an average spring rate of 1,200 lb/in. and a nonadjustable 2,400 lb preload. Figure 13 shows the measured force/stroke characteristics for this liquid spring assembly.

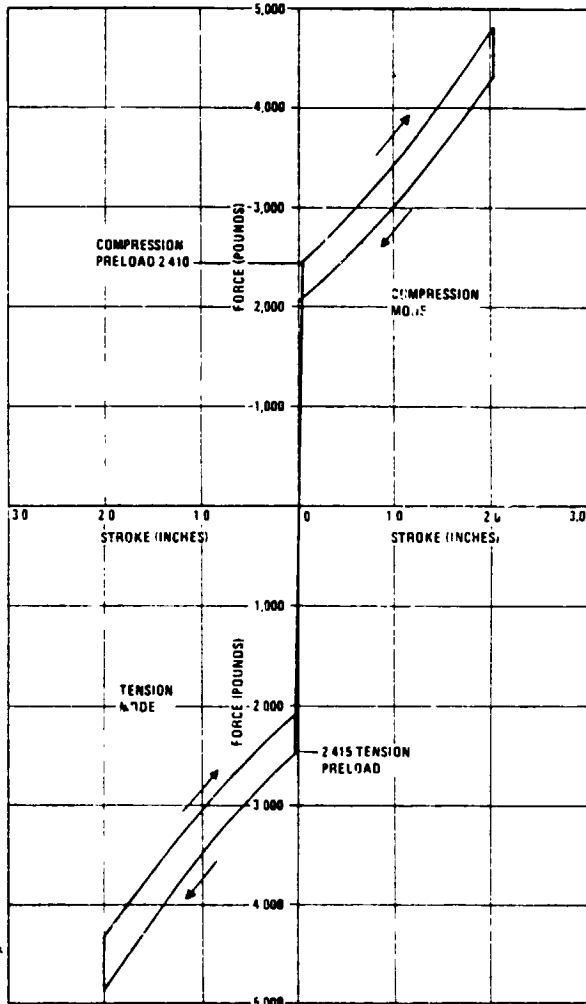


Figure 13. Force/stroke characteristics for dual liquid spring assembly.

Figure 14 shows the test setup for the dual liquid spring assembly and the stiff spacecraft beam with tip mass

Test results correlated well with analysis. Peak responses were generally predicted within 20% and almost always were conservatively higher than the test values. Figure 15, a typical comparison of predicted and measured vertical accelerations, shows good correlation between analysis and test. Our experience is that, particularly in nonlinear systems, it is difficult to mathematically model all damping mechanisms; this results in the predicted response being higher than measured. Of course, at specific points of lower amplitude (usually near a node of an important mode) the percentage error of the calculation may be higher, but this is usually of little design consequence.

CONCLUSIONS

Bilinear liquid springs are an effective means of reducing spacecraft loads due to Orbiter landing without increasing liftoff response. This attenuation system also substantially reduces the vertical reaction forces acting at the Orbiter/cargo support points during landing.

The analytical method for handling spring nonlinearity has been validated by dynamic model tests. Based upon correlation with test results, analytically predicted accelerations tend to be conservative.

Spacecraft peak acceleration response to Orbiter landing is relatively insensitive to spacecraft cantilever bending frequency when the liquid spring system is incorporated.

For a given liquid spring preload, spacecraft peak acceleration response to Orbiter landing can be reduced by reducing the spring constant at the expense of increased spacecraft dynamic deflection. Spacecraft deflections, however, are surprisingly small for practical values of spring constant.

ACKNOWLEDGMENTS

The authors are indebted to Messrs. Ed Bock and Ted Draper of General Dynamics Convair Division for their efforts in perfecting the liquid spring concept.

REFERENCES

1. Dreyer, W. M., and Huntington, R. G., United States Patent 4,043,524, "Support and Load Alleviation System for Space Vehicles," 23 August 1977.
2. Read, H. D., "Non-Linear Response Using Normal Modes," AIAA Paper 74-138, February 1974.
3. Hintz, R. M., "Analytical Methods in Component Modal Synthesis," *AIAA Journal*, Vol. 13, No. 8, August 1975, pp 1007-1016.
4. Hurty, W. C., "Dynamic Analysis of Structural Systems Using Component Modes," *AIAA Journal*, Vol. 3, No. 4, April 1965, pp 678-685.



Figure 14. Test setup for stiff spacecraft and dual liquid springs.

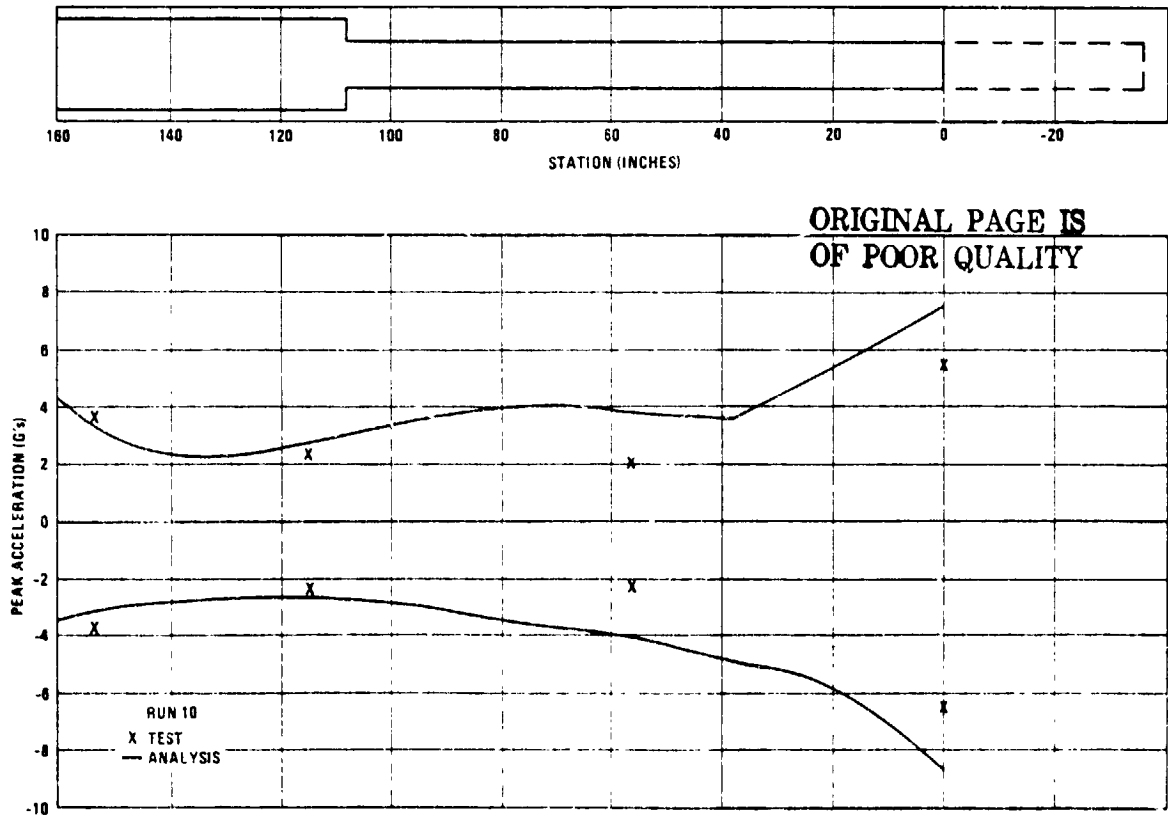
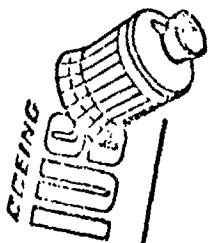


Figure 15. Calculated and measured peak accelerations for stiff spacecraft, adjustable liquid spring, 2,400 lb preload



PRECEDING PAGE BLANK NOT FILMED

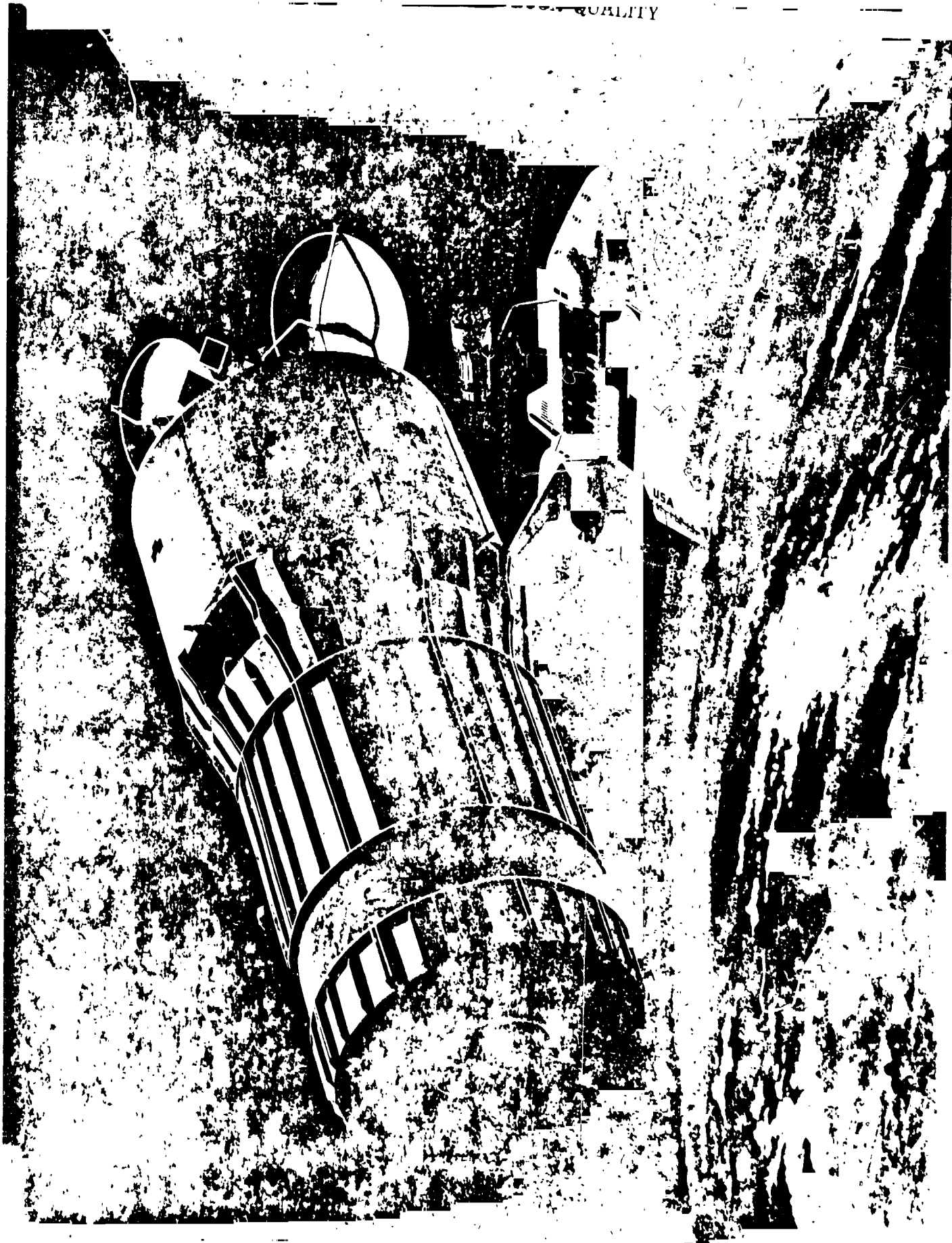
Low Response Suspension System
for
Orbiter Payloads

S.M. Church
Boeing Aerospace Co.

LOW RESPONSE SUSPENSION SYSTEM FOR CRBITER PAYLOADS

A SUSPENSION SYSTEM FOR SUPPORTING THE INERTIAL UPPER STAGE (IUS) AND ITS PAYLOADS HAS BEEN DEVELOPED FOR USE IN THE SPACE SHUTTLE VEHICLE. THE IUS IS BEING DEVELOPED BY BOEING AEROSPACE COMPANY FOR THE U.S. AIR FORCE UNDER CONTRACT NO. F04701-78-C-0040. THIS PRESENTATION DESCRIBES THE REQUIREMENTS, ANALYSES APPROACH, DESIGN CONCEPT, AND PERFORMANCE OF THE LOW RESPONSE SYSTEM.

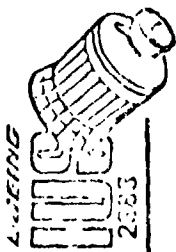
ORIGINAL PAGE IS
QUALITY



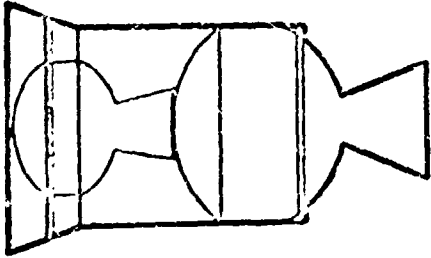
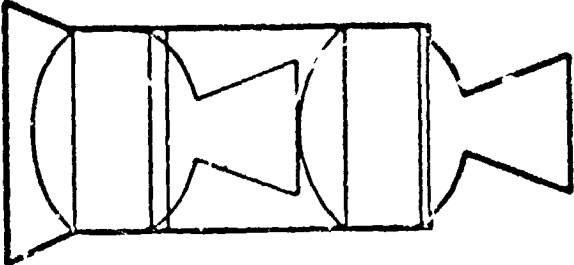
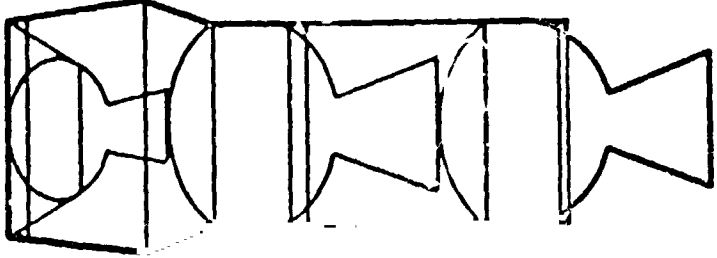
INERTIAL UPPER STAGE

THE INERTIAL UPPER STAGE (IUS) IS A TWO OR THREE STAGE SOLID PROPELLANT SPACE BOOSTER DESIGNED TO BE CARRIED BY THE SPACE SHUTTLE VEHICLE AND DELIVER SPACE-CRAFT TO HIGH ENERGY ORBITS. IN THE TWO STAGE CONFIGURATION, IT IS 12 1/2 FEET LONG, 7 1/2 FEET IN DIAMETER AND WEIGHS 32,000 POUNDS. IT IS SUPPORTED IN THE ORBITER BY TWO CRADLES OR AIRBORNE SUPPORT EQUIPMENT (ASE) AND WILL LAUNCH 1950 - 5000 POUND SPACECRAFT INTO GEOSYNCHRONOUS ORBITS AND 6000 POUND SPACECRAFT INTO 12 HOUR ORBITS. THE WEIGHT BREAKDOWN OF THE ORBITER CARGO IS AS FOLLOWS:

IUS	32000
ASE	8500
SPACECRAFT	2000 - 6000
BALLAST (CARGO C.G. CONTROL)	0 - 4250
	<hr/>
	42500 - 52750 POUNDS

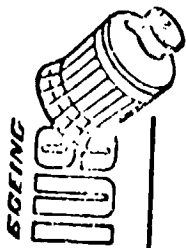


Shuttle IUS Vehicle Family

			
CONFIGURATION	TWO-STAGE	NASA TWIN-STAGE	THREE-STAGE SPINNER
CAPABILITY	5,000 LBS. TO GEOSYNCHRONOUS	11,000 LBS. TO MARS	3,300 LBS. TO JUPITER

SHUTTLE IUS VEHICLE FAMILY

THE IUS FAMILY CONSISTS OF THREE BASIC VEHICLES, A TWO STAGE FOR ORBITAL PAYLOADS AND A NASA TWIN AND THREE STAGE SPINNER FOR INTER-PLANETARY MISSIONS. THIS STUDY ADDRESSES THE TWO STAGE CONFIGURATION ONLY SINCE IT IS TO LAUNCH EXISTING SPACECRAFT DESIGNED FOR EXPENDABLE LAUNCH SYSTEMS. THE LARGER IUS CONFIGURATIONS HAVE TOTAL CARGO WEIGHTS CLOSE TO THE 65000 LB ORBITER CAPABILITY AND THE SPACECRAFT ARE NOT YET DESIGNED.

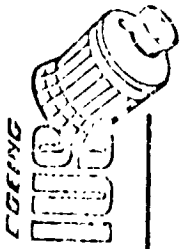


IUS/ASE Design Requirements

- Reduce spacecraft responses during liftoff and landing.
- Minimize loads in the spacecraft.
- Minimize IUS and spacecraft accelerations derived from the orbiter forcing functions.
- The dampers, isolators and additional supports shall be considered.

IUS/ASE DESIGN REQUIREMENTS

THE SYSTEM SPECIFICATION SS-STIS-100, VOL.3 REQUIRES THAT THE IUS/ASE SYSTEM BE DESIGNED TO LIMIT SPACECRAFT RESPONSES DURING ORBITER EVENTS AND THAT A LOAD ALLEVIATION STUDY BE UNDERTAKEN TO DETERMINE MEANS OF ACCOMPLISHING THIS.



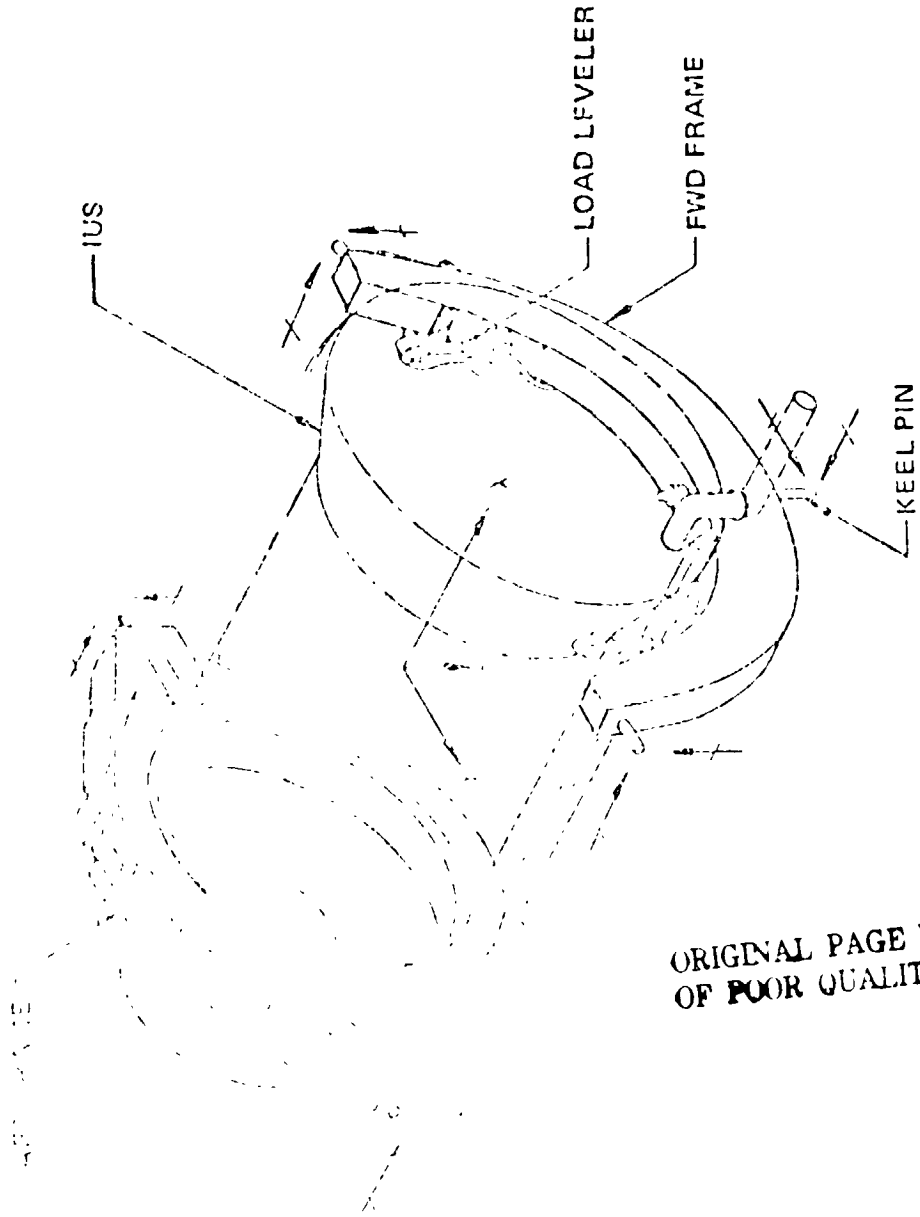
ASE Design Goals

- Control spacecraft loads to levels comparable to expendable launch systems.
- Insensitive to reference spacecraft configuration parameters.
- Insensitive to orbiter design evolution.
- Reusable (100 missions).
- Determinate interface with orbiter.
- Adaptable to existing ASE concept.

ASE DESIGN GOALS

THE ASE SHOULD PRODUCE SPACECRAFT LOADS NO HIGHER THAN EXPENDABLE LAUNCH SYSTEMS SO THAT EXISTING SPACECRAFT NEED NOT BE SUBSTANTIALLY REDESIGNED. IN ADDITION, THE ASE SHOULD BE SUCH THAT SPACECRAFT LOADS ARE NOT SENSITIVE TO SMALL CHANGES IN ORBITER, IUS AND SPACECRAFT DESIGN PARAMETERS. IT MUST BE REUSABLE FOR 100 MISSIONS AND IT IS DESIRABLE TO HAVE A DETERMINATE INTERFACE WITH THE ORBITER TO PREVENT COUPLING WITH THERMAL AND ELASTIC DEFORMATIONS AND ASSURE THAT THE INTERFACE ALLOWABLE LOADS ARE NOT EXCEEDED.

Design Concept



ORIGINAL PAGE IS
OF POOR QUALITY

DESIGN CONCEPT

THE PRELIMINARY DESIGN CONCEPT WAS A STRENGTH DESIGNED ASE SIZED FOR PRELIMINARY LOAD FACTORS DEFINED IN THE SYSTEM SPEC. IT HAD SEPARATE FORWARD AND AFT CRADLES AND UTILIZED A LOAD LEVELER IN THE FORWARD ASE TO ACHIEVE A DETERMINATE INTERFACE WITH THE ORBITER

THE AXIAL LOAD WAS REACTED BY THE AFT ASE AT THE ORBITER LONGERONS AND THE LATERAL LOAD BY THE FORWARD ASE KEEL FITTING. THIS STRENGTH DESIGNED CONCEPT PROVIDED A MUCH STIFFER AFT ASE THAN THE FORWARD ASE BECAUSE OF GEOMETRY AND LOAD DISTRIBUTIONS.

DEPLOYMENT WAS ACCOMPLISHED BY PIVOTING UP TO 90° ABOUT THE AFT ASE TRUNNION AND SEPARATION MADE BY A SPRING SYSTEM BETWEEN THE IUS AND ASE.

Analysis Procedure

• 30 unrestrained normal modes.

• Detailed models (200-300 degrees of freedom).
• Simplified models.

• Frequency.

• Detailed models (500 degrees of freedom).
• Simplified models.

• Loading conditions.

• SSV lift-off.

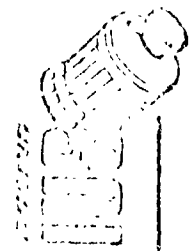
• Abort landing.

• Method.

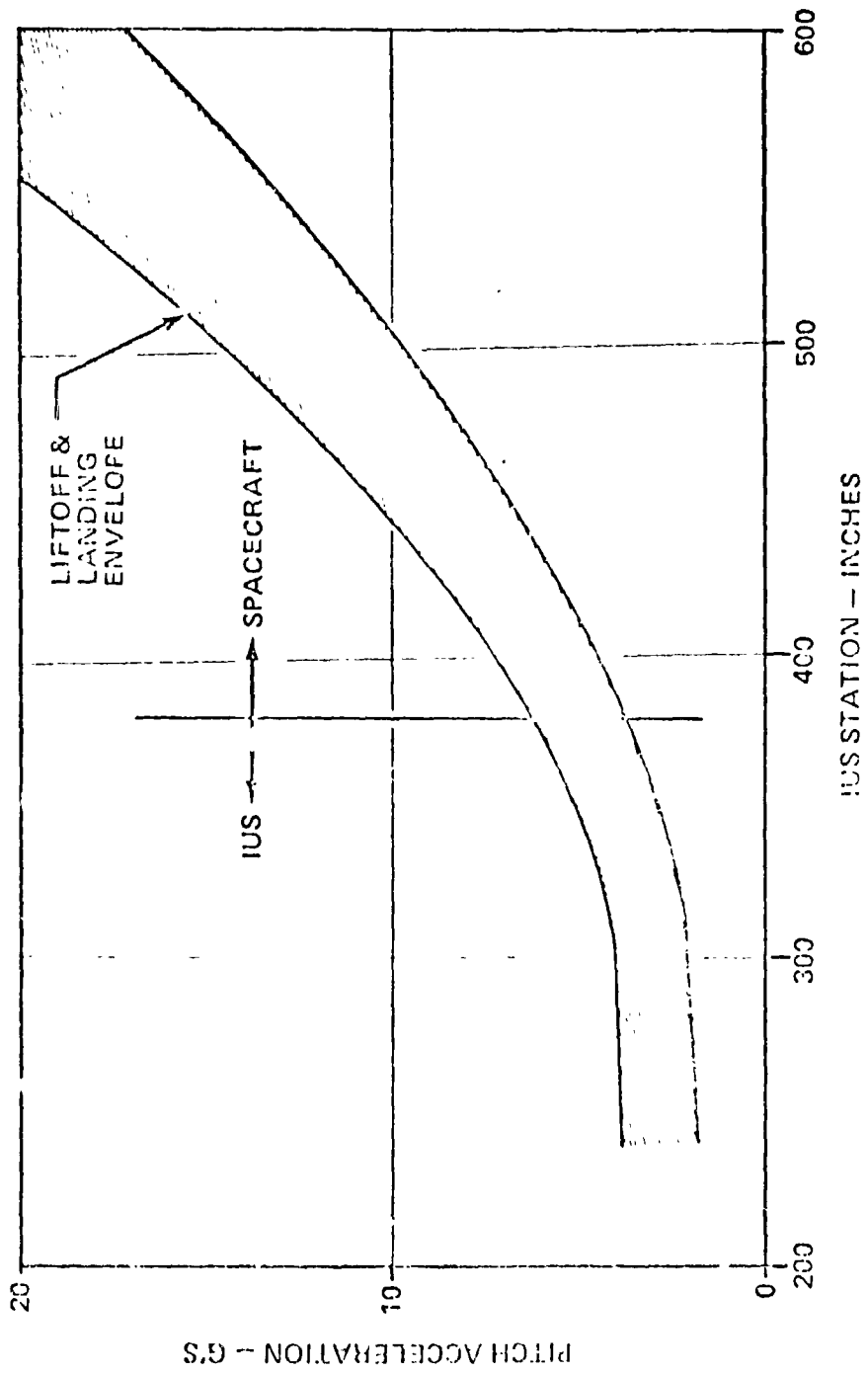
• Three body merge using modified Benfield-Hruda approach in NASTRAN.

ANALYSIS PROCEDURE

THE DYNAMIC ANALYSIS CONSISTS OF A THREE BODY MODAL MERGE USING THE BENFIELD-HRUDA BRANCH MODE TECHNIQUE IN NASTRAN. THIS METHOD WAS AGREED TO BY SAMSO, NASA-JSC, ROCKWELL AND BOEING AND USES ORBITER UNRESTRAINED MODES (WITH UNLOADED INTERFACE ATTACH POINTS AND RESIDUAL FLEXIBILITY COEFFICIENTS) AND SUPPORTED ELASTIC MODES AND CONSTRAINT MODES OF THE IUS AND SPACECRAFT. THIS METHOD IS ALSO ADAPTABLE TO USING STIFFNESS MATRICES DIRECTLY OR FINITE ELEMENT REPRESENTATIONS. THE RESULTING COMBINED MODAL REPRESENTATION IS SUBJECTED TO ORBITER LIFTOFF AND ABORT LANDING FORCING FUNCTIONS PROVIDED BY ROCKWELL INTERNATIONAL TO OBTAIN RESPONSES AND LOADS.



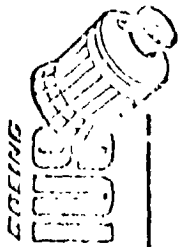
IUS/Spacecraft Results Strength Designed IUS/ASE



ORIGINAL PAGE IS
OF POOR QUALITY

IUS/SPACECRAFT RESULTS

THE RESULTS OF THE STRENGTH DESIGNED SYSTEM WITH A TYPICAL SPACECRAFT (3000 LB, 10 HZ) INDICATED VERY HIGH SPACECRAFT RESPONSES FOR BOTH LIFTOFF AND LANDING. SPACECRAFT RESPONSE WAS DOMINATED BY IUS/SPACECRAFT PITCHING IN THE 5-7 HZ RANGE WHICH WAS IN THE VICINITY OF THE ORBITER EXCITATIONS. ATTEMPTS TO REDUCE THESE RESPONSES BY MODEST ASE STIFFNESS CHANGES WERE UNSUCCESSFUL. LOADS SHOWN DO NOT INCLUDE ANY UNCERTAINTY FACTOR.



Parametric Loads Study

Objective: Establish ASE parameters that minimize spacecraft response loads.

Basis: Simplified IUS, ASE and spacecraft models with detailed orbiter.

- ASE variables.
 - Stiffness center tuning.
 - Vertical stiffness.
 - Axial stiffness.
 - ASE dampers.
- IUS variables.
 - Bending stiffness.
- Spacecraft variables.
 - Spacecraft weight.
 - Spacecraft center of gravity.
 - Spacecraft cantilever frequency.
- Configuration variables.
 - Trunnion centerline offset.

PARAMETRIC LOADS STUDY

A COMPREHENSIVE PARAMETRIC TRADE STUDY WAS CONDUCTED TO ESTABLISH ASE STIFFNESS AND DAMPING CHARACTERISTICS THAT MINIMIZE SPACECRAFT RESPONSE LOADS DURING ORBITER LIFTOFF AND LANDING. A WIDE RANGE OF SPACECRAFT WEIGHTS, C.G. HEIGHTS, AND STIFFNESSES WERE ANALYZED USING SIMPLIFIED MODELS OF THE SPACECRAFT, IUS, AND ORBITER.

SPACECRAFT WEIGHTS 1,200, 2,600, 5,000 LBS

SPACECRAFT C.G. AT 67, 103.5, 162 INCHES

SPACECRAFT CANTILEVER FREQUENCY 2.2 TO 14 HZ

ASE VERTICAL STIFFNESS 24,600 TO 1,500,000 LB./IN

ASE AXIAL STIFFNESS 112,000 TO 4,800,000 LBS/IN

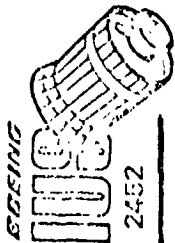
FORWARD ASE DAMPING 100 TO 2,000 LBS/IN/SEC

TRUNNION CENTERLINE OFFSET 0 AND 14 INCHES

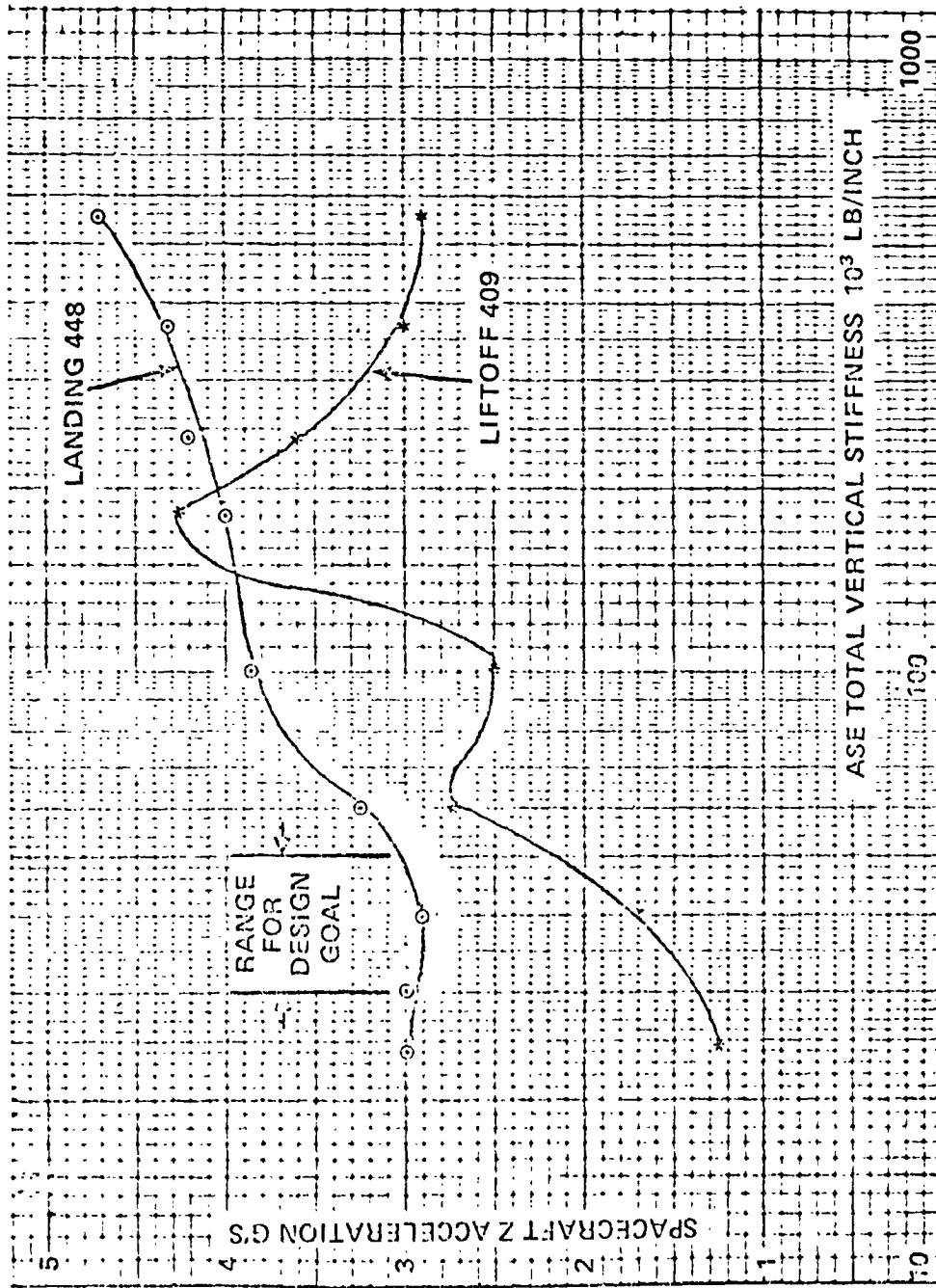
IUS STIFFNESS .50, 1.0, AND 2.0 X NOMINAL

A SIMPLIFIED MODEL OF THE IUS/ASE/SPACECRAFT WAS DEVELOPED THAT ALLOWED STRUCTURAL CHANGES TO BE MADE EASILY AND TO SUBSTANTIALLY REDUCE COMPUTER COSTS. (FACTOR OF = 10) IN EXCESS OF 90 DIFFERENT RUNS WERE MADE TO EVALUATE RESPONSE SENSITIVITY TO THE VARIOUS DESIGN PARAMETERS. THE SIMPLIFIED APPROACH HAS BEEN SUBSTANTIATED BY SUBSEQUENT DETAILED ANALYSES. THIS STUDY CONCENTRATED ON REDUCING THE VERTICAL RESPONSES SINCE THESE WERE THE BIGGEST PROBLEM AREAS.

THE ASE STIFFNESS TUNING, VERTICAL STIFFNESS AND ASE DAMPERS WERE THE SIGNIFICANT PARAMETERS FROM THIS STUDY AND WILL BE COVERED IN THE SUBSEQUENT CHARTS.



Vertical Stiffness Trade Tuned System

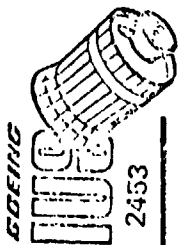


- IUS/DSP/ORBITER 5.3G
- LANDING NO. 448.
- * LIFTOFF NO. 409
- SHEAR CENTER
ALIGNED WITH C.G.

ORIGINAL PAGE IS
OF POOR QUALITY

VERTICAL STIFFNESS TRADE

THE VERTICAL STIFFNESS TRADE WAS CONDUCTED BY VARYING THE COMBINED AFT AND FORWARD ASE VERTICAL STIFFNESS AND ALSO VARYING THE FORE-AFT VERTICAL STIFFNESS DISTRIBUTION. THIS WAS DONE OVER A RANGE OF 24,000 LB/IN TO 1,500,000 LB/IN. THE RESULTS INDICATED THAT LOADS WERE MINIMIZED WHEN THE VERTICAL STIFFNESS SHEAR CENTER COINCIDED WITH THE CARGO CENTER OF GRAVITY AND WHEN ASE SUPPORTED FREQUENCIES ARE REDUCED TO UNDER 4 HZ AS CANTILEVERED FROM A RIGID ORBITER. THE MINIMUM SPACECRAFT EQUIVALENT CENTER OF GRAVITY VERTICAL ACCELERATION IS PLOTTED VERSUS TOTAL VERTICAL STIFFNESS. BASED ON THESE RESULTS, A VERTICAL STIFFNESS OF 40,000 LB/INCH WAS SELECTED AS THE BEST COMPROMISE BETWEEN SPACECRAFT ACCELERATION AND DEFLECTION.

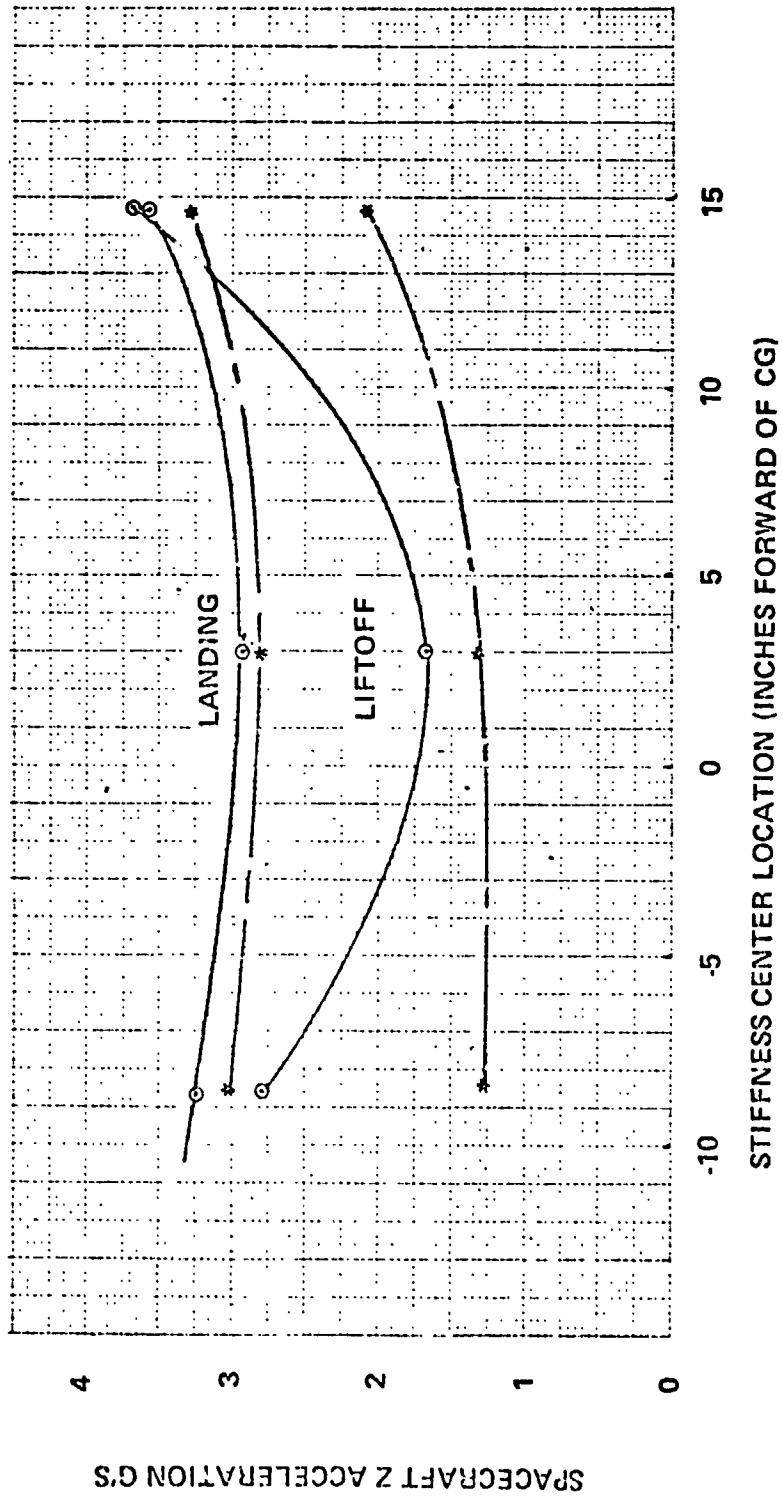


Shear Center Tuning/Damping Sensitivity

IUS/DSP/ORBITER 5.3G
ASE VERTICAL STIFFNESS = 40,000 LB/IN

- NO DAMPING
- * DAMPING C = 1500 LB-SEC/INCH

ORIGINAL PAGE IS
OF POOR QUALITY



SHEAR CENTER/CENTER OF GRAVITY ALIGNMENT
SENSITIVITY

SEVERAL SENSITIVITY STUDIES WERE CONDUCTED USING 40,000 LB/INCH VERTICAL STIFFNESS FOR THE ASE. THESE INCLUDED:

SHEAR CENTER ALIGNMENT - LIFTOFF ACCELERATIONS QUITE SENSITIVE, INCREASING 50% WITH A CENTER OF GRAVITY OFFSET OF 12 INCHES. THE ADDITION OF DAMPERS TO THE FORWARD ASE REDUCED THE ACCELERATION AND THE SENSITIVITY.

IUS STIFFNESS - INSENSITIVE OVER A \pm 50% RANGE

SPACECRAFT SIZE - LARGER SPACECRAFT HAVE LOWER RESPONSES



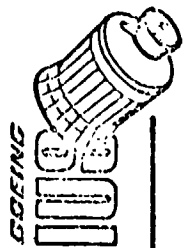
Parametric Study Results

MINIMIZE SPACECRAFT RESPONSE

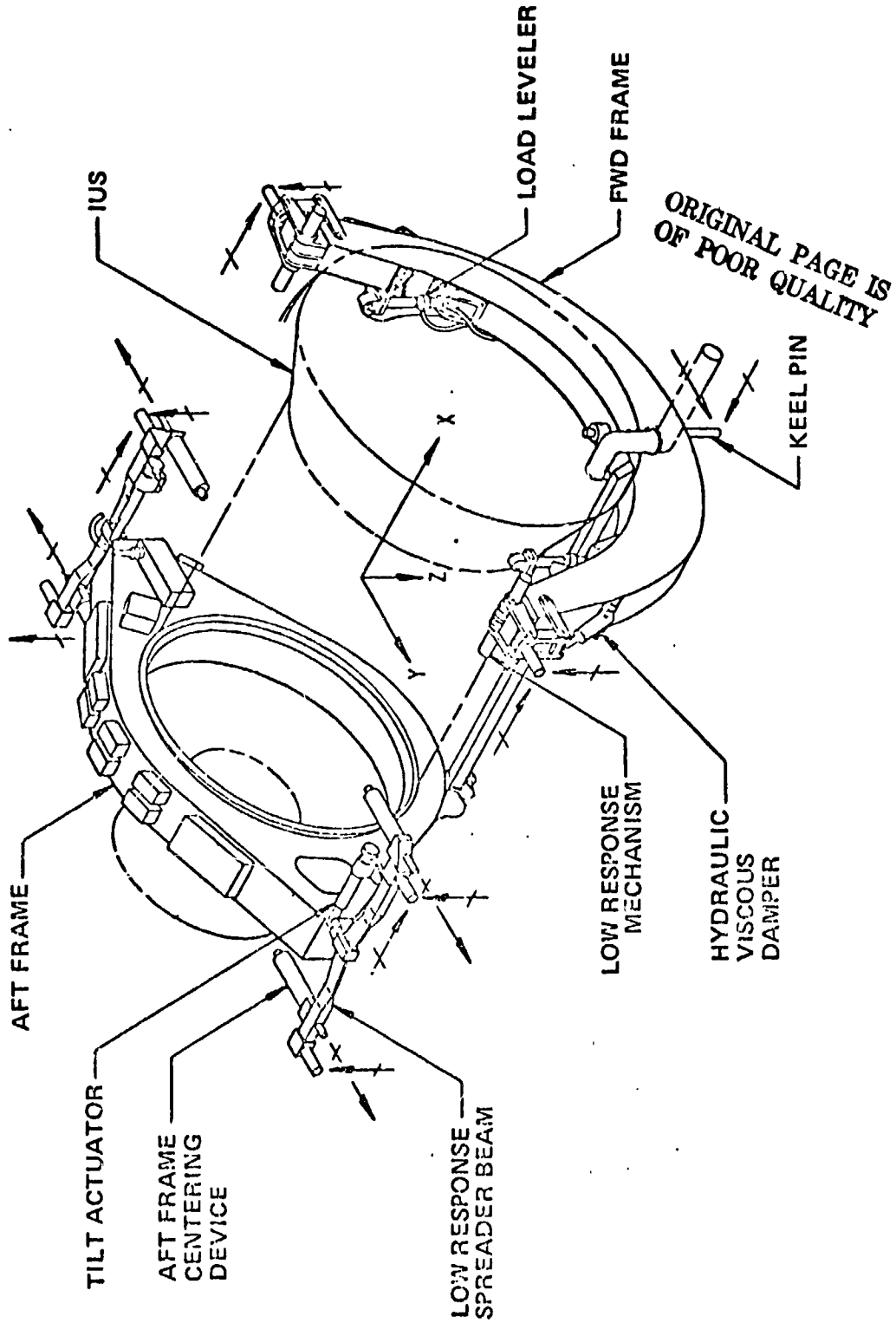
PARAMETER	CONCLUSION
ASE SHEAR CENTER ALIGNMENT WITH IUS/SC CG	ALIGNMENT REQUIRED. 50 TO 70% OF VERTICAL STIFF AT FWD ASE.
ASE VERTICAL STIFFNESS	PROV'DE SUSPENDED FREQUENCIES < 3.5 HZ.
IUS/SPACECRAFT STIFFNESS	PROVIDE 2ND PITCH MODE FREQ > 10 HZ. REQUIRED SC CANTILEVER FREQ > 10 HZ.
AFT ASE AXIAL STIFFNESS	AXIAL SUSPENDED FREQ ≈ 6.0 HZ. ~ NOT SENSITIVE PARAMETER.
IDEALIZED S/C RESPONSE LOADS AT CG (UNCERTAINTY FACTOR = 1.0)	LANDING ≈ 3.0 G LIFTOFF ≈ 2.0 G
DAMPING AT FWD ASE	SIGNIFICANTLY REDUCES L/O LOADS ≈ 25%. REDUCES SENSITIVITY TO CG/SHEAR CENTER ALIGNMENT. REDUCES IUS/SC REQUIRED STIFFNESS
14 INCHES TRUNNION/CG OFFSET	SMALL EFFECT ON LOADS.
REDUCED SC STIFFNESS	INCREASED PITCHING MOTION-HIGHER TIP ACCELERATIONS.

PARAMETRIC STUDY RESULTS

PRIMARY CONCLUSIONS GENERATED BY THE PARAMETRIC STUDY ARE SUMMARIZED ON THIS TABLE. THE MOST IMPORTANT CONSIDERATIONS FOR MINIMIZING SPACECRAFT RESPONSE LOADS ARE ASE SHEAR CENTER ALIGNMENT WITH IUS/C.G. AND ASE VERTICAL STIFFNESS. VERTICAL STIFFNESS MUST BE REDUCED TO PROVIDE SUSPENDED PITCH AND VERTICAL FREQUENCIES BELOW 3.5 HZ. IDEALIZED ASE STIFFNESSES WILL LIMIT EQUIVALENT SPACECRAFT C.G. RESPONSES TO 3.0 AND 2.0 G FOR LANDING AND LIFTOFF RESPECTIVELY. EQUIVALENT SPACECRAFT C.G. RESPONSE IS DEFINED AS SPACECRAFT IUS INTERFACE BENDING MOMENT DIVIDED BY SPACECRAFT WEIGHT TIMES C.G. HEIGHT.



IUS Two Stage Low Response System

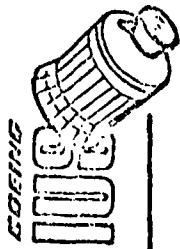


IUS/TWO STAGE LOW RESPONSE SYSTEM

THE ASE DESIGN TO PROVIDE THESE CHARACTERISTICS CONSISTS OF A FOUR-BAR LINKAGE WITH TORSION BAR SUSPENSION AT THE FORWARD ASE AND A SPREADER BEAM LEAF SPRING SYSTEM AT THE AFT ASE. THIS DESIGN PROVIDES THE FOLLOWING EFFECTIVE STIFFNESS:

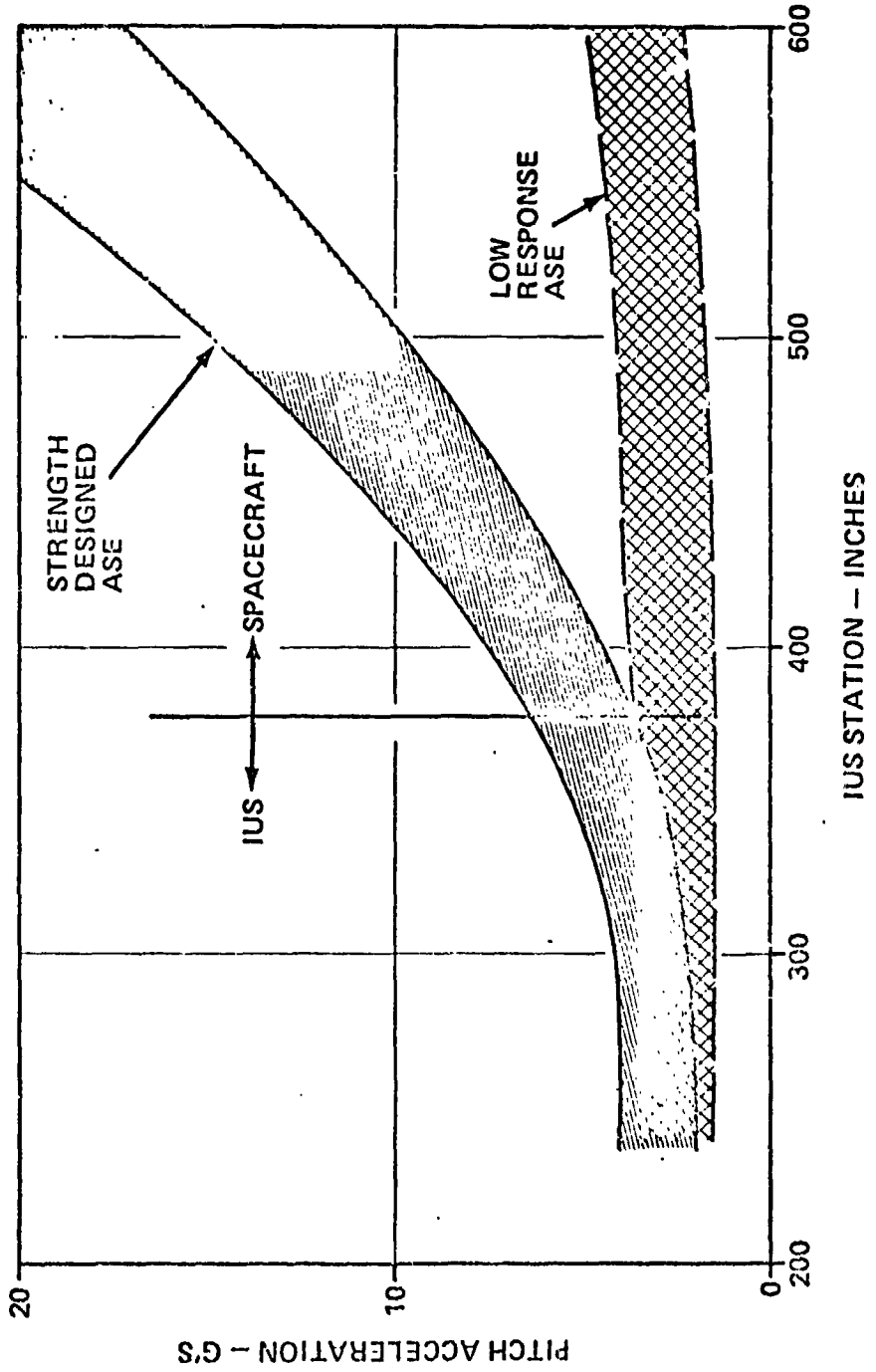
AFT ASE AXIAL	85,000	LB/INCH
AFT ASE VERTICAL	16,000	LB/INCH
FWD ASE VERTICAL	24,000	LB/INCH

HYDRAULIC DAMPERS ARE PROVIDED AT THE FORWARD ASE THAT PROVIDE 5% - 25% OF CRITICAL DAMPING TO THE FUNDAMENTAL MODES OF THE SYSTEM.



IUS/Spacecraft Results

ENVELOPE OF PRIMARY STRUCTURE RESPONSE DURING ORBITER LIFTOFF AND LANDING EVENTS



IUS/SPACECRAFT RESULTS WITH LOW RESPONSE ASE

THE LOW RESPONSE SYSTEM PROVIDES A DRAMATIC REDUCTION IN VERTICAL SPACECRAFT LOADS. KEEPING THE PITCH FREQUENCY BELOW 3.5 HZ DECOUPLES THE CARGO FROM THE ORBITER AND RESULTS IN LOADS TYPICALLY LESS THAN 3 G'S. THE ORBITER INTERFACE LOADS ARE WITHIN ALLOWABLES WITH COMFORTABLE MARGINS. THE DAMPER MAKES THE SYSTEM INSENSITIVE TO SPACECRAFT CHANGES. THIS SYSTEM IS EFFECTIVE FOR THE RANGE OF REFERENCE AND TRANSITION SPACECRAFT EVALUATED (1950 - 6000#). VERTICAL DEFLECTIONS ARE LESS THAN 3.0 INCHES AT THE ASE. SPACECRAFT RELATIVE DEFLECTION AT THE TIP ARE IN THE RANGE OF 3 TO 7 INCHES. SPACECRAFT DEFLECTIONS DID NOT INCREASE SIGNIFICANTLY BECAUSE PITCH MOTION WAS ESSENTIALLY ELIMINATED.

THESE RESULTS HAVE BEEN VALIDATED BY INDEPENDENT ANALYSES CONDUCTED BY AEROSPACE CORPORATION, ROCKWELL INTERNATIONAL AND MARTIN MARIETTA CORPORATION. STUDIES ARE UNDERWAY ASSESSING THE IMPACT OF THIS SYSTEM ON THE ORBITER FLIGHT CONTROL SYSTEM.



Summary

- **Low response system minimizes spacecraft load.**
- **Design goals have been achieved.**
- **Approach has been validated by independent analyses.**
- **System is being implemented on two stage ASE.**

PRECEDING PAGE BLANK NOT FILMED

DEVELOPMENT
OF A LOADS CRITERIA
FOR SPACE TELESCOPE

WM. B. HAILE
LOCKHEED MISSILES AND SPACE COMPANY



DEVELOPMENT OF A LOADS CRITERIA FOR SPACE TELESCOPE

610

OBJECTIVE

TO DEFINE THE MAXIMUM EXPECTED STRUCTURAL LOADS FOR DESIGN
OF THE SPACE TELESCOPE

METHOD

ANALYTICALLY COMPUTED LOADS ARE MULTIPLIED BY A FACTOR TO
ACCOUNT FOR VARIABILITIES

PROBLEM

TO DEFINE ACCEPTABLE LOAD VARIABILITY FACTORS



THE SPACE TELESCOPE

A HIGH PRECISION OPTICAL TELESCOPE FOR SCIENTIFIC INVESTIGATION OF THE
HEAVENS

- PRIMARY MIRROR 94 INCH DIAMETER
- TOTAL WEIGHT 22000 POUNDS
- 14 FOOT DIAMETER, 44 FEET LONG
- RESOLUTION APPROX 7 TIMES BETTER THAN LARGEST EARTH

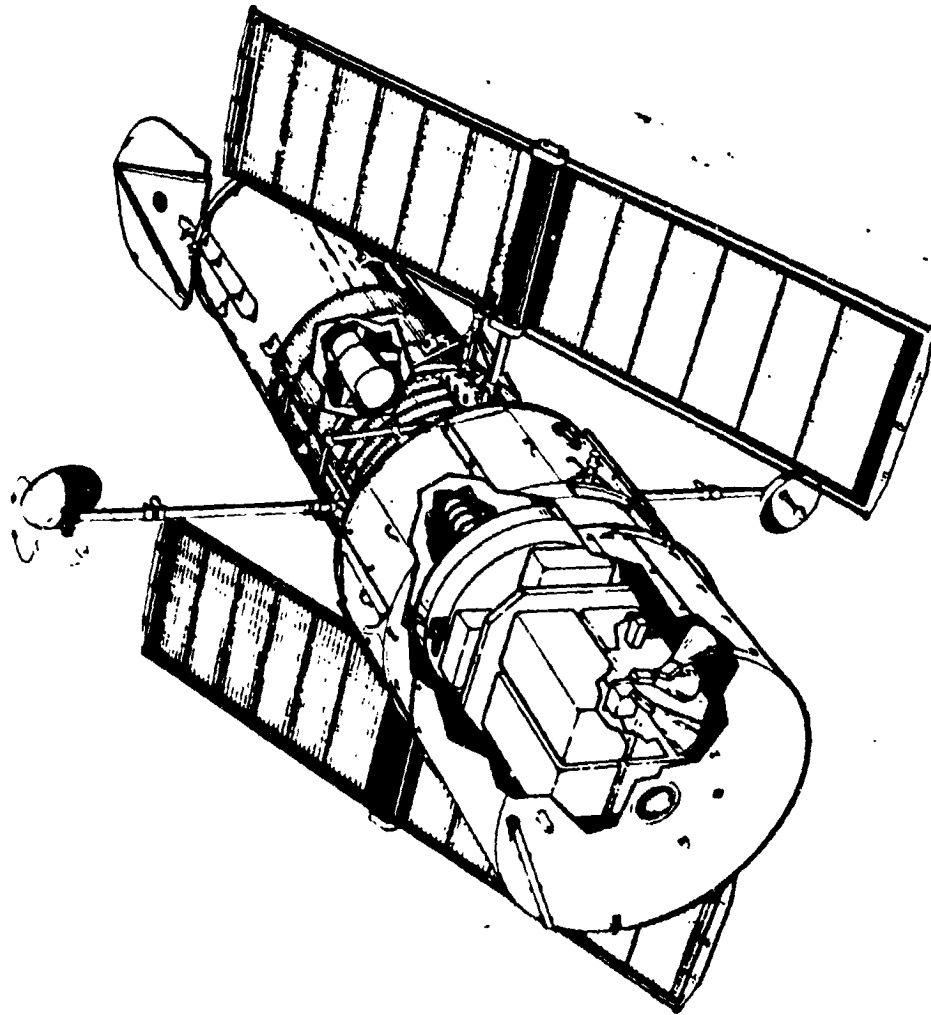
BASED TELESCOPES

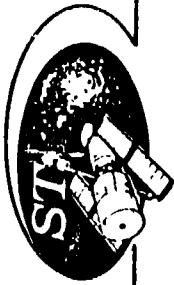
- FINE POINTING ERROR BUDGET 0.0070 ARC-SEC FROM ALL

SOURCES

- DESIGNED TO USE SPACE SHUTTLE FOR INSERTION INTO ORBIT AND RETURN TO EARTH FOR REFURBISHMENT
- STRUCTURE DESIGNED FOR A COMBINATION OF ON-ORBIT PERFORMANCE, SHUTTLE INDUCED LOADS, AND CONTROL SYSTEM CONSTRAINTS

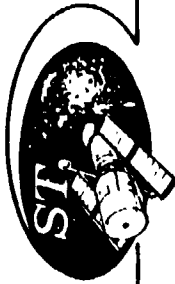
THE SPACE TELESCOPE



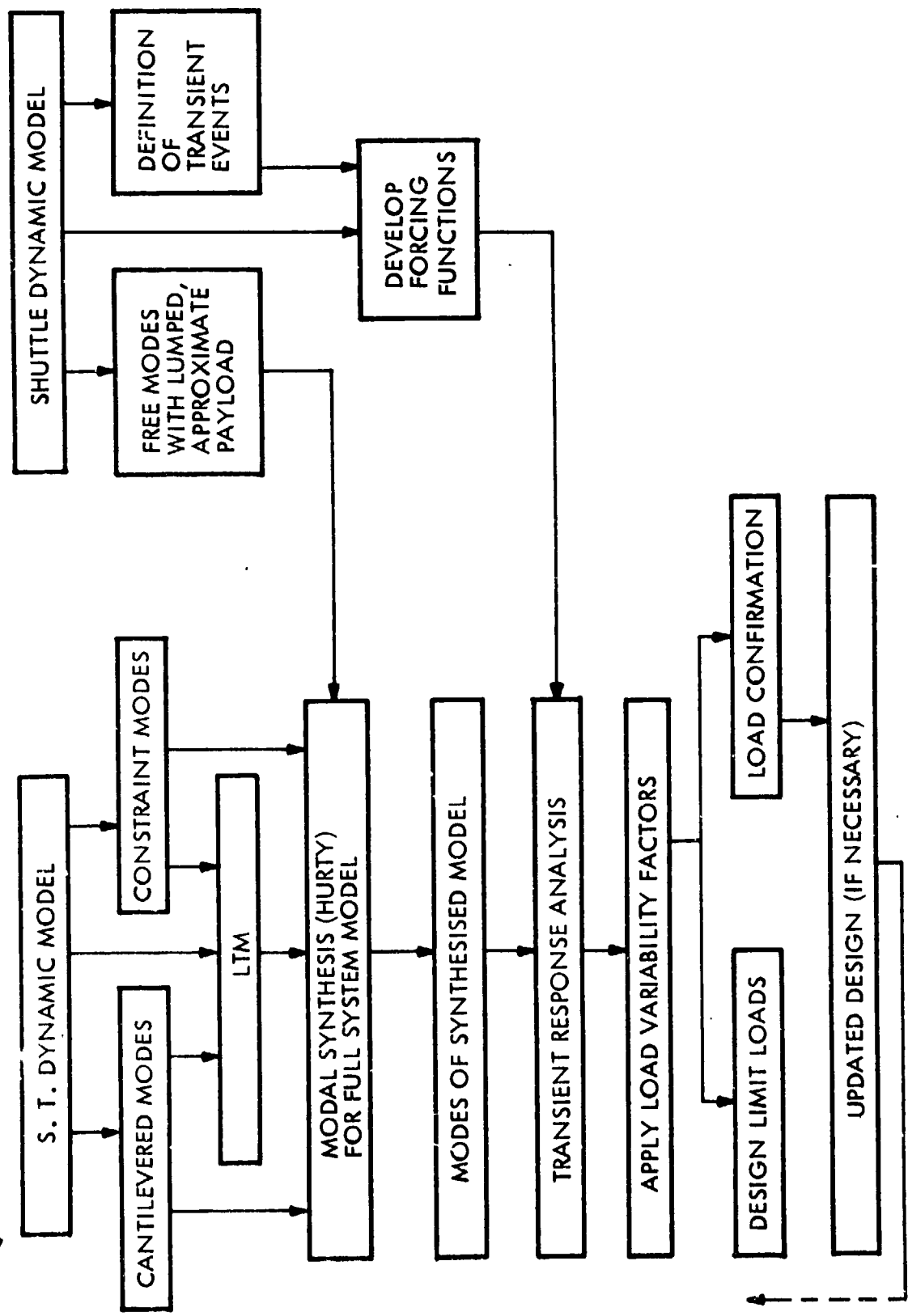


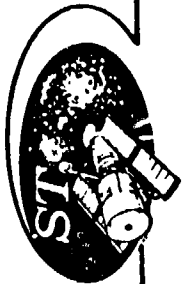
TYPES OF DESIGN FACTORS

	USE	TO ACCOUNT FOR	VALUE FOR SPACE TELESCOPE
LOAD VARIABILITY FACTOR	DYNAMIC G-LEVELS	FINITE ELEMENT MODEL FIDELITY FORCING FUNCTION UNCERTAINTY POTENTIAL DESIGN CHANGES	VARIABLE (TO BE DISCUSSED)
	YIELD SAFETY FACTOR	ANALYTICAL APPROXIMATIONS MATERIAL UNCERTAINTY MANUFACTURING TOLERANCE (NO STATIC TEST PROGRAM)	2.0
ULTIMATE SAFETY FACTOR	YIELD STRESS, LOCAL CRIPPLING ULTIMATE STRESS		3.0
COMPONENT LOAD FACTORS	COMPONENT MECHANICAL DESIGN	ALL OF ABOVE	VARIABLE, WT VERSUS FREQ VERSUS G-LEVEL



TYPICAL ST LOADS ANALYSIS CYCLE



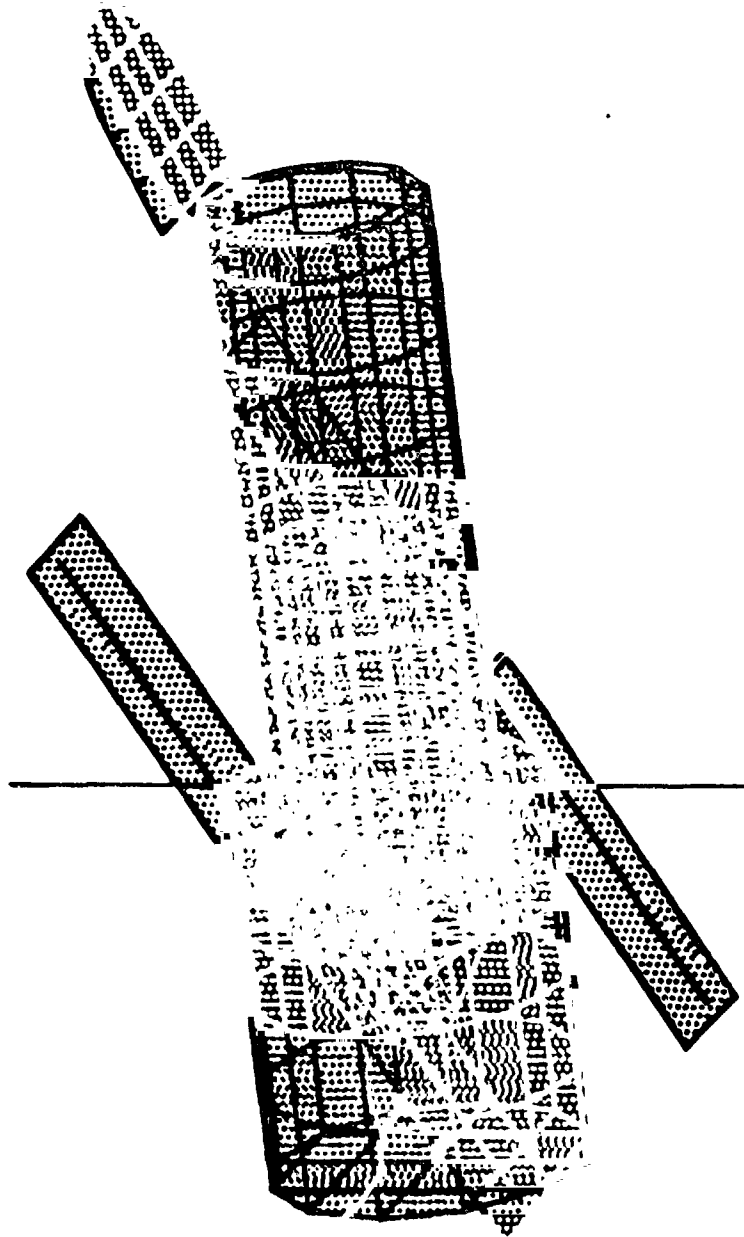


SPACE TELESCOPE DYNAMIC MODEL

- DETAILED FINITE ELEMENT MODEL WITH 5000 DEG OF FREE
- 120 CANTILEVERED MODES UP TO 72 Hz (LIFTOFF/LANDING)
- SIX DEG OF FREEDOM INTERFACE WITH SHUTTLE
- COUPLED TO SHUTTLE BY MODAL SYNTHESIS USING HURTY'S METHOD (CANTIL AND CONSTRAINT MODES)
- MODAL TEST VERIFICATION OF MODEL BEFORE FINAL LOADS ANALYSIS CYCLE
- NO STATIC TEST PROGRAM



SPACE TELESCOPE DYNAMIC MODEL (ON ORBIT)





SPACE SHUTTLE UNCERTAINTY

- MODEL IS NOT YET TEST VERIFIED
- FORCING FUNCTIONS BASED ON LIMITED SET OF ANALYTICAL DATA
- NONLINEAR LANDING FORCES ARE APPROXIMATED
- PAYLOAD RESPONSES HAVE INCREASED WITH NEW SHUTTLE MODELS
 - UP TO 50% INCREASE IN Z
 - UP TO 250% INCREASE IN Y
 - SMALL INCREASE IN AXIAL X
- MODEL DATA IS IN THE FORM OF FREE SYSTEM MODES WHICH CONVERGE SLOWLY IN MODAL SYNTHESIS ANALYSES
 - LIFTOFF, 300 MODES TO 66 Hz
 - LANDING, 300 MODES TO 157 Hz



COMBINING SUBSYSTEM LOAD FACTORS

- LOAD FACTORS REPRESENT RANDOM VARIATIONS OF UNCERTAINTIES
- RANDOM VARIATIONS CAN BE COMBINED IN SEVERAL WAYS:

(1) CONSERVATIVE PRODUCT

$$K_{TOTAL} = K_{STS} K_{ST} K_{SA} \dots$$

(2) R.S.S. (UNCORRELATED PROCESSES)

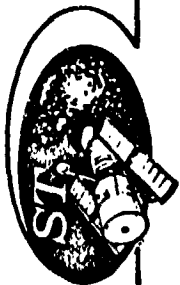
$$K_{TOTAL} = 1 + \sqrt{(K_{STS}^{-1})^2 + (K_{ST}^{-1})^2 + (K_{SA}^{-1})^2} + \dots$$

(3) SUM (PERFECTLY CORRELATED PROCESSES)

$$K_{TOTAL} = 1 + (K_{STS}^{-1}) + (K_{ST}^{-1}) + (K_{SA}^{-1}) + \dots$$

- THE WAY TO COMBINE LOAD FACTORS IS UNCLEAR
- SPACE TELESCOPE USES THE CONSERVATIVE PRODUCT

SUBSYSTEM	FACTOR
SPACE SHUTTLE	K_{STS}
SPACE TELESCOPE	K_{ST}
OTHER SUB-ASSEMBLIES	K_{SA}



LOAD VARIABILITY FACTORS FOR SPACE TELESCOPE

FOR PRELIMINARY LOADS CYCLE

	K _{STS}	K _{ST}	K _{TOTAL}
LIFTOFF X - AXIAL	1.25	1.25	1.56
Y	2.00	1.25	2.50
Z	1.50	1.25	1.88
LANDING X - AXIAL	1.25	1.25	1.56
Y - LATERAL	1.25	1.25	1.56
Z - VERTICAL	1.15	1.25	1.44

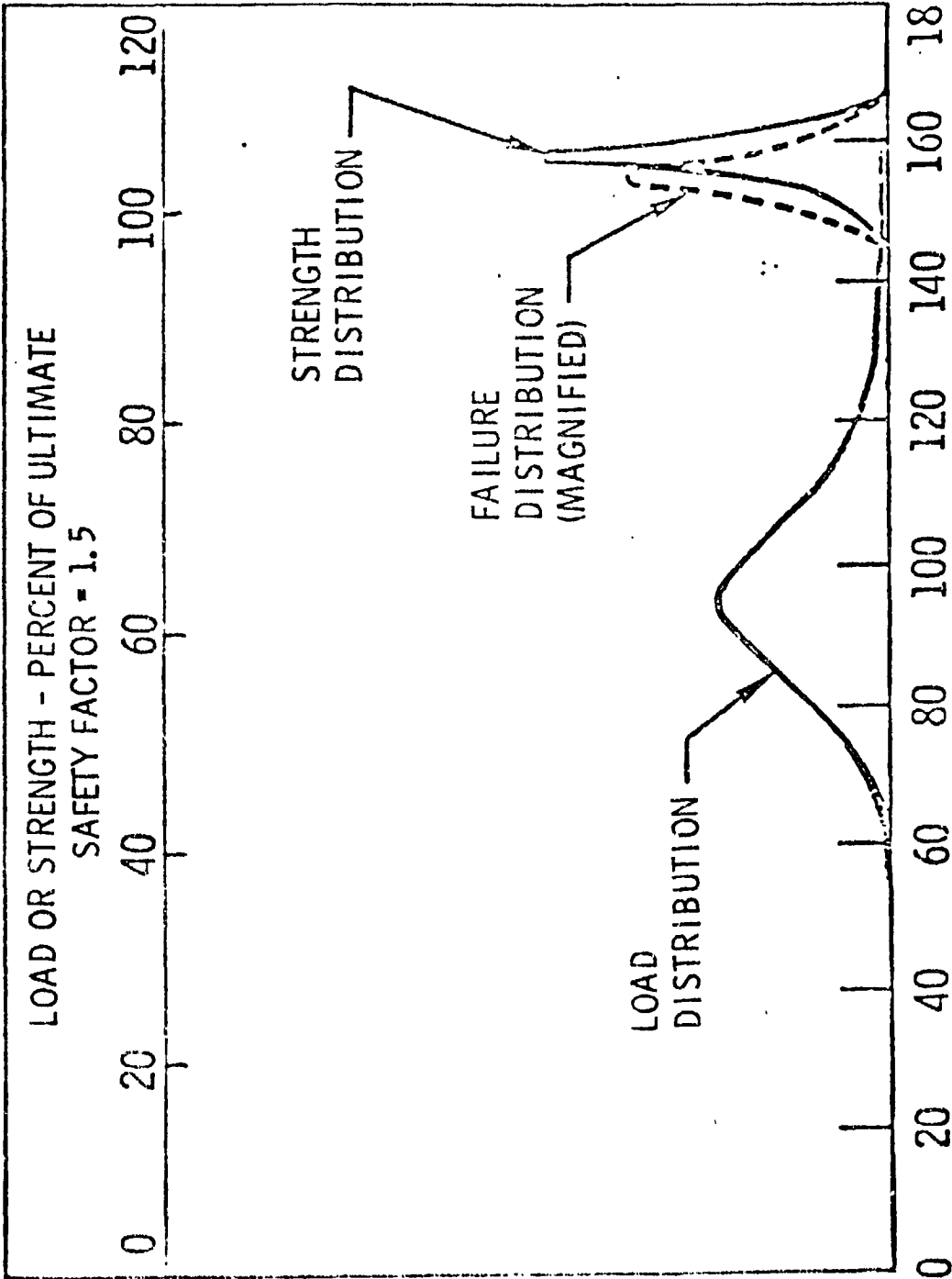


CONCLUDING COMMENTS

- LOAD VARIABILITY FACTORS ARE BASED ON ENGINEERING JUDGEMENT AND EXPERIENCE WITHOUT A RIGOROUS MATHEMATICAL CRITERION (STATISTICAL STUDY OF CONSTRUCTOR EXPERIENCE WOULD BE HELPFUL)
- A "BEST METHOD" SHOULD BE DEVELOPED FOR COUPLING THE SPACECRAFT AND THE SHUTTLE MODELS
- THE MODAL TEST PROGRAM AND FLIGHT DATA WILL BUILD CONFIDENCE IN SHUTTLE MODELS AND DECREASE THE UNCERTAINTY FACTORS

EP2785 ORGANIZATION:	MSFC/EP46	MARSHALL SPACE FLIGHT CENTER	NAME: N. SCHLEMMER
		STRUCTURAL CRITERIA	DATE: NOVEMBER 1978

- INTRODUCTION
- SAFETY FACTORS
- FATIGUE FACTOR
- FUTURE CONSIDERATION
- SUMMARY



LOAD OR STRENGTH - PERCENT OF ULTIMATE
SAFETY FACTOR = 1.5

PROBABILITY DENSITY FUNCTION

EP2804

ORGANIZATION:

MARSHALL SPACE FLIGHT CENTER

NAME:

N. SCHLEMMER

MSFC/EP46

STRUCTURAL CRITERIA

DATE:

NOVEMBER 1978

STRUCTURAL SAFETY FACTORS

- INTENTIONAL OVER-DESIGN
- CHOICE IS PRIMARILY INFLUENCED BY
 - PERSONNEL SAFETY
 - AMOUNT OF TESTING

- WHERE PERSONNEL SAFETY IS INVOLVED ● INFLUENCE OF STRUCTURAL TESTING
- FSU/FSU = 1.1/1.4 PLUS STRUCTURAL TESTING
- EXAMPLES: SPACE SHUTTLE
 - EXTERNAL TANK
 - SOLID ROCKET BOOSTER
 - ORBITER
 - SPACELAB
 - PALLET
 - MODULE
 - SKYLAB
 - SATURN VEHICLE
- FSU/FSU = 2.0/3.0; NO TESTING
- EXAMPLES: VARIOUS SPACELAB EXPERIMENTS
- MOST GROUND SUPPORT EQUIPMENT
- NO STRUCTURAL TESTING
- SAFETY FACTORS: 2.25 TO 3.00
- EXAMPLES
 - HEAO A FSULT = 3.00
 - HEAO B FSULT = 2.25
 - HEAO C FSULT = 2.75
 - SKYLAB PAYLOAD SHROUD 3.00
 - GSE 3.00
 - TELEOPERATOR 2.25
- STRUCTURAL TESTING REQUIRED
- SAFETY FACTORS: 1.25 TO 1.40
- EXAMPLES
 - EXTERNAL TANK 1.40
 - SOLID ROCKET BOOSTER 1.40/1.25
 - SKYLAB 1.25/1.40
 - INERTIAL UPPER STAGE 1.40

EP-2781

ORGANIZATION:

MSFC/EP46

MARSHALL SPACE FLIGHT CENTER
STRUCTURAL CRITERIA

NAME: N. SCHLEMMER
DATE: NOVEMBER 1978

SUMMARY OF GOVERNMENT AND INDUSTRY PRACTICE

ORGANIZATION	MANNED SYSTEMS AND CONDITIONS INVOLVING PERSONNEL SAFETY			UNMANNED SYSTEMS AND CONDITIONS NOT INVOLVING PERSONNEL SAFETY				
	YIELD FACTOR	ULTIMATE FACTOR	CYCLE FACTOR	TESTS REQUIRED	YIELD FACTOR	ULTIMATE FACTOR	CYCLE FACTOR	TESTS REQUIRED
AIR FORCE WPAFB	NONE	1.50	2.0	ULTIMATE LOAD AND FATIGUE	1.00	1.25	2.0	PROOF LOAD OF FLIGHT ARTICLE
FAA	NONE	1.50	4.0	ULTIMATE LOAD AND FATIGUE	NONE	1.20	4.0	ULTIMATE LOAD AND FATIGUE
NASA-LANGLEY	1.15	1.50		ULTIMATE LOAD	1.15	1.50		ULTIMATE LOAD
NASA-GODDARD					1.35 TO 1.50	1.65 TO 2.00		ULTIMATE LOAD
JPL						1.25 (1.75 PV)	2.0 TO 3.0	ULTIMATE LOAD
BELL AEROSPACE		1.50		ULTIMATE LOAD				
BRISTOL AEROSPACE					1.33	1.50		TEST TO YIELD FACTOR
MDAC		1.40	4.0	ULTIMATE LOAD		1.25		

TYPICAL STRUCTURAL DESIGN FACTORS FOR SPACE VEHICLES
 REFERENCE: DRAFT DESIGN CRITERIA MONOGRAPH "STRUCTURAL DESIGN FACTORS" (NASA LANGLEY)

<u>AGENCY/COMPANY</u>	<u>PROGRAM</u>	<u>YIELD FACTOR</u>	<u>ULTIMATE FACTOR</u>
JSC/R.I	APOLLO CM & LES	1.0	1.50 (TESTED)
JSC/MDAC	GEMINI	1.0	1.36
JSC/MDAC	MERCURY	1.0	1.50
JSC/GAEC	APOLLO LEM	1.35	1.50
MSFC	SATURN	1.1	1.40
MSFC/MDAC	SKYLAB	1.1 (TESTED)	1.40 (TESTED)
		2.0 (UNTESTED)	3.00 (UNTESTED)
JSC/LMSC	AGENA	1.0	1.25 (TESTED)
JSC/LMSC	POLARIS	1.0	1.25
JSC/GDC	ATLAS/CENTAUR	1.0	1.25
USAF/MMC	TITAN	1.0	1.25
GSFC	NIMBUS	1.2	1.50
JPL	MARINER, VIKING, RANGER	1.0	1.25
NASA & USAF/MDAC	THOR/DELTA	1.0 (TESTED)	125 (TESTED)
			1.50 (UNTESTED)

EP2805

ORGANIZATION:

MSFC/EP46

MARSHALL SPACE FLIGHT CENTER

STRUCTURAL CRITERIA

NAME:

N. SCHLEMMER

DATE:

NOVEMBER 1978

FATIGUE ANALYSIS

● BASIC INPUT FROM LOADS SPECIALIST

● LOAD MAGNITUDES

● LOADS DISTRIBUTION

● LOADS VARIATION WITH TIME

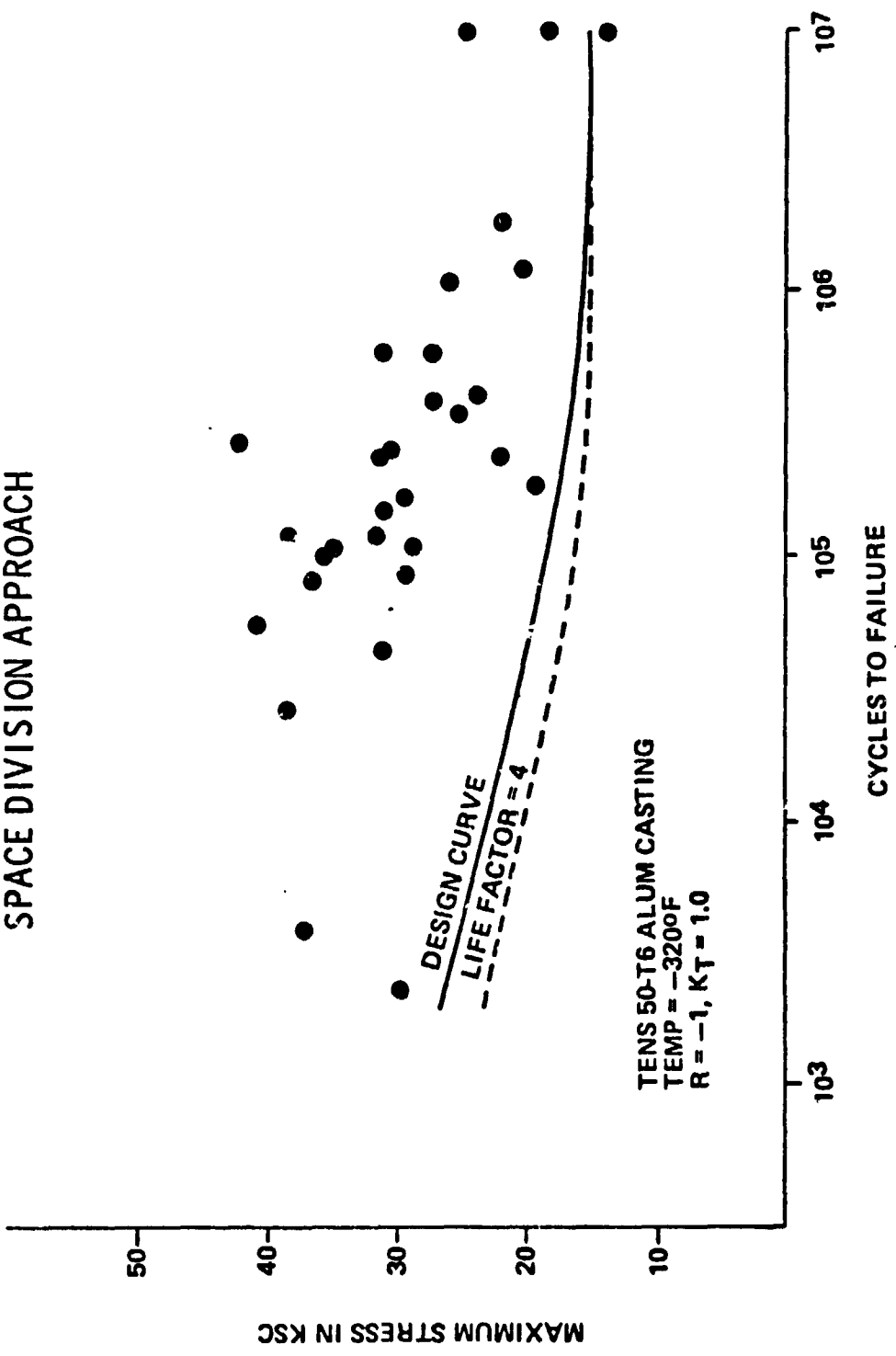
● CONFIGURATION

● MATERIALS DATA

● STRESS ANALYSIS

● FATIGUE LIFE

SPACE DIVISION APPROACH



EP7788

ORGANIZATION:

MSFC/EP46

MARSHALL SPACE FLIGHT CENTER

STRUCTURAL CRITERIA

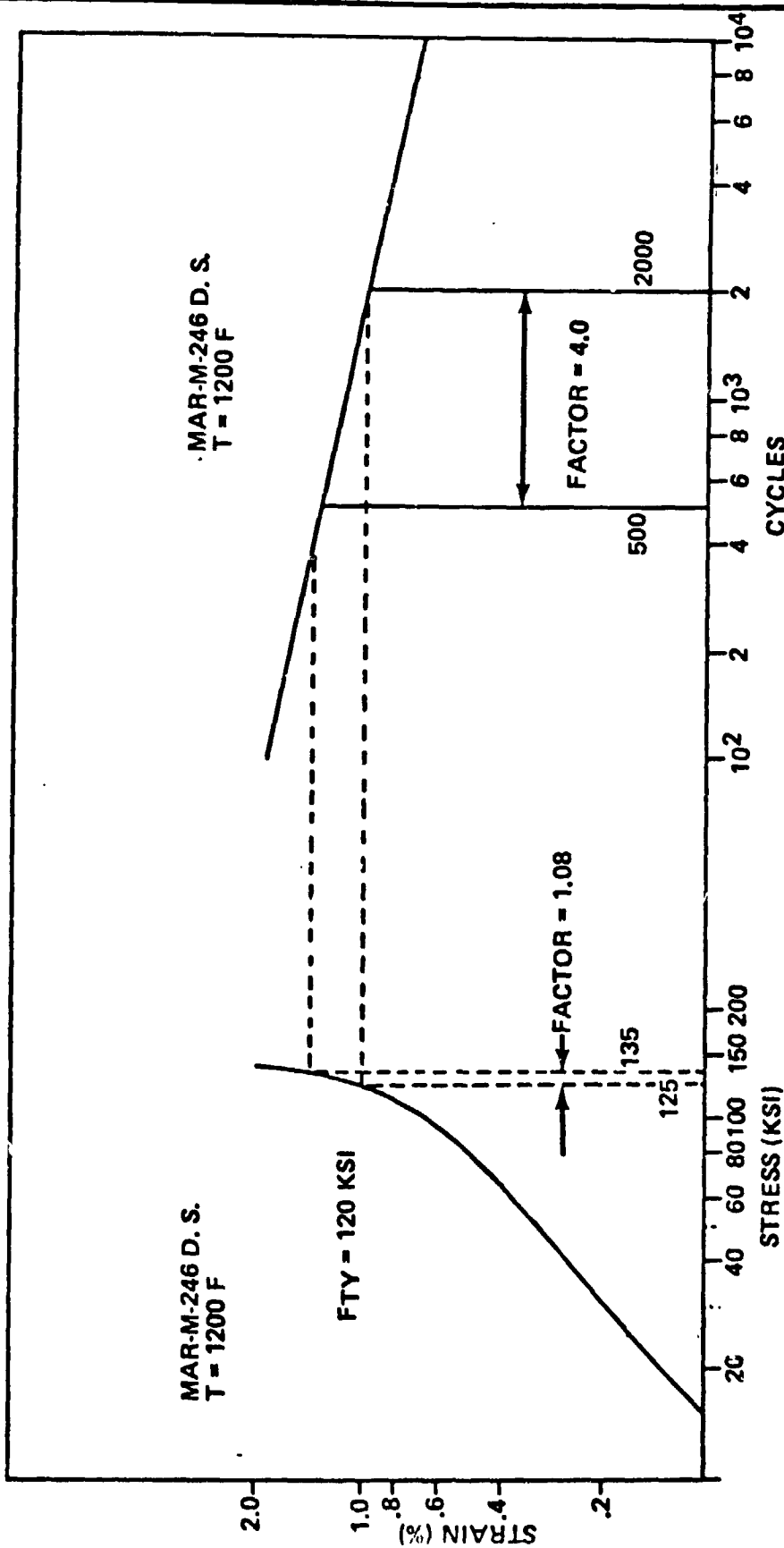
NAME:

N. SCHLEMMER

DATE:

NOVEMBER 1978

STRESS-STRAIN-CYCLES RELATIONSHIPS IN THE LOW CYCLE RANGE



STRUCTURAL CRITERIA

MSFC/EP46

SUMMARY

- MSFC APPLICATION OF SAFETY FACTORS
- QUASI STEADY STATE CONDITIONS
- FATIGUE CONDITIONS
- CONSIDERATION FOR FUTURE FATIGUE CRITERIA
- MORE REALISTIC
- MORE CONSERVATIVE

AN APPROACH FOR
ESTABLISHING PRELIMINARY STRUCTURAL DESIGN
REQUIREMENTS FOR SHUTTLE PAYLOADS

J. I. McPHERSON
D. A. R. NELSON, JR.
S. BRANDT

PRESENTED AT
PAYLOAD FLIGHT LOADS PREDICTION
METHODOLOGY WORKSHOP
14-16 NOVEMBER 1978
MARSHALL SPACE FLIGHT CENTER



BACKGROUND

*THE SHUTTLE SYSTEM IS BEING DEVELOPED AS A VEHICLE TO TRANSPORT CARGO TO SPACE. SOME FUNCTIONAL CHARACTERISTICS OF THE SHUTTLE ARE SIMILAR TO THOSE OF OTHER CARGO TRANSPORTS.

- LARGE NUMBER OF PAYLOADS
- WIDE VARIETY OF PAYLOADS
- MANIFESTS OF MULTIPLE PAYLOADS
- FREQUENT MISSIONS

*IN THE DESIGN OF CARGO FOR AIR, RAIL, AND WATER TRANSPORT SYSTEMS, THERE IS LITTLE REQUIREMENT FOR COMPLEX INTERFACES OF INDIVIDUAL CARRIER OR CARGO DETAILS. LIKEWISE, A PRELIMINARY PAYLOAD DESIGN APPROACH WITH MINIMUM NEED FOR COMPLEX INTERFACES WITH SHUTTLE DEVELOPMENTAL AND OPERATIONAL DETAILS IS DESIRABLE.

INTRODUCTION

OBJECTIVE: DEVELOP METHODOLOGY TO REDUCE PAYLOAD CONTRACTORS NEED TO INTERFACE WITH LARGE DETAILED SHUTTLE STRUCTURAL ANALYSES.

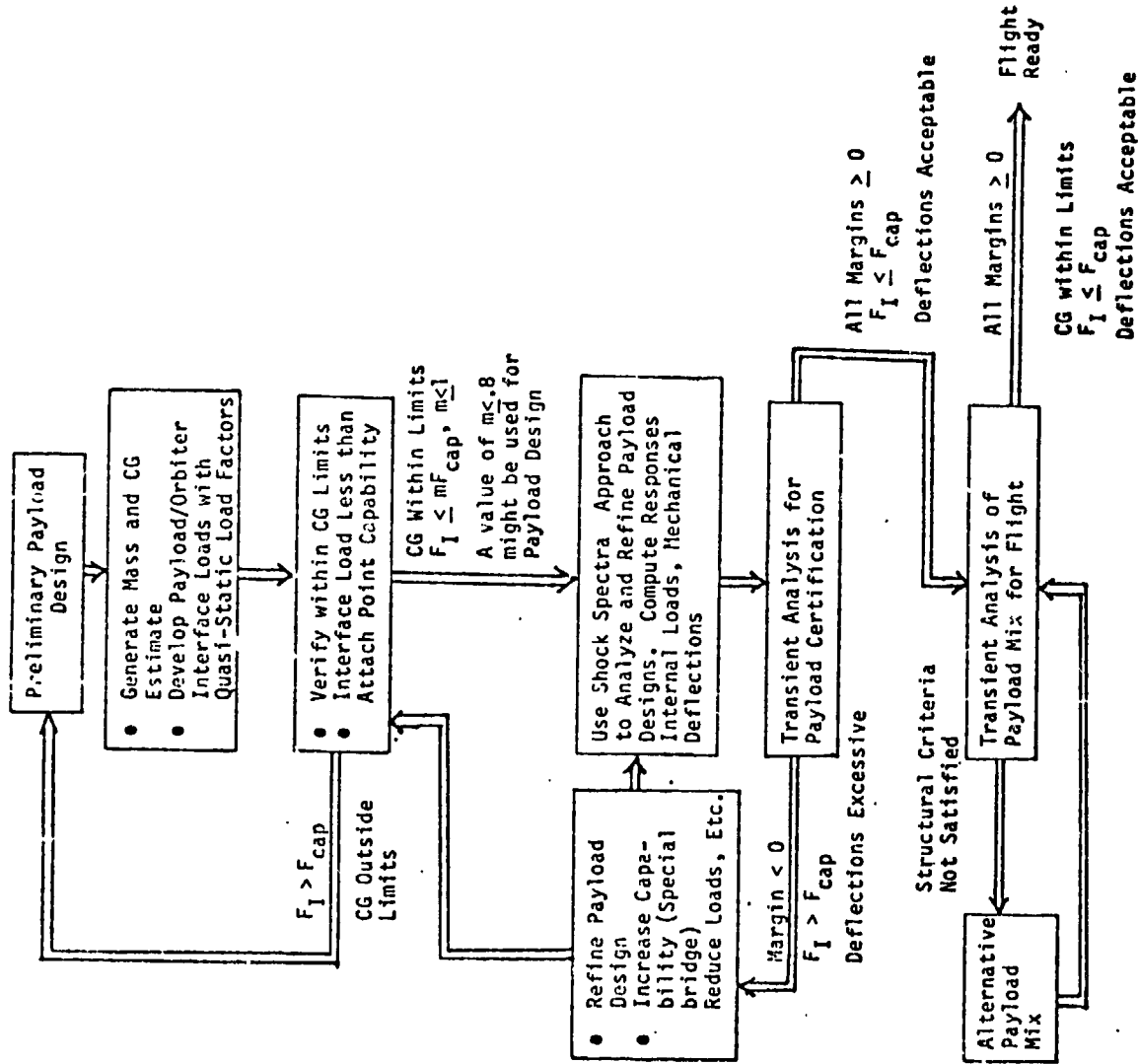
APPROACH: A MULTIPLE METHOD TECHNIQUE IS BEING STUDIED FOR SPACECRAFT STRUCTURAL DESIGN

- *LOAD FACTOR METHOD FOR INITIAL DESIGN LOADS GENERATION
- *SHOCK SPECTRA (RESPONSE SPECTRA) APPROACH FOR PRELIMINARY DESIGN PHASE
- *TRANSIENT ANALYSIS FOR FINAL DESIGN VERIFICATION AND FLIGHT READINESS CERTIFICATION

POTENTIAL BENEFITS:

- *PAYLOAD CONTRACTOR
 - INCLUDE PAYLOAD DYNAMICS IN EARLY DESIGN PHASE
 - REDUCE PERTURBATIONS TO PAYLOAD DESIGN CAUSED BY CHANGES IN SHUTTLE STRUCTURE AND/OR ENVIRONMENT (FORCING FUNCTIONS)
 - PROVIDE RAPID RESPONSE ASSESSMENT METHOD FOR PAYLOAD DESIGN SUPPORT
- *SHUTTLE ORGANIZATION
 - PRELIMINARY STRUCTURAL EVALUATIONS OF MULTIPLE PAYLOAD MANIFESTS
 - SCREENING OF PAYLOADS PRIOR TO CERTIFICATION ANALYSIS

POSSIBLE PAYLOAD STRUCTURAL DESIGN CYCLE



ORIGINAL PAGE IS OF POOR QUALITY

ORIGINAL PAGE IS
OF POOR QUALITY

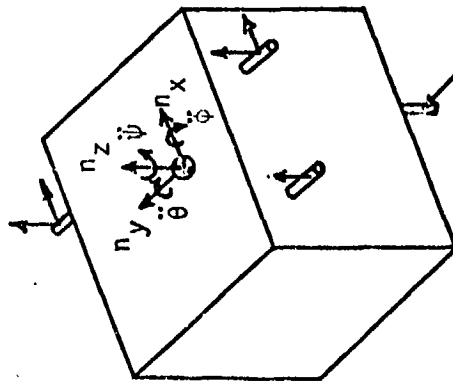
LOAD FACTOR APPROACH

*BACKGROUND

- GENERALLY USED FOR ANALYSIS WHEN LARGE TRANSIENTS ARE NOT ANTICIPATED
- ESPECIALLY SUITED TO EARLY DESIGN STUDIES

*CHARACTERISTICS

- SIMPLE METHOD TO APPLY
- MAXIMUM ELASTIC RESPONSES CANNOT BE DETERMINED WITH LOAD FACTOR APPROACH (ESTIMATES OF PROFILES COULD BE MADE)
- DISTRIBUTION ASSUMPTIONS NEEDED FOR INDETERMINATE SYSTEMS



LOAD FACTOR APPROACH (CONTINUED)

REQUIRES THAT SUITABLE LOAD FACTORS ARE AVAILABLE WHICH CAN BE USED IN CONJUNCTION WITH THE MASS AND GEOMETRIC PROPERTIES OF THE ITEM BEING DESIGNED (SHUTTLE PAYLOAD LOAD FACTORS ARE GIVEN IN ICD 2-19001, "SHUTTLE ORBITER/CARGO STANDARD INTERFACES," AND JSC 07700, "LEVEL II PROGRAM DEFINITION AND REQUIREMENTS, VOL. XIV, SPACE SHUTTLE SYSTEM PAYLOAD ACCOMMODATIONS")

- SHUTTLE LOAD FACTORS ARE ASSUMED INDEPENDENT OF PAYLOAD LOCATION IN RAY AND PAYLOAD ELASTIC CHARACTERISTICS
- COMPARISONS OF ATTACH POINT LOADS ESTIMATED WITH LOAD FACTORS AND ATTACH POINT CAPABILITIES CAN BE USED IN THE ASSESSMENT OF ATTACH POINT SELECTIONS

SHOCK SPECTRA METHOD

*BACKGROUND

- A SHOCK SPECTRA/IMPEDANCE METHOD WAS USED BY JPL ON THE MARINER JUPITER SATURN PROJECT
- A SHOCK SPECTRA TECHNIQUE WAS EMPLOYED IN THE DESIGN OF THE HARPOON MISSILE

*CHARACTERISTICS

- QUICK TURN AROUND METHOD FOR DESIGN SUPPORT
- COMPARATIVELY INEXPENSIVE
- REQUIRES ATTACH POINT INTERFACE RESPONSE DATA FROM ANALYSIS OR PREVIOUS FLIGHTS TO ESTABLISH ENVELOPE
- USE OF SHOCK SPECTRA ENVELOPES REDUCES SENSITIVITY TO SHUTTLE SYSTEM MODEL AND FORCING FUNCTION CHANGES
- DEPENDENT ON PAYLOAD DAMPING ESTIMATE
- NO PHASING OF LOAD (USUALLY CONSERVATIVE)
- PREDICTIONS/CONFIDENCE SHOULD IMPROVE WITH EXPERIENCE

TRANSIENT ANALYSIS TECHNIQUE

*BACKGROUND

- CLASSICAL APPROACH USED FOR ANALYSIS OF TRANSIENT CONDITIONS
- RIGOROUS APPROACH FOR HARDWARE CERTIFICATION

*CHARACTERISTICS

- ACCURATE METHOD WHICH CAN RESULT IN LIGHT WEIGHT DESIGN
- DOES NOT REQUIRE PREVIOUS FLIGHT DATA
- SLOW RESPONSE FOR STRUCTURAL DESIGN SUPPORT
- SENSITIVE TO DESIGN MODIFICATIONS
- EXPENSIVE
- MODELS/DATA FROM MULTIPLE ORGANIZATIONS MUST INTERFACE
 - QUALITY OF OTHER PAYLOAD MODELS WHICH SHARE PAYLOAD BAY
 - MAINTENANCE OF SHUTTLE MODELS AND FORCING FUNCTIONS

USE OF SHOCK SPECTRA METHOD
IN PAYLOAD DESIGN

*GENERATE A PAYLOAD BASE FIXED MODAL MODEL AND A LOAD TRANSFORMATION MATRIX

$$\begin{bmatrix} M_C & | & M_{CE} \\ \hline M_{CE}^T & | & 1 \end{bmatrix} \begin{Bmatrix} \ddot{X}_B \\ \ddot{Q}_E \end{Bmatrix} + \begin{bmatrix} 0 & | & 0 \\ \hline 0 & | & 2\zeta\omega_N \end{bmatrix} \begin{Bmatrix} \dot{X}_B \\ \dot{Q}_E \end{Bmatrix} + \begin{bmatrix} K_C & | & 0 \\ \hline 0 & | & \omega_N^2 \end{bmatrix} \begin{Bmatrix} X_B \\ Q_E \end{Bmatrix} = \begin{Bmatrix} F_B \\ 0 \end{Bmatrix} \quad (1)$$

$$\left\{ \begin{array}{l} \text{INTERNAL LOADS} \\ \text{STRESSES} \\ \text{RELATIVE PHYSICAL} \\ \text{MOTION} \\ \text{ETC.} \end{array} \right\} = [LTM] \left\{ \ddot{Q}_E \right\} \quad (2)$$

FOR THE ITH MODE

$$\ddot{Q}_{E_I} + 2\zeta\omega_{N_I} \dot{Q}_{E_I} + \omega_{N_I}^2 Q_{E_I} = - \left\{ M_{CE} \right\}_I^T \left\{ \ddot{X}_B \right\} \quad (3)$$

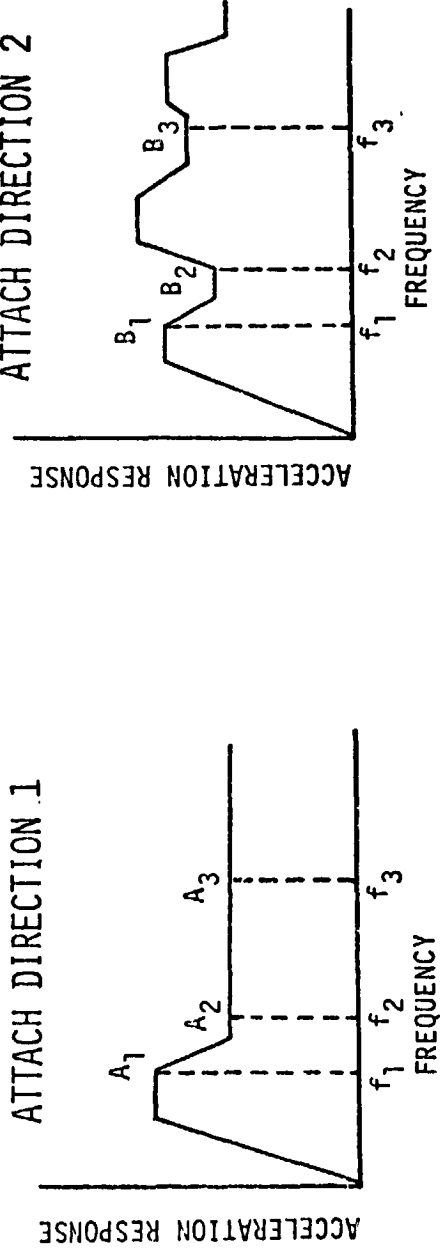
THE SHOCK SPECTRUM METHOD IS BASED ON

$$\ddot{X}_R + 2\zeta\omega \dot{X}_R + \omega^2 X_R = -\ddot{X}_B \quad (4)$$

NOTE THAT EQS. (3) AND (4) ARE SIMILAR WITH THE EXCEPTION OF THE TIME INDEPENDENT QUANTITIES $\left\{ M_{CE} \right\}_I$.

USE OF SHOCK SPECTRA METHOD
IN PAYLOAD DESIGN (CONTINUED)

*INTERROGATE SHUTTLE SHOCK SPECTRA ENVELOPES AND DETERMINE MODAL RESPONSES



$$\ddot{q}_{E1} = M_{CE1,1} A_1 + M_{CE2,1} B_1 + \dots$$

$$\ddot{q}_{E2} = M_{CE1,2} A_2 + M_{CE2,2} B_2 + \dots$$

$$\vdots$$

$$\ddot{q}_{EM} = M_{CE1,M} A_M + M_{2,M} B_M + \dots$$

*COMPUTE DESIRED PAYLOAD DESIGN PARAMETERS WITH LTM AND STATISTICAL MODAL SUMMATION APPROACH (PEAK + RSS)

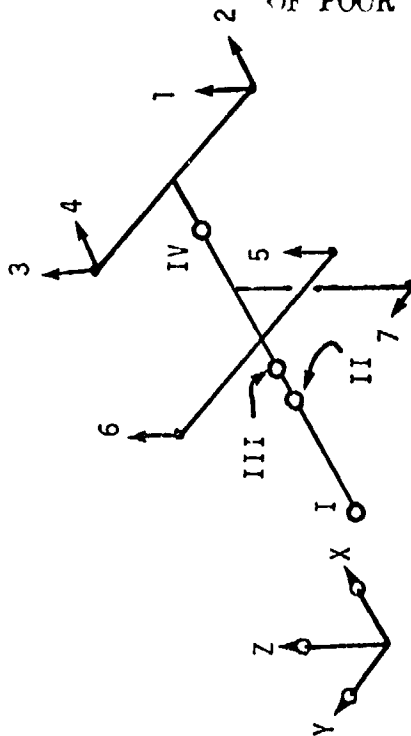


PAYLOAD EXAMPLE USING "EXACT" SHOCK SPECTRA

*MAXIMUM ACCELERATIONS WERE ESTIMATED AT FOUR PAYLOAD POINTS USING THE SHOCK SPECTRA FOR THE CONSTRAINED PAYLOAD ATTACH POINT DEGREES OF FREEDOM.

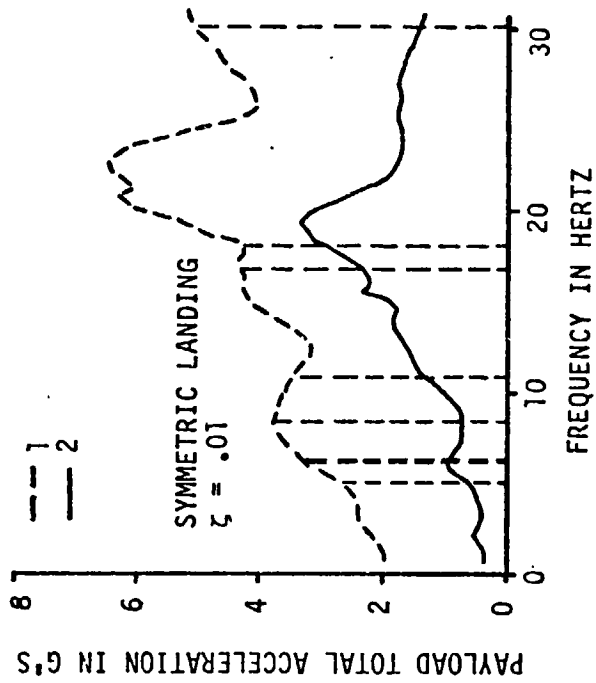
*IN THIS EXAMPLE, ACCELERATION PREDICTIONS ARE INDEPENDENT OF ENVELOPING PROCEDURE -- ATTACH POINT SHOCK SPECTRA WERE DEVELOPED FROM TRANSIENT ANALYSIS RESULTS FOR THE SPECIFIC PAYLOAD AND UNIQUE FLIGHT CONDITION.

SCHEMATIC OF PARAMETRIC PAYLOAD



ORIGINAL PAGE IS
OF POOR QUALITY

ATTACH POINT SHOCK SPECTRA



PAYLOAD EXAMPLE USING "EXACT" SHOCK SPECTRA (CONTINUED)

RESPONSE PREDICTIONS
SYMMETRIC LANDING CONDITION

LOCATION	DIRECTION	ACCELERATION PREDICTION (G'S)		
		TRANSIENT ANALYSIS	SHOCK SPECTRA	
			PEAK + RSS	RSS
I	X	1.03	.79	.65
	Y	.0012	.0006	.0004
	Z	4.62	4.62	3.27
II	X	.92	.59	.58
	Y	.0014	.0008	.0006
	Z	4.78	5.39	3.83
III	X	.92	.59	.58
	Y	.0018	.0005	.0005
	Z	4.46	5.22	3.75
IV	X	.89	.58	.56
	Y	.0011	.0004	.0003
	Z	3.13	5.33	4.88

*X-DIRECTION ACCELERATION PREDICTIONS ARE BEING FURTHER EVALUATED TO STUDY "STEADY-STATE" ACCELERATION CONTRIBUTIONS

SHUTTLE SHOCK SPECTRA ENVELOPES

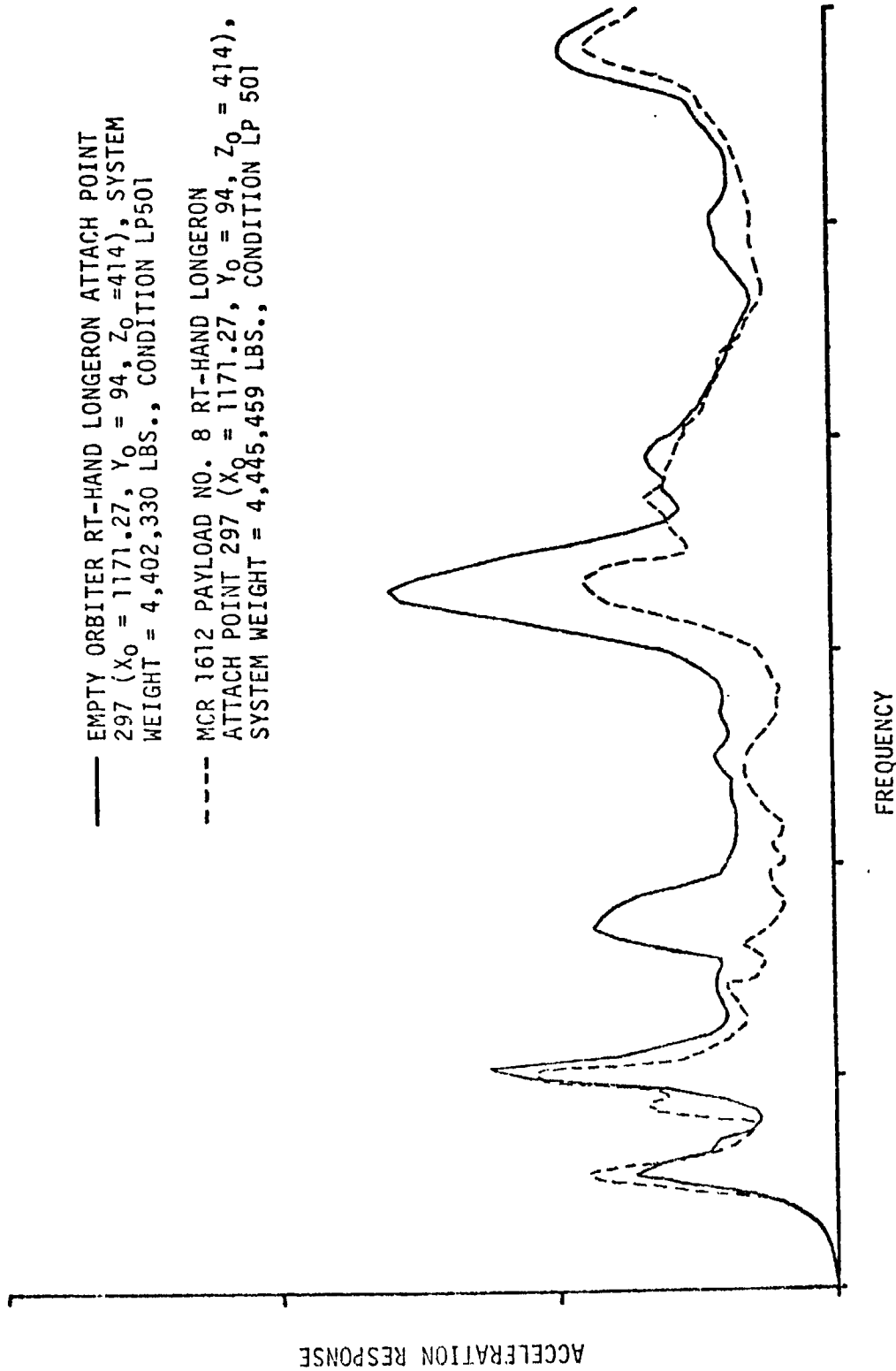
*ESTABLISH FORMAT FOR SHOCK SPECTRA ENVELOPES

- PARAMETERS TO BE INVESTIGATED
 - PAYLOAD MASS - EMPTY ORBITER, LIGHT AND HEAVY PAYLOADS
 - CONSTRAINED PAYLOAD FREQUENCIES - SHUTTLE RESONANCE FREQUENCIES
 - PAYLOAD GEOMETRY - ATTACH POINT SPACING, CANTILEVERED PAYLOAD
 - PAYLOAD TO ORBITER ATTACH POINT LOCATIONS - FORWARD BAY, MIDDLE BAY, AFT BAY
 - DAMPING
 - ABOVE ITEMS IN MULTIPLE PAYLOAD SITUATIONS
- APPROACHES TO BE CONSIDERED
 - INCLUDE ALL PEAKS OR ENVELOPE AT LOWER LEVELS
 - MULTIPLE POINT BASE DRIVE OR SINGLE POINT BASE DRIVE - ROTATIONAL MOTION, REDUNDANT SUPPORT SYSTEMS
 - SEPARATE OR COMMON ENVELOPES FOR DIFFERENT CATEGORIES OF FLIGHT CONDITIONS - LIFTOFF, LANDING

*INVESTIGATE USE OF REDUCTION FACTORS OR NOTCHING OF ENVELOPES

- PAYLOAD MASS
- INTERFACE FORCES VERSUS FACTORED ORBITER ATTACH POINT CAPABILITY
- SHOCK SPECTRA SHAPE AND RELATIVE IMPEDANCE (JPL)

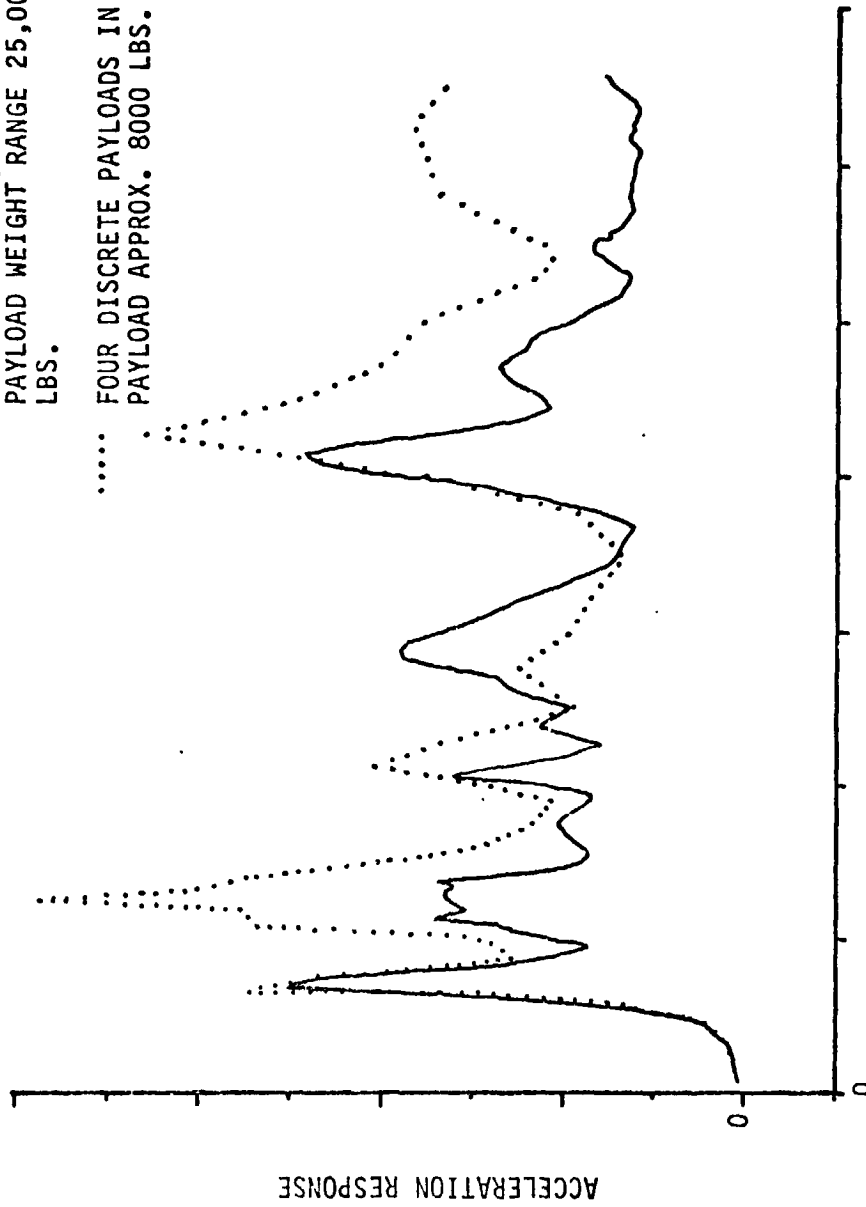
ATTACH POINT MAXIMUM Z-DIRECTION ACCELERATION AT LIFTOFF



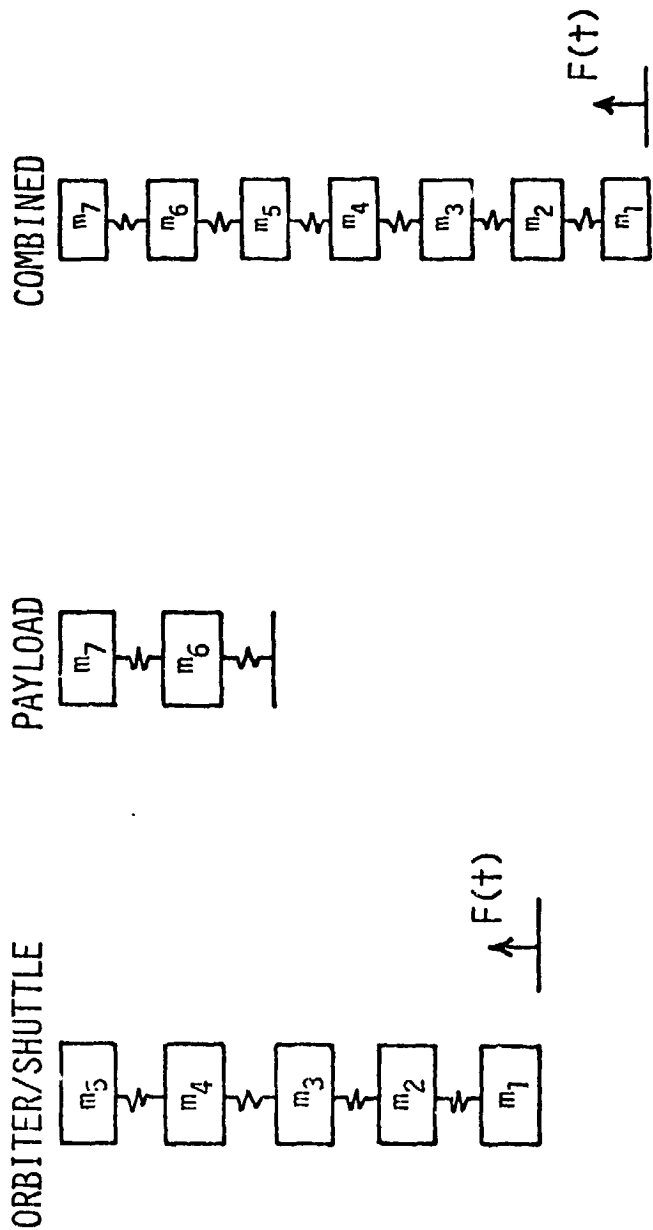
ENVELOPE OF PAYLOAD ATTACH POINT MAXIMUM
Z-DIRECTION ACCELERATION RESPONSES FOR
LIFTOFF CONDITIONS

— SELECTED MCR 1612 PAYLOADS, 20 PAYLOAD
CONFIGURATIONS, SINGLE PAYLOAD IN BAY,
PAYLOAD WEIGHT RANGE 25,000 TO 43,000
LBS.

..... FOUR DISCRETE PAYLOADS IN BAY, EACH
PAYLOAD APPROX. 8000 LBS.



PARAMETRIC STUDY



OBJECTIVE: INVESTIGATE EFFECTS OF PAYLOAD MASS VARIATIONS AND SHUTTLE/PAYLOAD FREQUENCY TUNING ON PAYLOAD RESPONSE.

METHOD: VARY PAYLOAD CHARACTERISTICS (MASS, CONSTRAINED FREQUENCIES) TO OBTAIN MATRIX OF PAYLOADS. COMPARE PAYLOAD RESPONSES COMPUTED FOR COMBINED SYSTEM.

SUMMARY

*A MULTIPLE METHOD ANALYSIS APPROACH IS BEING EXAMINED FOR USE IN PAYLOAD DESIGN AND PAYLOAD CERTIFICATION

- LOAD FACTOR
- SHOCK SPECTRA
- TRANSIENT

*POTENTIAL FOR DECREASE IN THE NEED FOR TRANSIENT ANALYSES

- PAYLOAD DESIGN
- MULTIPLE PAYLOAD MANIFESTS

*DEVELOPMENT OF DESIGN GUIDELINES FOR THE SHOCK SPECTRA METHOD IS BEING STUDIED

- GENERATE SHOCK SPECTRA FROM AVAILABLE PREDICTED RESPONSE DATA
- SELECT FORMAT FOR PRESENTATION OF ENVELOPES OF SHOCK SPECTRA
- INVESTIGATE USE OF REDUCTION FACTORS
- EVALUATE PROPOSED APPROACHES

*THIS APPROACH IS BEING EVALUATED UNDER CONTRACT WITH NASA-JSC AS ONE OF MANY APPROACHES FOR SHUTTLE/PAYLOAD INTEGRATION

ESTIMATION OF PAYLOAD LOADS USING RIGID BODY INTERFACE ACCELERATIONS

By

Jay C. Chen

John A. Garba

Ben K. Wada



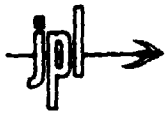
APPLIED MECHANICS TECHNOLOGY SECTION

JET PROPULSION LABORATORY

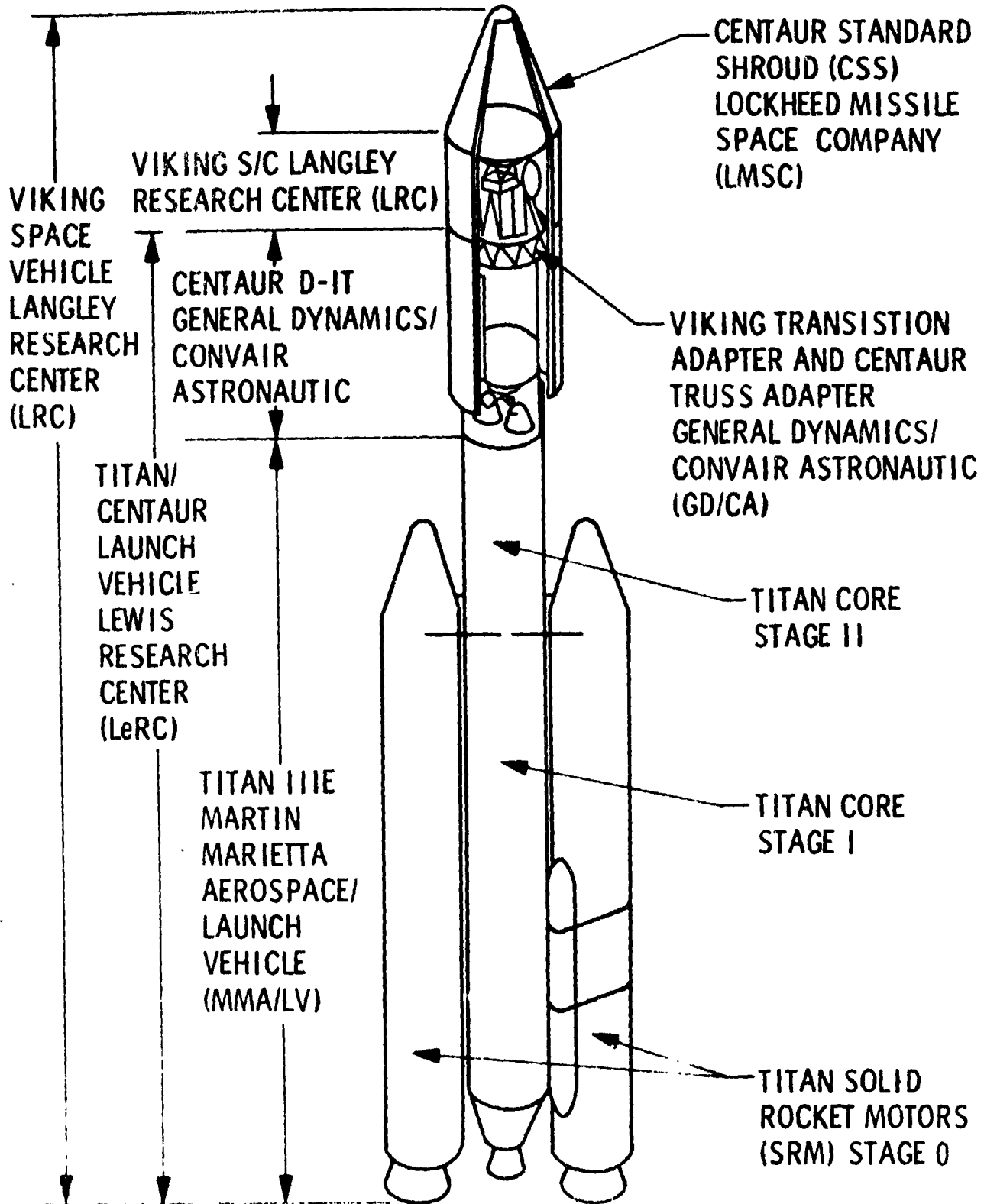
SPONSORED BY

OAST-NASA

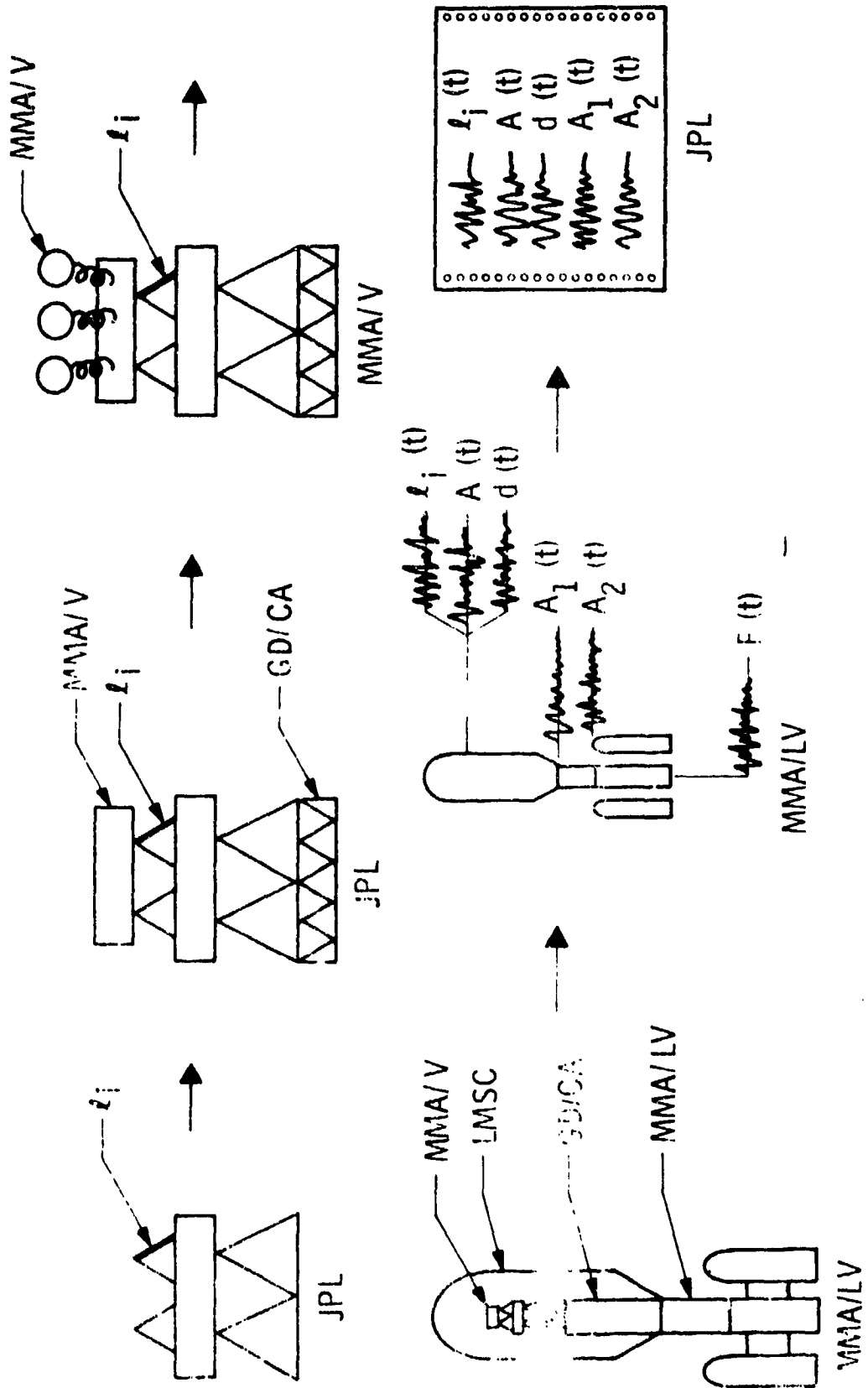
PRECEDING PAGE BLANK NOT FILMED



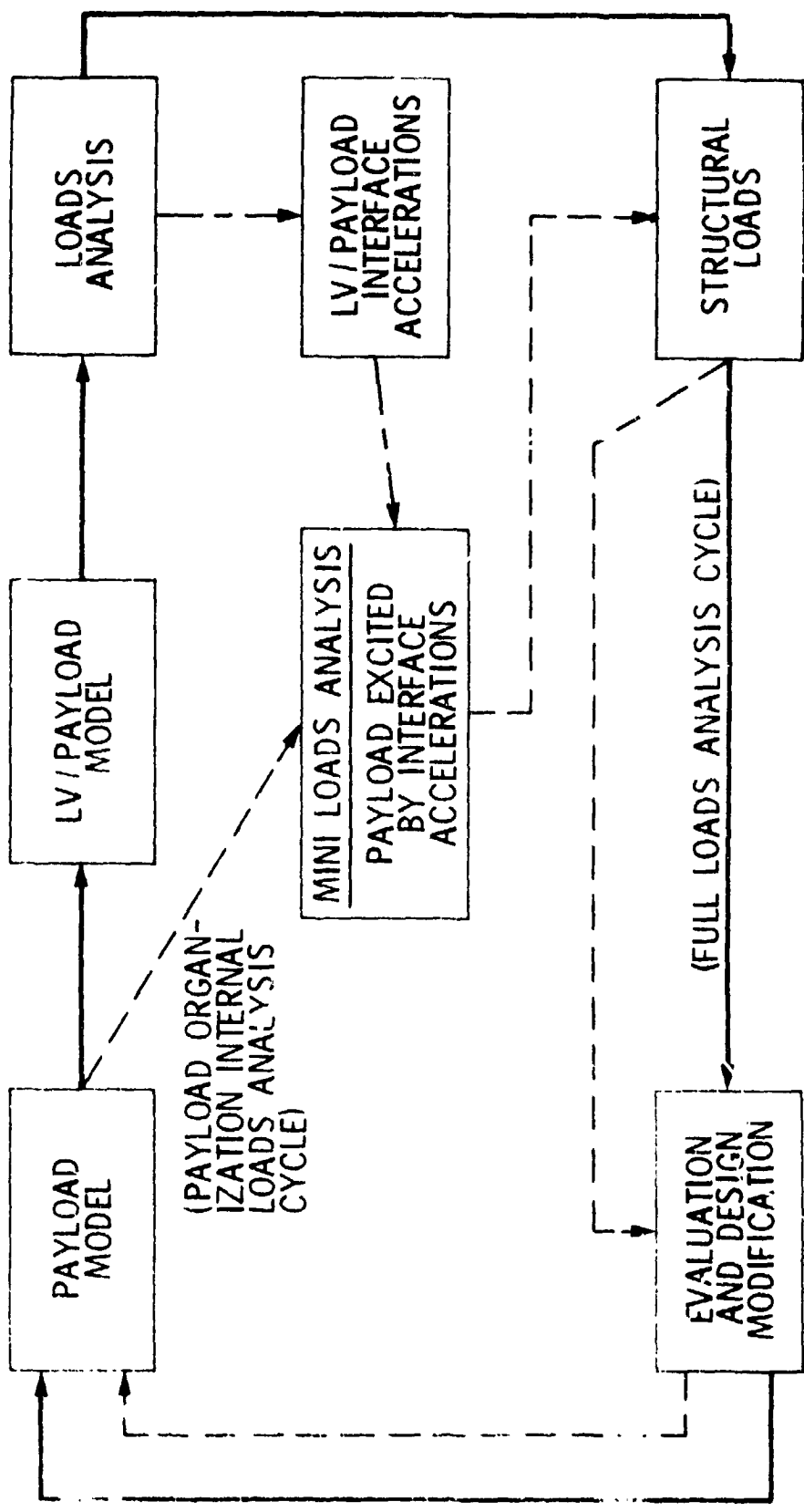
VIKING TITAN-CENTAUR VEHICLE



LOAD ANALYSIS PROCESS



DESIGN/LOADS ANALYSIS CYCLE



GOVERNING EQUATION FOR LAUNCH VEHICLE/PAYLOAD COMPOSITE MODEL

$$\begin{bmatrix} M_1 & 0 \\ 0 & M_2 \end{bmatrix} \begin{Bmatrix} \ddot{x}_1 \\ \ddot{x}_2 \end{Bmatrix} + \begin{bmatrix} K_{11} & K_{12} \\ K_{21} & K_{22} \end{bmatrix} \begin{Bmatrix} x_1 \\ x_2 \end{Bmatrix} = \begin{Bmatrix} F(t) \\ 0 \end{Bmatrix}$$

WHERE

$\{x_1\}$ AND $\{x_2\}$

= DISPLACEMENT VECTOR REPRESENTING THE LAUNCH VEHICLE AND THE PAYLOAD DEGREES-OF-FREEDOM, RESPECTIVELY.

$[M_1]$ AND $[M_2]$

= MASS MATRICES OF THE LAUNCH VEHICLE AND THE PAYLOAD, RESPECTIVELY.

$[K_{11}]$

= RESTRAINED STIFFNESS MATRIX OF THE LAUNCH VEHICLE.

$[K_{22}]$

= STIFFNESS MATRIX OF THE PAYLOAD CONSTRAINED AT THE INTERFACE.

$[K_{12}]^T$

= STIFFNESS MATRIX OF THE INTERFACE STRUCTURE WHICH CONNECTS THE PAYLOAD TO THE LAUNCH VEHICLE.

$\{F(t)\}$

= EXTERNAL FORCING FUNCTION VECTOR APPLIED TO LAUNCH VEHICLE ONLY.



PARTITION OF PAYLOAD MOTION

$$\{x_2\} = [\phi_R] \{x_1\} + \{x_e\}$$

→ RIGID BODY MOTION
→ ELASTIC MOTION

$$\left. \begin{aligned}
 [M_2] \{\ddot{x}_e\} + [k_{22}] \{x_e\} &= - [M_2] [\phi_R] \{\ddot{x}_1\} && \text{INTERFACE ACCELERATIONS} \\
 [M_1 + M_{rr}] \{\ddot{x}_1\} + [\phi_R]^T [M_2] \{\ddot{x}_e\} + [K_1] \{x_1\} &= \{F(t)\} \\
 &= [\phi_R]^T [M_2] [\phi_R]
 \end{aligned} \right\}$$

LAUNCH VEHICLE/RIGID PAYLOAD MODEL

$$[M_1 + M_{rr}] \{\ddot{y}\} + [K_1] \{y\} = \{F(t)\}$$

- USUALLY THE LAUNCH VEHICLE ORGANIZATION IS RESPONSIBLE FOR THE MODEL
- $[M_{rr}]$ IS ESTIMATED BY THE PAYLOAD ORGANIZATION EARLY IN THE PROJECT
- THE LAUNCH VEHICLE ORGANIZATION WILL PROVIDE THE INTERFACE ACCELERATION $\{\ddot{y}_1\}$, THE EIGENVECTORS AT INTERFACE $[\phi_1]$ AND THE EIGENVALUES $[\omega_1]$.

ORIGINAL PAGE IS
OF POOR QUALITY



PAYLOAD ELASTIC RESPONSE

$$\{x_e\} = [\phi_2] \{u_2\}$$

$$\{u_2\} = \{v_2\} + \{w_2\}$$

WHERE

$$\{\ddot{v}_2\} + 2[\rho_2][\omega_2] \{\dot{v}_2\} + [\omega_2^2] \{v_2\} = -[M_{er}] \{\ddot{y}_1\}$$

AND

$$\begin{bmatrix} 1 & \phi_1^T M_{re} \\ M_{er} \phi_1 & 1 \end{bmatrix} \begin{Bmatrix} \ddot{w}_1 \\ \ddot{w}_2 \end{Bmatrix} + \begin{bmatrix} 2\rho_1 \omega_1 & 0 \\ 0 & 2\rho_2 \omega_2 \end{bmatrix} \begin{Bmatrix} \dot{w}_1 \\ \dot{w}_2 \end{Bmatrix} + \begin{bmatrix} \omega_1^2 & 0 \\ 0 & \omega_2^2 \end{bmatrix} \begin{Bmatrix} w_1 \\ w_2 \end{Bmatrix} = \begin{bmatrix} -\phi_1^T M_{re} \ddot{y}_2 \\ 0 \end{bmatrix}$$

ORIGINAL PAGE IS
OF POOR QUALITY

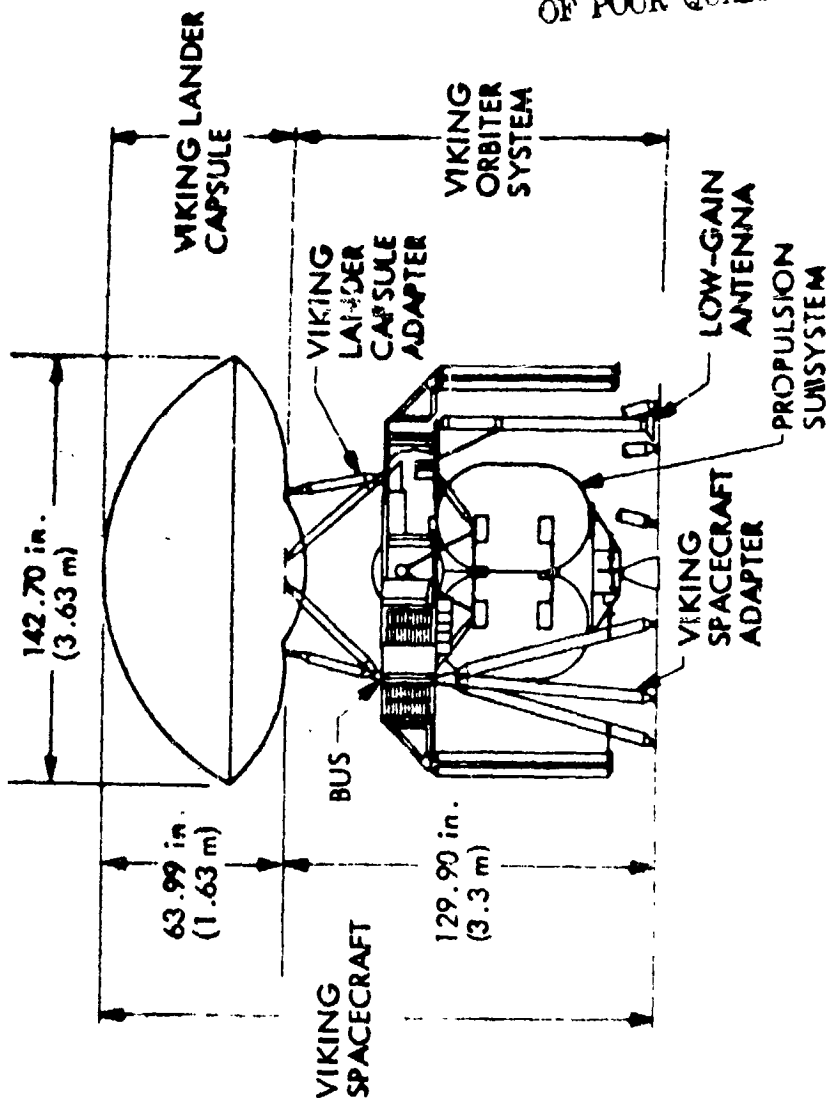
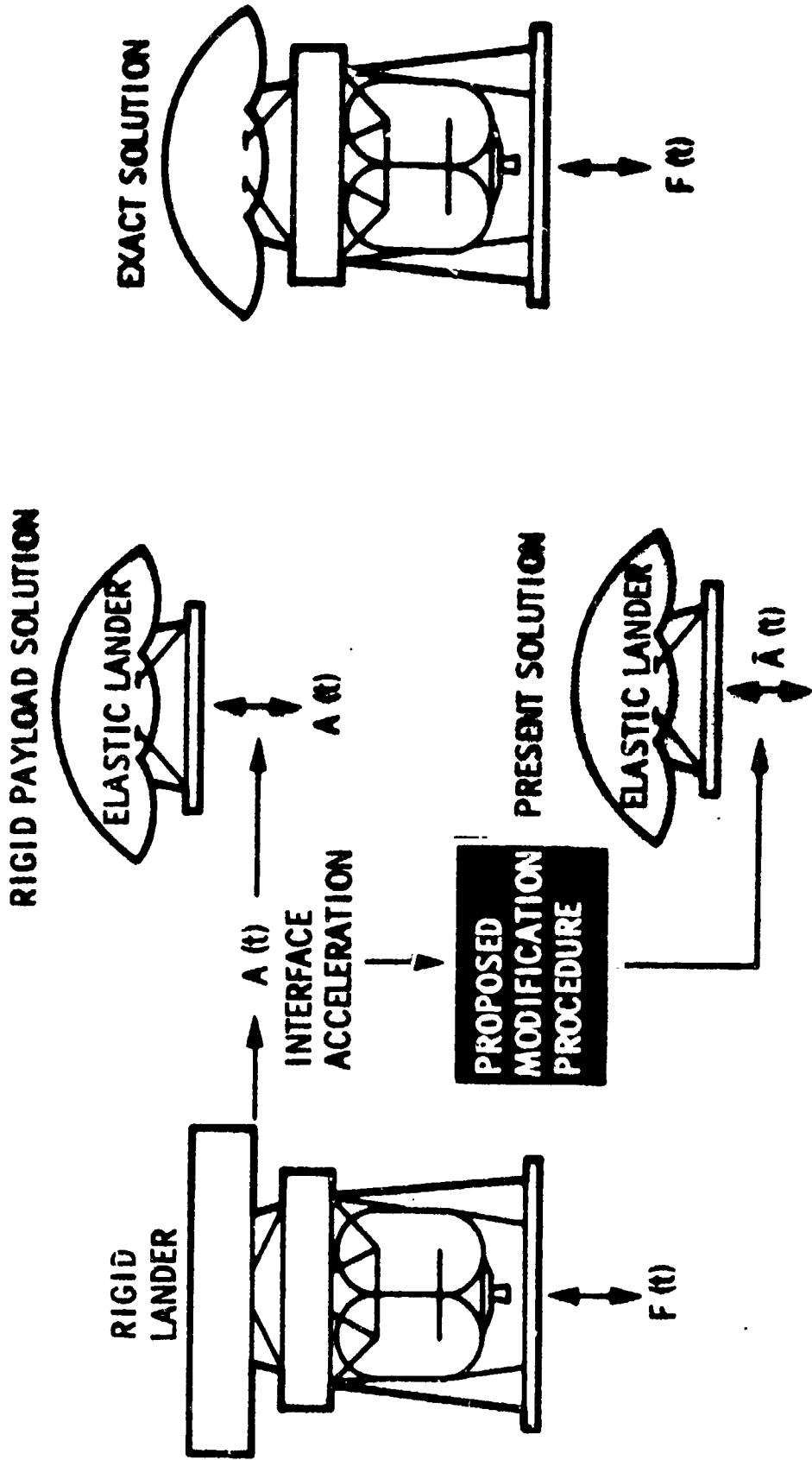


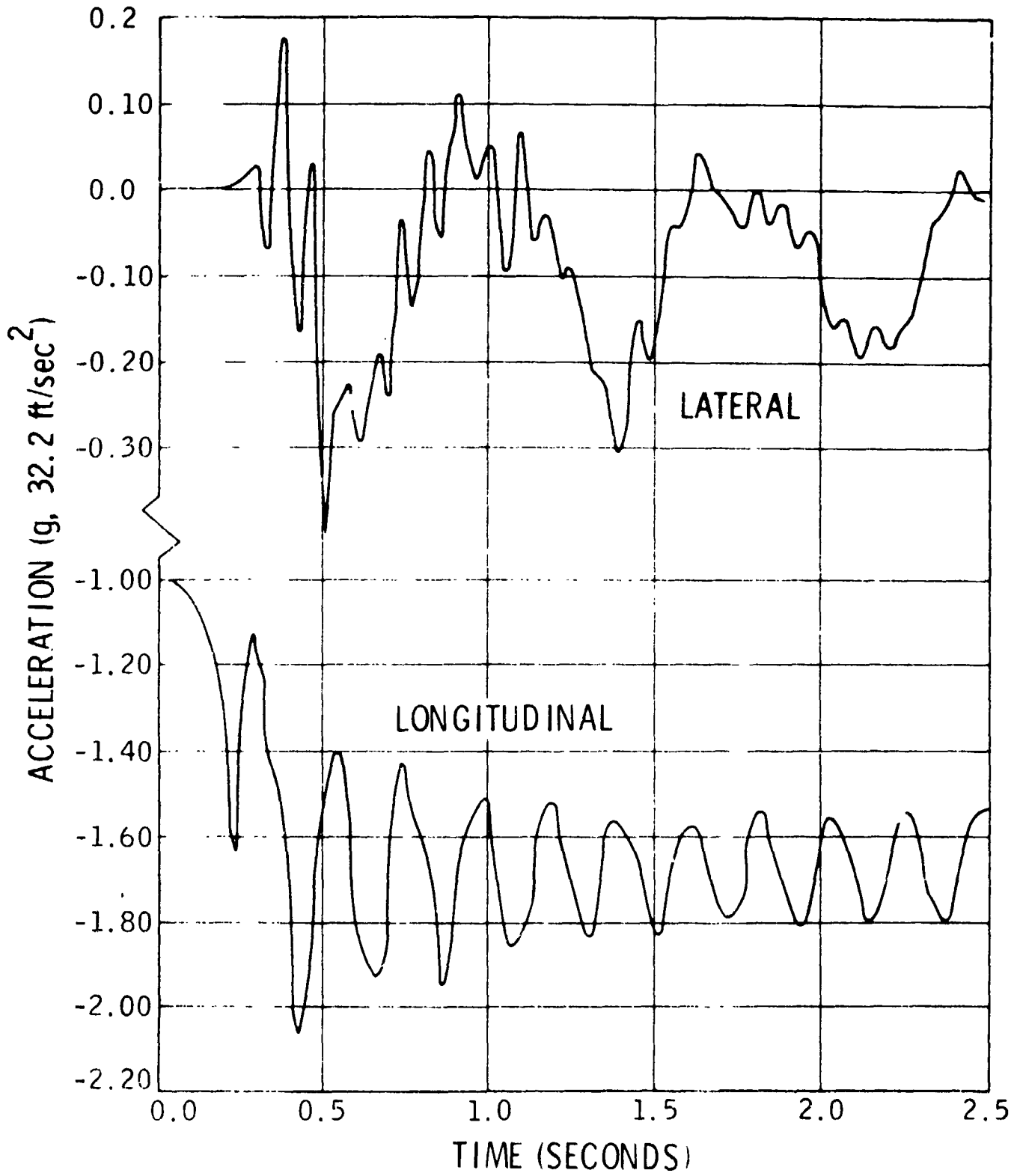
Fig 2



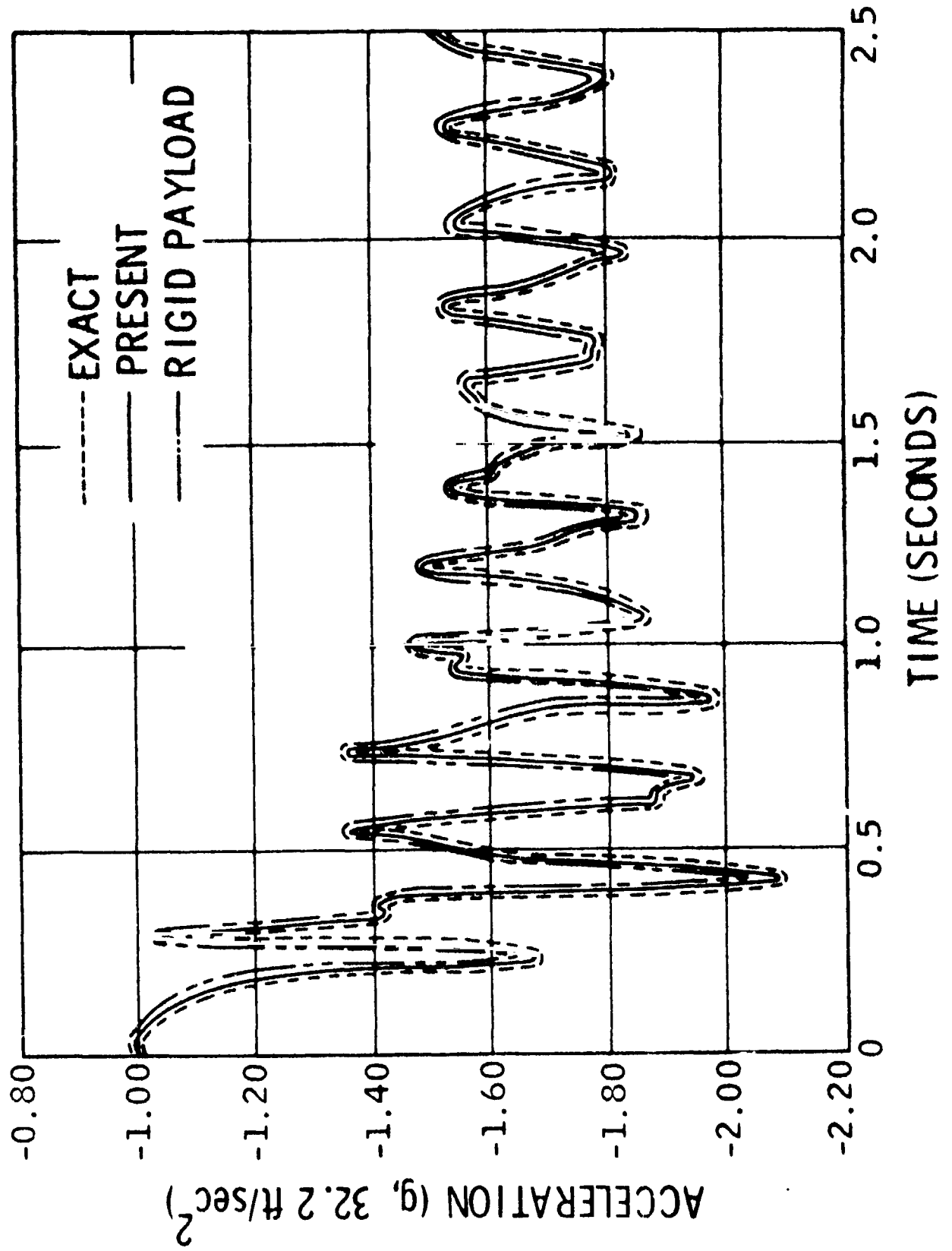
SAMPLE PROBLEM

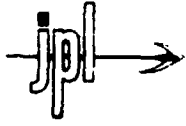


VIKING SPACECRAFT BASE ACCELERATION
FOR STAGE 0 IGNITION

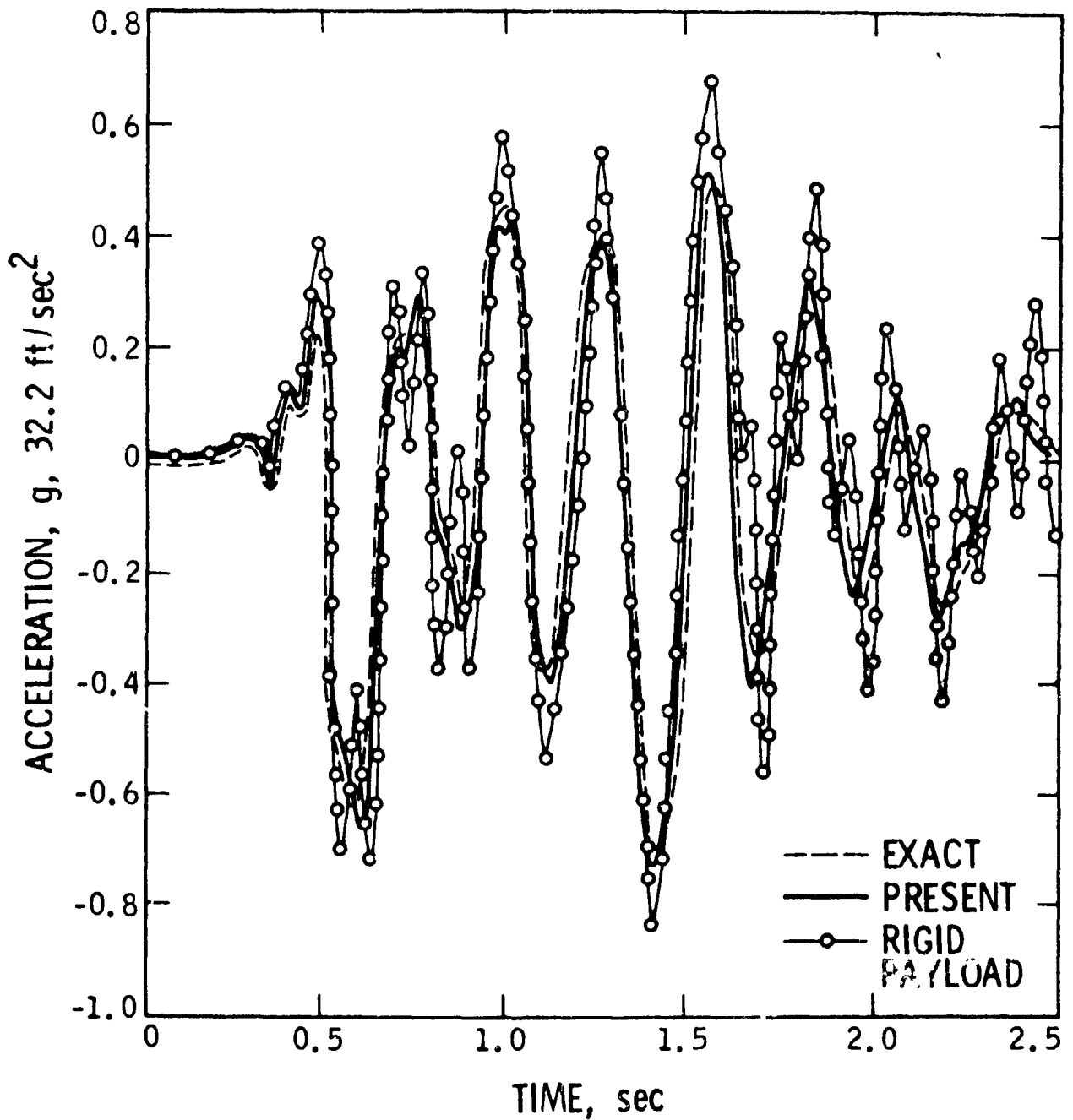


LANDER/ORBITER INTERFACE ACCELERATION -
LONGITUDINAL AT STAGE 0 IGNITION

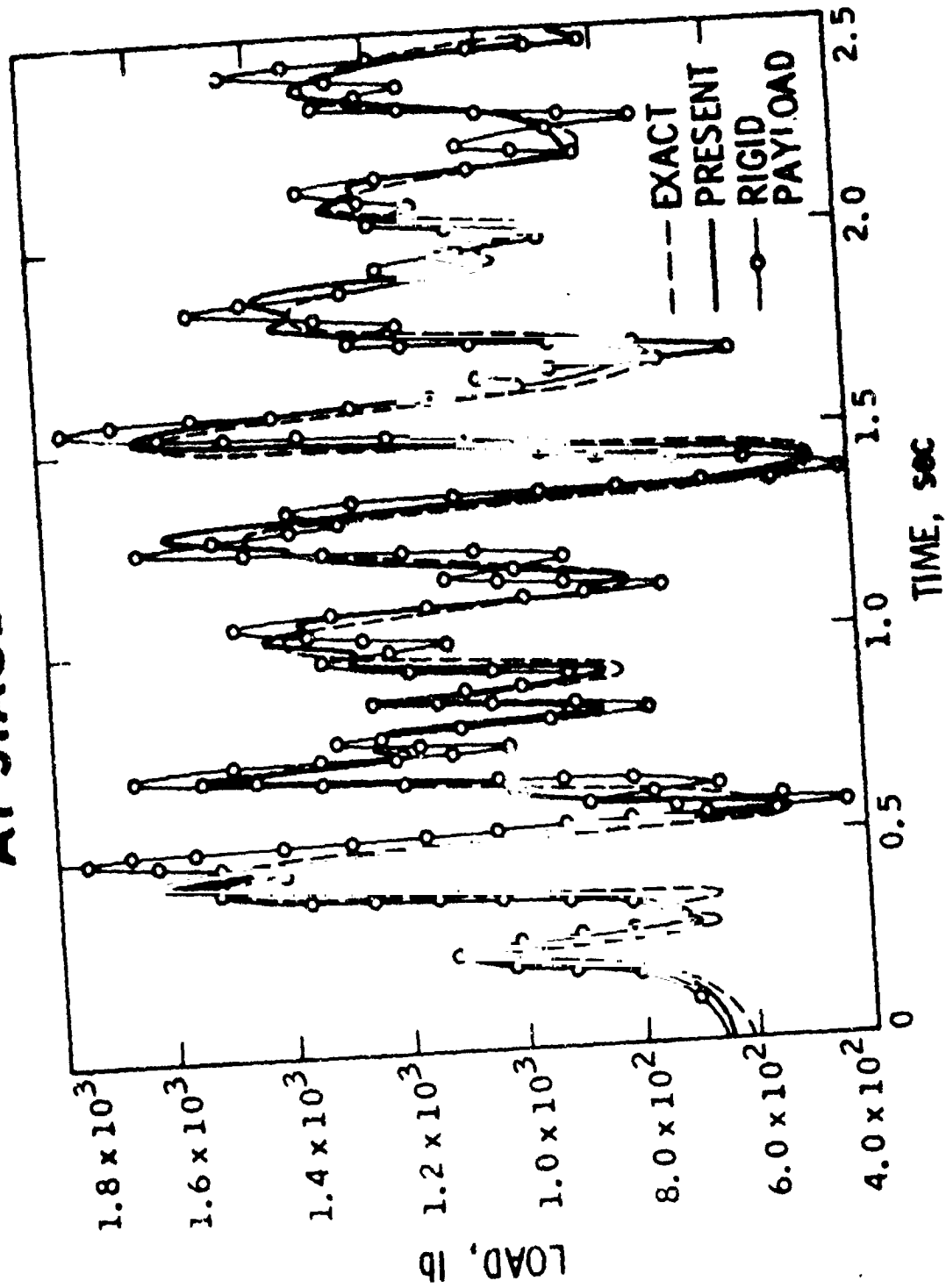




LANDER/ORBITER INTERFACE ACCELERATION-LATERAL AT STAGE 0 IGNITION



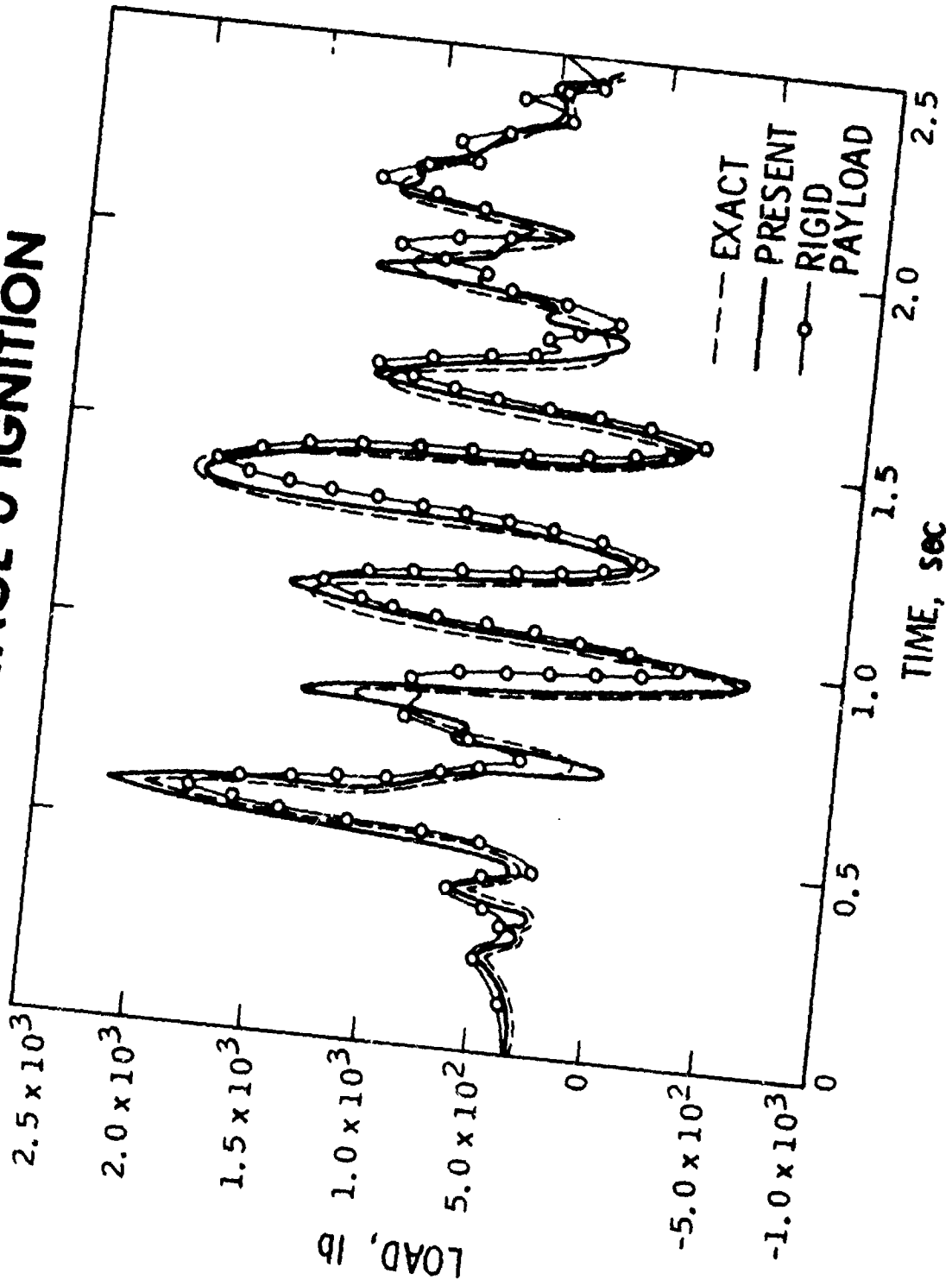
VLCA MEMBER 750 LOAD AT STAGE 0 IGNITION



10



VLCA MEMBER 754 LOAD AT STAGE 0 IGNITION





EXPERIENCES FROM SAMPLE PROBLEM

1. MODAL TRUNCATION

2. MODAL DAMPING

3. INITIAL CONDITIONS



SUMMARY

- **METHOD EXACT**
- **SUBJECT ONLY TO MODAL TRUNCATION**
- **ADVANTAGES**
- **CONTROL WITHIN ONE ORGANIZATION**
- **COST SAVINGS**
- **SCHEDULE ADVANTAGES**

PRECEDING PAGE BLANK NOT FILMED

MECHANICAL AND LOADS INTERFACE DEFINITIONS
FOR
PAYLOAD RETENTION LATCH ACTUATOR

NOVEMBER 16, 1978



AUTHORS:
VIC DURNELL
RUSS TAYLOR

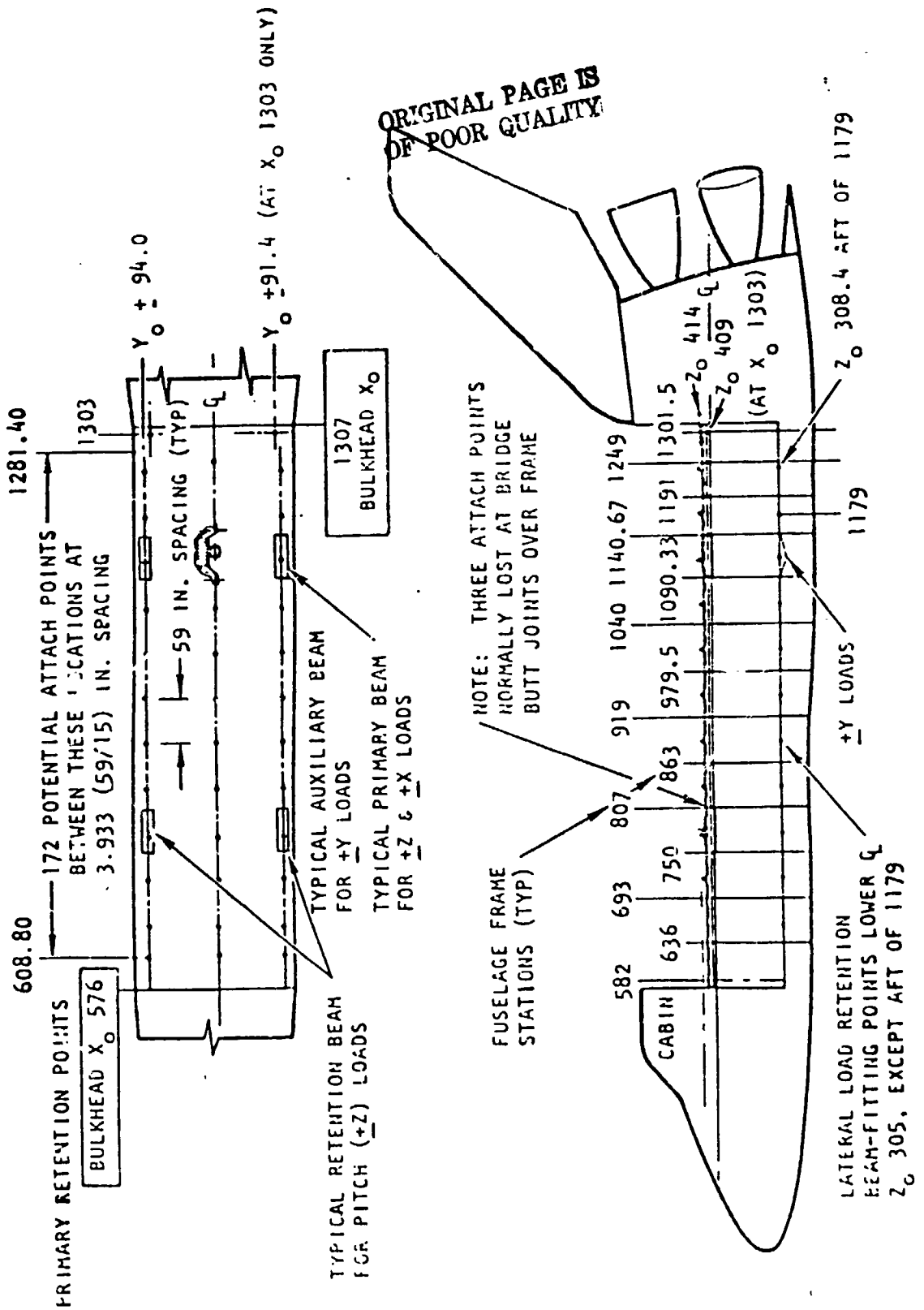
Payload Retention Latch Actuator

The purpose of this paper at the Payload Methodology Workshop is to help clarify the physical interface between the Shuttle Orbiter and the Payloads. The interfaces are always a major concern and require excellent communication to avoid systems problems very late in the program. It is our intent to make information available at this interface to system payload organizations.

The Payload Retention Latch Actuator (PRLA) employs a typical electro-mechanical actuator to drive a four-bar linkage. The combination of a very constrained envelope, very high loads, and extreme environmental conditions has been another one of the many challenges of making the Orbiter/Payload System come into reality.

A full-size plastic model of the PRLA has been very useful in demonstrating its concept and capability. The actuator portion (not shown), which is in the area of the handle, is also used to position the rendezvous radar on the Orbiter. The actuator starts with an input of high-speed, redundant AC motors driving through a 6262:1 gear train into the output shaft.

ORIGINAL PAGE IS
OF POOR QUALITY

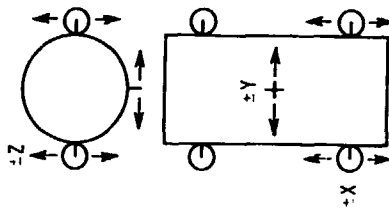
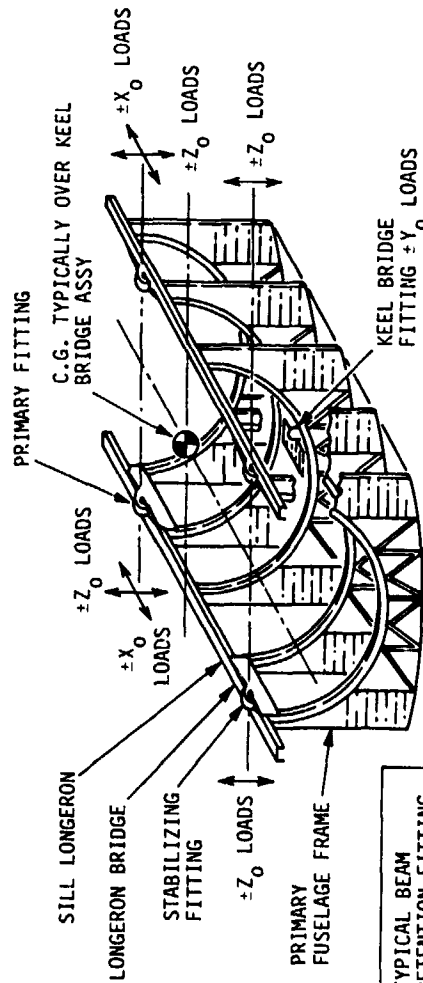


The Orbiter accommodates PRLA's in many locations

The Payload Retention Latch Actuators (PRLA's) are the lockdown and holding devices on the Orbiter that restrain the Payloads during launch and reentry. The PRLA is activated in space to release the Payloads for their insertion into orbit. It also can accept Payloads that have been in space and are being returned to earth. The Orbiter has been made extremely versatile to suit a great variety of sizes and shapes of Payloads. The viewgraph provides an overview of the many attach points.



5-POINT INSTALLATION (INDETERMINATE)



5-POINT INDETERMINATE
 (2 PRLA'S ±X, ±Y, ±Z LOADS)
 (2 PRLA'S ±Y, ±Z LOADS)
 (1 AKA ±Y LOADS)

ORIGINAL PAGE IS
 OF POOR QUALITY

Payload Installation into the Orbiter

The Payloads can be mounted into the Orbiter with either a 3-point, 4-point, or 5-point installation (indeterminate) possibility. The large and heavy Payloads would usually have a 5-point installation. All of the PRLA's secure the Payload in the + Z direction. Two of the PRLA's constrain the Payloads in the + X direction and with the aid of Y-Y guides and bumpers on the Payloads restrain them in the + Y direction. The other two PRLA's are free to float in the + X direction to accommodate dimensional changes between the Orbiter and Payloads and again restrain the Payloads in the Y-Y direction.

One Active Keel Actuator (AKA) is utilized per Payload to center the loads in the + Y direction. BASD also has this contract and information is available upon request.



PERFORMANCE:

- 30 SECONDS 2 MOTORS - OPERATIONAL
- 60 SECONDS 1 MOTOR - OPERATIONAL
- 15,000 LB LOAD TO SEAT TRUNNION
- 121,000 LB LIMIT LOAD LOCKED CONDITION
- 180,000 LB ULTIMATE LOAD (CRASH SURVIVAL)
- LIFE: 2,000 CYCLES

SIZE:

- 18" LONG X 14" HIGH X 6" WIDE
- WEIGHT: TOTAL PRLA - 84 POUNDS
ACTUATOR - 22 POUNDS

ENVIRONMENTS:

- TEMPERATURES +350°F TO -100°F OPERATING
- PRESSURE: AMBIENT TO SPARE VACUUM
- HUMIDITY: 0 - 100% RELATIVE

ORIGINAL PAGE IS
OF POOR QUALITY

PRLA Performance Specifications

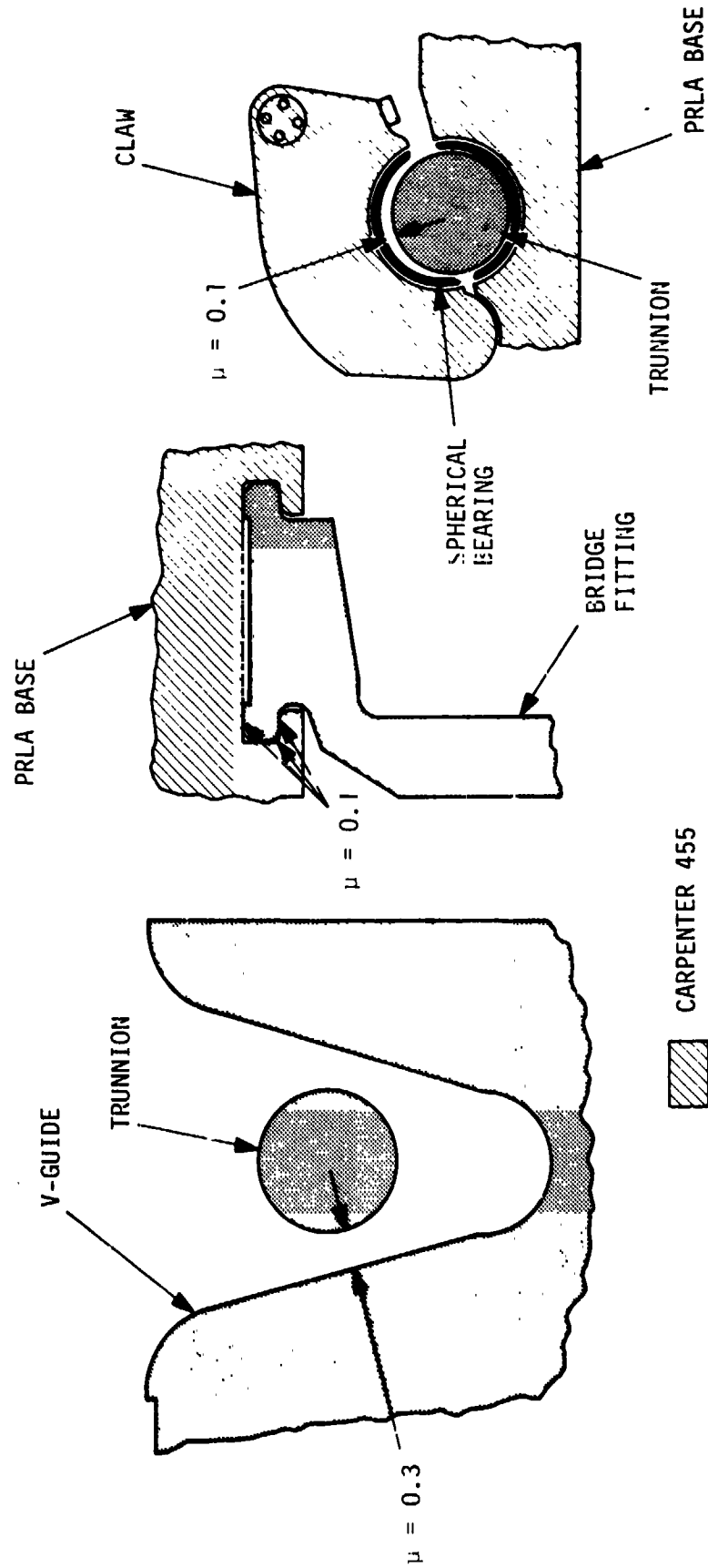
The performance of the PRLA has been tailored to meet the wide variety of expected payload interfaces on the first thirty-three Shuttle flights. The PRLA will close or open the claw within thirty seconds with both motors working or one minute when one motor is operational. It contacts the trunnion within two inches of the seat and increases the locking force up to 15,000 pounds to fully seat the Payload. Once latched, it can take limit loads of up to 121,000 pounds and still be operational. It must survive crash loads of 180,000 pounds without releasing the Payload.

Although the weight sounds high, the PRLA is very compact and efficient when you consider it must constrain the weight of forty-five automobiles.

Operating conditions are also a challenge. Temperatures range from +350°F to -100°F in both air and vacuum and in all humidity ranges.



FRICTION COEFFICIENT INTERFACE



Friction Coefficient Interface

The friction coefficient is a major specification requirement on the Payload Retention Latch Actuator (PRLA). The friction coefficient is the parameter that limits the loads into the Orbiter and limits the loads into the Payloads. In order to minimize the weight on both the Orbiter and the Payloads, a friction coefficient of 0.1 was determined early in the program to be an optimum choice.

The 0.1 friction coefficient applies between the PRLA and the Orbiter bridge rail. A positioning mechanism would allow up to one inch of X-X travel to accommodate anticipated dimensional differences between the Shuttle and the Payload.

The 0.1 coefficient of friction also applies between the PRLA and the payload trunnion. This allows for the trunnion to slide up to two and a half inches in the Y-Y direction during installation, orbit, space retrieval, and reentry.

The 0.3 coefficient of friction is required between the trunnion and the V-guide during payload integration into the Orbiter.



REQUIREMENT: FRICTION COEFFICIENT $\leq .07$
FOR APPARENT FRICTION COEFFICIENT OF $\leq .1$

PRESSURES: 2,000 TO 100,000 PSI

SPEEDS: STATIC TO 45 IN/MIN

LIFE: 20,000 CYCLES

ENVIRONMENT: ROOM AIR AND TEMPERATURE
COLD AIR -100°F
HOT AIR $+350^{\circ}\text{F}$
ROOM TEMP. VACUUM
COLD VACUUM -100°F
HOT VACUUM $+350^{\circ}\text{F}$

Friction Coefficient Requirements

The friction coefficient of 0.1 or less is a main interface requirement between the Payloads and Shuttle Orbiter. The high loads that can be exerted by some of the larger Payloads compounds the requirement by exerting a clamping action on the claw. This magnifies the loads on the claw and forces us to achieve a 0.07 friction coefficient in order to meet design intent.

The PRLA is intended to be a device that can accommodate all of the Payloads through Flight 33. This necessitates wide pressure requirements, considerable speed variation, and very hot and very cold environments in both air and vacuum conditions. Preliminary tests have revealed that friction coefficient goes down with increased pressure and is better at the slower speeds. Friction coefficient is adversely affected by cold temperatures and vacuum.

ORIGINAL PAGE IS
OF POOR QUALITY



THE INTERFACE PARAMETERS THAT AFFECT PAYLOAD ANALYSES ARE

- INTERFACE CLEARANCES
- STIFFNESS
- PAYLOAD CONSTRAINT LOADS
 - NEGLECTING FRICTION
 - CONSIDERING FRICTION
- PAYLOAD TRUNNION CONTACT STRESSES

Interface Parameters Affecting Payload Analysis

This chart is presented to introduce the topics to be covered on subsequent viewgraphs. It indicates the parameters at the interface that would affect static and dynamic analysis of payloads. Clearances affect dynamic analysis because of the non-linear force-deflection characteristics and the effects on stiffness. The effects of friction forces are of importance in determining loads on the payloads and whether slippage occurs between payload and interface during dynamic excitation. Payload trunnion contact stresses are vital in determining slippage loads because of the varying effects of coefficients of friction resulting from contact pressures.



INTERFACE CLEARANCES ARE NECESSARY

- TO PERMIT FREE MOTION BETWEEN PRLA AND PAYLOAD TRUNNION
- TO ALLOW PRLA TO MOVE FREELY ALONG ORBITER RAIL
- TO PREVENT CLAMPING OR BINDING BETWEEN MATING PARTS

HOWEVER THE PRLA-TO-TRUNNION CLEARANCE

- RESULTS IN HIGHER INTERFACE CONTACT STRESSES
- PRODUCES NONLINEAR STIFFNESS PROPERTIES THAT COMPLICATE DYNAMIC ANALYSIS

Interface Clearances

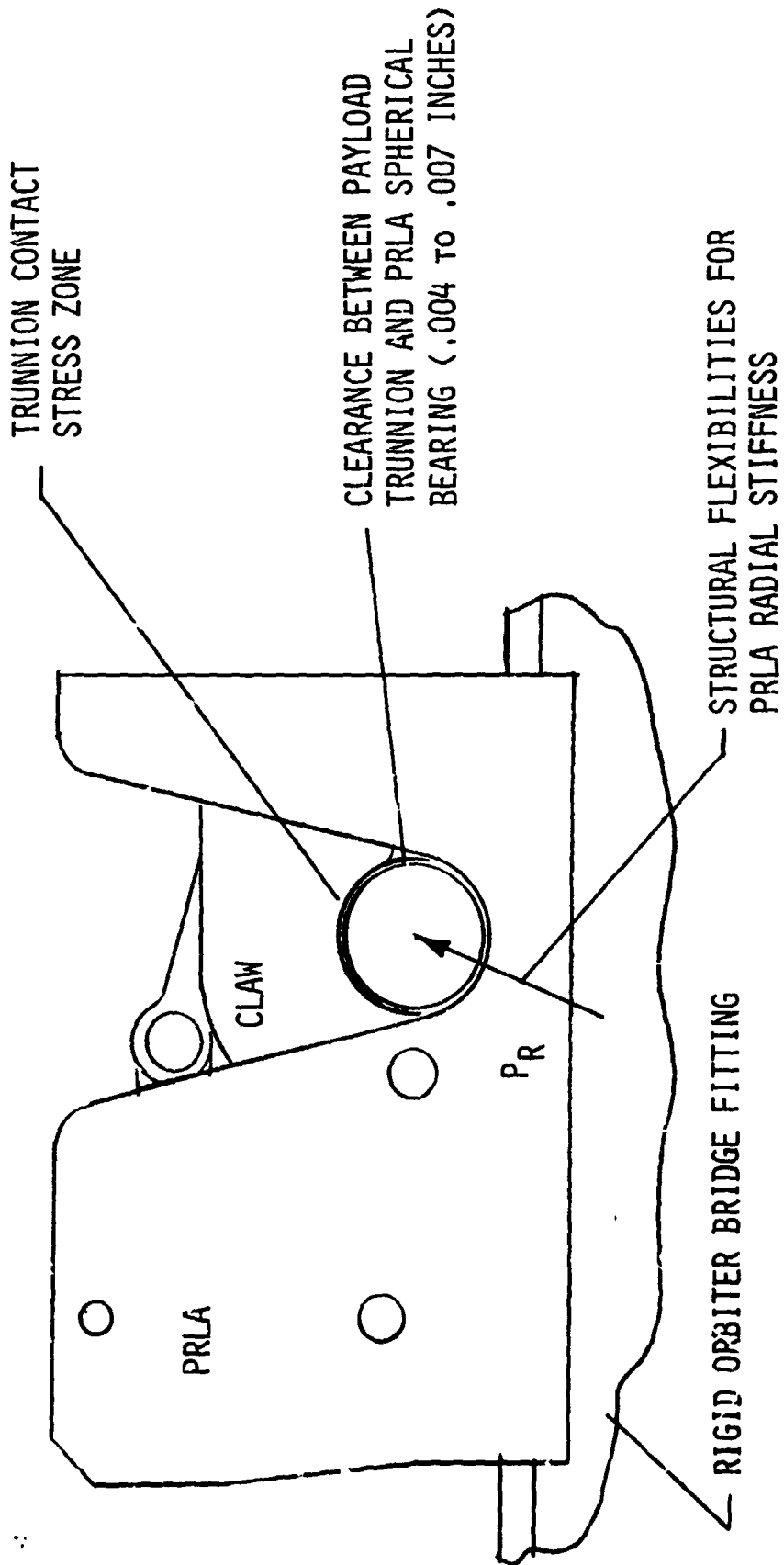
Clearance between the interface and payload trunnion is necessary to assure that free motion exists. Binding could cause loads along friction direction to exceed the 10 percent allowed. It could also cause difficulty in freeing a payload when required. The interface must be free to slide along Orbiter bridge rails and therefore clearances must exist there.

The clearances between trunnion and PRLA are undesirable from the standpoint that trunnion contact pressures are higher which can be detrimental if the lubrication material breaks down under the pressure. In addition, clearances create non-linear force-deflection data which complicates dynamic modeling and analysis.

**ORIGINAL PAGE IS
OF POOR QUALITY**



THE PARAMETERS CONSIDERED FOR PRLA ANALYSIS ARE



Analysis Parameters

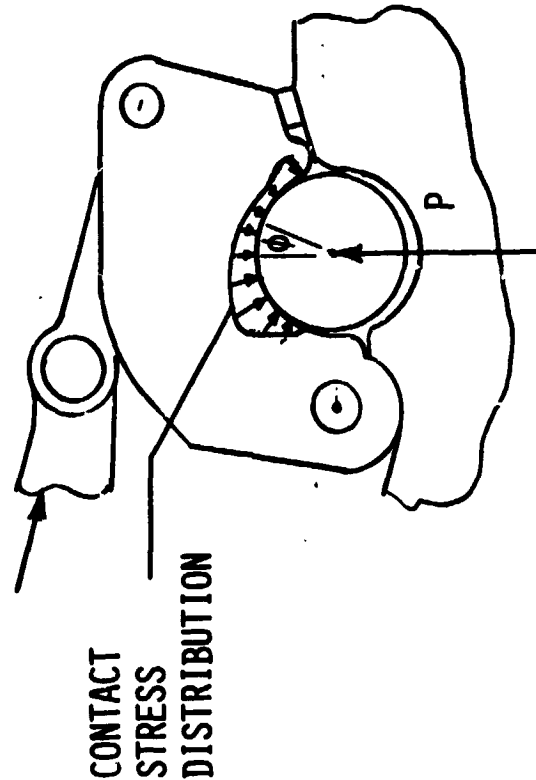
This chart reveals the parameters that were used in the to-date analysis of the PRLA interface. Apparent coefficients of friction must be less than or equal to 0.1. Clamping action of the claw on the trunnion creates trunnion normal loads exceeding the radial load by factors of 1.4 and possibly more. Clearances help reduce the clamping load and thus are considered even though they complicate the analysis effort.

The total structure was considered in addition to clearances to determine radial stiffness at the trunnion. Current analysis is based on a rigid Orbiter bridge fitting. Subsequent analysis will consider a flexible rail of the bridge fitting since pressure loads on the Orbiter bridge structure are intolerably high.



NASTRAN MODELS HAVE BEEN CREATED

- TO DETERMINE STRESS DISTRIBUTIONS IN CRITICAL PARTS FOR USE IN FRACTURE MECHANICS ANALYSIS
- TO DETERMINE LOADING DISTRIBUTIONS ON FRICTION SURFACES
- TO EVALUATE THE TOTAL NORMAL LOAD ON A FRICTION INTERFACE TO ARRIVE AT REAL COEFFICIENT OF FRICTION REQUIREMENTS



$$\mu_R = \frac{P \mu A}{\int W dA} \leq 0.1$$

WHERE

$$P = \int W \cos \phi dA$$

R = REAL

A = APPARENT

NASTRAN Models

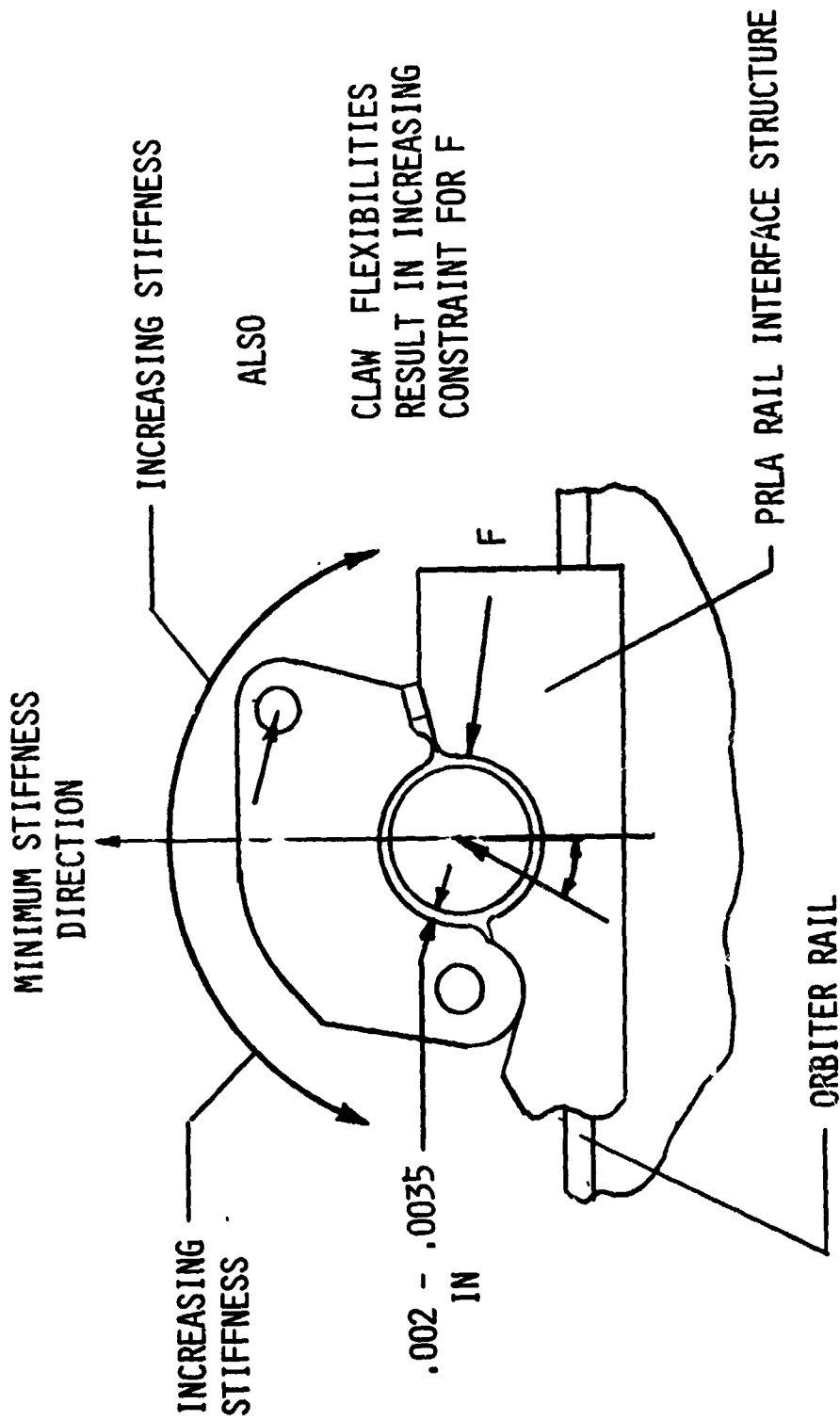
The NASTRAN finite element structural analysis program has been used to determine stiffness and internal stress distribution for the PRLA structure. Currently, separate models exist for the claw and for the Orbiter bridge interface structure. Parts of the PRLA structure are critical from a fracture mechanics viewpoint and thus a reasonably accurate stress analysis is required.

The NASTRAN model of the claw allows a determination of the normal pressure loads on the trunnion. This provides a basis for determining the real coefficient of friction required so that an apparent coefficient of friction goal of 0.1 may be achieved.

ORIGINAL PAGE IS
OF POOR QUALITY



THE CLAW MODEL SHOWED VARIABLE RADIAL STIFFNESS



Claw Radial Stiffness Studies

The radial stiffness of the claw is currently being studied for variable radial load and angle of loading.

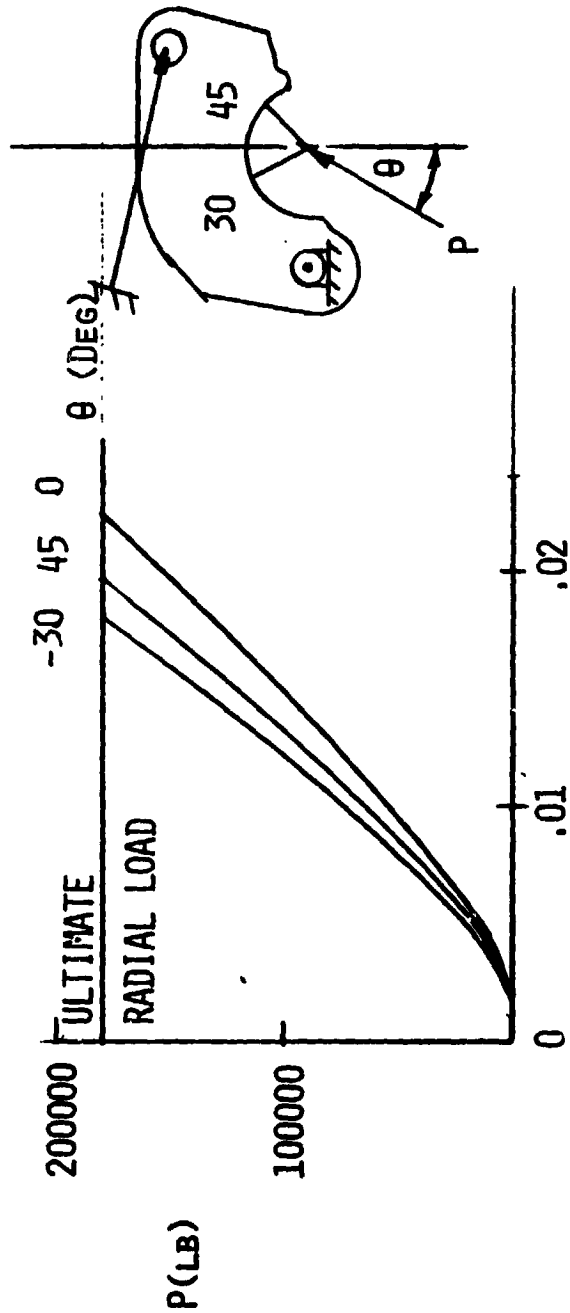
This chart shows that stiffness is a minimum at a loading orientation that is normal to the Orbiter bridge fitting rail. The results have been based on a radial clearance between trunnion and PRLA of 0.002 inches. As the radial load is applied at positive angles as shown radial stiffness increases. For these angles the PRLA rail interface structure becomes increasingly effective because of claw flexibilities. If this did not happen the claw stresses would be prohibitive. As the radial load is applied at negative angles the radial stiffness increases and the PRLA rail interface structure becomes ineffective.

ORIGINAL PAGE IS
OF POOR QUALITY



STIFFNESS CURVES WERE DERIVED USING THE MODEL

- FOR VARIOUS TRUNNION LOAD ORIENTATIONS
- AND FOR UP LOADING ON THE CLAW



FORCE-DEFLECTION CURVES ARE BASED ON TRUNNION CENTERED AT SPHERICAL BEARING AND 0.004 INCH DIAMETRAL CLEARANCE.

Radial Stiffness Curves

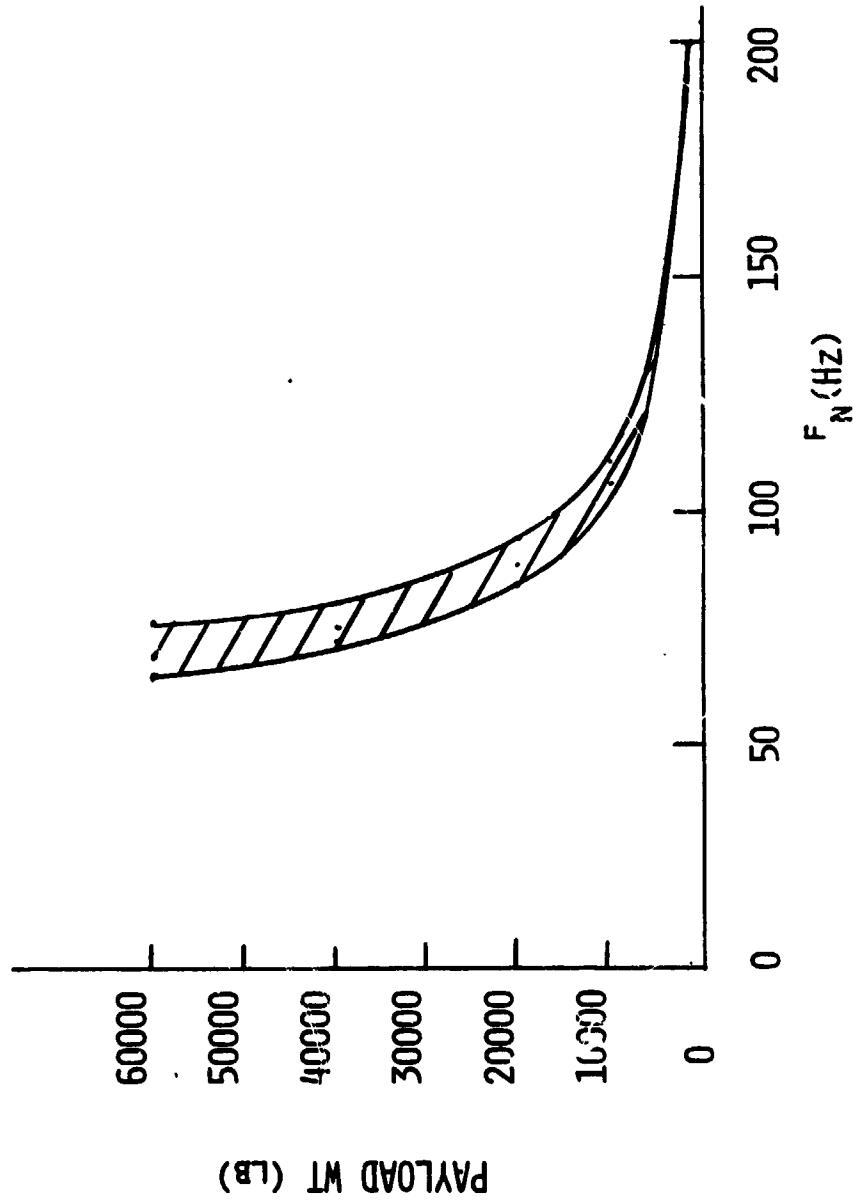
The NASTRAN model of the claw was used to derive radial stiffness data considering an up loading over an angular range of -30 degrees to +45 degrees from vertical. Although not presented it is expected that a down loading would show a higher stiffness because the load is directed more directly toward the Orbiter bridge rail. The curves shown on this chart account for a 0.002 inch radial clearance. As indicated on the previous chart the greatest deflection occurs for an up load applied normal to the bridge rail.

In addition to radial stiffness the PRLA would be flexible in a direction along the trunnion axis. This stiffness is not addressed in this paper.

**ORIGINAL PAGE IS
OF POOR QUALITY**



THE APPROXIMATE FREQUENCY OF VARIOUS PAYLOADS WOULD BE



- WITH 25 PERCENT MASS AT EACH OF FOUR INTERFACES
- A 5g RESPONSE LOAD
- AN AVERAGE STIFFNESS FROM THE PRECEDING CURVES

Payload Frequencies

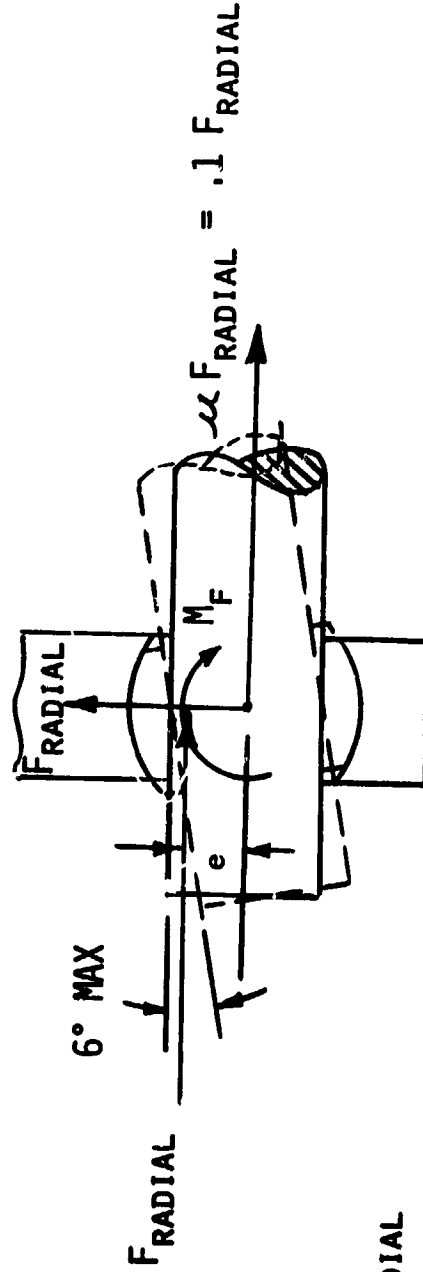
Approximations of payload resonance are shown on this chart based on rigid payloads and on the force-deflection curves of a previous chart. It is impossible to accurately determine resonance because of the non-linear spring rates and because each payload mounting configuration is different.

The curves are based on assuming 25 percent of the payload is mounted on each of 4 PRLA's. It is estimated that the payload response is 5g's and the spring rate is linear between zero and the point of maximum response load. This assumption results in higher frequencies especially for small payloads.



CONSTRAINT LOADS ON THE PAYLOAD CONSIST OF

- THE DIRECT RADIAL LOADS (F_{RADIAL}) ON THE TRUNNION
- FRICTION INDUCED LOADS (μF_{RADIAL}) PARALLEL TO THE TRUNNION AXIS BASED ON LIMIT RADIAL LOAD
- FRICTION INDUCED MOMENTS



$$M_f = \mu e F_{\text{RADIAL}}$$

= 18150 INCH POUNDS MAXIMUM

Payload Constraint Loads

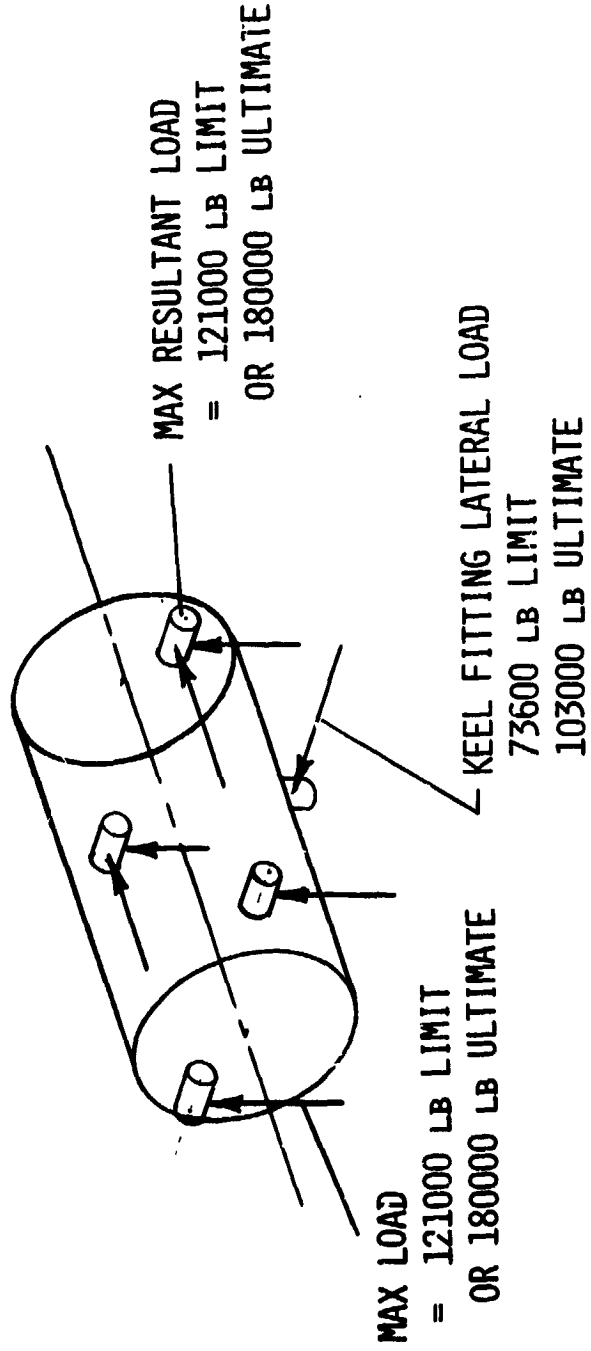
The message from this chart is that friction loads are induced on the payload trunnion; as a result of a direct radial load between PRLA and trunnion. These friction-induced loads are a side load parallel to the trunnion axis and a moment load induced at the PRLA spherical trunnion support bearing. The side load can be 10 percent of the radial load and maximum value is 12100 pounds based on limit loads.

The friction moment acting on a payload trunnion is a function of the trunnion radial load and the eccentricity of the friction load acting on the PRLA spherical bearing. It can be any value between zero and the maximum value of 0.1 times the direct radial times the eccentricity. For a PRLA limit design load of 121000 pounds the maximum moment is approximately 18000 inch pounds.



IF FRICTION IS NEGLECTED

- A FIVE-POINT MOUNTED PAYLOAD IS CONSTRAINED AS SHOWN



Trunnion Loads Neglecting Friction

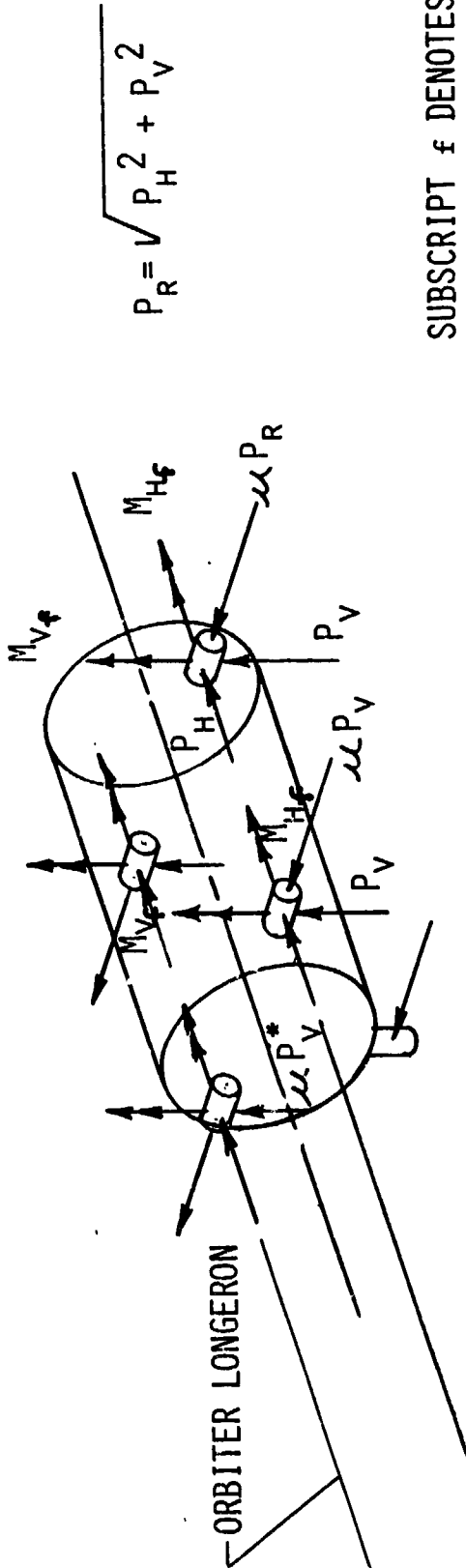
Payload trunnion loads are described on this chart for a five point attachment to the Orbiter payload bay considering that friction is neglected. The loading directions are shown and magnitudes for limit and ultimate loads at the PRLA interface. The limit radial load on a PRLA is 121000 pounds and the ultimate load is 180000 pounds.

The loads on the Orbiter keel are 73600 pounds limit and 103000 pounds ultimate. Ball Corporation is providing an Active Keel Assembly (AKA) but this is not addressed in this paper.



IF MAXIMUM FRICTION IS CONSIDERED

- A FIVE-POINT MOUNTED PAYLOAD IS CONSTRAINED AS SHOWN



$$P_R = \sqrt{P_H^2 + P_V^2}$$

SUBSCRIPT ϕ DENOTES
FRICTION FORCE

LOADS ON BOTH LONGERONS SIMILAR

* FRICTION LOAD BETWEEN ORBITER RAIL AND PRLA

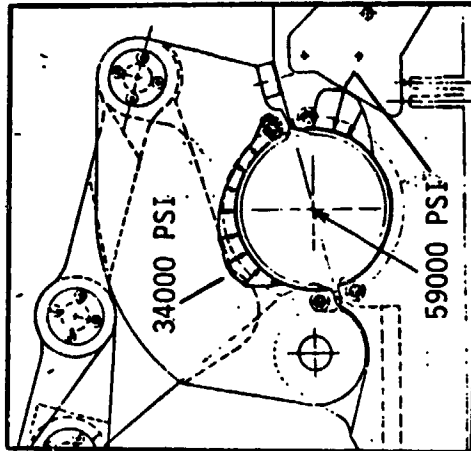
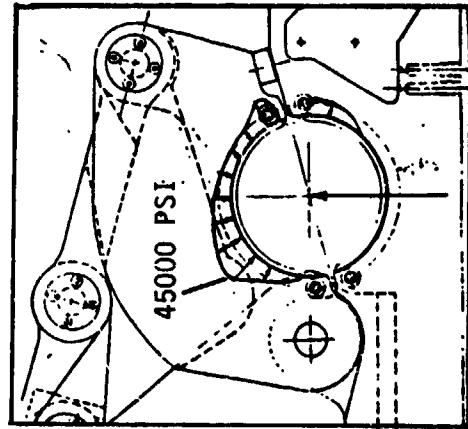
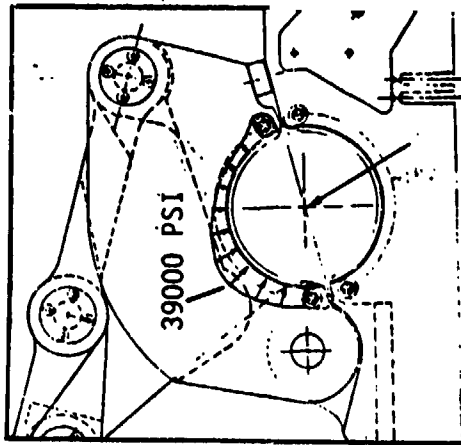
Trunnion Loads Considering Friction

The five point payload mount is again shown with direct radial loading accompanied by friction loading. The loading involves friction loads and moments at the four trunnion points. The payload should be investigated for the most critical combination of radial and friction loads imposed upon it.



PAYLOAD TRUNNION CONTACT STRESSES

- PEAK AT AN APPROXIMATE VALUE OF 60000 PSI
- ARE HIGHEST AT EDGES OF PRLA CLAW



Payload Trunnion Contact Stresses

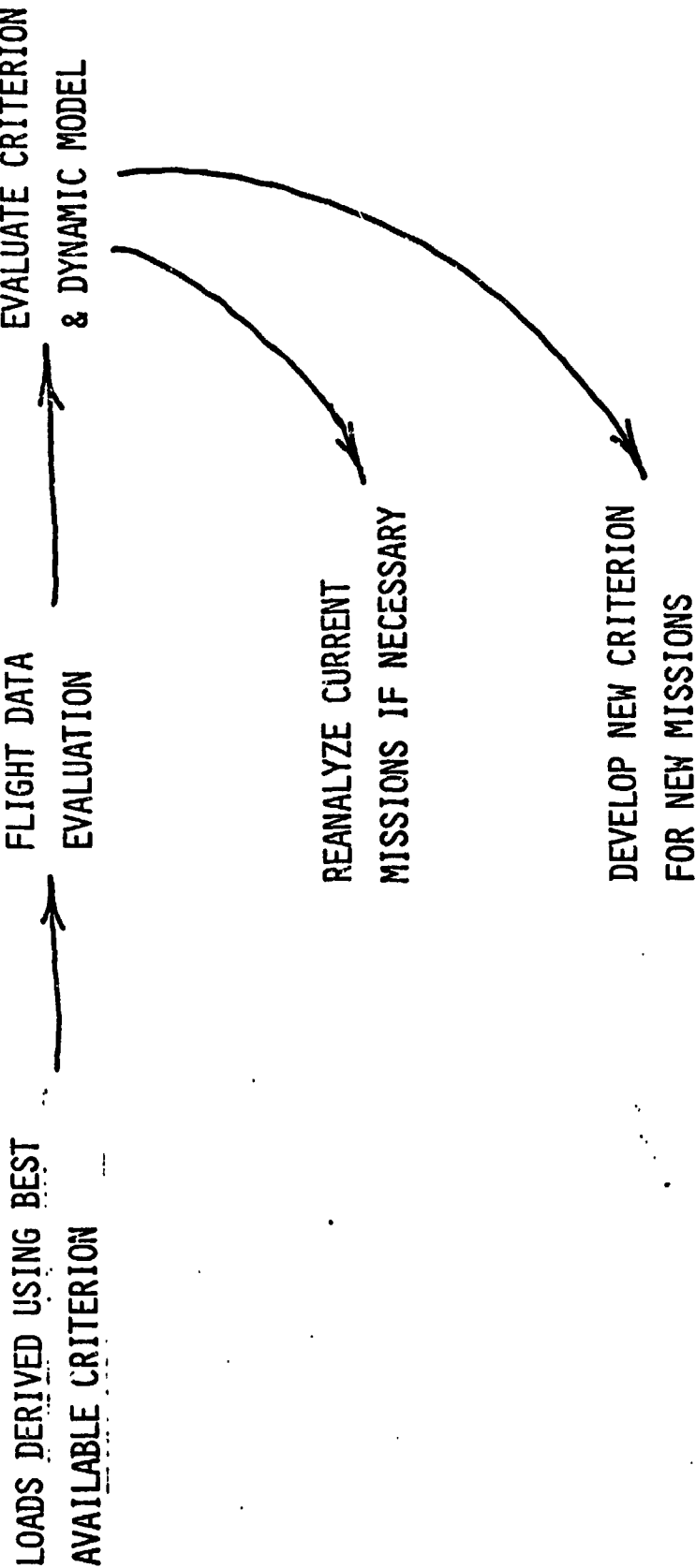
Payload trunnion contact stresses are most significant from a friction material standpoint. Coefficients of friction decrease with increases in pressure but many materials tend to break down at a contact pressure in excess of 50000 or 60000 psi.

Average contact pressures from a radial load of 121000 pounds are about 20000 psi over the projected area of the trunnion to PRLA interface. Because of claw flexibilities peak contact pressures are as high as 60000 psi. These stresses occur along the inner and outer edges of the claw.

PAYLOAD RESPONSE MEASUREMENTS ON ATLAS/CENTAUR
AND TITAN/CENTAUR MISSIONS AND THEIR USE IN
DEVELOPMENT OF LOADS CRITERION

T. GERUS
LeRC

ATLAS/CENTAUR AND TITAN/CENTAUR
LOAD CRITERION DEVELOPMENT



ATLAS/CENTAUR MISSION SUMMARY

1962 TO PRESENT

<u>MISSION</u>	<u>NUMBER</u>
R&D FLIGHTS	8
SURVEYORS	7
ATS	2
OAO	3
MARINER	5
INTELSAT IV	8
PIONEER	4
INTELSAT IVA	6
COMSTAR	3
FLTSATCOM	1
HEAD	1
<hr/>	<hr/>
TOTAL SAMPLE	48

SURVEYOR EXPERIENCE

- PRELIMINARY CRITERION - 2G SINE LONGITUDINAL
1G SINE LATERAL
- FINAL CRITERION - REDUCED (NOTCHED) SINE USING RESULTS
OF TRANSIENT ANALYSES OF TUNED GUSTS,
ENGINE TRANSIENTS
- FLIGHT EXPERIENCE - TUNED GUSTS, ENGINE TRANSIENT ANALYSES
ADEQUATE, BUT LAUNCH RELEASE TRANSIENT
FOUND TO CAUSE MOST CRITICAL PAYLOAD
LATERAL RESPONSE

LAUNCH TRANSIENT ANALYSIS EXPERIENCE

- RESPONSE CAUSED BY COUPLING BETWEEN LAUNCHER RELEASE MECHANISM AND LAUNCH VEHICLE
- DUE TO COMPLEXITY OF MECHANISM, UNABLE TO ACCURATELY RECONSTRUCT MEASURED FLIGHT RESPONSE
- FOLLOW-ON MISSION LOADS PREDICTIONS WERE BASED UPON FACTORING BEST AVAILABLE RECONSTRUCTION
- FACTOR REQUIRED WAS APPROXIMATELY 2

LAUNCH TRANSIENT IMPROVEMENT IMPLEMENTATION

- SIGNIFICANT REDUCTION IN LAUNCH TRANSIENT LOADS WERE DEMONSTRATED IN GROUND TEST USING "BACKPRESSURE"
- "BACKPRESSURE" WAS FIRST USED ON FLIGHT VEHICLE AC-36 ON SEPTEMBER 25, 1975
- FLIGHT DATA CONFIRMED SUCCESSFUL REDUCTION IN PAYLOAD LOADS WITH "BACKPRESSURE" ON ALL SUBSEQUENT LAUNCHES
- LOADS REDUCTION WAS SIGNIFICANT SO NEW LOADS CRITERION NEEDED TO BE DEVELOPED

NEW LOADS CRITERION DEVELOPMENT FOR ATLAS/CENTAUR PAYLOADS

- DEVELOPMENT WAS BASED UPON STATISTICAL EVALUATION OF THE MAGNITUDE AND SHOCK SPECTRA OF PAYLOAD ACCELEROMETER AND STRAIN GAGE DATA FOR ALL FLIGHT EVENTS.
- MOST CRITICAL PITCH PLANE RESPONSE OBSERVED DURING BOOSTER ENGINE SHUTDOWN, MOST CRITICAL YAW PLANE RESPONSE OBSERVED DURING BOOSTER PACKAGE JETTISON
- INITIAL RECONSTRUCTION OF FLIGHT MEASURED PITCH PLANE BENDING MOMENTS USING ENGINE DATA NOT ACCEPTABLE.
- REASONABLE RECONSTRUCTION OF PITCH PLANE BENDING MOMENTS MADE AFTER FINDING DYNAMIC MODEL ERROR.
- YAW PLANE RESPONSE DURING BOOSTER PACKAGE JETTISON BASED UPON DEVELOPMENT OF EQUIVALENT FORCING FUNCTION SINCE CAUSE OF YAW EXCITATION IS UNCERTAIN.

SUMMARY OF ATLAS/CENTAUR EXPERIENCE

- FLIGHT INSTRUMENTATION IDENTIFIED MOST CRITICAL LOADS EVENT AND PROVIDED MODELING CORRECTION COEFFICIENT.
- DYNAMIC MODELING ERROR IDENTIFIED AND CORRECTED USING FLIGHT RESPONSE DATA DURING NEW LOADS CRITERION DEVELOPMENT.
- YAW RESPONSE CRITERION DEVELOPED SOLELY BASED ON FLIGHT DATA SINCE IT IS VIRTUALLY IMPOSSIBLE TO MODEL THE YAW DISTURBANCE FORCES DURING BOOSTER PACKAGE JETTISON.

TITAN/CENTAUR MISSION SUMMARY

1974 - 1977

<u>MISSION</u>	<u>NUMBER</u>
R&D FLIGHT	1
HELIOS	2
VIKING	2
<u>VOYAGER</u>	<u>2</u>
TOTAL SAMPLE	7

TIJAN/CENTAUR-1 FLIGHT EXPERIENCE

- LATERAL RESPONSE OF PAYLOAD AT LIFT-OFF WAS ABOUT 3-SIGMA ALTHOUGH ALL KNOWN EXCITATION SOURCES WERE ABOUT NOMINAL
- ALL OTHER TRANSIENT EVENTS WERE WITHIN PREDICTED LIMITS
- POGO RESPONSE WAS OBSERVED DURING STAGE 1 FLIGHT

IMPACT OF IC-1 FLIGHT EXPERIENCE ON IC-2

- HIGH PAYLOAD LATERAL RESPONSE AT LIFT-OFF WAS ATTRIBUTED TO LAUNCH OVER-PRESSURE PHENOMENA.
- HOWEVER, THE LAUNCH OVERPRESSURE HAD TO BE MODIFIED SIGNIFICANTLY WHEN APPLIED TO THE IC-1 MODEL IN ORDER TO RECONSTRUCT THE MEASURED PAYLOAD RESPONSE.
- THIS MODIFIED LAUNCH OVERPRESSURE WAS THEN APPLIED TO THE IC-2 MODEL. THE RESULTANT LOADS ON THE HELIOS ANTENNA EXCEEDED THE ALLOWABLES.
- SPECIAL DYNAMIC LOADS TESTS PERFORMED ON HELIOS ANTENNA CAUSED STRUT STRUCTURAL FAILURE. ANTENNA WAS RETESTED USING THICKER WALL STRUTS AND PASSED; THICKER WALL STRUTS WERE USED ON BOTH HELIOS MISSIONS.
- HIGH POGO RESPONSE ATTRIBUTED TO SMALL POGO STABILITY MARGIN. CHANGED TITAN PRESSURIZATION SCHEME IN ORDER TO LOWER LINE FREQUENCY AND IMPROVE POGO STABILITY MARGIN.

TITAN/CENTAUR-2 (HELIOS) FLIGHT EXPERIENCE

- SHORT DURATION POGO RESPONSE OBSERVED PRIOR TO STAGE 1 SHUTDOWN
- HIGH ROLL RATE (≈ 11 DEGREES/SEC.) OBSERVED DURING SRM JETTISON
- ALL OTHER TRANSIENT EVENTS WERE WITHIN PREDICTED LIMITS

IMPACT OF IC-2 EXPERIENCE ON IC-3, 4 (VIKING)

- DEVELOPED OXIDIZER ACCUMULATOR TO STABILIZE POGO
- CAUSE OF ROLL TRANSIENT DETERMINED TO BE ROLL TORQUE ON VEHICLE AT HIGH MACH NUMBERS; ALL SYSTEMS WERE EVALUATED AND FOUND THAT THEY COULD TOLERATE MORE THAN TWICE IC-2 SO NO CHANGES WERE MADE

TITAN/CENTAUR-3 AND -4 (VIKING) FLIGHT EXPERIENCE

- SMALL UNPREDICTED RESPONSE OBSERVED ON VIKING STRAIN GAGES (30 PERCENT OF CAPABILITY) DURING CENTAUR POWERED FLIGHT.
- RESPONSE DETERMINED TO BE CAUSED BY ENGINE ACTUATORS COMMANDED FROM AUTOPILOT NOISE.
- LOADS REDUCED SIGNIFICANTLY ON SUBSEQUENT ATLAS/CENTAUR AND TITAN/CENTAUR FLIGHTS THROUGH AUTOPILOT FILTERING.

IMPACT OF IC-1 THROUGH IC-5 FLIGHT EXPERIENCE ON IC-6 AND -7 (VOYAGER)

- LIFT-OFF LOADS METHODOLOGY REFINED USING JPL TECHNIQUE AND USING ACCUMULATED TITAN/CENTAUR DATA
- ALL OTHER TRANSIENT EVENTS REVIEWED AND FOUND TO BE WITHIN PREFLIGHT PREDICTIONS

TITAN/CENTAUR-6 AND -7 (VOYAGER) EXPERIENCE

- BUFFETING RESPONSE LEVELS FAR IN EXCESS OF ALL PREVIOUS TITAN/CENTAUR EXPERIENCE
- SIGNIFICANT RANDOM LONGITUDINAL RESPONSE OBSERVED DURING STAGE 1 BURN
- SPACECRAFT LOADS DUE TO ABOVE EXPERIENCE WITHIN ALLOWABLES
- CAUSE OF INCREASED BUFFETING AND STAGE 1 RANDOM RESPONSE NEVER PURSUED SINCE THERE WERE NO FOLLOW-ON MISSIONS

OBSERVATIONS BASED UPON TITAN/CENTAUR AND ATLAS/CENTAUR EXPERIENCE

- FLIGHT PAYLOAD RESPONSE DATA HAS BEEN ESSENTIAL IN ORDER TO DERIVE REASONABLE LOADS CRITERION WHEN FORCING FUNCTIONS ARE NOT WELL KNOWN.
- SINCE MOST FLIGHT RESPONSE DATA WAS FOUND TO BE HIGHLY VARIABLE, A FLIGHT-BY-FLIGHT HISTORY OF THE ACCUMULATED DATA WAS INVALUABLE IN ARRIVING AT PREDICTED LOADS FOR THE FOLLOW-ON MISSIONS.
- DATA HAS ALSO BEEN VALUABLE IN VERIFYING DYNAMIC MODELS WHEN FORCING FUNCTIONS ARE KNOWN.



DELTA VEHICLE/SPACECRAFT DYNAMIC LOADS ANALYSIS
MODELING TECHNIQUES AND FORCING FUNCTION DEVELOPMENT

M. MARKOWITZ
MCDONNELL DOUGLAS ASTRONAUTICS CO.
HUNTINGTON BEACH, CALIFORNIA

PRECEDING PAGE BLANK NOT FILMED



DELTA VEHICLE/SPACECRAFT DYNAMIC LOADS ANALYSIS CYCLE

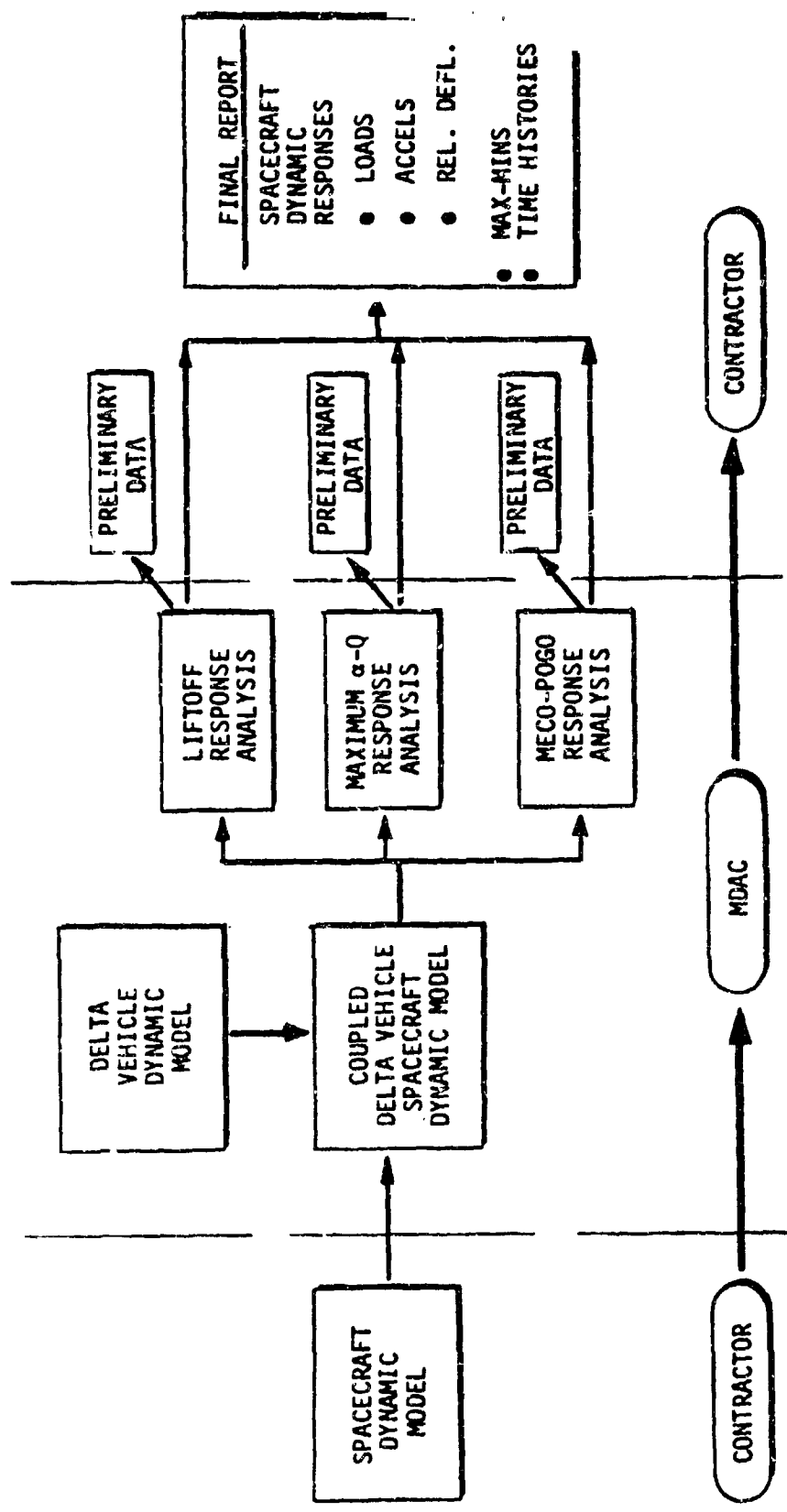
Spacecraft structural dynamic models are provided by the contracting agency to MDAC in one of three acceptable formats: (1) discrete mass and stiffness matrices, (2) constrained modal mass, stiffness, and load, acceleration, and deflection transformation matrices, and (3) NASTRAN bulk data decks.

The standard load cycle involves MDAC coupling the spacecraft to the appropriate Delta vehicle dynamic model and calculating maximum expected (2σ level) dynamic responses for three flight conditions. Transient responses predicted for liftoff define the governing lateral load used for spacecraft design. Transient response to wind gust penetration at maximum α - q predicts the critical dynamic relative deflections between spacecraft and fairing to ensure no interference occurs during flight. Sinusoidal responses for pogo are combined with the main engine cut-off (MECO) quasi-static vehicle acceleration responses to define the spacecraft maximum axial loading condition.

Preliminary transmittal of response data are made available to the contracting agency after completion of each flight condition analysis. Time history accelerations and/or spacecraft generalized coordinate accelerations are made available in computer tape or card format to the contracting agency for use in their detailed loads evaluation. A final report documenting the complete analysis is supplied to the contracting agency generally four months after MDAC receipt of spacecraft model.



DELTA VEHICLE/SPACECRAFT DYNAMIC LOADS ANALYSIS CYCLE





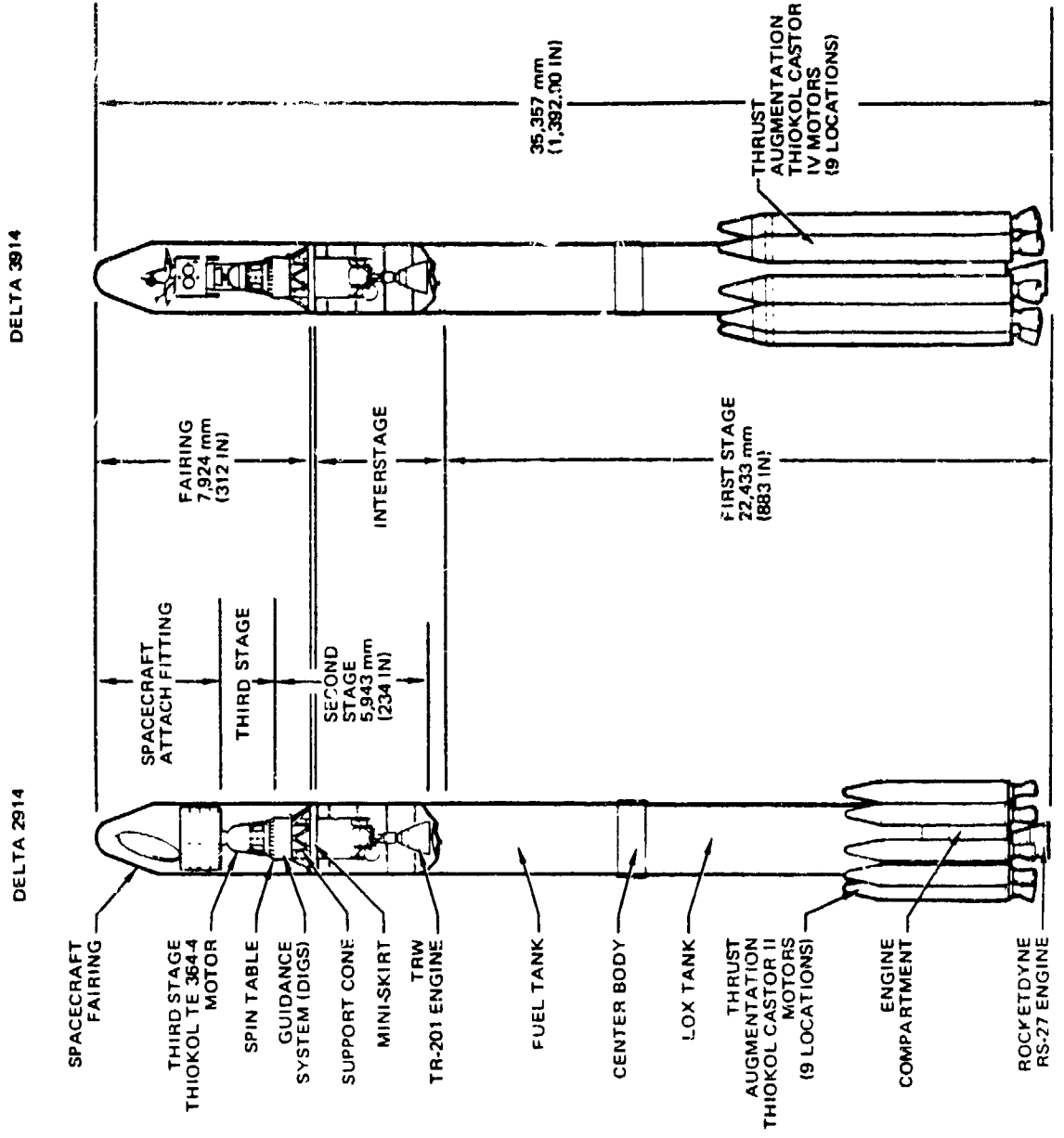
DELTA 2914 AND 3914 CONFIGURATION LAUNCH VEHICLES

MDAC offers two basic Delta launch vehicles, the 2914 and 3914 configurations, both of which can accommodate a third stage propulsion system. The two vehicles are basically identical with the distinct exception of the strap-on solid propellant motors.

The first stage liquid propellant booster is powered by an RS-27 main engine and is initially augmented by externally-mounted solid motors: Castor II variety for the 2914 vehicle, and Castor IV variety for the 3914 vehicle. In general, six Castor II motors are ignited during liftoff and the remaining three at altitude. Only five Castor IV motors are ignited during liftoff with the remaining four ignited at altitude. The solid propellant motors are jettisoned after they burn out.



DELTA 2914 AND 3914 CONFIGURATION LAUNCH VEHICLES





3914 DELTA VEHICLE DYNAMIC MODEL SCHEMATIC

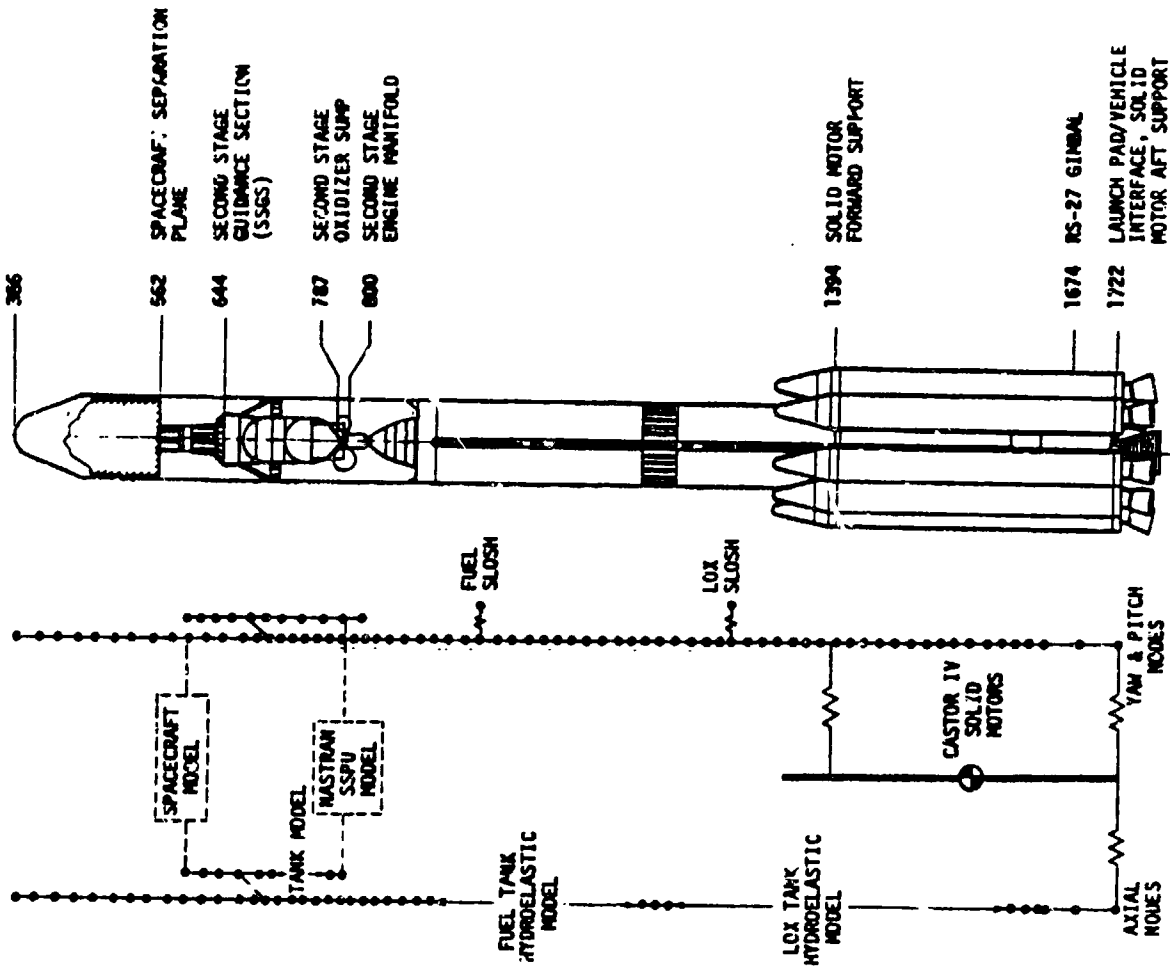
The Delta launch vehicle structural dynamic model is constructed from an assemblage of substructure models. The vehicle model possesses degrees of freedom for three planes of motion and two rotational axes; torsional motion of the vehicle is not modeled.

Dynamic representation of a majority of the vehicle is represented by Timoshenko beam lateral and axial planar models constructed in MDAC computer program "DA02". Structures modeled in this manner include: attach fittings, third stage, guidance section w/support truss, second stage tanks (lateral only), fairing, interstage, main fuel tank (lateral only), centerbody, main LOX tank (lateral only), LOX skirt, and boattail.

Longitudinal models of the first stage and second stage propellant tanks are constructed using computer program DYNASOR. This program generates mass and stiffness matrices for axisymmetric shells partially filled with an incompressible fluid.

NASTRAN Computer code is used to idealize the RS-27 main engine, second stage engine, and second stage panel/bottles assembly. The six degrees of freedom models provide the detail required for specific loads application and high frequency response analysis.

Main tank propellant slosh modes are represented as simple single degree of freedom dynamic models. Bending compliance for separation bands and separation bolt joints is represented by localized bending stiffness.





3914 DELTA VEHICLE
DYNAMIC MODEL
SCHEMATIC

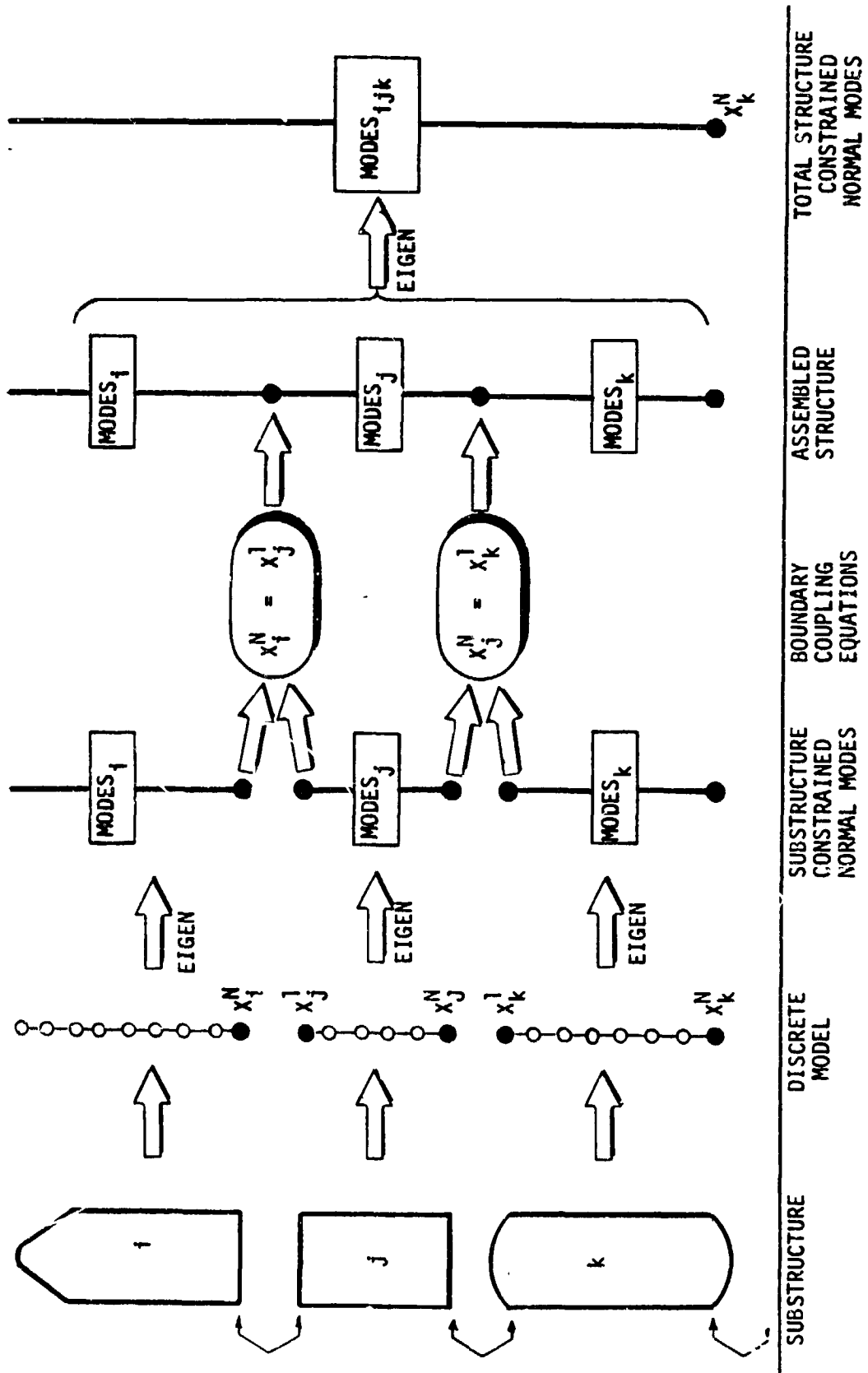


DELTA VEHICLE SUBSTRUCTURE MODELING AND ASSEMBLY TECHNIQUE

The Delta vehicle structural dynamic model is generated from an assemblage of substructure models using Hurty's method of component mode synthesis. Discrete models of the various substructures are generated. Fixed constraint normal modes and constraint shapes are calculated as are any necessary internal load and displacement transformations. Boundary coupling equations are used to assemble the various models at their discrete degree of freedom interfaces. These common internal interfaces are included with the i , j and k modal coordinates as the new set of generalized coordinates. Generally, an additional solution of this set of equations is used to calculate a reduced number of generalized coordinates which can be back-transformed to recover discrete internal loads and displacements.



DELTA VEHICLE SUBSTRUCTURE MODELING AND ASSEMBLY TECHNIQUE





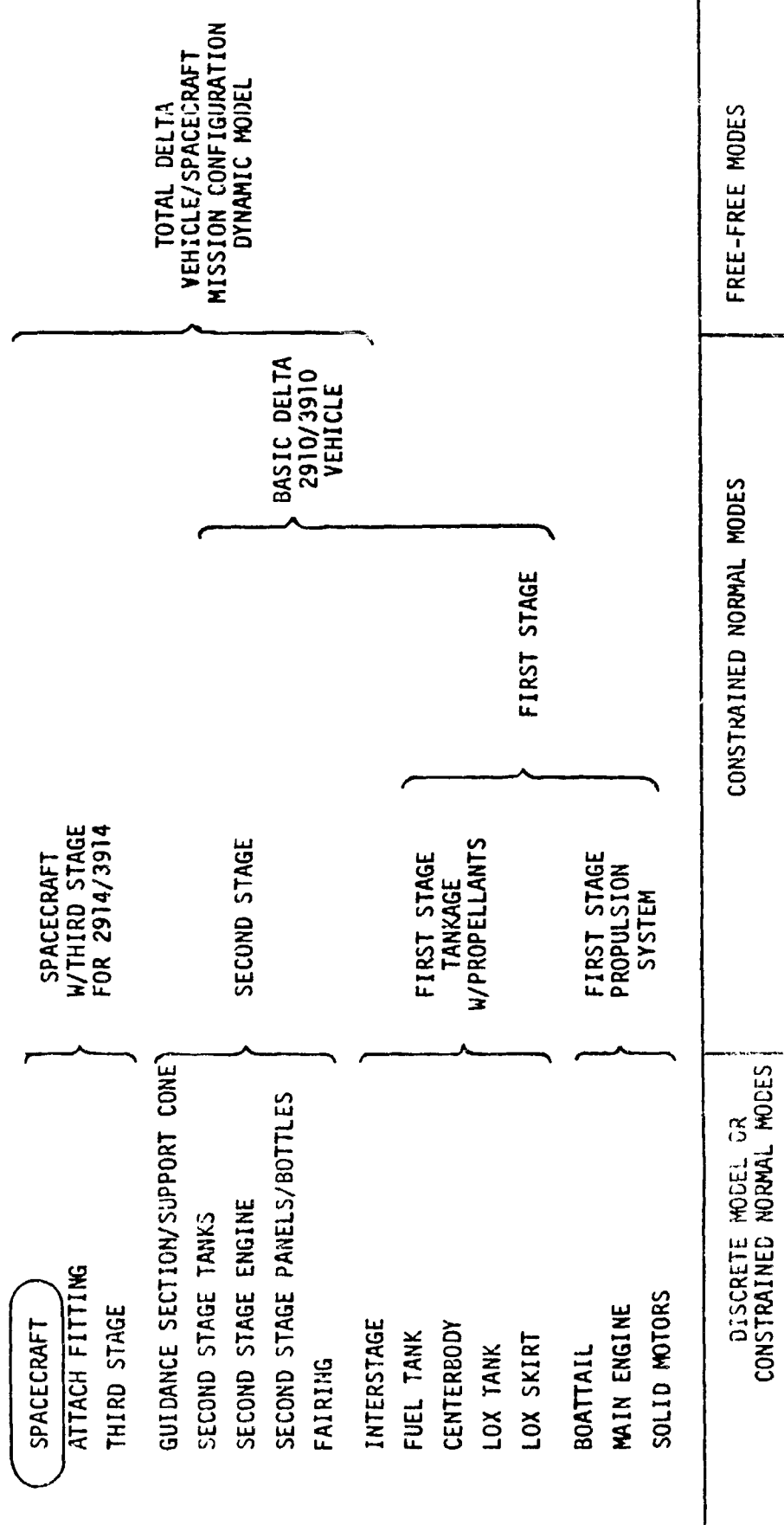
DELTA VEHICLE/SPACECRAFT MODEL ASSEMBLY FLOWCHART

All levels of Delta vehicle substructure models are retained in discrete and/or modal format on a library tape. Matrix abstraction routines, using MDAC Computer code SA48, are written to perform any level of substructure coupling. The basic levels of assemblage are organized so that structure common to all Delta vehicle configurations are fully constructed (e.g., third stage, second stage). A reasonable number of modes is retained for each substructure (> 100 Hz) so that adequate dynamic response characteristics are assured in the final model.

The basic Delta 2910 and 3910 vehicle dynamic models can either accommodate a third stage or simply represent the two-stage configuration. The total Delta vehicle/spacecraft mission configuration dynamic model is represented as free-free modes with frequency content > 50 Hz.



DELTA VEHICLE/SPACECRAFT DYNAMIC MODEL ASSEMBLY FLOWCHART





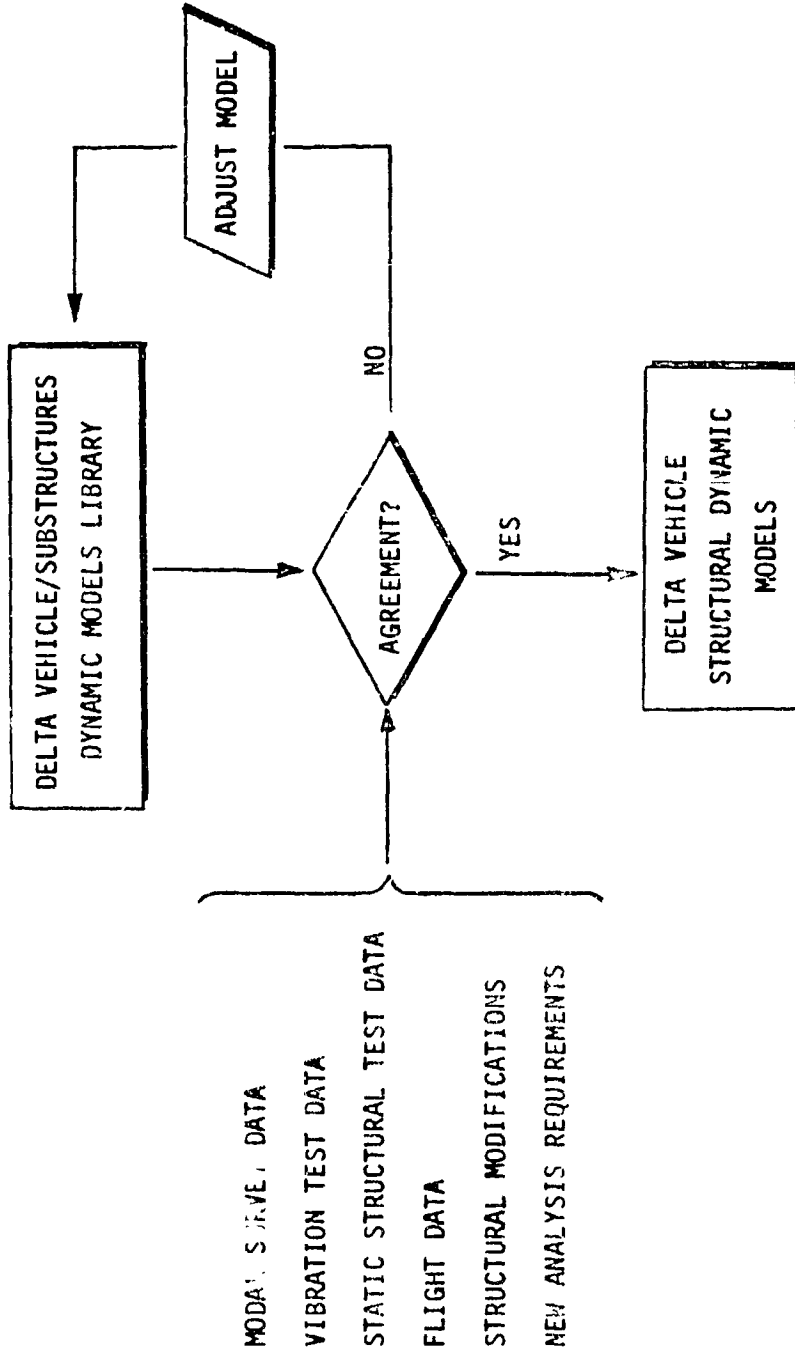
DELTA VEHICLE DYNAMIC MODEL MODIFICATION PROCESS

The Delta vehicle structural dynamic model has been modified, when necessary, to reflect structural characteristics exhibited in modal survey, vibration test, and flight data. Static test data is used as a basis for stiffness definition of structural elements if no dynamic data is available.

Flight acceleration data have been used to modify the Delta vehicle dynamic model to better match lateral frequencies and modeshapes, dominantly excited during lift-off. Better tank modeling was incorporated into the model so as to provide close agreement between analysis and flight axial modes, a necessary requirement for an associated pogo stability analysis. Structural design modifications would result in adjustment of the dynamic model only if they affect the vehicle dynamics in the frequency range of interest.



DELTA VEHICLE DYNAMIC MODEL MODIFICATION PROCESS





DELTA VEHICLE LIFTOFF RESPONSE ANALYSIS

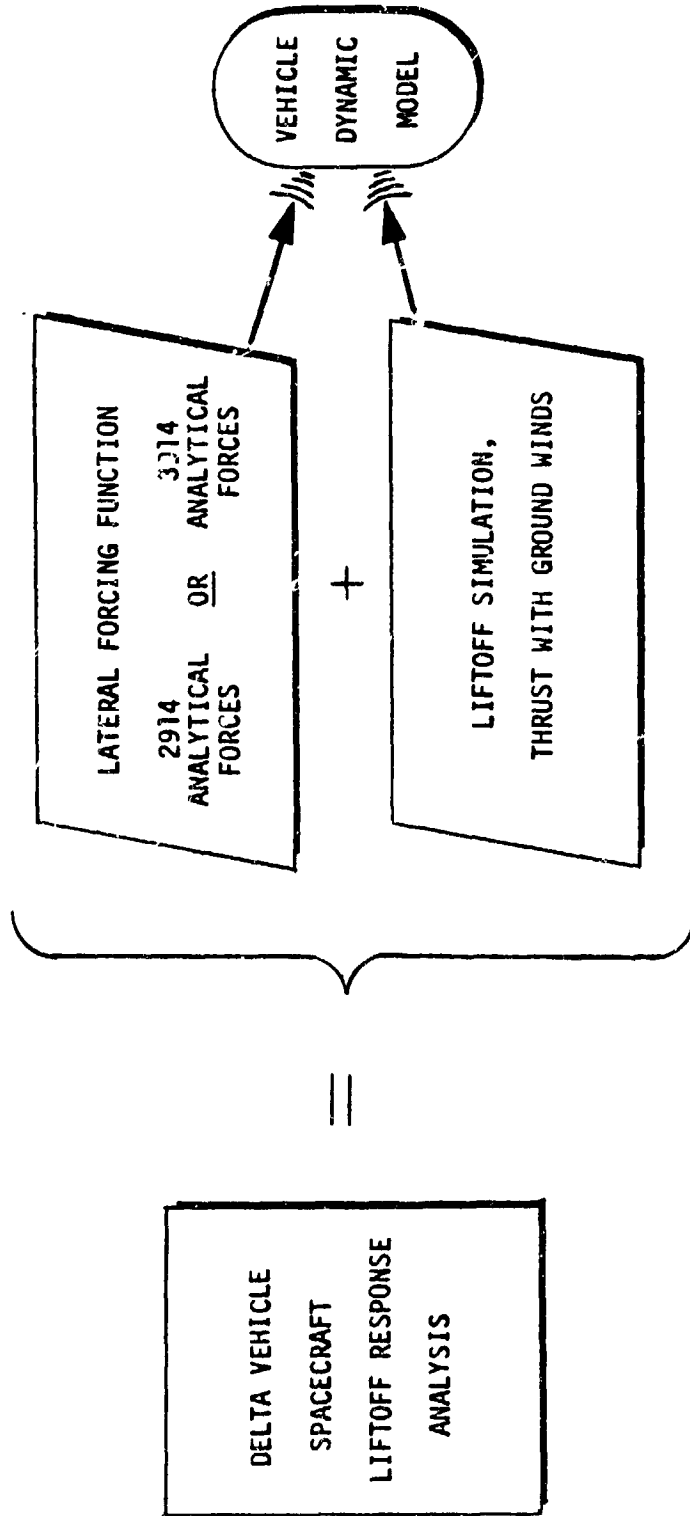
The Delta vehicle liftoff dynamic response analysis considers two sources of vehicle excitation: (1) lateral excitation resulting from mechanical and acoustic forces during ignition of the RS-27 main engine and the solid propellant motors, and (2) lateral wind induced excitation as influenced by the interaction of the vehicle and launch pad while the engine and solid motor thrusts forces accelerate the vehicle.

MDAC attempted to identify the lateral forces acting on the vehicle during ignition at liftoff through an extensive evaluation of ground and flight test data. MDAC determined it necessary to develop a set of synthesized lateral forces that, complementing the vehicle dynamic model, would analytically produce lateral dynamic responses with peak value and frequency content representative of measured flight responses.

Vehicle lateral responses from the analytical lateral forcing functions are combined with the responses calculated to occur due to thrust and ground winds. These combined responses define the maximum expected (2 σ level) spacecraft and vehicle accelerations and loads predicted for the liftoff event.



DELTA VEHICLE LIFTOFF RESPONSE ANALYSIS





2914 DELTA VEHICLE LIFTOFF LATERAL FORCING FUNCTION DEVELOPMENT

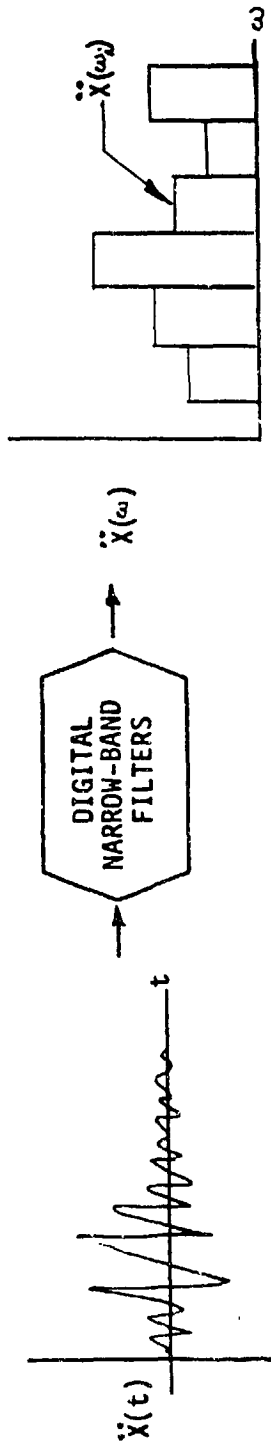
The lateral forcing function used in 2914 Delta liftoff analysis represents a transfer of frequency domain data, measured on Delta vehicles during liftoff with negligible winds present, to a synthesized pulse forcing function in the time domain. This forcing function is not meant to be quantitatively or qualitatively realistic.

Lateral accelerations $\ddot{X}(t)$ measured at the guidance compartment during liftoff are reduced by digital narrow-band filters to obtain acceleration as a function of discrete frequency bands, $\ddot{X}(\omega)$.

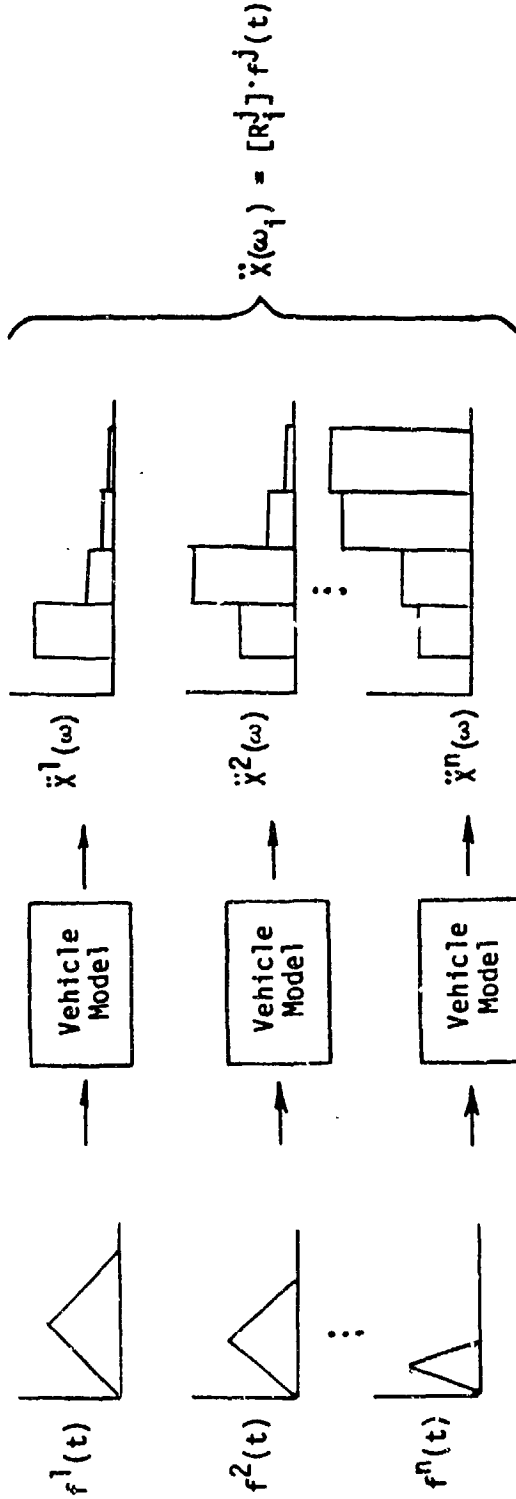
Triangular pulse forces produce residual responses vs. frequency that are a function of the duration of the pulse. A series of these pulse forces, the duration of which were selected to produce maximum response at the 2 Hz, 4 Hz, 9 Hz and 18 Hz ranges, were applied to the free-free dynamic model. The relationship of acceleration levels as a function of frequency $\ddot{X}_i(\omega)$ for each of the pulse forces $f_i(\omega)$, using the vehicle dynamic model as the transfer function, is used to calculate the proper pulse force levels and phasing so as to produce the desired vehicle lateral accelerations $\ddot{X}(\omega_i)$.

2914 DELTA VEHICLE LIFTOFF LATERAL FORCING FUNCTION DEVELOPMENT

1 FILTER MEASURED FLIGHT DATA TO OBTAIN $\ddot{X}(\omega)$



2 CALCULATE VEHICLE RESIDUAL RESPONSE TO UNIT TRIANGULAR PULSES OF VARYING DURATION





2914 DELTA VEHICLE LIFTOFF LATERAL FORCING FUNCTION DEVELOPMENT

The response transformation $[R]$ is inverted to obtain the force level and phase for each pulse f_i so as to produce the required acceleration residual response $\dot{X}(\omega_i)$. The final synthesized lateral function $F(t)$ is formulated as a direct summation of these individual pulse forces.

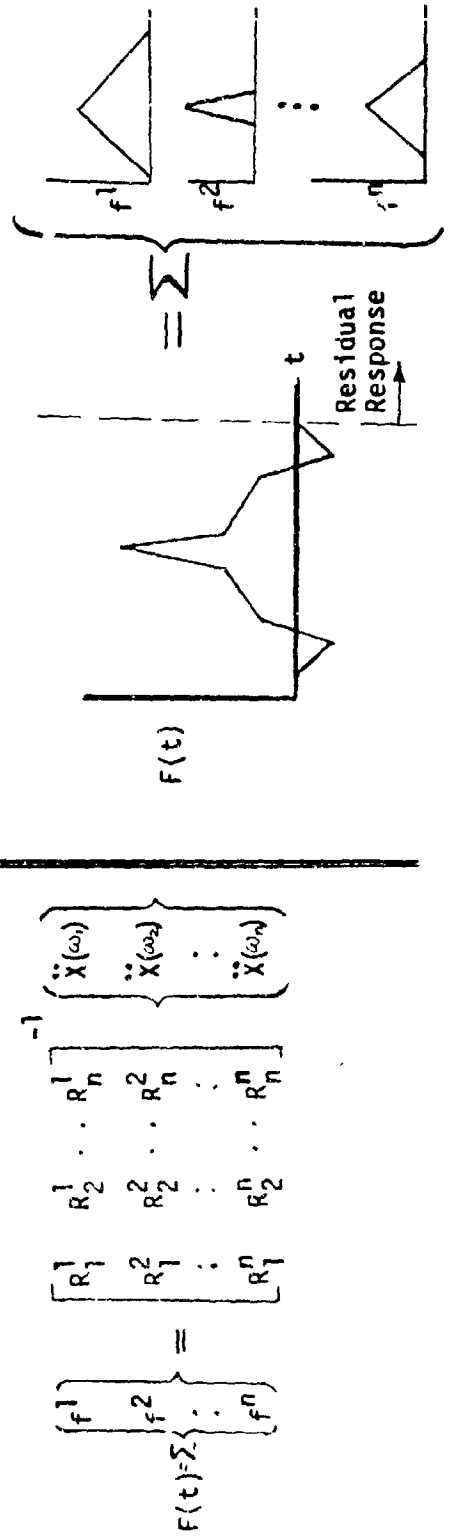
The forcing function magnitude was adjusted so as to produce maximum expected (2σ level) guidance compartment lateral acceleration levels, calculated from statistical evaluation of measured flight accelerations.

Measured lateral accelerations from a typical 2914 Delta launch compare favorably to 2σ level predictions for the mission. The predicted responses possess the acceleration level and frequency content as exhibited in flight.

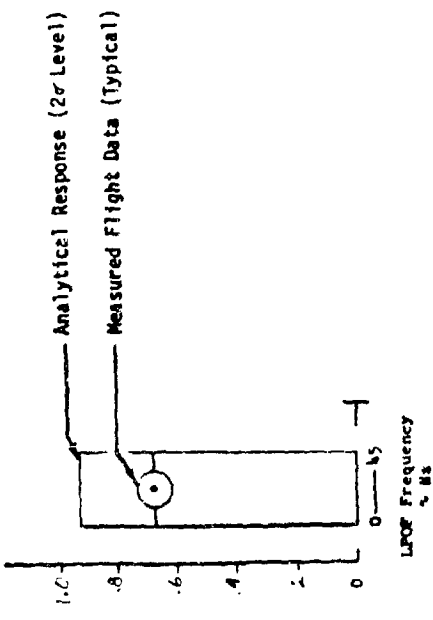
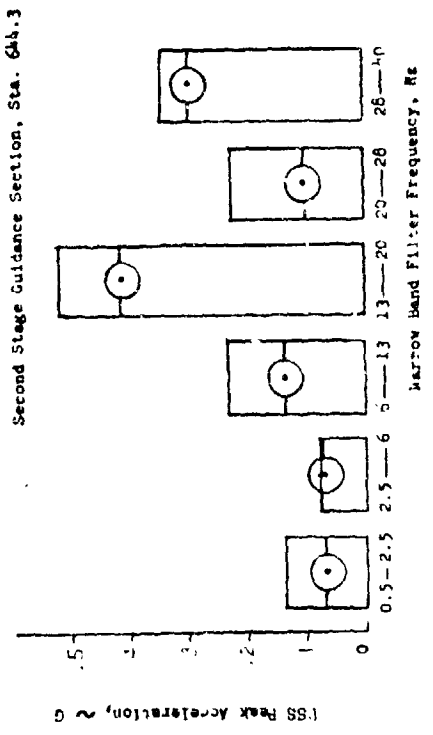


2914 DELTA VEHICLE LIFTOFF LATERAL FORCING FUNCTION DEVELOPMENT

3 SOLVE FOR FORCE AMPLITUDE AND PHASE; FORCING FUNCTION IS SUM OF PULSES



4 COMPARE ANALYTICAL RESPONSES WITH FLIGHT DATA





2914 DELTA VEHICLE LIFTOFF LATERAL FORCING FUNCTION

The 2914 Delta vehicle liftoff lateral forcing function consists of two synthesized pulse forces, one applied to vehicle station 697, and the other applied to the RS-27 Gimbal Block. Two response cases are performed in which the forcing function is applied in the two orthogonal (yaw or pitch) axes since the lateral vehicle response can occur in any lateral direction. Responses for any arbitrary vehicle azimuth can be calculated by appropriately vector summing the separate yaw and pitch case responses.

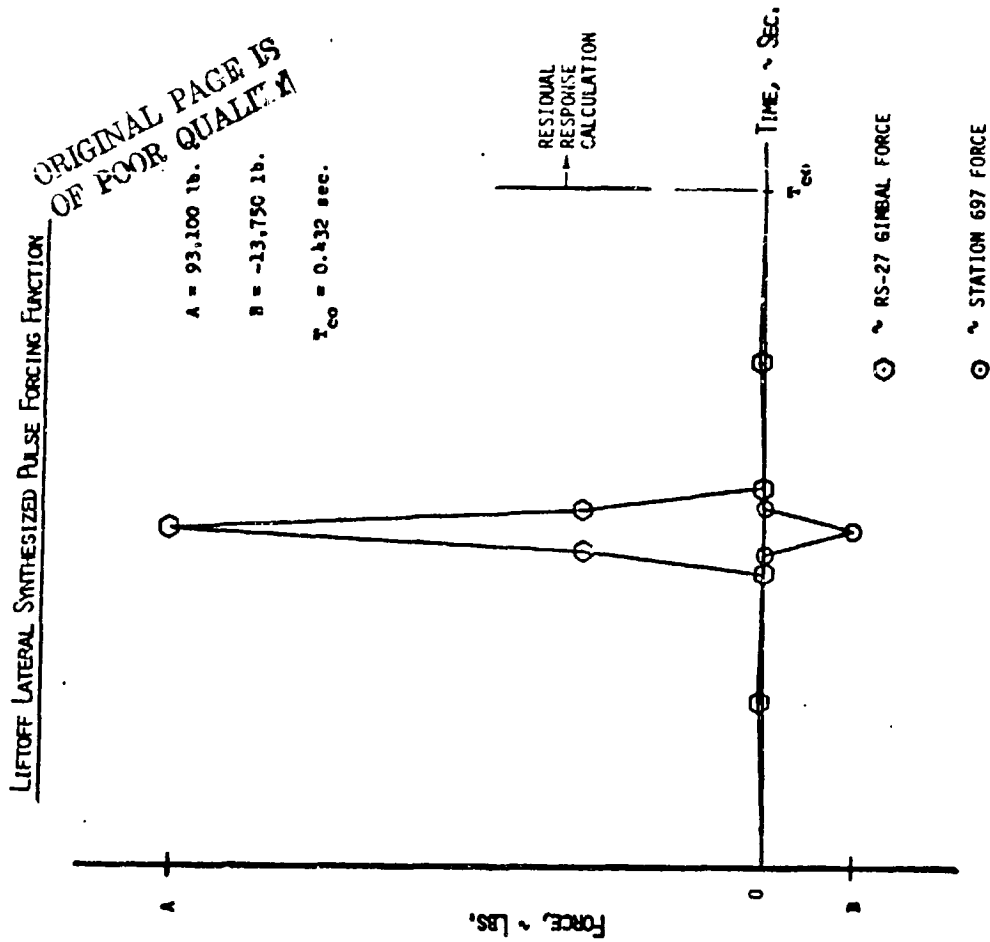
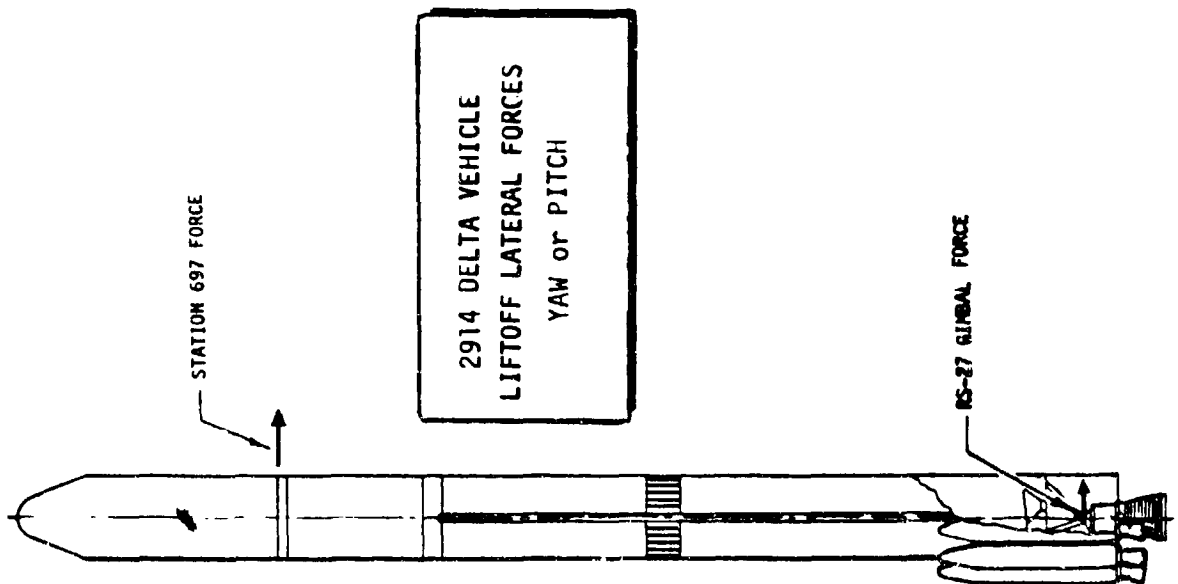
The pulse forcing function residual responses are defined as maximum expected (2σ level) since the forces were adjusted so as to reproduce 2σ level guidance compartment accelerations, calculated from statistical evaluation of measured flight data.

The forcing function is applied to free-free modes of the vehicle, frequency content from 0 Hz to > 45 Hz. Responses are calculated with $\Delta t = 0.0025$ seconds for a post-pulse duration of 1.5 seconds. Modal damping of 1.5 percent of critical is used for all modes.

ORIGINAL PAGE IS
OF POOR QUALITY



2914 DELTA VEHICLE LIFTOFF LATERAL FORCING FUNCTION



ORIGINAL PAGE IS
OF FOUR QUALITY



3914 DELTA VEHICLE LIFTOFF LATERAL FORCING FUNCTION DEVELOPMENT

For the 3914 Delta vehicle, the development of the lateral forcing function simulating the phenomena occurring during liftoff is based on analytically matching the measured pitch and yaw acceleration time histories at the guidance compartment for a mission with negligible wind effects. The method of Finite Fourier Transform (FFT) is used to produce an analytical force with proper amplitude and frequency content.

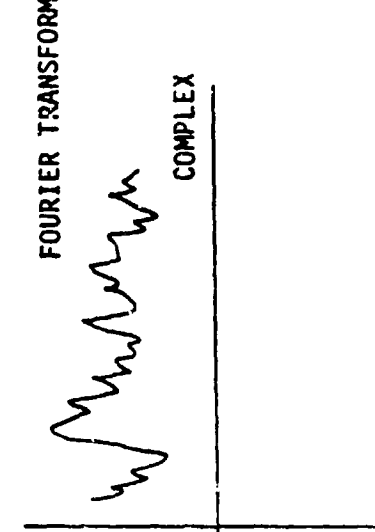
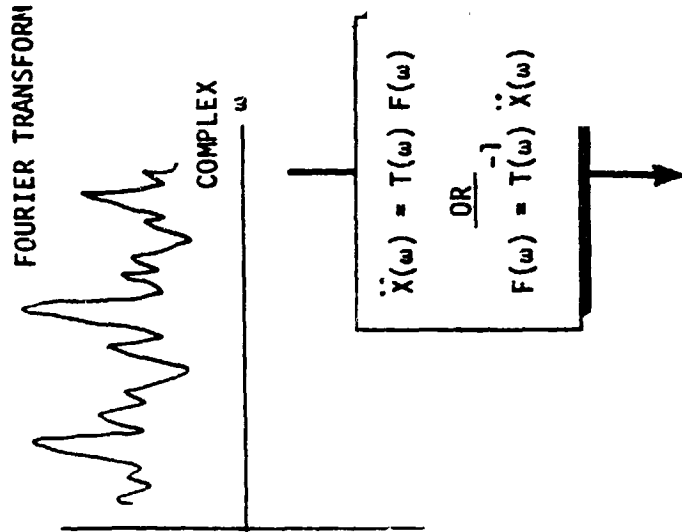
Transformation of the response from the time domain to the frequency domain is accomplished via Finite Fourier Transform. This results in a set of Fourier coefficients corresponding to the assumption that the data can be approximated as a superposition of harmonic waveforms (sine and cosine) whose amplitudes and phase are given by the Fourier coefficients. The purpose of transformation to the frequency domain is to permit use of the frequency response of the model (an excitation/response representation of the model) to calculate excitation as a function of frequency.

The structural response equations governing the calculation of force from acceleration are given in Vol. 2, Section 23-34, of the Harris and Crede Shock and Vibration Handbook. $T(\omega)$ represents the analytical model transfer function or mechanical admittance, while $T^{-1}(\omega)$ represents the mechanical impedance. In general, both are complex matrices, but are reduced to scalar values when only one force and one response are related.

Back-transformation of the force spectra to the time domain is accomplished by superimposing the harmonic waveforms whose amplitudes and phase are given by the force spectra (Fourier coefficients). The result is a time history of the forcing function, $F(t)$, which will force the model to respond at the appropriate degree of freedom as defined by flight data.



3J14 DELTA VEHICLE LIFTOFF LATERAL FORCING FUNCTION DEVELOPMENT





3914 DELTA VEHICLE LIFTOFF LATERAL FORCING FUNCTION

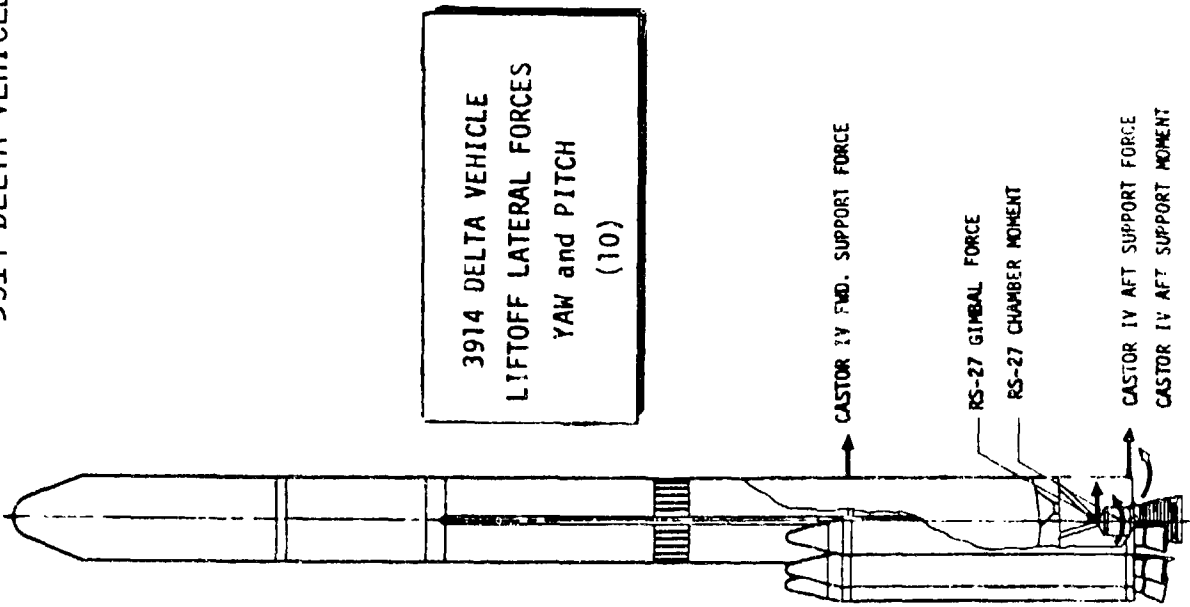
The 3914 Delta vehicle liftoff lateral forcing function consists of a total of ten forces and moments applied to the vehicle, five in the yaw axis and five in the pitch axis. The pitch and yaw forces and moments are fixed in direction since they are based on directionally discriminated flight measurements.

The forcing function produces maximum expected (2σ level) vehicle/spacecraft lateral responses. The forces were adjusted so as to produce 2σ level guidance compartment accelerations, calculated from statistical evaluation of measured flight data.

The forces are applied to free-free modes of the vehicle, frequency content from 0 Hz to > 45 Hz. Responses are calculated with $\Delta t = 0.0025$ seconds for a duration of 2.0 seconds. Modal damping of 1.5 percent of critical is used for all modes.

ORIGINAL PAGE IS
OF POOR QUALITY

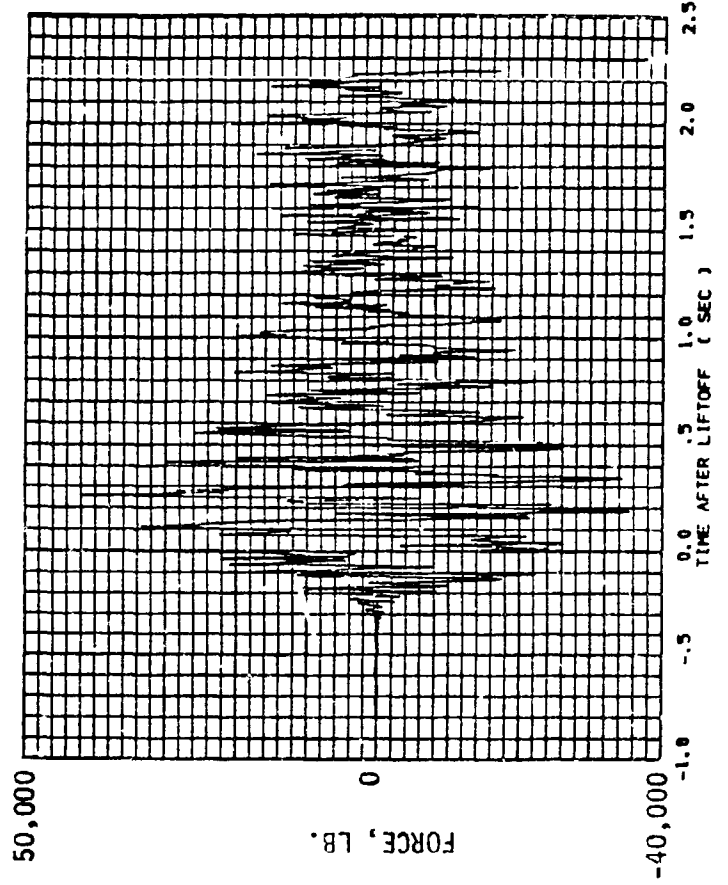
3914 DELTA VEHICLE LIFTOFF LATERAL FORCING FUNCTION



3914 DELTA VEHICLE
LIFTOFF LATERAL FORCES
YAW and PITCH
(10)

TYPICAL FORCE TIME HISTORY (1 OF 10)

DELTA 3914 L/O TWO SIGMA LATERAL EXCITATION, YAW
RS-27 GIMBAL BLOCK FORCE





3914 DELTA VEHICLE LIFTOFF LATERAL FORCING FUNCTION

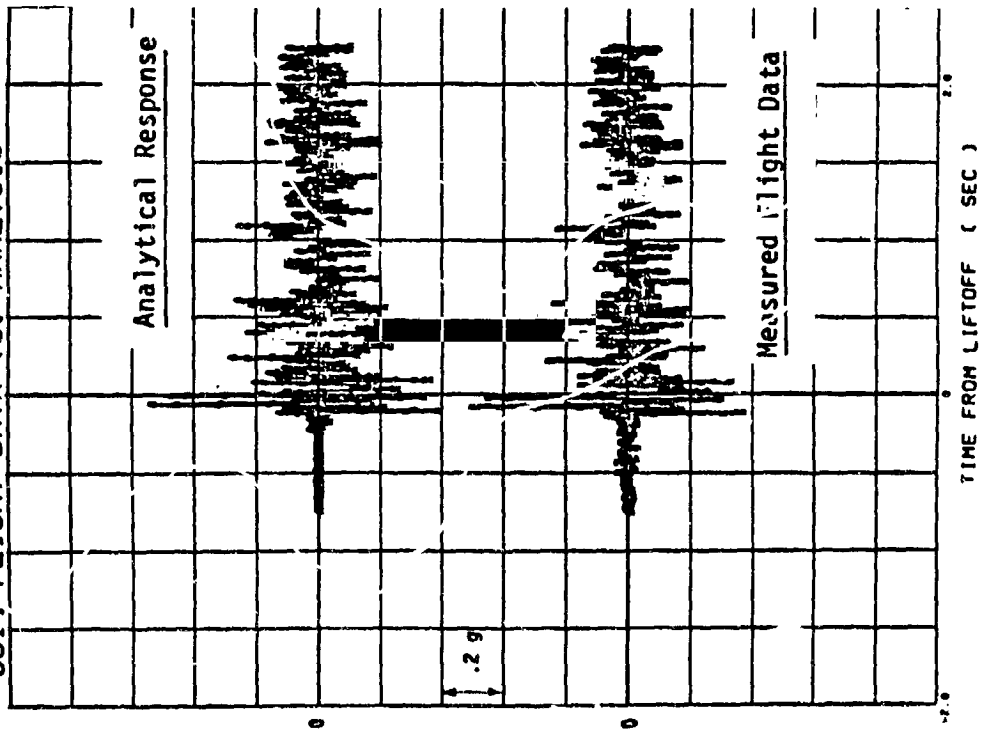
The lateral forcing function for the 3914 Delta vehicle was developed so that the time history analytical response matches the measured flight data from which it was developed. Digital narrow-band filter analyses of the analytical and measured accelerations are compared to assure that amplitude and frequency content are in agreement.

Since the lateral forcing is generated to match measured data in the time domain, the forcing function can be time correlated with measured thrust time histories. Consequently, the analytical lateral responses and the thrust/wind responses from a launch pad simulation analysis can be time correlated and summed to simulate time-phased triaxial combination of spacecraft structure loads and accelerations.



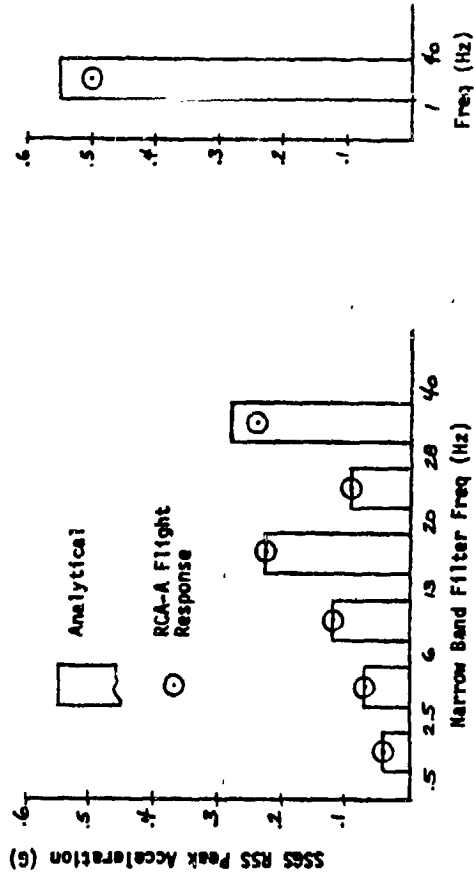
3914 DELTA VEHICLE LIFTOFF LATERAL FORCING FUNCTION

3914 FLIGHT DATA VS. ANALYSIS



RCA-A (3914 MEAN VALUE) LATERAL LIFTOFF

PEAK VALUE LATERAL UPPER STAGE ACCELERATIONS COMPARISON OF MEASURED FLIGHT LEVELS TO YAW (Y) ANALYSIS LEVELS



ORIGINAL PAGE OF POOR QUALITY

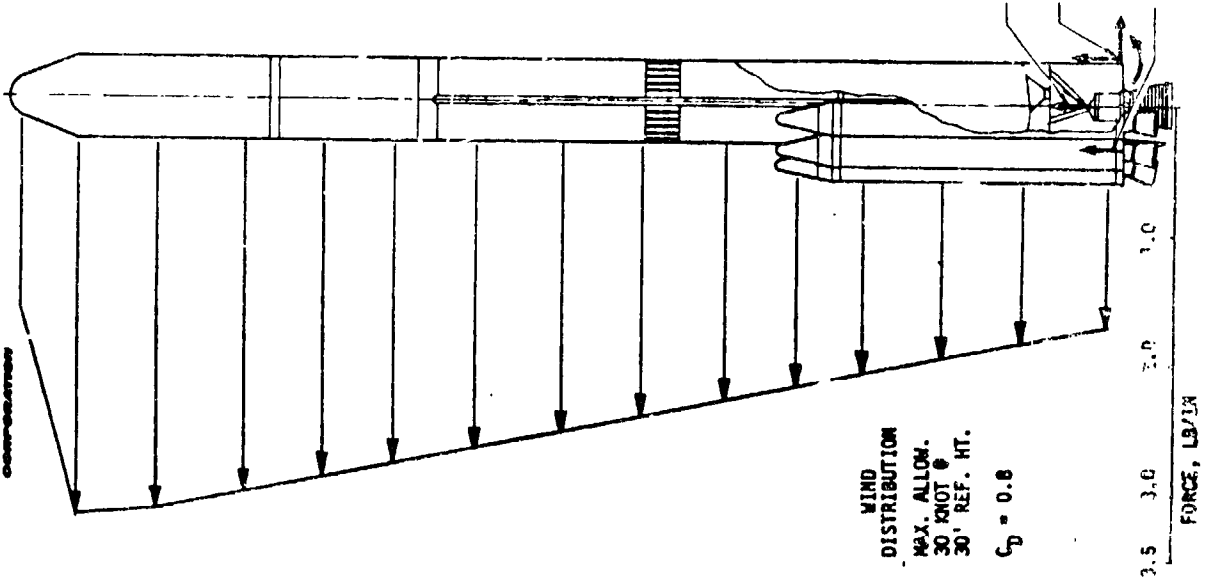


DELTA VEHICLE/LAUNCH PAD LIFTOFF SIMULATION - THRUST WITH GROUND WINDS

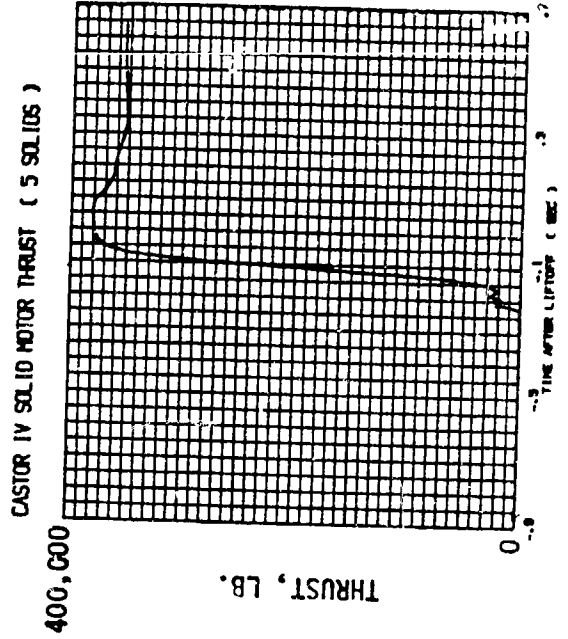
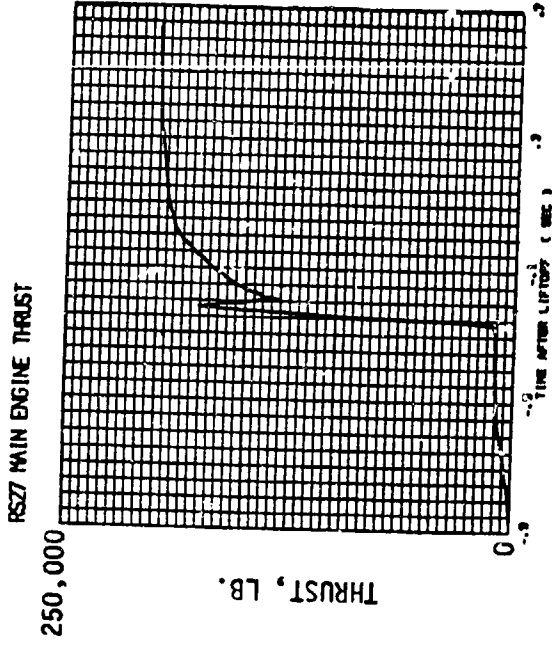
To calculate the effect of maximum allowable ground winds and thrust on spacecraft response, an analytical simulation of the vehicle lifting off from the launch pad was developed. Computer code was written that couples a flexible representation of the launch pad to the dynamic model of the Delta vehicle spacecraft. Thrust forces from main engine and solid motor ignition, modified to reflect 2σ level values, are applied to the vehicle. The resultant launch pad/vehicle interface loads, moments are monitored and adjusted as the vehicle begins first motion, clears launch pins, and becomes free of pad restraint. The total set of thrust and pad interface forces are compatible for application to free-free modes of the vehicle.

Responses from this liftoff simulation analysis are combined with those obtained using the appropriate lateral forcing function to define the maximum expected spacecraft responses predicted to occur during liftoff.

DELTA VEHICLE/LAUNCH PAD LIFTOFF SIMULATION - THRUST WITH GROUND WINDS



PROCEED TO PAGE 19 FOR FURTHER ANALYSIS





DELTA VEHICLE MAXIMUM α -Q RESPONSE ANALYSIS

Maximum α -Q is analyzed because the aerodynamic loads produce relative dynamic deflections between the spacecraft and vehicle fairing, which when combined with static deflections and manufacturing tolerances, define minimum spacecraft/fairing clearances for the mission.

Eight lateral load cases are considered which consist of four wind shear gust shapes $G(t)$ applied to the free-free vehicle dynamic model in the two orthogonal lateral axes. Using the recommended gust shapes from NASA SP-8035, NASA SPACE VEHICLE DESIGN CRITERIA, "Wind Loads During Ascent", June 1970, four selected wind shear depths are utilized to simulate the maximum aerodynamic gust loading conditions which occur at a flight time of 37 seconds for 2914 vehicles and at 55 seconds for 3914 vehicles.

The lateral forcing function for the maximum α -Q response analysis is given by

$$F(X,t) = F_{MAX}(X) \cdot G(t)$$

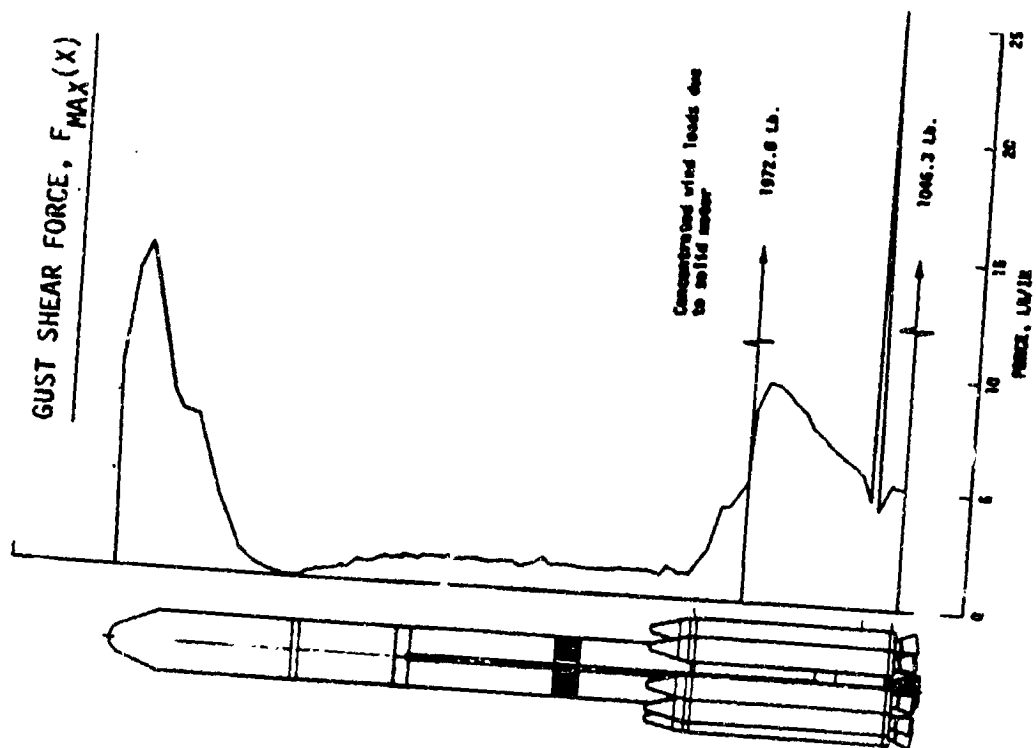
where $F_{MAX}(X)$ is the 2σ level lateral aerodynamic gust force discretized at a number of vehicle stations, and $G(t)$ is the wind shear gust shape. The duration (a) is calculated by the time the vehicle requires to penetrate a depth of 30 meters, per NASA SP-8035. The time (ℓ) is adjusted so that the gust duration ($2a + \ell$) is tuned to excite vehicle lateral modes between 2 Hz and 7 Hz. Instantaneous gust immersion is assumed. Modal damping of 1.5 percent of critical is used for all modes.



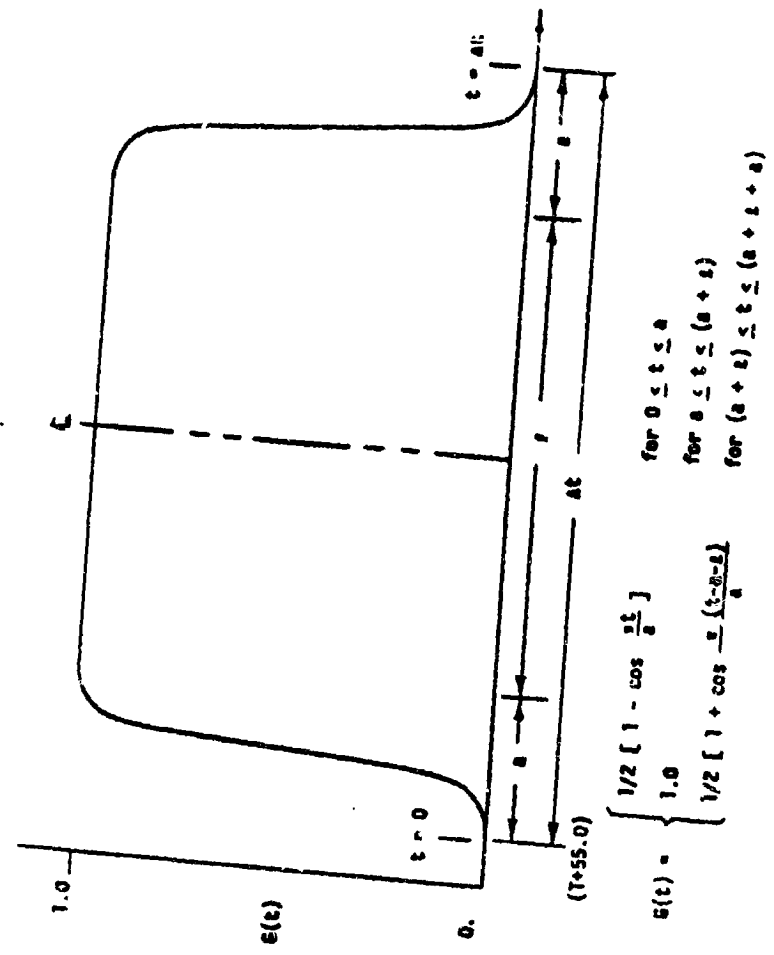
DELTA VEHICLE MAXIMUM αQ RESPONSE ANALYSIS

FORCING FUNCTION $F(X, t) = F_{MAX}(X) \cdot G(t)$

GUST SHEAR FORCE, $F_{MAX}(X)$



GUST SHAPE COEFFICIENT, $G(t)$





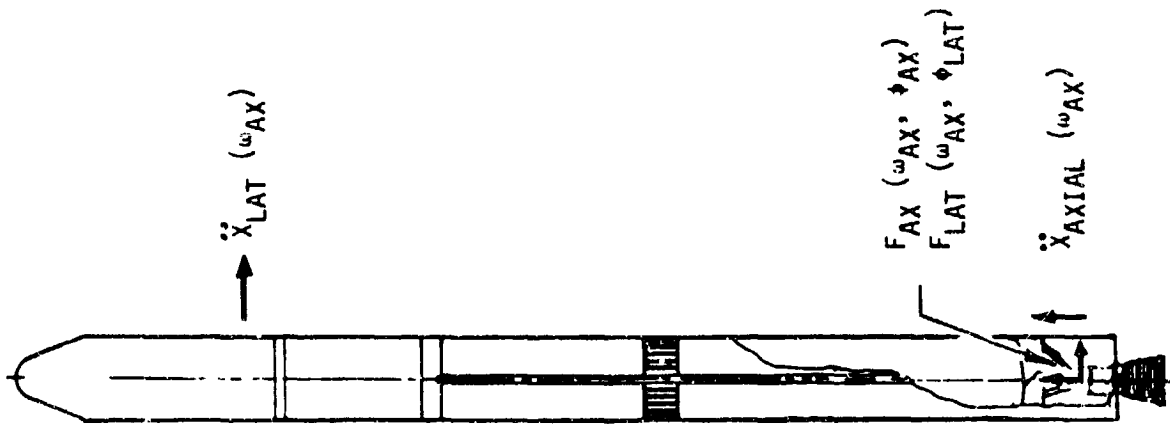
DELTA VEHICLE MECO POGO SINUSOIDAL RESPONSE ANALYSIS

A frequency response analysis is performed for determining the combined quasi-static and maximum expected (2σ level) sinusoidal responses on spacecraft and launch vehicle structure during pogo which occurs just prior to main engine cut-off (MECO) at 228 seconds in flight.

The dynamic responses are the result of axial and lateral sinusoidal forces applied to the RS-27 engine gimbal block at the fundamental axial vehicle frequency, which is predicted to be the pogo frequency. The applied forces are sized so as to recover specified criteria accelerations in the axial and lateral axes. Relative phasing of these accelerations is defined to be zero degrees for analytical simplicity. Spacecraft and vehicle response loads and accelerations are expressed as amplitude and relative phase. Modal damping of 1.5 percent of critical is used for all the free-free vehicle modes.

The vehicle dependent quasi-static axial acceleration responses are combined with the dynamic responses to define maximum and minimum expected value acceleration and loads predicted to occur for the MECO pogo flight event.

DELTA VEHICLE MECO POGO SINUSOIDAL RESPONSE ANALYSIS



CRITERIA:

$$\dot{X}_{AX}(\omega_{AX}) @ 0^\circ \text{ PHASE}$$

$$\dot{X}_{LAT}(\omega_{AX}) @ 0^\circ \text{ PHASE}$$

SINUSOIDAL FORCES:

$$\left\{ \begin{array}{l} F_{AX}(\omega_{AX}, \phi_{AX}) \\ F_{LAT}(\omega_{AX}, \phi_{LAT}) \end{array} \right\} = \left[\begin{array}{l} [T(\omega)] \\ \text{Complex} \end{array} \right] \left\{ \begin{array}{l} \ddot{X}_{AX}(\omega_{AX}) \\ \ddot{X}_{LAT}(\omega_{AX}) \end{array} \right\}$$

TOTAL RESPONSE:

$$\ddot{X}_{MAX, MIN} = \ddot{X}_{QUASI-STATIC} \pm |\ddot{X}(\omega_{AX})|$$

SPACELAB STRUCTURAL ASSESSMENT
BY COMPARATIVE ANALYSIS - DR. ROBERT L. MANN,
MCDONNELL DOUGLAS TECHNICAL SERVICES COMPANY

This paper describes a technique for determining whether the Spacelab structure is structurally capable of accommodating specific payload configurations. The process involves use of finite element models and post processor programs to compare mission peculiar loads with maximum as-run test loads. Loads analysis, model verification, capability matrix construction, post processor program and output formats are described.

PRECEDING PAGE BLANK NOT FILMED



SPACELAB STRUCTURAL ASSESSMENT
BY COMPARATIVE ANALYSIS

CHART No. 1
DATE 16 Nov 1973
SPEAKER R. L. MANN

SPACELAB = STANDARD MODULAR COMPONENTS
+ MISSION DEPENDENT EQUIPMENT
+ MISSION PECULIAR EQUIPMENT AND EXPERIMENTS

- MANY PAYLOAD CONFIGURATIONS
 - FREQUENT FLIGHTS
- NEEDING

QUICK, LOW COST STRUCTURAL EVALUATION



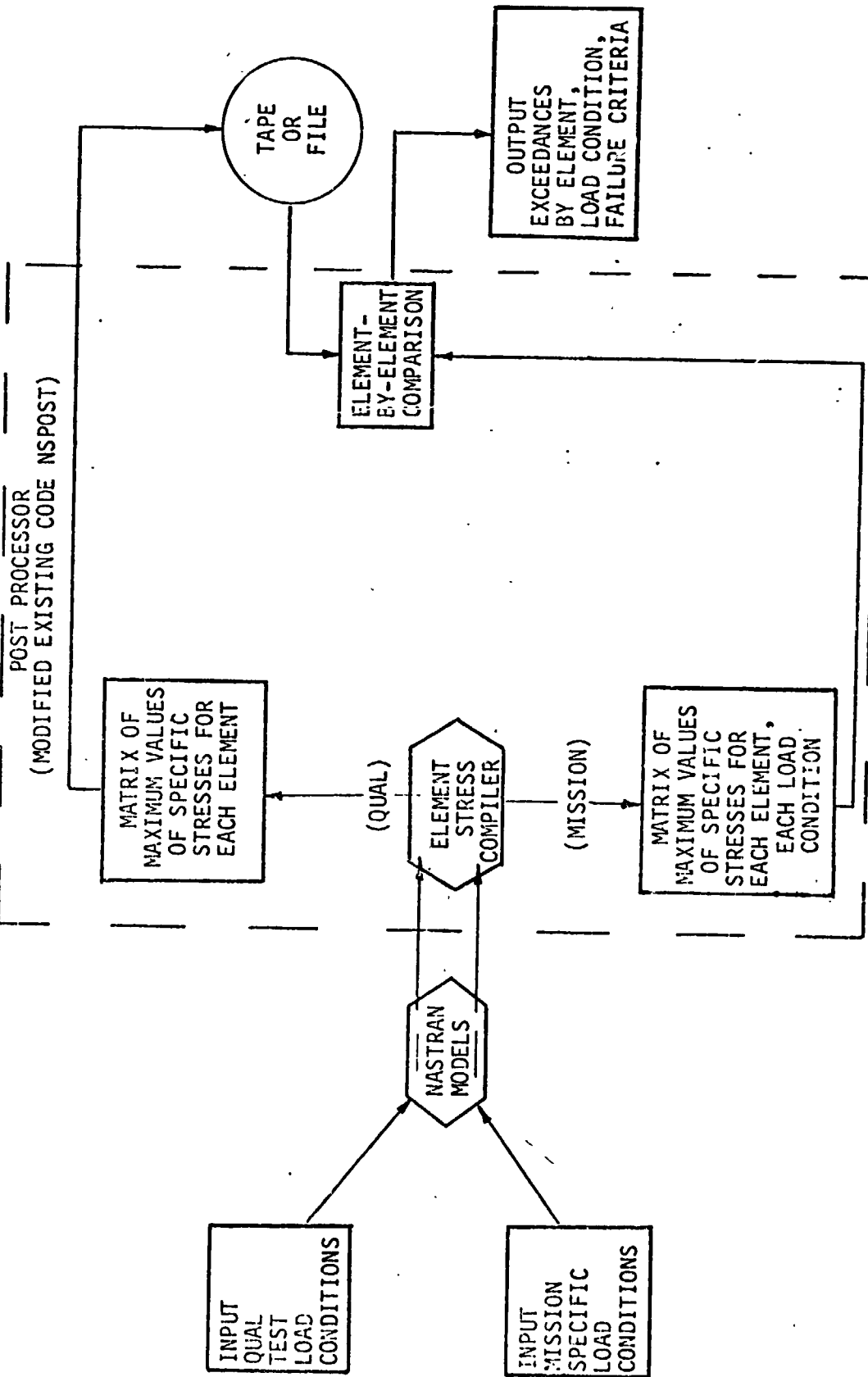
SPACELAB STRUCTURAL ASSESSMENT
BY COMPARATIVE ANALYSIS

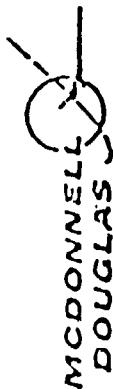
CHART No. 3
DATE 16 Nov 1978
SPEAKER R. L. MANN

PROGRAM DEVELOPMENT

- o ALTER NASTRAN TO OUTPUT ELEMENT STRESS TABLE
- o WRITE POST-PROCESSOR TO CALCULATE CRITICAL STRESS LOADINGS (CSL FILE)
- o WRITE ROUTINE TO READ CSL FILE AND COMPARE WITH REFERENCE VALUES (CSLREF)
- o OUTPUT DEFINES EXCEEDANCES - ELEMENT TYPE, LOADING TYPE, CONDITION, EXCEEDANCE FACTOR (%)

NASTRAN STRUCTURAL EVALUATION POST PROCESSOR





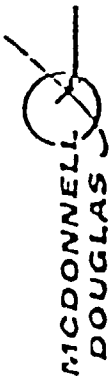
SPACELAB STRUCTURAL ASSESSMENT
BY COMPARATIVE ANALYSIS

CHART No. 2
DATE 16 NOV 1978
SPEAKER R. L. MANN

APPROACH

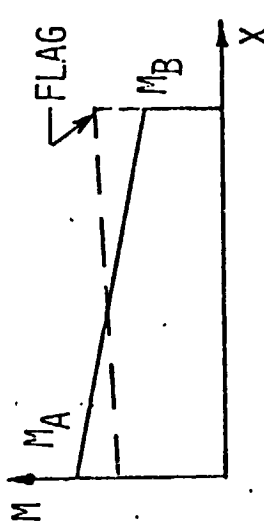
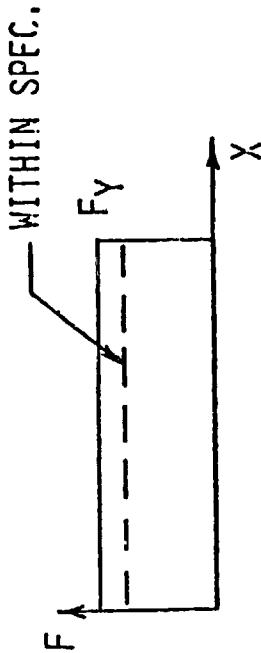
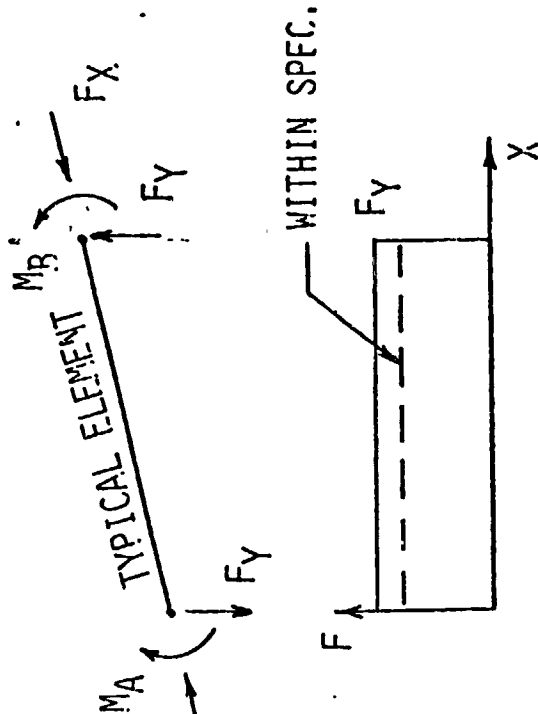
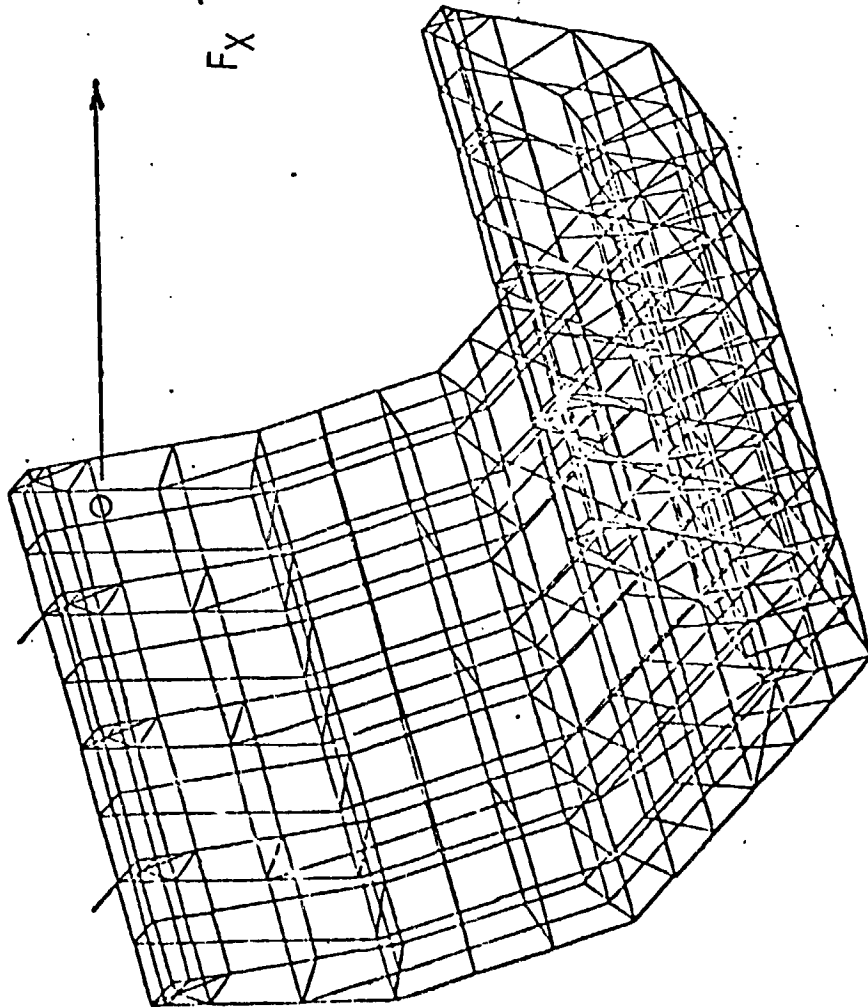
- o ESTABLISH "BASELINE" ELEMENT LOADS ENVELOPE FROM QUALIFICATION LOAD CASES
- o PERFORM LOADS ANALYSIS FOR MISSION PAYLOAD
- o COMPARE CALCULATED ELEMENT LOADS WITH "BASELINE" LOADS
- o FLAG EXCEEDANCES
- o DEVELOP A SUITABLE COMPUTER ROUTINE TO DO THE JOB

ORIGINAL PAGE IS
OF POOR QUALITY



SPACELAB STRUCTURAL ASSESSMENT
BY COMPARATIVE ANALYSIS

CHART No. 15
DATE 16 Nov 1978
SPEAKER R. L. MANN



— BASELINE LOADS ENVELOPE
- - - FLIGHT LIMIT LOADS



SPACECRAFT STRUCTURAL ASSESSMENT
BY COMPARATIVE ANALYSIS

CHART No. 6
DATE 16 NOV 1978
SPEAKER R. L. MAHN

SPECIFIC STRESSES TO BE USED IN EVALUATION

ELEMENT TYPE	STRESS	FAILURE CRITERIA COVERED
BAR (CBAR)	1. MAX. COMBINED 2. MIN. COMBINED 3. MIN. AXIAL (-ONLY)	1. TENSION 2. LOCAL INSTABILITY 3. EULER COLUMN
ROD (CROD, CONROD)	1. MAX. AXIAL 2. MIN. AXIAL (-ONLY)	1. TENSION 2. EULER COLUMN
PLATES (CQUAD, CTRIA)	1. MAX. VON MISES (EITHER SURFACE) 2. MAX. VON MISES * (MIDSURFACE - SEE REMARKS)	1. YIELD 2. INSTABILITY
MEMBRANES (CQDMEM, CTRMEM)	1. MAX. VON MISES 2. MAX. VON MISES * (SPECIAL CONSIDERATIONS - SEE REMARKS)	1. YIELD 2. INSTABILITY
SHEAR PANELS (CSHEAR)	1. MAX. SHEAR	1. SHEAR
SPRINGS (CELAS)	1. MAX. LOAD (STRESS)	1. LOAD (STRESS)

ORIGINAL PAGES
OF POOR QUALITY

* MAXIMUM VALUE IDENTIFIED UNDER ONE OF THE FOLLOWING CONDITIONS:

- a. σ_1 and $\sigma_2 < 0$
- b. $\sigma_1 < 0$ and $|\sigma_1| > |\sigma_2|$
- c. $\sigma_2 < 0$ and $|\sigma_2| > |\sigma_1|$

where σ_1 and σ_2 are principal stresses.



SPACELAB STRUCTURAL ASSESSMENT
BY COMPARATIVE ANALYSIS

CHART No. 7
DATE 16 Nov 1978
SPEAKER R. L. MANN

CONCLUDING REMARKS

- o INFLUENCE SIMILARITY - VERIFICATION BY TEST
- o CHECKOUT IN PROGRESS
- o MSFC INSTALLATION SCHEDULED DECEMBER 1978

MCDONNELL DOUGLAS TECHNICAL SERVICES COMPANY, INC. SPACELAB DIVISION



**A GENERALIZED MODAL
SHOCK SPECTRA METHOD
FOR SPACECRAFT LOADS ANALYSIS**

BY

**MARC TRUBERT
MOKTAR SALAMA**



OBJECTIVE OF LOADS ANALYSIS

THE DETERMINATION OF THE INTERNAL LOADS IN A SPACECRAFT STRUCTURE SUBJECTED TO A DYNAMIC LAUNCH ENVIRONMENT IS AN ITERATIVE PROCESS AIMED AT THE ULTIMATE SIZING OF THE STRUCTURE. THE PROCESS IS ITERATIVE SINCE THE INTERNAL LOADS ARE DEPENDENT UPON ITS MASS AND STIFFNESS DISTRIBUTION AS WELL AS THEIR INTERACTION WITH THE LAUNCH VEHICLE. IT IS NOT A SIMPLE FLIGHT SIMULATION BUT IT LOOKS FOR THE WORSE POSSIBLE CASE TO ESTABLISH A BOUND OF THE LOADS USED FOR THE SIZING OF THE STRUCTURE. SOME OF THE KEY PARAMETERS THAT DOMINATE THE LOADS ANALYSIS ARE TIMELINESS OF THE SIZING, COST, WEIGHT AND LOW SENSITIVITY TO ITERATIVE CHANGE IN THE DESIGN.

jpd →

OBJECTIVE OF LOADS ANALYSIS

- DETERMINE BOUNDS FOR LOADS IN SPACECRAFT STRUCTURE FOR LOW FREQUENCY (≤ 40 Hz)
- NOT A FLIGHT SIMULATION
- ESTABLISH WORSE CASES
- CRITICAL ITEMS
 - EARLY DEFINITION OF DESIGN LOADS
 - LOW SENSITIVITY TO DESIGN CHANGES
 - WEIGHT
 - COST

jpd →

SHOCK SPECTRA METHOD

BY DEFINITION THE SHOCK SPECTRA IS THE MAXIMUM AMPLITUDE OF THE RESPONSE OF A SIMPLE OSCILLATOR TO A GIVEN BASE MOTION. THEREFORE, IT IS INHERENTLY A BOUND AND THE SHOCK SPECTRA CONCEPT IS WELL SUITED FOR LOADS ANALYSIS SINCE THE ANALYSIS IS AIMED AT THE DETERMINATION OF A BOUND.

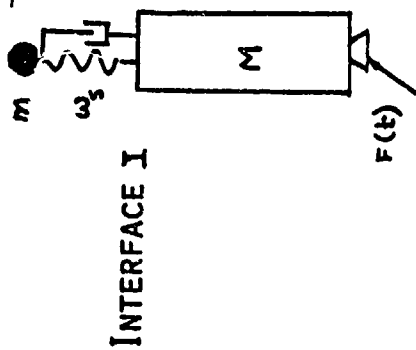
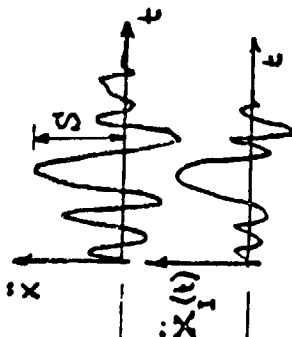
THE SHOCK SPECTRA OF THE RESPONSE OF THE UNLOADED LAUNCH VEHICLE AT ITS INTERFACE WITH A SPACECRAFT TO BE CARRIED BY THE LAUNCH VEHICLE GIVES DIRECTLY THE MAXIMUM LOAD IN THE SPRING OF THE OSCILLATOR. A BASIC ASSUMPTION IS THAT THE MASS OF THE OSCILLATOR IS INFINITELY SMALL SO THAT IT DOES NOT CHANGE THE RESPONSE OF THE LAUNCH VEHICLE.

$\frac{1}{|j\omega|}$ →

SHOCK SPECTRA METHOD

- SHOCK SPECTRA DEFINITION
 - SIMPLE OSCILLATOR, NEGLIGIBLE MASS
 - BASE MOTION $\ddot{x}_1(t)$
 - MAXIMUM AMPLITUDE S FOR RANGE OF OSCILLATOR RESONANCE ω_3
(IT IS A BOUND)

- SHOCK SPECTRA OF UNLOADED LAUNCH VEHICLE



INTERFACE I

LAUNCH VEHICLE

- NO CHANGE OF $x_1(t)$
- MAX. LOAD IN SPRING = $m * S_{peak}$

$m \ll M$

GENERALIZED SHOCK SPECTRA METHOD

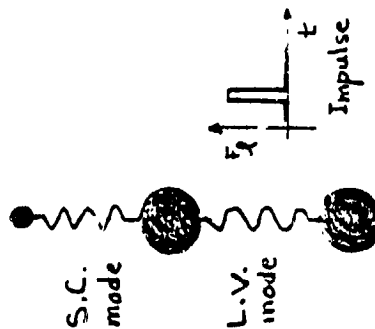
WHEN A REAL SPACECRAFT IS PLACED ON THE LAUNCH VEHICLE IT AFFECTS THE RESPONSE OF THE INTERFACE. THE SHOCK SPECTRA METHOD FOR LOADS ANALYSIS CONSISTS IN

- TREATING EACH MODE OF THE SPACECRAFT AS AN OSCILLATOR
- INTRODUCING THE CHANGE OF THE INTERFACE ACCELERATION DUE TO THE PRESENCE OF THE FINITE MASS OF THE SPACECRAFT
- THIS INTERFACE ACCELERATION IS BROKEN DOWN INTO ITS MODAL COMPONENTS CORRESPONDING TO EACH OF THE LAUNCH VEHICLE MODES ALONE OR WITH A RIGID MASS
- THE LAUNCH VEHICLE FORCING FUNCTION IS DECOMPOSED INTO DELTA FUNCTIONS GENERALIZED FORCE FOR EACH LAUNCH VEHICLE MODE.
- THE SHOCK SPECTRA IS COMPUTED FOR EACH MODAL RESPONSE OF THE LAUNCH VEHICLE, (MODAL SHOCK SPECTRA) RATHER THAN FOR THE PHYSICAL DEGREES OF FREEDOM OF THE INTERFACE. THE MODAL SHOCK SPECTRA CONTAINS BOTH THE STRUCTURE AND THE FORCING FUNCTION CHARACTERISTICS. SINCE THE MODAL RESPONSE IS AN OVERALL PROPERTY, IT IS LITTLE AFFECTED BY THE PRESENCE OF THE SPACECRAFT.



GENERALIZED SHOCK SPECTRA METHOD

- LAUNCH VEHICLE LOADED BY A SPACECRAFT OF FINITE MASS
 - SPACECRAFT MODE TAKEN AS OSCILLATOR
 - SPACECRAFT CHANGES INTERFACE RESPONSE
 - TAKE LAUNCH VEHICLE MODE ALONE OR WITH RIGID MASS ONLY
 - INTERFACE RESPONSE DECOMPOSED INTO LAUNCH VEHICLE MODAL RESPONSES $\ddot{q}_f(t)$
 - USE SHOCK SPECTRA OF MODAL RESPONSE INSTEAD OF INTERFACE
 - MODAL RESPONSE IS AN OVERALL STRUCTURAL PARAMETER
 - CONTAINS LAUNCH VEHICLE AND FORCING FUNCTION CHARACTERISTICS
 - INSENSITIVE TO PRESENCE OF SPACECRAFT
 - LAUNCH VEHICLE FORCING FUNCTION DECOMPOSED INTO IMPULSE DELTA FUNCTIONS FOR EACH LAUNCH VEHICLE MODE





GENERALIZED SHOCK SPECTRA METHOD

- BOUND OF MODAL LOAD = $(m_{eff})_s S_l C_{sl} = (m_{eff})_s Q_{sl}$

Q_{sl} : GENERALIZED SHOCK SPECTRA = $S_l C_{sl}$

C_{sl} : ACCOUNTS FOR INTERACTION BETWEEN LAUNCH VEHICLE AND SPACECRAFT

$$C = C_{sl} \left(\frac{m_{eff}}{M_{eff}}, \frac{\omega_l}{\omega_s}, (\xi_s + \xi_p) \right) \quad 0 < C < 1.0$$

S_l : SHOCK SPECTRA OF LAUNCH VEHICLE MODAL RESPONSE (CORRECTED)

- TUNING
 - LOCAL TUNING BETWEEN NEIGHBORING L/V & S/C NATURAL FREQUENCIES
 - OVERALL TUNING MAXIMIZE $\left(\sum_{s,l} Q_{sl}^2 \right)$ SHIFTING ENTIRE SPECTRUM OF L/V W.R.T. S/C FREQUENCIES

GENERALIZED SHOCK SPECTRA
(SIMPLIFIED FORMULA)

$$Q_{s\Omega} = \frac{\omega_1 F_{01}}{\sqrt{\Delta\Omega^2 + 4\beta^2}} e^{-\alpha \frac{2\beta}{\Delta\Omega}}$$

$$\Delta\Omega = \sqrt{\mu_{sr} + (1-R)^2}$$

$$2\beta = \xi_1 R + (1 + \mu_{sr}) \xi_{1s}$$

$$\alpha = \tan^{-1} \left(\frac{\Delta\Omega}{2\beta} \right)$$

$$R = \frac{\omega_1}{\omega_s}$$

$$\begin{aligned} \mu_{sr} &= \text{effective mass ratio (S.C. modes / L.V. mode } \Omega) \\ &= \left(\langle m_{si} \rangle \{ \Phi_{i, \Omega} \}^2 \right) / \left(1 + \left(\langle M_{si} \rangle \{ \Phi_{i, \Omega} \} \right)^2 \right) \end{aligned}$$

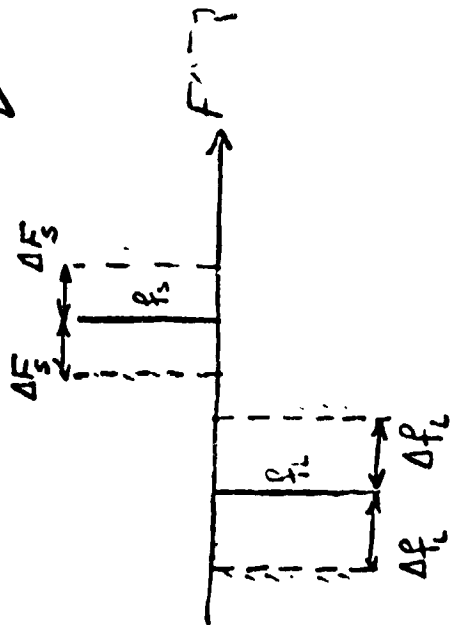
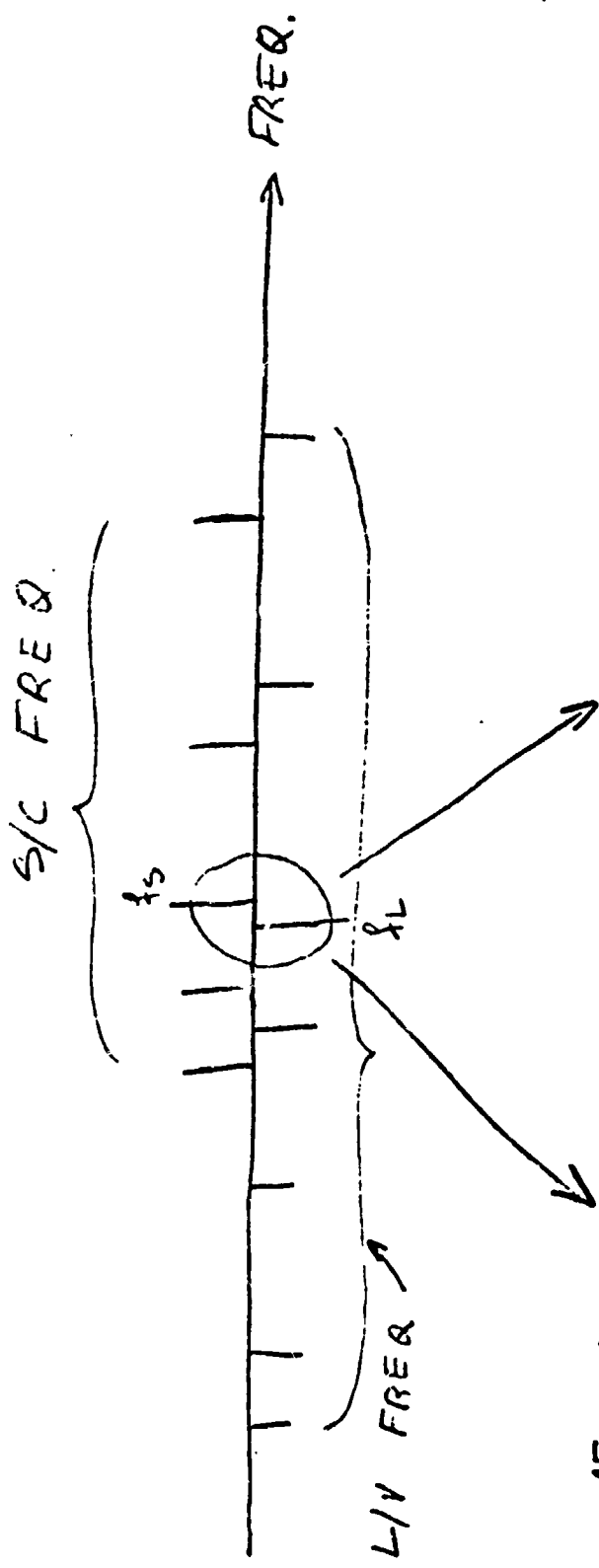


GENERALIZED SHOCK SPECTRA METHOD

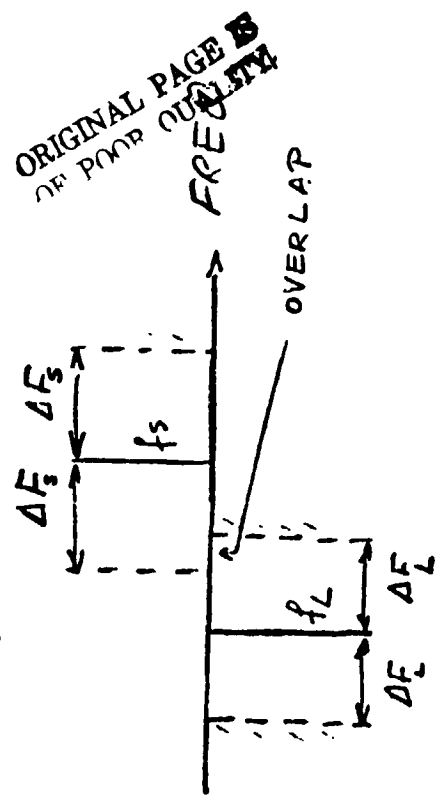
THE BOUND OF THE MODAL LOAD IS THE PRODUCT OF THE MODAL SHOCK SPECTRA S_L BY THE EFFECTIVE MASS M_{EFF} OF THE SPACECRAFT MODE AND CORRECTED BY A COEFFICIENT C_{SL} LESS THAN UNITY THAT INTRODUCES THE CHANGE OF INTERFACE ACCELERATION DUE TO THE PRESENCE OF A FINITE MASS OF THE SPACECRAFT.

THE BOUNDS CORRESPONDING TO EACH MODAL LOAD FOR EACH MEMBER ARE COMBINED IN A ROOT-SUM-SQUARED MANNER OVER THE SPACECRAFT MODES AND THE LAUNCH VEHICLE MODES TO GIVE A BOUND OF THE TOTAL LOAD.

TUNING



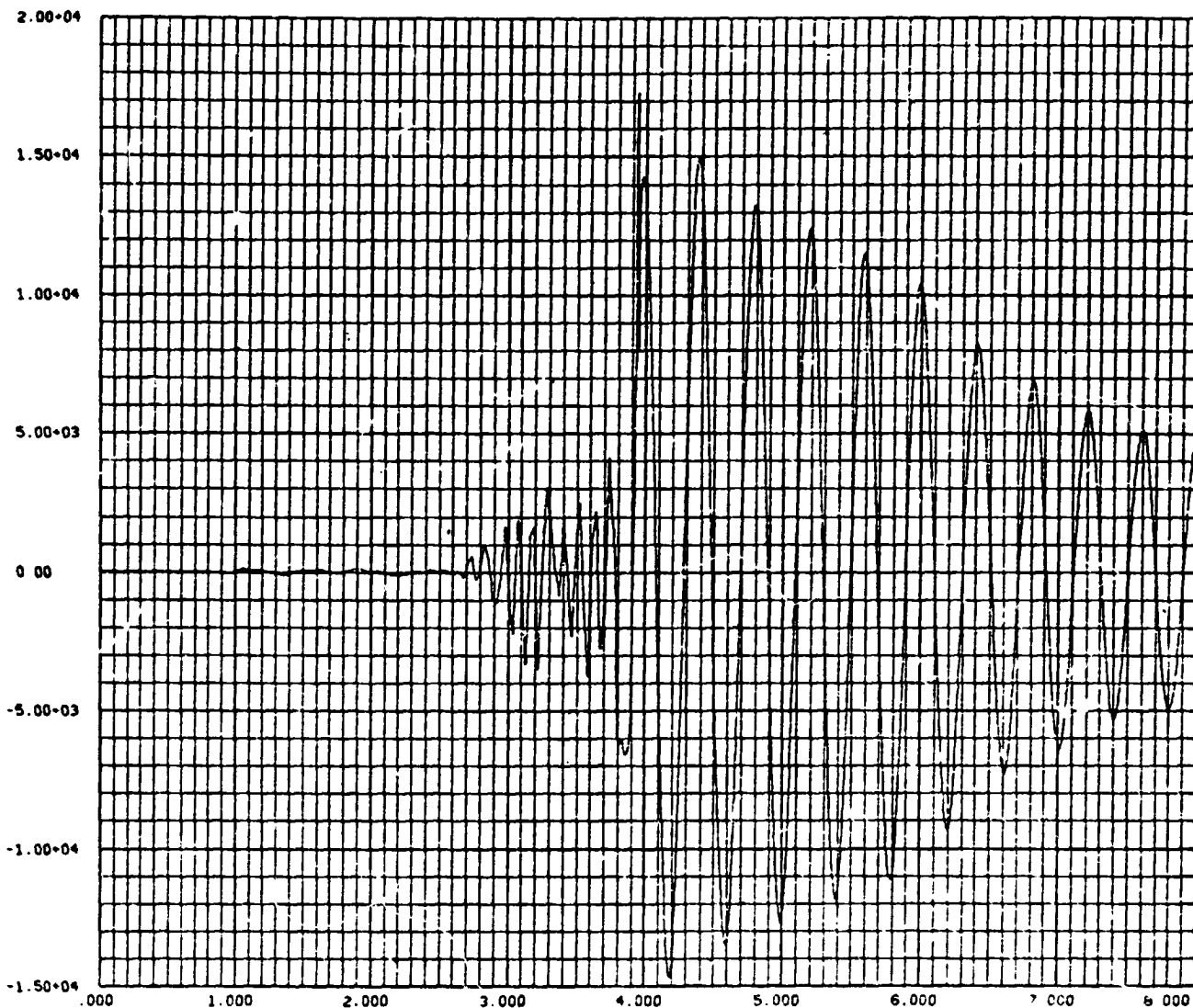
WORSE CASE
 $\frac{f_s}{f_L} \rightarrow \frac{f_s - \Delta F_s}{f_L + \Delta F_L}$
 PARTIAL TUNING



WORSE CASE
 $\frac{f_s}{f_L} = 1$
 PERFECT TUNING

ORIGINAL PAGE 13
 OF POOR QUALITY

$\ddot{q}_{10}(t)$



TIME (SEC)
ACCELERATION (G, S)

CALIBED L/O LP 549 MODEL GL10:4 11/06/78 MODE 10

SAMPLE RATE 250

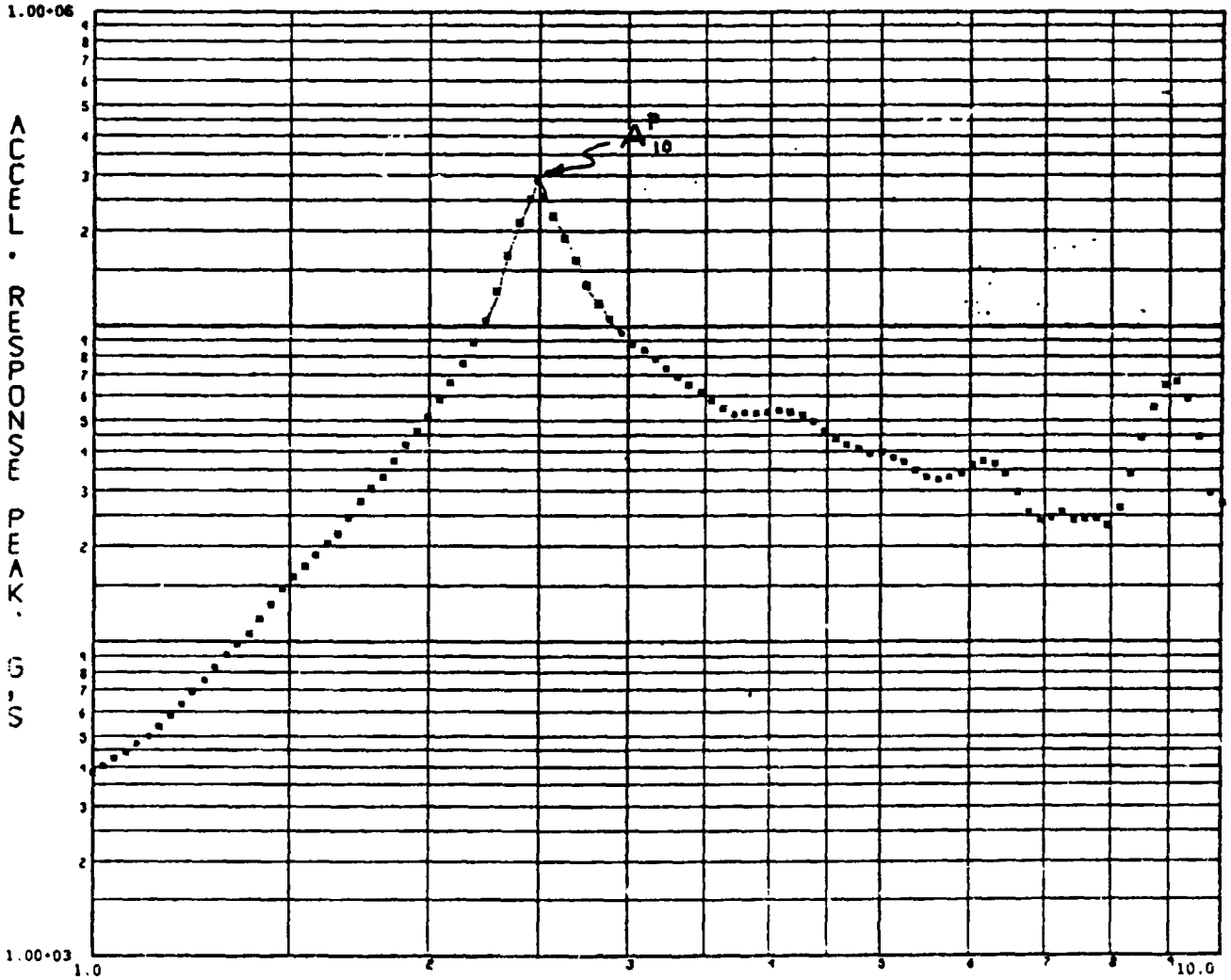
START TIME .0000

TIME INCREMENT 0.0000

DECKID 1

TAPEID *

A₁₀



FREQUENCY (CPS)
SHOCK SPECTRUM

GALILEO L/O LP 549 MODEL CL1014 11/06/78 MODE 10

SAMPLE RATE 250.

START TIME .0000

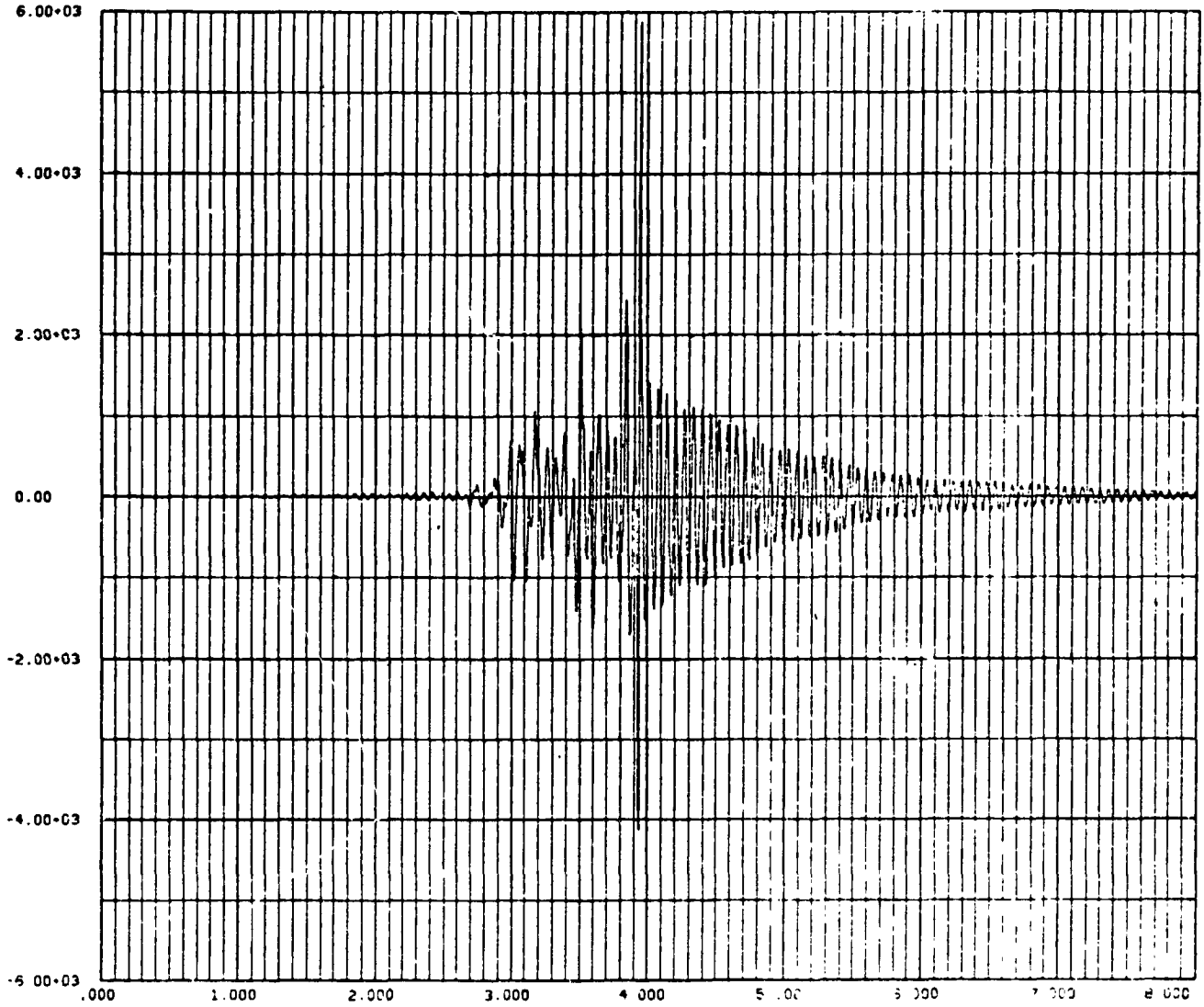
0 100.00

DECKID 1A

TIME INCREMENT 0.0000

TAPEID *

$\ddot{q}_1(t)$



TIME (SEC)
ACCELERATION.....(G, S)

GALILEO L/O LP 549 MODEL GL1014 11/06/78 MODE 01

SAMPLE RATE 250

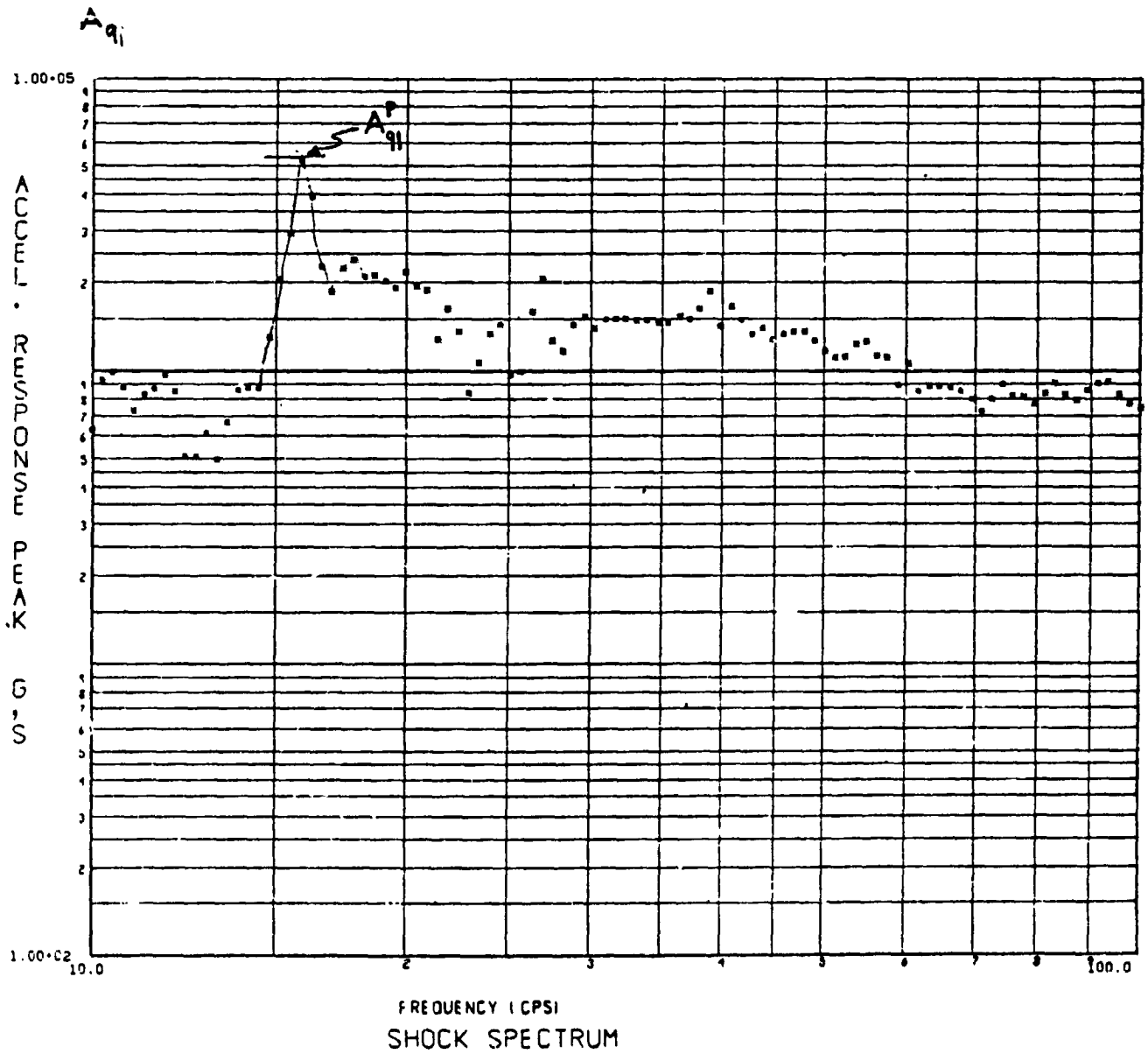
START TIME .0000

TIME INCREMENT 0.000

DECKID 1

TAPEID -

ORIGINAL PAGE IS
OF POOR QUALITY

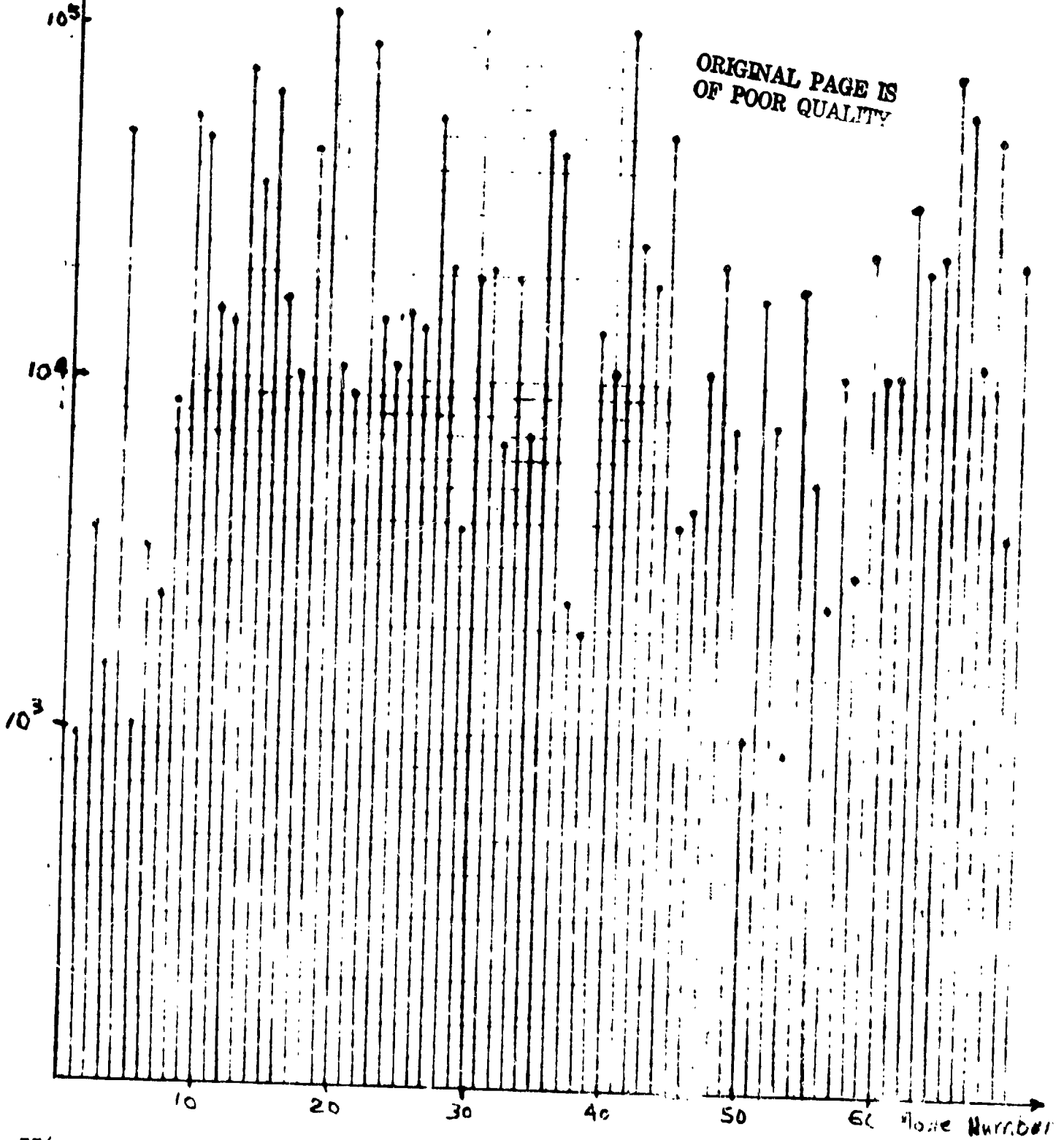


GALILEO L/O LP 549 MODEL GL1014 11/06/78 MODE 91
START TIME .0000
DECHID 1A

SAMPLE RATE 250.
Q 100.00
TIME INCREMENT 8.0000
TAPEID *

$\omega_1 \omega_2$

EQUIVALENT GENERALIZED FORCES



jpl →

121

GENERALIZED SHOCK SPECTRA METHOD

- BOUND F_A OF TOTAL LOAD IN MEMBERS
 - ALL SPACECRAFT MODES
 - ALL LAUNCH VEHICLE MODES
 - ROOT SUM SQUARED TECHNIQUE

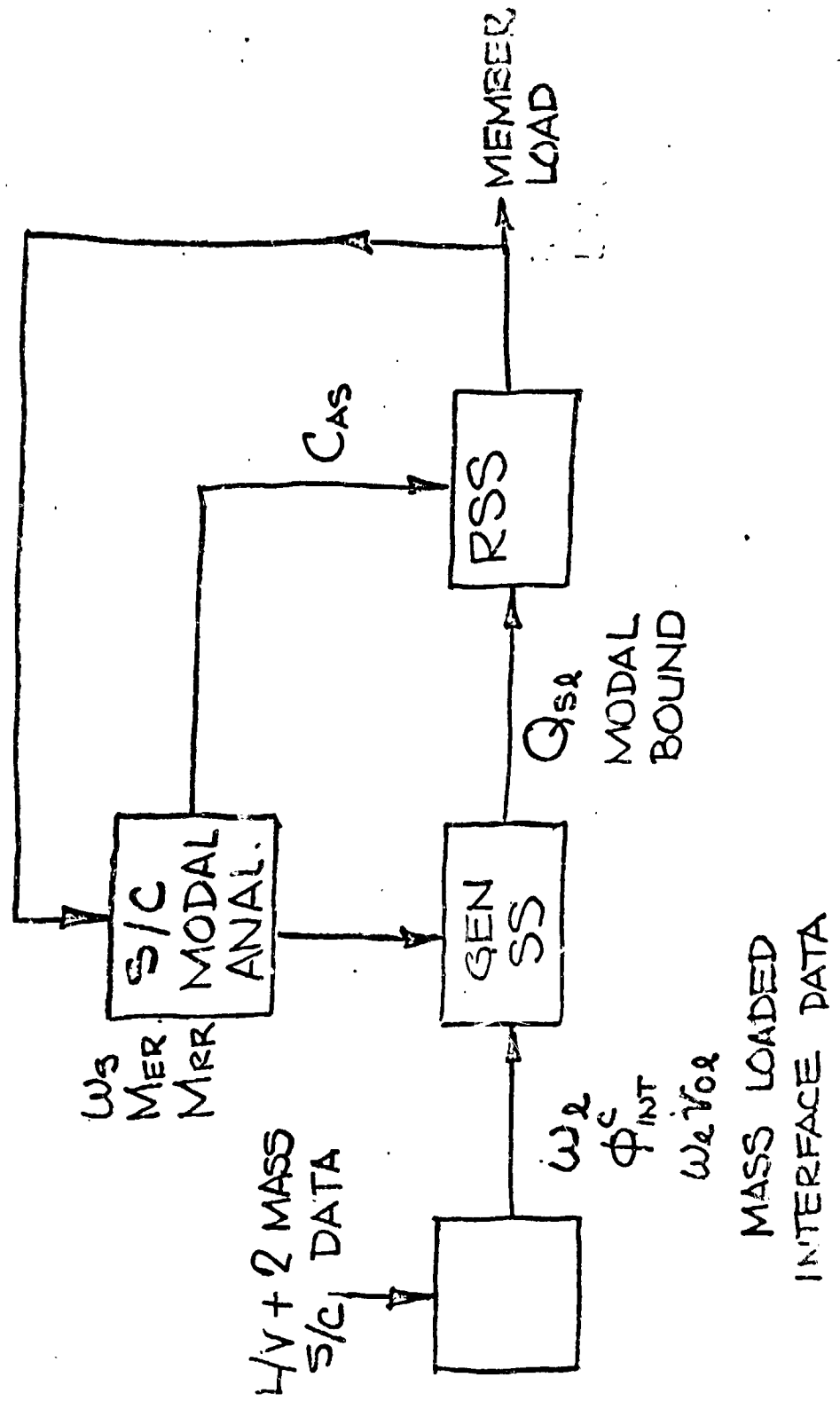
$$F_A = \sqrt{\sum_S (C_{AS}^2 \sum_I Q_{SI}^2)}$$

C_{AS} : MODAL STRESS

GENERALIZED SHOCK SPECTRA METHOD

- THE SHOCK SPECTRA METHOD REQUIRES THAT THERE HAS BEEN A PREVIOUS DYNAMIC ANALYSIS DONE FOR THE LAUNCH VEHICLE ALONE OR WITH A DUMMY VERY SIMPLE SPACECRAFT MODEL, THE RESULTS OF WHICH ARE USED TO ESTABLISH
 - THE AMPLITUDE OF THE DELTA FUNCTION FOR EACH MODAL FORCING FUNCTION
 - THE INTERACTION BETWEEN THE LAUNCH VEHICLE AND THE SPACECRAFT
- THE ADVANTAGES OF THE SHOCK SPECTRA METHOD ARE
 - AVOID COSTLY TRANSIENT ANALYSIS FOR THE SPACECRAFT
 - INTRODUCE ADVERSE TUNING BETWEEN SPACECRAFT MODES AND LAUNCH VEHICLE MODES
 - LOW SENSITIVITY TO LATE CHANGE IN THE DESIGN
 - IN HOUSE LOADS ANALYSIS FOR THE SPACECRAFT FOR FAST INTERACTION BETWEEN ANALYSIS AND DESIGN

GENERALIZED SHOCK SPECTRA METHOD



MASS LOADED
INTERFACE DATA



GENERALIZED SHOCK SPECTRA METHOD

- REQUIREMENT
 - PREVIOUS TRANSIENT ANALYSIS FOR LAUNCH VEHICLE
 - ALONE
 - OR WITH A RIGID MASS
 - OR WITH DUMMY
- ADVANTAGES
 - IN HOUSE LOADS ANALYSIS FOR SPACECRAFT
 - EARLY LOADS DEFINITION
 - LOW COST
 - ADVERSE TUNING BUILT IN (WORSE CASE)
 - LOW SENSITIVITY TO DESIGN CHANGES
- APPLICATION
 - CURRENTLY USED ON GALILEO

148



THE SHOCK SPECTRA METHOD WAS USED TO ESTABLISH PRELIMINARY DESIGN LOAD FACTORS FOR THE SPACECRAFT THAT ARE CONSERVATIVE BOUNDS, FUNCTION OF

- A) THE MASS OF A SPACECRAFT COMPONENT
- B) THE DAMPING ξ_1 OF THE LAUNCH VEHICLE AND THE DAMPING ξ_s OF THE SPACECRAFT

DATA AVAILABLE FROM THE LAUNCH VEHICLE ANALYSIS ON A SINGLE SPRING MASS MODEL AND PAST EXPERIENCE WERE USED TO ESTABLISH F_0 and \dot{N}_0

ORIGINAL PAGE IS
 OF POOR QUALITY

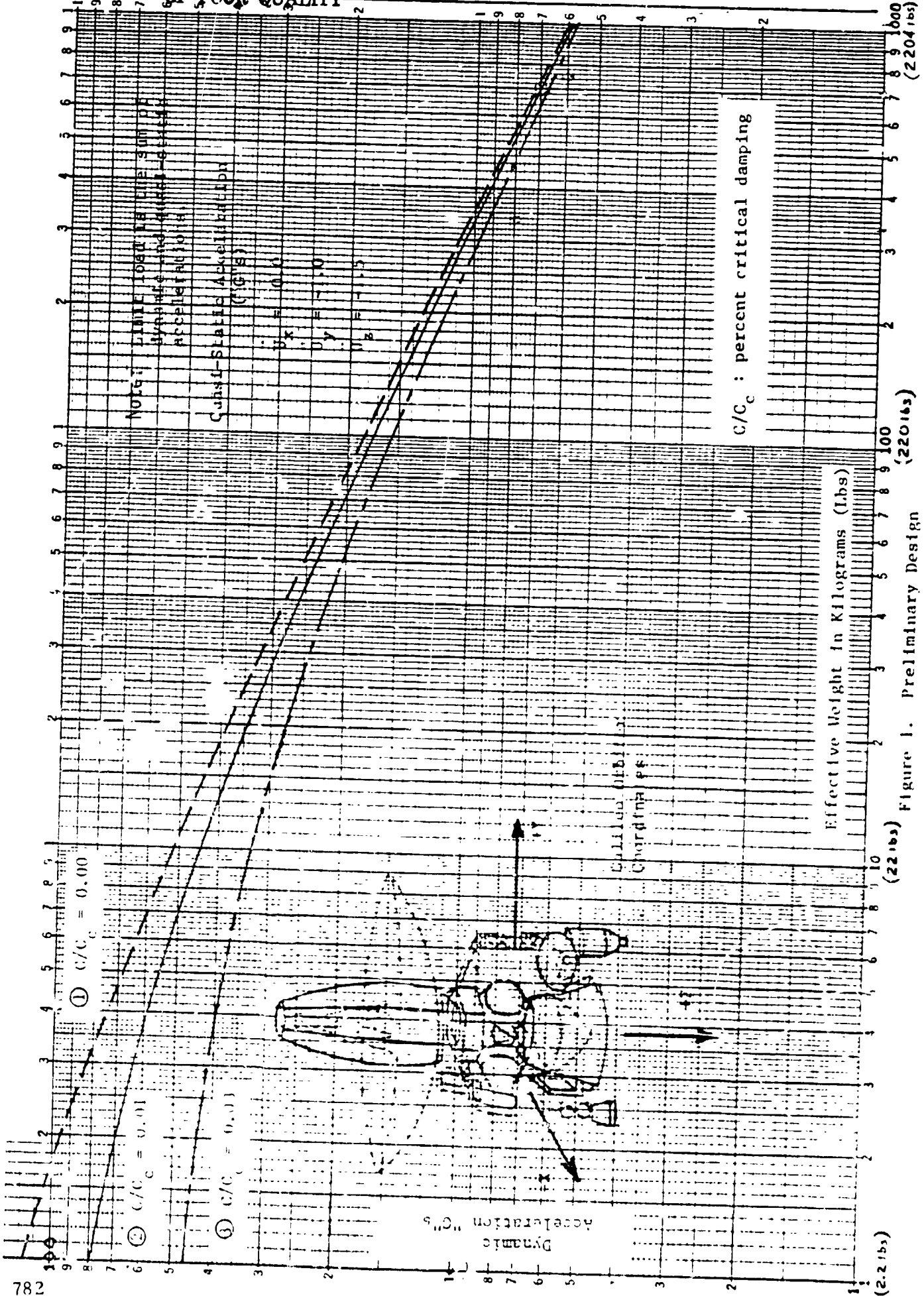


Figure 1. Preliminary Design
 Limit Loads for Galileo Orbiter



SPACECRAFT PRELIMINARY DESIGN LOADS

- ASSUME SPACECRAFT (OR COMPONENT) FREQUENCY TUNED TO A VEHICLE MODE
- ACCELERATION OF C.G. OF COMPONENT

$$G = \frac{F_0}{\sqrt{\frac{m}{M} + (\xi_s + \xi_A)^2}} e^{-\alpha \frac{\xi_s + \xi_A}{\sqrt{\frac{m}{M}}}}$$

m, M SPACECRAFT AND LAUNCH VEHICLE EFFECTIVE MASSES

ξ_s, ξ_A SPACECRAFT AND LAUNCH VEHICLE DAMPINGS

M, F_0 DETERMINED FROM RESPONSE ANALYSIS OF SINGLE MASS,
SPEC, EXPERIENCE

PRECEDING PAGE BLANK NOT FILMED

THE APPLICATION OF FLIGHT DATA TO IMPROVING
PAYLOAD RESPONSE PREDICTION

By

BRANTLEY R. HANKS

NASA LANGLEY RESEARCH CENTER

PROBLEMS OF FLIGHT RESPONSE PREDICTION

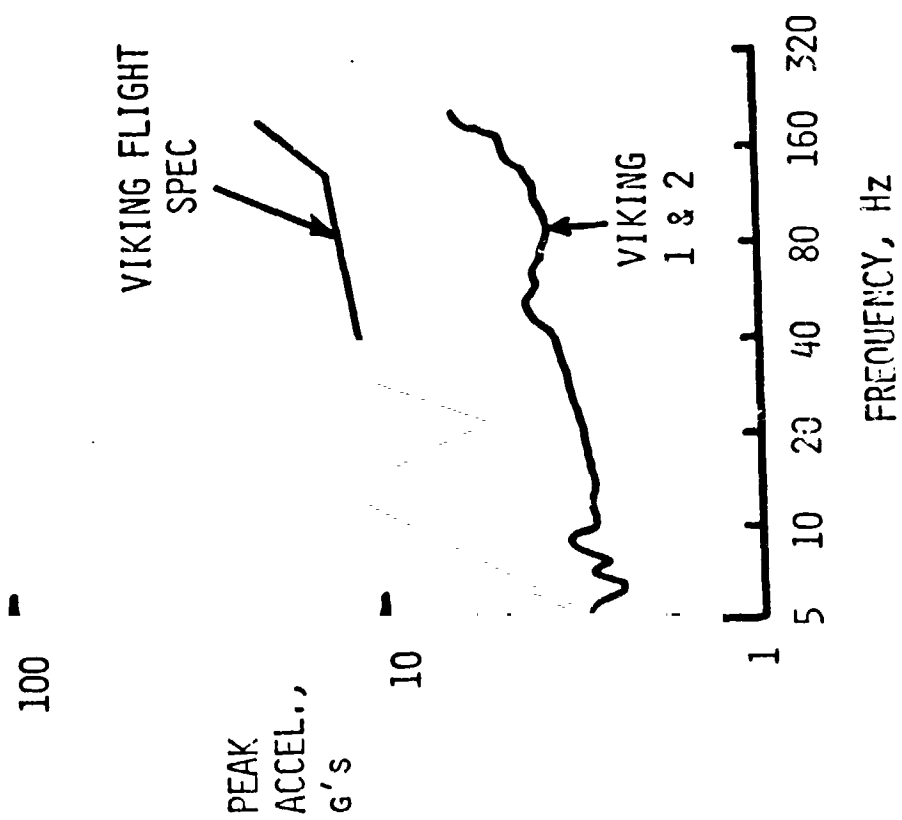
Past experience with the prediction of payload flight response has not been good. For example, the acceleration spectrum used for design and flight acceptance testing of the Viking payloads is compared in the figure with the envelope for the peaks of all such spectra measured in actual flight. The payload was considerably overdesigned, sometimes by a factor of four. If the fact that an equivalent sine test was used for acceptance is considered, design conservatism becomes even greater. Yet using similar prediction methods, other payloads predicted responses have been unconservative. Future needs for reducing payload costs require more accurate design environments which are payload-centered rather than heavily dependent on a large launch vehicle analytical model.

PROBLEMS OF FLIGHT RESPONSE PREDICTION

PAST EXPERIENCE

FUTURE NEEDS

- LESS CONSERVATIVE DESIGN
- PAYLOAD-CENTERED RESPONSE PREDICTION METHODS



OBSTACLES TO SOLUTION

Improvement over past experience in payload flight response prediction is needed for the space shuttle in order to reduce costs of payloads. However, the problem is more complicated than in the past for several reasons. The shuttle/payload system is non-axisymmetric and otherwise more complicated analytically than previous launch vehicles. Inputs to payloads must be considered for both landing and liftoff, and these are orthogonal to each other. Large payloads will affect these inputs, particularly in landing where the payload comprises a significant portion of the vehicle weight. High level acoustic inputs to payloads may occur at frequencies low enough to excite some structural modes normally excited only by mechanical inputs. Finally, a myriad of payload attachment locations and combinations with other payloads will be involved and these will not usually be known in the design stage.

OBSTACLES TO SOLUTION

- COMPLEXITY OF SHUTTLE/PAYLOAD SYSTEM
- PAYLOAD AFFECTS INPUTS
- ACOUSTIC AND DYNAMIC LOADS OVERLAP IN FREQUENCY
- DIFFERENT PAYLOAD LOCATIONS, MASS, STIFFNESS, VOLUME, AND FLIGHT CONDITIONS

SOLUTION APPROACH

Because of the complexity of the payload response prediction problem for the shuttle, it is believed that an advanced technology program for measuring and analyzing flight responses on the shuttle could produce a significantly better prediction capability.

SOLUTION APPROACH

- ADVANCED TECHNOLOGY FLIGHT MEASUREMENTS WITH MODERN DATA ANALYSIS AND APPLICATIONS EMPLOYED

NEW TOOLS FOR USE WITH FLIGHT DATA

Technology advancements in recent years have led to the development of several new tools which could significantly improve the usefulness of measured flight data. Most past applications of flight data have been to assure that underdesign or failure did not occur and, as such, the data was not properly acquired or adequately analyzed for improving the prediction process. Some of the new tools available for future rectifying of this situation are shown in the following figures.

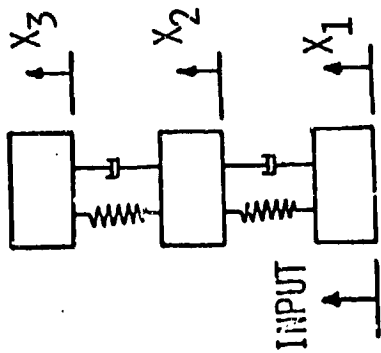
NEW TOOLS FOR USE WITH MEASURED FLIGHT DATA

SHAPED FILTER IMPROVES FREQUENCY DOMAIN FLIGHT RESPONSE PREDICTION

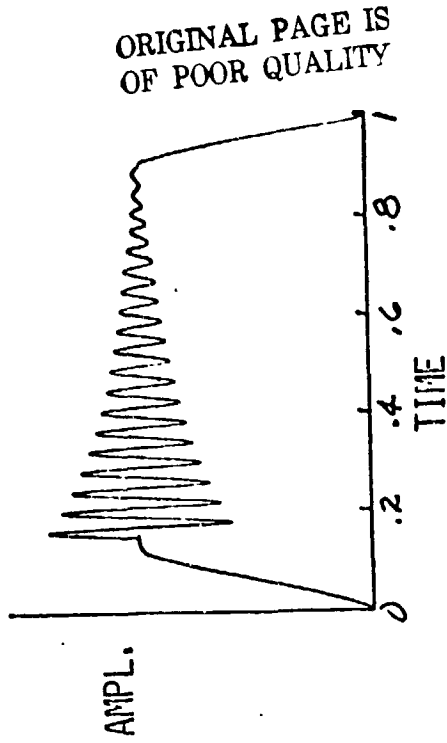
The prediction of flight loads is normally conducted using time integration of the equations of motion for the launch vehicle payload system subjected to predicted inputs. This is an expensive analytical process; and, for physical interpretation of results, a conversion to the frequency domain is still needed. Solution directly in the frequency domain would be less expensive in computer time. However, past experience with such solutions has shown them to produce poor representations of actual peak flight loads because of ^{poor} maintenance of phase relations between modes in the analysis. Recent studies by Martin Marietta Corporation have shown this to be the result of the method used to treat slowly-varying thrust components in the flight response. This figure shows a comparison of a frequency domain analysis transformed to the time domain with a time integration analysis for a simple three-degree-of-freedom system using two different methods of treating the thrust effects. DC level removal, the normal way of conducting such analyses, produces poor agreement between the methods. However, shaping the DC level removal filter to the flight curve gives very good agreement. Use of this method with actual flight data should provide a less expensive analytical prediction method for payload developers.

SHAPED FILTER IMPROVES FREQUENCY DOMAIN FLIGHT RESPONSE PREDICTION

SYSTEM

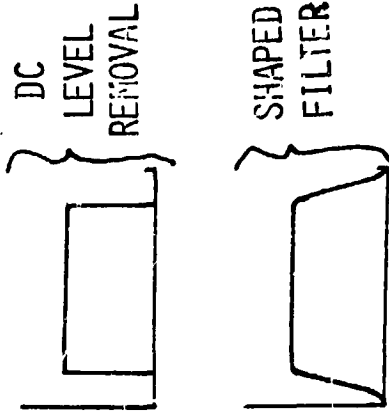


INPUT

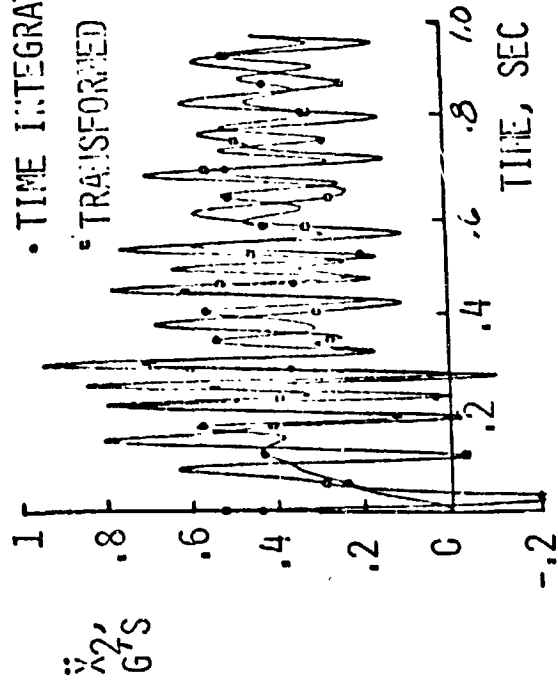


ORIGINAL PAGE IS OF POOR QUALITY

DATA WINDOWS

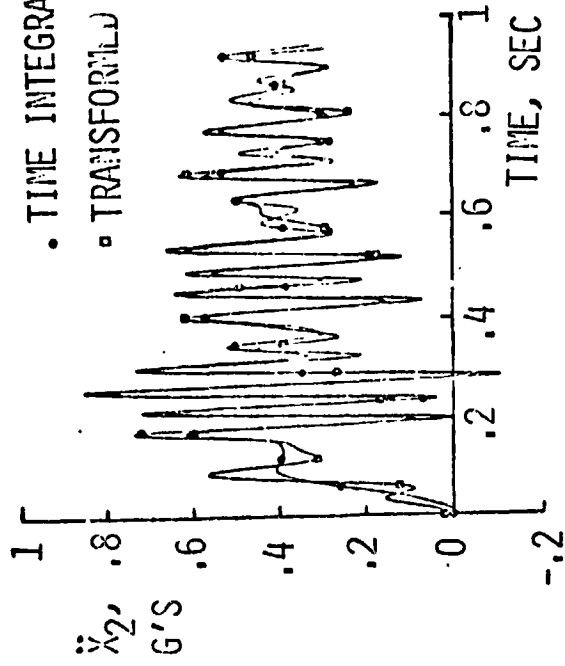


RESPONSE WITH DC LEVEL REMOVED



• TIME INTEGRATION
• TRANSFORMED FREQ.

RESPONSE WITH SHAPED FILTER



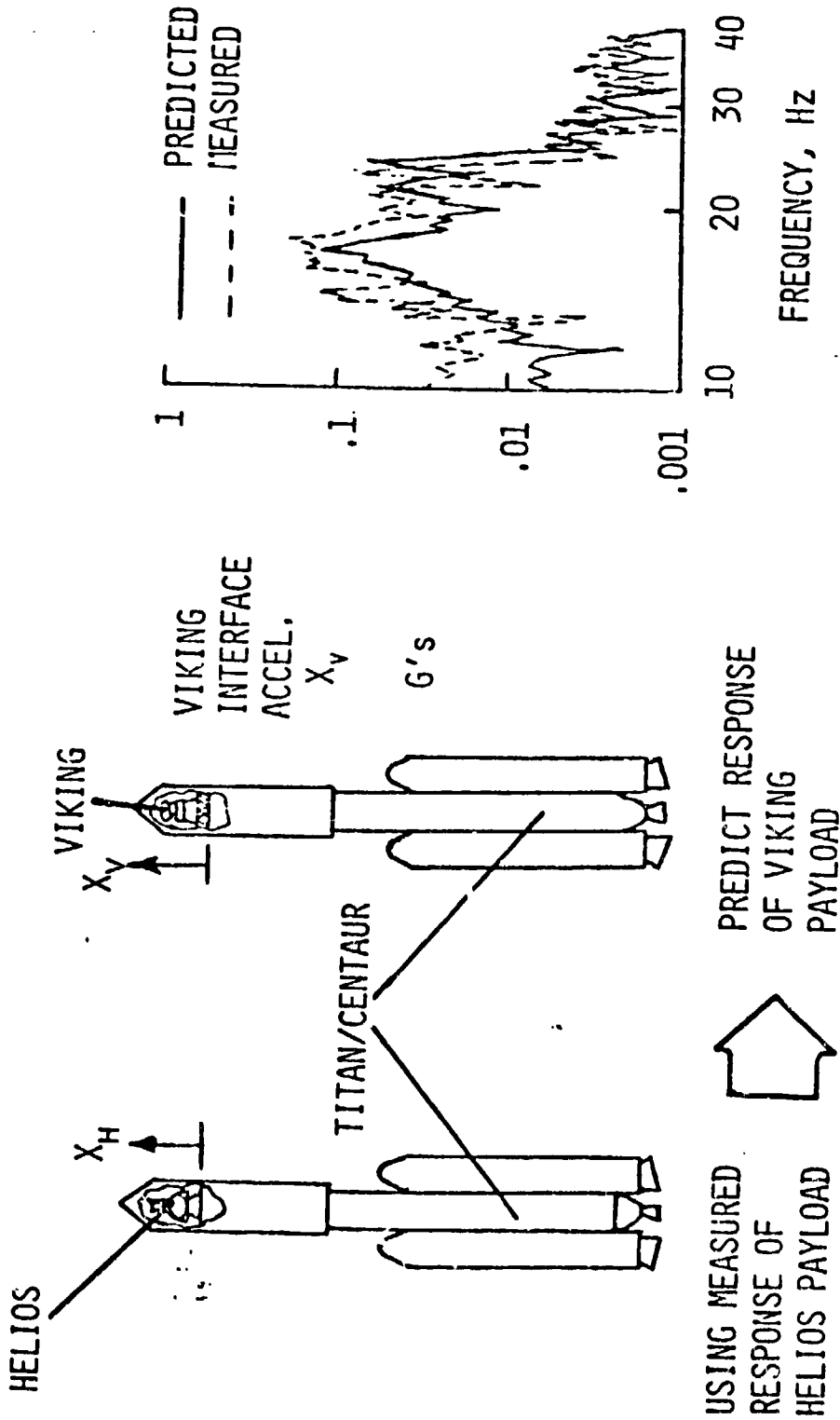
• TIME INTEGRATION
• TRANSFORMED FREQ.

ORIGINAL PAGE IS OF POOR QUALITY

IMPEDANCE ANALYSES ALLOW EXTRAPOLATION OF MEASURED FLIGHT RESPONSES

Impedance methods of dynamic response prediction are the dynamic equivalent to static influence coefficients. They involve point-to-point relationships rather than the complete degrees of freedom of the entire launch vehicle/payload modal analysis. They are therefore simpler and less expensive to use and are well suited to a payload developer for quick-turn-around analysis. Accuracy can be a problem, however; and measured responses, particularly at some payload interfaces, are needed to improve their accuracy. In a redesign mode or in the design of a new payload for similar flight conditions and locations as measured ones, impedance techniques can be used in a ratio mode to predict the response of the new payload. This figure shows an example of such a prediction (conducted by Martin Marietta Corporation) for Viking payloads using measured data from the Helios payload. The data was ill-suited to the purpose because it was obtained for a different purpose, but the result is still much better than the prediction actually used for Viking design which was shown in figure 1.

IMPEDANCE ANALYSES ALLOW EXTRAPOLATION OF MEASURED FLIGHT RESPONSES

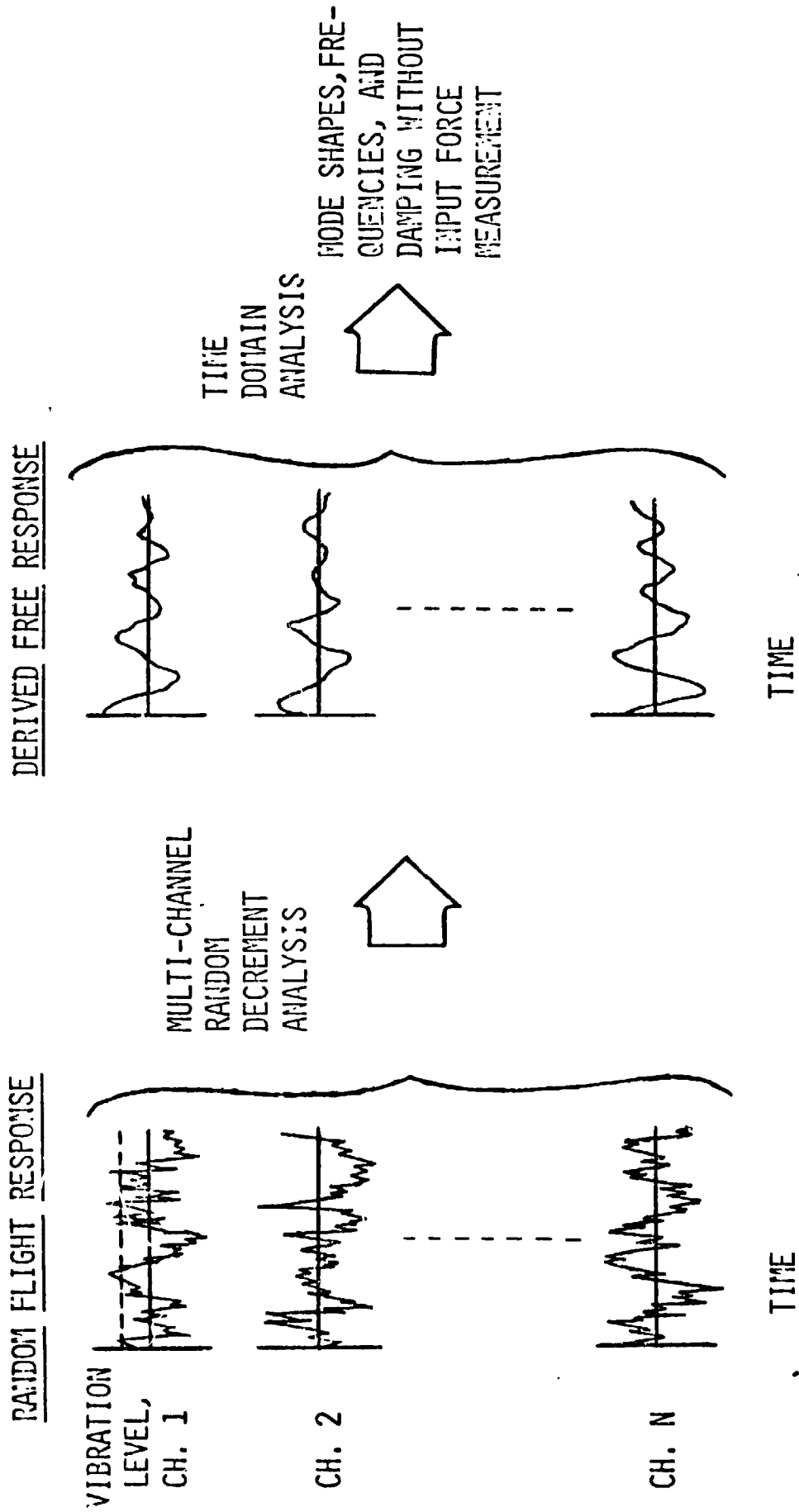


ORIGINAL PAGE IS
OF POOR QUALITY

TIME DOMAIN ANALYSIS DETERMINES MODAL PARAMETERS FROM FLIGHT DATA

The time domain modal test method developed by S. R. Ibrahim of Old Dominion University and the Langley Research Center enables the determination of complete modal parameters from random or transient data without input force measurement. As such, it is applicable to determining, for the first time, the modes of the launch vehicle/payload system under actual flight conditions. Application of this method to measured flight data on the shuttle and some of its payloads could considerably improve information for analytical model verification.

TIME-DOMAIN ANALYSIS DETERMINES MODAL PARAMETERS FROM FLIGHT DATA



OTHER PROMISING NEW TECHNOLOGY APPLICABLE TO FLIGHT DATA

Several additional new technology tools are under development which would further improve flight response prediction and/or design if properly measured data were available. The automated modification of analytical models to match measured modes would be particularly useful if measured flight modes were obtained using the time domain data analysis approach. The improved mass matrix thus obtained could then be used with the measured modal parameters to obtain input forcing functions. Other promising technology involves the replacing of sine-wave-equivalent to flight transients in qualification tests with actual flight transients and the use of partial coherence functions to determine what relative portions of a measured response are due to mechanical and acoustic inputs.

ORIGINAL PAGE IS
OF POOR QUALITY

OTHER PROMISING NEW TECHNOLOGY APPLICABLE TO FLIGHT DATA

- AUTOMATED MATCHING OF ANALYTICAL MODEL TO TEST DATA
- INPUT FORCE IDENTIFICATION
- TRANSIENT SIMULATION IN QUALIFICATION TESTS
- PARTIAL COHERENCE FUNCTIONS FOR DETERMINING LOAD INPUT PATHS

ORIGINAL PAGE IS
OF POOR QUALITY

DYNAMIC FLIGHT MEASUREMENTS FOR IMPROVED RESPONSE PREDICTION

Use of the foregoing new technology is best served by measurement in flight of certain needed quantities. These include launch vehicle, payload, and launch vehicle/payload interface responses. Care should be taken to maintain a known phase relationship between these measurements in order to obtain complete system modes. Because low frequency acoustic inputs may contribute to structural response, proper filtering is needed on both acoustic and vibration measurements to allow correlation between the two. Finally, a high dynamic range is desirable to allow accurate data and to minimize ranging problems on measurement gains.

DYNAMIC FLIGHT MEASUREMENTS FOR IMPROVED RESPONSE PREDICTION

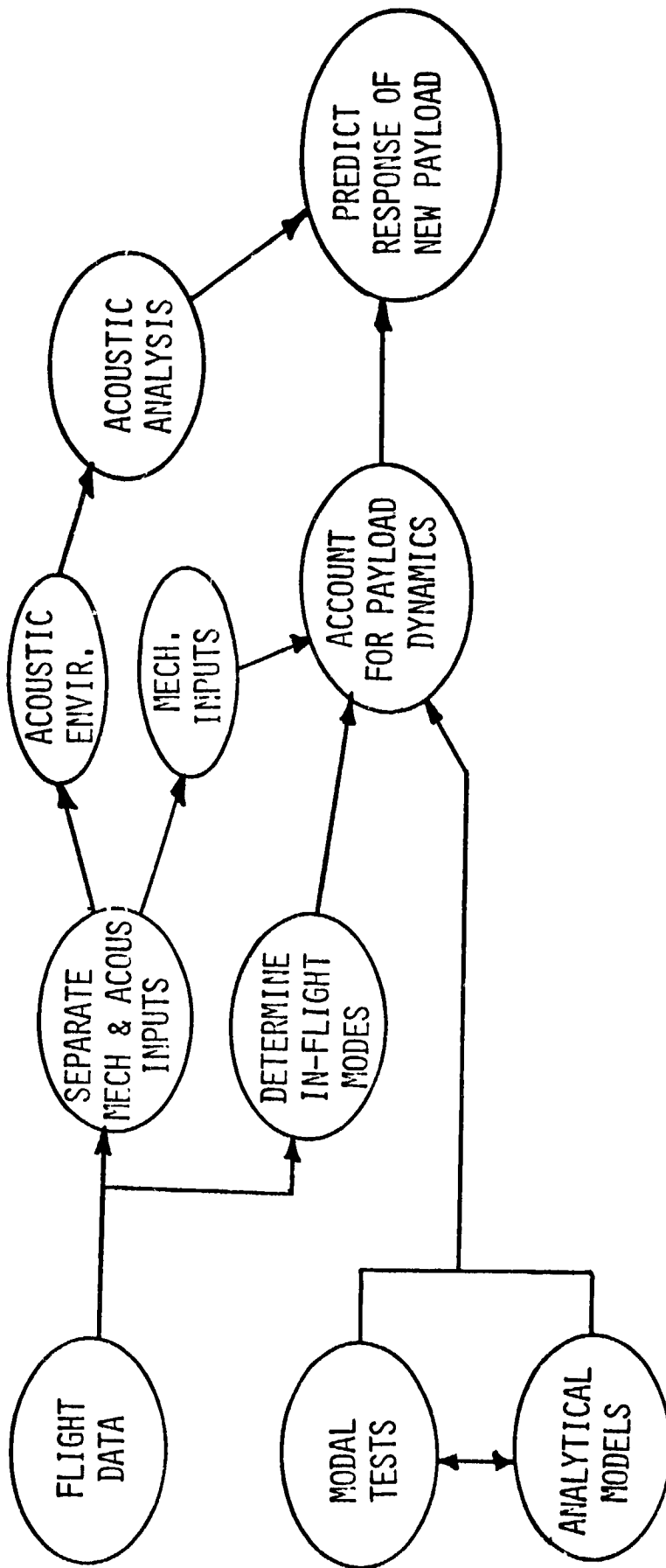
- **LOADS AND/OR VIBRATIONS AT PAYLOAD ATTACHMENTS**
- **PAYLOAD VIBRATION DISTRIBUTION**
- **CORRESPONDING LAUNCH VEHICLE VIBRATION DISTRIBUTION**
- **VIBRATION AND ACOUSTIC MEASUREMENTS WITH IDENTICAL FILTERING**
- **HIGH DYNAMIC RANGE ON ALL MEASUREMENTS**

**ORIGINAL PAGE IS
OF POOR QUALITY**

APPLICATION OF DYNAMIC FLIGHT DATA

This chart shows the flow of data in applying the aforementioned new technology tools to measured flight data in order to improve payload flight response prediction.

APPLICATION OF DYNAMIC FLIGHT DATA

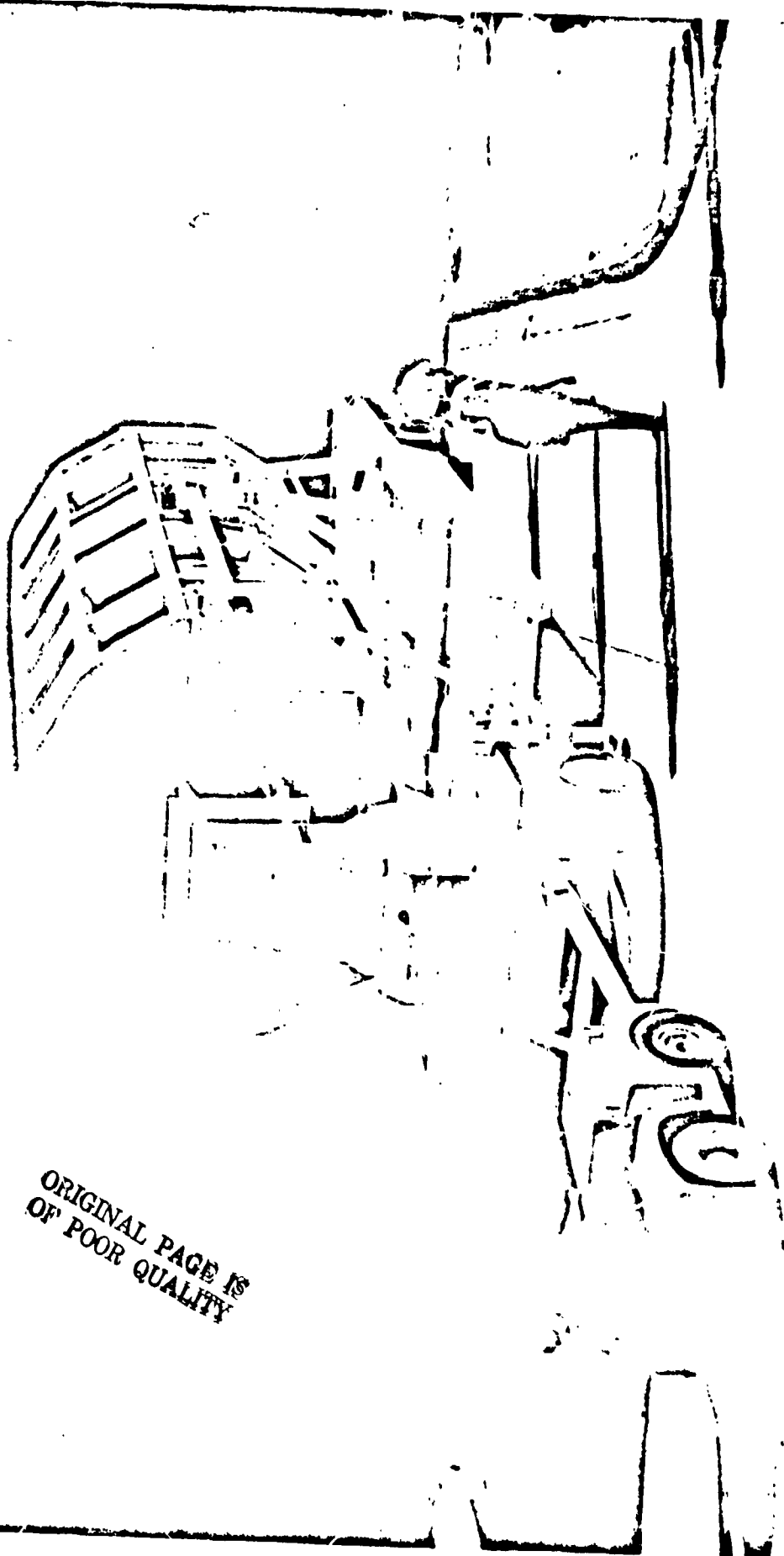


LONG DURATION EXPOSURE FACILITY (LDEF) SHUTTLE PAYLOAD

The LDEF payload, shown in this photograph, will carry a dynamic environment measurement system in its flight on the shuttle in the 1980-81 time frame. It is 30 feet long, 14 feet in diameter, and weighs about 20,000 pounds. It is to be released to orbit for about six months and then picked up by the shuttle for return to earth. Vibration and acoustic environments will be measured during launch and return flights.

LONG DURATION EXPOSURE FACILITY (LDEF) SHUTTLE PAYLOAD

ORIGINAL PAGE IS
OF POOR QUALITY



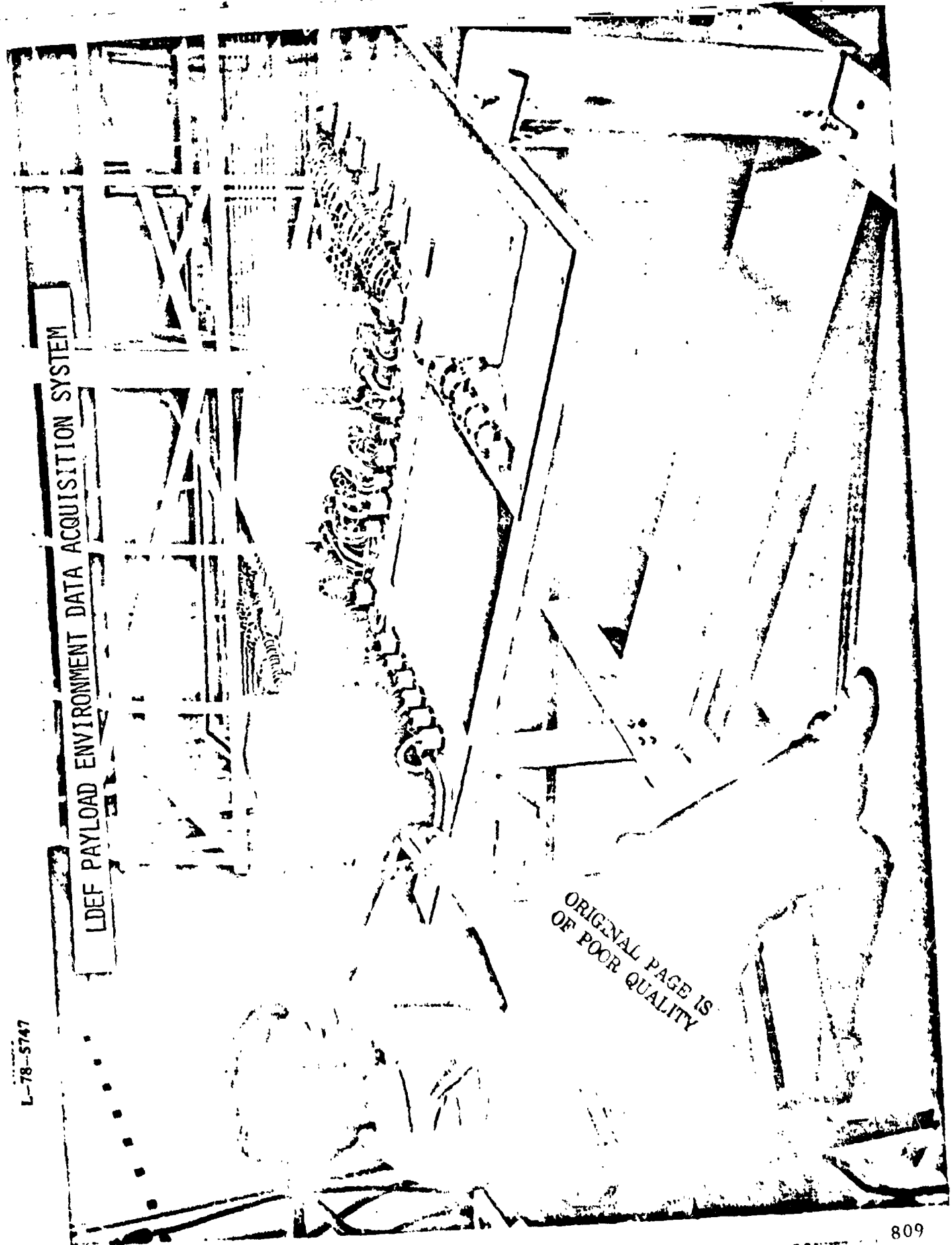
LDEF PAYLOAD ENVIRONMENT DATA ACQUISITION SYSTEM

This photograph shows the data acquisition system under development for the LDEF dynamic flight environment measurements. The system is a battery-powered, eight-bit digital system mounted on the LDEF payload. Data is recorded on a shuttle-mounted tape recorder via a hard-wired link.

;

L-78-5747

LDEF PAYLOAD ENVIRONMENT DATA ACQUISITION SYSTEM



ORIGINAL PAGE IS
OF POOR QUALITY

LDEF/SBEM FINAL DESIGN

The LDEF Shuttle Bay Environments Measurement (SBEM) System will contain these sensors and design characteristics for dynamics measurements. It also contains thermal and pressure measuring sensors (not shown). The strain gage bridges noted are for load sensing trunnions at the payload attachments to the shuttle. The system has excellent characteristics for technology oriented measurements with the exception of dynamic range. A comparison range of 48 dB was necessitated by cost constraints.

LDEF/SBEM FINAL DESIGN

SENSORS

- 7 MICROPHONES (10-2.0 KHZ)
- 1 MICROPHONE (10-4.5 KHZ)
- 9 ACCELEROMETERS (10-2.0 KHZ)
- 16 ACCELEROMETERS (2-75 HZ)
- 20 INPUT LOAD STRAIN GAGE BRIDGES (0-75 Hz)

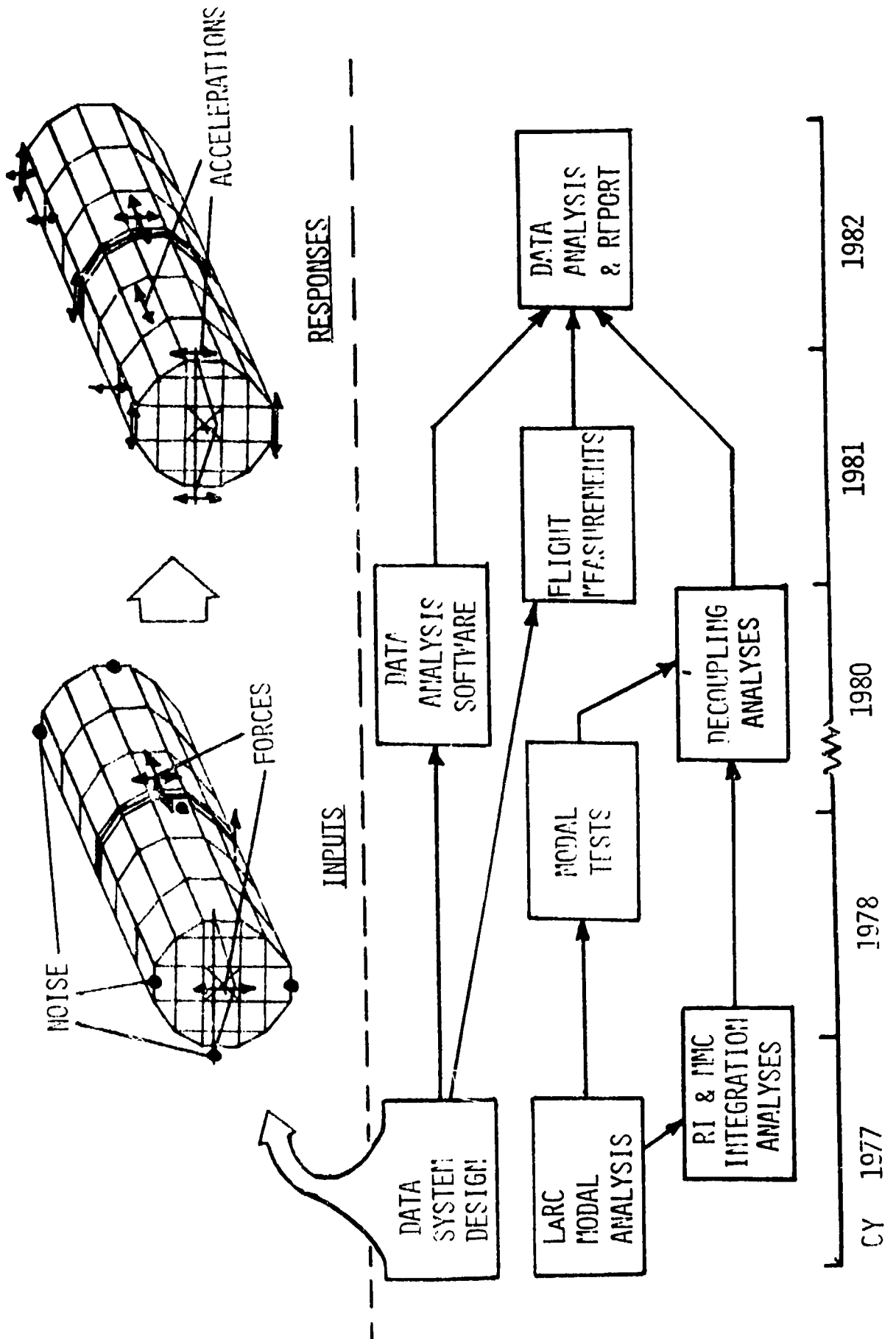
SYSTEM CHARACTERISTICS

- 48 DB DYNAMIC RANGE
- 1% SYSTEM ACCURACY (EXCEPT SENSORS)
- CROSS-SPECTRA CAPABILITY
 - 3° PHASE @ 60 Hz ALL CHANNELS
 - 5° PHASE @ 1500 Hz H.F. CHANNELS

STATUS OF LDEF FLIGHT EXPERIMENT

The LDEF flight measurements experiment is well into the development stage. The data system has been designed, initial modal analyses and loads integration analyses have been performed, and modal tests are nearing completion. Flight schedule is somewhat nebulous at this point as a final flight assignment has not been received. A flight sometime in early 1981 is expected, however.

STATUS OF IDEF FLIGHT EXPERIMENT



PRECEDING PAGE BLANK NOT FILMED

EQUIVALENT PULSE DETERMINATION FOR
STAGE ZERO IGNITION OF TITAN/CENTAUR
FORCING FUNCTION RECONSTRUCTION

BY

M. TRUBERT





BACKGROUND

- HELIOS TITAN/CENTAUR FLIGHT SHOWED STRONG RESPONSE AT STAGE ZERO IGNITION
- OVERPRESSURE CONDITION
- WAS NOT FULLY REPRESENTED BY ANALYSIS, UNDERESTIMATED
- MATHEMATICAL REPRESENTATION NEEDED FOR VOYAGER LOADS ANALYSIS
- GOAL
 - CHOOSE A STRUCTURAL MODEL
 - DETERMINE EQUIVALENT FORCING FUNCTION

ORIGINAL PAGE IS
OF POOR QUALITY



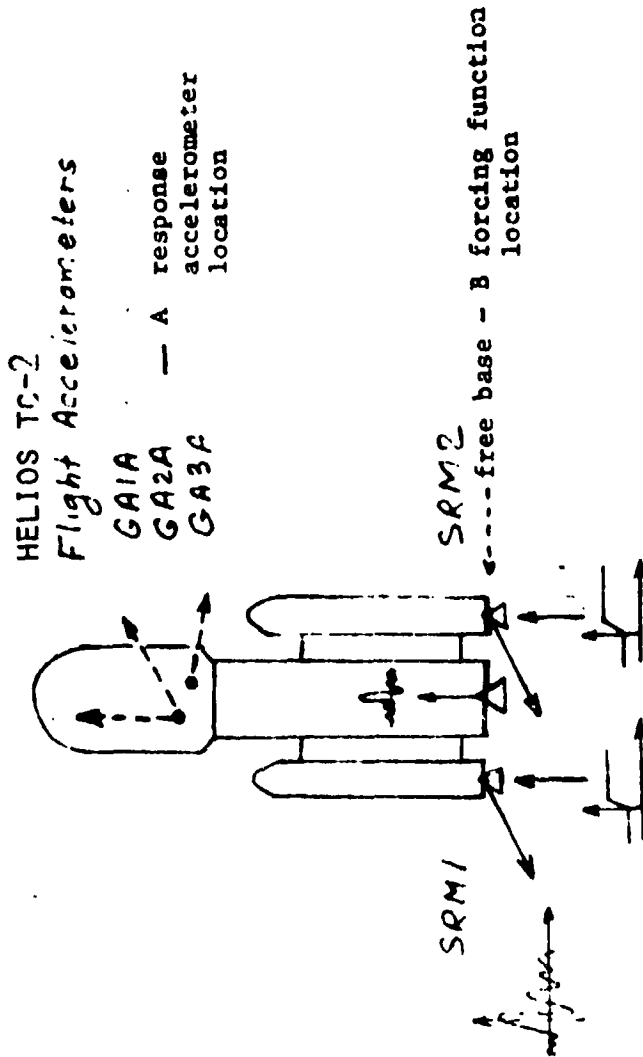
MODELING

- LAUNCH VEHICLE ON LAUNCHING PAD VERY COMPLEX AND MODEL WAS NOT AVAILABLE
- MAX RESPONSE OCCURRED AFTER TAKE-OFF
 - FREE-FREE MODEL ADEQUATE AND SIMPLER
- METHOD
 - FORCING FUNCTION ADJUSTED TO MATCH RESPONSE BY TRIAL AND ERROR
 - ABOUT 40 MODES TITAN/CENTAUR/HELIOS
 - FREQUENCY DOMAIN SOLUTION



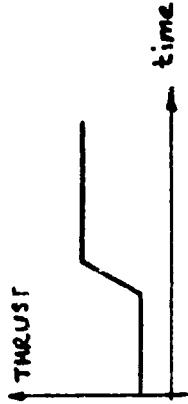
TITAN/CEITAU
STAGE ZERO IGNITION
EQUIVALENT FORCING FUNCTION

ORIGINAL PAGE IS
OF POOR QUALITY





TYPES OF PULSES



1. THRUST BUILD-UP

2. IMPULSE

COMBINATION OF EXPONENTIAL COSINES

$$\text{TIME} \quad \sum_{n=1}^{n_0} \phi_n e^{-\xi_n \omega_n t} \cos(\omega_n \sqrt{1-\xi_n^2} t)$$

$$\text{FREQUENCY} \quad F(f) = \sum_{n=1}^{n_0} \phi_n \frac{2 \xi_n \left(\frac{f}{f_n}\right)^2 + i \frac{f}{f_n} \left[1 - \left(\frac{f}{f_n}\right)^2\right]}{\left[1 - \left(\frac{f}{f_n}\right)^2\right]^2 + 4 \xi_n^2 \left(\frac{f}{f_n}\right)^2}$$

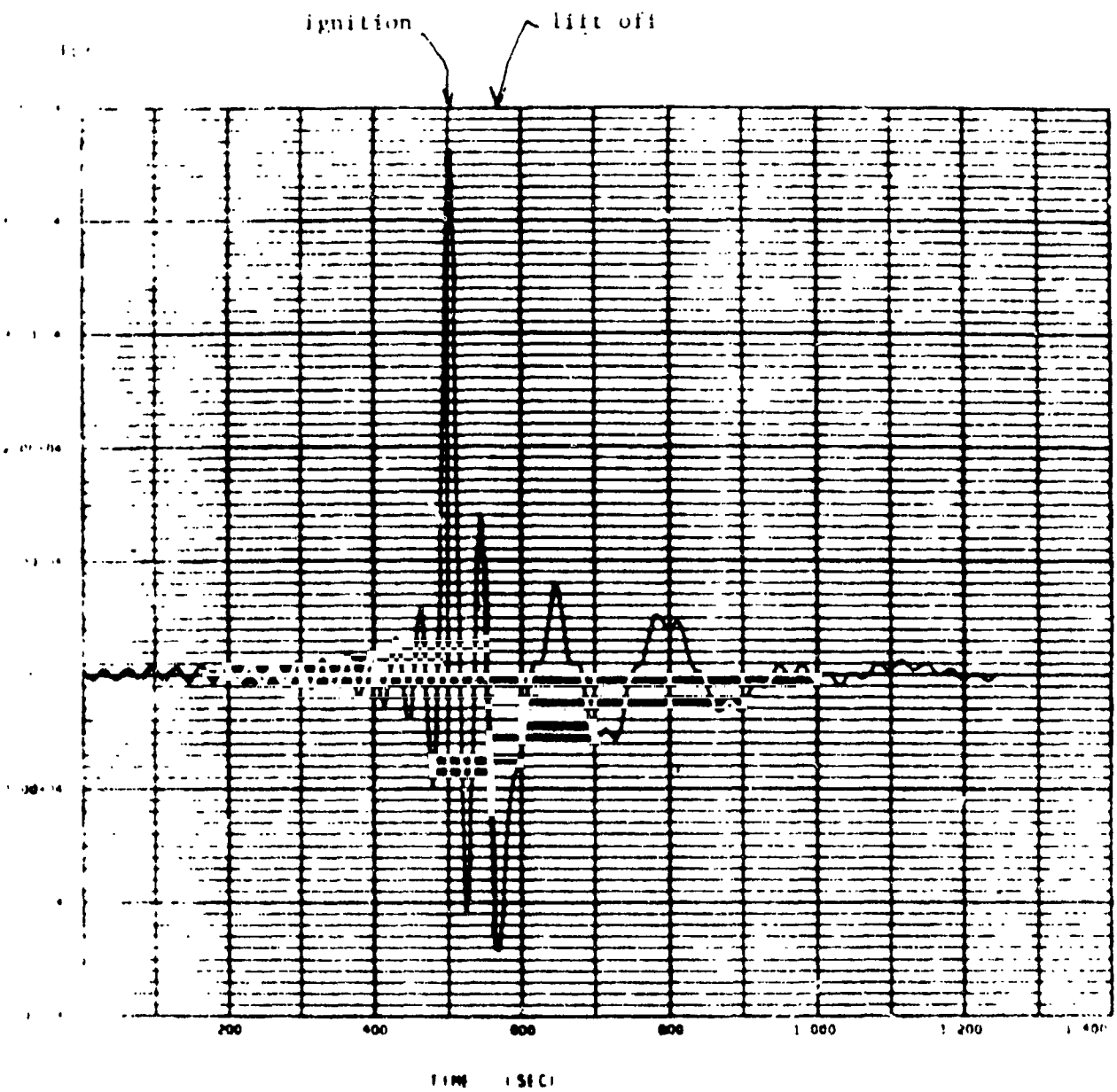


MATCHING

ORIGINAL PAGE IS
OF POOR QUALITY

ADJUST ϕ_n, ω_n, ξ_n TO :

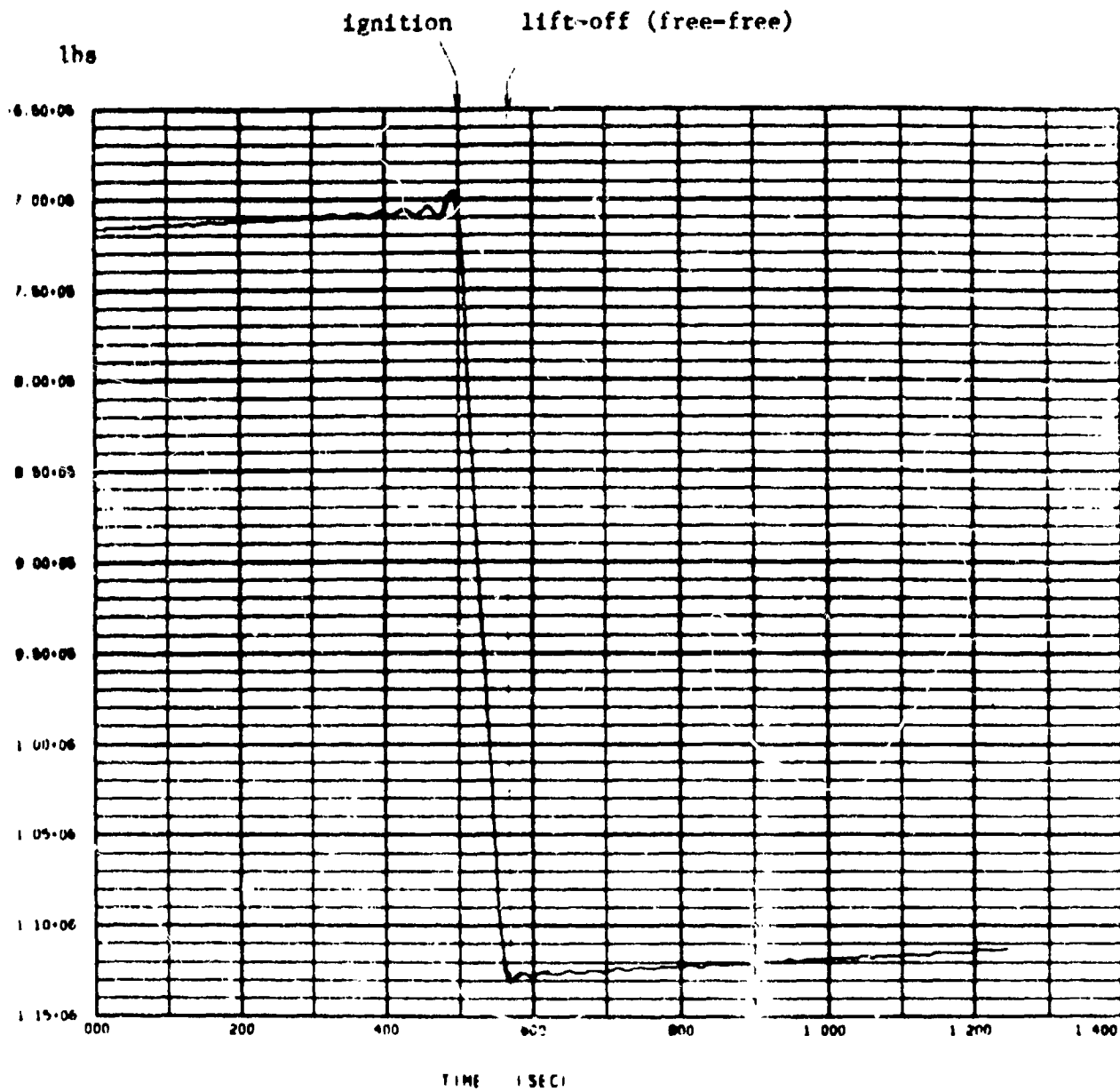
1. MATCH SHOCK SPECTRA OF CALCULATED
RESPONSE WITH FLIGHT DATA
2. ONLY SIMILAR CHARACTER FOR TIME HISTORY
NO DETAIL MATCHING
3. THREE DEGREES OF FREEDOM MATCHED
2 LATERAL
1 AXIAL



DATA FILE: IGNITION HELIOS 1 21 300 SAMPLE RATE 200
 NAME: 0000 TIME INCREMENT 1 2500
 (R = 1) TAPE ID -

Fig. 2. Lateral Pulse - Yaw - SKM1 and SKM2
 (Pitch = Yaw x 4.0)

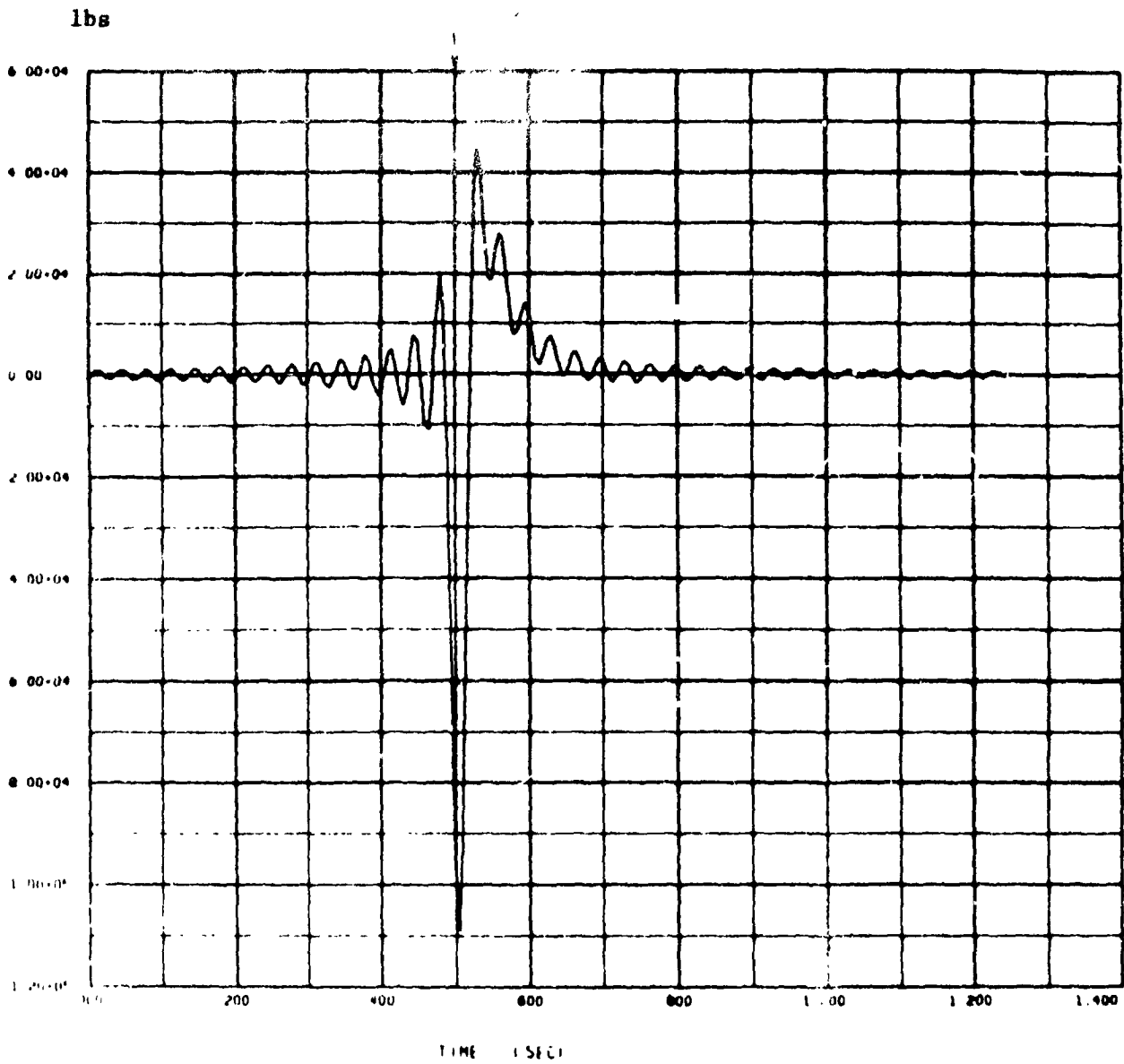
ORIGINAL PAGE IS
OF POOR QUALITY



STAGE 0 FORCING FUNCTION (MELLOS) 21-300 SAMPLE RATE 200
START TIME 0000 TIME MEASUREMENT 1.2500
DELTA ID 1 TAP .

Fig. 3. Longitudinal Forcing Function on SRM1 and SRM2 (No thru differential)

ignition 11% off (free-free)



NAME OF FORMING FUNCTION (MELT) 2 21 306

SAMPLE RATE 200

START TIME 0000

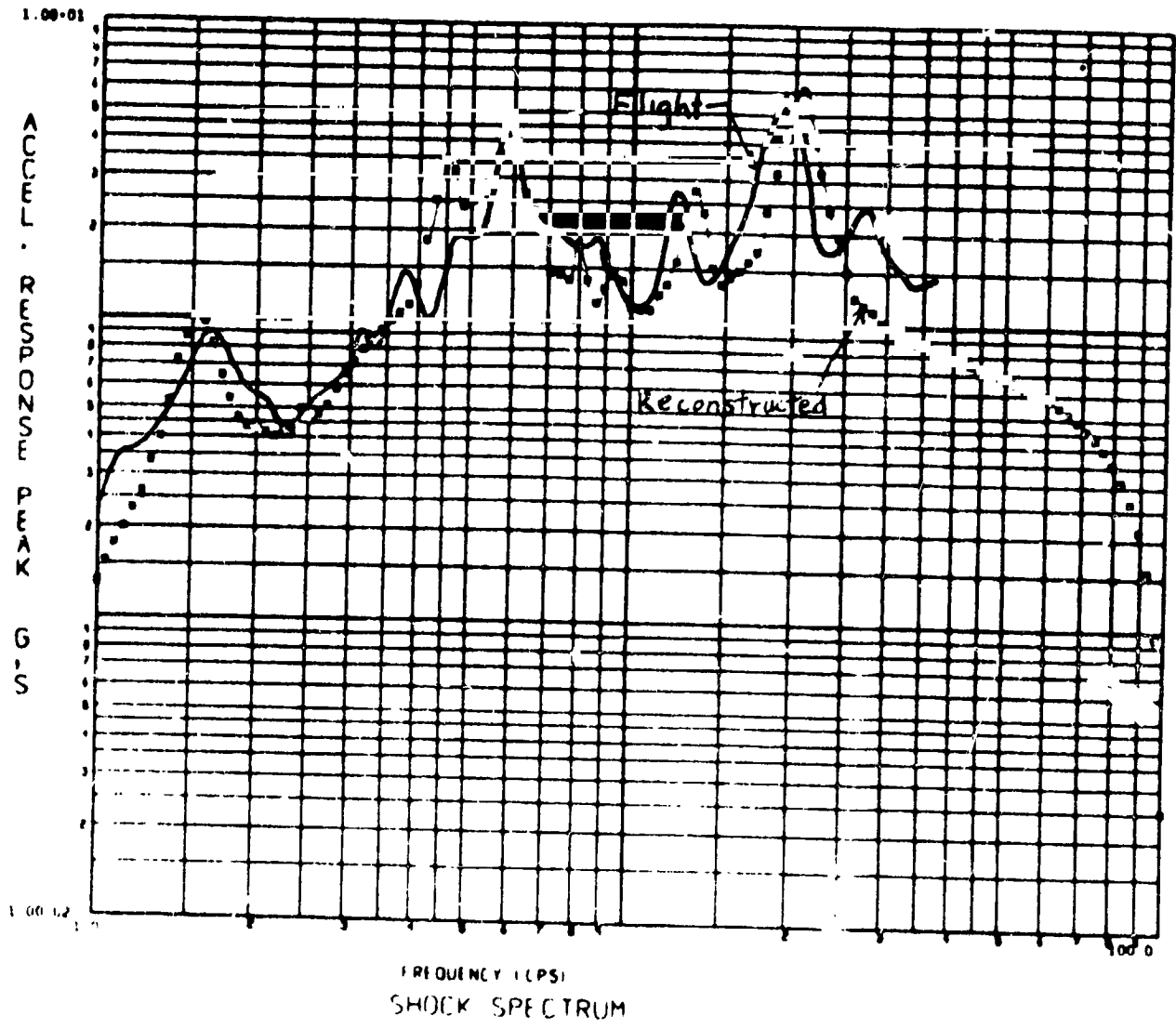
TIME INCREMENT 1.2500

ORCID 1

TAPEID *

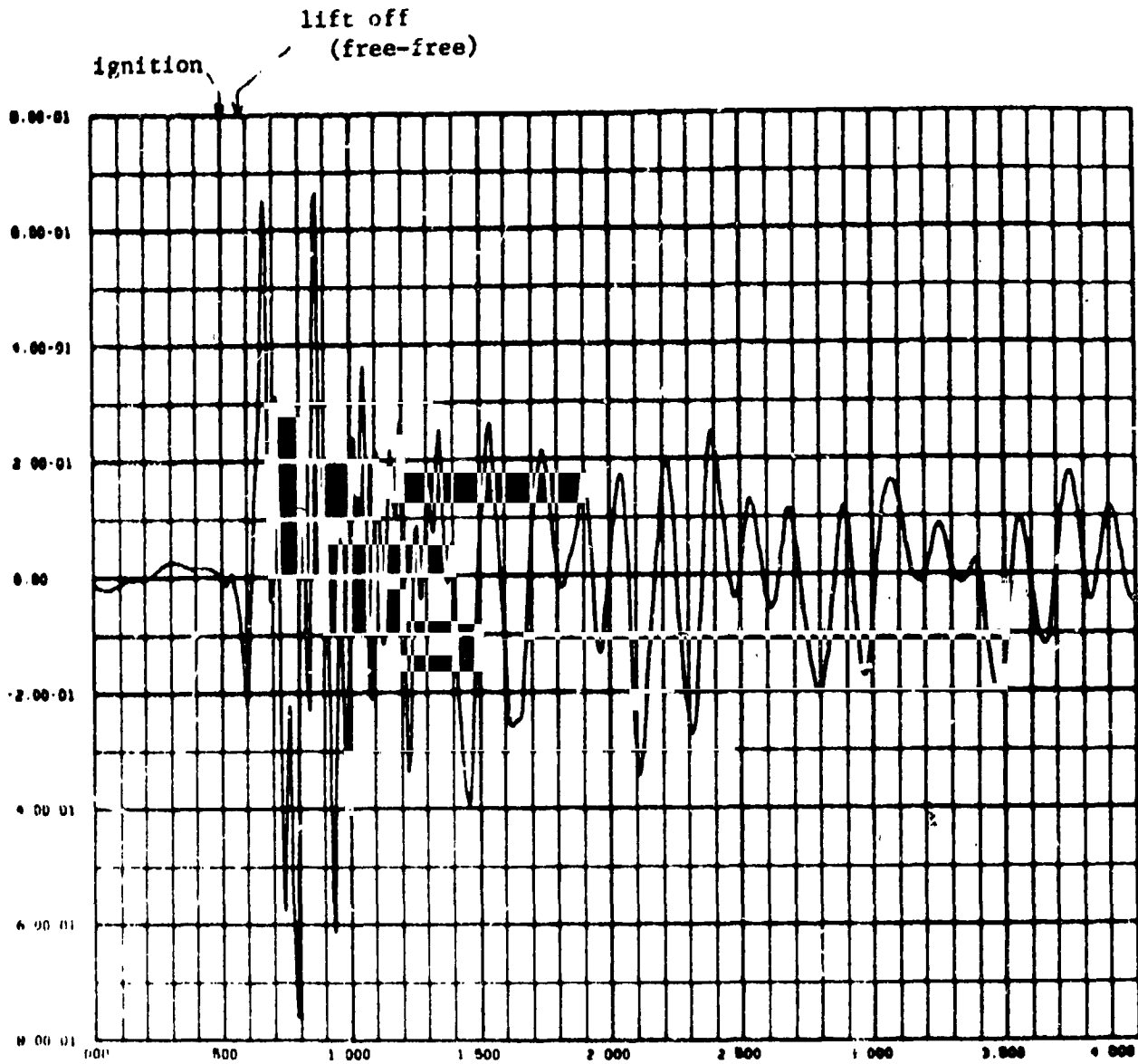
Fig. 4. Longitudinal Pulse - Cor

ORIGINAL PAGE IS
OF POOR QUALITY



HEI	1000/1.000	11 1503	SAMPLE RATE	200
START TIME	0000		0	30.00
DATE	10		TIME INCREMENT	4.0000
			TAPE ID	

Fig. 9. Helios TC-2 - Lateral - 100A



TIME (SEC)
ACCELERATION... (G, S)

RECORD CORE

Y 11 1503

SAMPLE RATE 100

START TIME 0000

TIME INCREMENT 0.0000

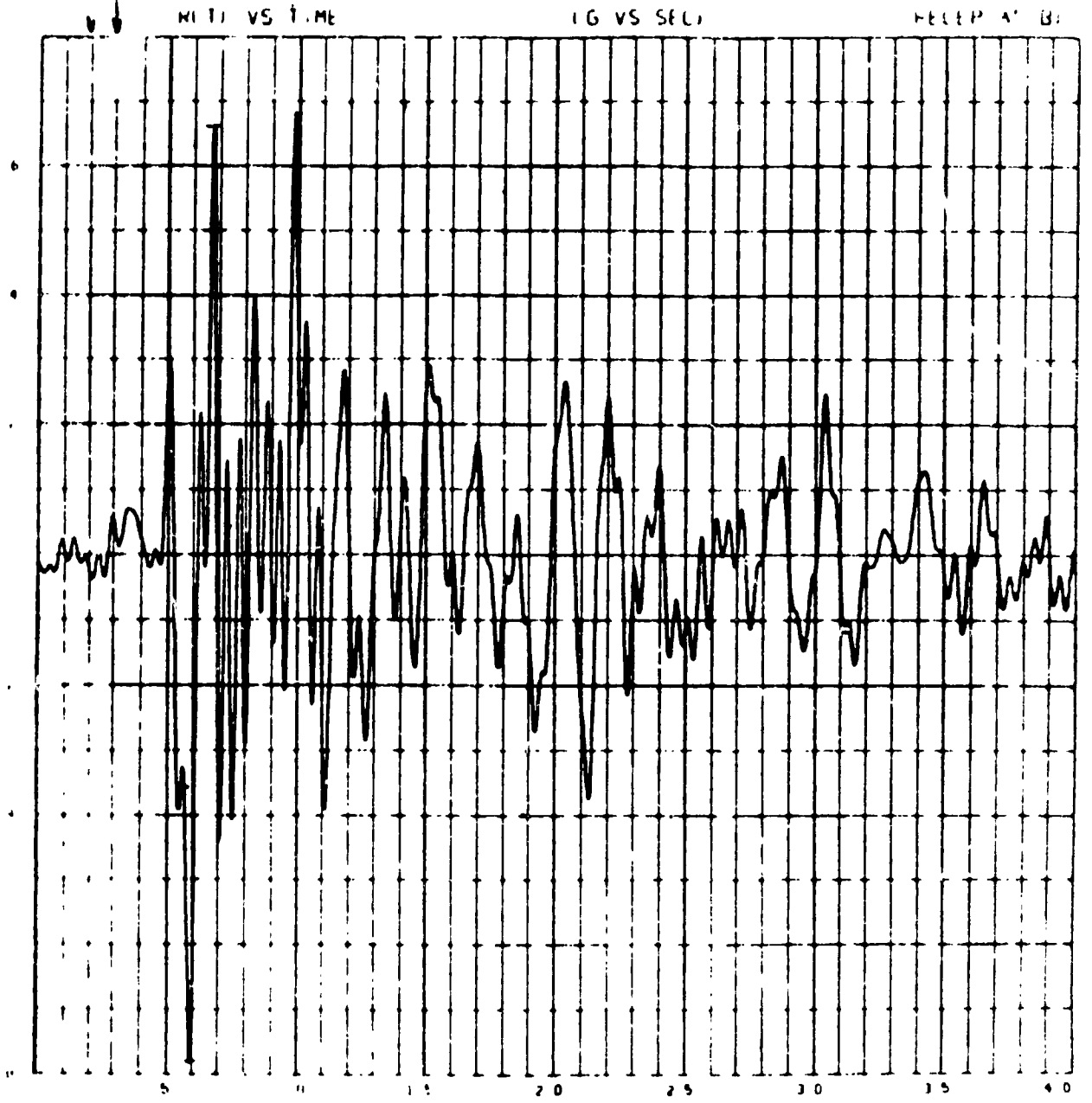
DE FILE 1

TAPED -

ORIGINAL PAGE IS
OF POOR QUALITY

Fig. 6. Helios TC-2 - Lateral GAGE
Reconstructed

approx. ignition approx. lift off

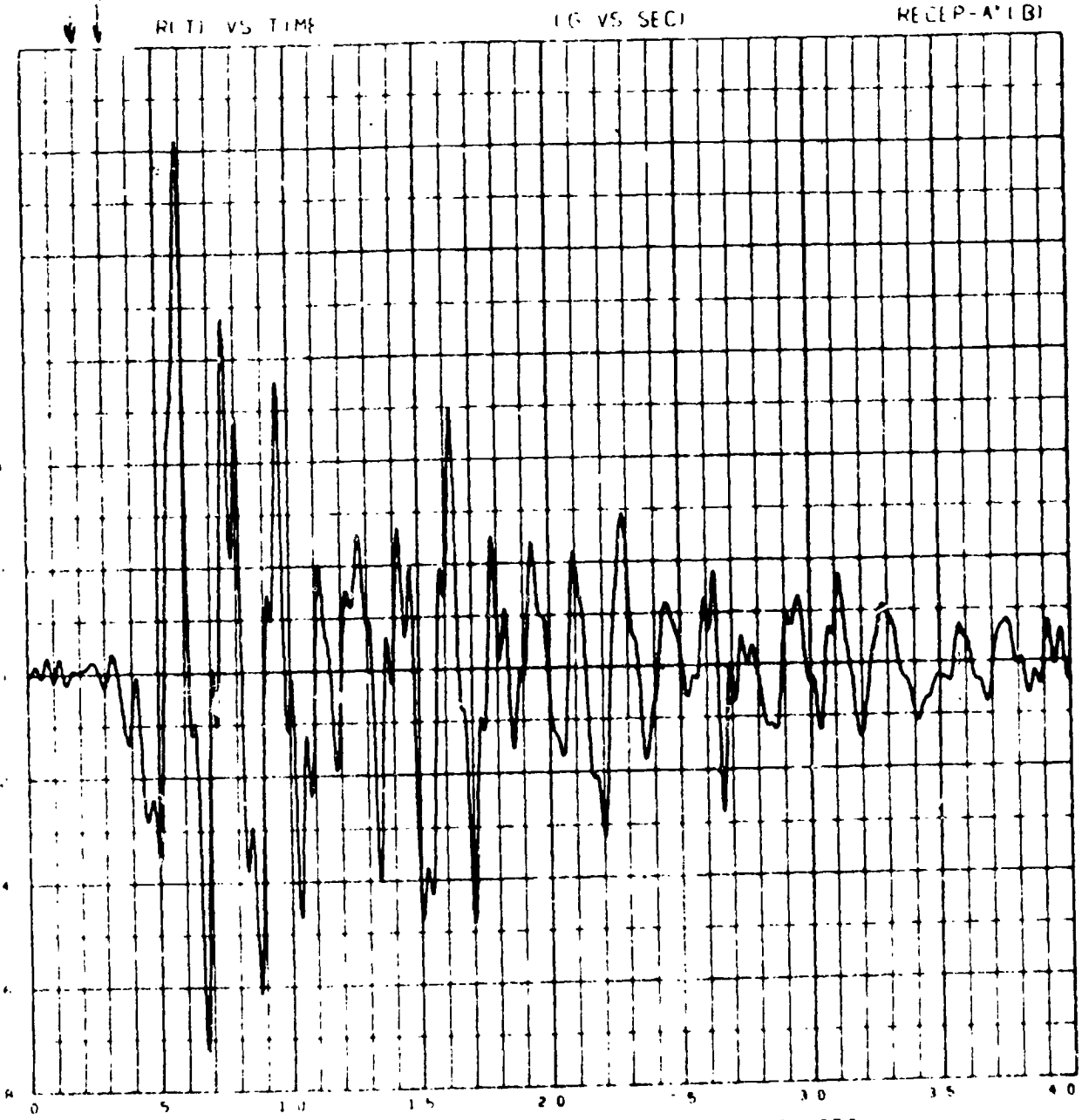


DATA TITLE: ACCELERATIONS AT LAUNCH 5:21:75 400 SPS
 CHANNEL: 0000000000 2:100 000000 PLS PLOTTED: 1 600000-04 MAX NO PLS: 1 000000-03 24 ME 4 1 000
 FILTER CHAN: 000 0 400 START: 000
 END: 997
 DATE: 11/07/75

Fig. 7. Helios TC-2 - Lateral A
Flight Data

approx.
ignition

approx.
lift off



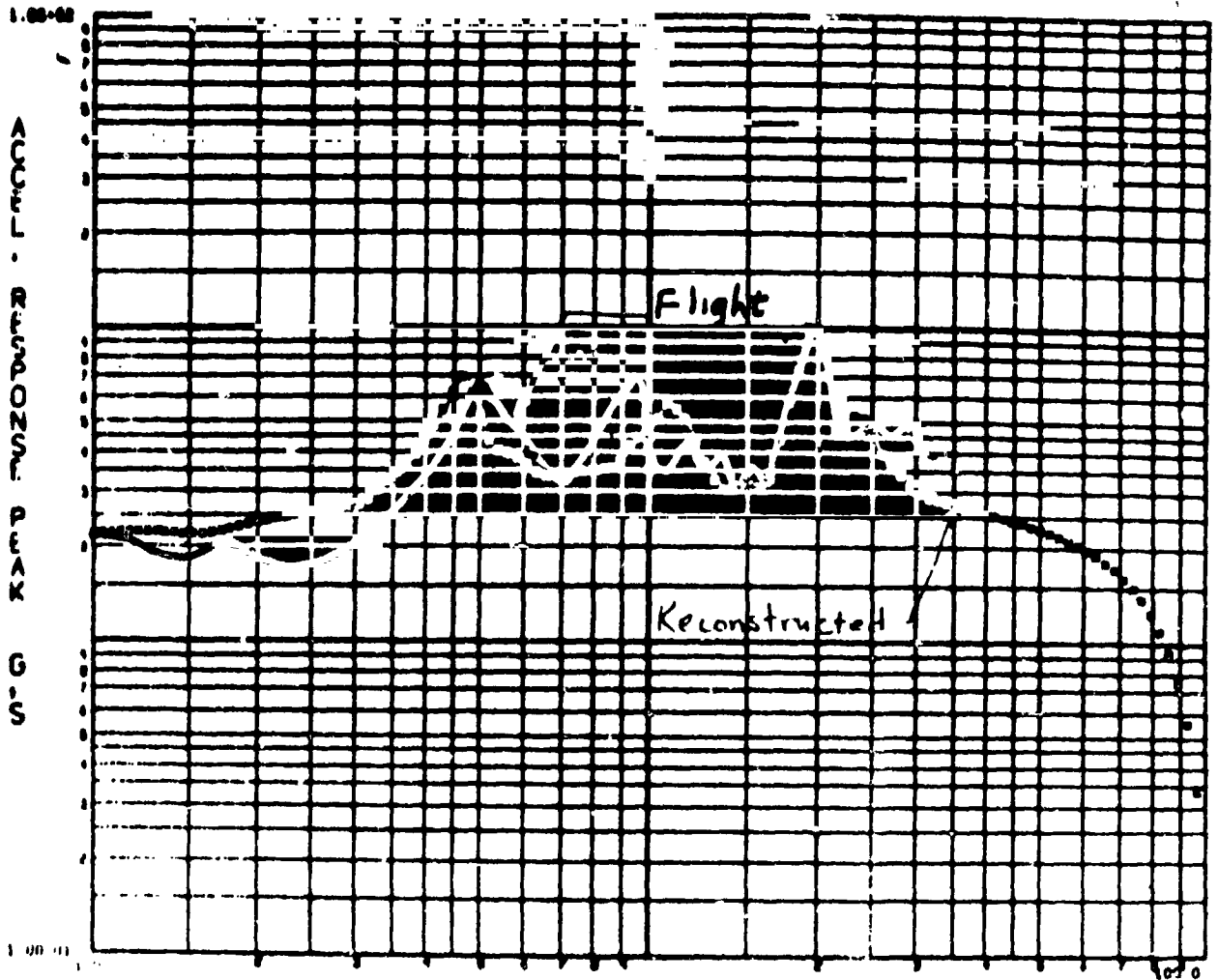
FLIGHT DATA TC-2 ACCELERATIONS AT LAUNCH 5.1175 400 SPS
CHANNEL 10 D NUMBER DELTA 1 TIME AG PTS PLOTTED MAX. PTS
1 2 2 000000-00 1.00000 1.000000 1.600000-03 1.00000-03
RECORD NUMBER 100H FILTER CHAR EQU 0 TIME START 0
TAPE SOURCE LXC1 PFA 400 END 3

24 Hz filter

PL 1, M. O. R. M. 75, 11, 07, 11, 07, 1108

Fig. 10. Helios TC-2 Lateral GABA Flight Data

ORIGINAL PAGE IS
OF POOR QUALITY



FREQUENCY (CPS)
SHOCK SPECTRUM

NO. 100/000

11-1963

SAMPLE RATE 200

TAPE TIME 0000

C 50 00

RECORD 10

TIME INCREMENT 4 0000

TAPE ID *

Fig. 11. Helios TC-2 - Longitudinal - LALA

Table 4. Comparison of Maximum Peak to Peak Amplitudes of the Time Histories

Accelerometer Location	Flight in g's	Calculated in g's
GALA	2.02	2.36
GAZA	1.44	1.41
GA3A	1.74	1.75
$\sqrt{(GA2A)^2 + (GA3A)^2}$	2.26	2.25



SPACELAB PAYLOAD AND SHUTTLE LAUNCHED
SPACECRAFT LOADS ANALYSIS METHODS

E. J. KUHAR

ORIGINAL, PAGE IS
OF POOR QUALITY

PURPOSE

TO DESCRIBE METHODOLOGY USED FOR SHUTTLE PAYLOAD
LOADS ANALYSIS

- SPACECRAFT ANALYSIS
- SPACELAB PAYLOAD ANALYSIS

METHODOLOGY VARIES DEPENDING
ON PAYLOAD CHARACTERISTICS

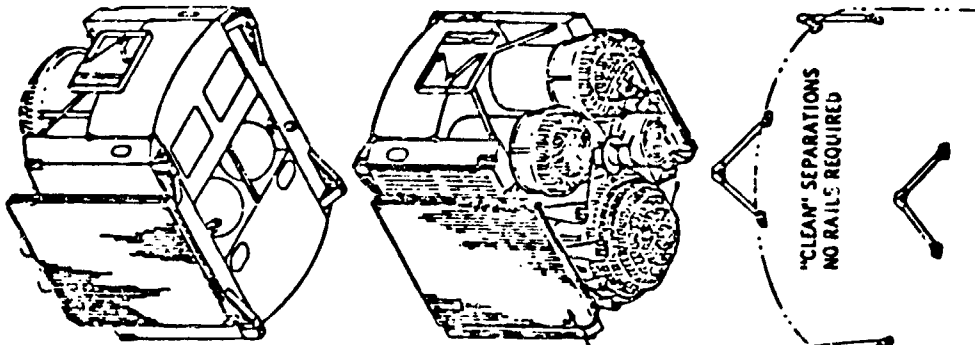


DSCS III STACKED LAUNCH CONFIGURATIONS

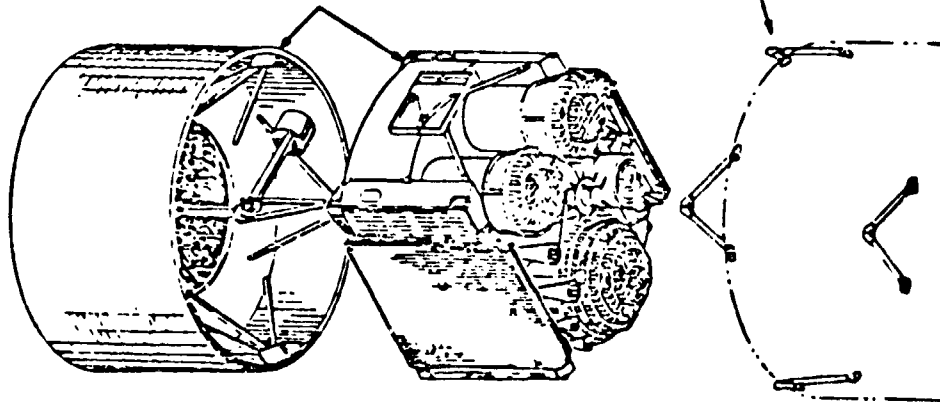


ORIGINAL PAGE IS
OF POOR QUALITY

DSCS III/DSCS III LAUNCH



DSCS III/DSCS II LAUNCH



- DSCS II
INTERFACE
- BASICALLY UNCHANGED
 - SAME STATION
 - SAME SEPARATION HARDWARE
 - STIFF RADIAL LOAD PATH PROVIDED BY DSCS II

HARD MOUNT
SOLAR ARRAYS

TRUSS ADAPTER
REMAINS WITH
BOOSTER

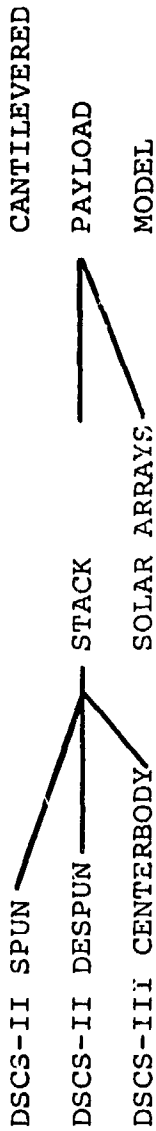


**GENERAL
ELECTRIC**

MODELING APPROACH



- NASTRAN MODEL OF DSCS-III CENTERBODY (3000 DOF)
- NASTRAN MODEL OF DSCS-III SOLAR ARRAY (1000 DOF)
- MODAL MODEL OF DSCS-II (236 D-DOF)
 - SPUN (133 D-DOF)
 - DESPUN (103 D-DOF)
- MODAL SYNTHESIS OF SPACECRAFT



FINAL MODEL CONTAINS 624
 PHYSICAL DOF USING 200 DOF
 EIGENVALUE SOLUTIONS



**GENERAL
ELECTRIC**

DYNAMIC MODEL DATA REQUIREMENTS



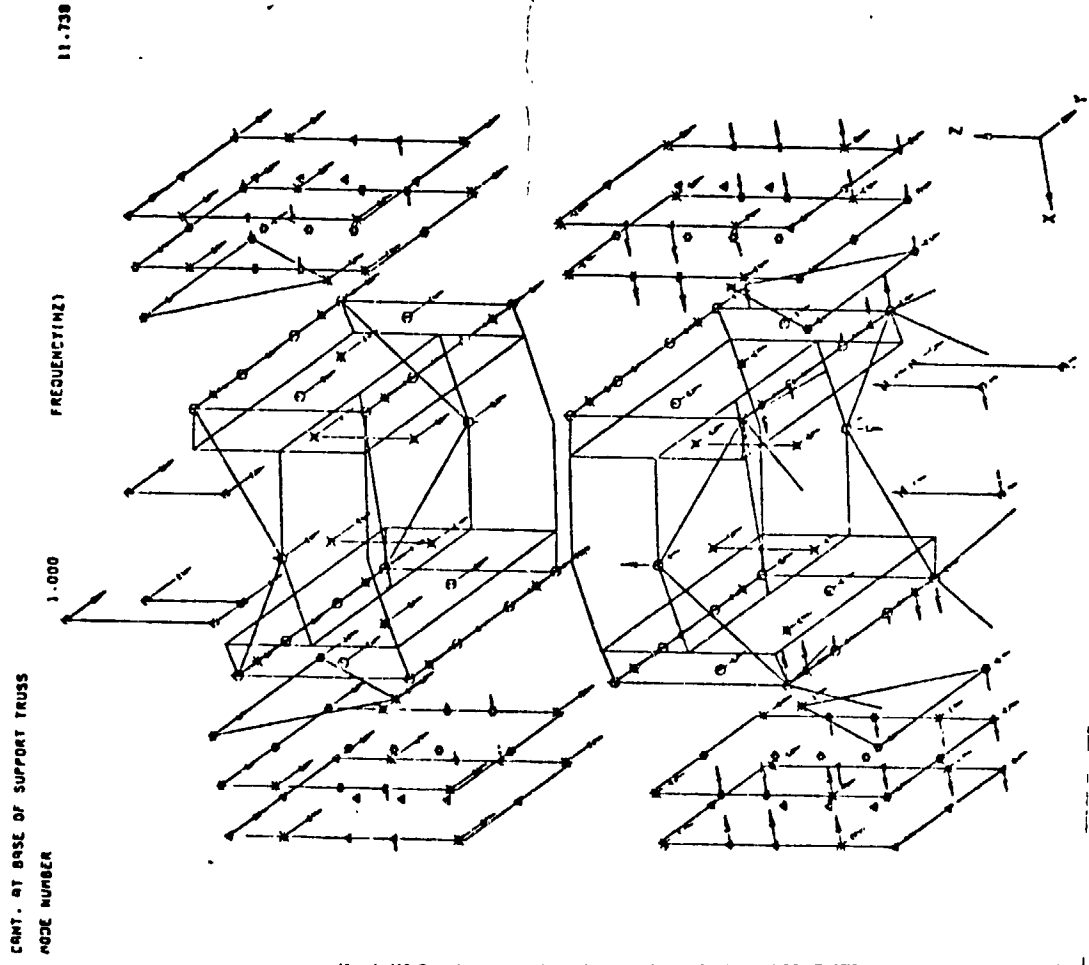
space division

- SUBSTRUCTURE MODES/FREQUENCIES
ATTACHMENT COORDINATES INCLUDED IN SUBSTRUCTURE
DOFS
- SUBSTRUCTURE COUPLING STIFFNESS MATRICES
RELATES ATTACHMENT COORDINATES BETWEEN 2
SUBSTRUCTURES

NOTE: SUBSTRUCTURE FREE/FREE STIFFNESS MATRIX RETRIEVED AT THIS POINT
FOR FUTURE ANALYSIS

ORIGINAL PAGE IS
OF POOR QUALITY

STACKED MODEL MODE SHAPE





**GENERAL
ELECTRIC**



space division

LOAD TRANSFORMATION MATRIX (LTM)

PHYSICAL LTM

$$[L] = [U_D] \{X\} \quad [L] = [U_L] \{F\}$$

$$[U_D] = [U_L] [K]$$

MODAL LTM

$$\{\dot{X}\} = [K]^{-1} \{F\}$$

$$\{F\} = -[M] \{\ddot{X}\}$$

$$\{\ddot{X}\} = [\phi] \{\ddot{q}\}$$

$$[L] = [T] \{\ddot{q}\}$$

$$\text{WHERE } [LTM] = [T] = - [U_D] [K]^{-1} [M] [\phi]$$

REVISED MODAL LTM

$$\{X\} = \{X^a\} + \{X^b\}$$

$$[L] = [T] \{\dot{q}\} + [V] \{X_B\}$$

ORIGINAL PAGE IS
OF POOR QUALITY



**GENERAL
ELECTRIC**

LOADS TRANSFORMATION METHOD



space division

$$\left\{ \begin{array}{l} \text{LOADS} \\ \text{STRESS} \\ \text{DEFLECTION} \end{array} \right\} = \begin{bmatrix} T_1 \\ T_2 \\ T_3 \end{bmatrix} + \left\{ \begin{array}{l} q \\ -q \\ \vdots \\ X_B \end{array} \right\} \begin{bmatrix} V_1 \\ V_2 \\ V_3 \end{bmatrix} \quad \{x_B\}$$

DSCS-II

$$T_1 = [U_D^{II}] \begin{bmatrix} K_{II}^{-1} & 0 \\ 0 & M_{BB} \end{bmatrix} \begin{bmatrix} \phi_N \\ \phi_C \\ 0 \\ I \end{bmatrix}$$

$$V_1 = [U_D^{II}] \begin{bmatrix} \phi_C \\ I \end{bmatrix}$$

DSCS-III

$$T_2 = - [U_D^{III}] \begin{bmatrix} K_{II}^{-1} & 0 \\ 0 & M_{BB} \end{bmatrix} \begin{bmatrix} \phi_N \\ \phi_C \\ 0 \\ I \end{bmatrix}$$

$$V_2 = [U_D^{III}] \begin{bmatrix} \phi_C \\ I \end{bmatrix}$$

INERTIAL
LOADS

$$T_3 = [R]^T \begin{bmatrix} M_{II} & 0 \\ 0 & M_{BB} \end{bmatrix} \begin{bmatrix} \phi_N \\ \phi_C \\ 0 \\ I \end{bmatrix}$$

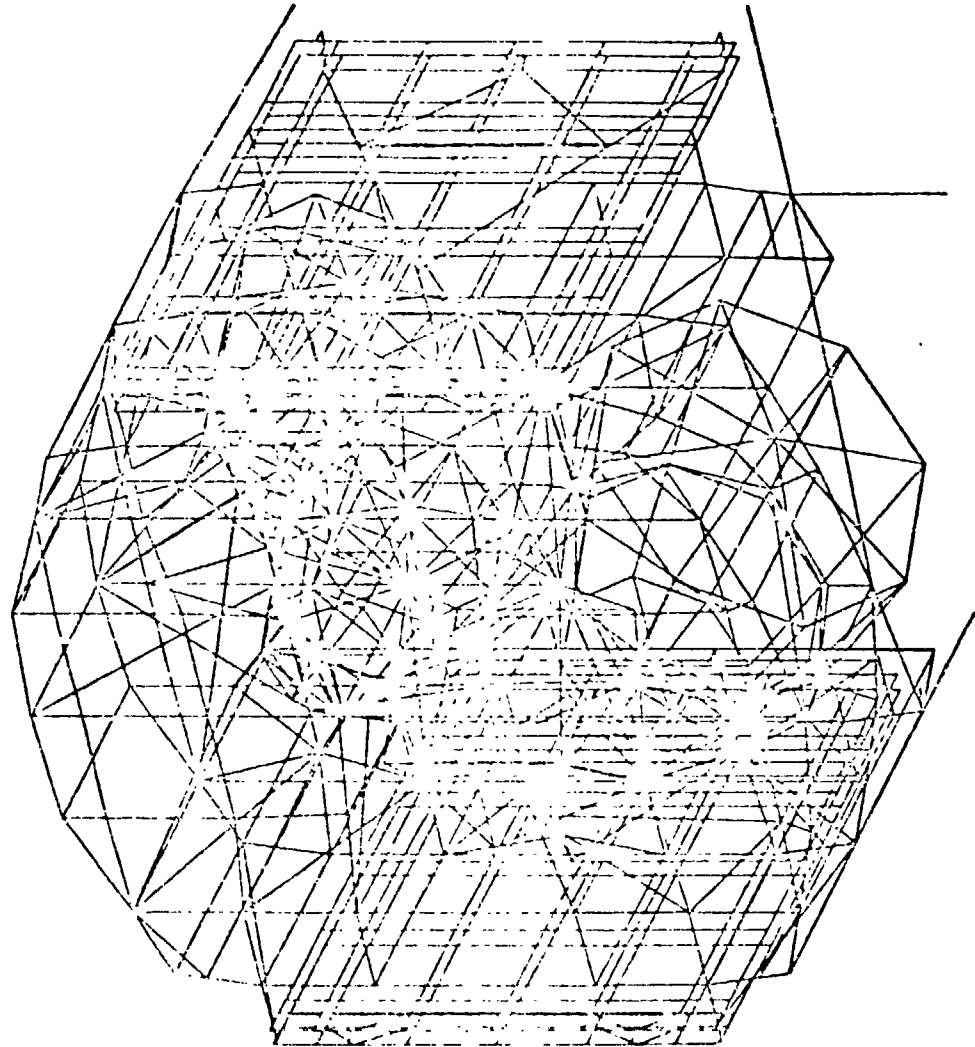
$$V_3 = 0$$

LOADS DETERMINED SEPARATELY
FOR EACH SPACECRAFT



space division

FINITE ELEMENT MODEL



GENERAL
ELECTRIC

ORIGINAL PAGE IS
OF POOR QUALITY



**GENERAL
ELECTRIC**

LTM DATA REQUIREMENTS



space division

- SUBSTRUCTURE FREE/FREE STIFFNESS MATRICES
- SUBSTRUCTURE COUPLING STIFFNESS MATRICES
- SUBSTRUCTURE MASS MATRICES
- COUPLED SYSTEM MODES AND FREQUENCIES



**GENERAL
ELECTRIC**

DATA TRANSMITTAL



space division

DSCS-II

- FREE-FREE MODES/FREQUENCIES
- WEIGHT MATRIX
- FREE-FREE STIFFNESS MATRIX
- UNIT DEFLECTION MATRIX
- COORDINATES
- RATTLESACE EQUATION
- CHECK DATA

(236 DOF)

DSCS-II/III

- CANTILEVERED MODES/
FREQUENCIES
- CONSTRAINT MODES
- WEIGHT MATRIX
- BOUNDARY MASS AND
STIFFNESS MATRICES
- COORDINATES
- RATTLESACE EQUATIONS
- LOAD TRANSFORMATION
MATRICES
- CHECK DATA

(130 MODES)

RESULTS

- STATISTICAL
ACCELERATIONS (MIN/
MAX)
- STATISTICAL LOADS
(MIN/MAX)
- CLEARANCES

(941 ITEMS)

**ORIGINAL PAGE IS
OF POOR QUALITY**

PAYLOAD CAN BE ATTACHED TO
ANY L/V STRUCTURE



**GENERAL
ELECTRIC**

LOAD CYCLES



- PRELIMINARY LOAD CYCLE
- SDM
- VERIFICATION LOAD CYCLE



MODELING APPROACH



- DETAILED FINITE ELEMENT MODEL
- SIMPLIFIED DYNAMIC MODEL

ORIGINAL PAGE IS
OF POOR QUALITY



**GENERAL
ELECTRIC**

ACPL LOADS METHODOLOGY



- DESIGN CRITERIA
 - MINIMUM RESONANT FREQUENCY - 35 HZ
 - LIMIT LOAD FACTOR (VARIES WITH WEIGHT AND RESONANT FREQUENCY)
- VERIFICATION LOADS
 - SIMPLIFIED MODEL (< 10 NODES)

LOADS NOT HIGHLY
DEPENDENT ON DYNAMIC
CHARACTERISTICS BY DESIGN



**GENERAL
ELECTRIC**

CONCLUSIONS



space division

- METHODOLOGY HAS BEEN DEVELOPED FOR COMPLEX PAYLOAD ANALYSIS
- COMPLEXITY OF ANALYSIS WILL VARY DEPENDING ON PAYLOAD REQUIREMENTS
- MODAL SYNTHESIS IS AN EFFECTIVE APPROACH FOR LOADS ANALYSIS

**ORIGINAL PAGE IS
OF POOR QUALITY**

PRECEDING PAGE BLANK NOT FILMED

PANEL SUMMARY AND TECHNOLOGY RECOMMENDATIONS

Moderator: Dr. Amos, NASA Headquarters

Panel:

- Mr. D. Stone, Rockwell
- Mr. R. Gatto, Rockwell
- Dr. R. Herzberg, Lockheed
- Mr. D. Wade, JSC
- Dr. M. Card, LaRC
- Mr. R. Ryan, MSFC
- Dr. J. Hill, University of Alabama
- Dr. R. Craig, University of Texas

**ORIGINAL PAGE IS
OF POOR QUALITY**

REPRESENTING THE DYNAMICS COMMUNITY AT THE OAST/MSFC SPONSORED WORKSHOP ON PAYLOAD LOADS TECHNOLOGY, WE, THE SUMMARY PANEL, MAKE THE FOLLOWING RECOMMENDATIONS AND STATEMENT:

"THE DYNAMICS COMMUNITY FULLY SUPPORTS THE REQUIREMENT FOR MEASUREMENTS OF DYNAMIC LOADS AND OTHER ENVIRONMENTAL EFFECTS DURING SPACE SHUTTLE FLIGHTS. MEASUREMENTS ARE RECOMMENDED TO BE TAKEN FROM BOTH THE SHUTTLE AND PAYLOAD. WE RECOMMEND FURTHER THAT ALL NASA, DOD, AND CIVIL AGENCIES USING THE SHUTTLE SUPPORT SUCH MEASUREMENTS AND COOPERATE TO DEVELOP A PLAN FOR DATA COLLECTION, ANALYSIS, AND USE. MEMBERS OF THE DYNAMICS COMMUNITY PRESENT AT THIS WORKSHOP AGREE TO SUPPORT FLIGHT MEASUREMENTS AND WILL ACTIVELY WORK TOWARD ESTABLISHMENT OF SOME FORM OF DATA GATHERING AND ANALYSIS SYSTEM."

M. F. CARD
LANGLEY RESEARCH CENTER

SUMMARY AND TECHNOLOGY RECOMMENDATIONS
PAYLOAD FLIGHT LOADS PREDICTION
METHODOLOGY WORKSHOP

MSFC

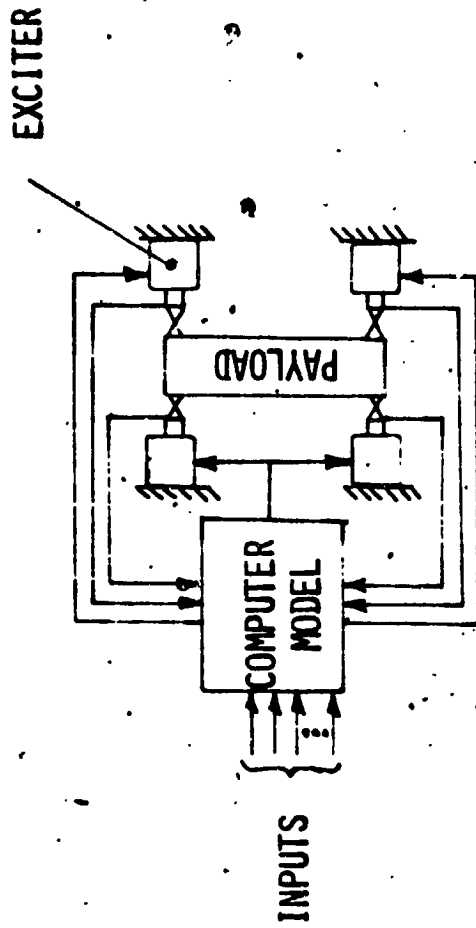
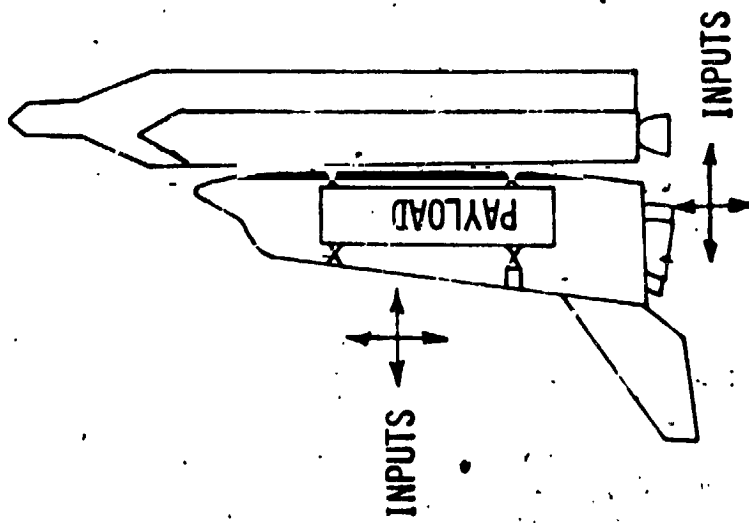
Nov. 14-16, 1978

ORIGINAL PAGE IS
OF POOR QUALITY

PAYLOAD DYNAMICS

- o GND TEST TECHNIQUES
- o FLUID-STRUCTURE MODELING
- o MODAL COUPLING

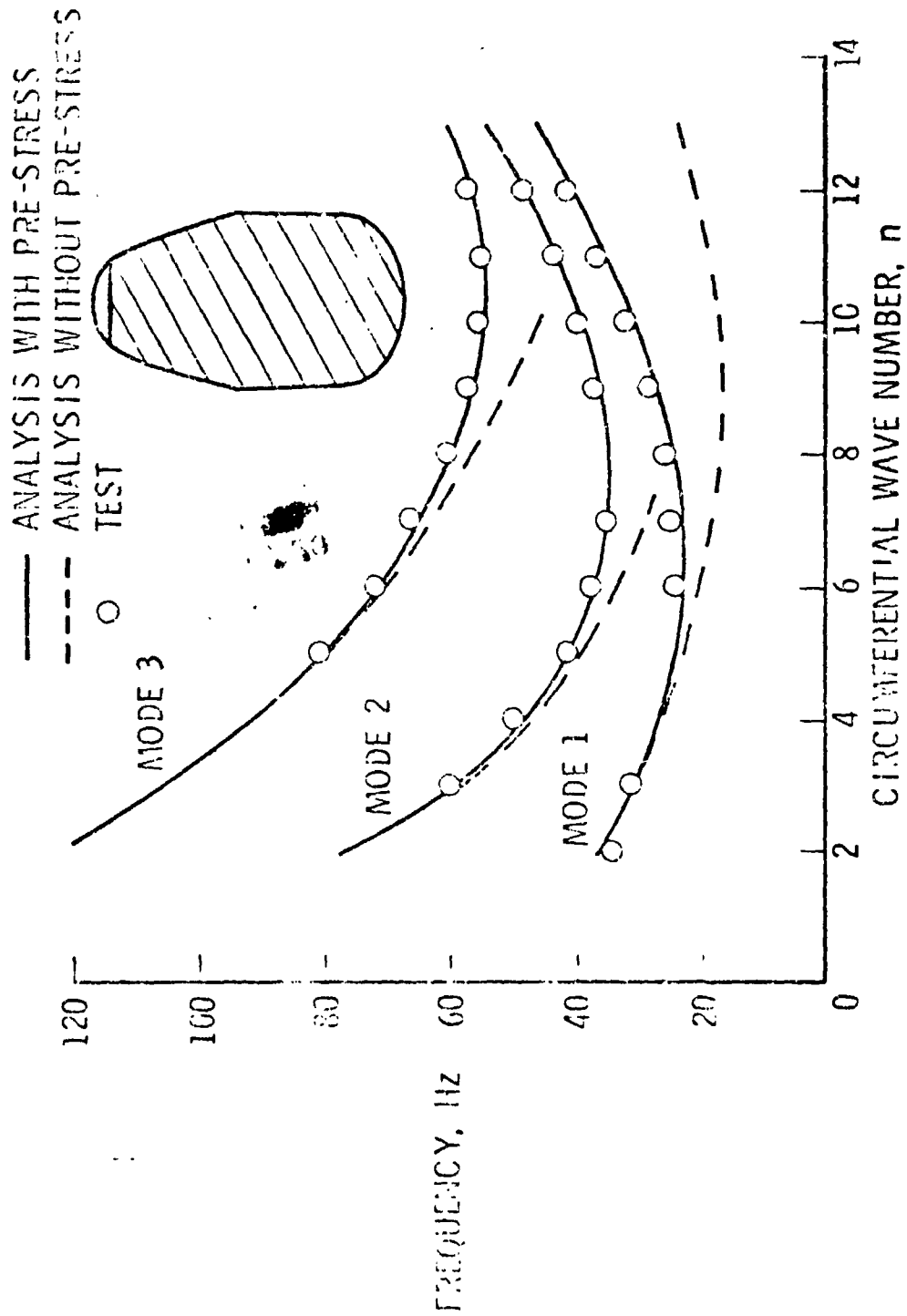
MAKE A PAYLOAD UNDER TEST THINK IT IS IN A SHUTTLE VEHICLE!



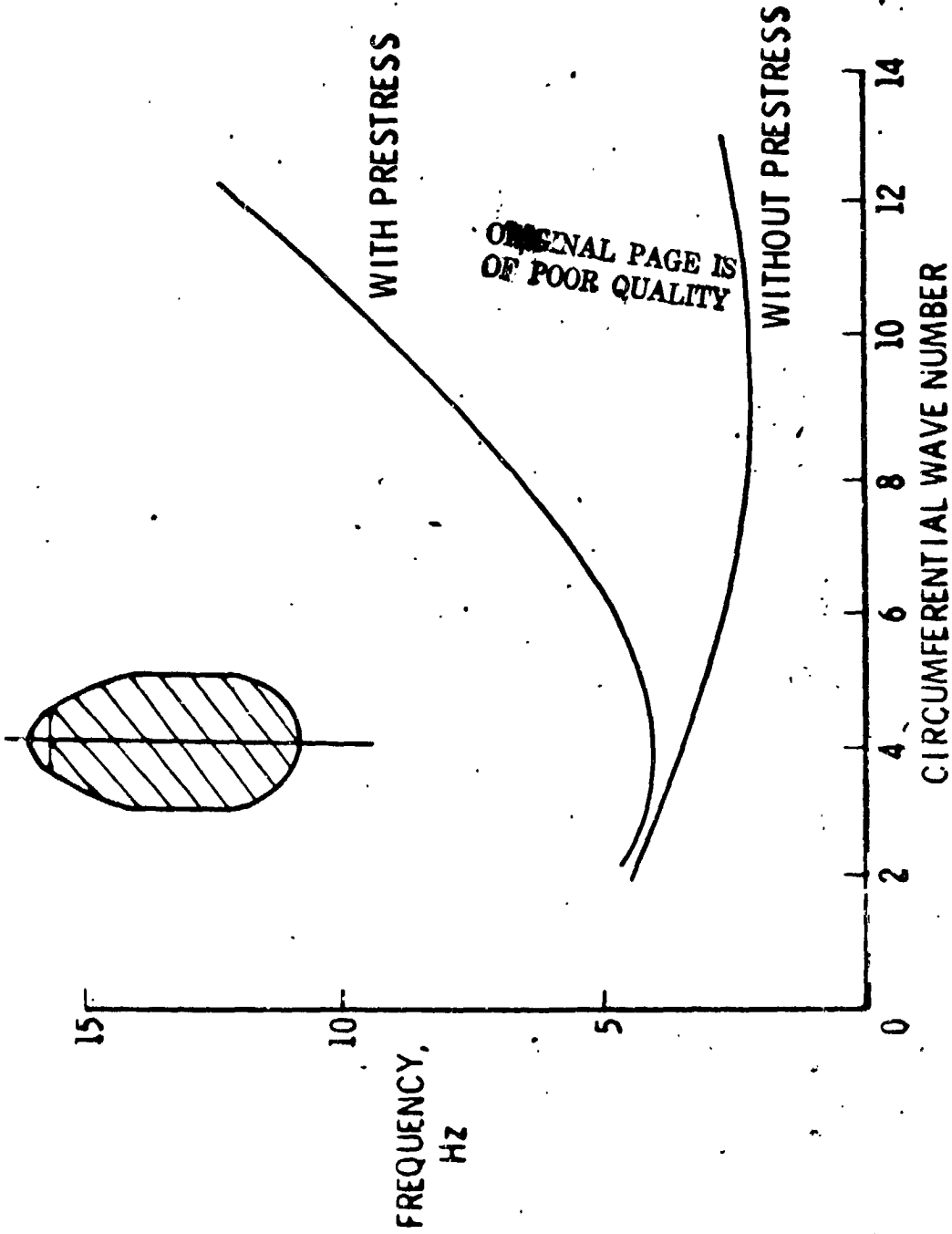
WITH MATH-MODEL/PAYLOAD TEST

REPLACE VEHICLE/PAYLOAD TEST
ORIGINAL PAGE IS
POOR QUALITY

NATURAL FREQUENCIES OF NEARLY FULL $\frac{1}{2}$ SCALE SHUTTLE LOX TANK



NATURAL FREQUENCIES OF
NEARLY FULL SCALED UP LOX TANK



RESONANCE IN MULTI-BODY VIBRATION ANALYSIS DEMONSTRATED

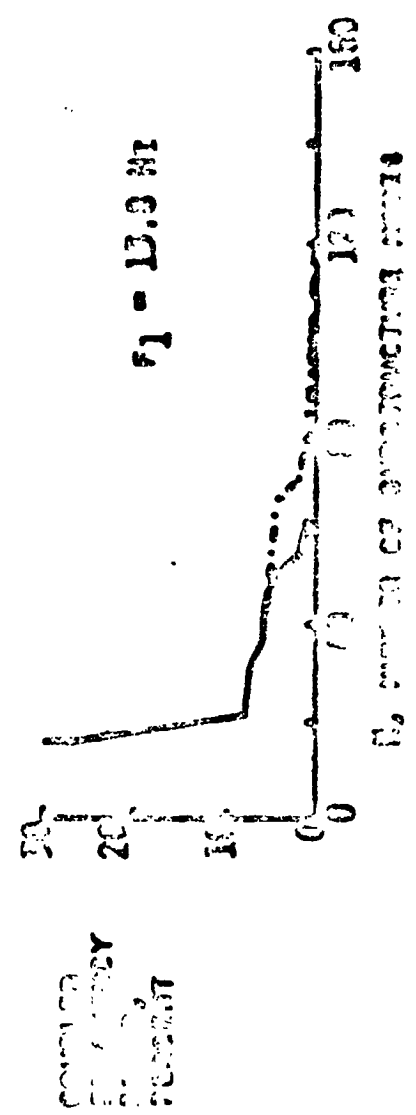
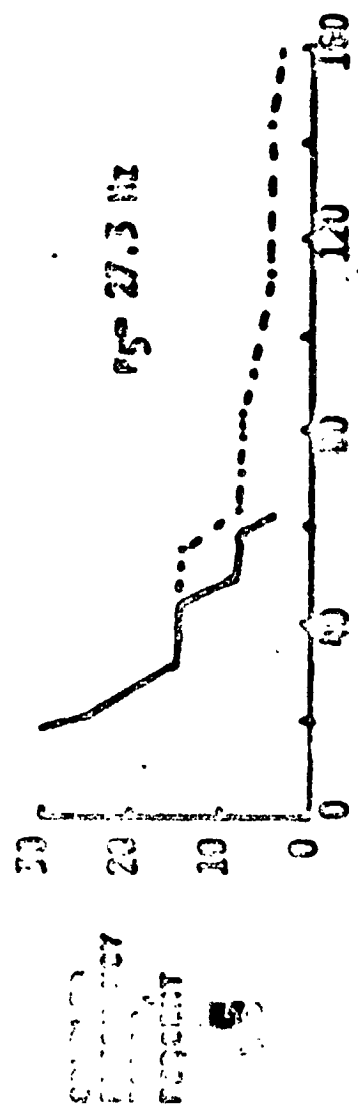


FIGURE 1

ORIGINAL PAGE IS OF POOR QUALITY

FIGURE 2

FIGURE 3

LOAD SUPPRESSION

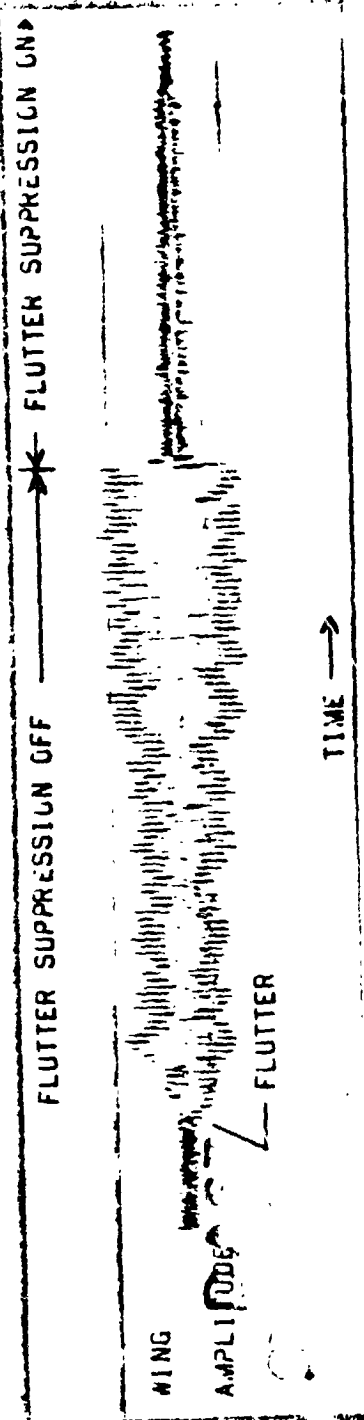
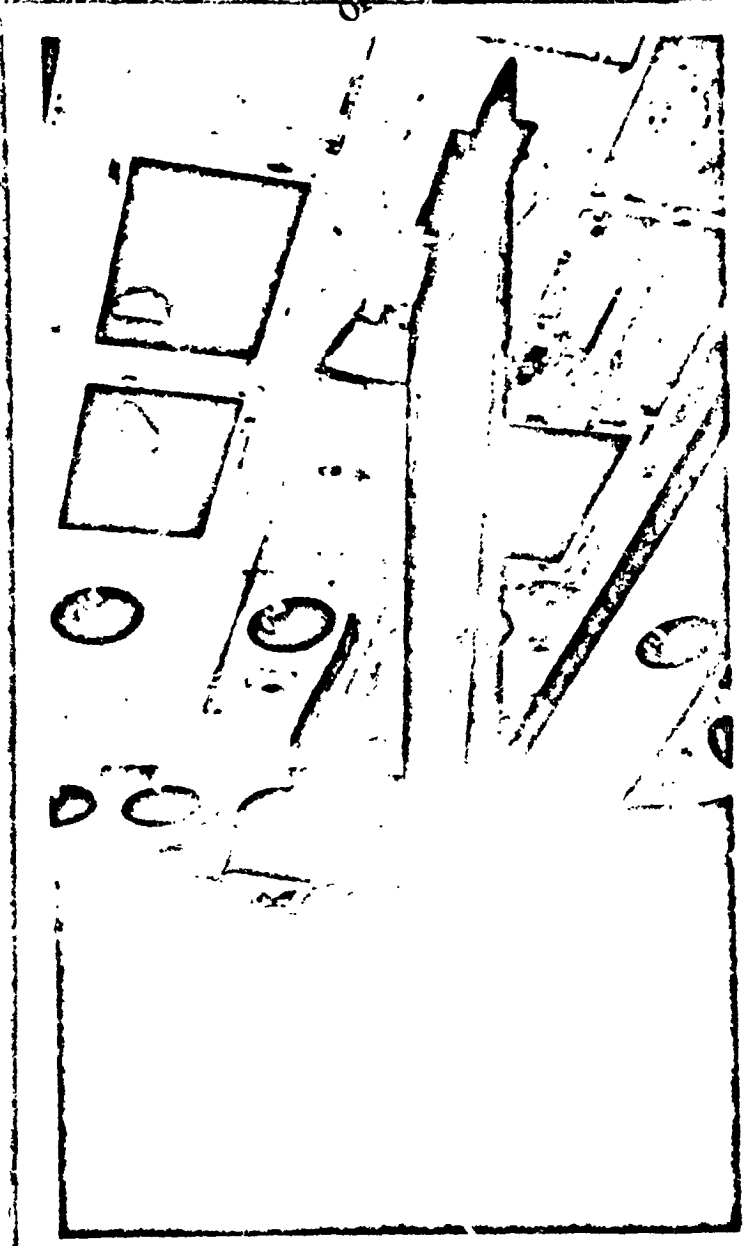
(AERONAUTICS)

- o WING FLUTTER (ACTIVE)
- o STORE FLUTTER (ACTIVE)
- o LANDING GEAR (ACTIVE)
- o CABIN NOISE (PASSIVE)

ORIGINAL PAGE IS
OF POOR QUALITY

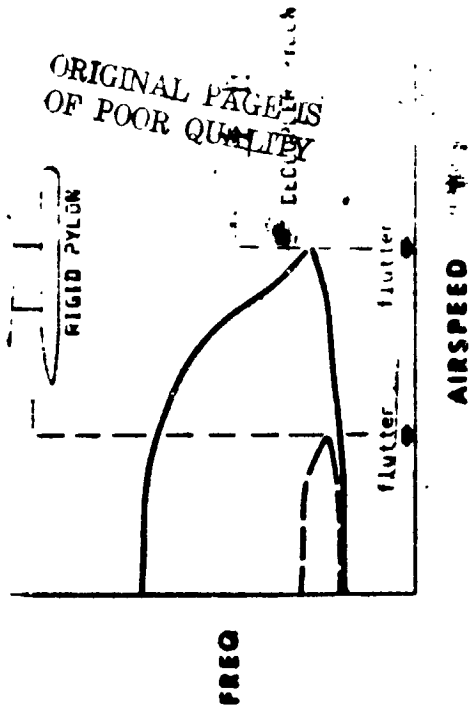
DAST WING FLUTTER SUPPRESSION SYSTEM SHOWN EFFECTIVE IN TDT TESTS

ORIGINAL PAGE IS OF POOR QUALITY

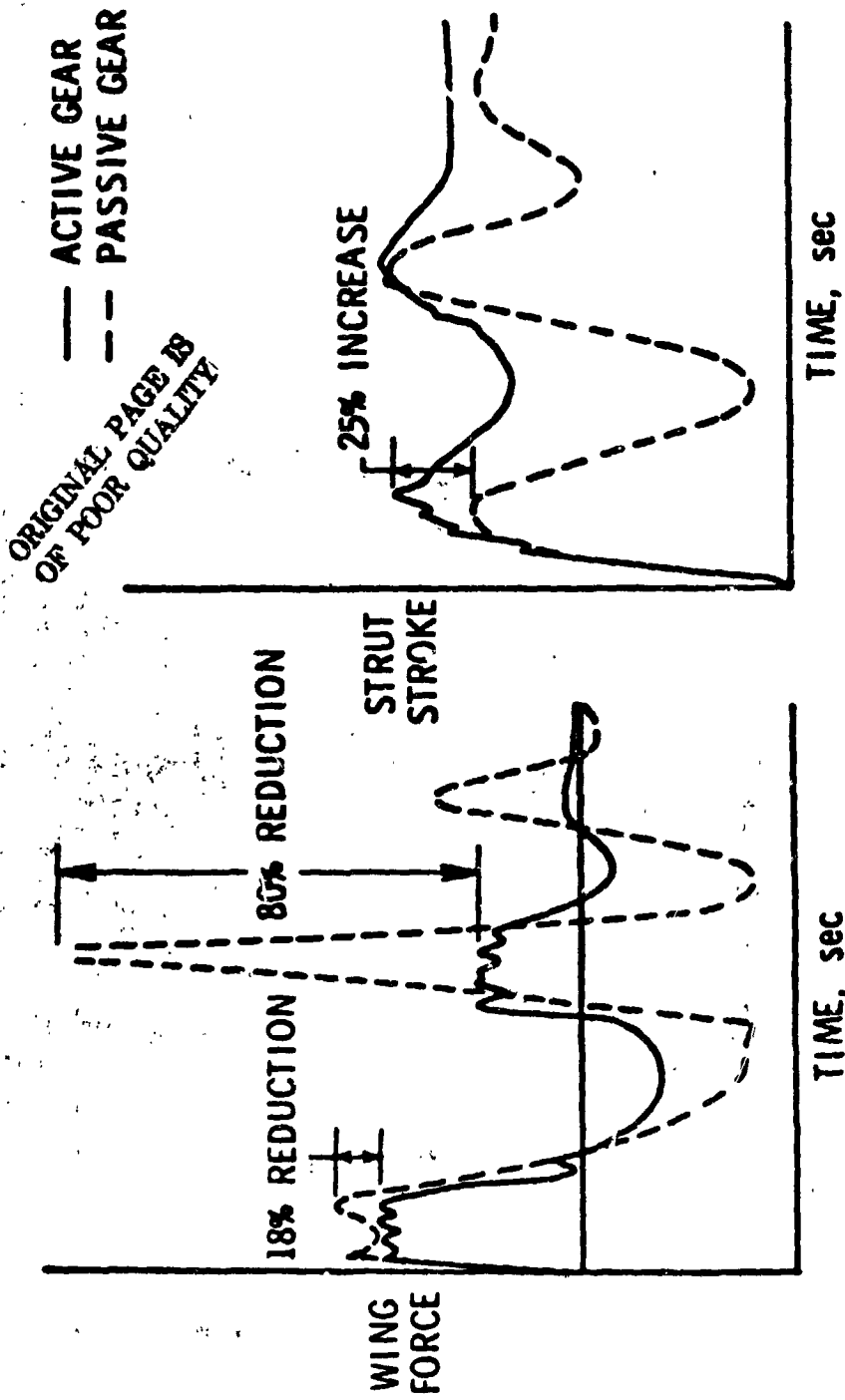


WING-STORE DECOUPLER PYLON

ALLEVIATES FLUTTER

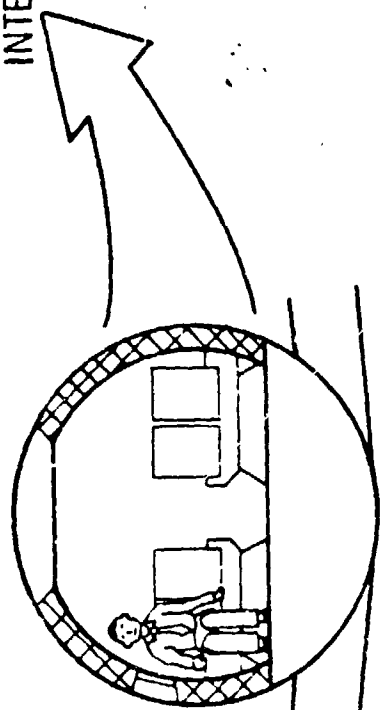
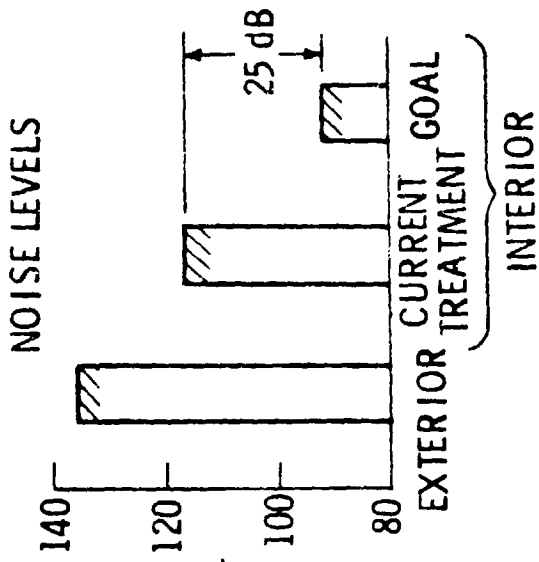
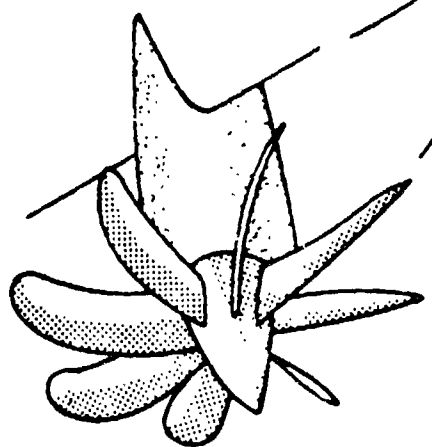


ANALYTICAL RESULTS FOR ACTIVE AND PASSIVE GEARS



PROP-FAN INTERIOR NOISE

SOURCE NOISE DEFINITION



SIDEWALL NOISE CONTROL

ORIGINAL PAGE IS
OF POOR QUALITY

ORIGINAL PAGE IS
OF POOR QUALITY

LARGE SPACE STRUCTURES

- o LOADS/DESIGN CRITERIA
- o FLEXIBILITY MYTHS
- o CONTROLS NEEDS

LOAD SOURCES FOR LARGE SPACE STRUCTURES

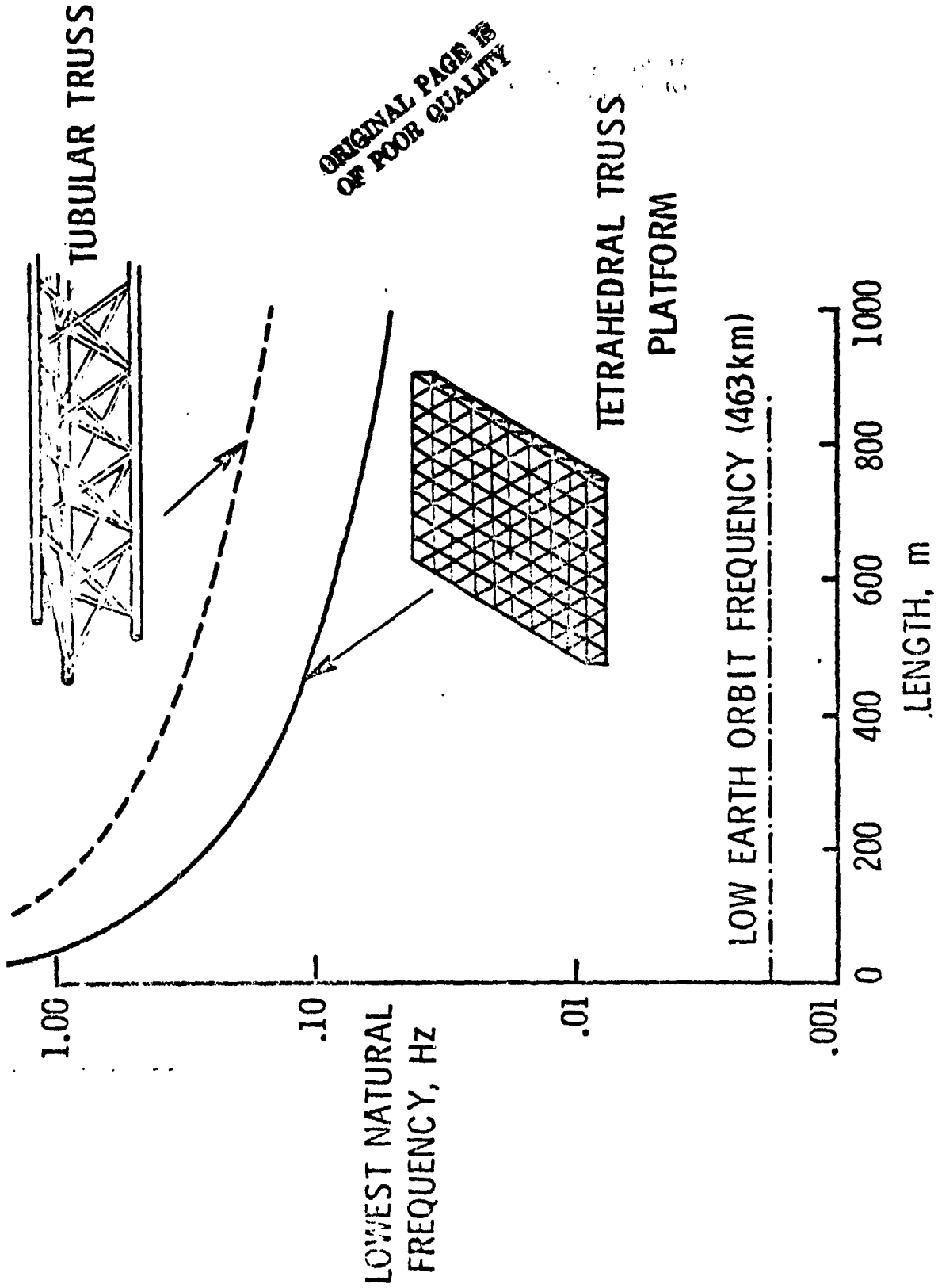
SYSTEM

SIGNIFICANT INSIGNIFICANT DEPENDEN

	SIGNIFICANT	INSIGNIFICANT	DEPENDEN
● GROUND HANDLING AND BOOST		X	
● DEPLOYMENT	X		
● ASSEMBLY	X		
● CONTROL			
● ATTITUDE	X		
● SURFACE			X
● GRAVITY		X	
● THRUSTING			
● ORBIT MAINTENANCE AND CHANGE	X		
● MANEUVERING			X
● DOCKING			
● DURING CONSTRUCTION			X
● DURING OPERATION		X	
● OPERATIONS			
● MACHINERY			X
● MAN MOVEMENTS		X	
● ENVIRONMENT			
● THERMAL			X
● AERODYNAMIC, MAGNETIC, SOLAR PRESSURE		X	

ORIGINAL PAGE IS OF POOR QUALITY

LOWEST FREQUENCIES OF LARGE PLATFORMS AND BEAMS





NASA
L-78-3916

ORIGINAL PAGE IS
OF POOR QUALITY

TECHNOLOGY RECOMMENDATIONSSPACE PAYLOADS

- o GREATER EMPHASIS ON ACTIVE LOAD SUPPRESSION AND DAMPING
- o NEED FOR BETTER MODELING TECHNIQUES AND MORE RATIONAL METHODS FOR CORRECTING ANALYSIS MODELS
- o MSFC CONSIDER SERIOUSLY SPACE LAB DYNAMICS LOADS EXPERIMENT

LARGE SPACE STRUCTURES

- o DEFINITION OF LOADS/DESIGN CRITERIA
- o LESS EMPHASIS ON FLEXIBILITY OF STRUCTURES
- o NASA SHOULD ADOPT "PRACTICAL APPLICATIONS" OF ARPA OPTICAL DYNAMICS/CONTROLS TECHNOLOGY

MODE SURVEY TESTING

- DIGITAL FREQUENCY-DOMAIN METHODS

- SOFTWARE DEPENDENCE

- CURVE-FIT ALGORITHMS, ETC.

- "TECHNIQUE"

- (WINDOWS, ZOOM, EDITING, ETC.)

- EXCITATION

- RANDOM, FAST-SINE, IMPACT

- SINGLE-POINT, MULTI-POINT

- MULTI-POINT SINE TESTING

- TUNING

- TIME-DOMAIN METHODS

- REL. TO F-D METH., LIMITATIONS

ORIGINAL PAGE IS
OF POOR QUALITY

MODAL SYNTHESIS METHODS

- COMPONENT MODEL
 - RESIDUAL FLEXIBILITY
 - ARBITRARY INTERFACE
- COUPLING PROCEDURE
 - FORM OF SYSTEM EQUATIONS
 - EFFICIENCY
- COMPATIBILITY WITH TEST PROC.
 - STATIC
 - GUT
- DAMPING

ORIGINAL PAGE IS
OF POOR QUALITY

PANEL SESSION - QUESTIONS AND RESPONSES

Card to Gatto

Do you feel there is an active program to reduce cost of integration on the Shuttle?

Gatto:

This is a broad question. In the area that I have cognizance of, yes, there is. In the real world, it is not structured for high priorities and funds. To make tools more efficient requires service of our better people in the program. It is not easy to take these people off of critical project efforts and assign them to methodology improvement programs. Yahata is very active in this. This problem has been brought to the attention of management. Management has been very receptive. We are trying to do our part; we are getting some efficiency in calculation techniques.

Stone:

Rockwell has devoted discretionary resources to this topic. Use of interactive graphic computers was added to the design effort and has been successful. We are trying to cut down on turnaround time for doing analysis. Interfaces have been set up for direct communication between people involved.

Hill to Card:

The papers on reducing loads focused primarily on landing cantilever loads in the Orbiter. Might you be able to design an optimal mechanical device to give an index to performance? Same kind of device that has been done for flutter based on measure of index for performance.

Card:

In terms of Langley's work, these techniques have been applied in a practical sense but there could be something new still out.

Ryan:

This optimized index of performance has been done in control work, and we are getting beneficial results and insights. Using the work done on active flutter suppression and control as a basis, we could and should develop performance indexes for loads on payloads and go from there.

Wade to Herzberg:

Is there a need for payloads to understand criteria that Shuttle has used in order to understand how much conservatism is used in loads and forcing functions? There was one workshop with payload users which described criteria used on Shuttle. Would you suggest we continue this as a normal service?

Herzberg:

Not sure which workshop you are talking about. I'm thinking more of a straightforward interchange between people who are critically responsible for the payload. Do not think a workshop is the right forum; just having access to technical information is all that is required.

Wade:

The Structural/Mechanical Working Group perhaps would be a good forum for anyone who has a payload to fly on Shuttle. These are technical interchange meetings. I suggest it be done there.

Herzberg:

In the Marshall involvement on Shuttle at Lockheed, emphasis has been placed on uncertainty factors on Shuttle and payload model. Recent modal test results should help reduce these. Can we expect to receive this type results of ground vibration test?

Ryan:

If people want it, NASA and MSFC and other Centers would be happy to respond to the payload community. Particularly, let Don Wade or me know. I'm sure we can do this. Information on dynamic test and follow-on test could be provided or discussed in another meeting.

Wade:

For Air Force payloads, post test data correlation has been sent when completed to the PIC contractor, Aerospace, and SAMSO.

Simondi:

You reach CDR on payloads two years prior to launch. Changes after CDR are expensive and not desired. Effect on cargo element and cargo dynamic analysis are at the 18 months point. Why is this acceptable?

Wade:

It is not until 18 months before the flight manifest is defined; consequently, it is not practical to run a verification analysis until the manifest of the configuration is defined. This is why we show 18 months. The final verification load analysis is planned to be finished 6 months prior to flight. In some cases, much of the verification of models for payloads are not accomplished until then; therefore, judgement has been standard. Special requests for payload verification at some other time are run. For example, we are willing to do this on TDRS. We are running somewhat early to support ground test program to be run at 9 months prior to flight. We try to be flexible within reason, but we have to establish the manifest first.

Simondi:

ORIGINAL PAGE IS
OF POOR QUALITY

In final design analysis just prior to CDR, if you don't have knowledge of cargo at this point, doesn't this give problems?

Wade:

Problem is one primarily of interaction of payload with whatever else is riding --not a big driver. The more sensitive thing appears to be the position in the payload bay, which depends quite a bit on dynamics of the payload. Some payloads are insensitive to position; others are sensitive. You put more than one model in the payload bay in different positions so the position can be checked on loads. Our standard service is to perform final verification analysis only. Design analysis of the payload description is not what you want run when you want it run; therefore, you should run payloads in several places of the bay with spectrum of payloads from very low to high frequencies.

Pengelley:

In the past ten years, there has been almost infinite increase in our ability to handle linearized eigenvalue solutions for real, undamped problems. During this time, hardly anyone has learned anything on nonlinear structures. We can't get rid of clearances and joints in payload design and fabrication. We are still seeing nonlinearities, parametric excitation, damping, structural damping, viscous damping. We need work on damping predictions and nonlinearities.

Wada:

I have put together a paper for the university on how to handle damping. Everybody uses simplified approach--1 percent for modal coupling. Ninety-nine percent use this approach. Nonlinearities cannot be defined. Different type of damping for each different joint. Almost nobody can define input parameters for damping.

Pengelley:

Is it a lack of knowledge of what to put in?

Ryan:

Everyone has taken the easy way out with 1 percent. We need simple models generated on physical insight instead of large finite element systems. We can't depend entirely on computers, but must depend on physics.

Herzberg:

The problem of damping goes back as far as 1870; no progress has been made. We will never make any progress unless there is a large volume of experimental data. This is one area where the universities must help us.

Craig:

True, the universities would like to make contribution.

Hill:

Mathematical tools to model, in principle, have been around. To handle large eigenvalue problems, these tools are not practical. Computers can handle problems without damping, can handle mass. Trying to develop best linear model for damping.

Simondi and Keegan:

Noticed Shuttle is paying a lot of attention to liftoff and landing loads. Talked about buildup rate of liquids, etc. There is an absence of discussions on transonic buffeting and how it might affect spacecraft loads. After Voyager, we wonder what thoughts are on pursuing this?

Wade:

Ran combined flutter buffet model of configuration for both ascent and descent. Looked at buffet levels. Probably biggest concern are loads on vertical tail as opposed to payloads. Load checks are made at transonic Mach number. Transonic loads were low; therefore, we thought there is enough margin. Were able to tolerate buffet levels we expected. No significant overall vehicle response to buffet from tests.

Gatto:

This is similar to what we have done. During descent, coming back, operate with rudder deployed open. Buffeting is something we will have to wait on flight experience to see if testing has been adequate. Liftoff and landing are where payload dynamics are of interest to Shuttle vehicle design. These are only two out of many flight events that are important.

Wade:

Everyone should use other conditions to be sure they are not overlooked something, particularly high q loading conditions. Loads man should look at overall load cases.

From the floor:

For payload performance capability increases, will you be going to weight reduction or thrust augmentation? Do you foresee affect on loads analysis or acoustic environment?

Wade:

Don't envision there will be very much effect. Will be some changes in bridge fairings on Orbiter to take weight out of bridges. Bridge design has been based on Orbiter capability, not on payload requirements. This will allow some weight reduction in some of the bridges. Different primary

ORIGINAL PAGE IS
OF POOR QUALITY

ORIGINAL PAGE IS
OF POOR QUALITY

solid rocket boosters are being considered, where the thrust for rocket is equal to their weight. Ignition acoustics and overpressure of solids environment could be worse at liftoff. We will need to look at max q alleviation again. We may have to reshape trajectory based on additional thrust and weight. Should not affect payload world very much.

Simondi and Keegan:

GSFC presentation on DATE appeared to support dynamics. If this is the case, considering state of funding, would the panel make comments to support or oppose operational measurement system?

Card:

Already cast vote.

Ryan:

We all want flight data. First Shuttle flights have instrumentation geared to remove uncertainty in vehicle parameters as we move downstream. Primarily for getting Shuttle ready for operational flight first. We have requested special instrumentation on first Spacelab flights for dynamic data.

Wade:

We do not have enough flight instruments. Not successful in getting everything desired in payload world. During OFT flights, biggest void was in getting enough accelerometers in the payload bay. System proposed on LDEF has a problem with 2 to 50 Hz accelerometers which cannot measure transient loads. Were able to get some 0 to 50 Hz in payload bay area. Encourage more thought be given to instrumentation on DATE especially in payload area. Also, get 0 to 50 Hz loads transducers on LDEF payload.

From the floor:

What is the status of payloads to flight on first Shuttle flights? Are they already designed?

Wade:

First launch will carry DFI to check out Shuttle system itself. Second flight is TRS to rescue Skylab, being developed at MSFC. CDR on TRS is this week. Third flight will contain OSTA-1. Experiments

are now being integrated into OFT payload through CDR. Payloads are now in development. Payload integration plans are being written.

From the floor:

Are there any guidelines to reduce loads?

Wade:

Frequencies that stay away from 2.5 Hz system.

Is there a publication of these guidelines forthcoming?

Wade:

Two attempts were made to do this, MCR 1612 and a study with the Air Force on load alleviation. We put out some guidelines which Boeing is using.

ORIGINAL PAGE IS
OF POOR QUALITY

APPROVAL

GOVERNMENT INDUSTRY WORKSHOP ON PAYLOAD LOADS TECHNOLOGY

The information in this report has been reviewed for security classification. Review of any information concerning Department of Defense or nuclear energy programs or activities has been made by the MSFC Security Classification Officer. This report, in its entirety, has been determined to be unclassified.



J. A. LOVINOOD

Director, Systems Dynamics Laboratory